AEROSPACE REPORT NO.
ATR-86(7126)-2

(2)

AD-A213 738

Final Report
Infrared Detector Array Test Program for the Kuiper Infrared Technology Experiment (KITE)

Prepared by

R. W. RUSSELL, G. M. BOYD, S. C. CHAPMAN, J. E. COX, D.J. EDELSOHN,
L. M. FRIESEN, J.. A. HACKWELL, A. M. KISHI, D. K. LYNCH, C. J. RICE,
AND G. S. ROSSANO
Space Sciences Laboratory

DTIC
ELECTE
OCT 26 1989
S B D

April 1987

Laboratory Operations
THE AEROSPACE CORPORATION
El Segundo, CA 90245

Prepared for

NATIONAL AERONAUTICS AND SPACE ADMINISTRATION
Ames Research Center
Moffett Field, CA 94035

Contract No. NAS2-12155

Development Group

THE AEROSPACE CORPORATION

PUBLIC RELEASE IS AUTHORIZED

DISTRIBUTION STATEMENT A

Approved for public release;
Distribution Unlimited

054

LABORATORY OPERATIONS

The Aerospace Corporation functions as an "architect-engineer" for national security projects, specializing in advanced military space systems. Providing research support, the corporation's Laboratory Operations conducts experimental and theoretical investigations that focus on the application of scientific and technical advances to such systems. Vital to the success of these investigations is the technical staff's wide-ranging expertise and its ability to stay current with new developments. This expertise is enhanced by a research program aimed at dealing with the many problems associated with rapidly evolving space systems. Contributing their capabilities to the research effort are these individual laboratories:

Aerophysics Laboratory: Launch vehicle and reentry fluid mechanics, heat transfer and flight dynamics; chemical and electric propulsion, propellant chemistry, chemical dynamics, environmental chemistry, trace detection; spacecraft structural mechanics, contamination, thermal and structural control; high temperature thermomechanics, gas kinetics and radiation; cw and pulsed chemical and excimer laser development including chemical kinetics, spectroscopy, optical resonators, beam control, atmospheric propagation, laser effects and countermeasures.

Chemistry and Physics Laboratory: Atmospheric chemical reactions, atmospheric optics, light scattering, state-specific chemical reactions and radiative signatures of missile plumes, sensor out-of-field-of-view rejection, applied laser spectroscopy, laser chemistry, laser optoelectronics, solar cell physics, battery electrochemistry, space vacuum and radiation effects on materials, lubrication and surface phenomena, thermionic emission, photo-sensitive materials and detectors, atomic frequency standards, and environmental chemistry.

Computer Science Laboratory: Program verification, program translation, performance-sensitive system design, distributed architectures for spaceborne computers, fault-tolerant computer systems, artificial intelligence, micro-electronics applications, communication protocols, and computer security.

Electronics Research Laboratory: Microelectronics, solid-state device physics, compound semiconductors, radiation hardening; electro-optics, quantum electronics, solid-state lasers, optical propagation and communications; microwave semiconductor devices, microwave/millimeter wave measurements, diagnostics and radiometry, microwave/millimeter wave thermionic devices; atomic time and frequency standards; antennas, rf systems, electromagnetic propagation phenomena, space communication systems.

Materials Sciences Laboratory: Development of new materials: metals, alloys, ceramics, polymers and their composites, and new forms of carbon; non-destructive evaluation, component failure analysis and reliability; fracture mechanics and stress corrosion; analysis and evaluation of materials at cryogenic and elevated temperatures as well as in space and enemy-induced environments.

Space Sciences Laboratory: Magnetospheric, auroral and cosmic ray physics, wave-particle interactions, magnetospheric plasma waves; atmospheric and ionospheric physics, density and composition of the upper atmosphere, remote sensing using atmospheric radiation; solar physics, infrared astronomy, infrared signature analysis; effects of solar activity, magnetic storms and nuclear explosions on the earth's atmosphere, ionosphere and magnetosphere; effects of electromagnetic and particulate radiations on space systems; space instrumentation.

AEROSPACE REPORT NO.
ATR-86(7126)-2

Final Report
Infrared Detector Array Test Program for the Kuiper Infrared Technology Experiment (KITE)

Prepared by

R. W. RUSSELL, G. M. BOYD, S. C. CHAPMAN, J. E. COX, D.J. EDELSOHN,
L. M. FRIESEN, J.. A. HACKWELL, A. M. KISHI, D. K. LYNCH, C. J. RICE,
AND G. S. ROSSANO
Space Sciences Laboratory

April 1987

Laboratory Operations
THE AEROSPACE CORPORATION
El Segundo, CA 90245

Prepared for

NATIONAL AERONAUTICS AND SPACE ADMINISTRATION
Ames Research Center
Moffett Field, CA 94035

Contract No. NAS2-12155

Development Group

PUBLIC RELEASE IS AUTHORIZED

Aerospace Report No.
ATR-86(7126)-2

FINAL REPORT

INFRARED DETECTOR ARRAY TEST PROGRAM FOR THE KUIPER INFRARED TECHNOLOGY EXPERIMENT (KITE)

Prepared by

R. W. Russell, G. M. Boyd, S. C. Chapman, J. E. Cox, D. J. Edelsohn, L. M. Friesen, J. A. Hackwell, A. M. Kishi, D. K. Lynch, C. J. Rice, and G. S. Rossano,

Space Sciences Laboratory

April 1987

Laboratory Operations
THE AEROSPACE CORPORATION
El Segundo, CA 90245

Prepared for

NATIONAL AERONAUTICS AND SPACE ADMINISTRATION
Ames Research Center
Moffett Field, CA 94035

Contract No. NAS2-12155

LABORATORY OPERATIONS

The Aerospace Corporation functions as an "architect-engineer" for national security projects, specializing in advanced military space systems. Providing research support, the corporation's Laboratory Operations conducts experimental and theoretical investigations that focus on the application of scientific and technical advances to such systems. Vital to the success of these investigations is the technical staff's wide-ranging expertise and its ability to stay current with new developments. This expertise is enhanced by a research program aimed at dealing with the many problems associated with rapidly evolving space systems. Contributing their capabilities to the research effort are these individual laboratories:

Aerophysics Laboratory: Launch vehicle and reentry fluid mechanics, heat transfer and flight dynamics; chemical and electric propulsion, propellant chemistry, chemical dynamics, environmental chemistry, trace detection; spacecraft structural mechanics, contamination, thermal and structural control; high temperature thermomechanics, gas kinetics and radiation; cw and pulsed chemical and excimer laser development including chemical kinetics, spectroscopy, optical resonators, beam control, atmospheric propagation, laser effects and countermeasures.

Chemistry and Physics Laboratory: Atmospheric chemical reactions, atmospheric optics, light scattering, state-specific chemical reactions and radiative signatures of missile plumes, sensor out-of-field-of-view rejection, applied laser spectroscopy, laser chemistry, laser optoelectronics, solar cell physics, battery electrochemistry, space vacuum and radiation effects on materials, lubrication and surface phenomena, thermionic emission, photosensitive materials and detectors, atomic frequency standards, and environmental chemistry.

Computer Science Laboratory: Program verification, program translation, performance-sensitive system design, distributed architectures for spaceborne computers, fault-tolerant computer systems, artificial intelligence, microelectronics applications, communication protocols, and computer security.

Electronics Research Laboratory: Microelectronics, solid-state device physics, compound semiconductors, radiation hardening; electro-optics, quantum electronics, solid-state lasers, optical propagation and communications; microwave semiconductor devices, microwave/millimeter wave measurements, diagnostics and radiometry, microwave/millimeter wave thermionic devices; atomic time and frequency standards; antennas, rf systems, electromagnetic propagation phenomena, space communication systems.

Materials Sciences Laboratory: Development of new materials: metals, alloys, ceramics, polymers and their composites, and new forms of carbon; nondestructive evaluation, component failure analysis and reliability; fracture mechanics and stress corrosion; analysis and evaluation of materials at cryogenic and elevated temperatures as well as in space and enemy-induced environments.

Space Sciences Laboratory: Magnetospheric, auroral and cosmic ray physics, wave-particle interactions, magnetospheric plasma waves; atmospheric and ionospheric physics, density and composition of the upper atmosphere, remote sensing using atmospheric radiation; solar physics, infrared astronomy, infrared signature analysis; effects of solar activity, magnetic storms and nuclear explosions on the earth's atmosphere, ionosphere and magnetosphere; effects of electromagnetic and particulate radiations on space systems; space instrumentation.

ion For
GRA&I ☑
AB ☐
unced ☐
cation
By
Distribution/
Availability Codes
Dist	Avail and/or Special
A-1	

Report No.
ATR-86(7126)-2

FINAL REPORT
INFRARED DETECTOR ARRAY TEST PROGRAM FOR THE
KUIPER INFRARED TECHNOLOGY EXPERIMENT (KITE)

Prepared

R. W. Russell

G. M. Boyd

S. C. Chapman

J. E. Cox

D. J. Edelsohn

L. M. Friesen

J. A. Hackwell

A. M. Kishi

D. K. Lynch

C. J. Rice

G. S. Rossano

Approved

E. M. Randall, Head
Mathematics and Analysis Department
Space Sciences Laboratory

H. R. Rugge, Director
Space Sciences Laboratory
Laboratory Operations

ABSTRACT

Three two-dimensional infrared arrays have been tested under flight conditions on the NASA-Ames Research Center Kuiper Airborne Observatory (KAO). Two series of 3 flights each were undertaken. Two of the arrays were manufactured by Aerojet ElectroSystems Company; these were a 16 x 32 pixel Si:Bi bulk array and a 16 x 32 pixel Si:As MC^2 (impurity band conduction) array. The third array, a BIBIB (back-illuminated blocked impurity band) Si:As detector, with 10 x 50 pixels, was manufactured by Rockwell International. This report concentrates on several aspects of general array performance observed during the sixth flight, during which each of the arrays was mounted on the telescope. Each array was exposed to background radiation from the telescope and the atmosphere and each was able to detect a star. The performance characteristics of representative array pixels are presented in some detail, while tables show the performance of all pixels as a set. Anomalies and other unusual characteristics of the data are discussed, linking each characteristic to its apparent source in the arrays themselves, the associated multiplexers, or other elements of the array electronics system. The techniques and nature of the flatfielding required and correction for local background are also addressed. Properties of the noise and the uniformity of the arrays are examined in detail with tables and gray-scale plots.

Acknowledgments

The success of the KITE project was due to extensive efforts by a large number of people. Numerous individuals at the Army's Ballistic Missile Defense Advanced Technology Center (now U.S. Army Strategic Defense Command), Teledyne Brown Engineering in Huntsville, and Ames Research Center played important roles. Dave Pollock of TBE played a key role in the collimation of the KAO telescope between flights, and Doug Elgin of TBE lent significant guidance in the planning of the observations. Carl Gillespie and the flight and ground crews at NASA-Ames gave many hours of dedicated support. We particularly want to thank Bob Keever of the Boeing Aircraft Company for his enthusiasm and willingness to take on tasks as needed, and for supplying us data on floppy disc to replace some of the lost 28-track data.

We wish to give special recognition to Bob Macklin of SSL, who constructed the isolation interface to the arrays, wrote the software to transmit floppy disc files to the VAX, and was the key person coaxing data onto and off from the 28-track recorder. Thus, the presence of data in this report is in large measure due to his efforts. We also wish to especially thank the array teams at Aerojet ElectroSystems Company and at Rockwell International who were dedicated to making their arrays perform in the best manner possible. Many fruitful discussions were held with the technical people over the course of the project.

Table of Contents

List of Figures and Tables

I. SUMMARY

Three two-dimensional infrared arrays have been tested under flight conditions as part of the Kuiper Infrared Technology Experiment (KITE) sponsored by the U. S. Army Ballistic Missile Defense Advanced Technology Center (BMDATC), now the U.S. Army Strategic Defense Command (USASDC), in Huntsville, Alabama, and overseen by NASA-Ames Research Center in Mountain View, California. The arrays were tested under a variety of conditions in the laboratory, at groundbased telescopes, and, ultimately, under flight conditions aboard the Kuiper Airborne Observatory (KAO) which flies out of Ames.

The three arrays tested were 1) a Si:Bi bulk array with 16 x 32 pixels and 2) an Si:As MC^2 (impurity conduction band) array (also with 16 x 32 pixels), both of which were manufactured by Aerojet ElectroSystems Company (AESC), and 3) an Si:As BIBIB (back-illuminated Blocked Impurity Band) array with 10 x 50 pixels manufactured by Rockwell International. The purpose of the tests was to demonstrate the use of arrays of these types under flight conditions while evaluating both the performance of the arrays as well as limitations imposed by operation in an aircraft environment with a cooled telescope exposed to and viewing through the local ambient environment.

This report presents parameters quantifying the noise performance of each of the arrays by means of a number of related tables displaying values derived for every pixel. In addition, noise distributions are shown in detail for a number of representative channels in order to clarify the significance of parameter values found in the tables. The major conclusion to be drawn from these data is that, except when the detector array element itself was clearly damaged, the noise is well represented by a normal (or gaussian) distribution. There is no evidence for "excess" noise appearing as extended tails, nor for frequency-dependent noise. The only significant deviation from gaussian noise appears to be due to unevenly-spaced channels in the analog-to-digital converters, a common and well-known problem with successive-approximation encoders.

A good star detection was obtained with each of the arrays. The background measured by pointing the telescope just off the star was used to generate multipliers to flat-field each array. These values were then used

with values measured by pixels just above and below the star image to subtract the local background. The size of the star on the arrays was such that a pixel received approximately 15% of the available irradiance at the peak of the image, and less on pixels away from the peak. These star sightings have been used to determine a noise-equivalent power for each of the detector arrays. The system NEP is 1-2 x 10^{-13} $W/\sqrt{Hz}$ for each of the arrays. Taking into account the transmission through the telescope and dewar optics, the array NEP is ~5 x 10^{-14} $W/\sqrt{Hz}$. This indicates background limited performance. The scanning (chopping) secondary mirror was used to successfully demonstrate a time-delay-and-integrate mode of observation to improve the statistiscal significance (signal-to-noise) of the detection of a point source. This latter experiment has been discussed in detail in Boeing (Hibben et al. 1986) and TBE reports (Elgin 1985, Elgin 1986; Chu et al. 1986).

II. INTRODUCTION

The Kuiper Infrared Technology Experiment (KITE) is a U. S. Army-sponsored project to investigate such areas as atmospheric seeing effects, effects of aerodynamic factors on image quality, background radiance from the atmosphere and the telescope, and general implications and limitations in the use of IR arrays in an airborne environment. The program is built around the use of the Kuiper Airborne Observatory (KAO), a 4-engine C-141 jet transport into which has been built a 90-cm telescope optimized for infrared observations (Cameron 1976, Haughney and Mumma 1986, Elliott et al. 1989). The telescope has all-reflective optics in an altazimuth mount. It views out the left side of the aircraft at elevation angles between 35 and 72 degrees. Three state-of-the-art detector arrays were tested on the KAO under flight conditions. They were

1. Si:Bi Bulk Array
   16 x 32 pixels
   Aerojet ElectroSystems Company

2. Si:As MC^2 (Impurity Band Conduction) Array
   16 x 32 pixels
   Aerojet ElectroSystems Company

3. Si:As BIBIB (Back-Illuminated Blocked Impurity Band) Array
   10 x 50 pixels
   Rockwell International

The goals of the array work were

1. To demonstrate the use of state-of-the-art IR arrays in a working aircraft flight system.

2. To collect information on the characteristics of the arrays in an airborne environment subject to the ground currents, radio transmissions, and mechanical and acoustical vibrations which are an unavoidable part of that environment.

3. To evaluate the performance of the arrays, in particular in the following areas:

   a. To quantify the angular size of the IR image near 11 microns over a variety of time scales, and to measure the amount of motion of the image (blur size and jitter).

   b. To collect a database for evaluating the impact of varying aerodynamical parameters such as Mach number and cavity turbulence on the image quality.

4. To attempt an actual demonstration of system performance in a time-delay-and-integrate (TDI) mode.

5. To provide a database for subsequent use in studies of signal processing of extended sources, background variability and subtraction, and closely-spaced objects.

This final report will focus on tasks 1, 2 and 3, while providing general information pertinent to the use of the database as a generic resource. Task 4 was discussed briefly in the Annual Report (Russell et al., 1986) and more completely in reports from The Boeing Company and Teledyne Brown Engineering.

Russell et al. (1986) described aspects of the experiment, in particular the instrumentation, in some detail. The Annual Report presented a description of the hardware, field trips, and flight series conducted under this contract. In addition, the Annual Report presented some preliminary data analysis, specifically, detections of stars with each of the three arrays (Rockwell BIBIB, AESC Bulk and AESC MC^2) used for this program. Subsequent analyses have confirmed and refined the results presented in that document. The present final report will discuss several aspects of the analysis in more detail and will include a significantly larger quantity of data than the Annual Report, principally in the form of tables and plots of distributions of frequency of occurrence of various A/D count levels (ADCs), FFTs, etc. It is worth noting that all of the data presented to date still represent only a small fraction of all of that acquired under this program. In the present report, representative data for each array will be shown, with the format and pixels chosen to assist the reader in understanding which effects are linked to the arrays, which to the multiplexers, which to the digital electronics, etc. The most important parameters describing array performance during flight will be discussed in detail, including derivation of Noise Equivalent Power (NEP) and signal-to-noise ratio. There will also be a discussion of flat fielding, "local background" subtraction, and some of the general properties of the noise. We emphasize that, unlike many reports of this type, we show typical or representative images and noise data, not the "best" data available.

III. NOISE MEASUREMENTS

Noise is the most critical parameter that goes into estimating the overall performance of the detector array system used in this program. It is for this reason that we have concentrated so much of our effort in this Final Report upon measuring detector noise and upon discussing its probable source.

Although most of the results discussed below came from post-flight analysis of the data, the noise level of the detectors was monitored in three different ways during the flight. This real-time monitoring of the noise level allowed us to avoid any problems that might have been introduced by obvious electromagnetic interference, noise from bad contacts at cable connections, cabling microphonics, or other intermittent noise sources. During almost the entire flight, the Aerospace data acquisition system showed the array output as a colored "checkerboard" pattern that was updated at about 15 hertz. Each color in the display represented a different signal level, and visual monitoring of the display gave the operator a good idea of overall system performance. Most of the time the display showed the total array signal and the noise was less than one color interval in the display. The color monitor gave a better indication of noise during the time that the star position was "chopped" on and off the array. For this measurement the "on-star" and "off-star" signals were differenced, and the noise was readily visible on the screen. A qualititative idea of the signal-to-noise (S/N) ratio was given by the ease with which the star could be seen against the noise. A second method of monitoring the noise during flight was by feeding the output from one pixel (the hardware "quick-look" output) into an Ithaco lock-in amplifier which could be set to display the root-mean-square (rms) noise at any frequency between 10 and 100 hertz with a bandwidth of 1 hertz. Third, the same one-pixel output was fed into an HP 3582A spectrum analyzer which calculated the noise spectrum from a Fourier transform of the pixel signal. In flight, the spectrum analyzer occasionally showed a noise peak near 120 hertz. No hard record could be made of data from the lock-in amplifier or from the spectrum analyzer, although some Polaroids of the spectrum analyzer display were taken by TBE.

Each of the detector array systems generated analog voltages that were encoded by analog-to-digital converters (ADCs). The post-flight analysis of these data is discussed in the remainder of this section. These data were recorded in two ways. In principle, the most complete data set was to be recorded onto a 28-track digital tape recorder that had the bandwidth to store all ~ 500 pixels from every frame at rates corresponding to as little as 300 microseconds per frame. Technical problems with the 28-track recorder resulted in readable data being recorded only for the Rockwell BIBIB array. But data from every array were written onto 9-track tape by The Aerospace Corporation's 16-bit computer system. This computer was unable to record every frame at a 300 microsecond frame interval due to speed limitations in the computer. These files represent 3200 frames x 300 microseconds per frame or about 1 second of total integration time over a ~ 4-second period. Moreover, these frames were not uniformly sampled in time; sometimes every third and sometimes every fourth frame was stored depending upon the relative timing of the computer and array clocks. Nevertheless, these 3200-frame files recorded on 9-track tape represent a uniform data resource for all of the arrays, and it is these files that we have studied the most closely.

The first simple question that can be asked of the 9-track data is whether or not the noise is "normally" distributed (i.e. if there is a gaussian distribution of signal intensities). To study this, we have constructed histograms of the ADC counts from a representative 3200-frame file for each of the detector arrays tested. A large sample of these histograms is shown in Appendix A. Almost all of the pixels that are working show a gaussian-like peak that is centered on a single maximum. For comparison, the gaussian that best fits the mean and standard deviation of the sample is also shown, and is seen to be a good fit in almost all of the cases. A formal test of the shape of the distribution was made by computing the reduced χ^2 (or χ^2 per degree of freedom; see, e.g. Taylor, 1982). This is defined as:

$$\chi^2 = \{\Sigma[\frac{(\text{observed-expected})^2}{\text{expected}}]\}/(N-3) \ .$$

We have assumed that the standard deviation of the frequency of occurrence of a given ADC value is determined by Poisson statistics (i.e. is the square root of the frequency). Although inspection by eye shows that the gaussian distribution agrees quite well in shape and form with the measured distribution, in

all cases the formal χ^2 varies significantly from the expected value of approximately 1. The chance probability of occurrence of the measured χ^2 values is less than 10^{-4} in most cases.

To study further the source of the discrepancy between the spuriously high values of χ^2 and the otherwise apparently good fit between the data and a normal distribution, we computed higher moments of the ADC count distribution. To remain within accepted practice, we represented the third moment of the distribution by the Pearson "skewness", and the fourth moment by the "kurtosis." Formal definitions of the mean, variance, skewness, and kurtosis are as follows (see, e.g. Martin, 1971):

mean $$\bar{x} = \frac{\Sigma\, x_i}{N} \; ;$$

variance $$\sigma^2 = \frac{\Sigma\, (x_i - \bar{x})^2}{N - 1} \; ;$$

skewness, $$\beta_1 = \frac{[\Sigma(x_i - \bar{x})^3]^2}{[\Sigma(x_i - \bar{x})^2]^3} \; ;$$

kurtosis, $$\beta_2 = \frac{\Sigma(x_i - \bar{x})^4}{[\Sigma(x_i - \bar{x})^2]^2} \; .$$

For a gaussian distribution, the skewness, which measures the asymmetry of the distribution, is zero; the kurtosis, which measures the peakedness of the distribution, is 3. Close-to-ideal values of skewness and kurtosis are seen for almost all of the "working channels". Thus the high values of χ^2 must be explained by a mechanism other than a gross deviation from a normal distribution of the ADC counts. The explanation for high χ^2 that we favor is that the ADC has unevenly-spaced channels so that all voltage values are not equally represented in the encoder. This results in the deviations of the counts in a given channel not being properly represented by the Poisson distribution as calculated from the best-fit gaussian, and in a larger than expected value for the formal χ^2. For a given ADC channel, the relative values of χ^2 will be meaningful, but channel-to-channel variations will represent mainly the relative quality of the encoders.

As an example of the usefulness of reducing the ADC count distributions to four parameters (i.e., mean, standard deviation, skewness, and kurtosis), we observe that in instances when there were frames of zeros (which occurred for unknown reasons on AESC 9-track tapes), or when sync pulses had been incorrectly identified (as happened occasionally on some RI downloaded 28-track tapes) then the skewness and kurtosis increased by an order of magnitude over the values shown in Appendix A. At the same time, the mean and standard deviation were near those expected for "good" data; thus, the skewness and kurtosis were important warning flags of bad data.

As a further test of the frequency content of the array outputs, we used Fourier transforms to study a stream of RI data taken from the 28-track tape recorder. Figure 1 shows the amplitude spectrum of the noise vs. frequency for several representative pixels from the Rockwell BIBIB array. There is no evidence for 120 hertz interference, nor is there significant power over white noise at any other frequency. The 1/f noise component is also very slight. This result supports in all ways the conclusions about the gaussian distribution of the noise that we reached by studying the count distributions.

The major conclusion that we draw from the data shown in Appendix A and associated tables is that, except when the detector array element itself was damaged (see, e.g. column 12 of the AESC MC^2 array), the noise is well represented by a normal (or gaussian) distribution. There is no evidence for "excess" noise appearing as extended tails, nor for frequency-dependent noise. The only significant deviation from gaussian noise appears to be due to unevenly-spaced channels in the ADCs, a common and well-known problem with successive-approximation encoders.

Figure 1: Fourier amplitudes of the time-series output from several pixels in the Rockwell BIBIB array are shown. Each sequence was 3200 samples long with an interval of 300 microseconds; thus the first tick-mark at 400 represents a frequency of about 417 hertz. There is little evidence for low-frequency 1/f noise in the specta. Each plot is labeled by column and row number starting from zero. Thus, RI detectors ranged from column 0, row 0, to column 9, row 49.

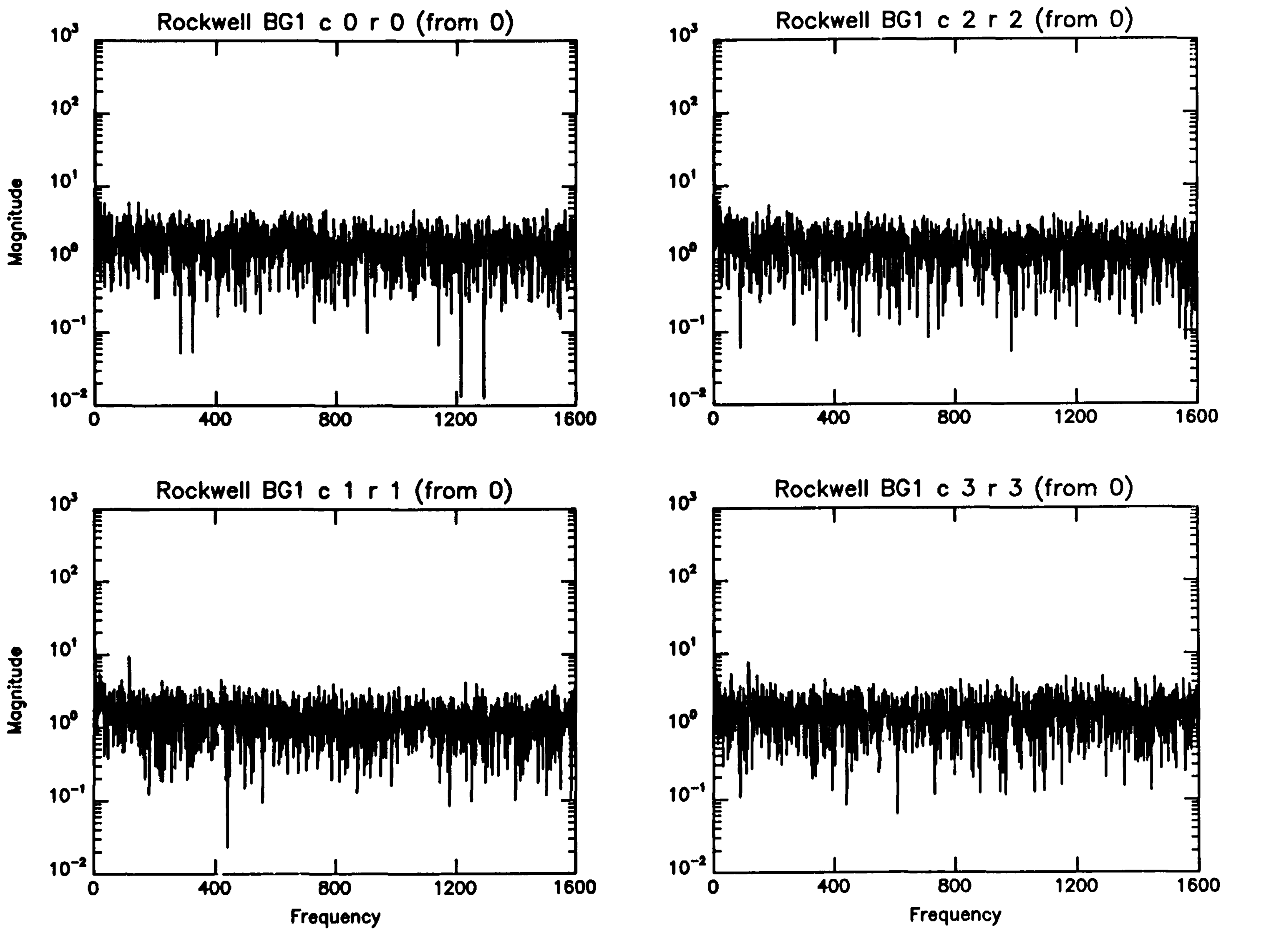

Rockwell BG1 c 0 r 0 (from 0)
Rockwell BG1 c 2 r 2 (from 0)
Rockwell BG1 c 1 r 1 (from 0)
Rockwell BG1 c 3 r 3 (from 0)
Magnitude
Frequency

Figure 1a

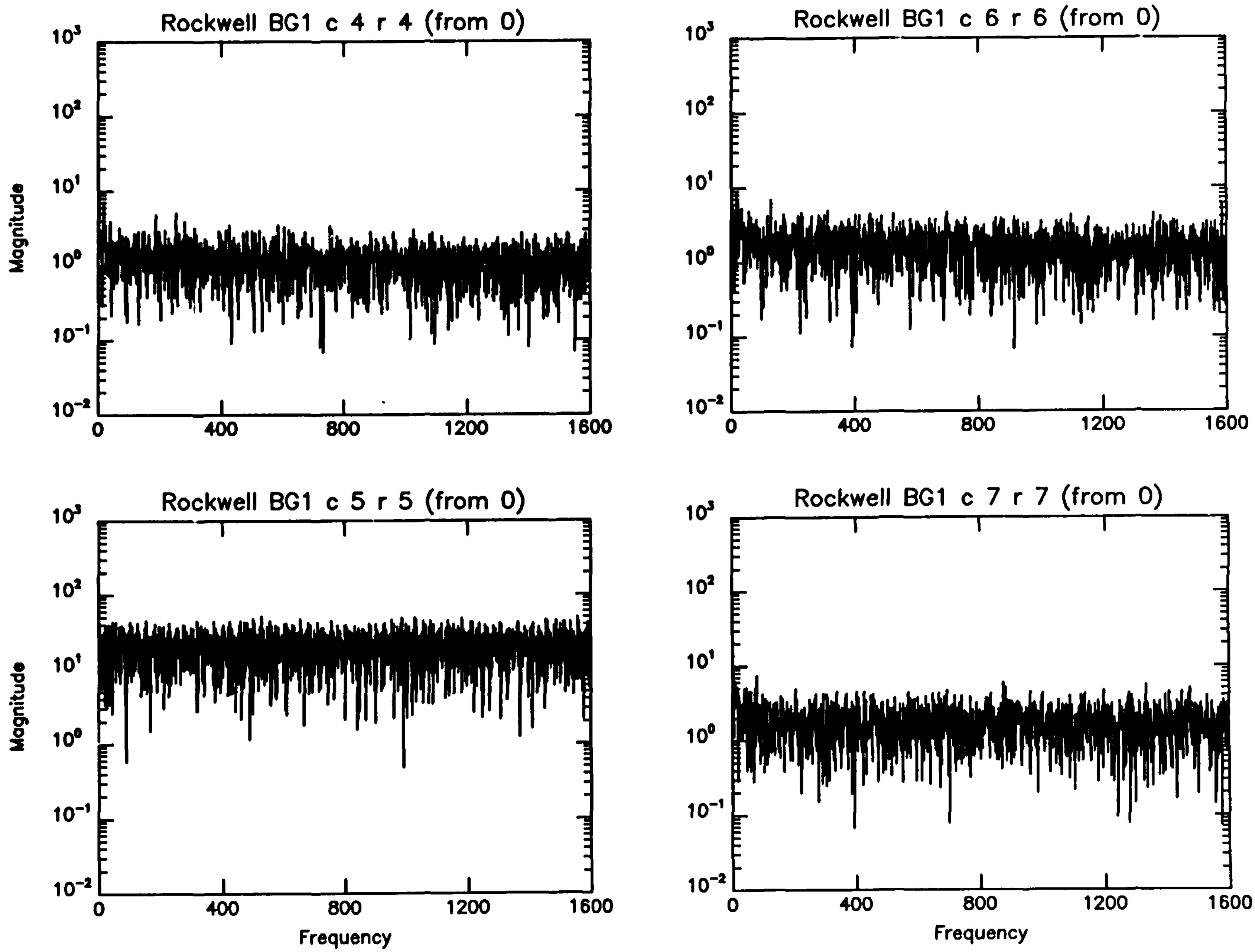
Rockwell BG1 c 4 r 4 (from 0)
Rockwell BG1 c 6 r 6 (from 0)
Rockwell BG1 c 5 r 5 (from 0)
Rockwell BG1 c 7 r 7 (from 0)
Magnitude
Frequency
10³
10²
10¹
10⁰
10⁻¹
10⁻²
0
400
800
1200
1600

Figure 1b

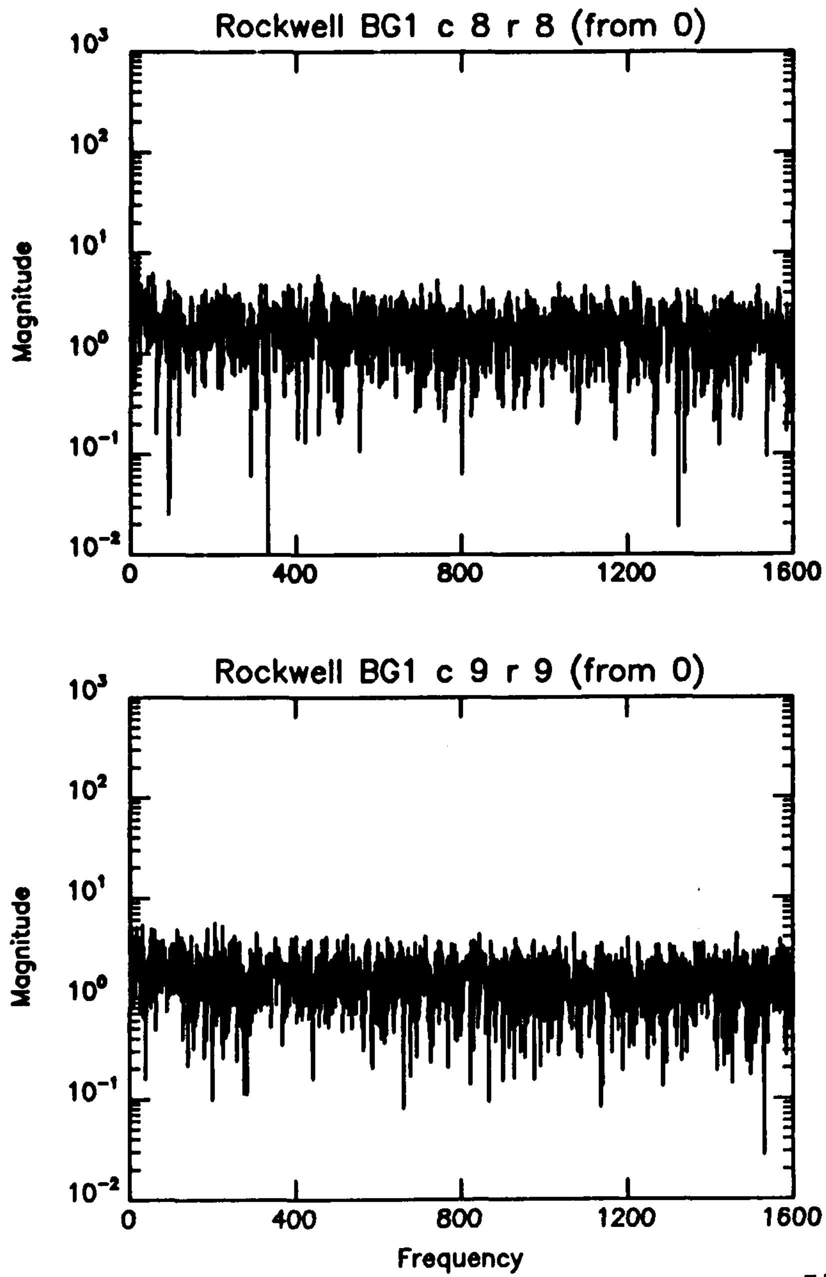
Rockwell BG1 c 8 r 8 (from 0)
Magnitude
10³
10²
10¹
10⁰
10⁻¹
10⁻²
0
400
800
1200
1600
Rockwell BG1 c 9 r 9 (from 0)
Magnitude
10³
10²
10¹
10⁰
10⁻¹
10⁻²
0
400
800
1200
1600
Frequency

Figure 1c

IV. STAR MEASUREMENTS

To reduce the noise measurements discussed above to absolute intensity values that are suitable for calculating Noise Equivalent Power (NEP) or D^* requires that the detector array be illuminated by a source of known brightness. We found that observations of bright infrared stars were the most suitable for testing the detectors under operating conditions. This section discusses the data reduction of such stellar measurements and the implications of the results.

As an example of our data-reduction technique, we discuss measurements made with the AESC MC^2 detector that are shown in Figure 2. The top center image of Figure 2 shows the mean for a 3200-frame file of a field that contains the infrared star Alpha Orionis; the bottom center image shows a 2700-frame mean on a field near the star that was made immediately after the star measurement. There is no obvious difference between the sets of measurements. The appearance of both is dominated completely by pixel-to-pixel variations in the detector responsivity/multiplexer characteristics modulating the appearance of the background signal, which was much greater than the star signal. The right hand side of Figure 2 shows the ratio of the average of the star frames to the background in the top image, and the combined standard deviation in the bottom image. Some vignetting effects can be seen on the top and left edges. This ratio has removed, to first order, the effects of different pixel-to-pixel responsivities/outputs and reveals the star. The principal reason that the star's signal was not visible on the "raw" frames is that, even though Alpha Orionis is one of the brightest infrared stars in the sky, it is only about 1% of the background intensity, and is therefore completely swamped by the unevenness of the array response. The principal lesson to be drawn here is that, if targets less bright than the background are to be viewed by these arrays, some "flat-fielding" will have to be done to remove the effects of pixel-to-pixel variations in the responsivity until more uniform arrays are routinely available. Arrays obtained recently have demonstrated ~1-5% uniformity and offer great promise for easier use. Figure 3 shows the same ratio data as Figure 2 but in the form of 3D plots. Note that the star is the slightly-extended source in the center of the frame. The other compact features are the result of "hot" or noisy pixels in the array. Optical vignetting on the left side (3 columns) and top (2 rows)

Figure 2: Imagery with the AESC MC^2 array. The top center image is the average of 3200 frames of 300 μsec each of raw data with the stellar source α Ori contained in the field of view. The standard deviation for each pixel is shown to the left. In the center bottom image is the average of 2700 frames of 300 μsec each of the sky near the star. Again, the standard deviation is shown to the left. Due to the large size of the background flux (mostly emitted by the telescope at the wavelength of 11 μm used here), compared to the star, these images are virtually indistinguishable. On the upper right is the flat-fielded image of the star as discussed in the text. The 148 pixels which yielded a ratio of less than .9955 have been set to black, and these pixels are mostly in the dead column and vignetted portions of the array. Pixels (0,2), (14,1), (15,5), (2,11), and (8,22) have been set to one. The place scale here is about 4.7"/pixel, or 23 μradians/pixel. The combined (square root of the sum of the squares) standard deviation of the flat fielded image is shown on the bottom right. For each array, the smallest and largest values plotted are given as "MIN" and "MAX".

AESC MC^2 ARRAY

STAR: α ORI = AFGL 836 = IRC + 10°100

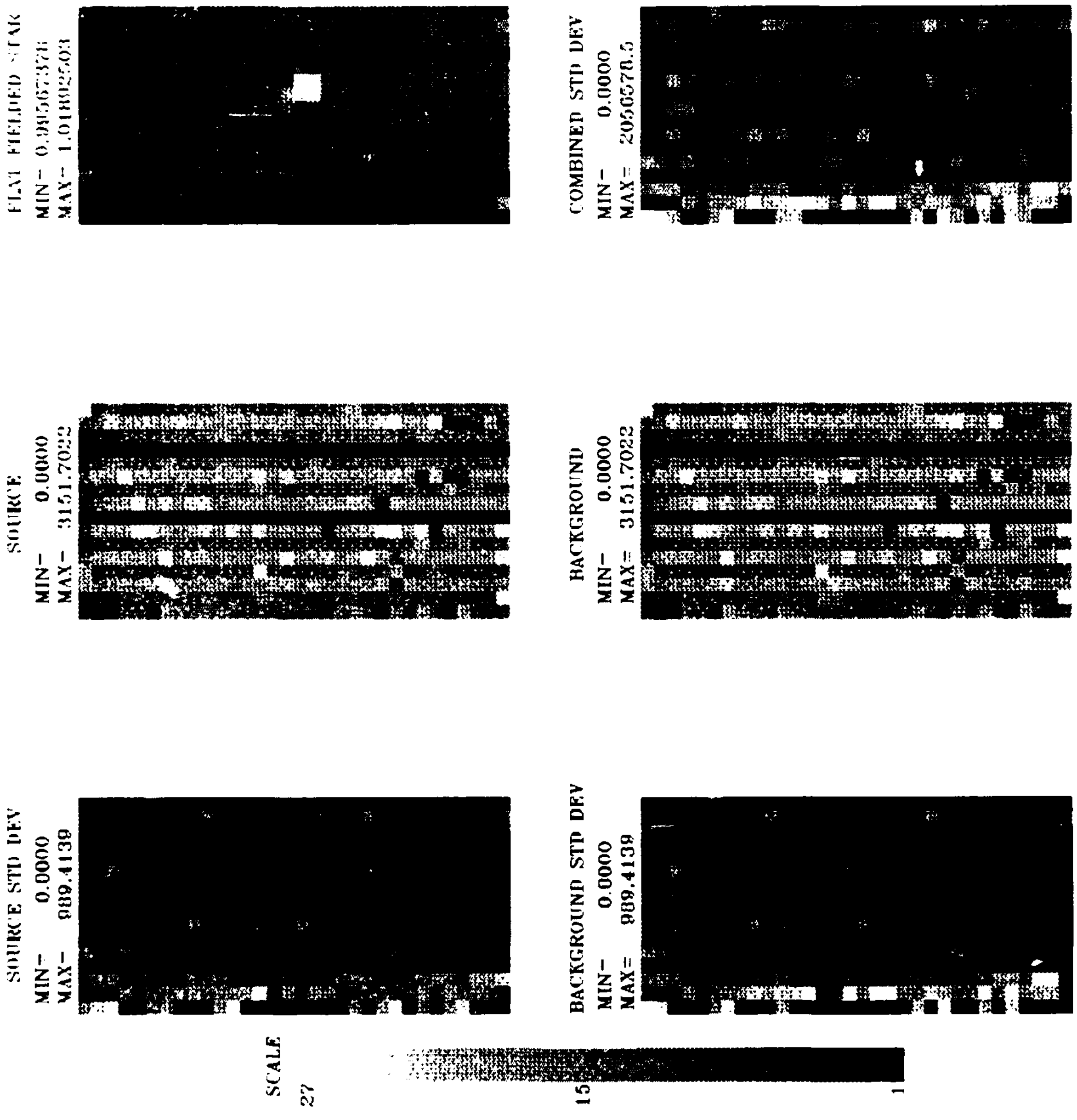

Figure 2

Figure 3: Surface plots of images obtained with the AESC MC^2 array. The flat-fielded image from Figure 2 is shown here as a 3D plot in 2 perspectives. The dead column and vignetted areas are plotted at the threshold. The stellar image, which covers several pixels due to the size of the image in flight as discussed in the text, is seen as the prominent spike. The five pixels set to 1.0 in Figure 2 are treated the same way here for clarity.

AESC MC^2 ARRAY

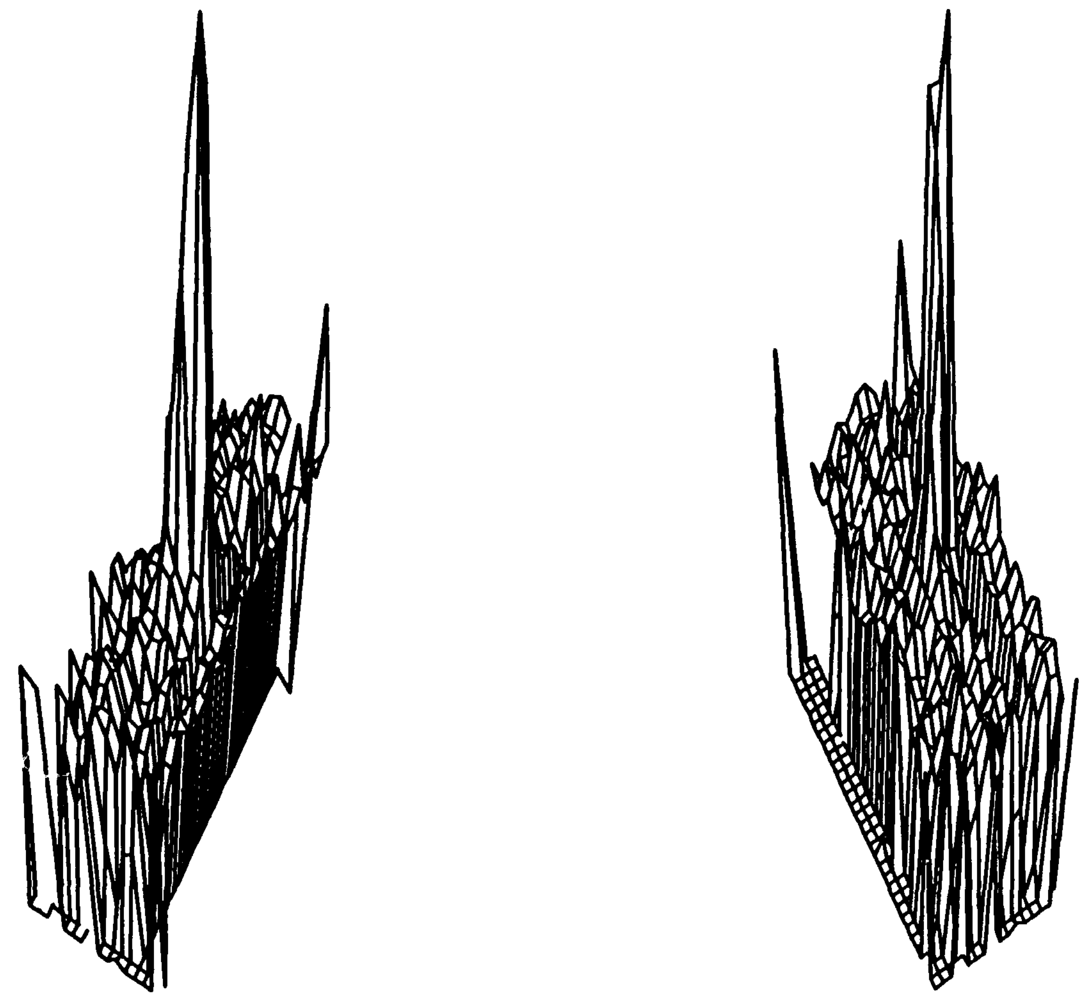

Figure 3

STAR: A ORI = AFGL 836 = IRC + 10°100

of the array results in a non-constant background that has been suppressed. These pixels were used to assess scattered light levels from the telescope vs. inside the dewar. Figures 4 and 5 are similar to Figures 2 and 3 but are for the AESC Bulk detector array. Note that the star in the case of the Bulk array is about 10 times brighter than that used for the MC^2 array. Very little (one row and one column) vignetting is seen with this sensor. Figures 6 and 7 show the same data for the Rockwell International BIBIB array looking at Alpha Ori, the same star viewed with the MC^2 array, but through a different spectral filter. The long dimension of the array was too large for the lens, so a few rows are partly vignetted on the top and bottom. Some of the original data (not necessarily that used for these images) for the AESC Bulk, the AESC MC^2 array, and the RI array are given in Appendix B.

Once a star has been identified on an array frame, its known brightness in the infrared can be used to calculate the effective array responsivity under operating conditions.

Because stars appear as unresolved point sources to our optical system, the analysis of a stellar image has the potential to tell us much about the overall optical quality of the telescope and array system. The stellar images shown in Figures 2-7 are smeared over several pixels, and are significantly larger than expected for the diffraction-limited point-spread function of the telescope. Other parts of the KITE program conducted by MIT (Elliot et al., 1989) demonstrated that the sources of the large images were not in the array or the array dewar optics, but were associated with the telescope and its environment.

The system NEP was calculated using the following procedure. The sequence of background frames obtained looking off-source were averaged, and the incident flux on the array from the combined background sources (sky plus telescope) assumed to be uniform. A table of multipliers' M_{ij}, was calculated by dividing a typical or average value of the signal on one pixel by each pixel's averaged response to the background, i.e.,

$$M_{ij} = \frac{S_{typical}}{\bar{S}_{ij}}$$

This table of multipliers was then matrix multiplied times the average of the frames obtained on-source to obtain the flat-fielded signals, SFF_{ij}:

$$SFF_{ij} = M_{ij} * S_{on\text{-}source\ ij}.$$

The rows just above and below the location of the image of the star were then averaged to obtain a "local background" to subtract from the rows containing the image of the star. The resulting (small) signal counts were summed and set equal to the total inband flux of the star. The fraction of the total counts measured on one pixel then represented the corresponding fraction of the star's flux being incident on that pixel, F_{ij}. The noise, obtained from the variance multiplied by the same matrix of flat-field multipliers $VFF_{ij} = M_{ij} * Variance_{ij}$ was then used in the calculation of the NEP for each pixel

$$NEP_{ij} = f_{ij} \frac{SFF_{ij}}{\sqrt{VFF_{ij}}} * \sqrt{\frac{1}{t_F}}$$

where t_F = frame time in seconds. In all the instances examined here, the resulting NEP was about 1-2 x 10^{-13} W/$\sqrt{\text{Hz}}$. This is significantly greater than the electrical NEP of the pixels as measured under low backgrounds in controlled laboratory conditions, and indicates these systems were background limited or limited by the electronics used on board the aircraft. As the noise was greatly reduced when the dewars were blanked off with a cold metal surface, we believed the systems were background limited.

Using reasonable values for telescope temperature from inflight sensors (~245K) and typical measured values for the effective emissivity of the KAO telescope of about 30%, one would expect a background limited (BLIP) NEP of less than 10^{-17} W/$\sqrt{\text{Hz}}$ for a .25 μm or .2 μm filter near 11 μm and a detector size of 23 μrad (4.7 arc sec) or 27 μrad (5.5 arcsec). Warm cabin air was known to be leaking into the field of view, warm cavity components were contained in the off-axis response cones of the dewars, and warmer components of the telescope and the dewar window were likely additional background sources, but would only raise the NEP to a few $\times 10^{-15}$. In order to account for the larger NEP that we measure, some additional source of white noise must be invoked, and the generally accepted scapegoats are the electronics and associated ground currents. There was insufficient time during the program to accurately assess this hypothesis--the FFT analysis after the fact showed no evidence of noise spikes at any particular frequency. We are left with systems which behaved as if they were background limited at a level (~10^{-13}

Figure 4: Imagery with the AESC Bulk Array. The layout of this figure follows that of Figure 2, but 3200 frames were used to calculate each of the averages, "source" and "background". In this case, however, no pixels had to be set to 1.0, and 27 pixels fell below the flat-field image threshold of .9955 and thus were set to black. Slight evidence for vignetting may be seen on the right and bottom of the array. The star used for this set of observations, CW Leo, is significantly brighter in the infrared (~ a factor of 10) than α Ori. Again, each pixel corresponds to about 4.7 arcsec or 23 μradians.

AESC BULK ARRAY

STAR: CW LEO = AFGL 1318 = IRC + 10°216

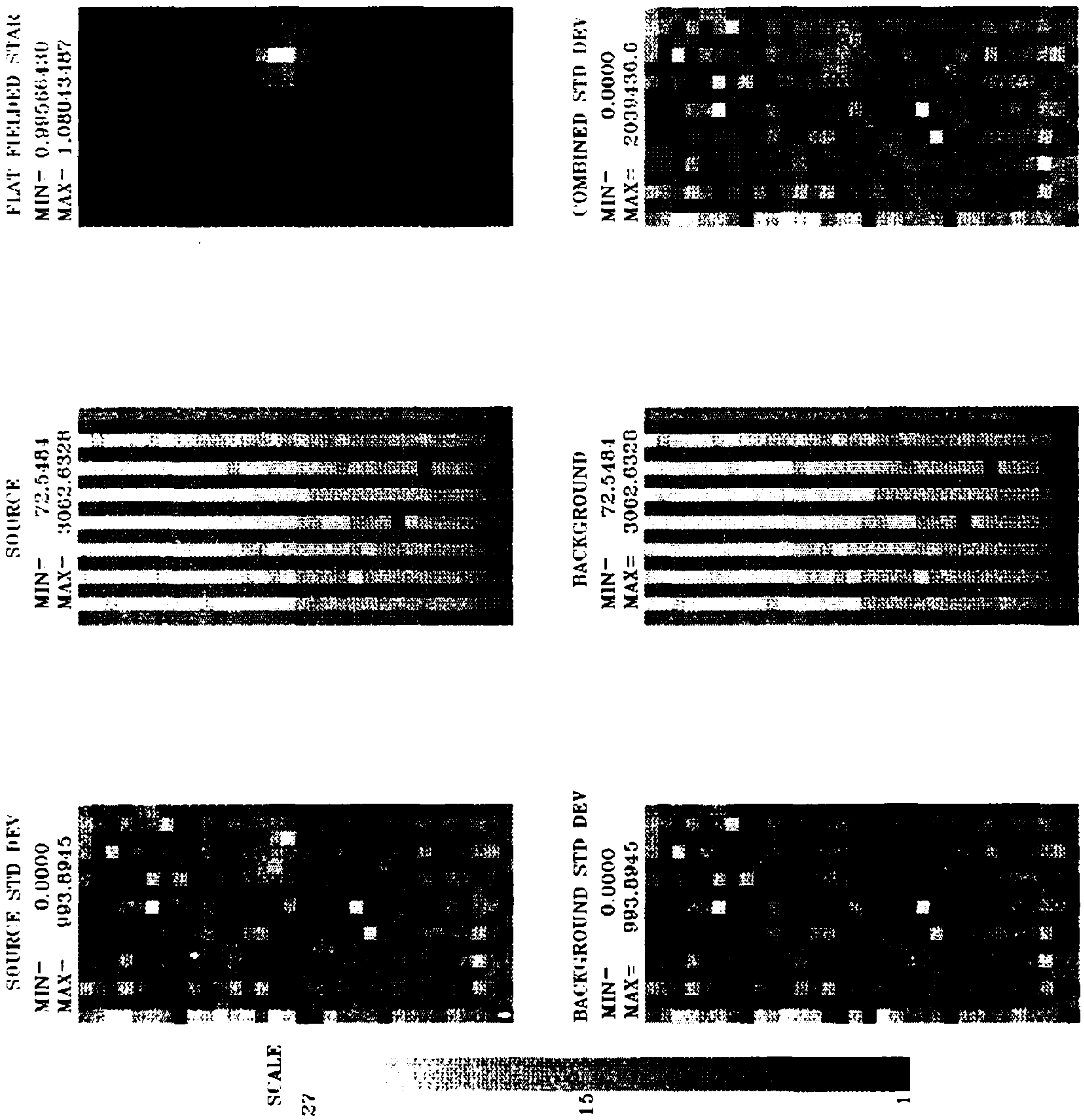

Figure 4

Figure 5: Surface plots of images obtained with the AESC Bulk Array. These plots follow the format of Figure 3. The brighter source permits a more detailed examination of the shape and intensity distribution in the image. The faintest sources studied were also detected with this array.

AESC BULK ARRAY

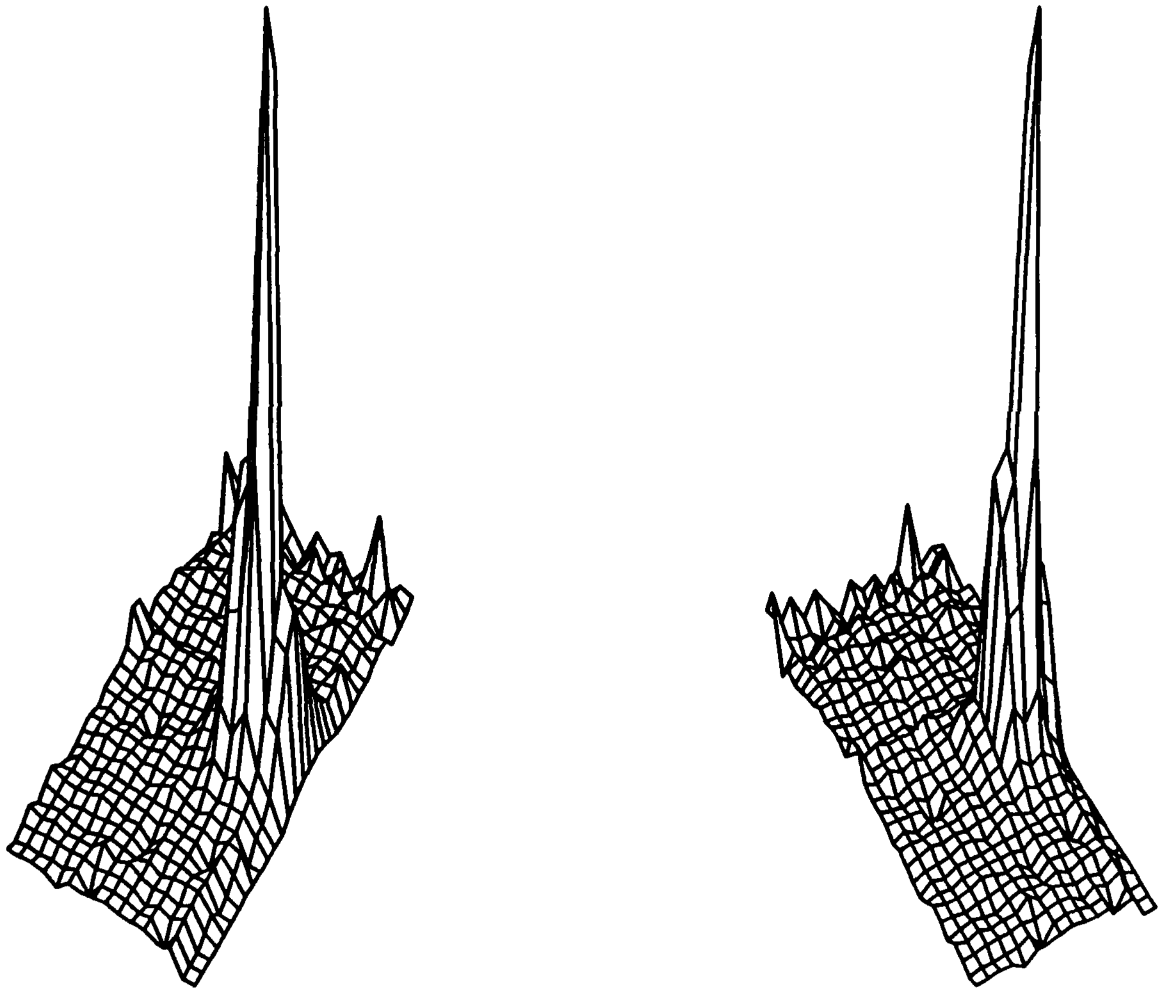

Figure 5

STAR: CW LEO = AFGL 1318 = IRC + 10°216

Figure 6: Imagery with the RI BIBIB Array. This array had a different format (10 x 50 vs. 16 x 32) and slightly larger pixel size (150 μm vs. 125 μm) compared to the arrays used to obtain the data in Figures 2-5. This resulted in each pixel corresponding to about 5.5 arcsec or 27 μrad; thus the images may appear a little more condensed. The same star, αOri, shown in the images in Figures 2 and 3 was used to obtain these data, but through a slightly different spectral filter. Also, only 126 frames were averaged to produce the "source" image, and 126 frames for the "background," in contrast to the much larger number of frames used for Figures 2-5. Again the threshold was set to .9955 for the flat-fielded image, and 6 pixels fell below that level and were then set to black. Pixel (9,8) was set to 1.0. Given the large height of this array, modest vignetting of the top and bottom of the array was inevitable as a result of the physical size constraints on the dewar optics.

RI BIBIB ARRAY

STAR: A ORI = AFGL 836 = IRC + 10°100

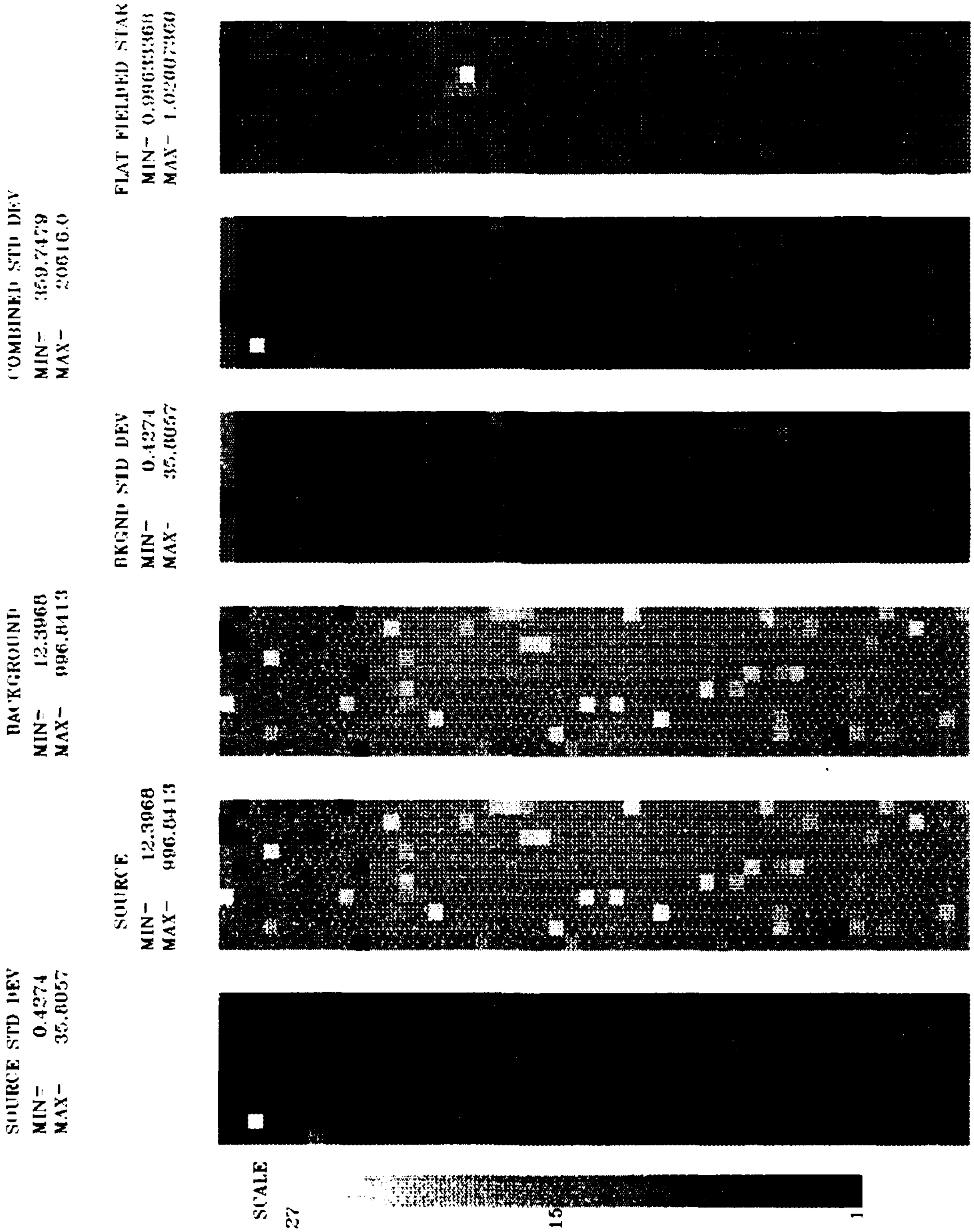

Figure 6

Figure 7: Surface plots of images obtained with the RI BIBIB Array. These plots follow the format of Figures 3 and 5, using a threshold of .9955 and pixel (9,8) set to 1.0. As discussed in the text, the structure in the surface away from the star is mostly due to multiplexer characteristics: a more recent array from RI exhibits virtually no structure and no dead or hot pixels.

RI BIBIB ARRAY

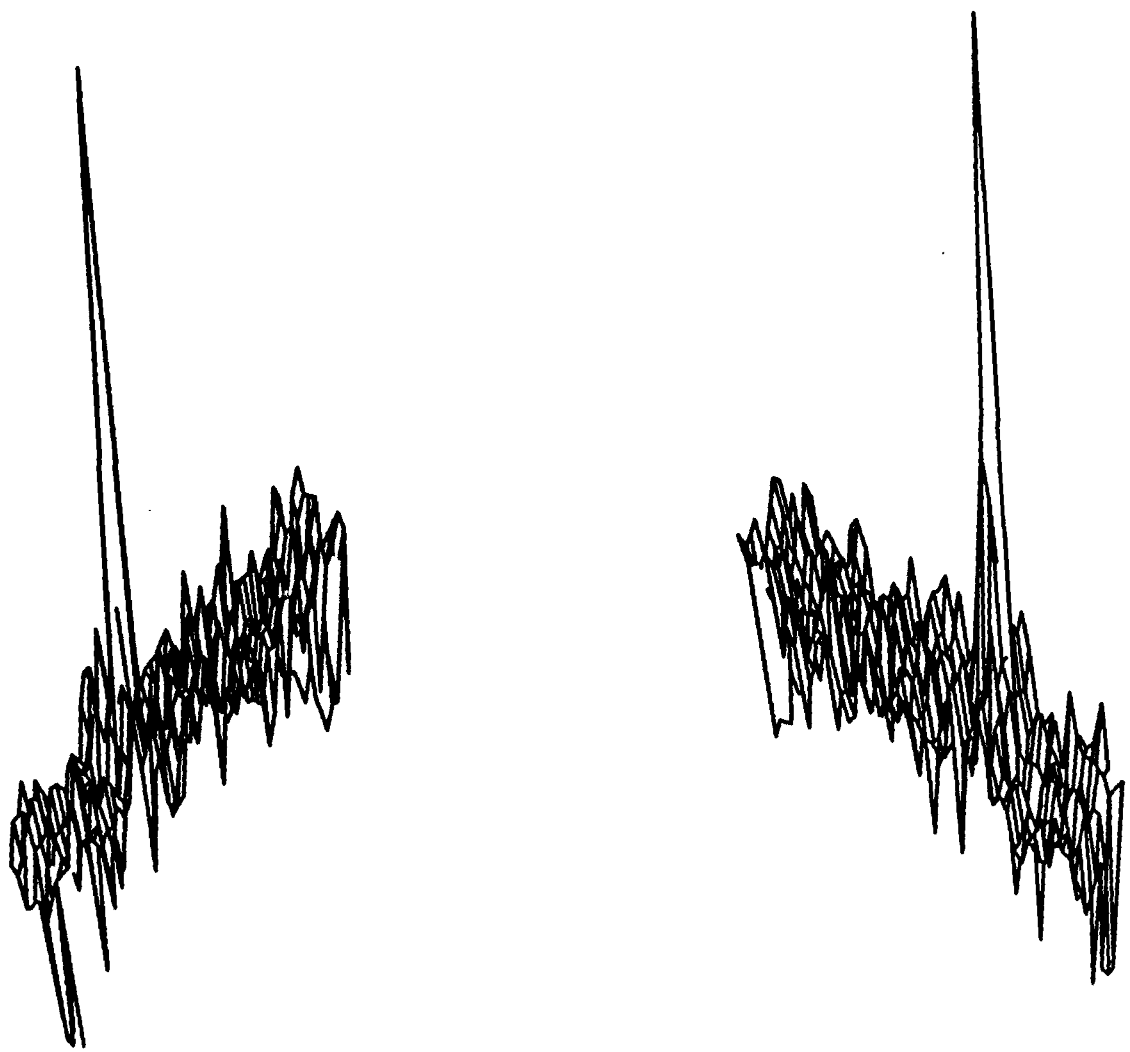

Figure 7

STAR: A ORI = AFGL 836 = IRC + 10°100

$W/\sqrt{Hz}$) comparable to the NEPs of astronomical sensors flown on the KAO at the time. It thus appears more likely that the limit was associated with the facility, rather than the KITE array sensor itself.

V. DISCUSSION AND CONCLUSIONS

For each of the three arrays studied in this program, measurements made during flight time on the Kuiper Airborne Observatory (KAO) concentrated on estimating noise and on observing infrared stars of known brightness. These measurements have allowed us to quantitatively characterize the performance and sensitivity of the three arrays while they were operating under conditions that stress mechanical, optical and electronic systems and while they were viewing a background that is typical of the airborne environment. Due to the use of different spectral filtering and bias voltages for the different arrays, the array performances must not be compared to each other.

All of the infrared arrays that we tested have large pixel-to-pixel variations in the responsivity. This results in the unprocessed array output looking very structured; this structure effectively hides stellar and other signals from the casual observer. Output from the arrays must be "flat-fielded" before it gives useful information. Even after flat-fielding, there are a number of completely insensitive ("dead") pixels and several very noisy ("hot") pixels that give no useful data. Table 1 lists these "unusual" channels.

The noise performance for each of the arrays is well represented by a normal (or gaussian) distribution. We find little evidence for excess noise that appears as "tails" in the signal distributions nor do we find any significant frequency-dependent noise. The only departure from a gaussian noise distribution seems to be caused by unevenly-spaced channels in the analog-to-digital converters. This is a common problem with successive-approximation encoders.

Infrared stars of known brightness were measured by all three of the arrays. These measurements allow us to convert the array signals into absolute units and thereby to estimate total sensor performance (arrays plus optics plus electronics). In general, we find that the overall Noise Equivalent Power (NEP) of each of the systems is remarkably similar ($1\text{-}2 \times 10^{-13}$ Watts/Hz$^{1/2}$) even though the AESC Bulk array uses a detector technology that is usually considered far from optimal. If the telescope and dewar optical transmissions are taken into account, we derive an NEP of $\sim 5 \times 10^{-14}$ watts/Hz$^{1/2}$. The stellar observations also show that the optical blur is

TABLE 1
Summary of Unusual Channels

Rockwell BIBIB Array

Dead Pixels (≤ 60 counts/sample)

0,9	1,41	5,1	5,9	7,0	7,1
7,6	8,0	9,1	9,8		

"Hot" Pixels (≥ 700 counts/sample)

1,37	1,42	2,14	2,29	3,0	3,24
3,26	5,35	6,3	7,20	7,21	8,11
8,46	9,18	9,19	9,27	9,36	

High Pixels (< hot pixels, but criteria depends on other adjacent pixels)

2,37	2,48	5,37	7,43	8,16	8,39
9,20	9,44				

Aerojet MC^2 Array

Dead Pixels

0,1	0,27	1,2	8,22	10,25	14,28
+all column 12					

"Hot" Pixels (≥ 1.5 X average for the column)

1,13	1,31	2,11	3,0	3,13	3,23
6,4	6,23	9,13	9,24	9,29	10,3
11,17	15,0	15,20			

High Pixels (< hot pixels, criteria depends on other adjacent pixels)

0,5	0,22	0,28	2,23	5,25	5,28
6,5	6,22	6,25	6,26	6,31	8,4
10,27	10,28	13,10	14,27	14,29	15,1
15,2	15,5	5,10	15,19	+all column 7	

Aerojet Bulk Array

Dead Pixels

0,30	7,23

Hot Pixels
none

High Pixels

1,25	8,23	11,25

NOTE: Pixels called out in (column, row) format.

larger than the ~ 2.5 arcsecond (12 microradians) diffraction-limit of a 36-inch telescope; the full width at half maximum of the image is typically 5-10 arcseconds (25-50 microradians). We cannot say whether this small additional blurring was caused by misfocus of the telescope and optics or by turbulence in the telescope cavity, but this size (~ 7") is consistent with the size quoted in the seeing study report which was also part of the KITE program (Elliott et al., 1989). In the seeing study, the 4 arcsecond image size was attributed to a combination of thermal gradients in the cavity, leakage of warm cabin air into the cavity, and to a lesser degree to mechanical motion of parts of the telescope, the residual miscollimation or misalignment of the telescope, and the effects of the boundary layer. On a subsequent flight with a fixed secondary (as opposed to the oscillating secondary used for the IR measurements) and with thermal gradients minimized and focus control improved, 3 arcsec images in the visible were obtained by Elliott et al. At that point, cavity turbulence effects and telescope effects (alignment, vibration, figure errors) were probably comparable at about 2 arcsec each, with a one arcsec contribution from the shear layer, and these were combined in quadrature. This is consistent with the Boeing result on jitter (Hibben et al. 1986), where the jitter of the IR image centroid was less than 1 arc sec on a variety of time scales.

In summary, the pixels in these array systems performed at about the level of sensitivity of individual detectors flown on astronomical missions by scientists using the KAO. The level of performance was somewhat worse than predicted by optical models, even after allowance was made for some excess background. No evidence was seen for anomalous 1/f noise in the arrays. The source of the extra white noise is not known for certain, but we suspect there was some excess multiplexer/electronics noise present, as there was not enough time to check out possible ground loops in detail, or to optimize the voltages used to drive the multiplexers. On the positive side, stars were cleanly detected with all three arrays. The time-delay-and-integrate experiment (TDI) was successfully completed with the results very close to theoretical predictions (Chu et al. 1986, Hibben et al. 1986). Successful techniques for acquiring, storing, and processing the data were developed and used, and flat fielding procedures and noise analysis techniques were successfully developed and are now available for use on other programs. Very small limits on jitter

of the IR image were measured, providing confidence that the use of an open port telescope on an airborne platform for IR imaging at the ≤ 5 μrad scale is feasible.

VI. REFERENCES

Cameron, R. M., 1976, Sky and Tel 52, 327.

Cangelosi, V. E., Taylor, P. H., Rice, P. F., 1979, Basic Statistics: A Real World Approach, Second Edition, West, NY, NY.

Chu, S. J., Elgin, D. L., Schmidt, E. D., 1986, "Optical Concepts Definition Analysis, Task 2.5: Sensor Definition and Technology Verification, Annual Report," Teledyne Brown Engineering, SAT 86-SDC-3031.

Elgin, D. L., 1985, "Optical Concepts Definition Analysis, Task 2.5: Sensor Definition and Technology Verification, Annual Report," Teledyne Brown Engineering SD85-BMDATC-2942.

Elgin, D. L., editor, 1986, "SDTV Data Analysis-Interim Report, Optical Concepts Definition Analysis, Task 2.5 Sensor Definition and Technology Verification," Teledyne Brown Engineering, SAT 86-SDC-2978.

Elliott, J. L., Dunham, E. W., Baron, R. L., Watts, A. W., Kruse, S. E., Rose W. C., and Gillespie, C. M., Jr., 1989, P.A.S.P. 101, 737-764.

Haughney, L. C. and Mumma, M. J., 1986, "NASA C141/KAO Comet Halley Observations" in Proc. of 20th ESLAB Symp on the Exploration of Halley's Comet, Heidelberg, 27-31 Oct. 1986, ESA-SP-250 (Dec. 1986) Vol. III, p. 215-221.

Hibben, T. N., Bloedel, E. D., Keever, R. R., 1986, "Kuiper Infrared Technology Experiment (KITE) Signal Processing: Final Technical Report, Doc. #2-3774-000-436, 30 Sept. 1986, Revised Jan. 1987.

Martin, B. R., 1971, Statistics for Physicists, Academic Press, New York.

Russell, R. W., Rossano, G. S., Lynch, D. K., Hackwell, J. A., Macklin, R. H., Murray, D., Retig, D. A., Rice, C. J., Roux, D. A., Young, R. M., Colon-Bonet, G. T., and Morse, T. C., 1986, Annual Report: Infrared Detector Array Test Program for the Kuiper Infrared Technology Experiment (KITE), Aerospace Corp. ATR-86A(7126)-1.

Taylor, J. R., 1982, Introduction to Error Analysis, Univ. Sci., Mill Valley, California.

Appendix A
Plots of Distributions of Output Signals

The plots on the following pages are designed to give the general reader a feeling for the data which can only come from seeing the behavior of representative pixel elements in some detail, while at the same time providing detailed information on the performance of those same pixels for the person interested in actual performance characteristics. For the latter person, in particular, the tables of averages, standard deviation, skew, and kurtosis found in the main body of the text will supply the equivalent numbers for all the elements of each array, permitting an overall view of the important question of uniformity across the array.

Each individual plot shown resembles at half scale the representative sample in Figure A1. The data are generated from 3200 frames at 307 microseconds per frame, or just under 1 second. During this period, test conditions have remained relatively constant, for example the star pointing will have been held constant to of the order of an arcsec (~5 μradians) and the background conditions will be steady to usually <1%. The heading of each graph gives a file code (which can be used to identify the conditions of the test), specifies the array, and indicates the column and row number of the pixel in question. Note that the column/row numbers use the computer convention of beginning at zero; thus the upper left pixel is 0,0 and the lower right pixel is either 15/32 (for Aerojet) or 9/49 (for Rockwell). During the period in question, each pixel will have 3200 values, distributed around some average value. The abscissa is count value; the ordinate is "frequency of occurrence" of each value, normalized to the number of times the most frequently occurring value appeared, which in the case of Figure A1 was 185. Thus if one were to add the frequency numbers for each count value shown, the total would be 3200/185. Equivalently, if one multiplied the plotted frequency of occurrence of each ADC value times the normalization for that graph one would obtain the number of times during the 3200 frames that that pixel gave the corresponding ADC level on the x axis. In addition to the measured frequency shown as a solid line, each graph shows the best fit gaussian distribution as a dotted line, also in histogram format to facilitate an eyeball comparison. In addition, a number of parameters of the measured distribution are shown in the upper right hand corner. These are, in order

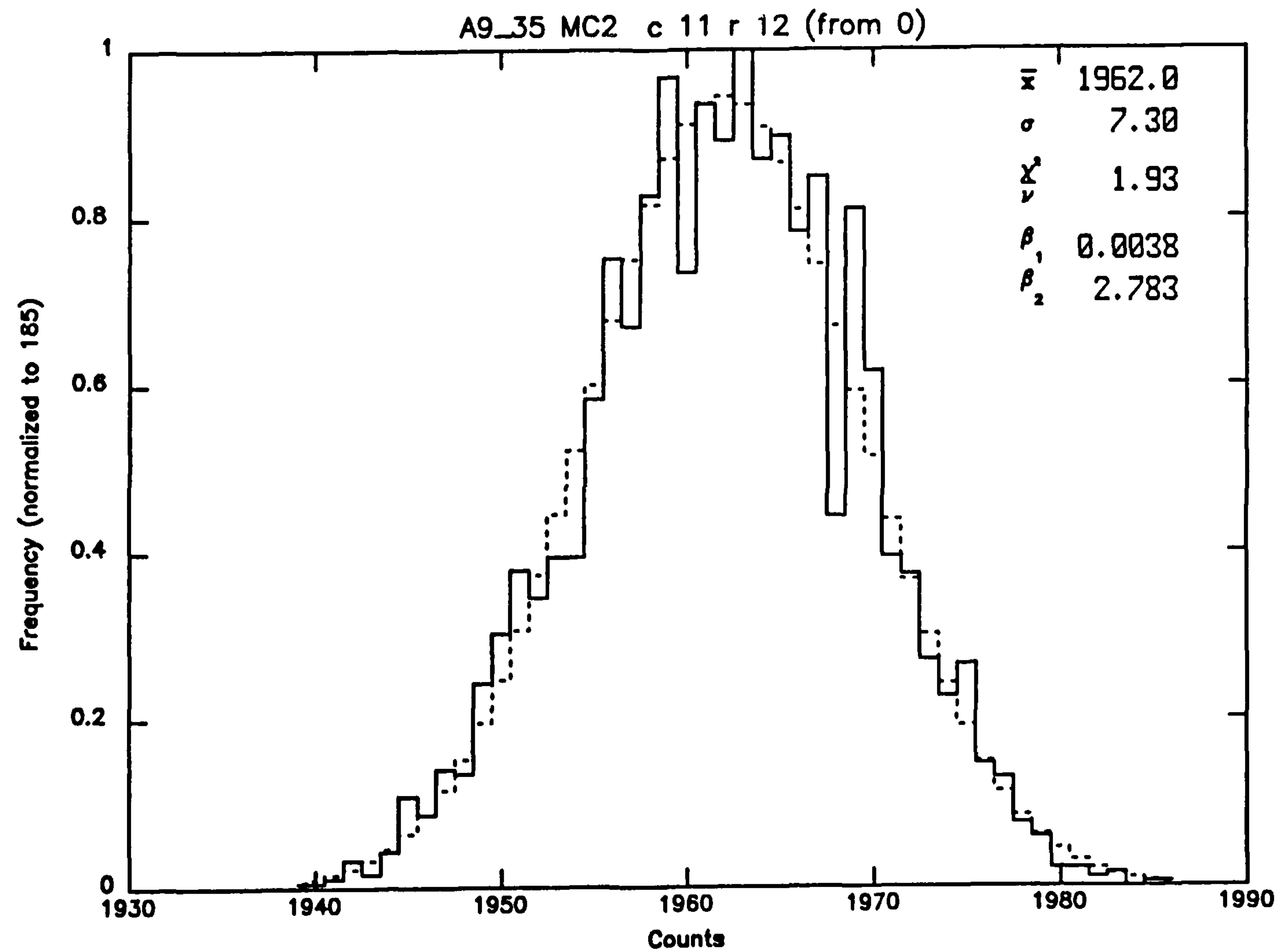

Figure A1. Example of plot format for display of distributions of count values Data are from file A9_35, a background measurement for the Aeroject MC^2 array. The pixel is from channel 11, row 12. Other parameters are discussed in the text.

from the top, average count value, sigma, chi-squared per degree of freedom, skew, and kurtosis. The mathematical definition and significance of each of these values are discussed in more detail in the main body of this report and below under the noise section. Note that the tables of average count value, etc. for the entire array found in the main report are keyed by the same file numbers found in the heading of each graph. This permits ready cross reference with individual pixel values shown here.

The arrangement of the individual plots into sets is made in a manner designed to permit contrasting of the signals seen by various columns, under various conditions, and/or with various arrays. First, all plots used are half the scale of Figure A1; thus 4 can be fit on each page. All sets are set up as column-to-column comparisons. Thus, for example, in Appendix A-1, two columns of data from the Rockwell BIBIB array are lined up with a row element from column 0 on the left and the same row element but from column 4 on the right. Not every row is represented in each set; the elements involved in each are called out in a cover sheet preceding each set. The cover sheet also briefly describes the test conditions obtaining for each data set and other relevant information.

APPENDIX A-1

Array: Rockwell BIBIB Array

	Left	Right
Elements:	Column 0; Rows 0-19	Column 4; Rows 0-19
Data Run:	Background #1	Background #1

Purpose: Comparison of column/row behavior for normal background.

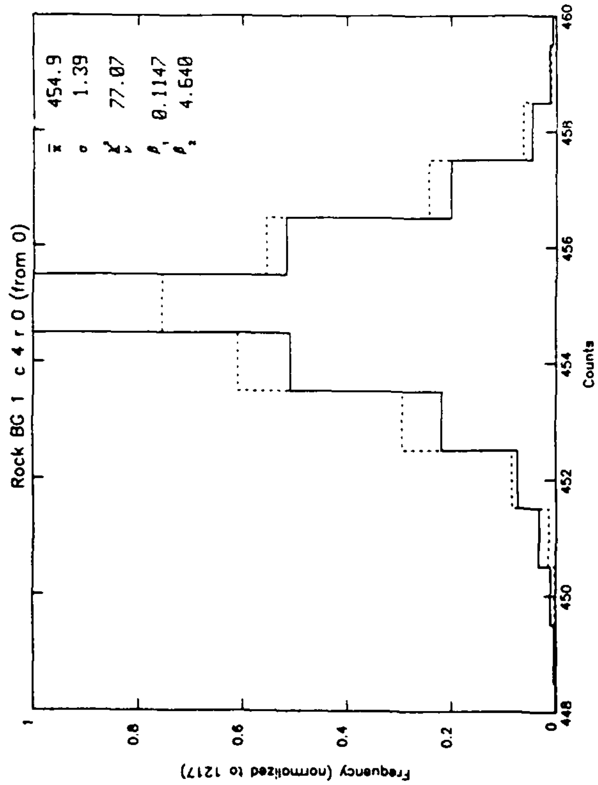

Rock BG 1 c 4 r 0 (from 0)
$\bar{x}$ 454.9
σ 1.39
χ^2_ν 77.07
β_1 0.1147
β_2 4.640
Frequency (normalized to 1217)
Counts

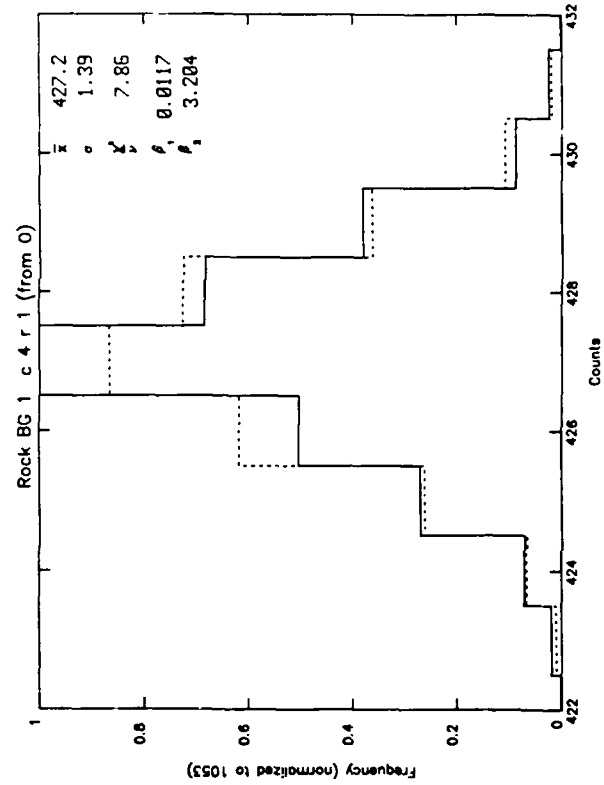

Rock BG 1 c 4 r 1 (from 0)
$\bar{x}$ 427.2
σ 1.39
χ^2_ν 7.86
β_1 0.0117
β_2 3.204
Frequency (normalized to 1053)
Counts

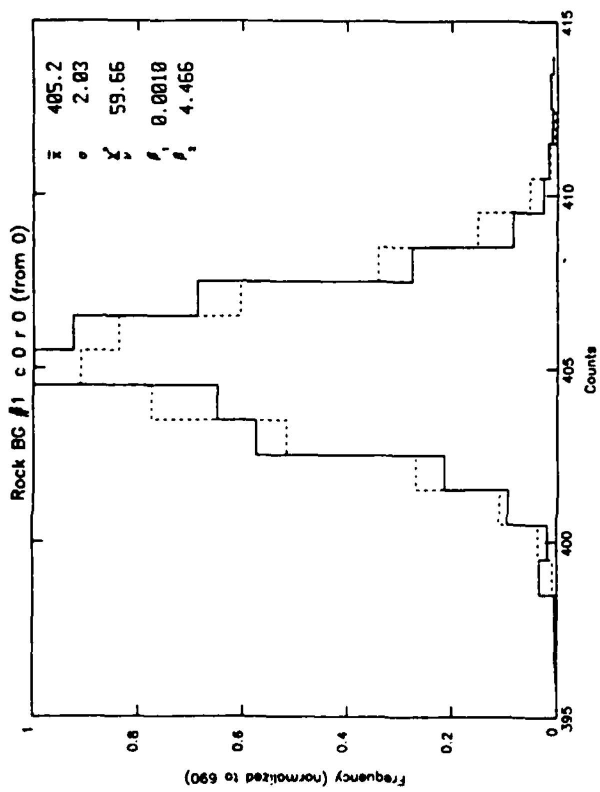

Rock BG #1 c 0 r 0 (from 0)
$\bar{x}$ 405.2
σ 2.03
χ^2_ν 59.66
β_1 0.0010
β_2 4.466
Frequency (normalized to 690)
Counts

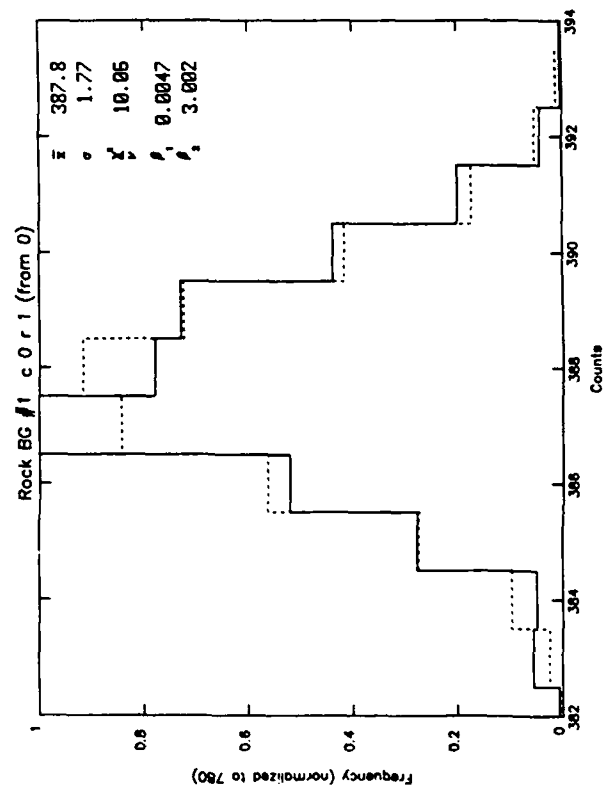

Rock BG #1 c 0 r 1 (from 0)
$\bar{x}$ 387.8
σ 1.77
χ^2_ν 10.06
β_1 0.0047
β_2 3.002
Frequency (normalized to 780)
Counts

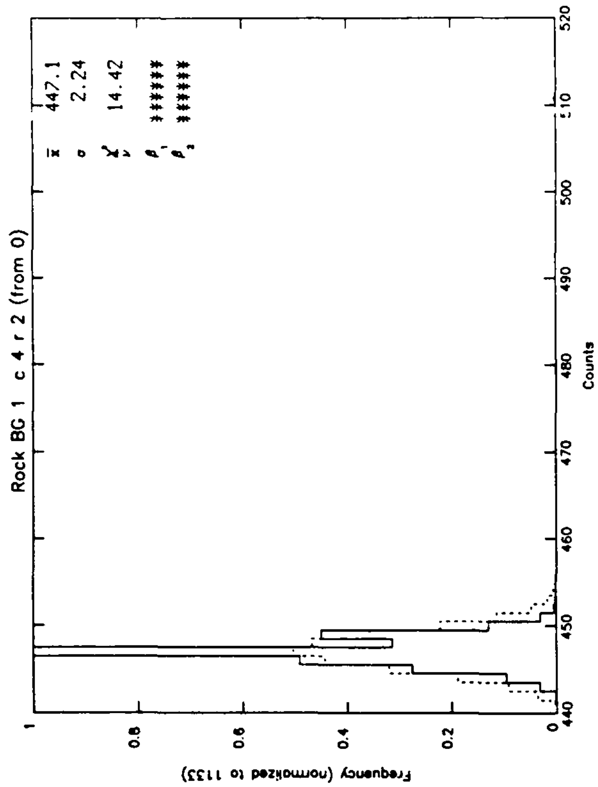

Rock BG 1 c 4 r 2 (from 0)
Frequency (normalized to 1133)
Counts
x̄ 447.1
σ 2.24
14.42
######
######

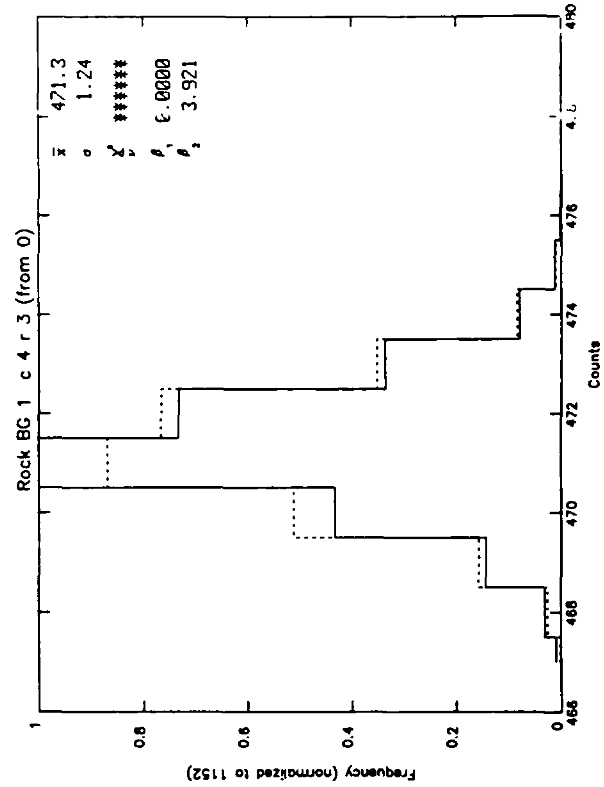

Rock BG 1 c 4 r 3 (from 0)
Frequency (normalized to 1152)
Counts
x̄ 471.3
σ 1.24
######
3.921

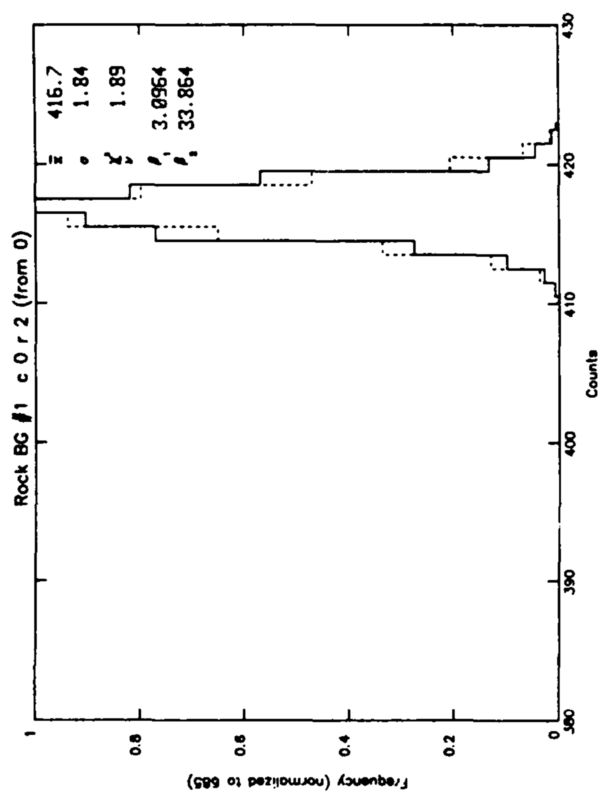

Rock BG #1 c 0 r 2 (from 0)
Frequency (normalized to 685)
Counts
x̄ 416.7
σ 1.84
1.89
3.0964
33.864

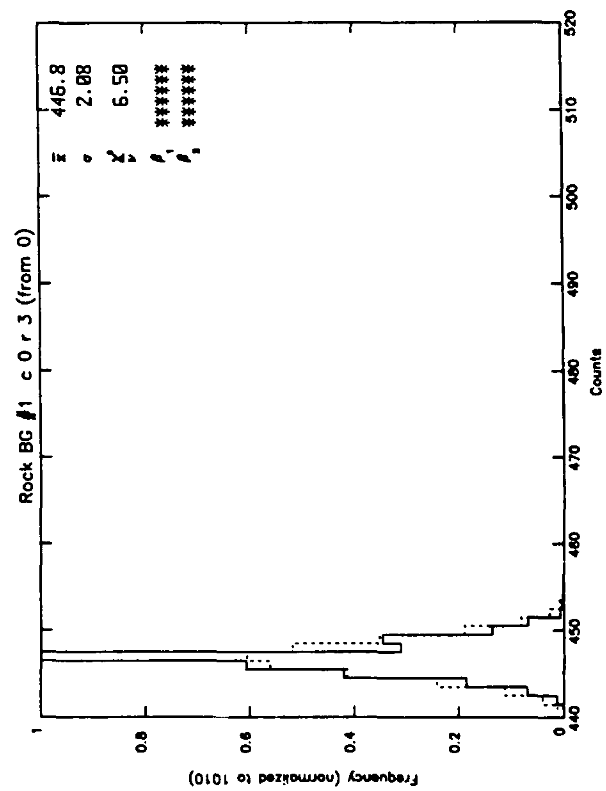

Rock BG #1 c 0 r 3 (from 0)
Frequency (normalized to 1010)
Counts
x̄ 446.8
σ 2.88
6.50
######
######

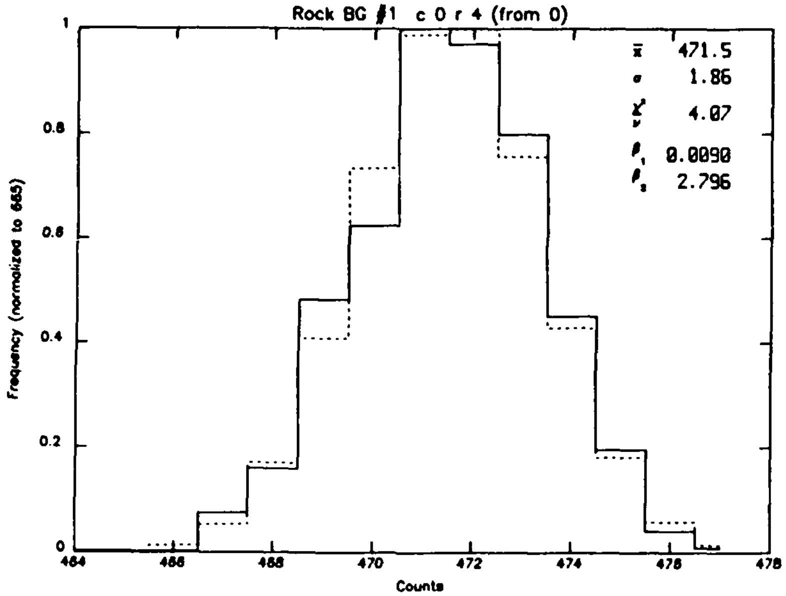
Rock BG #1 c 0 r 4 (from 0)
Frequency (normalized to 665)
Counts
x̄ 471.5
σ 1.86
χ^2_ν 4.07
β_1 0.0090
β_2 2.796

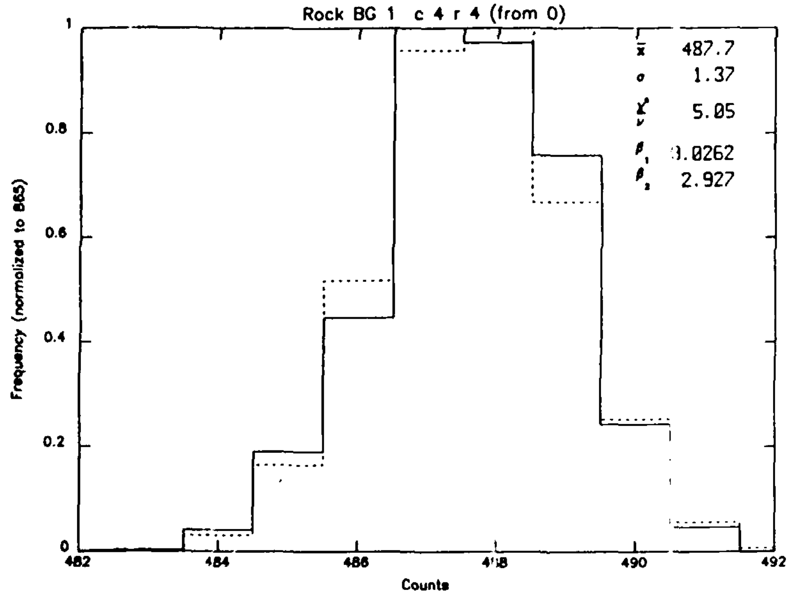
Rock BG 1 c 4 r 4 (from 0)
Frequency (normalized to 865)
Counts
x̄ 487.7
σ 1.37
χ^2_ν 5.05
β_1 0.0262
β_2 2.927

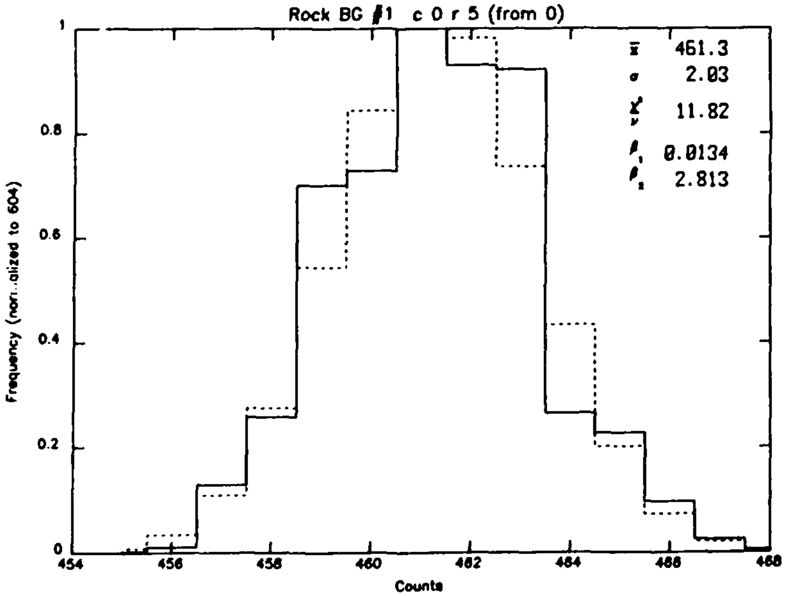
Rock BG #1 c 0 r 5 (from 0)
Frequency (normalized to 604)
Counts
x̄ 461.3
σ 2.03
χ^2_ν 11.82
β_1 0.0134
β_2 2.813

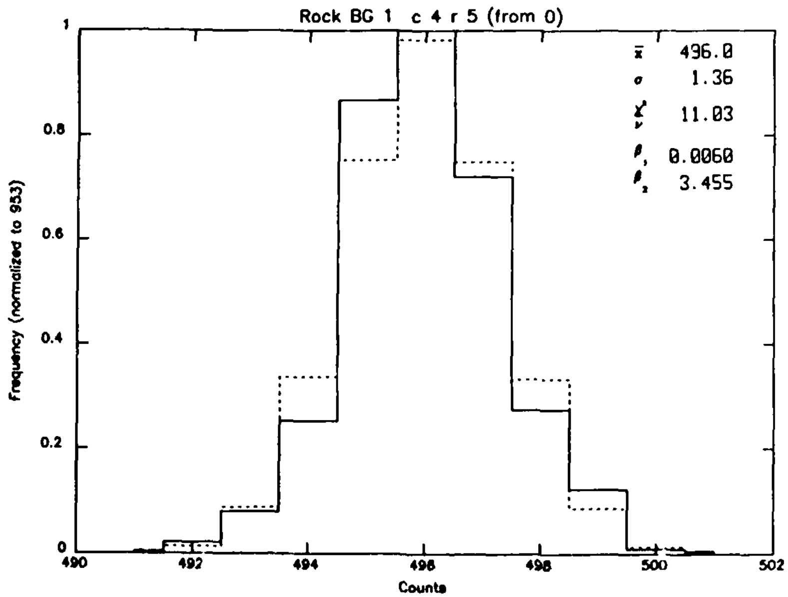
Rock BG 1 c 4 r 5 (from 0)
Frequency (normalized to 953)
Counts
x̄ 496.0
σ 1.36
χ^2_ν 11.03
β_1 0.0060
β_2 3.455

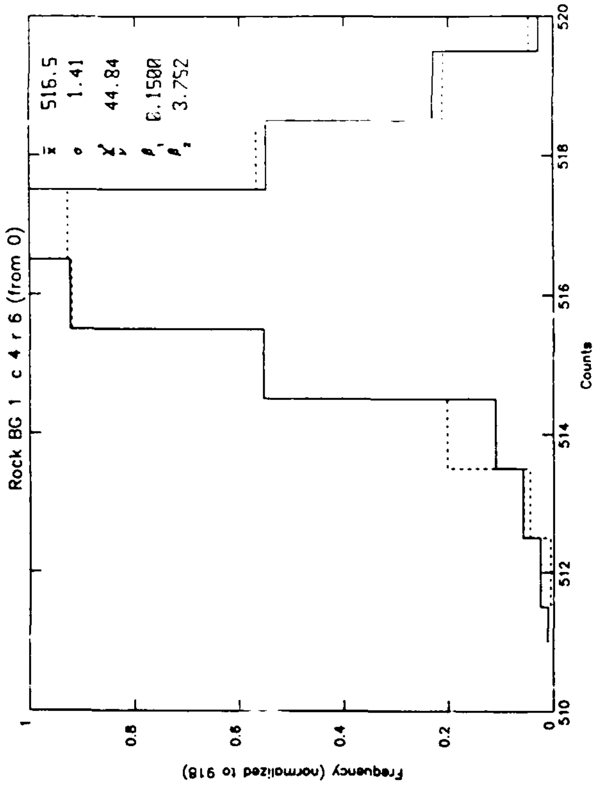
Rock BG 1 c 4 r 6 (from 0)
$\bar{x}$ 516.5
σ 1.41
χ^2_ν 44.84
β_1 0.1500
β_2 3.752
Frequency (normalized to 918)
Counts

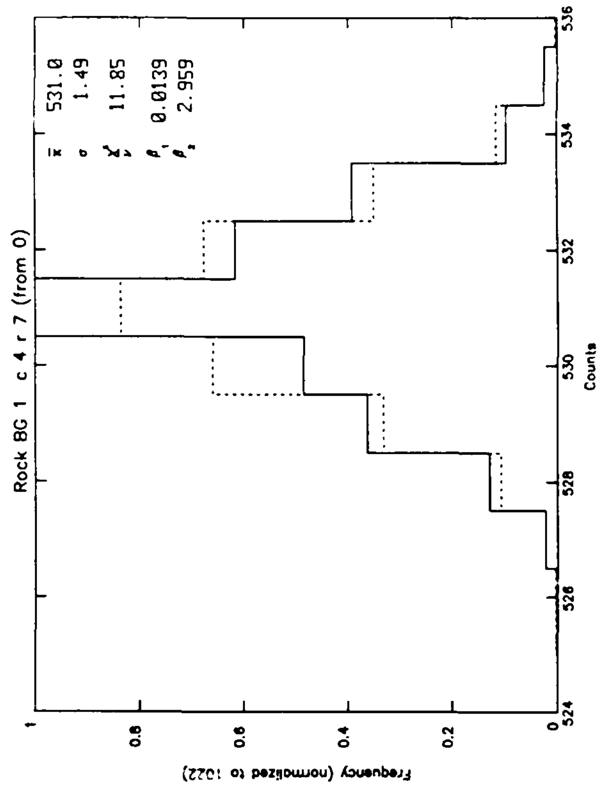
Rock BG 1 c 4 r 7 (from 0)
$\bar{x}$ 531.0
σ 1.49
χ^2_ν 11.85
β_1 0.0139
β_2 2.959
Frequency (normalized to 1022)
Counts

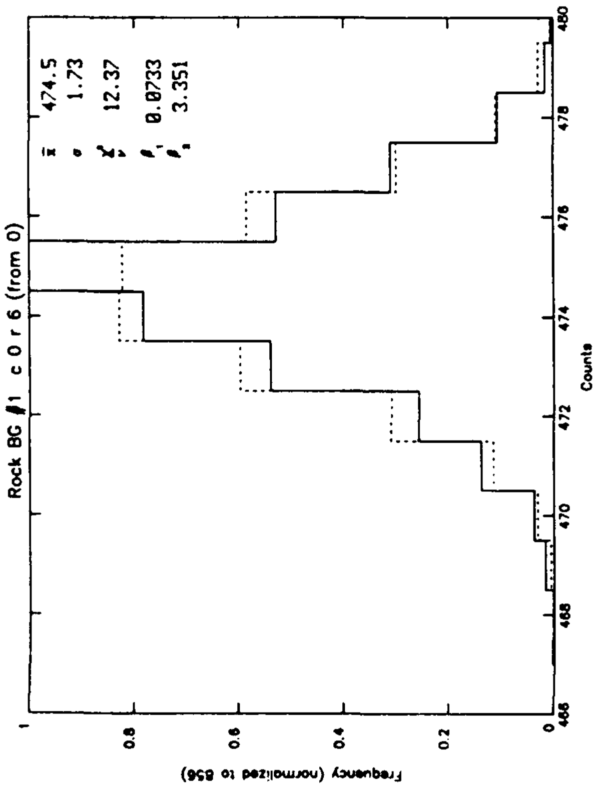
Rock BG #1 c 0 r 6 (from 0)
$\bar{x}$ 474.5
σ 1.73
χ^2_ν 12.37
β_1 0.0733
β_2 3.351
Frequency (normalized to 856)
Counts

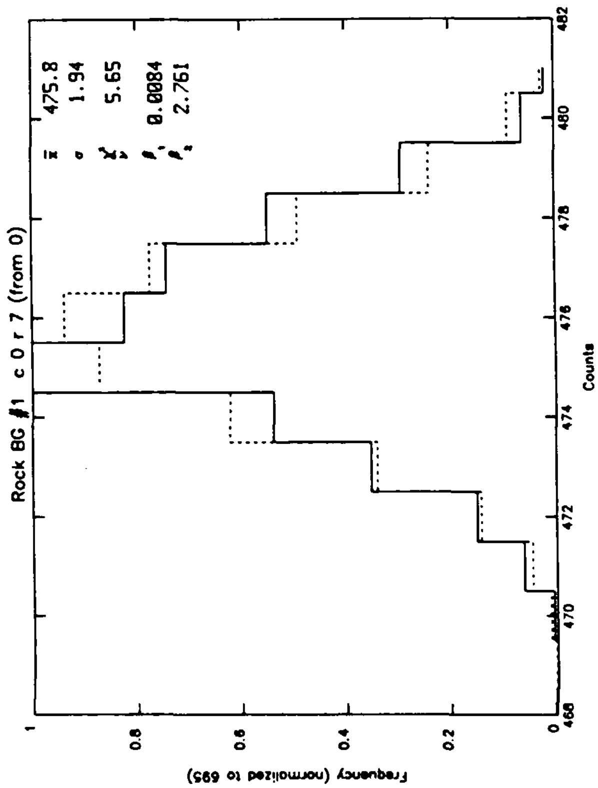
Rock BG #1 c 0 r 7 (from 0)
$\bar{x}$ 475.8
σ 1.94
χ^2_ν 5.65
β_1 0.0084
β_2 2.761
Frequency (normalized to 695)
Counts

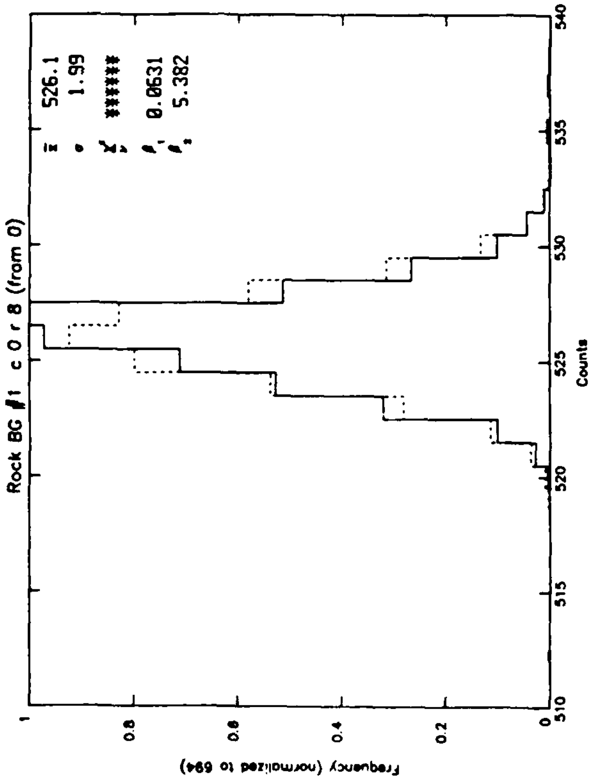
Rock BG #1 c 0 r 8 (from 0)
Frequency (normalized to 694)
Counts
x̄ 526.1
σ 1.99
χ²ν *****
β1 0.0631
β2 5.382

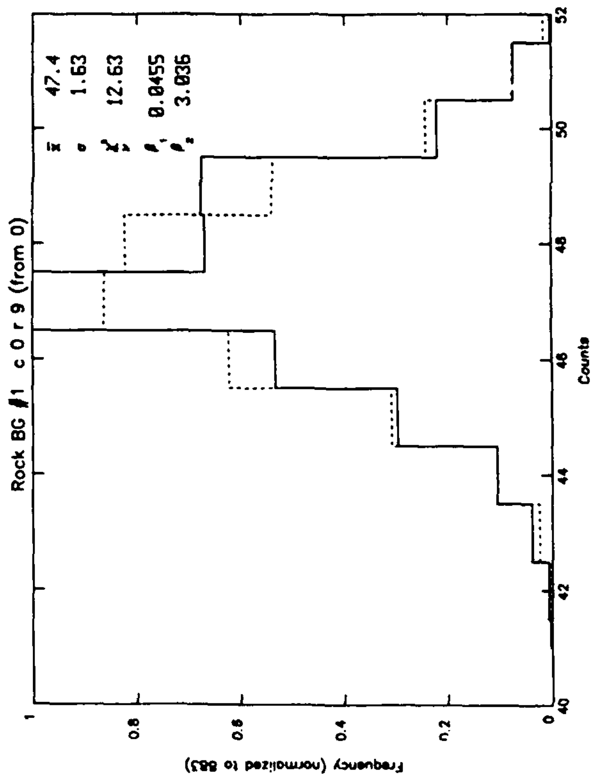
Rock BG #1 c 0 r 9 (from 0)
Frequency (normalized to 683)
Counts
x̄ 47.4
σ 1.63
χ²ν 12.63
β1 0.0455
β2 3.036

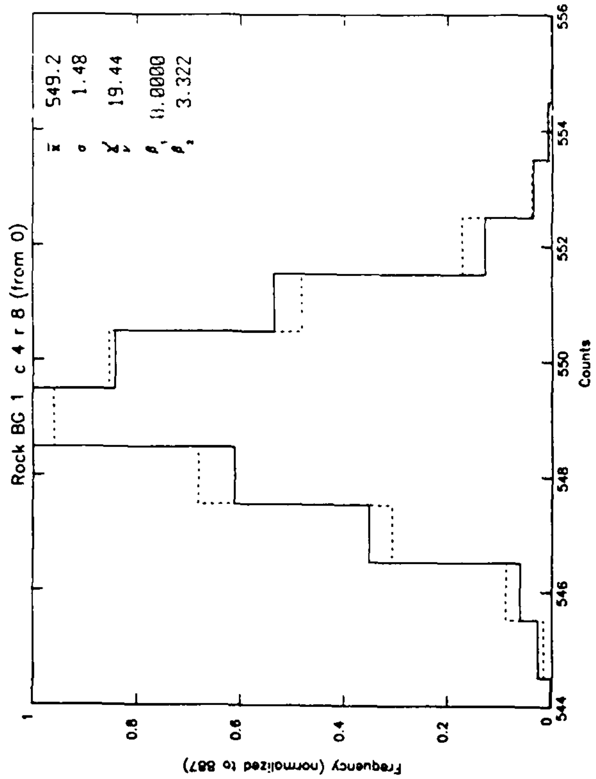
Rock BG 1 c 4 r 8 (from 0)
Frequency (normalized to 687)
Counts
x̄ 549.2
σ 1.48
χ²ν 19.44
β1 0.0000
β2 3.322

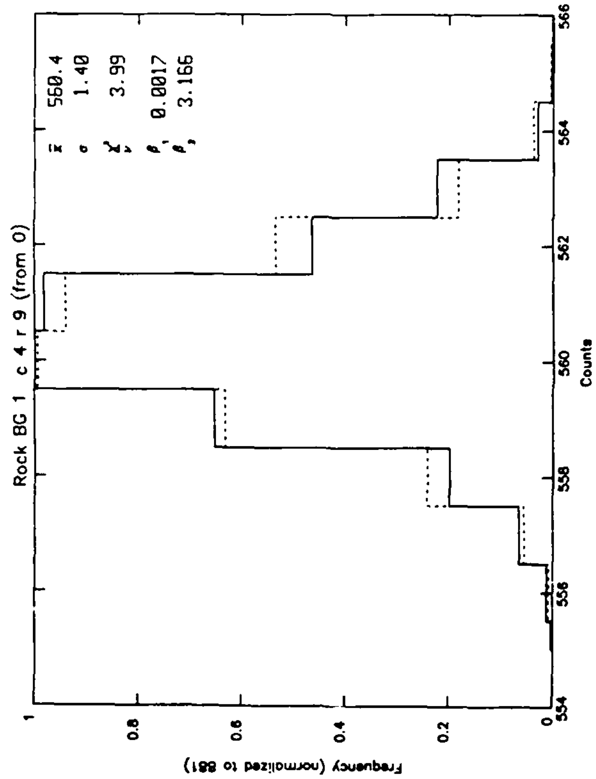
Rock BG 1 c 4 r 9 (from 0)
Frequency (normalized to 681)
Counts
x̄ 560.4
σ 1.40
χ²ν 3.99
β1 0.0017
β2 3.166

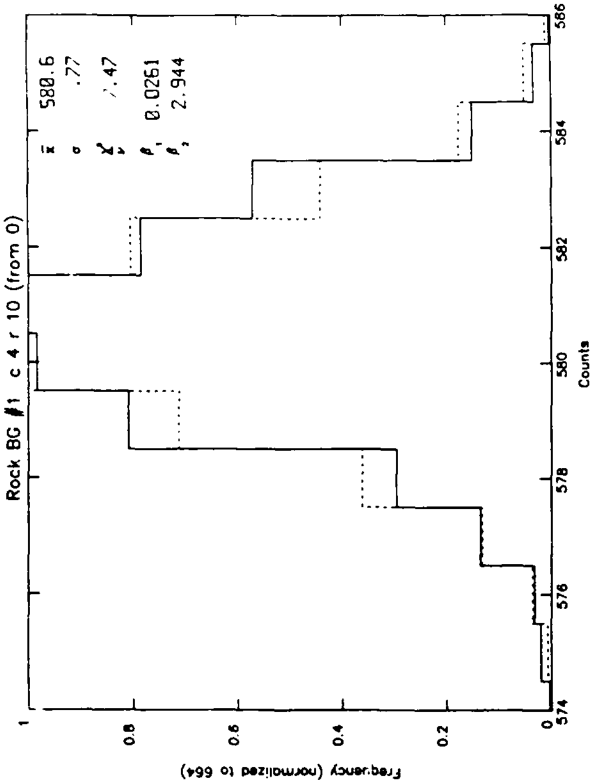
Rock BG #1 c 4 r 10 (from 0)
x̄ 580.6
σ .77
χ^2_ν ?.47
β_1 0.0261
β_2 2.944
Counts
Frequency (normalized to 664)

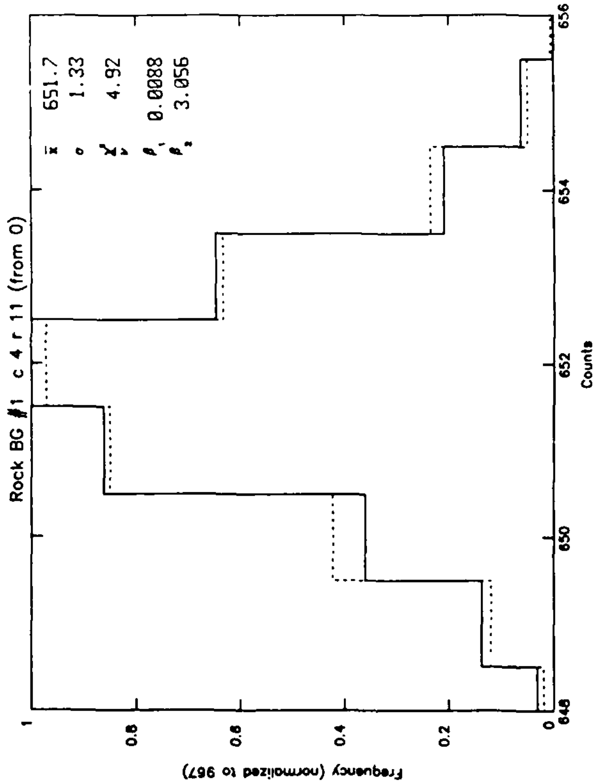
Rock BG #1 c 4 r 11 (from 0)
x̄ 651.7
σ 1.33
χ^2_ν 4.92
β_1 0.0088
β_2 3.056
Counts
Frequency (normalized to 967)

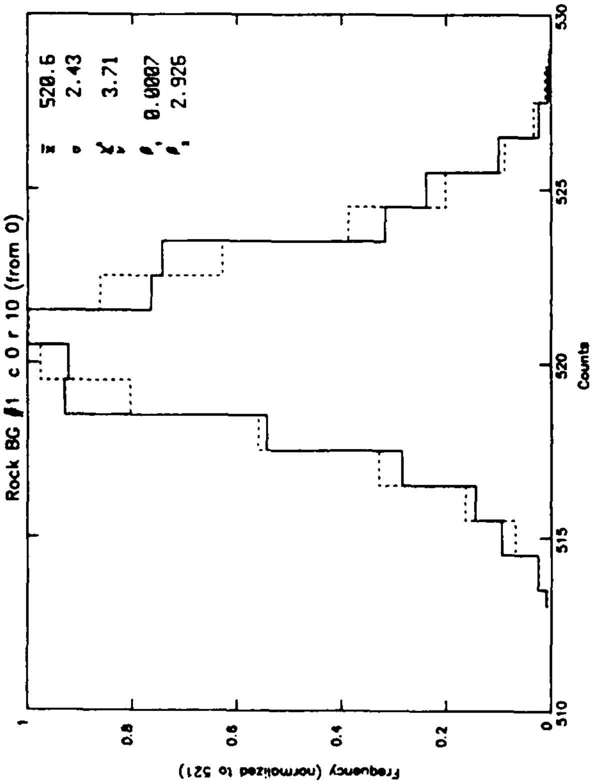
Rock BG #1 c 0 r 10 (from 0)
x̄ 520.6
σ 2.43
χ^2_ν 3.71
β_1 0.0007
β_2 2.926
Counts
Frequency (normalized to 521)

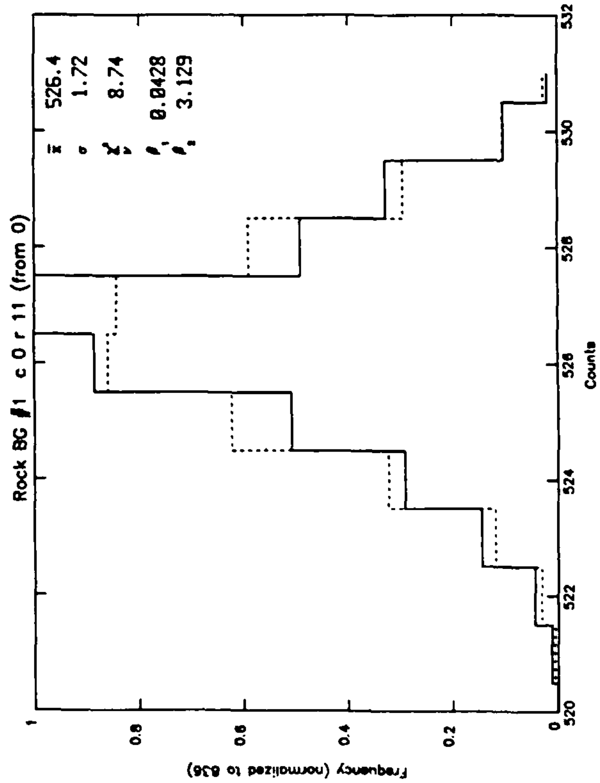
Rock BG #1 c 0 r 11 (from 0)
x̄ 526.4
σ 1.72
χ^2_ν 8.74
β_1 0.0428
β_2 3.129
Counts
Frequency (normalized to 836)

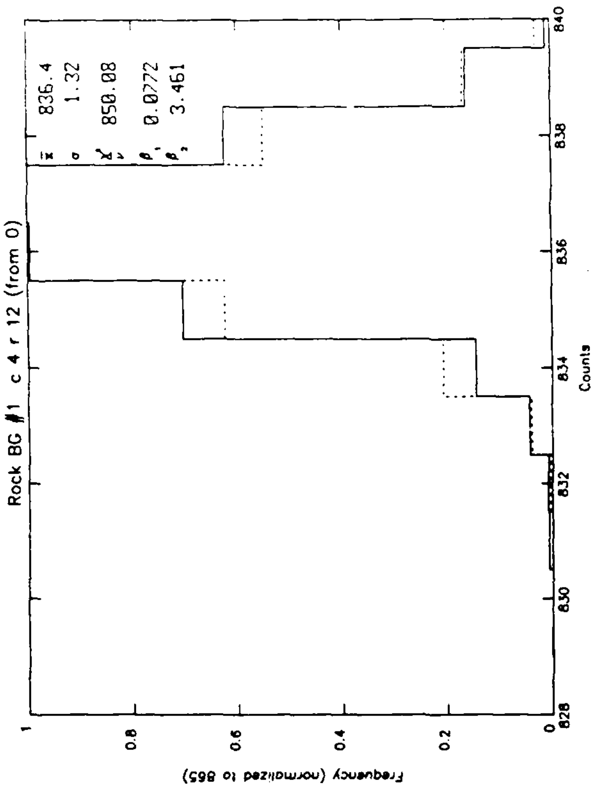

Rock BG #1 c 4 r 12 (from 0)
x̄ 836.4
σ 1.32
χ^2_ν 850.08
β_1 0.0772
β_2 3.461
Counts
Frequency (normalized to 865)

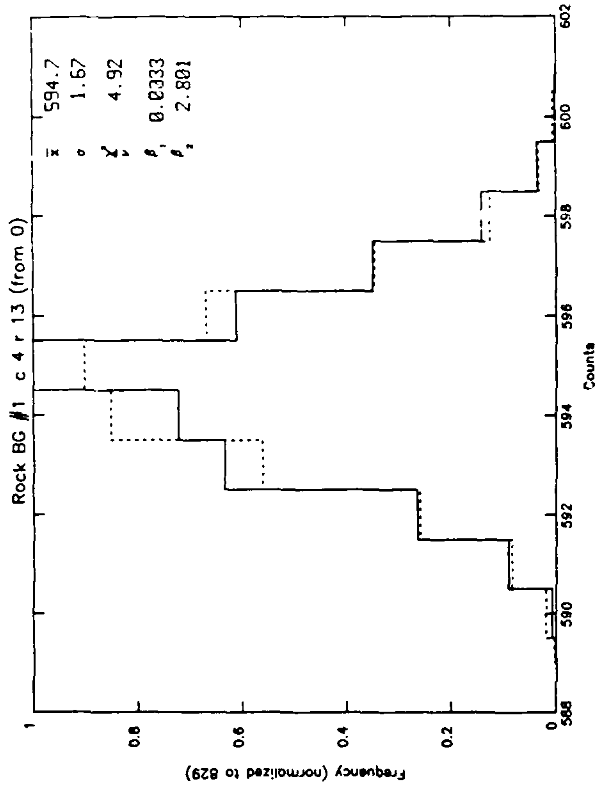

Rock BG #1 c 4 r 13 (from 0)
x̄ 594.7
σ 1.67
χ^2_ν 4.92
β_1 0.0333
β_2 2.801
Counts
Frequency (normalized to 829)

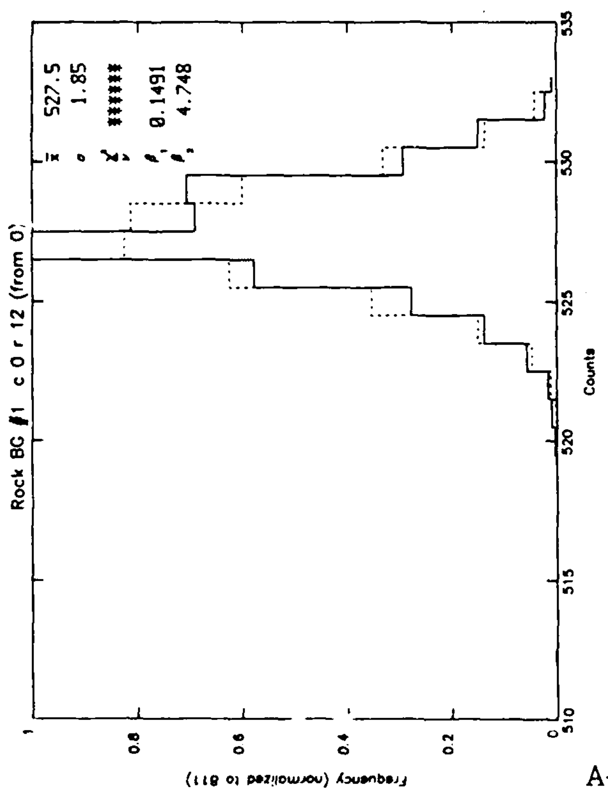

Rock BG #1 c 0 r 12 (from 0)
x̄ 527.5
σ 1.85
χ^2_ν *****
β_1 0.1491
β_2 4.748
Counts
Frequency (normalized to 811)

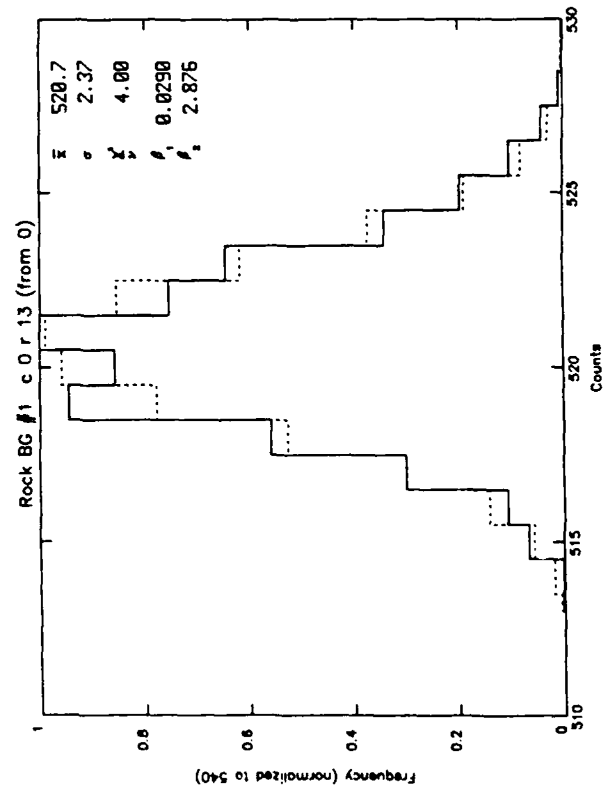

Rock BG #1 c 0 r 13 (from 0)
x̄ 520.7
σ 2.37
χ^2_ν 4.00
β_1 0.0290
β_2 2.876
Counts
Frequency (normalized to 540)

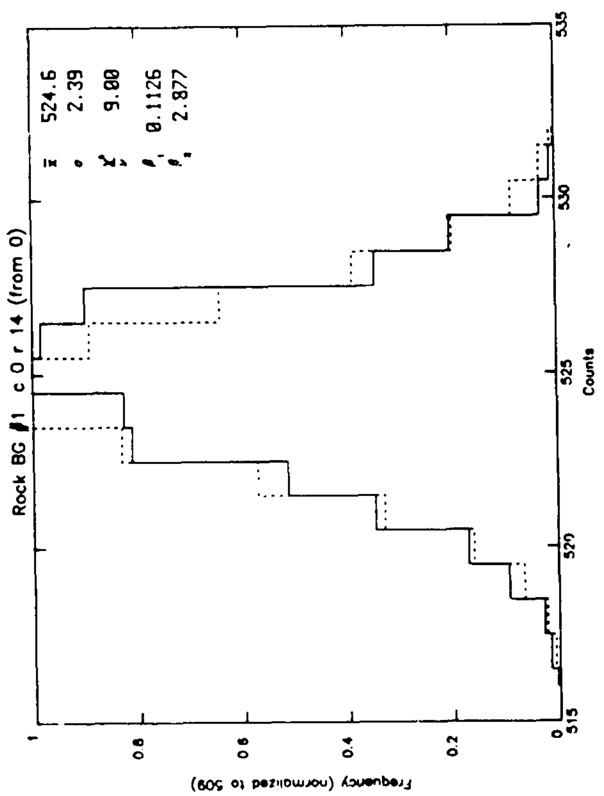
Rock BG #1 c 0 r 14 (from 0)
Frequency (normalized to 509)
Counts
$\bar{x}$ 524.6
σ 2.39
χ^2_ν 9.00
β_1 0.1126
β_2 2.877

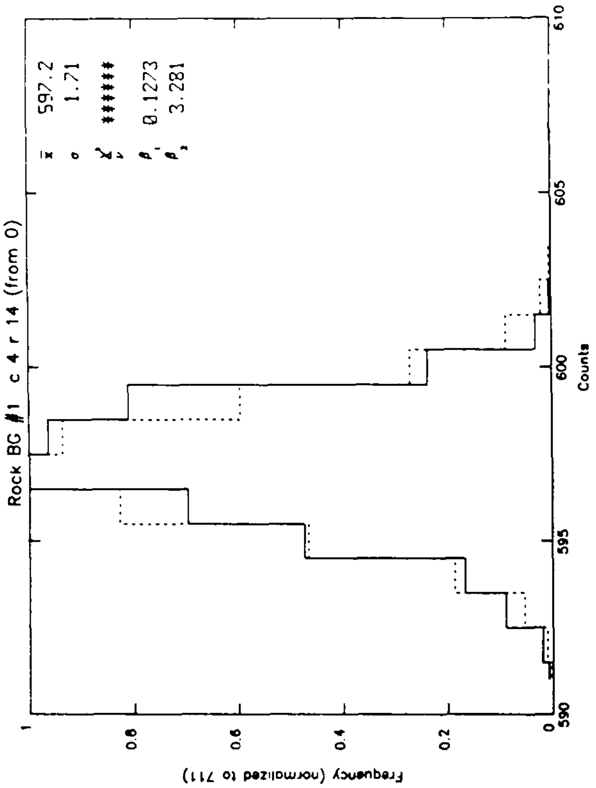
Rock BG #1 c 4 r 14 (from 0)
Frequency (normalized to 711)
Counts
$\bar{x}$ 597.2
σ 1.71
χ^2_ν ******
β_1 0.1273
β_2 3.281

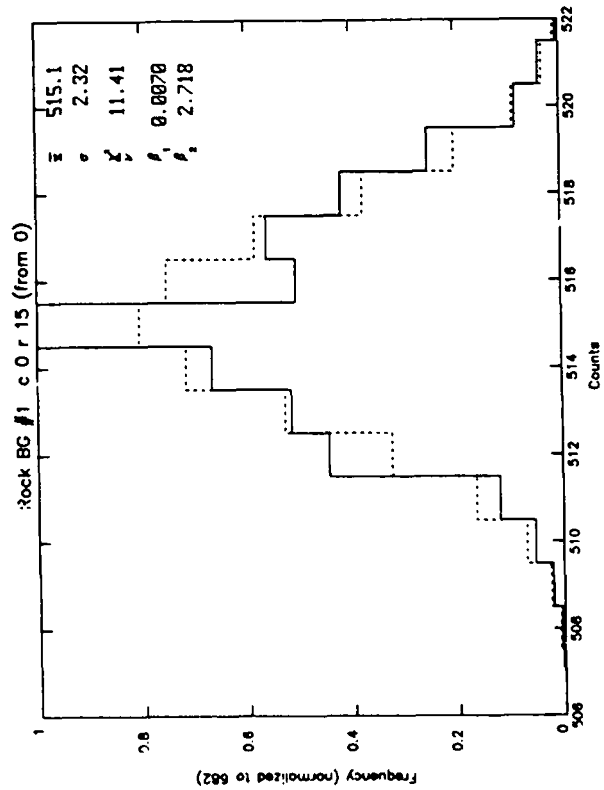
Rock BG #1 c 0 r 15 (from 0)
Frequency (normalized to 682)
Counts
$\bar{x}$ 515.1
σ 2.32
χ^2_ν 11.41
β_1 0.0070
β_2 2.718

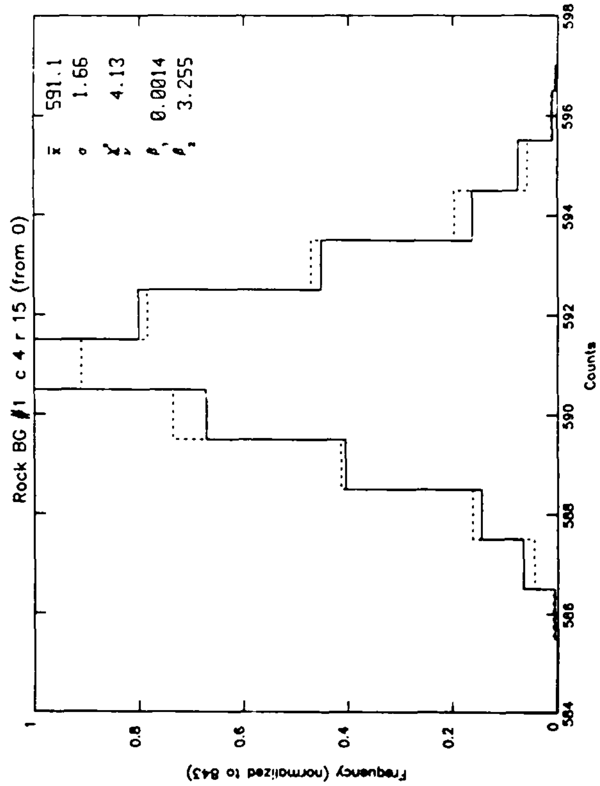
Rock BG #1 c 4 r 15 (from 0)
Frequency (normalized to 843)
Counts
$\bar{x}$ 591.1
σ 1.66
χ^2_ν 4.13
β_1 0.0014
β_2 3.255

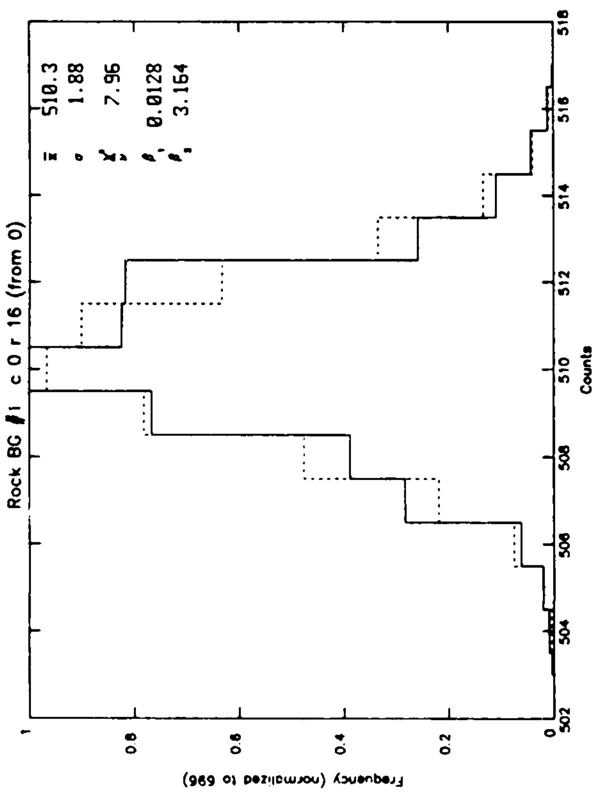
Rock BG #1 c 0 r 16 (from 0)
x̄ 510.3
σ 1.88
χ^2_ν 7.96
β_1 0.0128
β_2 3.164
Frequency (normalized to 686)
Counts

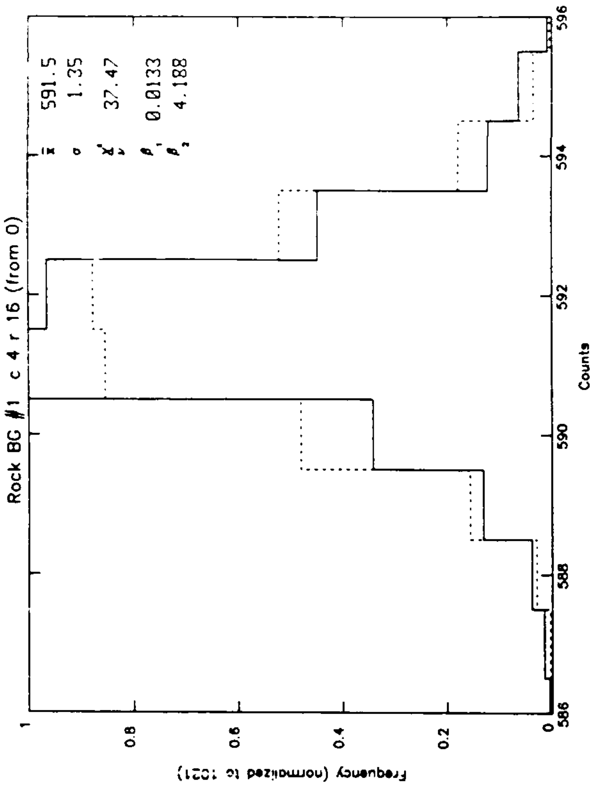
Rock BG #1 c 4 r 16 (from 0)
x̄ 591.5
σ 1.35
χ^2_ν 37.47
β_1 0.0133
β_2 4.188
Frequency (normalized to 1021)
Counts

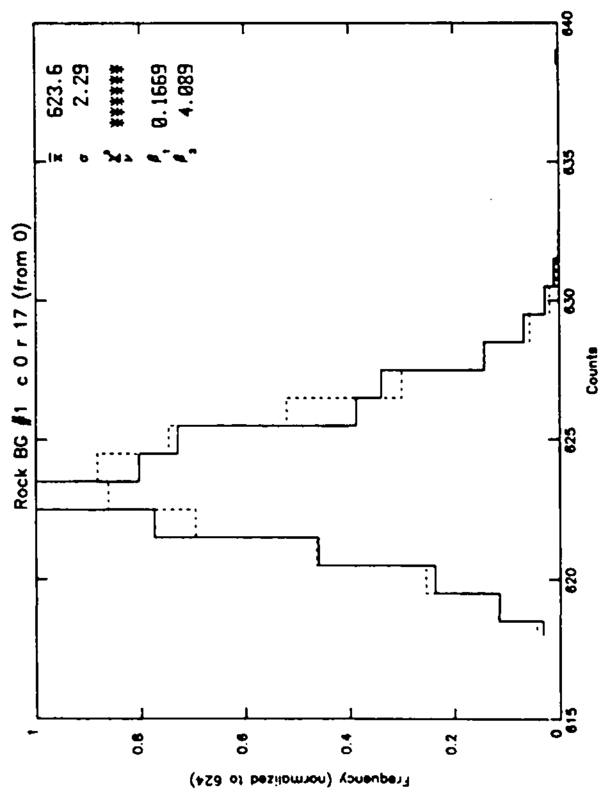
Rock BG #1 c 0 r 17 (from 0)
x̄ 623.6
σ 2.29
χ^2_ν *****
β_1 0.1669
β_2 4.089
Frequency (normalized to 624)
Counts

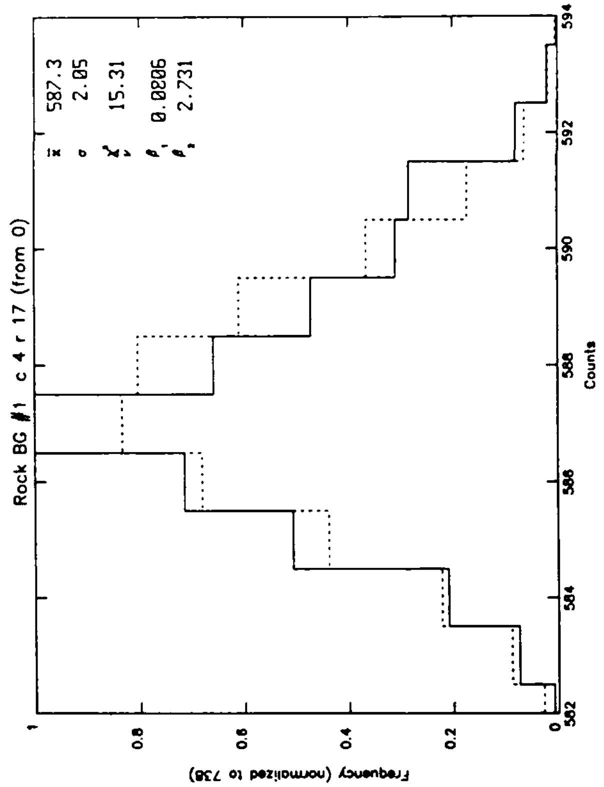
Rock BG #1 c 4 r 17 (from 0)
x̄ 587.3
σ 2.05
χ^2_ν 15.31
β_1 0.0806
β_2 2.731
Frequency (normalized to 738)
Counts

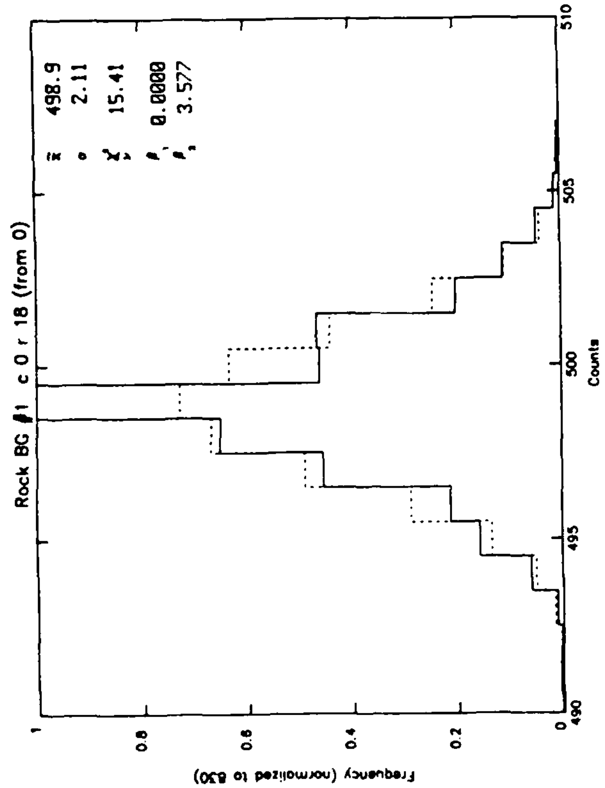
Rock BG #1 c 0 r 18 (from 0)
x̄ 498.9
σ 2.11
χ²ν 15.41
β1 0.0000
β2 3.577
Frequency (normalized to 630)
Counts

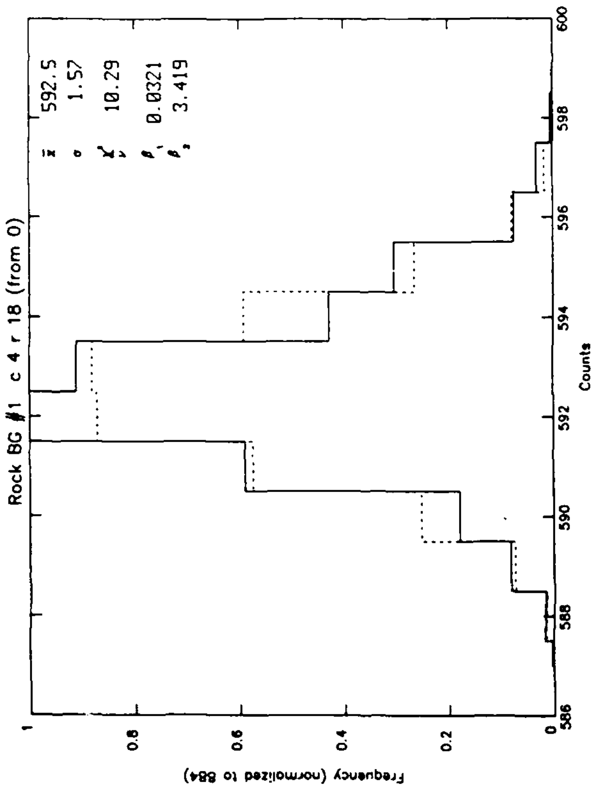
Rock BG #1 c 4 r 18 (from 0)
x̄ 592.5
σ 1.57
χ²ν 10.29
β1 0.0321
β2 3.419
Frequency (normalized to 884)
Counts

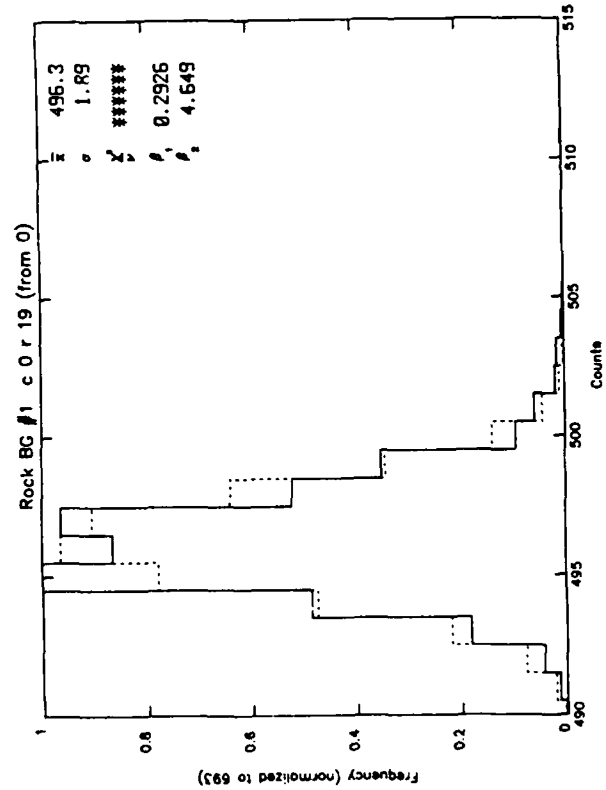
Rock BG #1 c 0 r 19 (from 0)
x̄ 496.3
σ 1.89
χ²ν *****
β1 0.2926
β2 4.649
Frequency (normalized to 693)
Counts

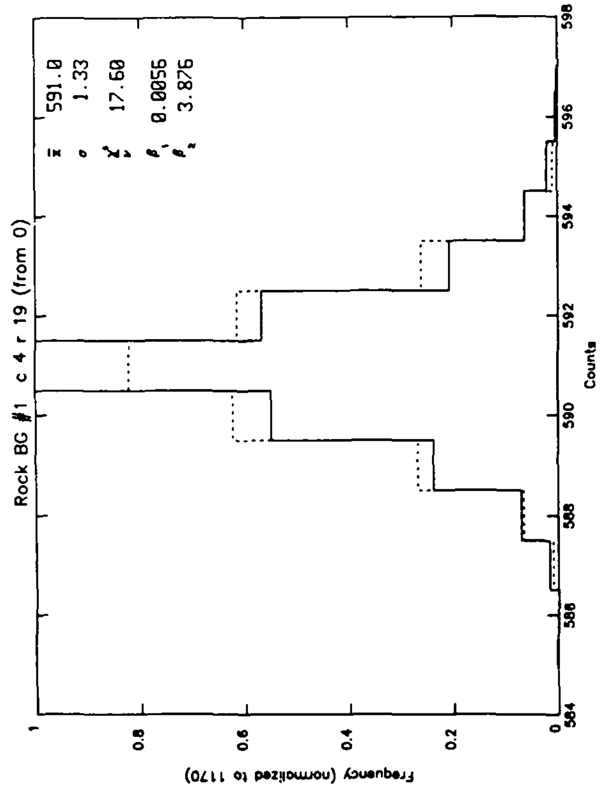
Rock BG #1 c 4 r 19 (from 0)
x̄ 591.0
σ 1.33
χ²ν 17.60
β1 0.0056
β2 3.876
Frequency (normalized to 1170)
Counts

APPENDIX A-2

Array: Rockwell BIBIB Array

	Left	Right
Elements:	Column 0; Rows 0-9	Column 4; Rows 0-19
Data Run:	Background #2	Background #3

Purpose: Comparison of the same detector elements for two different background measurements. Compare also with Appendix A-3 for other elements and with Appendix A-1 for another background measurement.

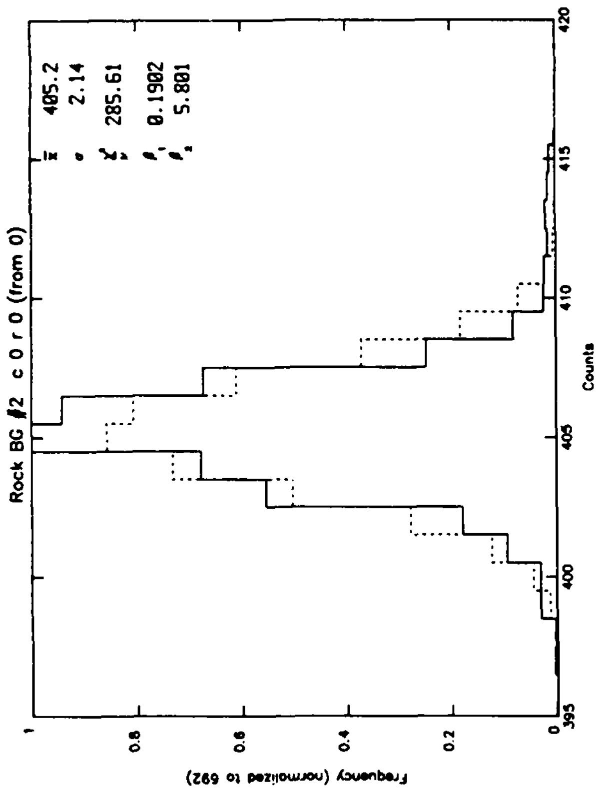
Rock BG #2 c 0 r 0 (from 0)
x̄ 405.2
σ 2.14
χ^2_ν 285.61
β_1 0.1902
β_2 5.801
Counts
Frequency (normalized to 692)

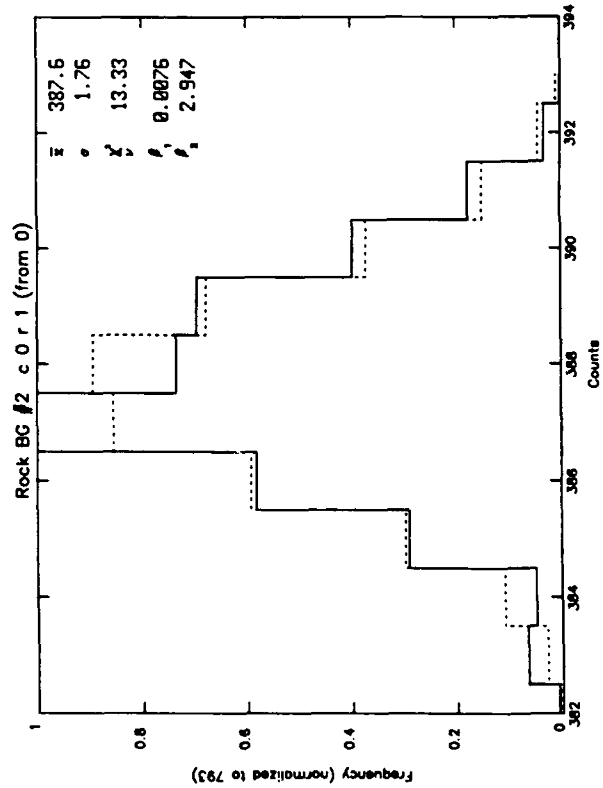
Rock BG #2 c 0 r 1 (from 0)
x̄ 387.6
σ 1.76
χ^2_ν 13.33
β_1 0.0076
β_2 2.947
Counts
Frequency (normalized to 793)

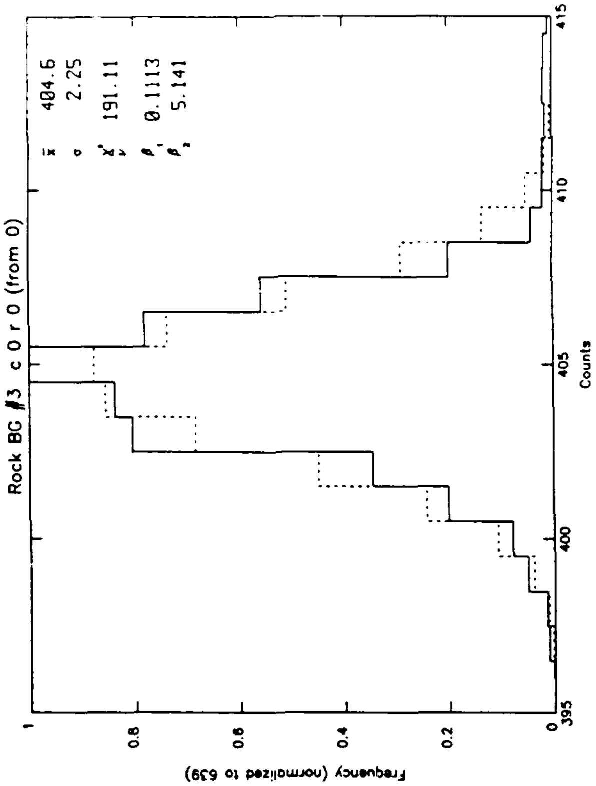
Rock BG #3 c 0 r 0 (from 0)
x̄ 404.6
σ 2.25
χ^2_ν 191.11
β_1 0.1113
β_2 5.141
Counts
Frequency (normalized to 639)

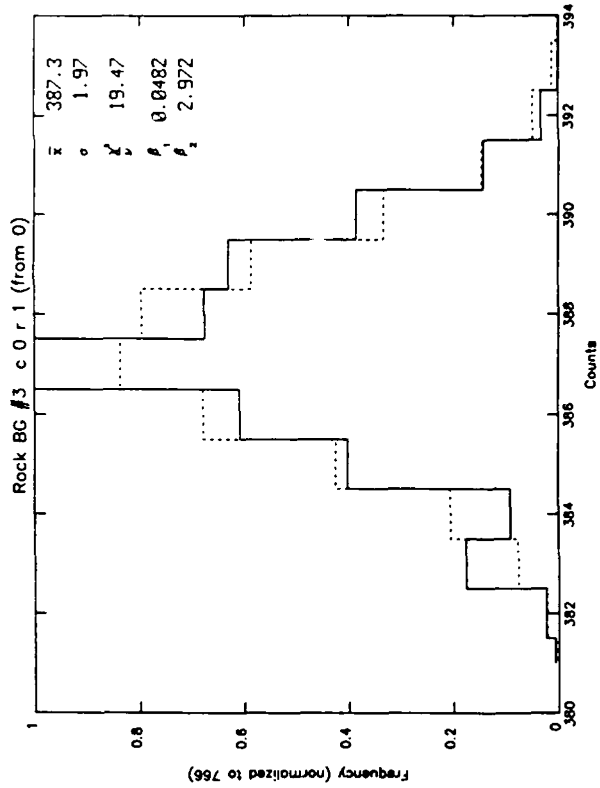
Rock BG #3 c 0 r 1 (from 0)
x̄ 387.3
σ 1.97
χ^2_ν 19.47
β_1 0.0482
β_2 2.972
Counts
Frequency (normalized to 766)

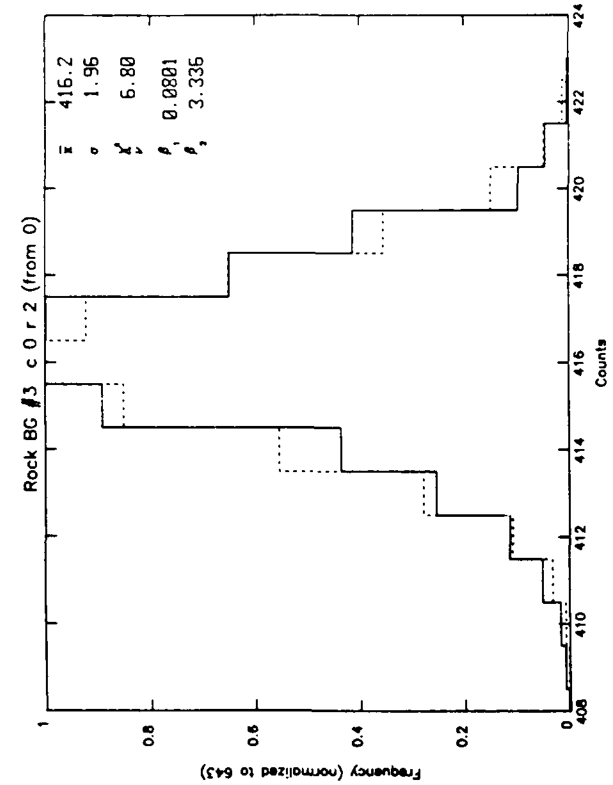

Rock BG #3 c 0 r 2 (from 0)
x̄ 416.2
σ 1.96
χ²ν 6.80
β₁ 0.0801
β₂ 3.336
Counts
Frequency (normalized to 643)

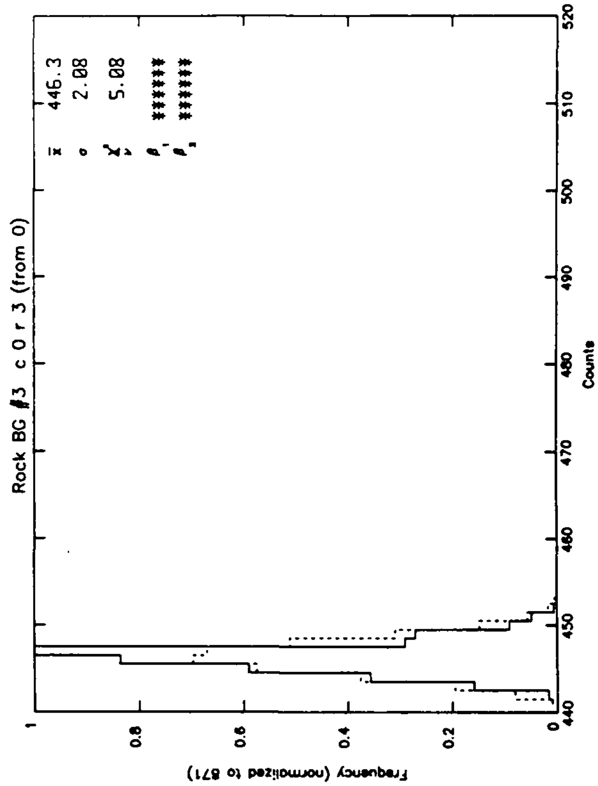

Rock BG #3 c 0 r 3 (from 0)
x̄ 446.3
σ 2.08
χ²ν 5.08
β₁ *****
β₂ *****
Counts
Frequency (normalized to 871)

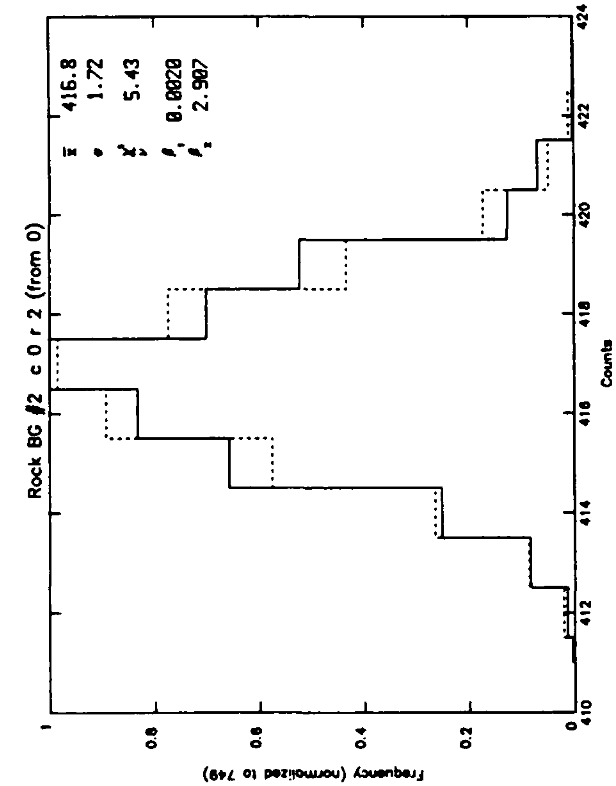

Rock BG #2 c 0 r 2 (from 0)
x̄ 416.8
σ 1.72
χ²ν 5.43
β₁ 0.0020
β₂ 2.907
Counts
Frequency (normalized to 749)

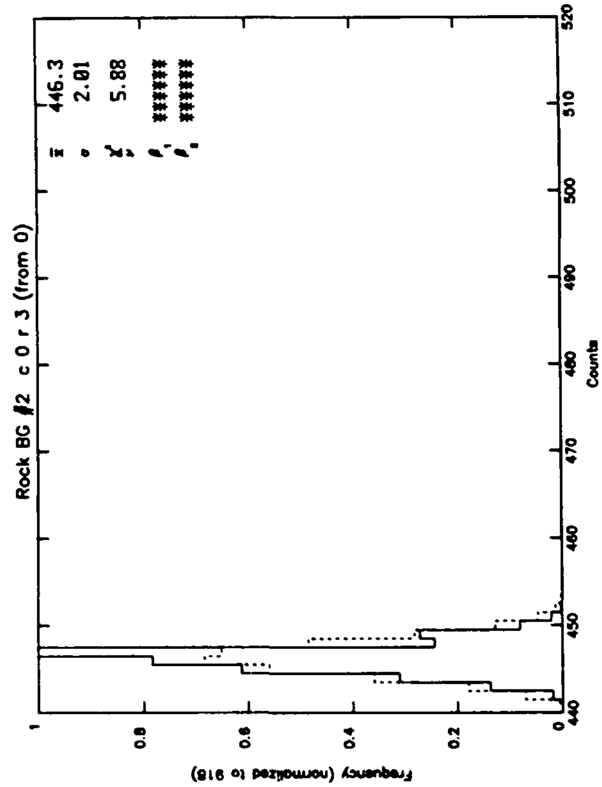

Rock BG #2 c 0 r 3 (from 0)
x̄ 446.3
σ 2.01
χ²ν 5.88
β₁ *****
β₂ *****
Counts
Frequency (normalized to 918)

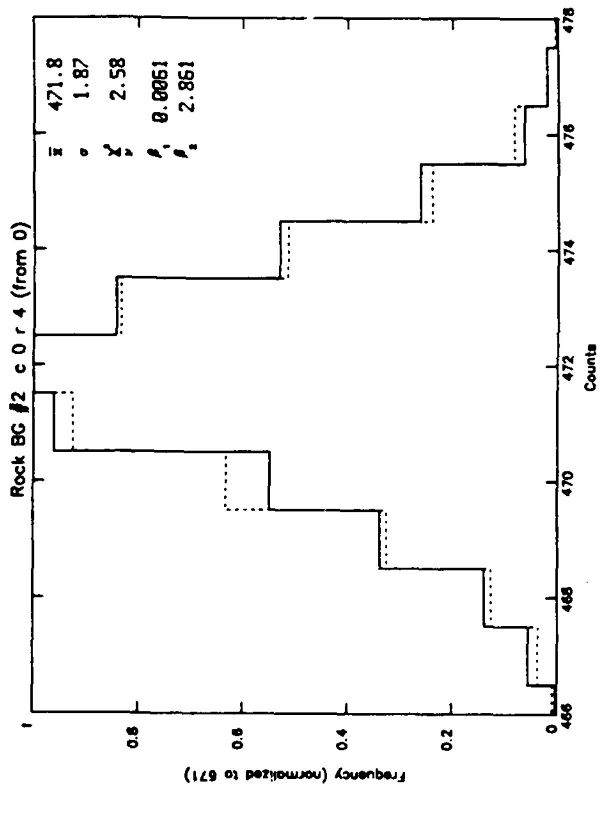
Rock BG #2 c 0 r 4 (from 0)
x̄ 471.8
σ 1.87
χ²ν 2.58
β1 0.0061
β2 2.861
Frequency (normalized to 671)
Counts

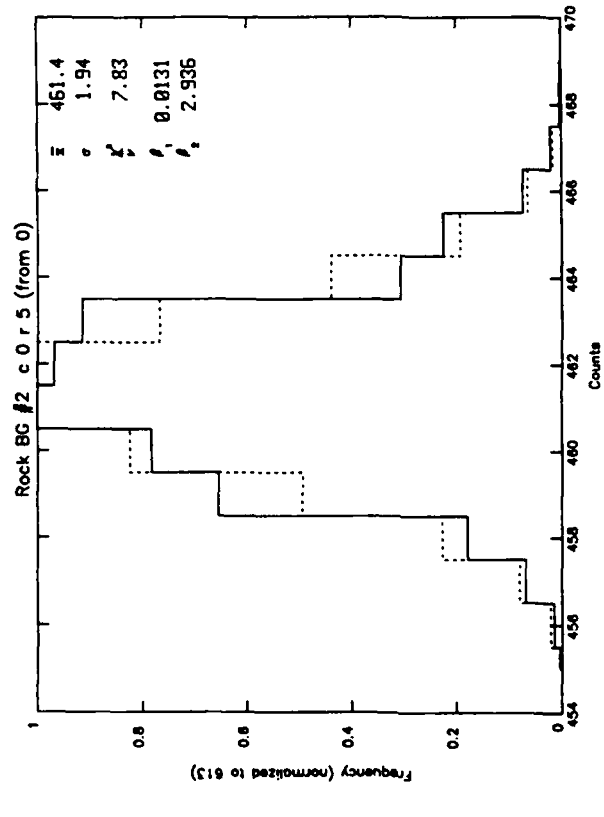
Rock BG #2 c 0 r 5 (from 0)
x̄ 461.4
σ 1.94
χ²ν 7.83
β1 0.0131
β2 2.936
Frequency (normalized to 613)
Counts

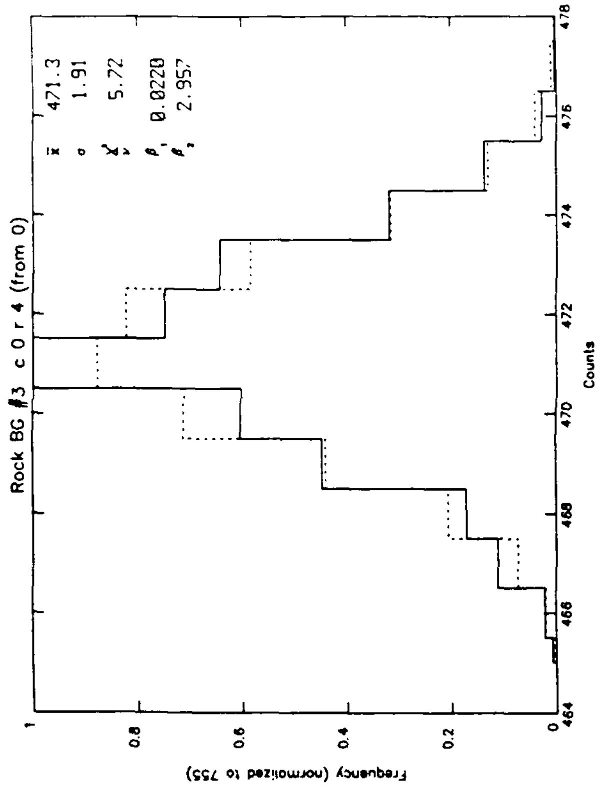
Rock BG #3 c 0 r 4 (from 0)
x̄ 471.3
σ 1.91
χ²ν 5.72
β1 0.0220
β2 2.957
Frequency (normalized to 755)
Counts

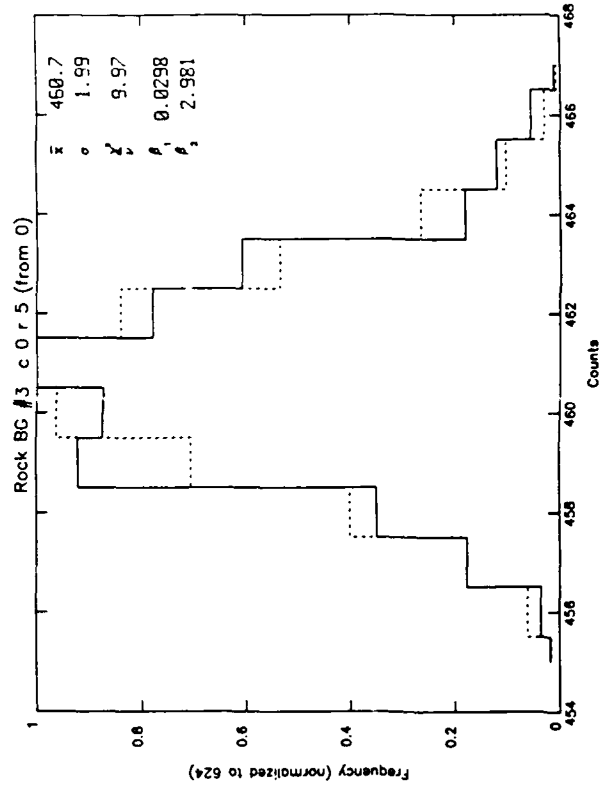
Rock BG #3 c 0 r 5 (from 0)
x̄ 460.7
σ 1.99
χ²ν 9.97
β1 0.0298
β2 2.981
Frequency (normalized to 624)
Counts

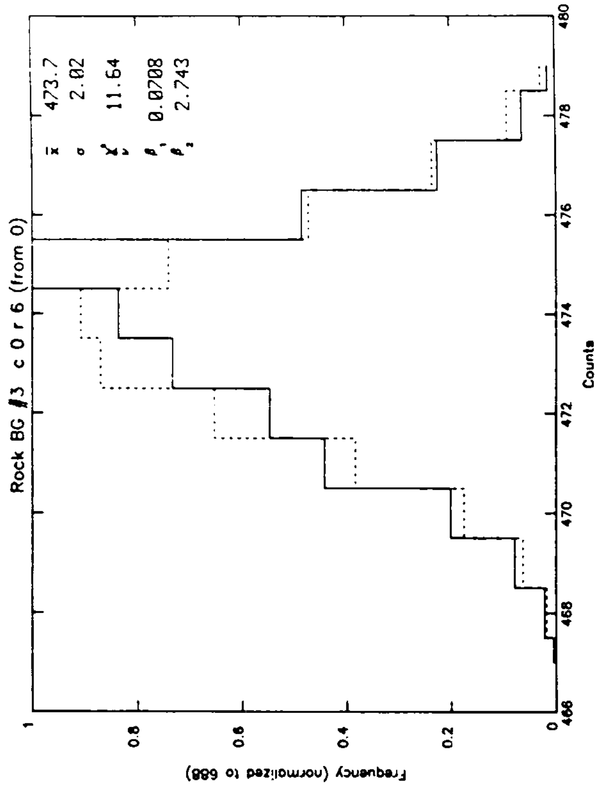
Rock BG #3 c 0 r 6 (from 0)
x̄ 473.7
σ 2.02
χ^2_ν 11.64
β_1 0.0708
β_2 2.743
Frequency (normalized to 688)
Counts

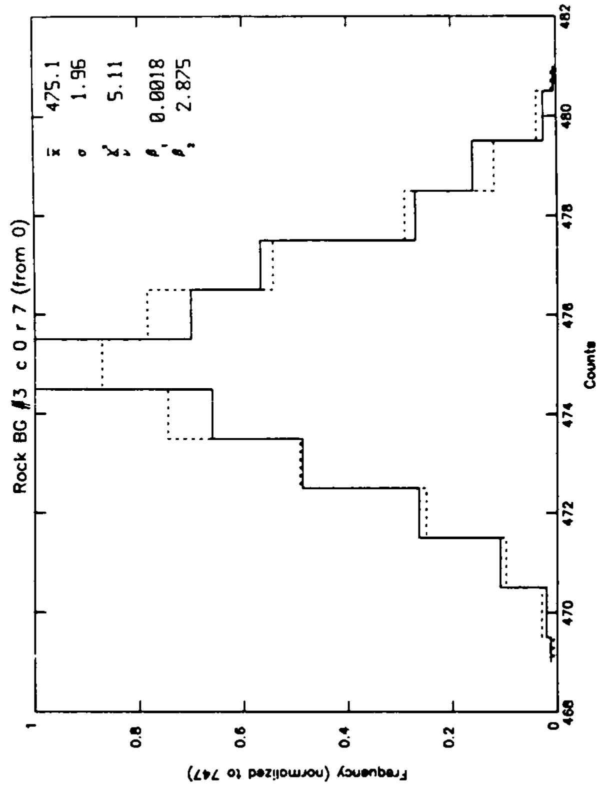
Rock BG #3 c 0 r 7 (from 0)
x̄ 475.1
σ 1.96
χ^2_ν 5.11
β_1 0.0018
β_2 2.875
Frequency (normalized to 747)
Counts

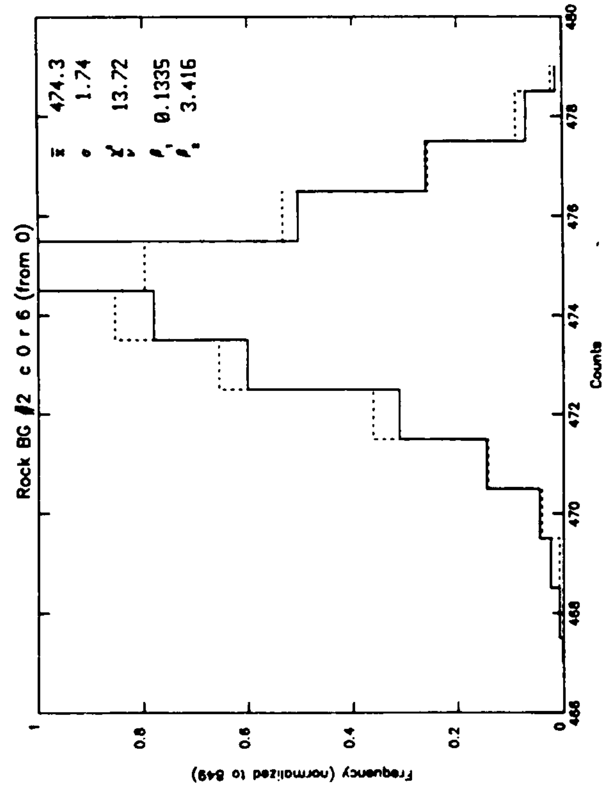
Rock BG #2 c 0 r 6 (from 0)
x̄ 474.3
σ 1.74
χ^2_ν 13.72
β_1 0.1335
β_2 3.416
Frequency (normalized to 849)
Counts

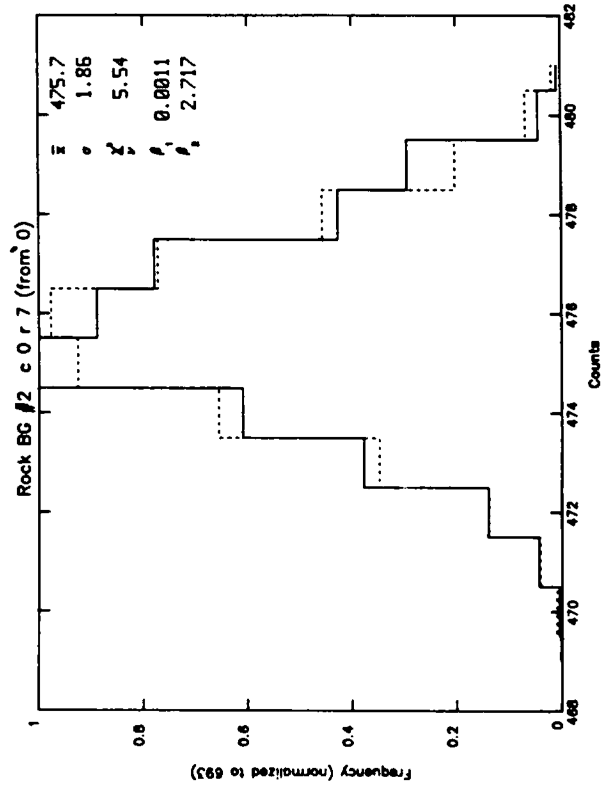
Rock BG #2 c 0 r 7 (from 0)
x̄ 475.7
σ 1.86
χ^2_ν 5.54
β_1 0.0011
β_2 2.717
Frequency (normalized to 693)
Counts

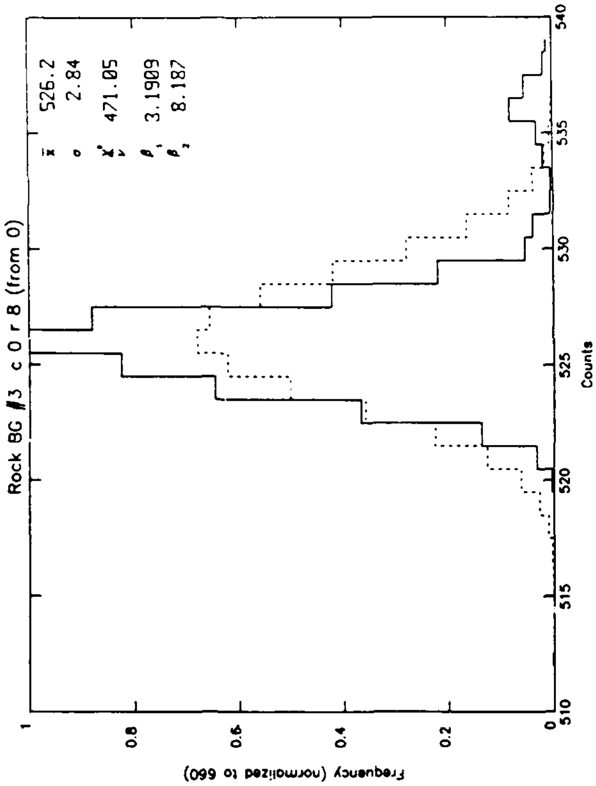
Rock BG #3 c 0 r 8 (from 0)
x̄ 526.2
σ 2.84
χ²ν 471.05
β₁ 3.1909
β₂ 8.187
Counts
Frequency (normalized to 660)

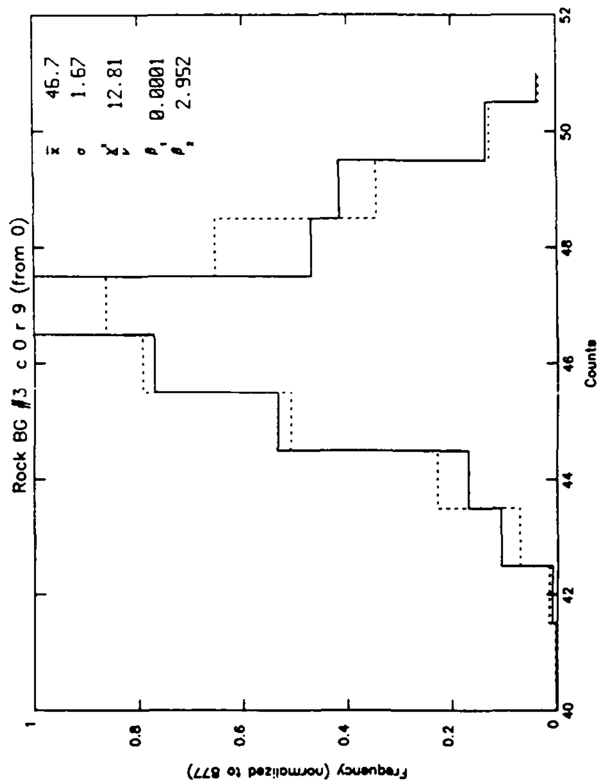
Rock BG #3 c 0 r 9 (from 0)
x̄ 46.7
σ 1.67
χ²ν 12.81
β₁ 0.0001
β₂ 2.952
Counts
Frequency (normalized to 877)

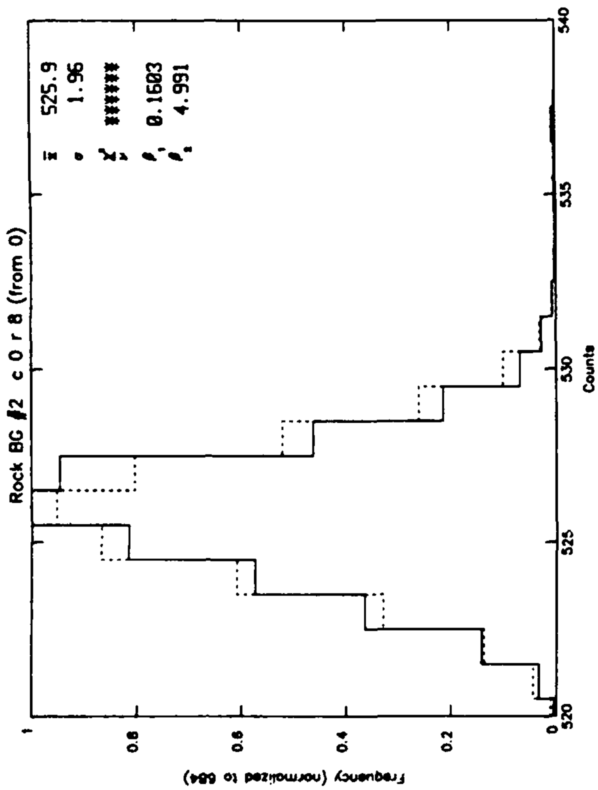
Rock BG #2 c 0 r 8 (from 0)
x̄ 525.9
σ 1.96
χ²ν ******
β₁ 0.1603
β₂ 4.991
Counts
Frequency (normalized to 684)

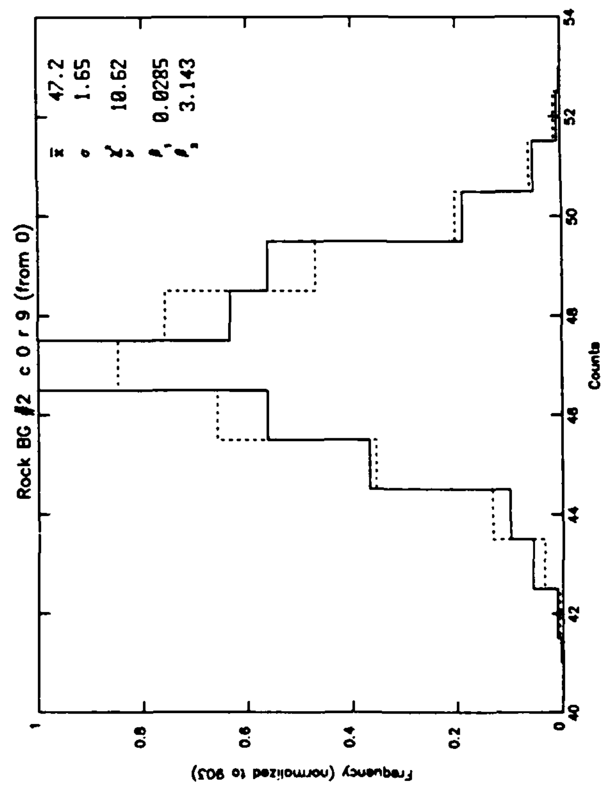
Rock BG #2 c 0 r 9 (from 0)
x̄ 47.2
σ 1.65
χ²ν 10.62
β₁ 0.0285
β₂ 3.143
Counts
Frequency (normalized to 903)

APPENDIX A-3

Array: Rockwell BIBIB Array

	Left	Right
Elements:	Column 4; Rows 30-39	Column 4; Rows 30-39
Data Run:	Background #2	Background #3

Purpose: Comparison of the same detector elements for two different background measurements. Compare also with Appendix A-2 for other elements and with Appendix A-1 for another background measurement.

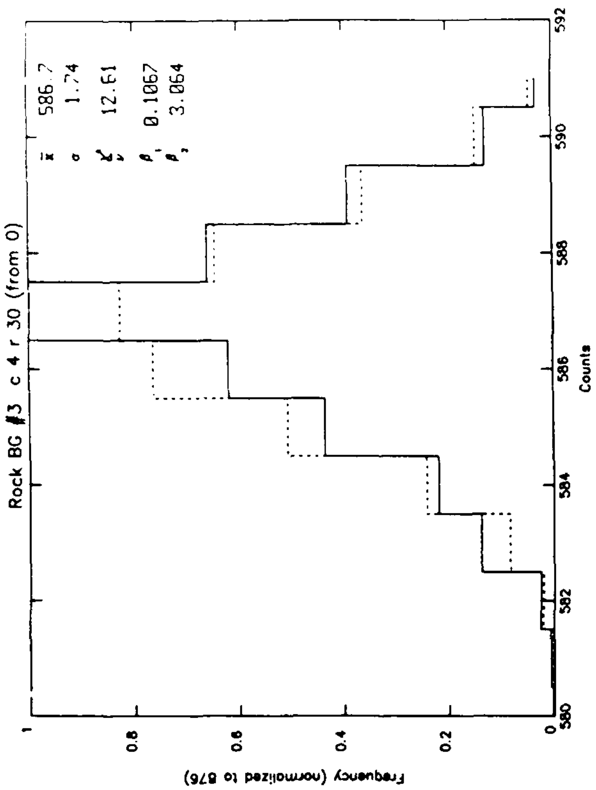
Rock BG #3 c 4 r 30 (from 0)
x̄ 586.7
σ 1.74
χ²ν 12.61
β1 0.1067
β2 3.064
Counts
Frequency (normalized to 876)

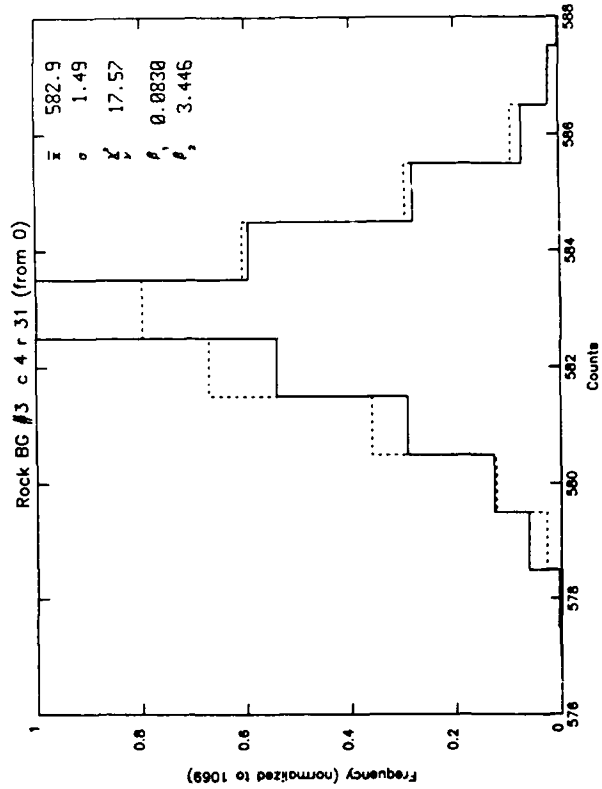
Rock BG #3 c 4 r 31 (from 0)
x̄ 582.9
σ 1.49
χ²ν 17.57
β1 0.0830
β2 3.446
Counts
Frequency (normalized to 1069)

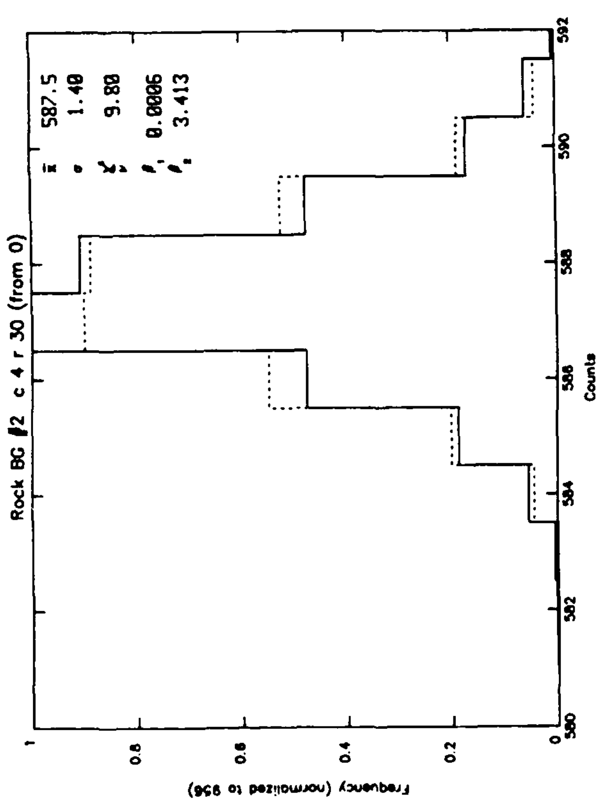
Rock BG #2 c 4 r 30 (from 0)
x̄ 587.5
σ 1.40
χ²ν 9.80
β1 0.0006
β2 3.413
Counts
Frequency (normalized to 956)

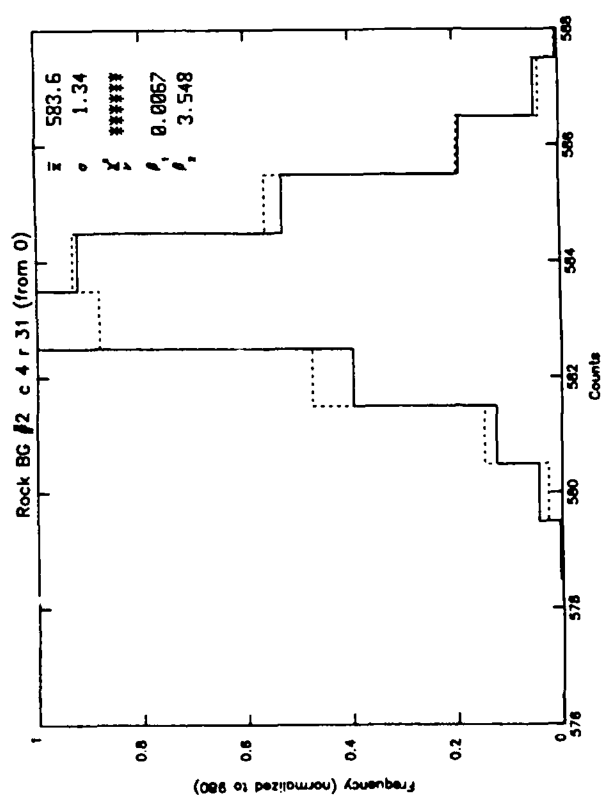
Rock BG #2 c 4 r 31 (from 0)
x̄ 583.6
σ 1.34
χ²ν *****
β1 0.0067
β2 3.548
Counts
Frequency (normalized to 980)

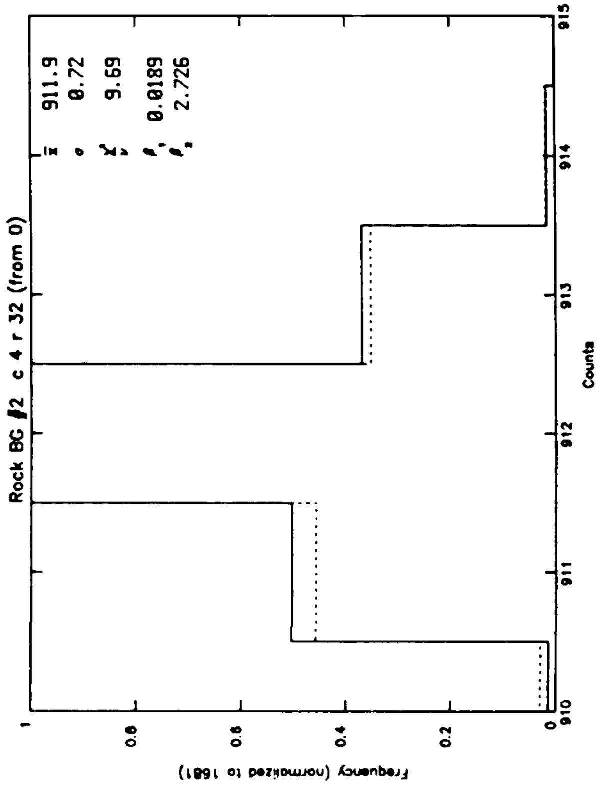

Rock BG #2 c 4 r 32 (from 0)
$\bar{x}$ 911.9
σ 0.72
χ^2_ν 9.69
β_1 0.0189
β_2 2.726
Counts
Frequency (normalized to 1681)

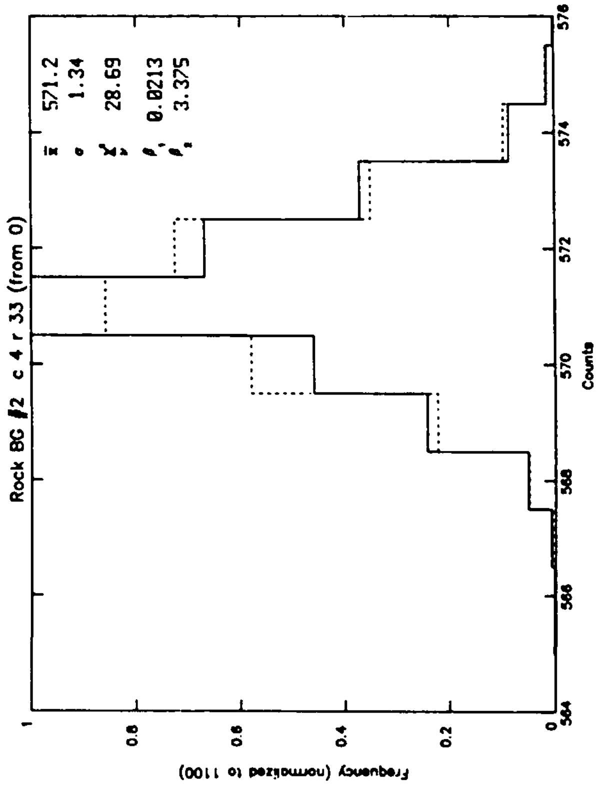

Rock BG #2 c 4 r 33 (from 0)
$\bar{x}$ 571.2
σ 1.34
χ^2_ν 28.69
β_1 0.0213
β_2 3.375
Counts
Frequency (normalized to 1100)

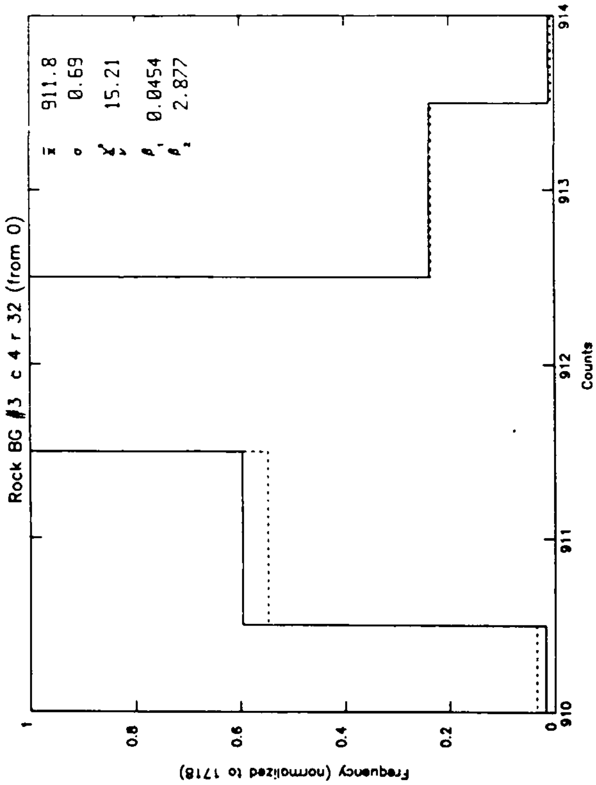

Rock BG #3 c 4 r 32 (from 0)
$\bar{x}$ 911.8
σ 0.69
χ^2_ν 15.21
β_1 0.0454
β_2 2.877
Counts
Frequency (normalized to 1718)

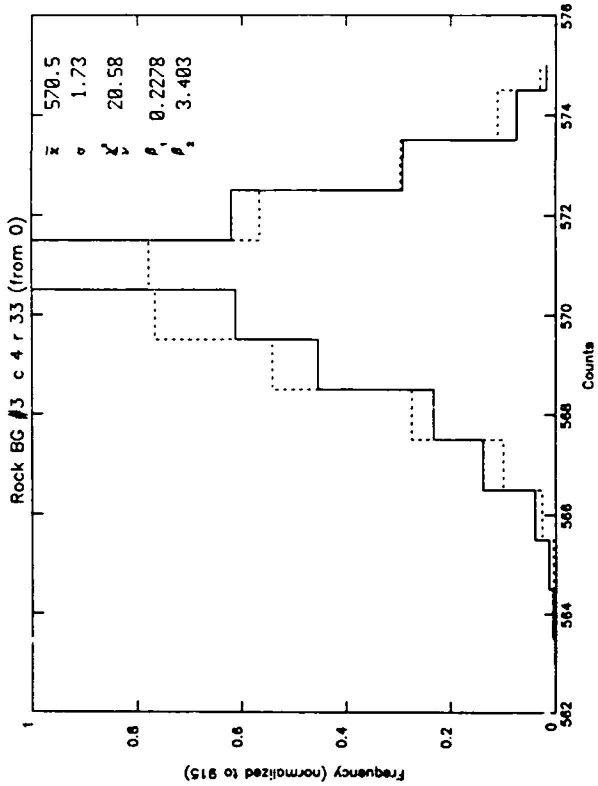

Rock BG #3 c 4 r 33 (from 0)
$\bar{x}$ 570.5
σ 1.73
χ^2_ν 20.58
β_1 0.2278
β_2 3.403
Counts
Frequency (normalized to 915)

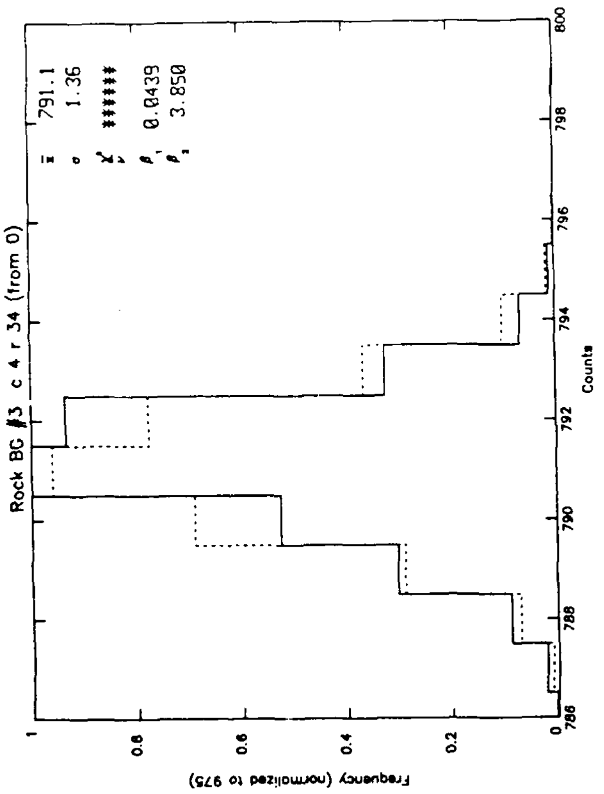
Rock BG #3 c 4 r 34 (from 0)
791.1
1.36
******
0.0439
3.850
Frequency (normalized to 975)
Counts

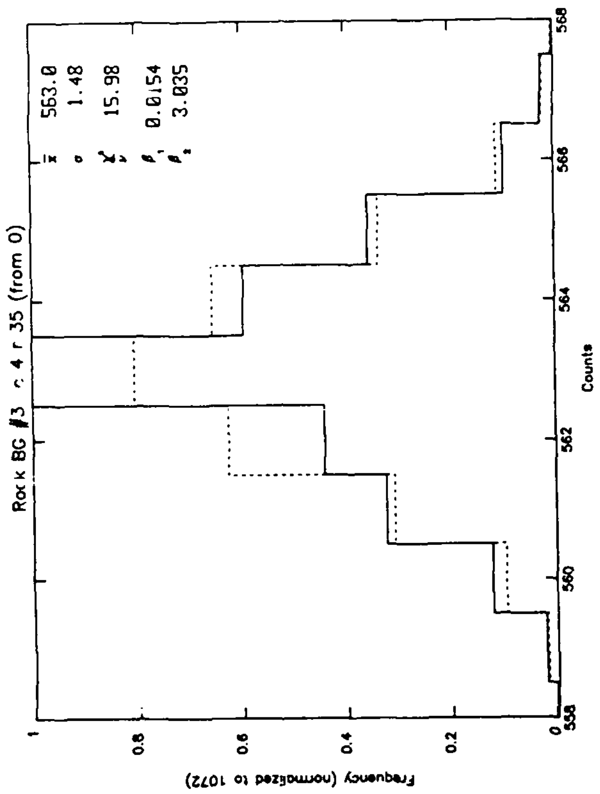
Rock BG #3 c 4 r 35 (from 0)
563.0
1.48
15.98
0.0154
3.035
Frequency (normalized to 1072)
Counts

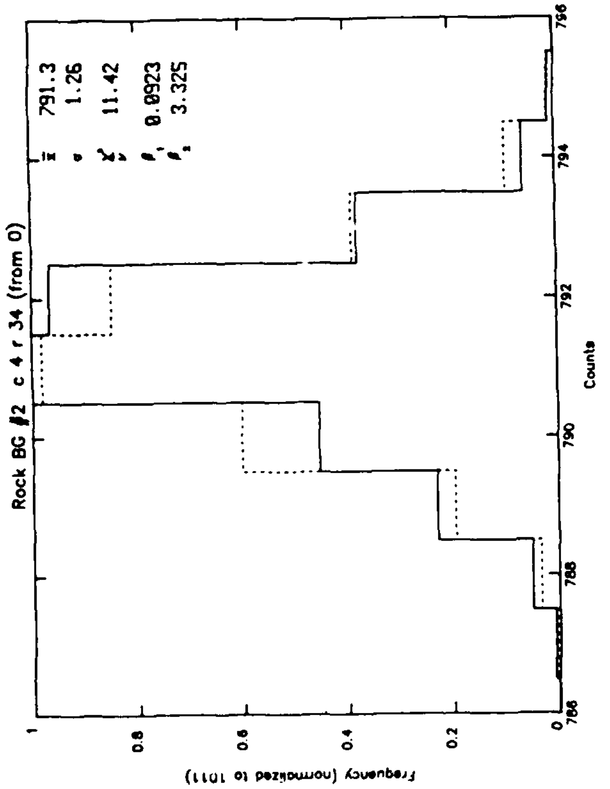
Rock BG #2 c 4 r 34 (from 0)
791.3
1.26
11.42
0.0923
3.325
Frequency (normalized to 1011)
Counts

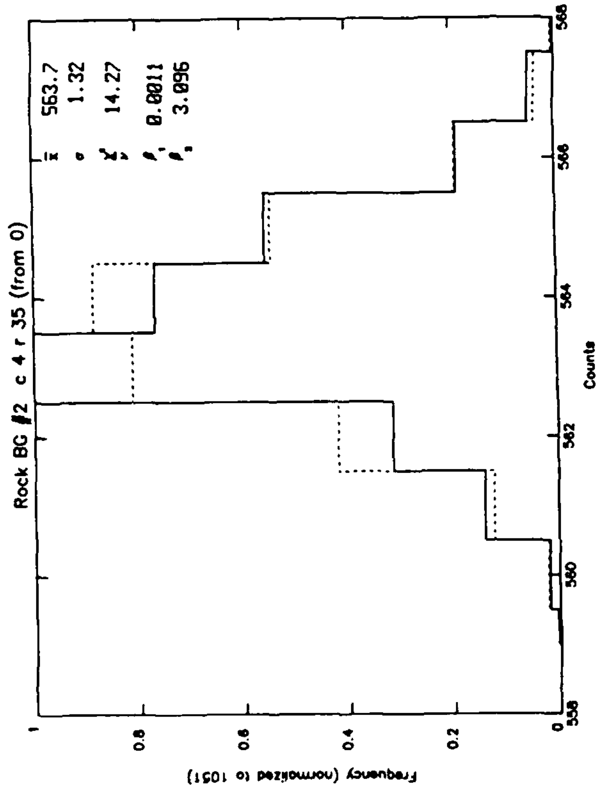
Rock BG #2 c 4 r 35 (from 0)
563.7
1.32
14.27
0.0011
3.096
Frequency (normalized to 1051)
Counts

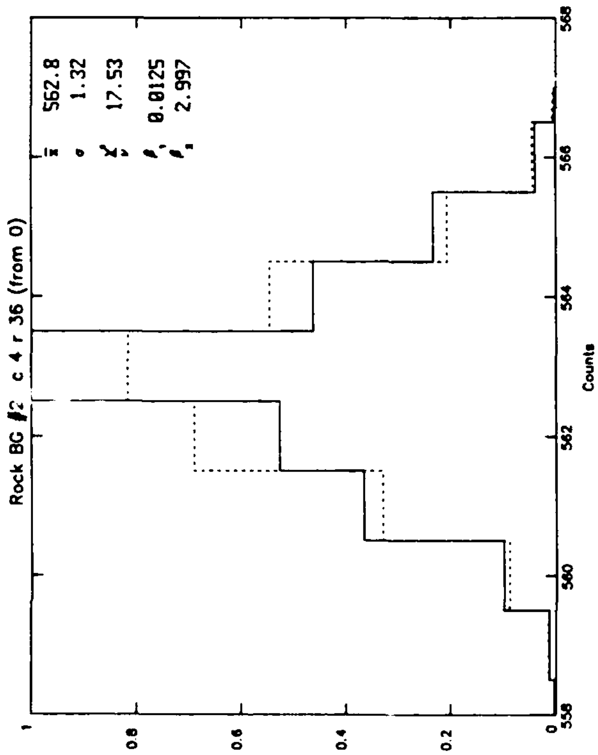
Rock BG #2 c 4 r 36 (from 0)
x̄ 562.8
σ 1.32
χ^2_ν 17.53
β_1 0.0125
β_2 2.997
Frequency (normalized to 1166)
Counts

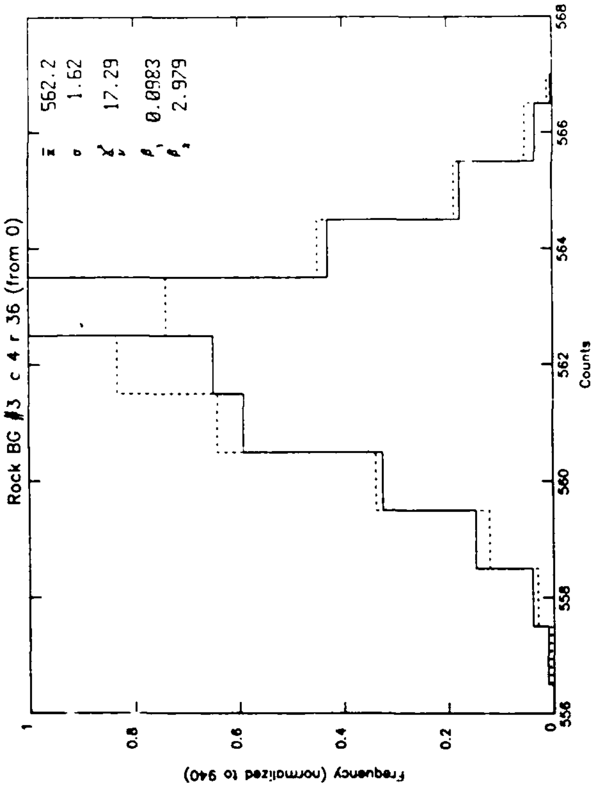
Rock BG #3 c 4 r 36 (from 0)
x̄ 562.2
σ 1.62
χ^2_ν 17.29
β_1 0.0983
β_2 2.979
Frequency (normalized to 940)
Counts

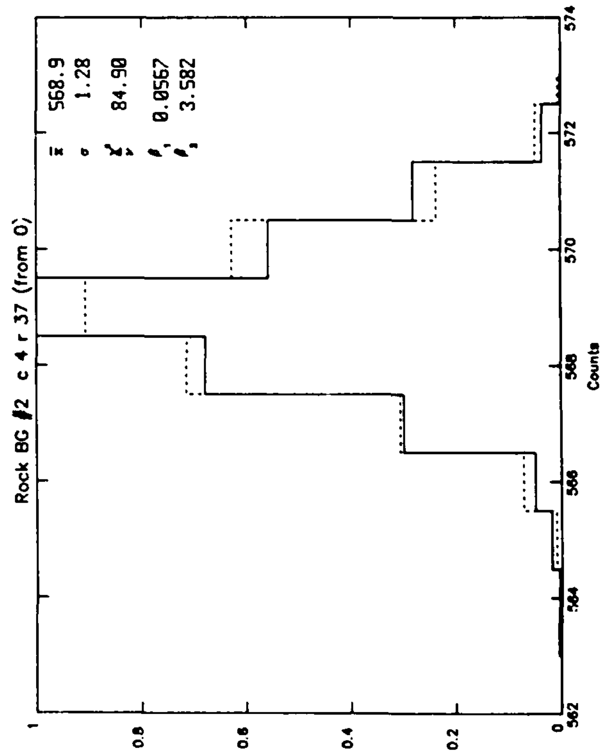
Rock BG #2 c 4 r 37 (from 0)
x̄ 568.9
σ 1.28
χ^2_ν 84.90
β_1 0.0567
β_2 3.582
Frequency (normalized to 1093)
Counts

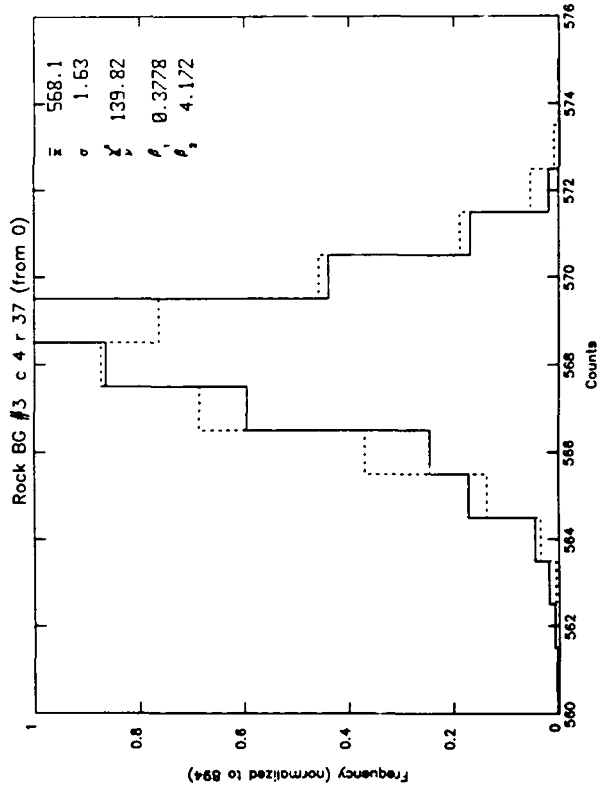
Rock BG #3 c 4 r 37 (from 0)
x̄ 568.1
σ 1.63
χ^2_ν 139.82
β_1 0.3778
β_2 4.172
Frequency (normalized to 894)
Counts

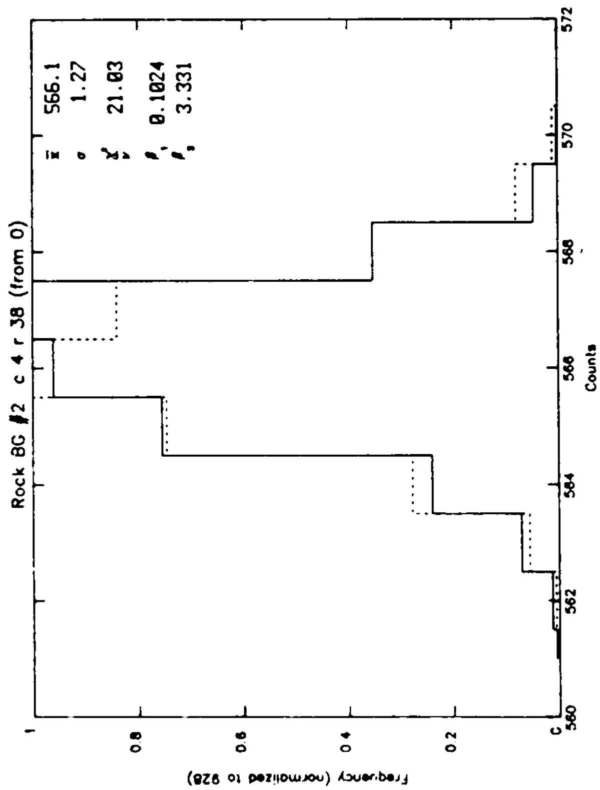
Rock BG #2 c 4 r 38 (from 0)
x̄ 566.1
σ 1.27
χ^2_ν 21.03
β_1 0.1024
β_2 3.331
Counts
Frequency (normalized to 928)

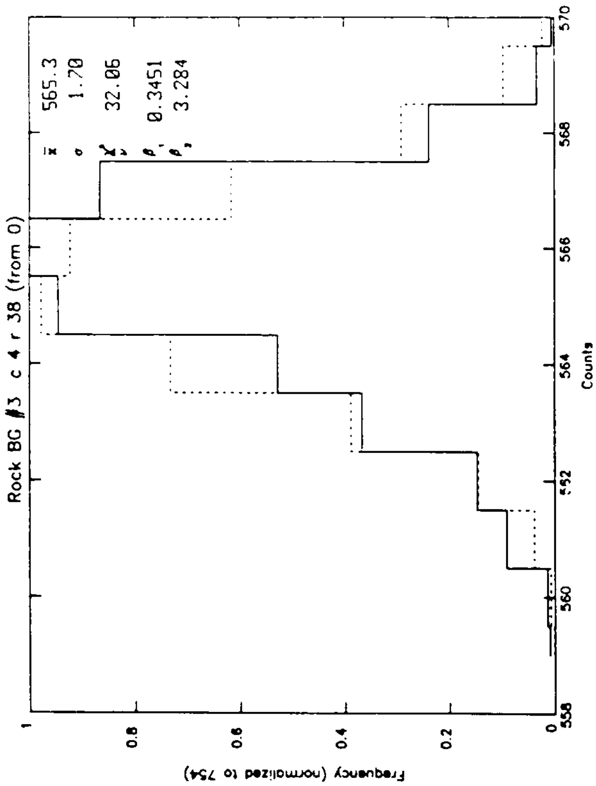
Rock BG #3 c 4 r 38 (from 0)
x̄ 565.3
σ 1.70
χ^2_ν 32.06
β_1 0.3451
β_2 3.284
Counts
Frequency (normalized to 754)

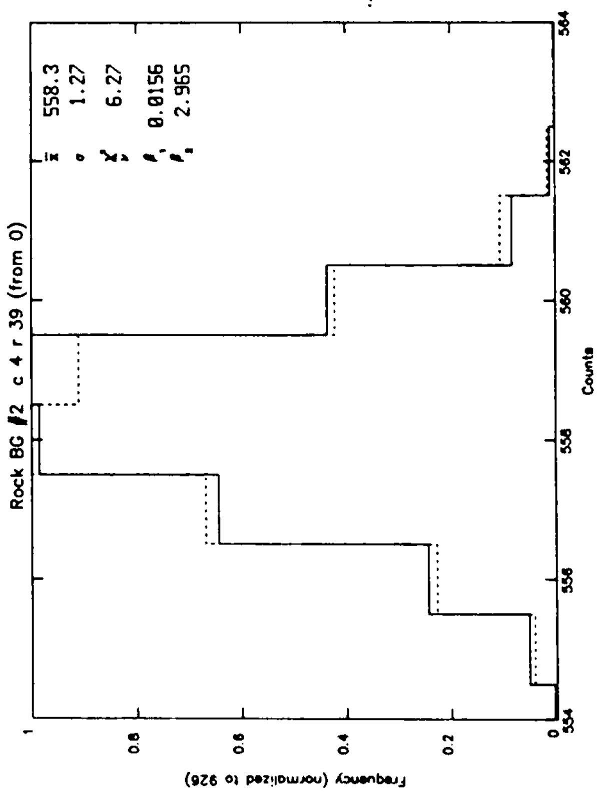
Rock BG #2 c 4 r 39 (from 0)
x̄ 558.3
σ 1.27
χ^2_ν 6.27
β_1 0.0156
β_2 2.965
Counts
Frequency (normalized to 926)

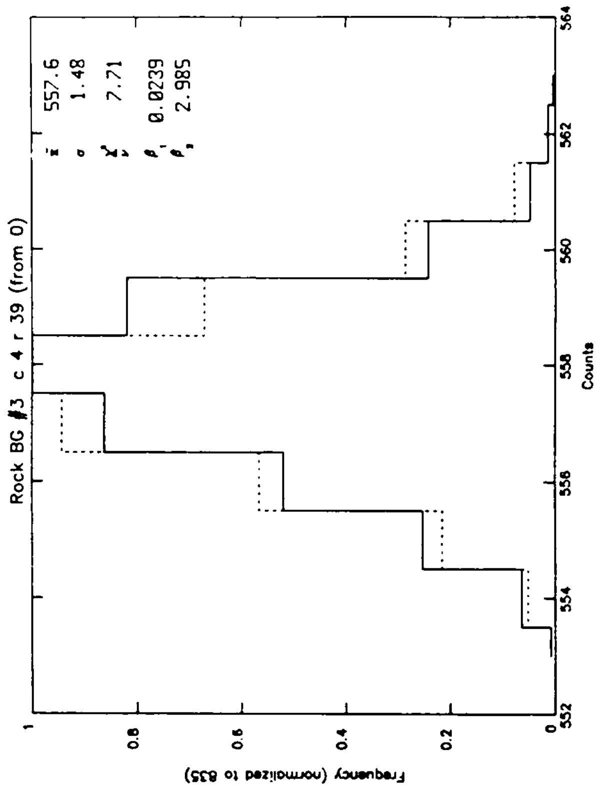
Rock BG #3 c 4 r 39 (from 0)
x̄ 557.6
σ 1.48
χ^2_ν 7.71
β_1 0.0239
β_2 2.985
Counts
Frequency (normalized to 835)

APPENDIX A-4

Array: Rockwell BIBIB Array

	Left	Right
Elements:	Column 0; Rows 0-19	Column 3; Rows 0-19
Data Run:	Star 1_637	Star 1_637

Purpose: Comparison of behavior of an even and an odd column for background and star in field.

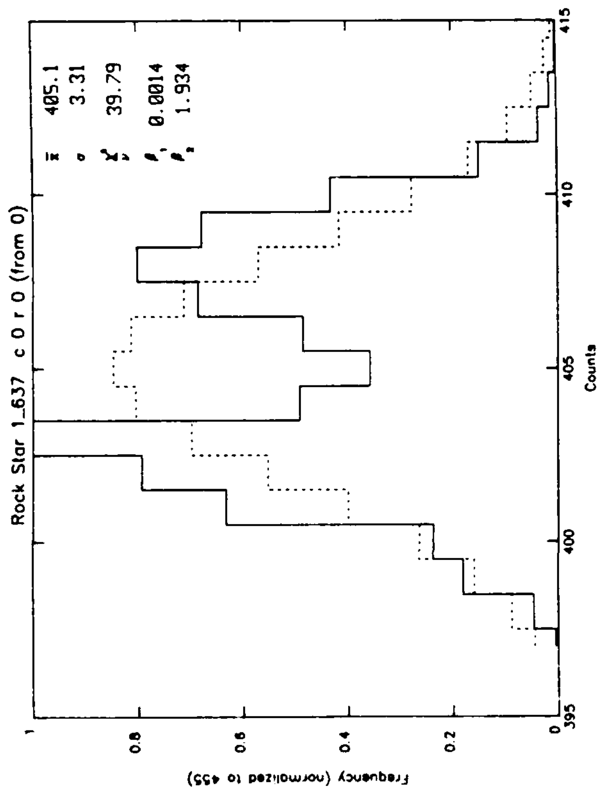

Rock Star 1_637 c 0 r 0 (from 0)
$\bar{x}$ 405.1
σ 3.31
χ^2_ν 39.79
β_1 0.0014
β_2 1.934
Frequency (normalized to 455)
Counts

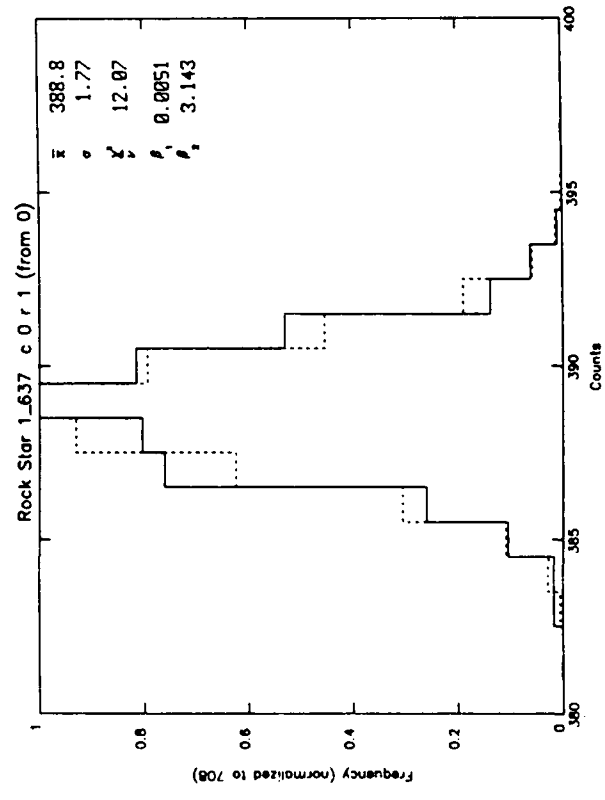

Rock Star 1_637 c 0 r 1 (from 0)
$\bar{x}$ 388.8
σ 1.77
χ^2_ν 12.07
β_1 0.0051
β_2 3.143
Frequency (normalized to 708)
Counts

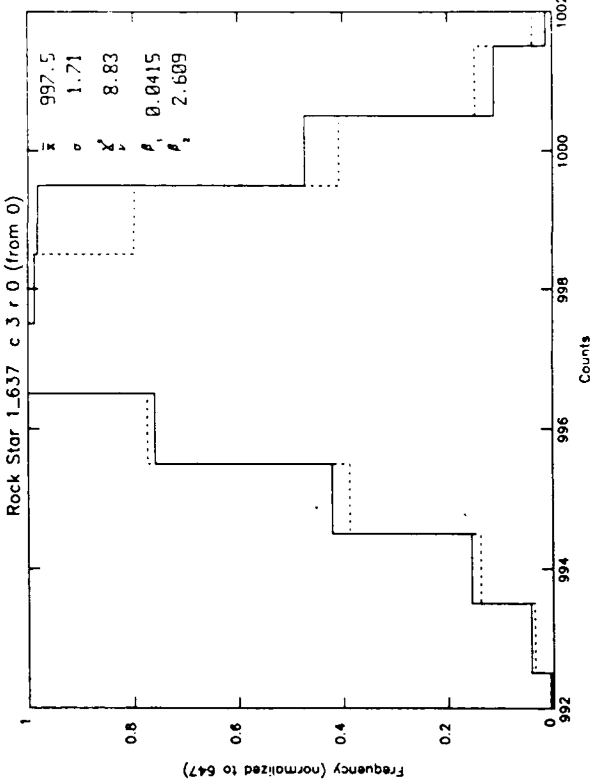

Rock Star 1_637 c 3 r 0 (from 0)
$\bar{x}$ 997.5
σ 1.71
χ^2_ν 8.83
β_1 0.0415
β_2 2.609
Frequency (normalized to 647)
Counts

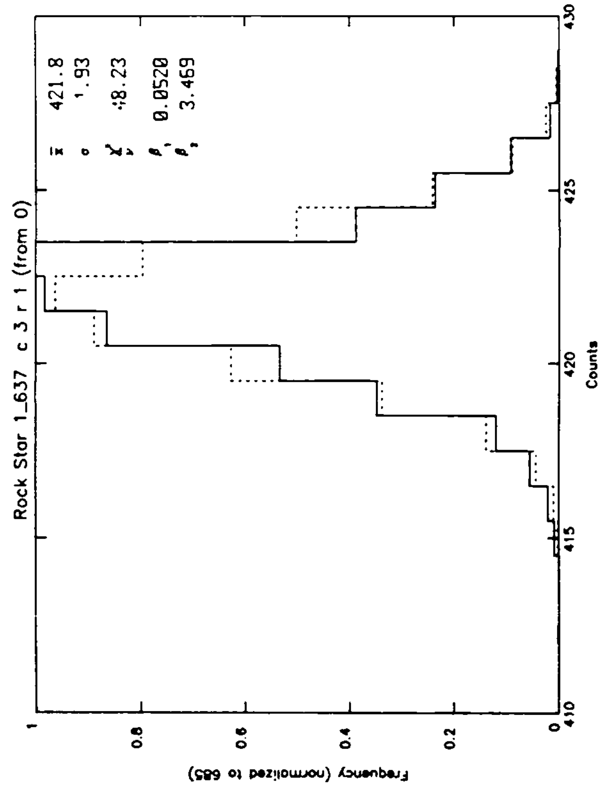

Rock Star 1_637 c 3 r 1 (from 0)
$\bar{x}$ 421.8
σ 1.93
χ^2_ν 8.23
β_1 0.0520
β_2 3.469
Frequency (normalized to 685)
Counts

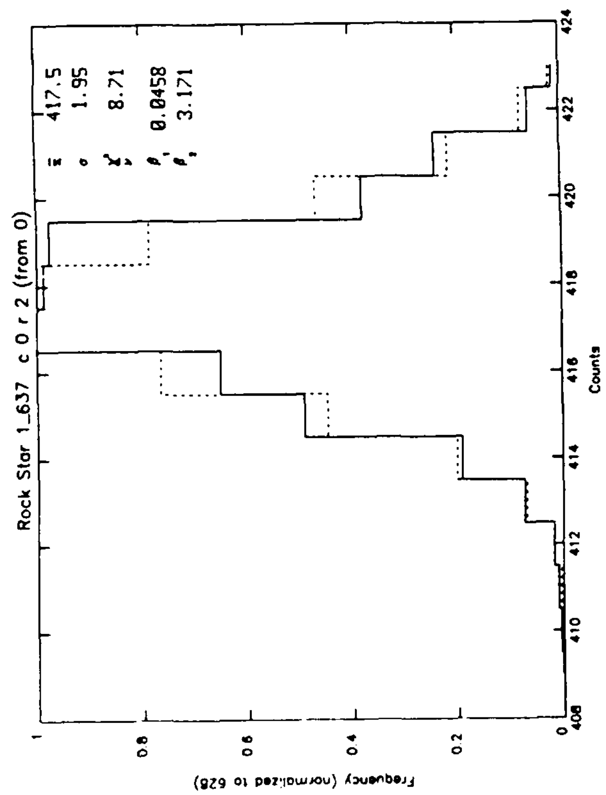
Rock Star 1_637 c 0 r 2 (from 0)
x̄ 417.5
σ 1.95
χ^2_ν 8.71
β_1 0.0458
β_2 3.171
Frequency (normalized to 628)
Counts

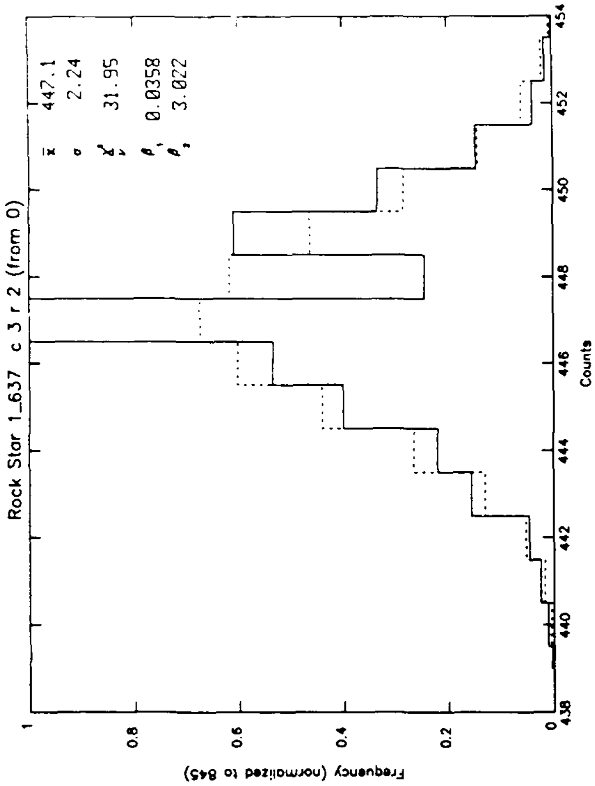
Rock Star 1_637 c 3 r 2 (from 0)
x̄ 447.1
σ 2.24
χ^2_ν 31.95
β_1 0.0358
β_2 3.022
Frequency (normalized to 845)
Counts

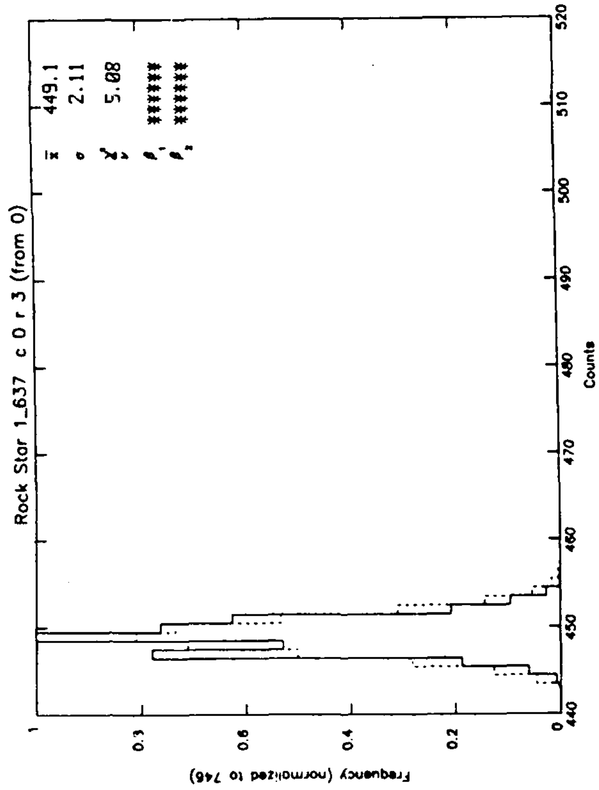
Rock Star 1_637 c 0 r 3 (from 0)
x̄ 449.1
σ 2.11
χ^2_ν 5.08
β_1 ******
β_2 ******
Frequency (normalized to 746)
Counts

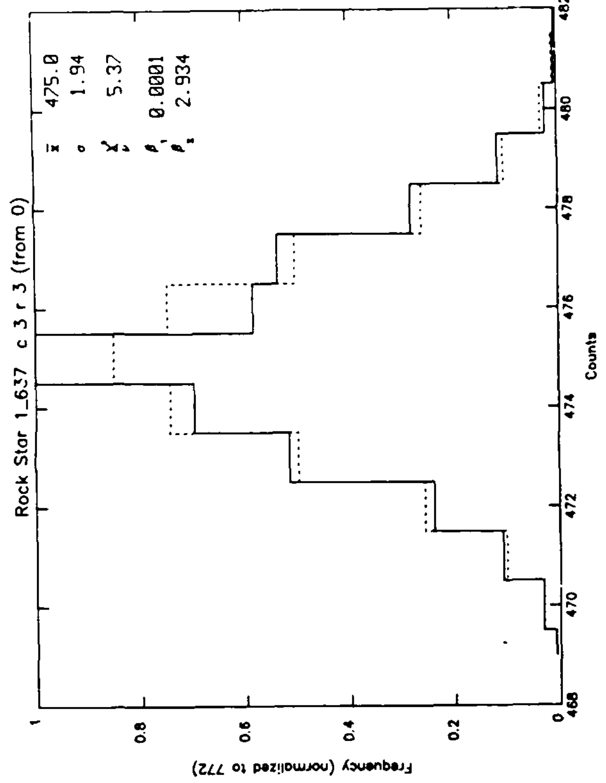
Rock Star 1_637 c 3 r 3 (from 0)
x̄ 475.0
σ 1.94
χ^2_ν 5.37
β_1 0.0001
β_2 2.934
Frequency (normalized to 772)
Counts

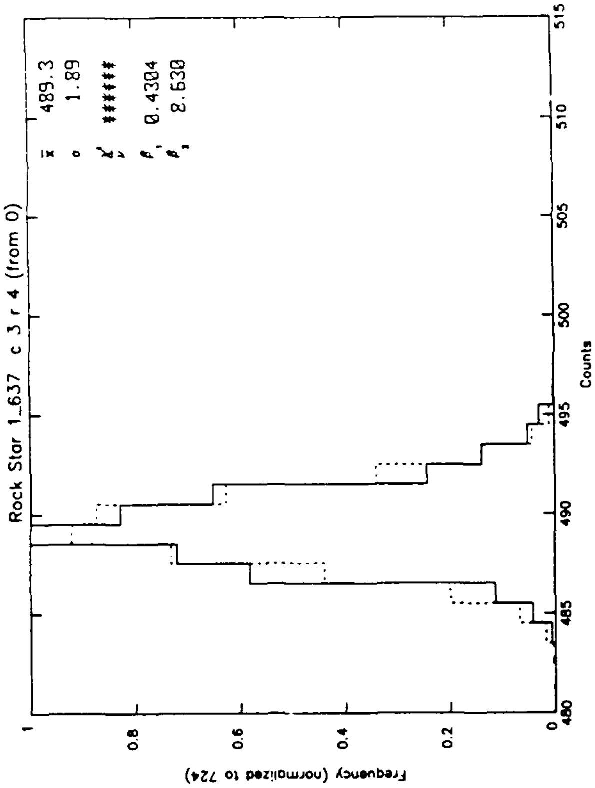

Rock Star 1_637 c 3 r 4 (from 0)
x̄ 489.3
σ 1.89
χ²ν ######
β1 0.4304
β2 8.638
Counts
Frequency (normalized to 724)

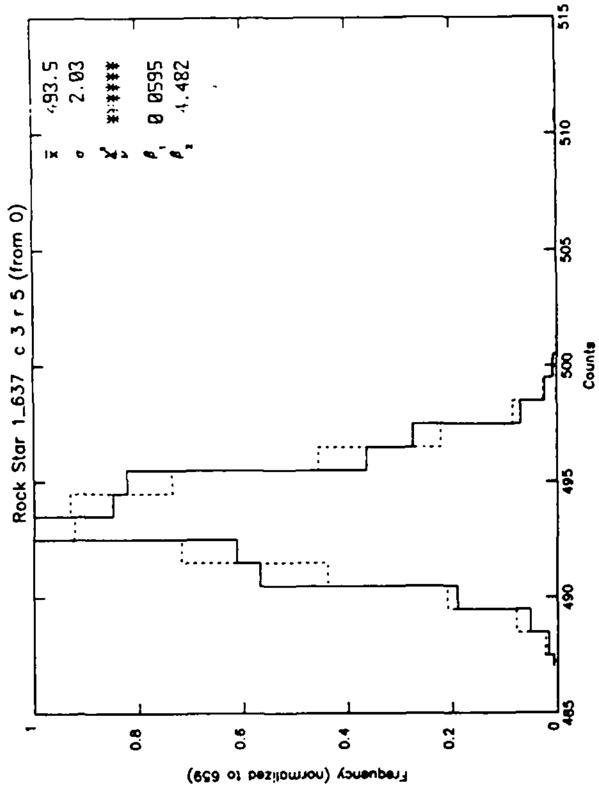

Rock Star 1_637 c 3 r 5 (from 0)
σ 2.03
β2 4.482
Counts
Frequency (normalized to 659)

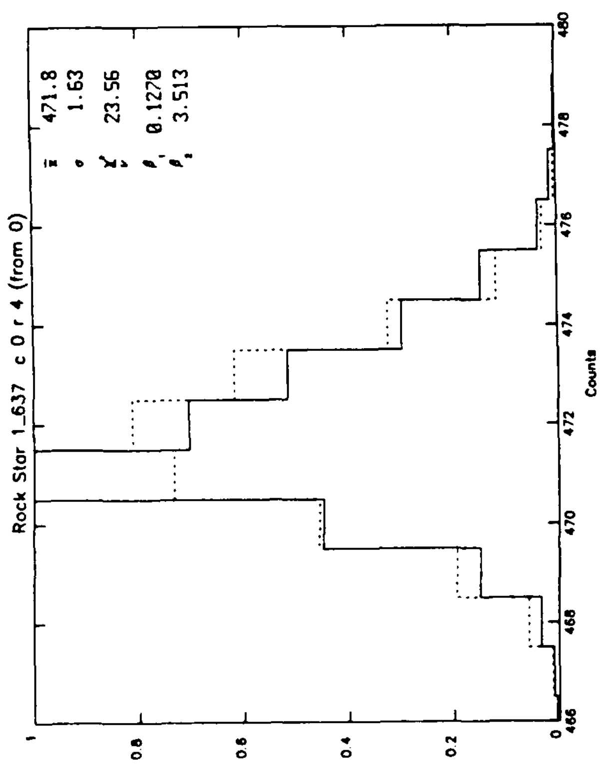

Rock Star 1_637 c 0 r 4 (from 0)
x̄ 471.8
σ 1.63
χ²ν 23.56
β1 0.1270
β2 3.513
Counts
Frequency (normalized to 952)

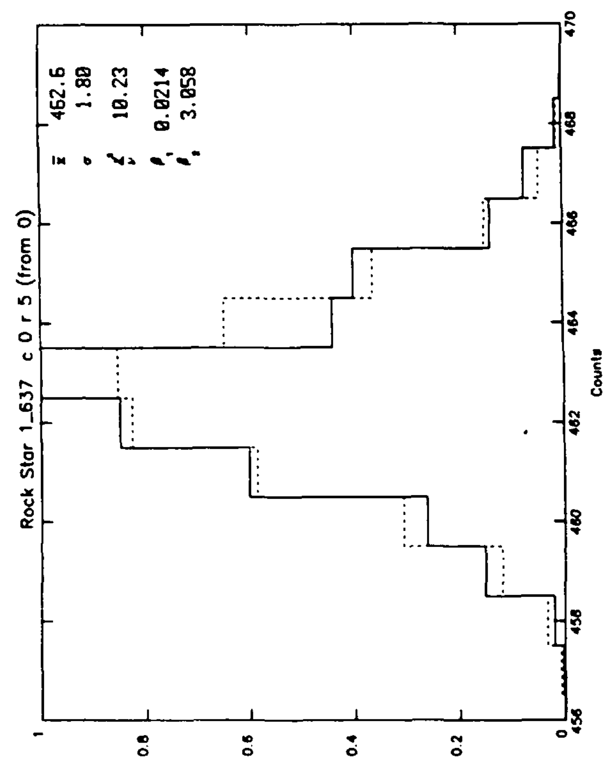

Rock Star 1_637 c 0 r 5 (from 0)
x̄ 462.6
σ 1.80
χ²ν 10.23
β1 0.0214
β2 3.058
Counts
Frequency (normalized to 809)

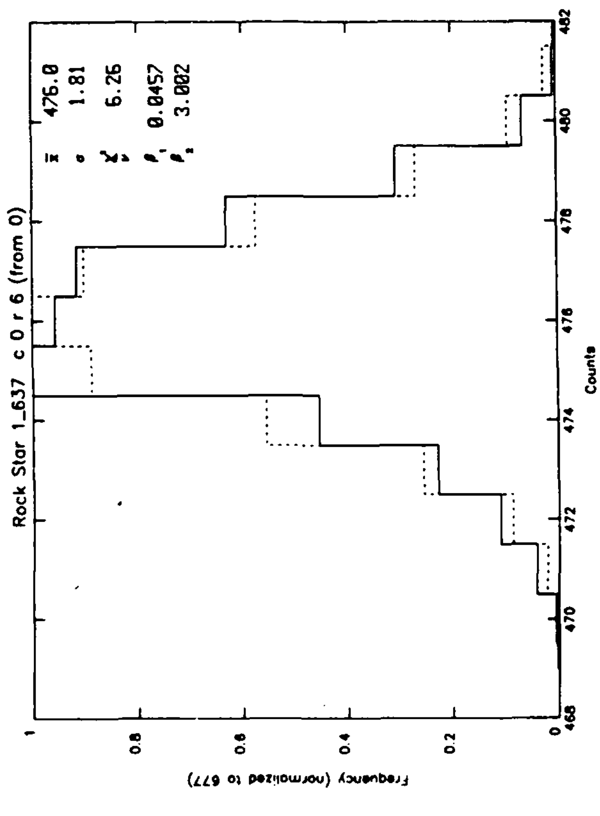
Rock Star 1_637 c 0 r 6 (from 0)
x̄ 476.0
σ 1.81
χ²ν 6.26
β₁ 0.0457
β₂ 3.002
Frequency (normalized to 677)
Counts

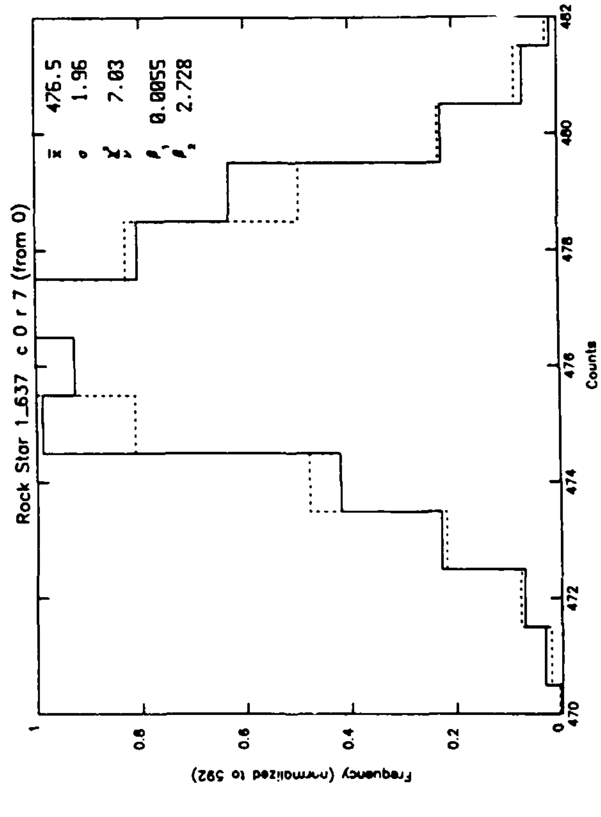
Rock Star 1_637 c 0 r 7 (from 0)
x̄ 476.5
σ 1.96
χ²ν 7.03
β₁ 0.0055
β₂ 2.728
Frequency (normalized to 592)
Counts

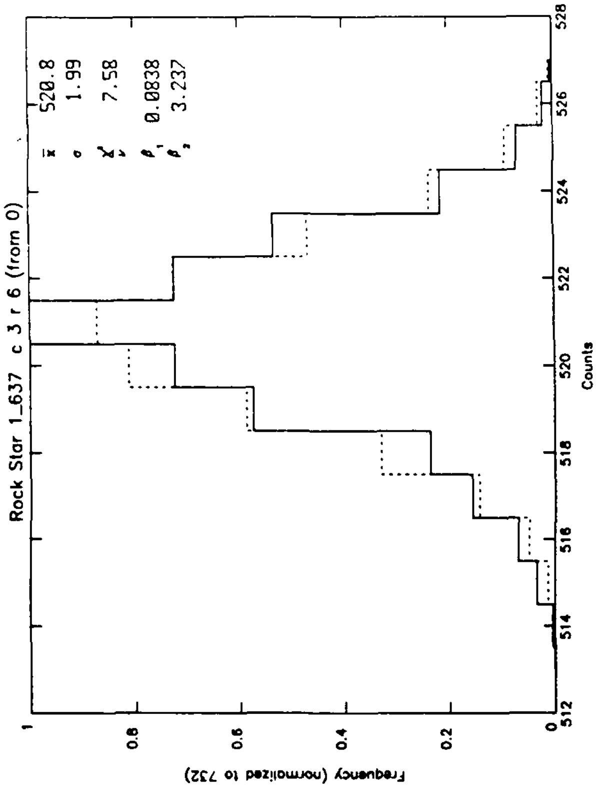
Rock Star 1_637 c 3 r 6 (from 0)
x̄ 520.8
σ 1.99
χ²ν 7.58
β₁ 0.0838
β₂ 3.237
Frequency (normalized to 732)
Counts

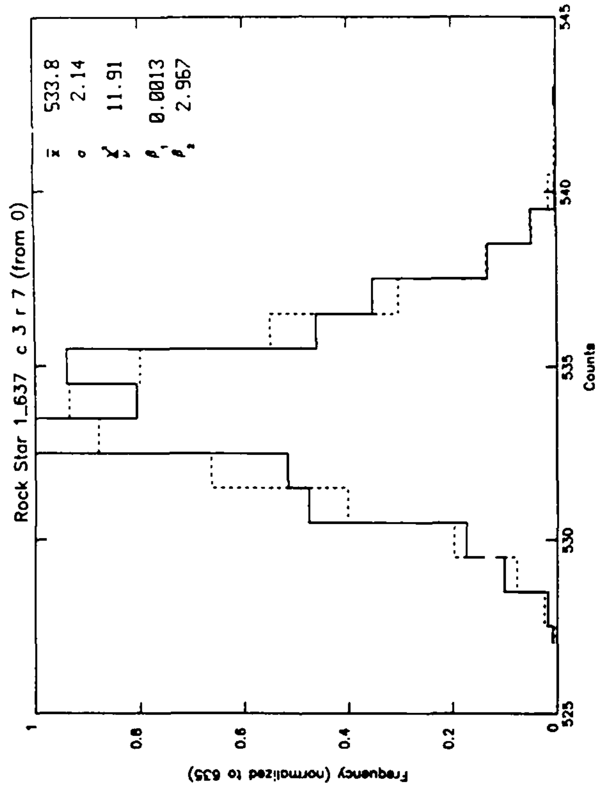
Rock Star 1_637 c 3 r 7 (from 0)
x̄ 533.8
σ 2.14
χ²ν 11.91
β₁ 0.0013
β₂ 2.967
Frequency (normalized to 635)
Counts

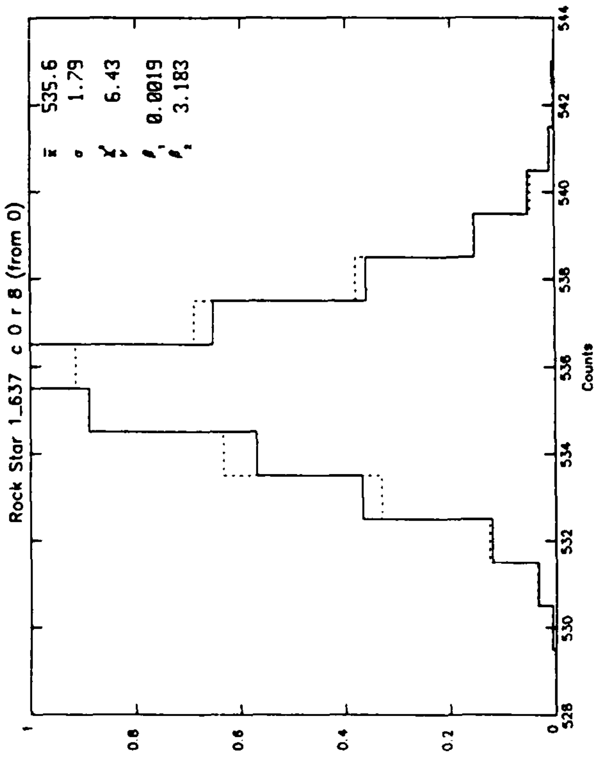
Rock Star 1_637 c 0 r 8 (from 0)
x̄ 535.6
σ 1.79
χ^2_ν 6.43
β_1 0.0019
β_2 3.183
Counts
Frequency (normalized to 759)

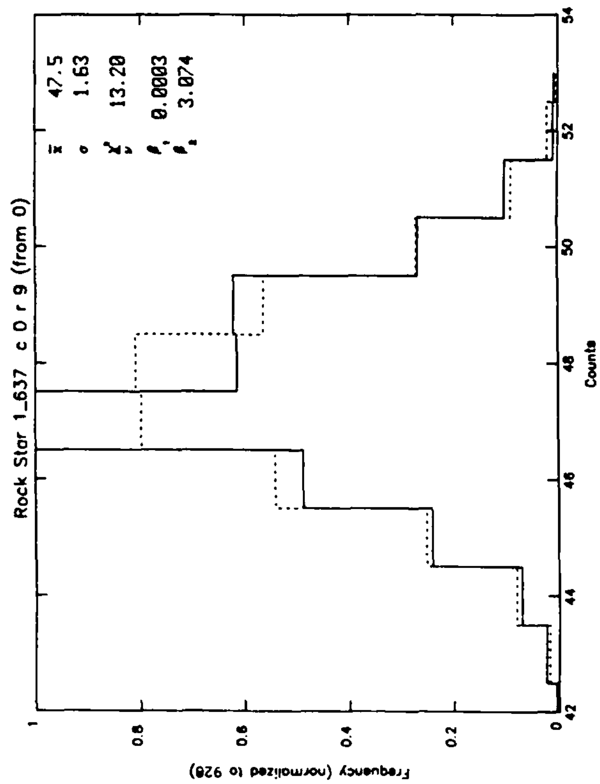
Rock Star 1_637 c 0 r 9 (from 0)
x̄ 47.5
σ 1.63
χ^2_ν 13.20
β_1 0.0003
β_2 3.074
Counts
Frequency (normalized to 928)

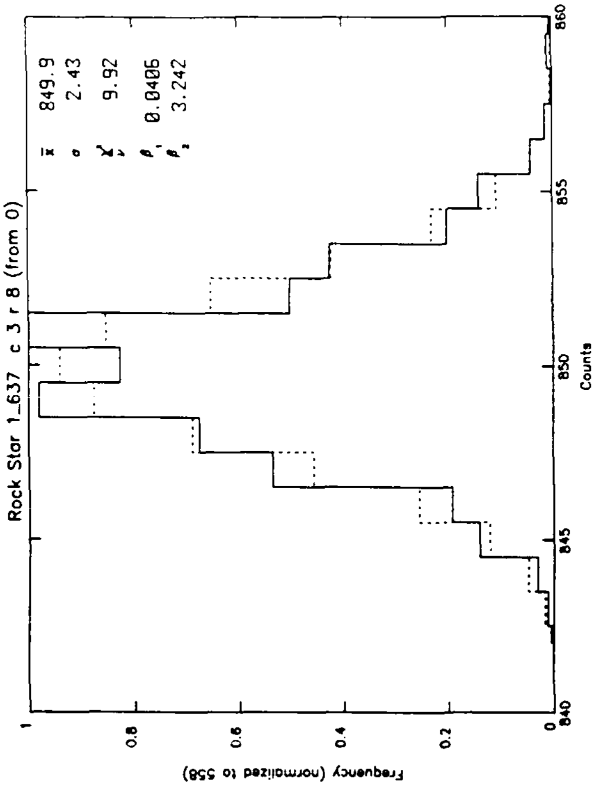
Rock Star 1_637 c 3 r 8 (from 0)
x̄ 849.9
σ 2.43
χ^2_ν 9.92
β_1 0.0406
β_2 3.242
Counts
Frequency (normalized to 558)

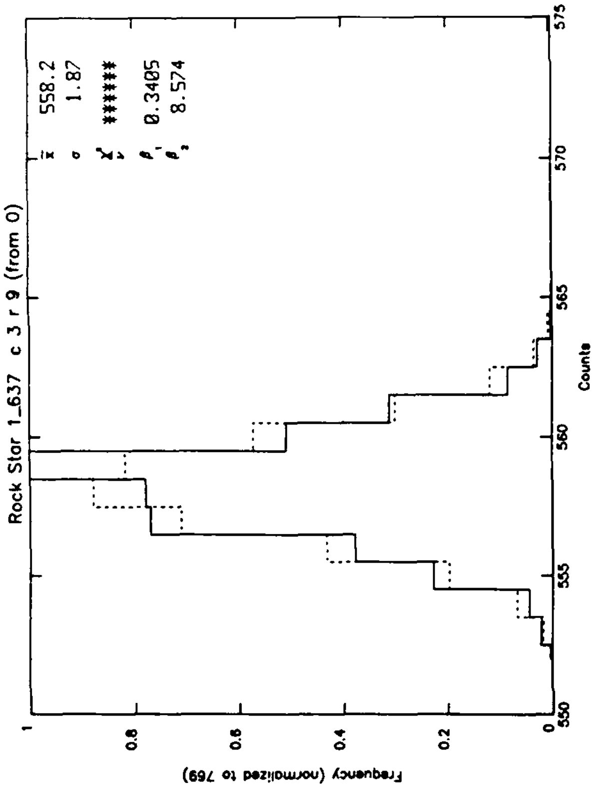
Rock Star 1_637 c 3 r 9 (from 0)
x̄ 558.2
σ 1.87
χ^2_ν *****
β_1 0.3405
β_2 8.574
Counts
Frequency (normalized to 769)

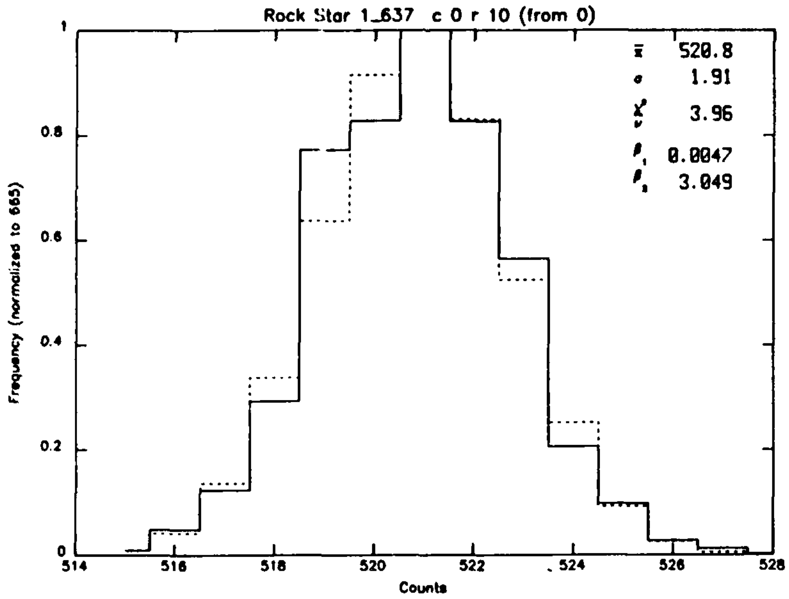
Rock Star 1_637 c 0 r 10 (from 0)
x̄ 520.8
σ 1.91
χ^2_ν 3.96
β_1 0.0047
β_2 3.049
Frequency (normalized to 665)
Counts

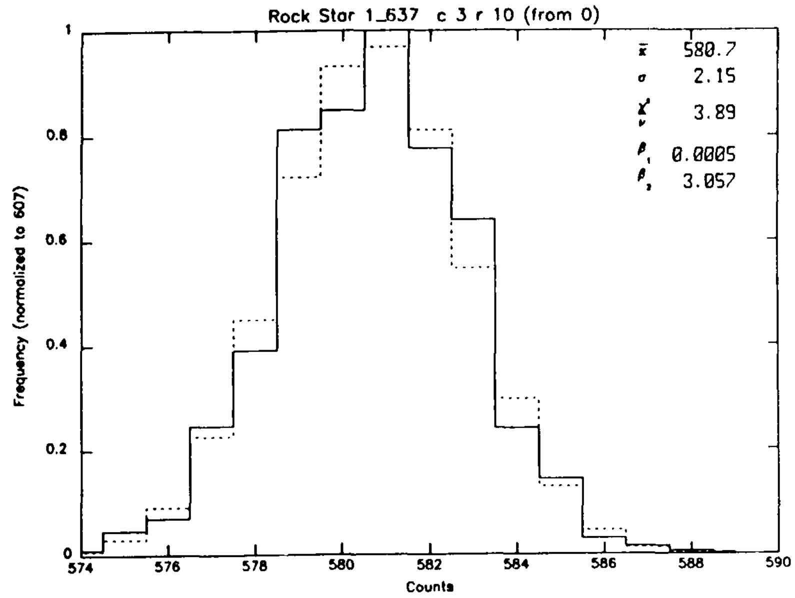
Rock Star 1_637 c 3 r 10 (from 0)
x̄ 580.7
σ 2.15
χ^2_ν 3.89
β_1 0.0005
β_2 3.057
Frequency (normalized to 607)
Counts

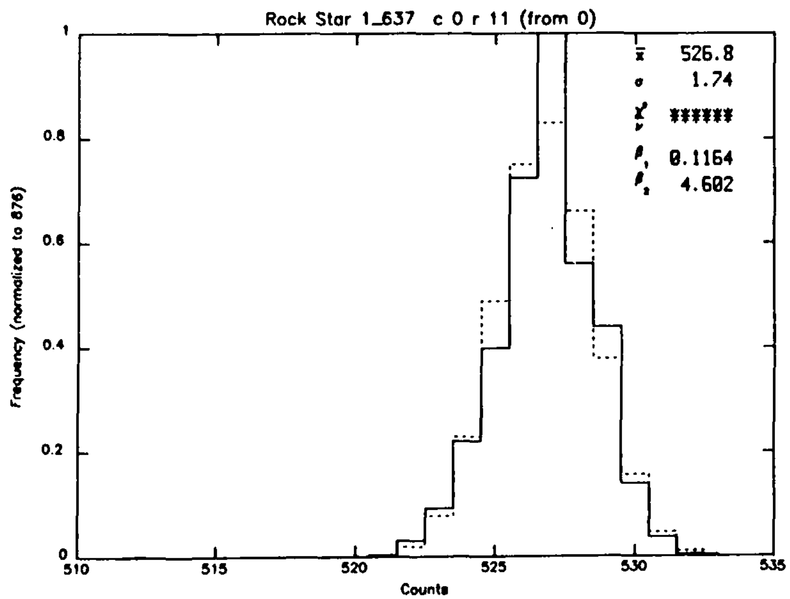
Rock Star 1_637 c 0 r 11 (from 0)
x̄ 526.8
σ 1.74
χ^2_ν ******
β_1 0.1164
β_2 4.602
Frequency (normalized to 876)
Counts

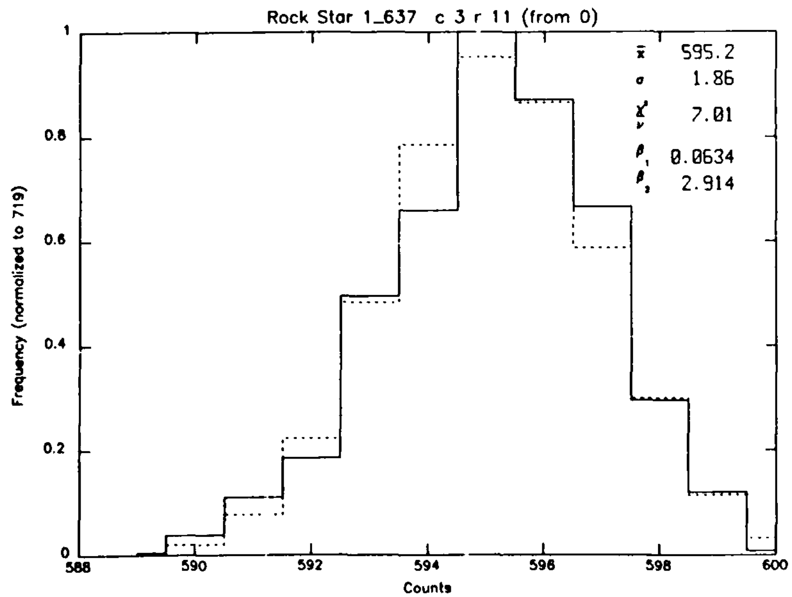
Rock Star 1_637 c 3 r 11 (from 0)
x̄ 595.2
σ 1.86
χ^2_ν 7.01
β_1 0.0634
β_2 2.914
Frequency (normalized to 719)
Counts

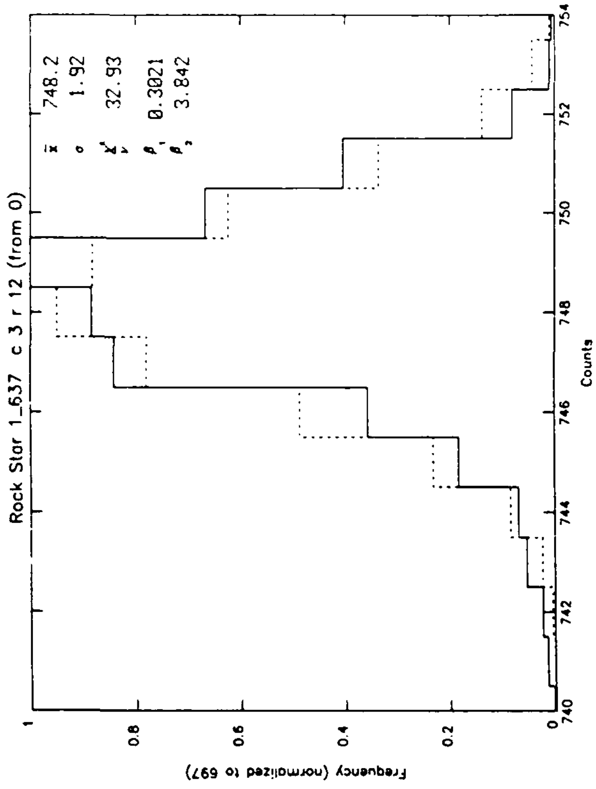
Rock Star 1_637 c 3 r 12 (from 0)
Frequency (normalized to 697)
Counts
x̄ 748.2
σ 1.92
χ²ν 32.93
β1 0.3021
β2 3.842

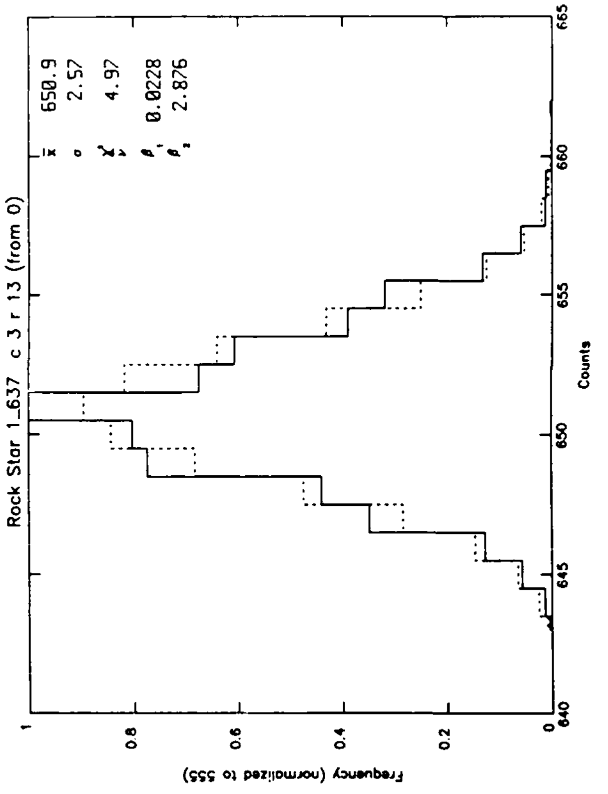
Rock Star 1_637 c 3 r 13 (from 0)
Frequency (normalized to 555)
Counts
x̄ 650.9
σ 2.57
χ²ν 4.97
β1 0.0228
β2 2.876

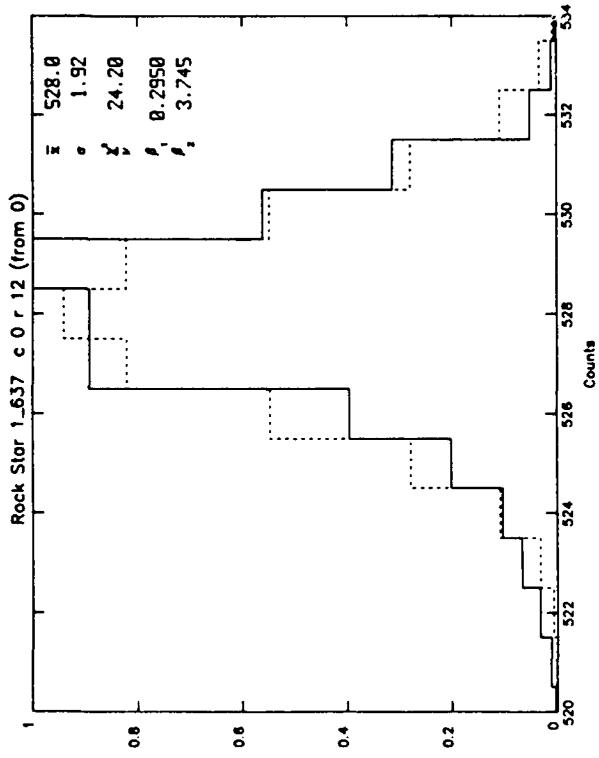
Rock Star 1_637 c 0 r 12 (from 0)
Frequency (normalized to 705)
Counts
x̄ 528.0
σ 1.92
χ²ν 24.20
β1 0.2950
β2 3.745

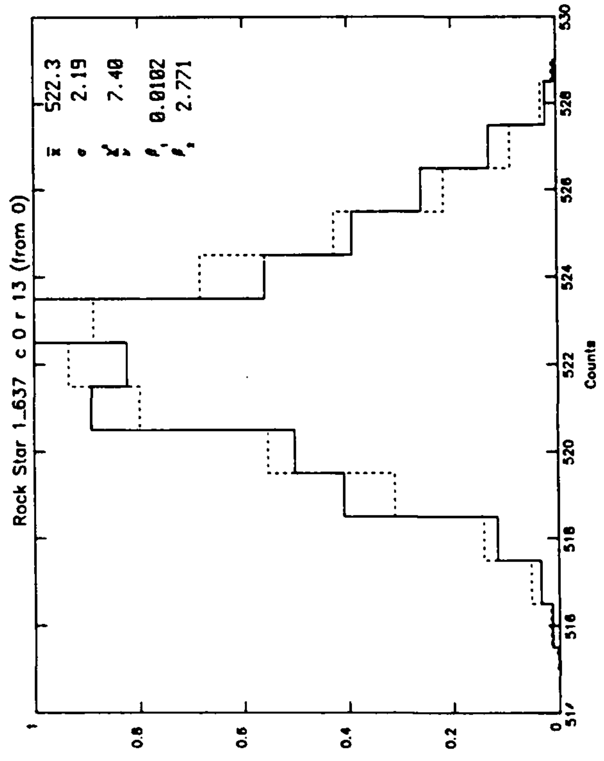
Rock Star 1_637 c 0 r 13 (from 0)
Frequency (normalized to 621)
Counts
x̄ 522.3
σ 2.19
χ²ν 7.40
β1 0.0102
β2 2.771

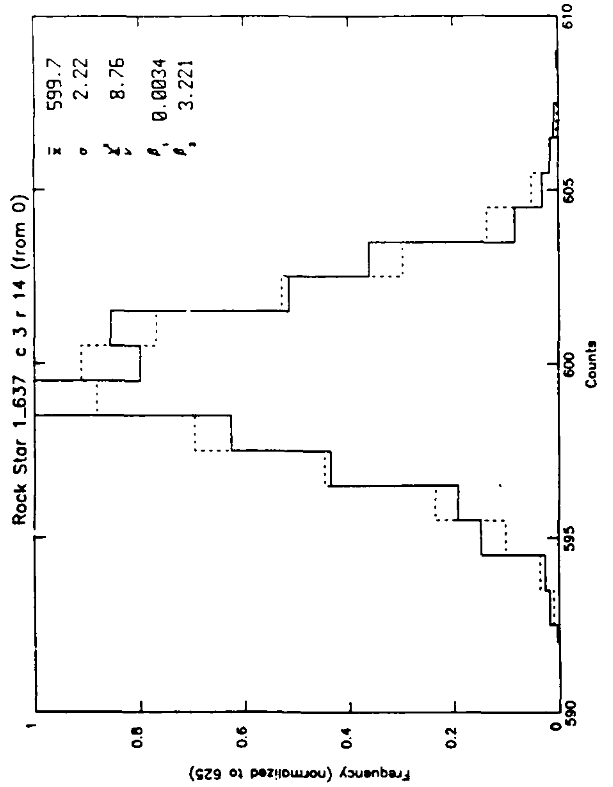
Rock Star 1_637 c 3 r 14 (from 0)
$\bar{x}$ 599.7
σ 2.22
χ^2_ν 8.76
β_1 0.0034
β_2 3.221
Counts
Frequency (normalized to 625)

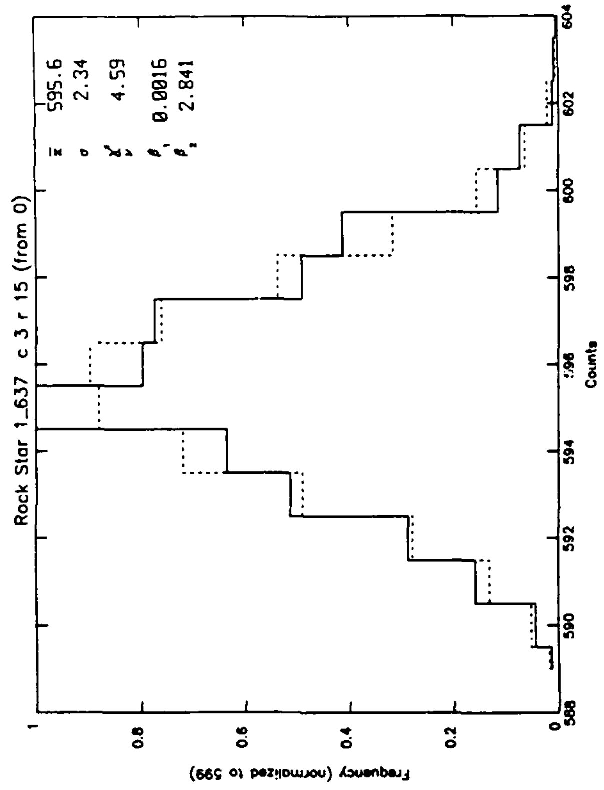
Rock Star 1_637 c 3 r 15 (from 0)
$\bar{x}$ 595.6
σ 2.34
χ^2_ν 4.59
β_1 0.0016
β_2 2.841
Counts
Frequency (normalized to 599)

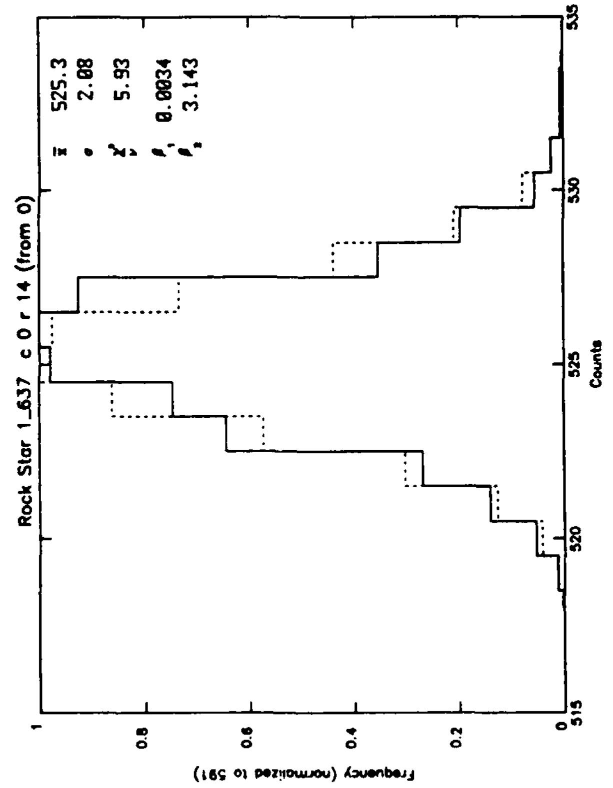
Rock Star 1_637 c 0 r 14 (from 0)
$\bar{x}$ 525.3
σ 2.08
χ^2_ν 5.93
β_1 0.0034
β_2 3.143
Counts
Frequency (normalized to 591)

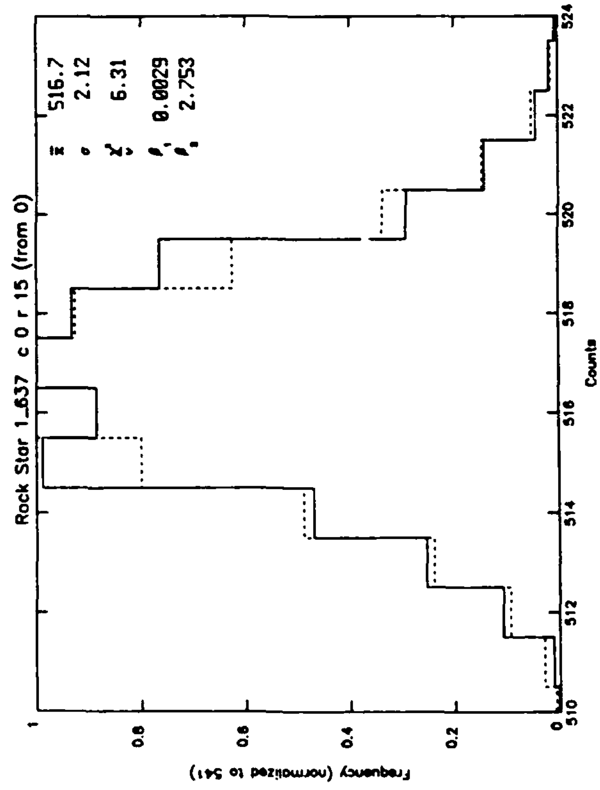
Rock Star 1_637 c 0 r 15 (from 0)
$\bar{x}$ 516.7
σ 2.12
χ^2_ν 6.31
β_1 0.0029
β_2 2.753
Counts
Frequency (normalized to 541)

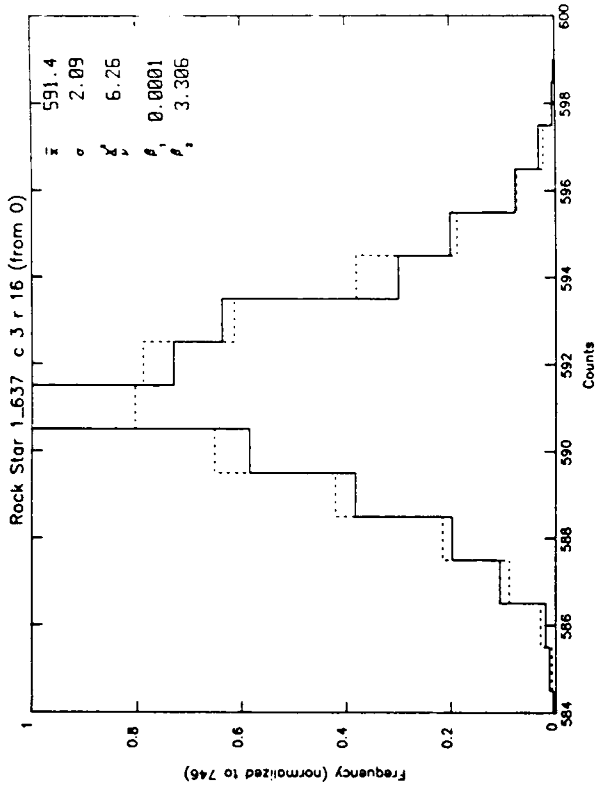
Rock Star 1_637 c 3 r 16 (from 0)
$\bar{x}$ 591.4
σ 2.09
χ^2_ν 6.26
β_1 0.0001
β_2 3.306
Frequency (normalized to 746)
Counts

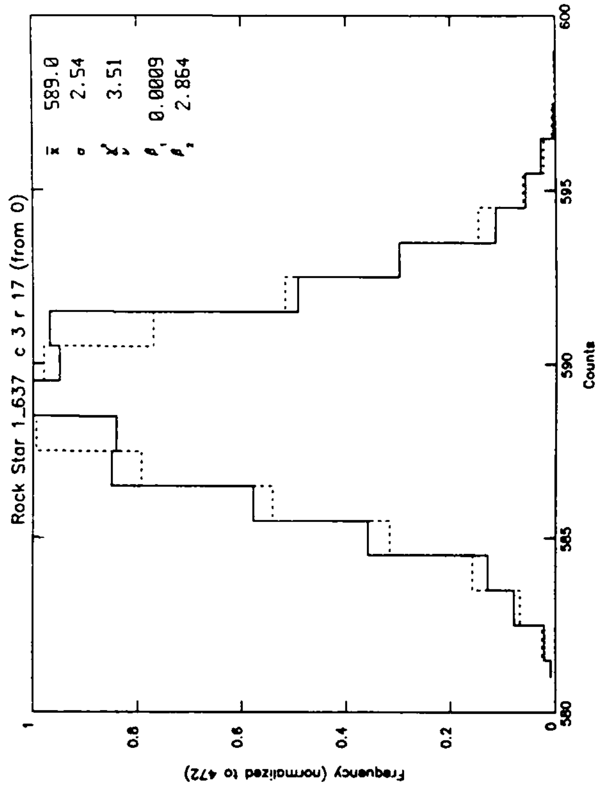
Rock Star 1_637 c 3 r 17 (from 0)
$\bar{x}$ 589.0
σ 2.54
χ^2_ν 3.51
β_1 0.0009
β_2 2.864
Frequency (normalized to 472)
Counts

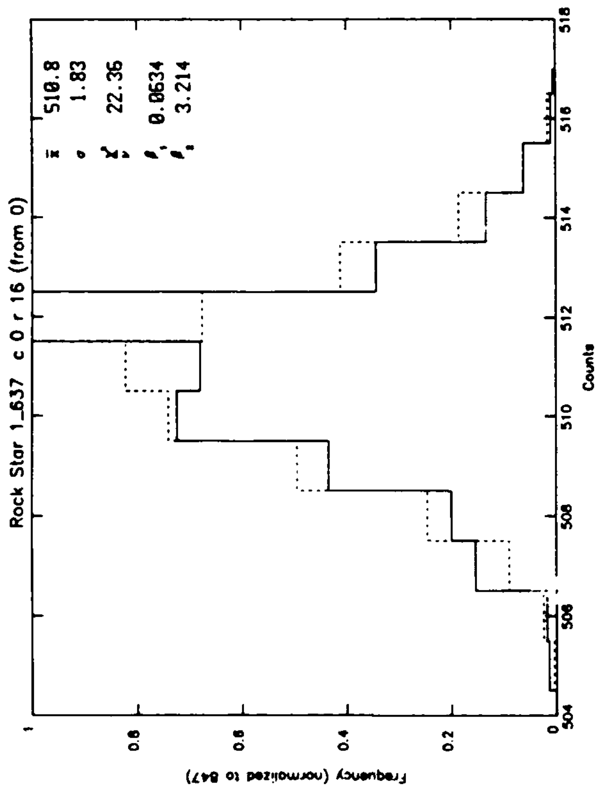
Rock Star 1_637 c 0 r 16 (from 0)
$\bar{x}$ 510.8
σ 1.83
χ^2_ν 22.36
β_1 0.0634
β_2 3.214
Frequency (normalized to 847)
Counts

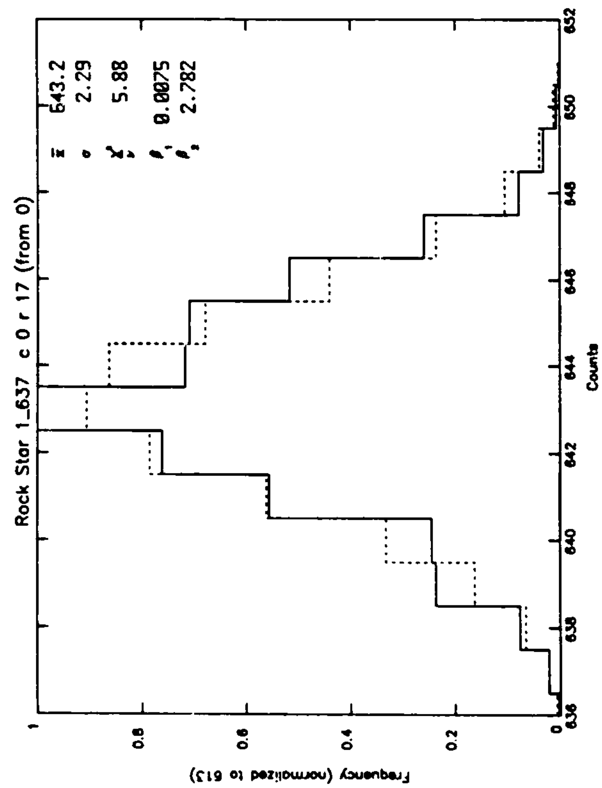
Rock Star 1_637 c 0 r 17 (from 0)
$\bar{x}$ 643.2
σ 2.29
χ^2_ν 5.88
β_1 0.0075
β_2 2.782
Frequency (normalized to 613)
Counts

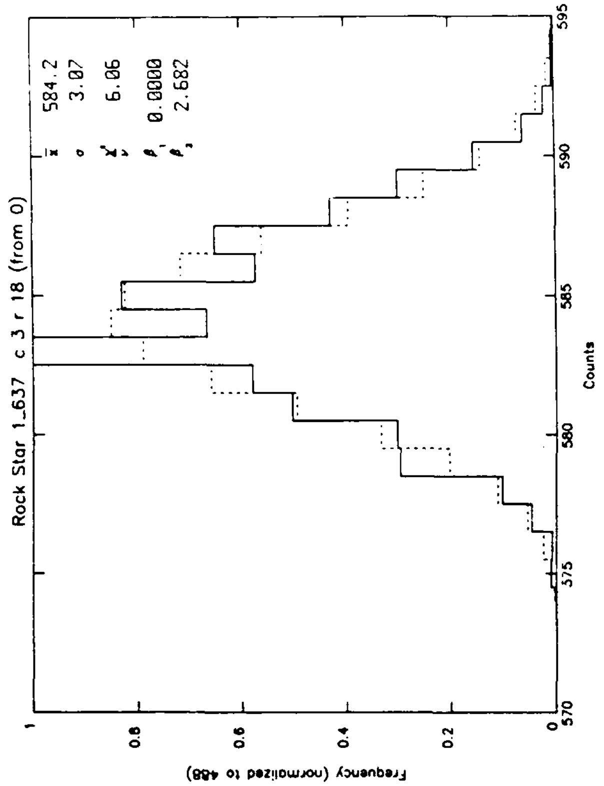
Rock Star 1_637 c 3 r 18 (from 0)
584.2
3.07
6.06
0.0000
2.682
Counts
Frequency (normalized to 488)

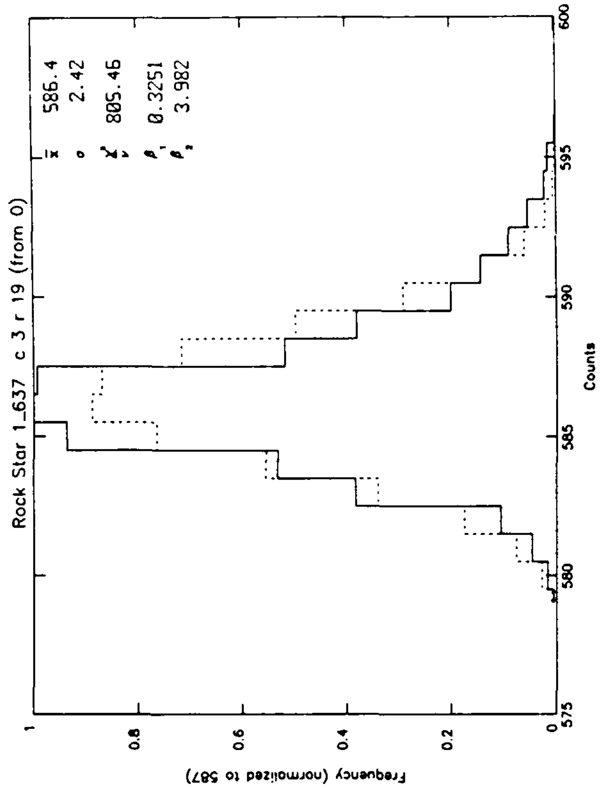
Rock Star 1_637 c 3 r 19 (from 0)
586.4
2.42
805.46
0.3251
3.982
Counts
Frequency (normalized to 587)

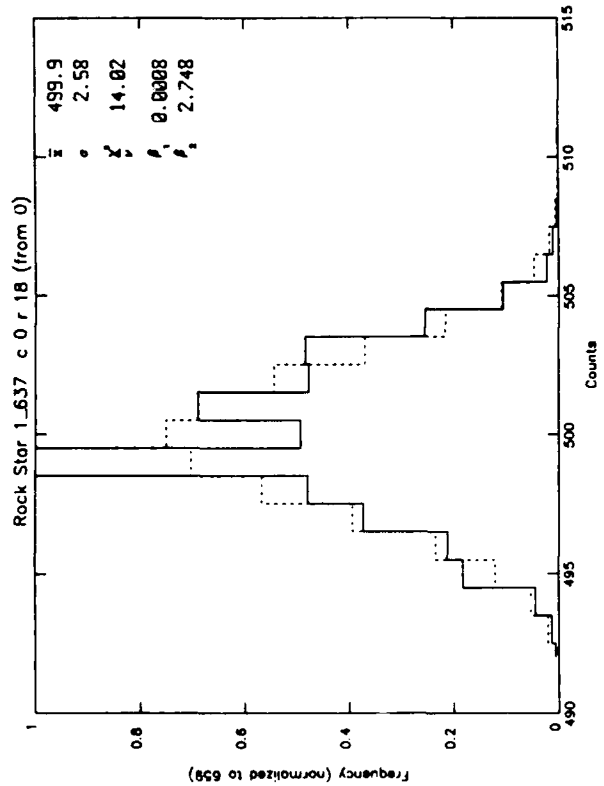
Rock Star 1_637 c 0 r 18 (from 0)
499.9
2.58
14.02
0.0008
2.748
Counts
Frequency (normalized to 658)

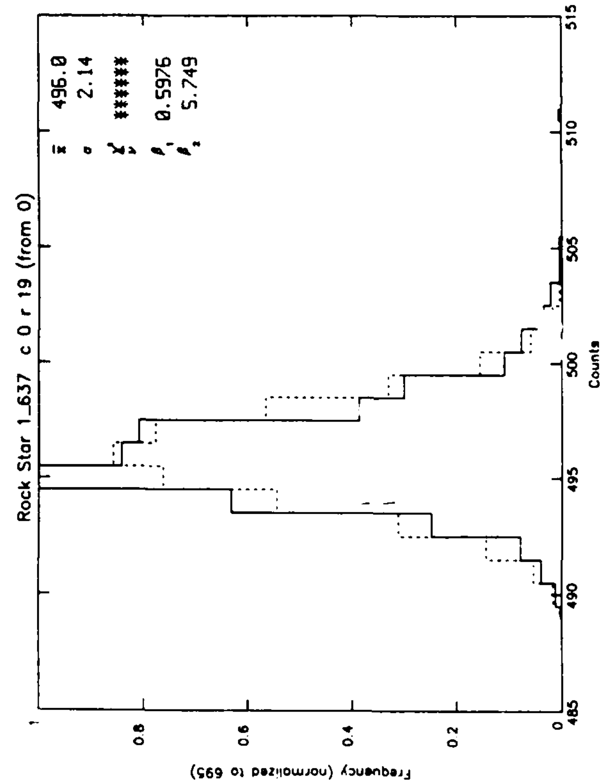
Rock Star 1_637 c 0 r 19 (from 0)
496.0
2.14
******
0.5976
5.749
Counts
Frequency (normalized to 695)

APPENDIX A-5

Array: Aerojet Bulk Array

	Left	Right
Elements:	Column 2; Rows 0-2, 15-17, 30, 31	Column 3, Rows 0-2, 15-17, 30, 31
Data Run:	Background all_17	Background all_17

Purpose: Comparison of column (even vs odd)/row behavior for normal background. Compare also with Appendices A-6 and A-7 for other columns on the same run. The full set (A-5 to A-7) gives representative results across the whole array from top to bottom and left to right.

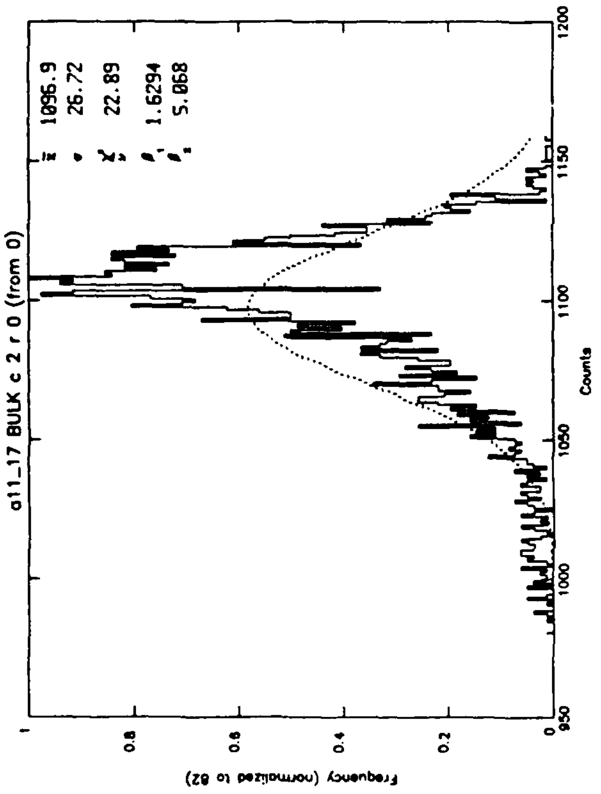
a11_17 BULK c 2 r 0 (from 0)
x̄ 1096.9
σ 26.72
χ²ν 22.89
β1 1.6294
β2 5.068
Frequency (normalized to 62)
Counts

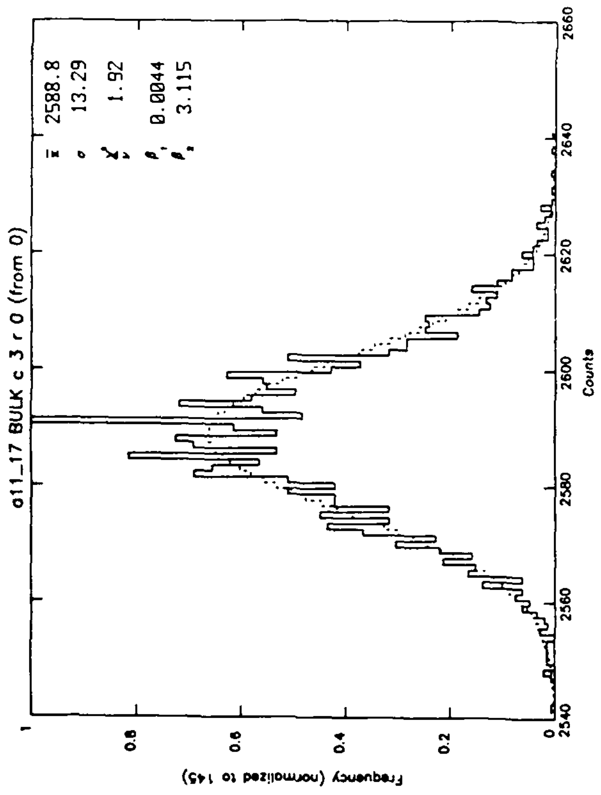
a11_17 BULK c 3 r 0 (from 0)
x̄ 2588.8
σ 13.29
χ²ν 1.92
β1 0.0044
β2 3.115
Frequency (normalized to 145)
Counts

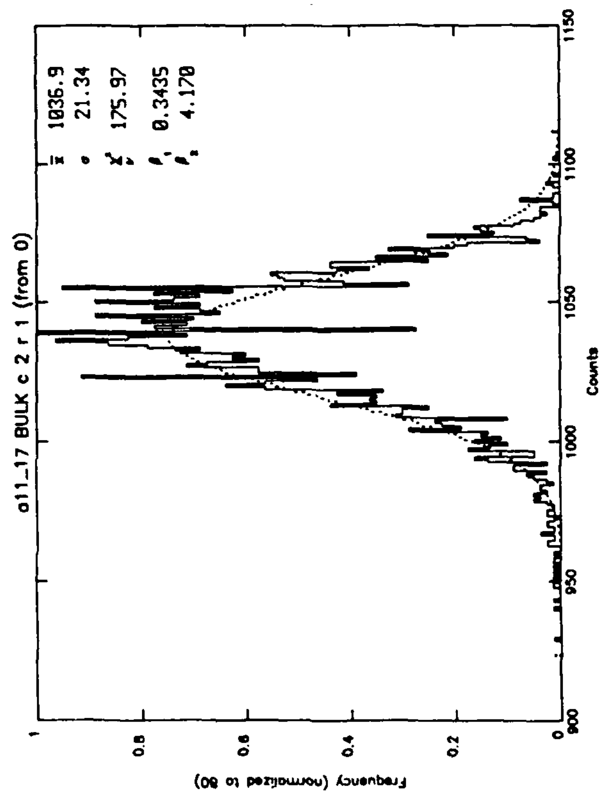
a11_17 BULK c 2 r 1 (from 0)
x̄ 1036.9
σ 21.34
χ²ν 175.97
β1 0.3435
β2 4.170
Frequency (normalized to 80)
Counts

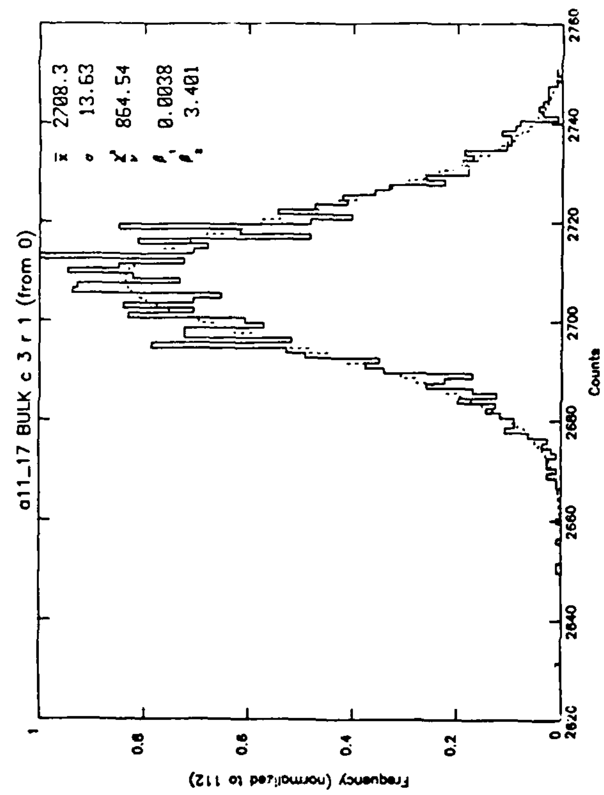
a11_17 BULK c 3 r 1 (from 0)
x̄ 2708.3
σ 13.63
χ²ν 864.54
β1 0.0038
β2 3.401
Frequency (normalized to 112)
Counts

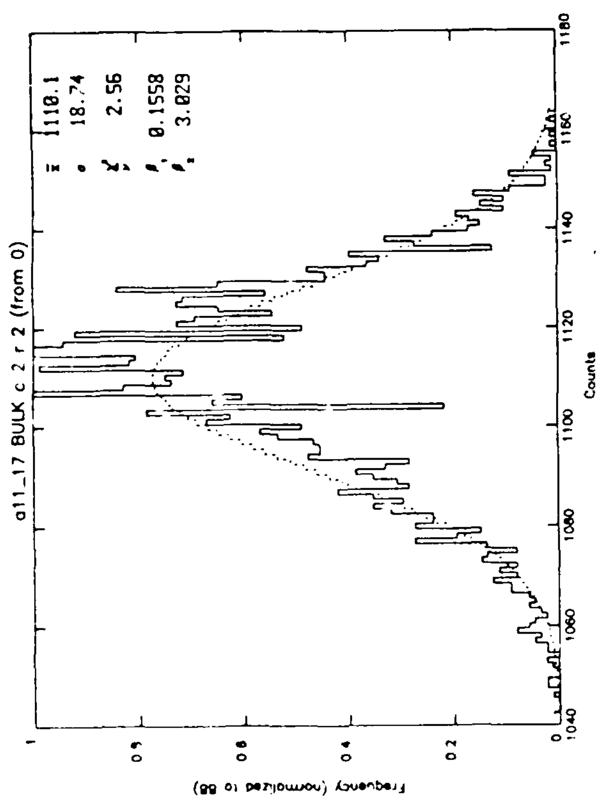
a11_17 BULK c 2 r 2 (from 0)
x̄ 1110.1
σ 18.74
χ^2_ν 2.56
β_1 0.1558
β_2 3.029
Frequency (normalized to 88)
Counts

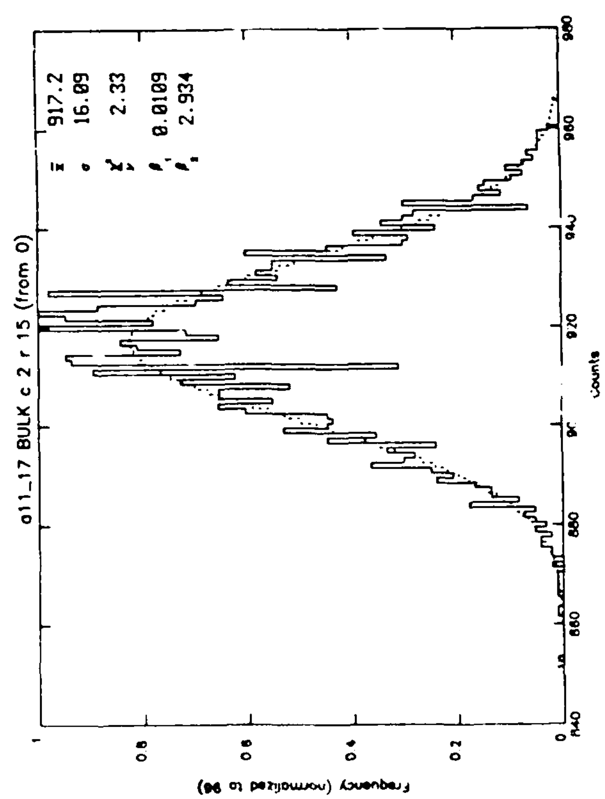
a11_17 BULK c 2 r 15 (from 0)
x̄ 917.2
σ 16.09
χ^2_ν 2.33
β_1 0.0109
β_2 2.934
Frequency (normalized to 96)
Counts

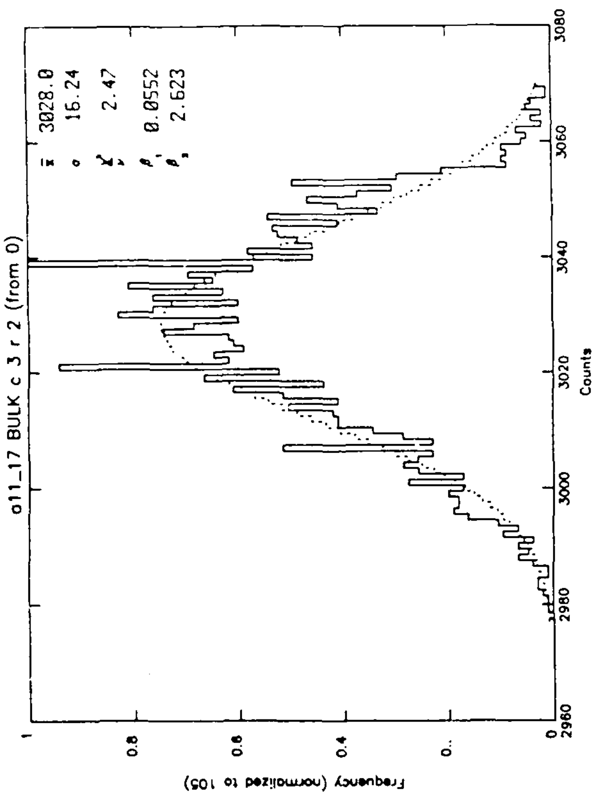
a11_17 BULK c 3 r 2 (from 0)
x̄ 3028.0
σ 16.24
χ^2_ν 2.47
β_1 0.0552
β_2 2.623
Frequency (normalized to 105)
Counts

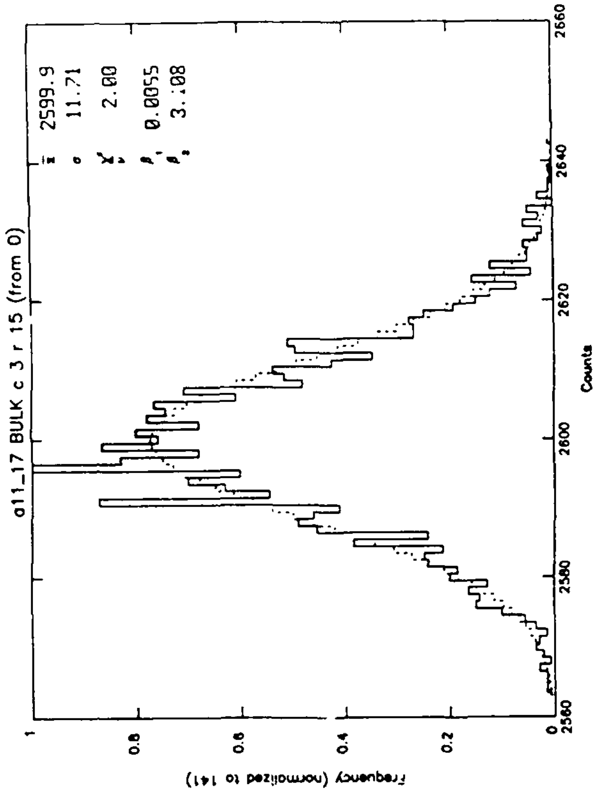
a11_17 BULK c 3 r 15 (from 0)
x̄ 2599.9
σ 11.71
χ^2_ν 2.00
β_1 0.0055
β_2 3.108
Frequency (normalized to 141)
Counts

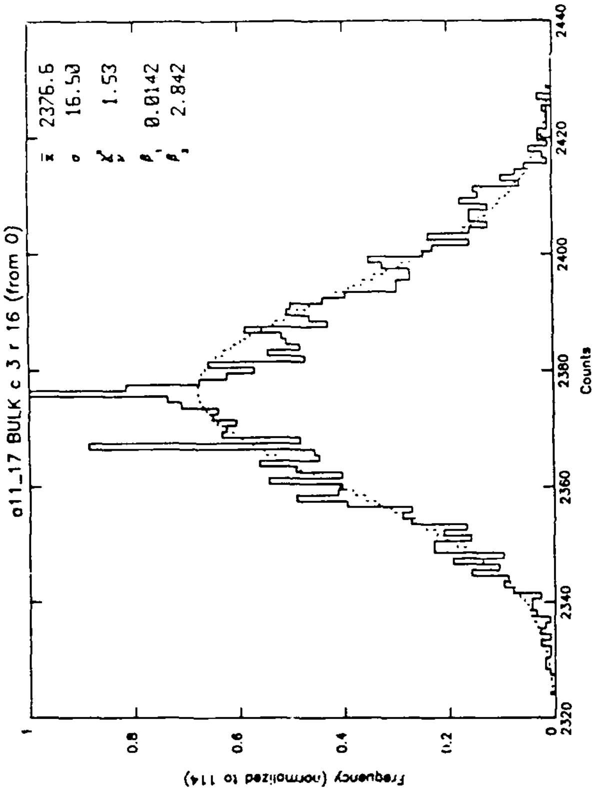
a11_17 BULK c 3 r 16 (from 0)
x̄ 2376.5
σ 16.50
χ^2_ν 1.53
β_1 0.0142
β_2 2.842
Counts
Frequency (normalized to 114)

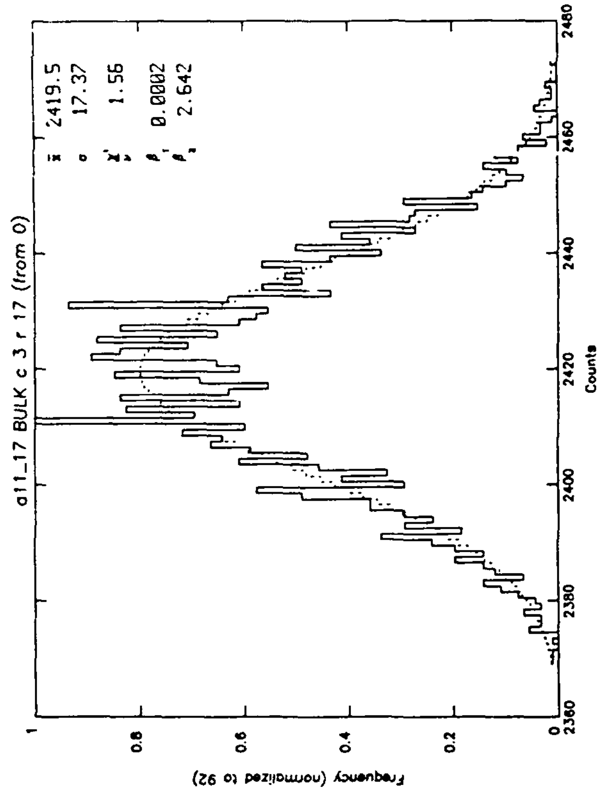
a11_17 BULK c 3 r 17 (from 0)
x̄ 2419.5
σ 17.37
χ^2_ν 1.56
β_1 0.0002
β_2 2.642
Counts
Frequency (normalized to 92)

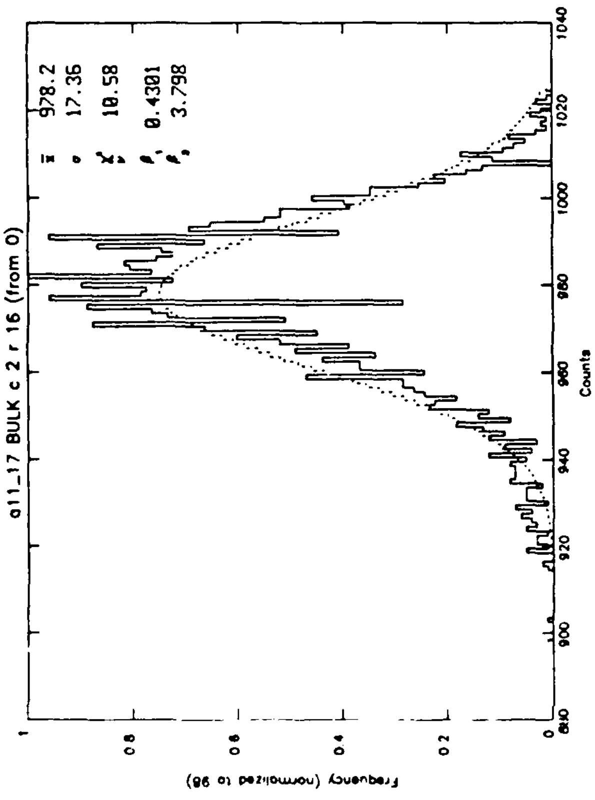
a11_17 BULK c 2 r 16 (from 0)
x̄ 978.2
σ 17.36
χ^2_ν 10.58
β_1 0.4301
β_2 3.798
Counts
Frequency (normalized to 98)

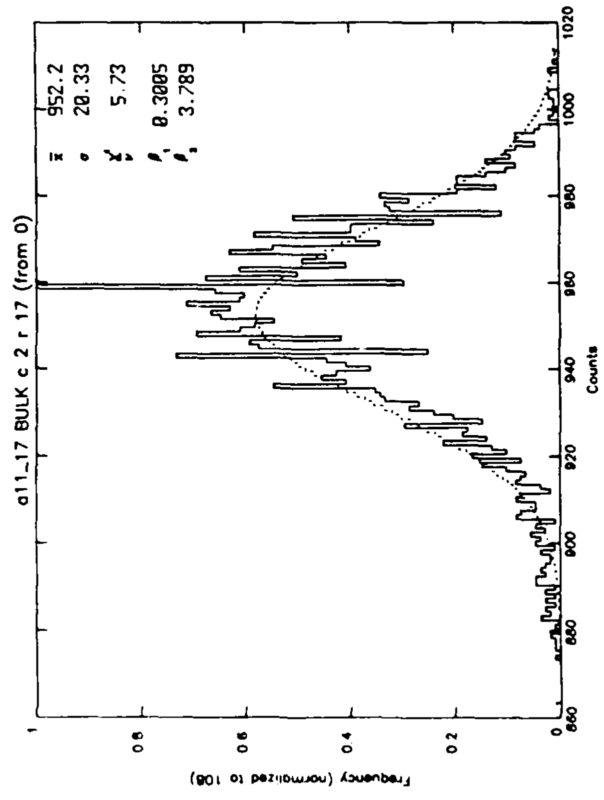
a11_17 BULK c 2 r 17 (from 0)
x̄ 952.2
σ 20.33
χ^2_ν 5.73
β_1 0.3005
β_2 3.789
Counts
Frequency (normalized to 108)

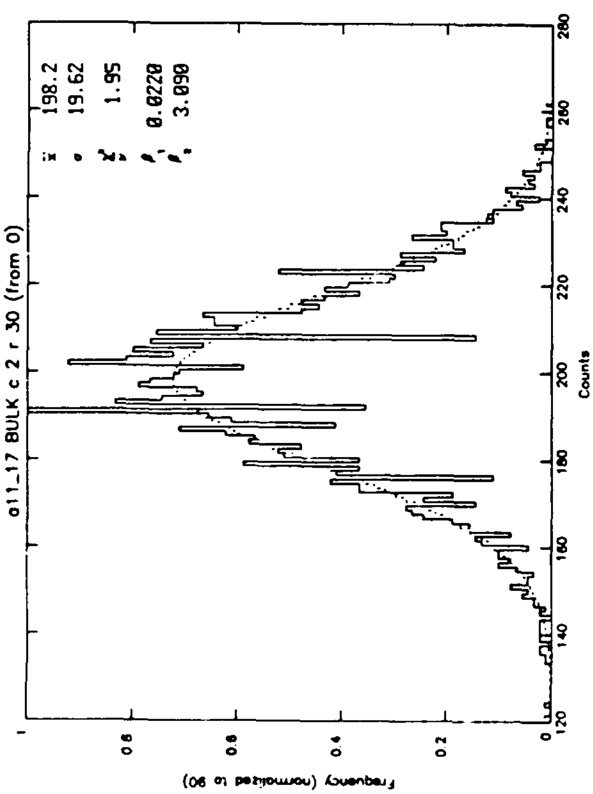
a11_17 BULK c 2 r 30 (from 0)
x̄ 198.2
σ 19.62
χ²ν 1.95
β1 0.0220
β2 3.090
Counts
Frequency (normalized to 90)

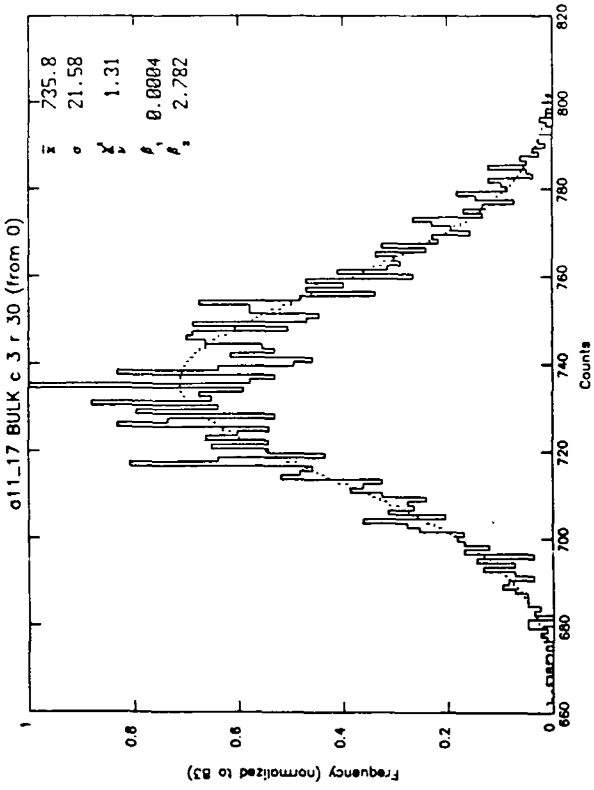
a11_17 BULK c 3 r 30 (from 0)
x̄ 735.8
σ 21.58
χ²ν 1.31
β1 0.0004
β2 2.782
Counts
Frequency (normalized to 83)

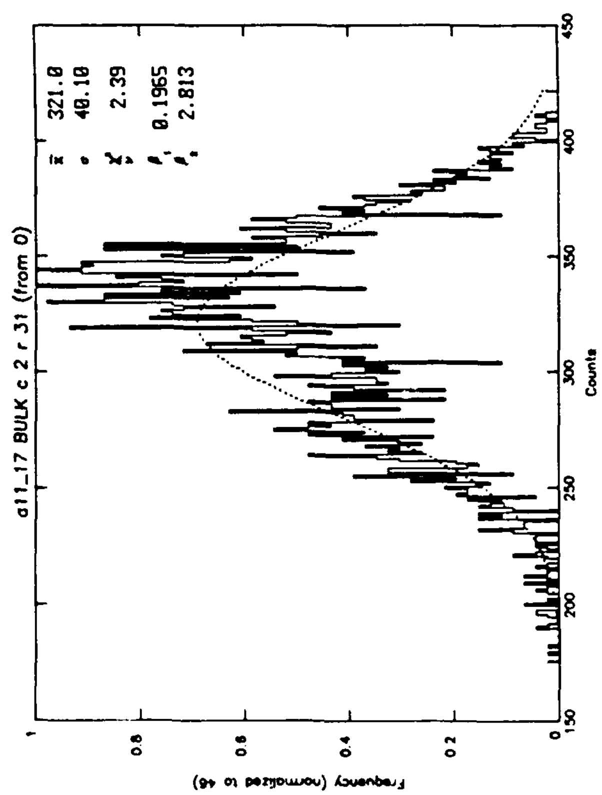
a11_17 BULK c 2 r 31 (from 0)
x̄ 321.0
σ 40.10
χ²ν 2.39
β1 0.1965
β2 2.813
Counts
Frequency (normalized to 46)

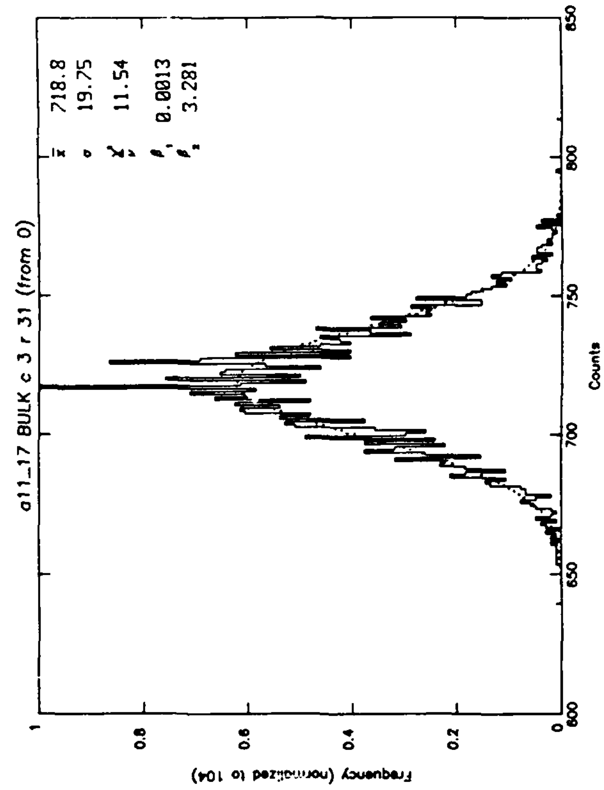
a11_17 BULK c 3 r 31 (from 0)
x̄ 718.8
σ 19.75
χ²ν 11.54
β1 0.0013
β2 3.281
Counts
Frequency (normalized to 104)

APPENDIX A-6

Array: Aerojet Bulk Array

	Left	Right
Elements:	Column 4; Rows 0-2, 15-17, 30, 31	Column 7, Rows 0-2, 15-17, 30, 31
Data Run:	Background all_17	Background all_17

Purpose: Comparison of column (even vs odd)/row behavior for normal background. Compare also with Appendices A-5 and A-7 for other columns on the same run. The full set (A-5 to A-7) gives representative results across the whole array from top to bottom and left to right.

a11_17 BULK c 4 r 0 (from 0)

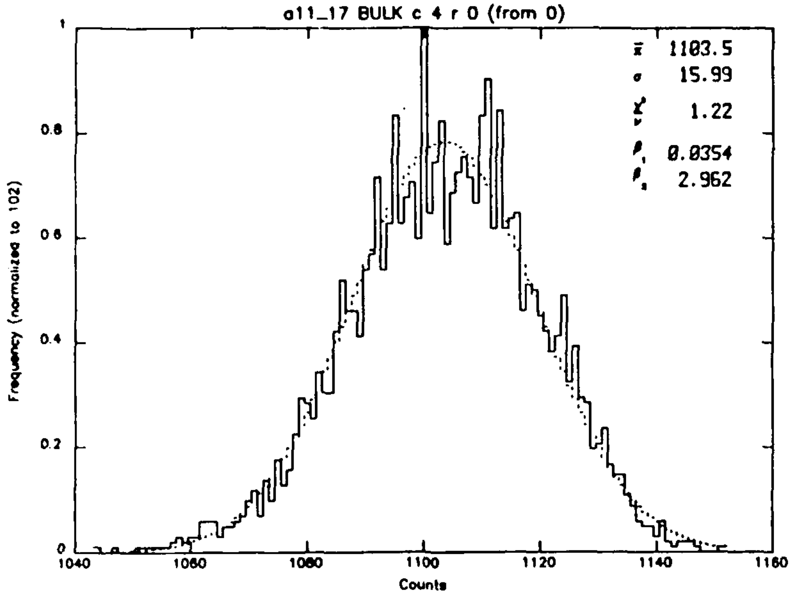

a11_17 BULK c 7 r 0 (from 0)

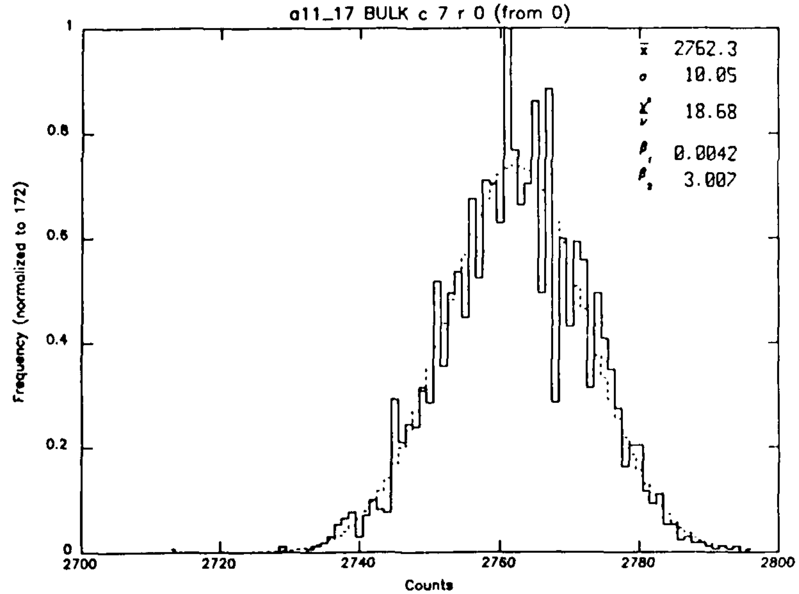

a11_17 BULK c 4 r 1 (from 0)

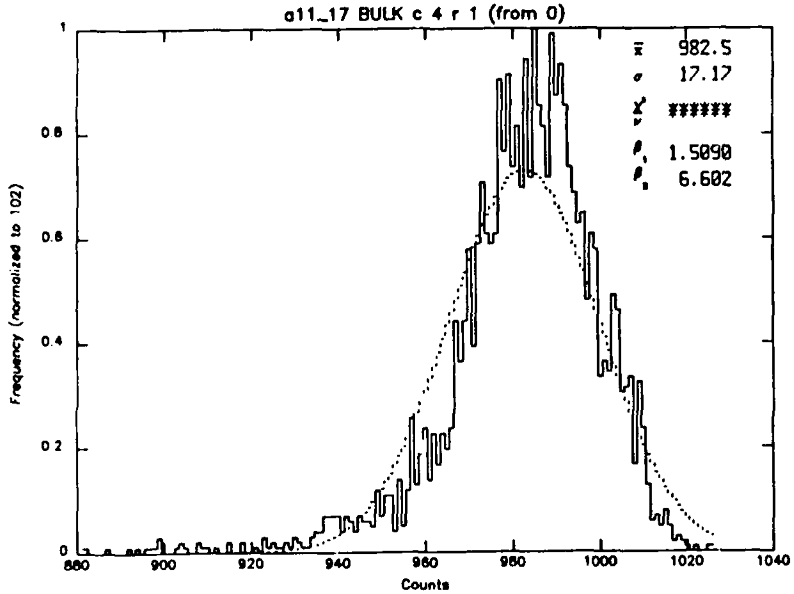

a11_17 BULK c 7 r 1 (from 0)

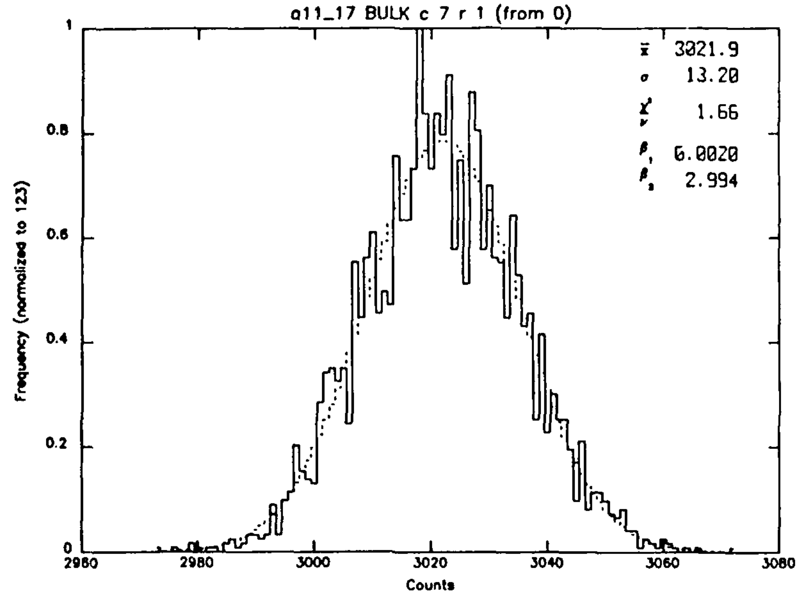

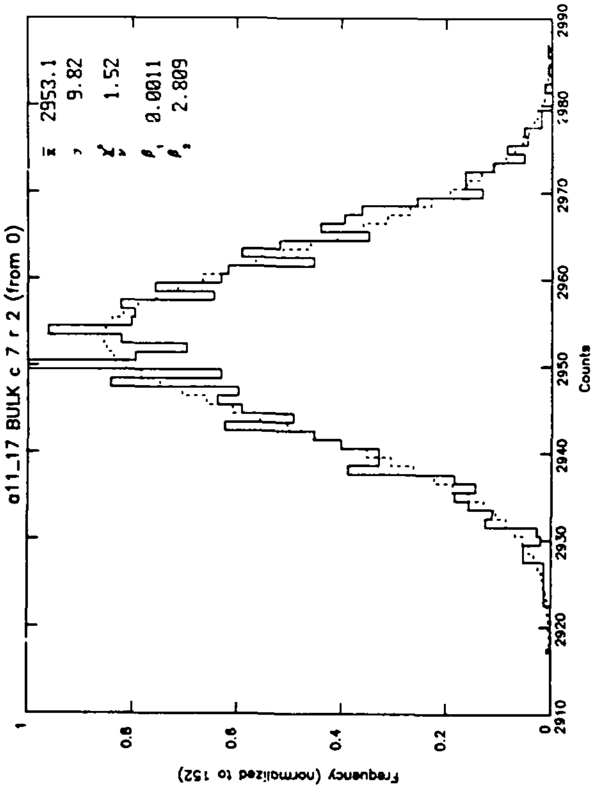
a11_17 BULK c 7 r 2 (from 0)
x̄ 2953.1
σ 9.82
χ² 1.52
β1 0.0011
β2 2.809
Frequency (normalized to 152)
Counts

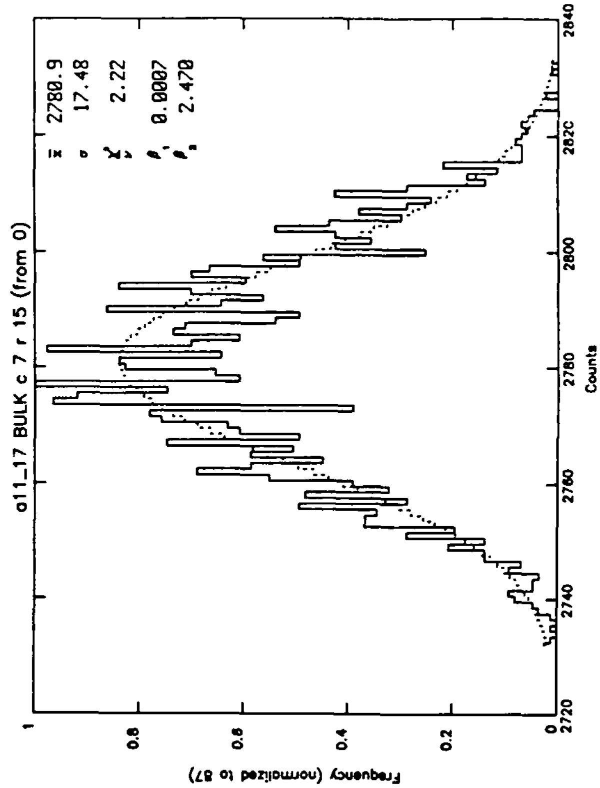
a11_17 BULK c 7 r 15 (from 0)
x̄ 2780.9
σ 17.48
χ² 2.22
β1 0.0007
β2 2.470
Frequency (normalized to 87)
Counts

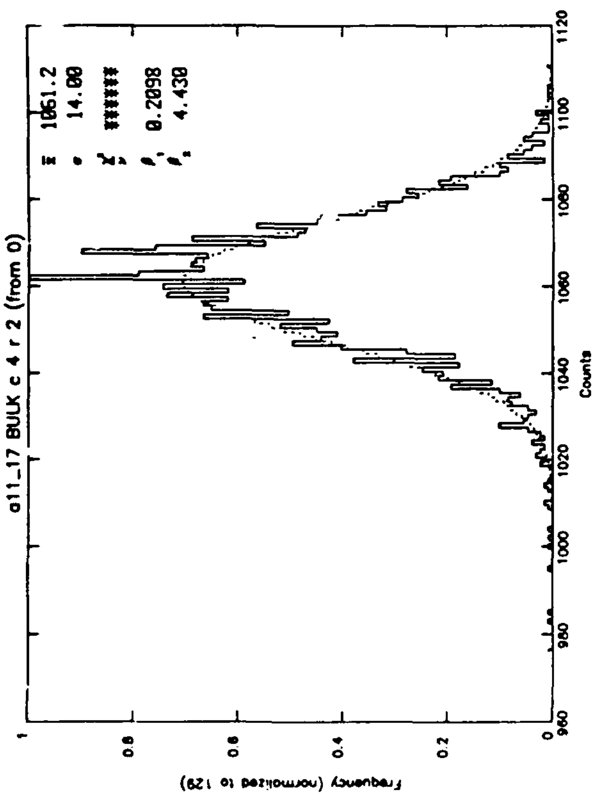
a11_17 BULK c 4 r 2 (from 0)
x̄ 1061.2
σ 14.00
χ² ******
β1 0.2098
β2 4.430
Frequency (normalized to 129)
Counts

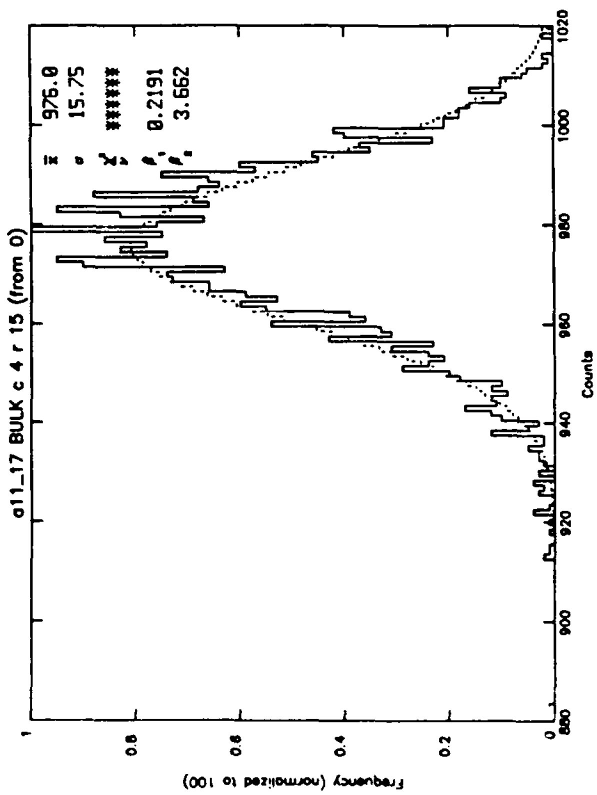
a11_17 BULK c 4 r 15 (from 0)
x̄ 976.0
σ 15.75
χ² *****
β1 0.2191
β2 3.662
Frequency (normalized to 100)
Counts

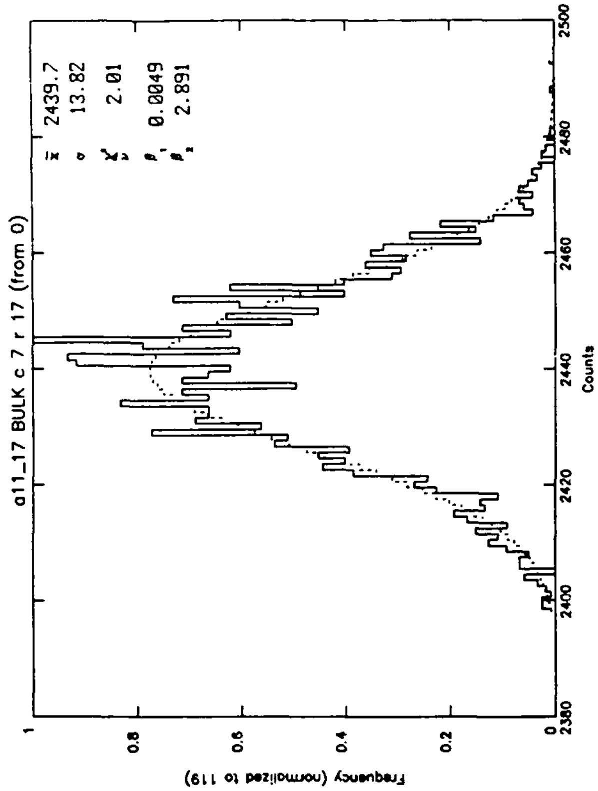

a11_17 BULK c 7 r 17 (from 0)
x̄ 2439.7
σ 13.82
χ^2_ν 2.01
β_1 0.0049
β_2 2.891
Frequency (normalized to 119)
Counts

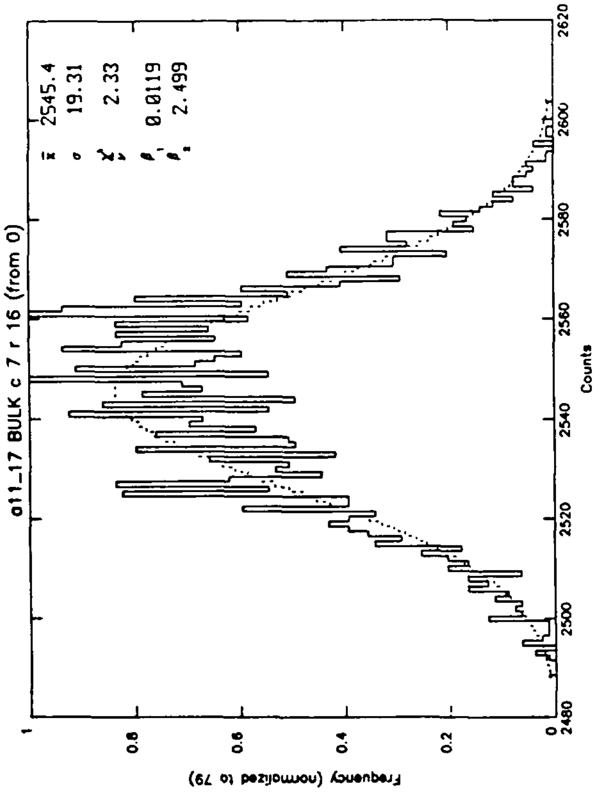

a11_17 BULK c 7 r 16 (from 0)
x̄ 2545.4
σ 19.31
χ^2_ν 2.33
β_1 0.0119
β_2 2.499
Frequency (normalized to 79)
Counts

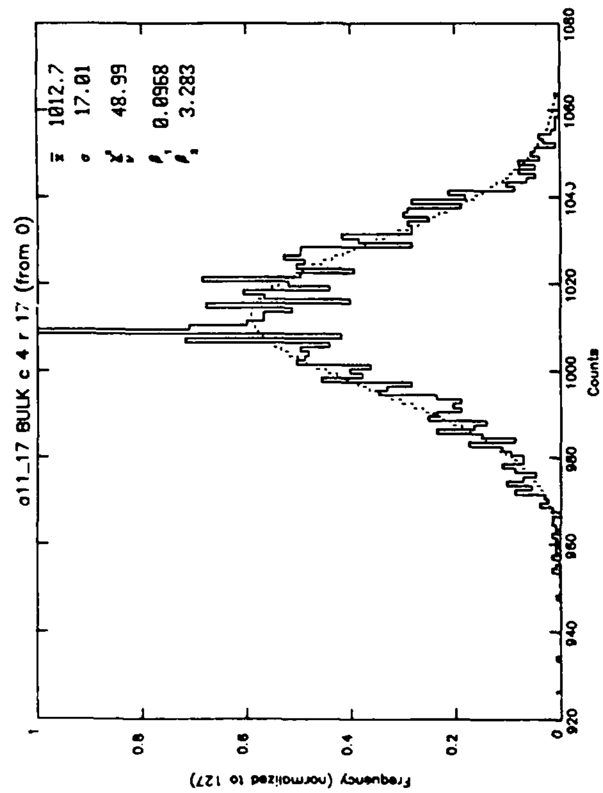

a11_17 BULK c 4 r 17 (from 0)
x̄ 1012.7
σ 17.01
χ^2_ν 48.99
β_1 0.0968
β_2 3.283
Frequency (normalized to 127)
Counts

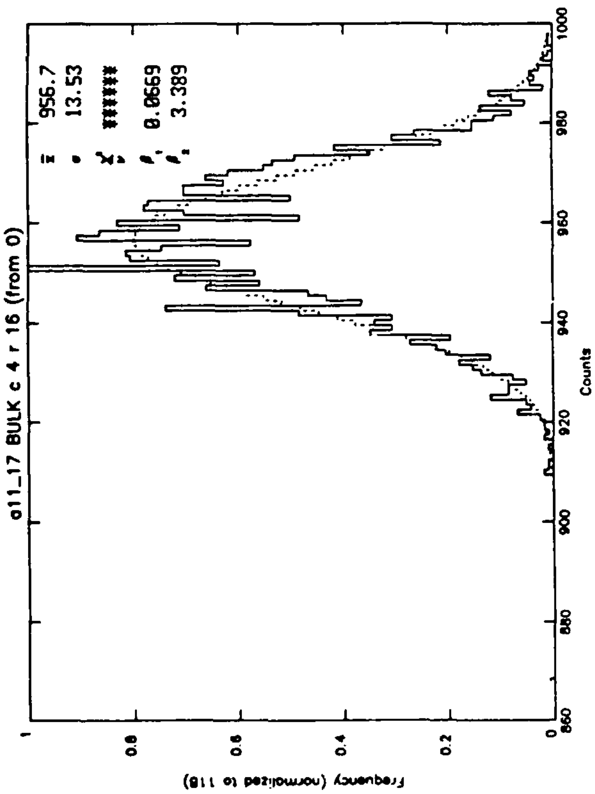

a11_17 BULK c 4 r 16 (from 0)
x̄ 956.7
σ 13.53
χ^2_ν ******
β_1 0.0669
β_2 3.389
Frequency (normalized to 118)
Counts

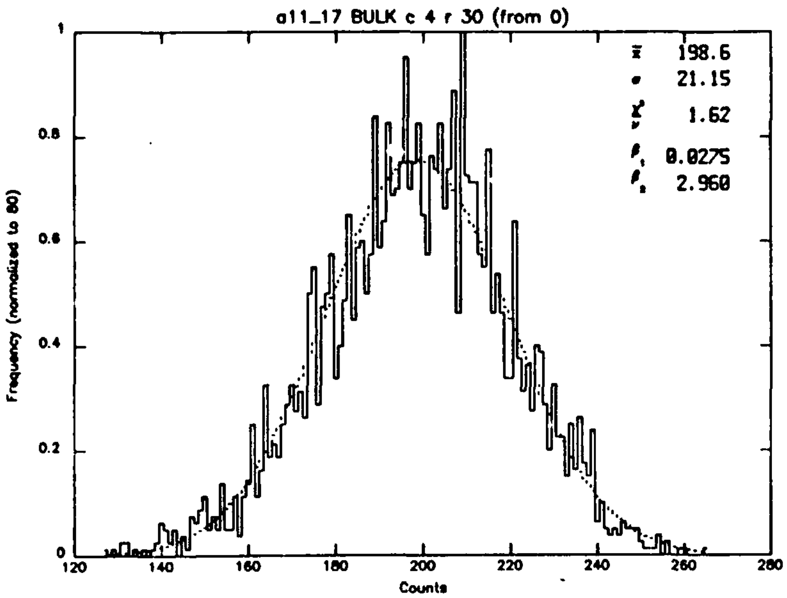
a11_17 BULK c 4 r 30 (from 0)
$\bar{x}$ 198.6
σ 21.15
χ^2_ν 1.62
β_1 0.0275
β_2 2.960
Frequency (normalized to 80)
Counts

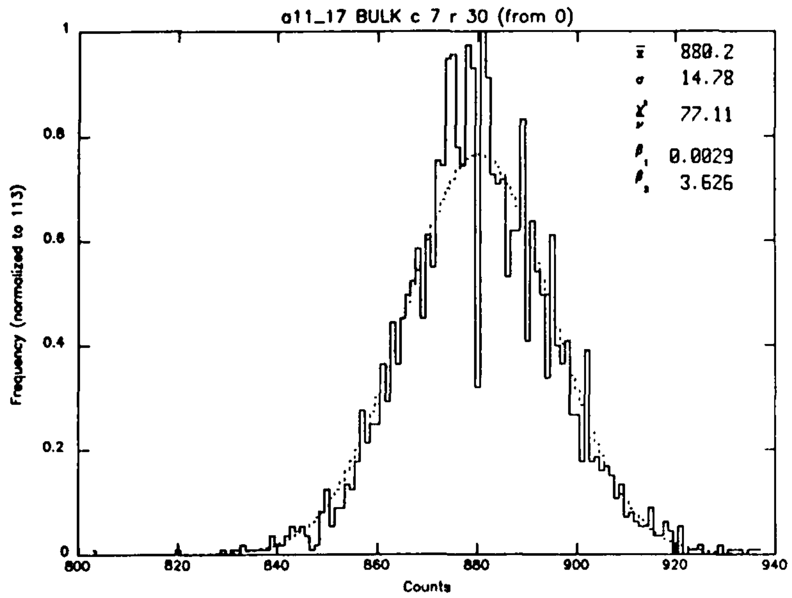
a11_17 BULK c 7 r 30 (from 0)
$\bar{x}$ 880.2
σ 14.78
χ^2_ν 77.11
β_1 0.0029
β_2 3.626
Frequency (normalized to 113)
Counts

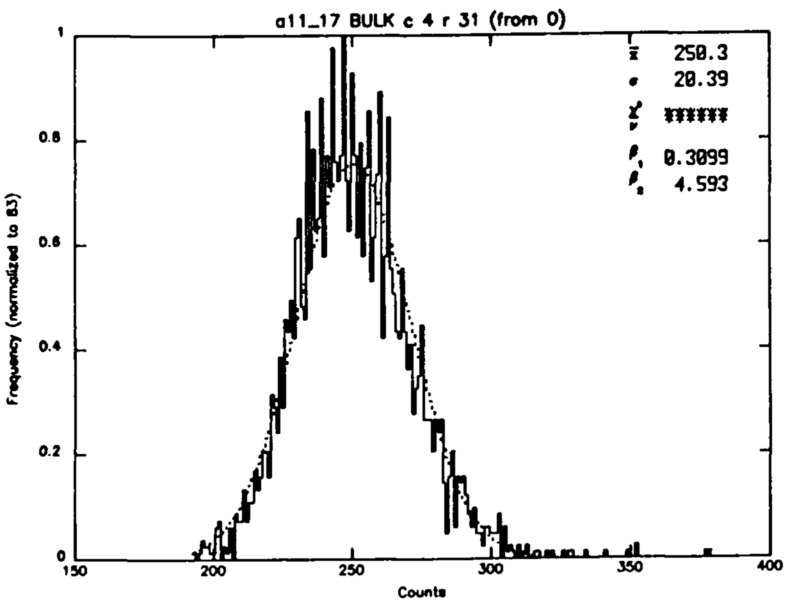
a11_17 BULK c 4 r 31 (from 0)
$\bar{x}$ 250.3
σ 20.39
χ^2_ν ******
β_1 0.3099
β_2 4.593
Frequency (normalized to 83)
Counts

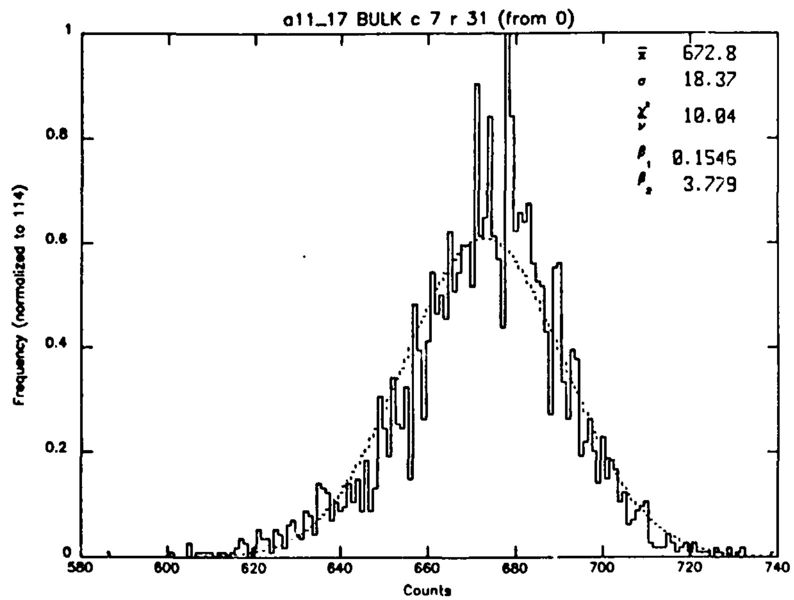
a11_17 BULK c 7 r 31 (from 0)
$\bar{x}$ 672.8
σ 18.37
χ^2_ν 10.04
β_1 0.1546
β_2 3.779
Frequency (normalized to 114)
Counts

APPENDIX A-7

Array: Aerojet Bulk Array

	Left	Right
Elements:	Column 11; Rows 0-2, 15-17, 30 31	Column 15, Rows 0-2, 15-17, 30, 31
Data Run:	Background all_17	Background all_17

Purpose: Comparison of column/row behavior for normal background. Compare also with Appendices A-5 and A-6 for other columns on the same run. The full set (A-5 to A-7) gives representative results across the whole array from top to bottom and left tc right.

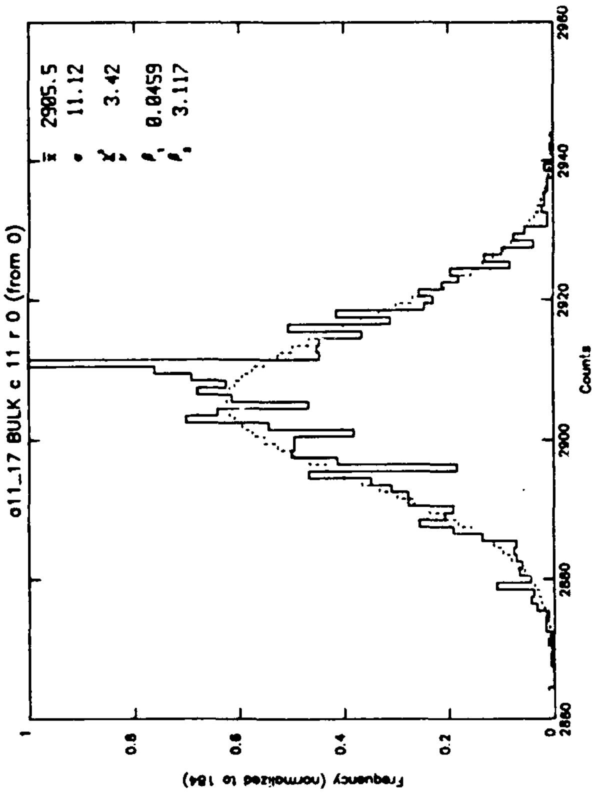
a11_17 BULK c 11 r 0 (from 0)
x̄ 2905.5
σ 11.12
χ²ν 3.42
β₁ 0.0459
β₂ 3.117
Frequency (normalized to 184)
Counts

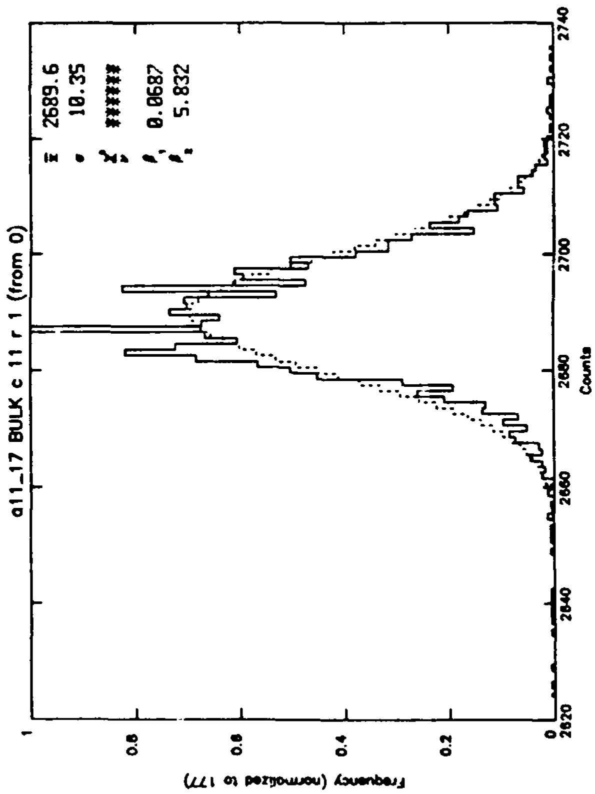
a11_17 BULK c 11 r 1 (from 0)
x̄ 2689.6
σ 10.35
χ²ν ******
β₁ 0.0687
β₂ 5.832
Frequency (normalized to 177)
Counts

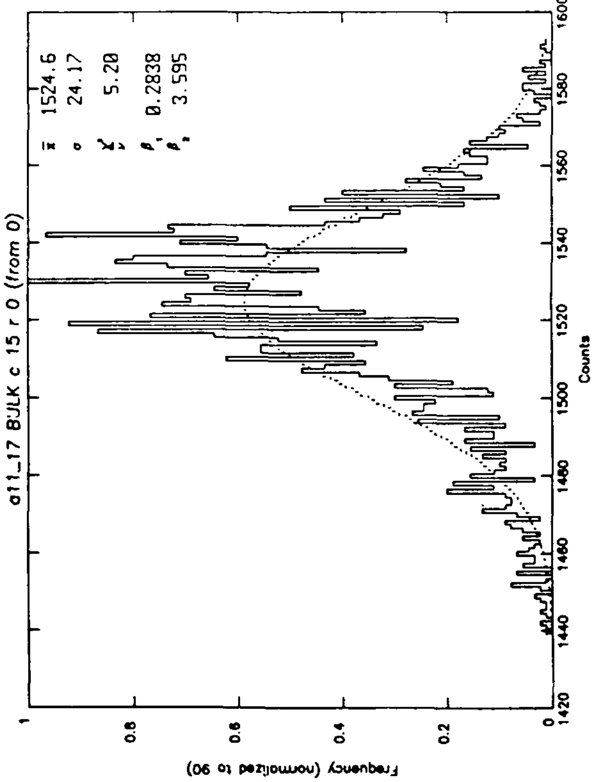
a11_17 BULK c 15 r 0 (from 0)
x̄ 1524.6
σ 24.17
χ²ν 5.20
β₁ 0.2838
β₂ 3.595
Frequency (normalized to 90)
Counts

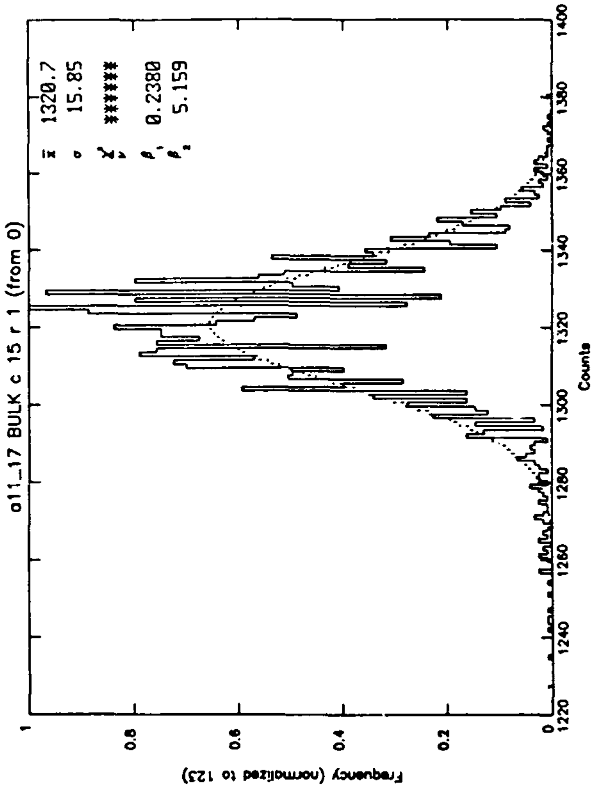
a11_17 BULK c 15 r 1 (from 0)
x̄ 1320.7
σ 15.85
χ²ν ******
β₁ 0.2380
β₂ 5.159
Frequency (normalized to 123)
Counts

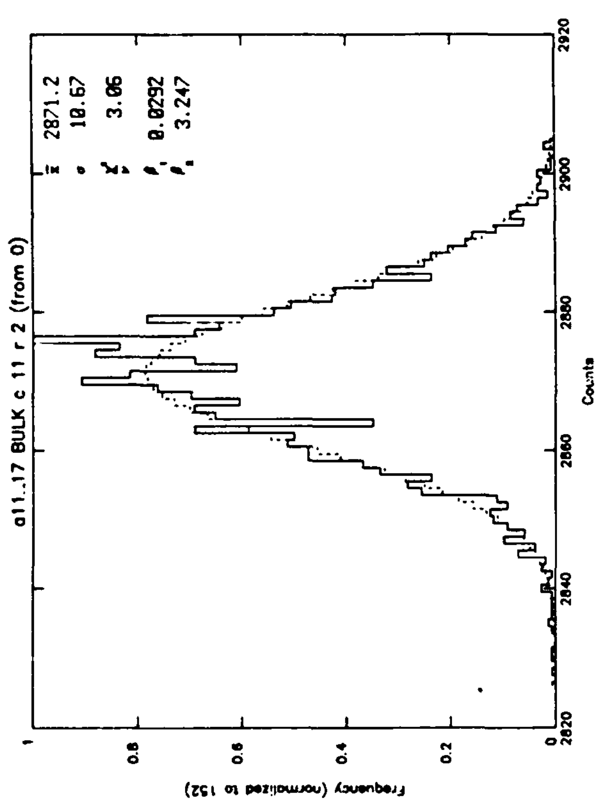
a11_17 BULK c 11 r 2 (from 0)
2871.2
10.67
3.06
0.0292
3.247
Frequency (normalized to 152)
Counts

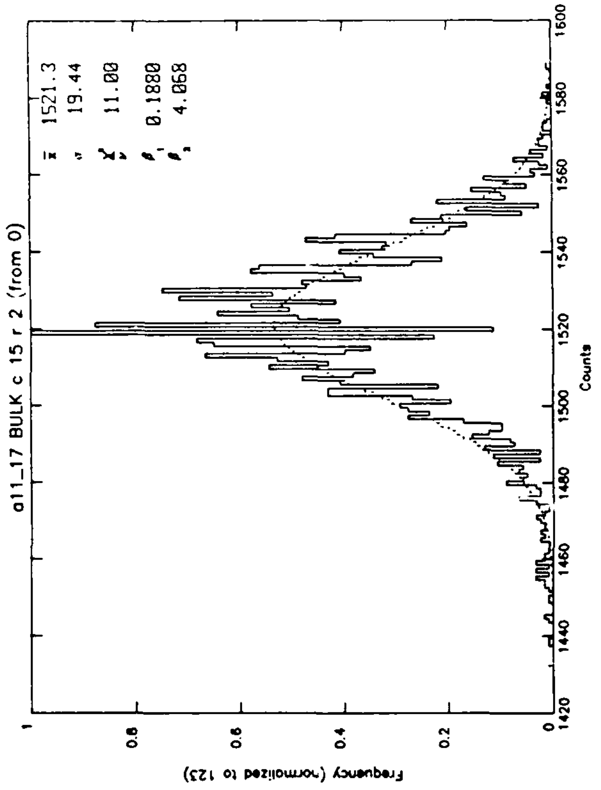
a11_17 BULK c 15 r 2 (from 0)
1521.3
19.44
11.00
0.1880
4.068
Frequency (normalized to 123)
Counts

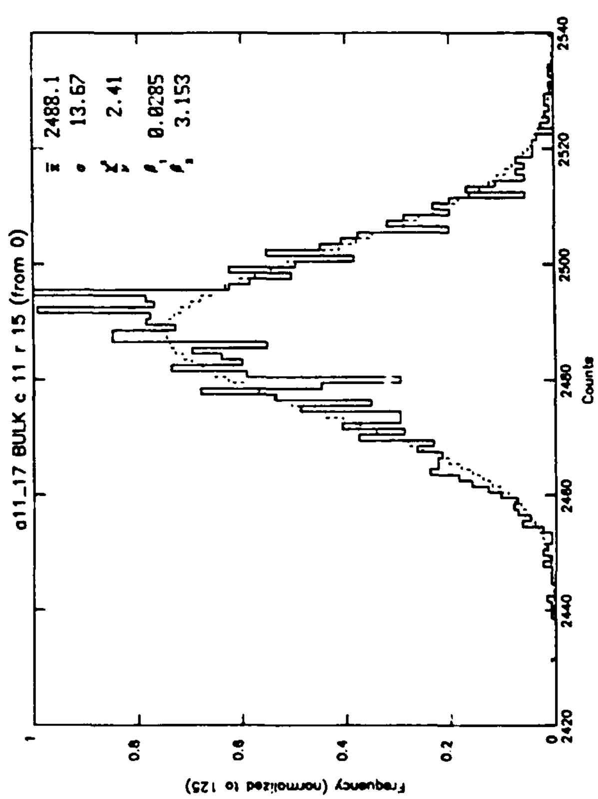
a11_17 BULK c 11 r 15 (from 0)
2488.1
13.67
2.41
0.0285
3.153
Frequency (normalized to 125)
Counts

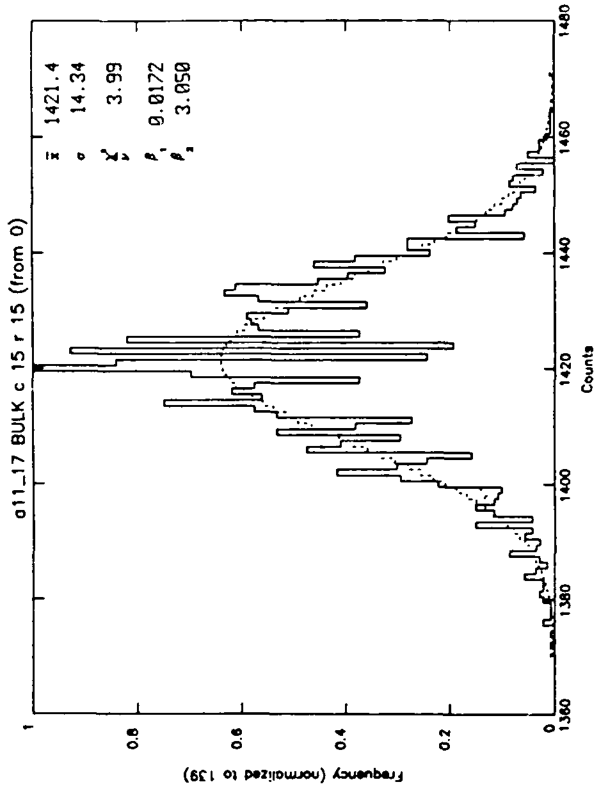
a11_17 BULK c 15 r 15 (from 0)
1421.4
14.34
3.99
0.0172
3.050
Frequency (normalized to 139)
Counts

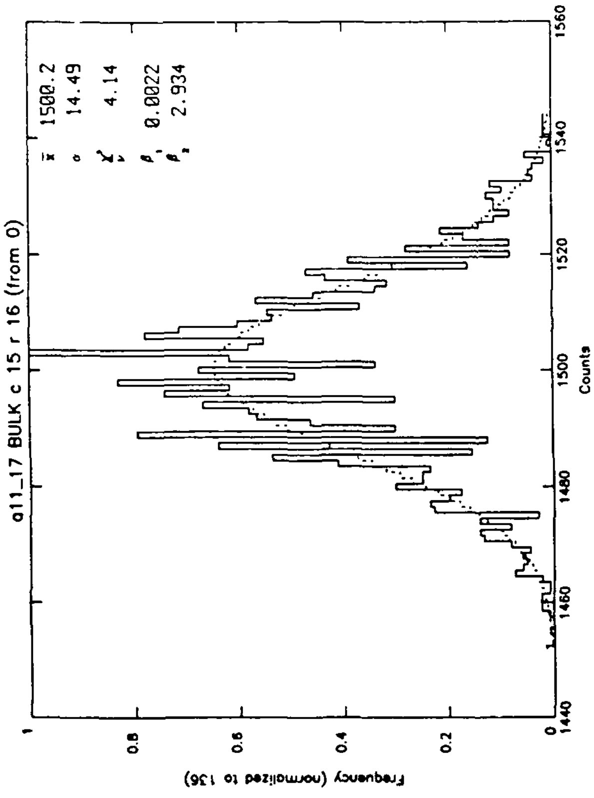
a11_17 BULK c 15 r 16 (from 0)
x̄ 1500.2
σ 14.49
χ^2_ν 4.14
β_1 0.0022
β_2 2.934
Frequency (normalized to 136)
Counts

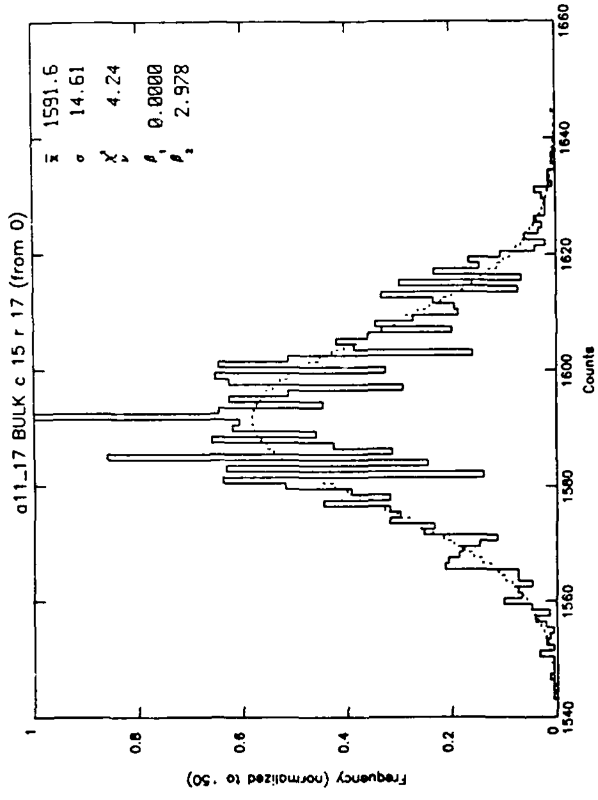
a11_17 BULK c 15 r 17 (from 0)
x̄ 1591.6
σ 14.61
χ^2_ν 4.24
β_1 0.0000
β_2 2.978
Frequency (normalized to 150)
Counts

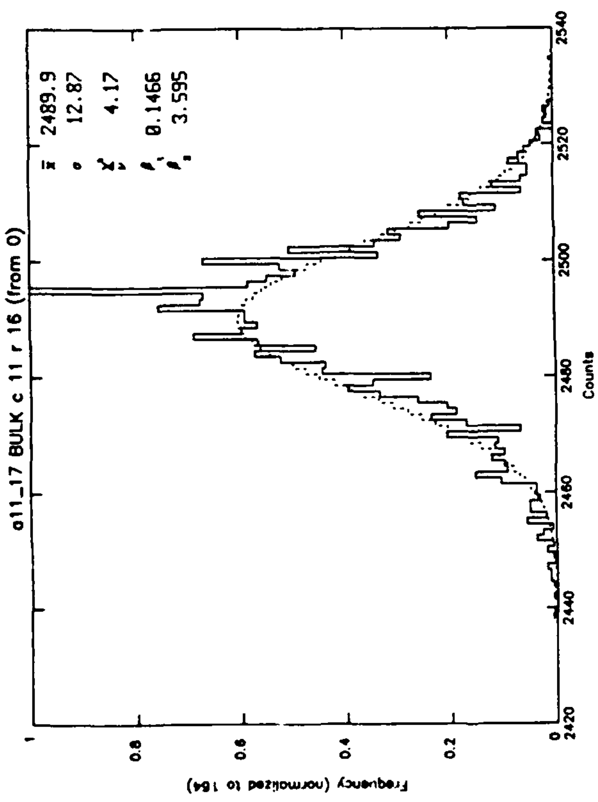
a11_17 BULK c 11 r 16 (from 0)
x̄ 2489.9
σ 12.87
χ^2_ν 4.17
β_1 0.1466
β_2 3.595
Frequency (normalized to 164)
Counts

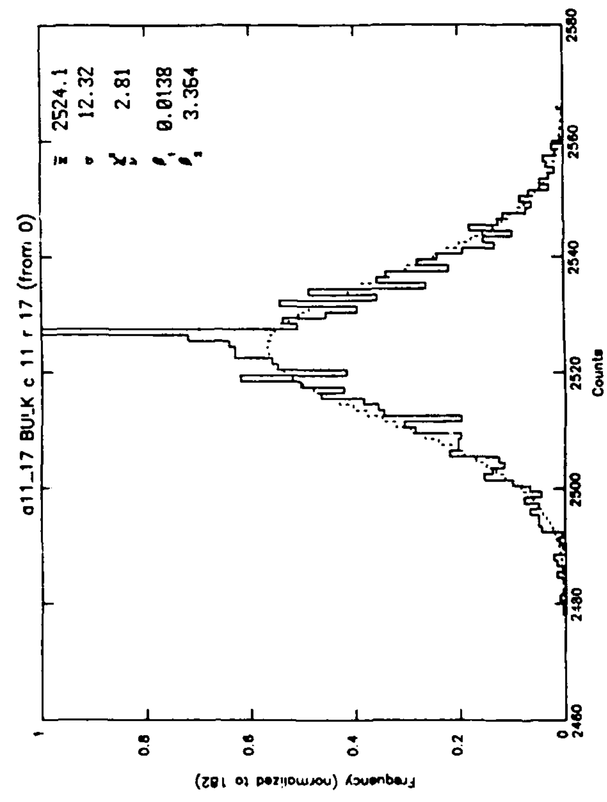
a11_17 BULK c 11 r 17 (from 0)
x̄ 2524.1
σ 12.32
χ^2_ν 2.81
β_1 0.0138
β_2 3.364
Frequency (normalized to 182)
Counts

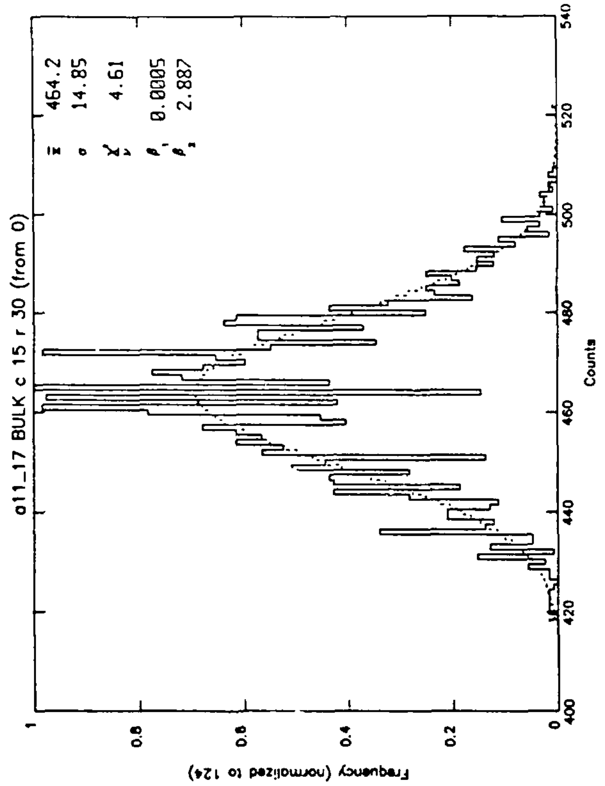
a11_17 BULK c 15 r 30 (from 0)
x̄ 464.2
σ 14.85
χ^2_ν 4.61
β_1 0.0005
β_2 2.887
Counts
Frequency (normalized to 124)

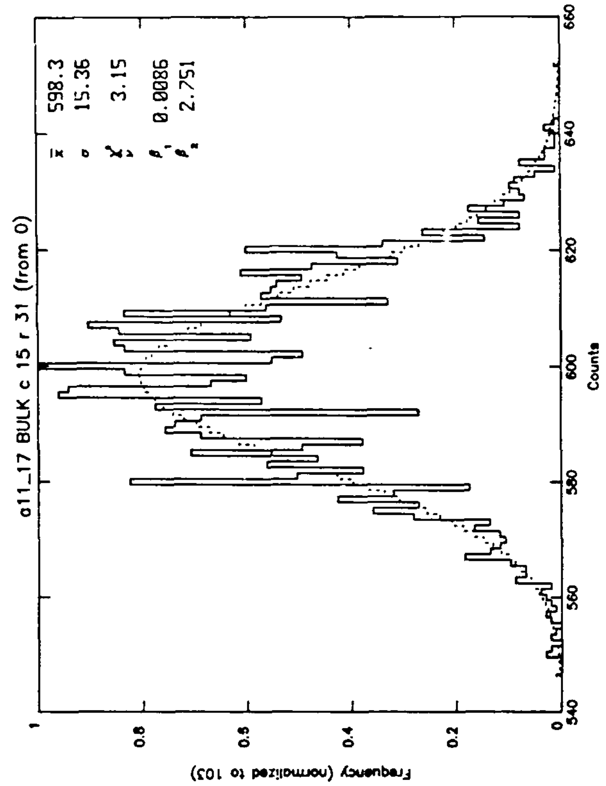
a11_17 BULK c 15 r 31 (from 0)
x̄ 598.3
σ 15.36
χ^2_ν 3.15
β_1 0.0086
β_2 2.751
Counts
Frequency (normalized to 103)

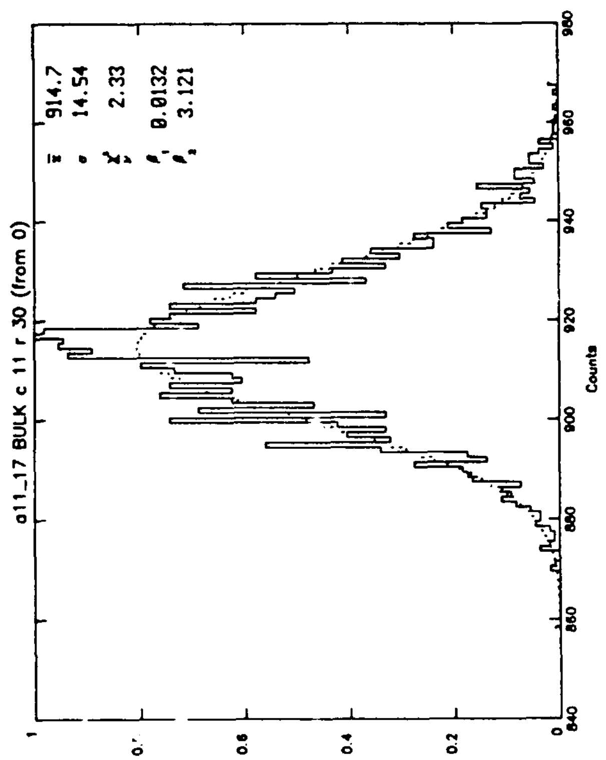
a11_17 BULK c 11 r 30 (from 0)
x̄ 914.7
σ 14.54
χ^2_ν 2.33
β_1 0.0132
β_2 3.121
Counts
Frequency (normalized to 109)

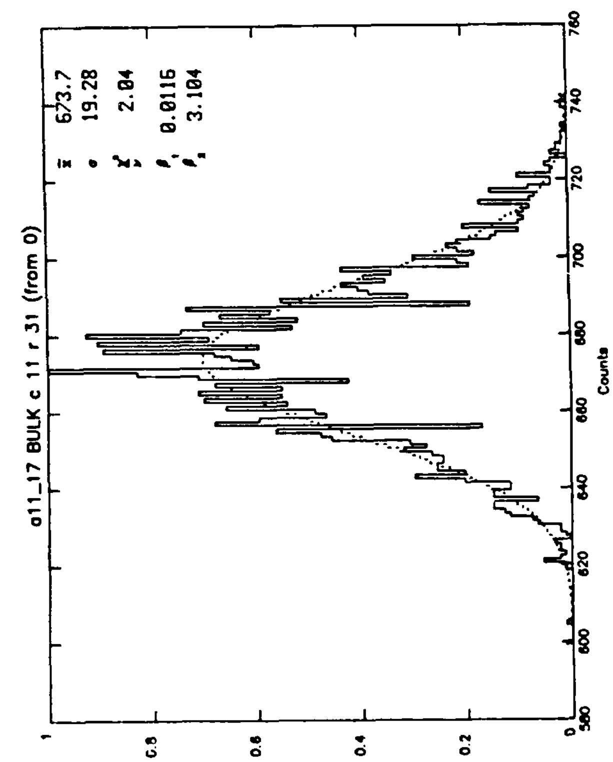
a11_17 BULK c 11 r 31 (from 0)
x̄ 673.7
σ 19.28
χ^2_ν 2.04
β_1 0.0116
β_2 3.104
Counts
Frequency (normalized to 94)

APPENDIX A-8

Array: Aerojet MC^2

	Left	Right
Elements:	Column 2; Rows 0-2, 15-17, 30, 31	Column 3, Rows 0-2, 15-17, 30, 31
Data Run:	Background a9_35	Background a9_35

Purpose: Comparison of column (even vs odd)/row behavior for normal background. Compare also with Appendices A-9 and A-10 for other columns on the same run. The full set (A-8 to A-10) gives representative results across the whole array from top to bottom and left to right. Compare also with Appendices A-11 to A-13 from a different run.

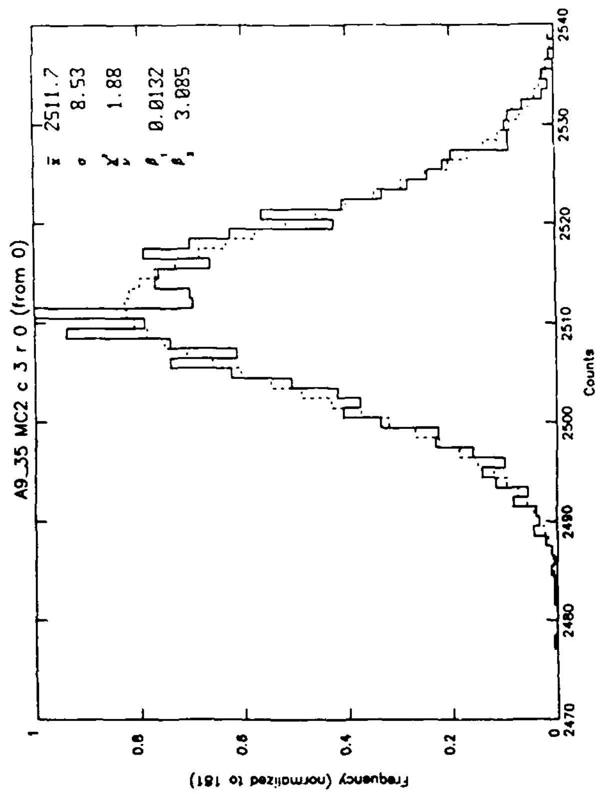

A9_35 MC2 c 3 r 0 (from 0)
2511.7
8.53
1.88
0.0132
3.085
Counts
Frequency (normalized to 181)

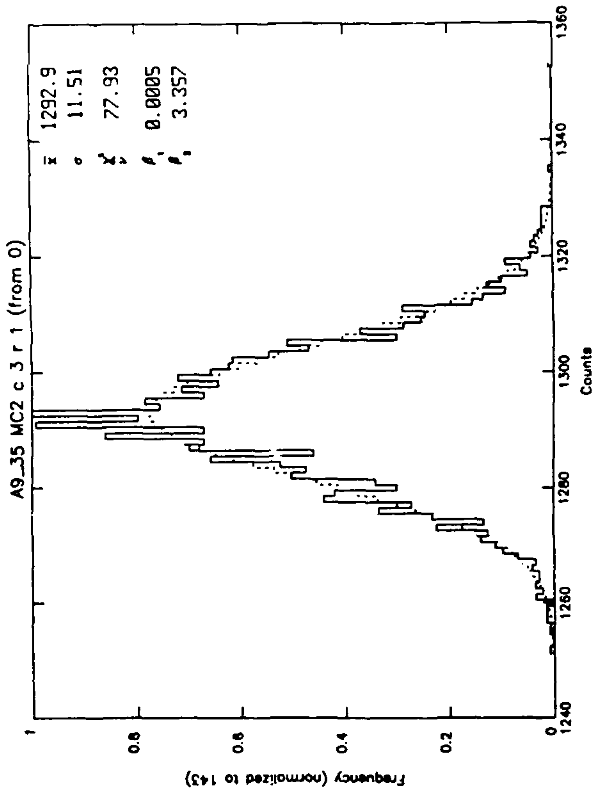

A9_35 MC2 c 3 r 1 (from 0)
1292.9
11.51
77.93
0.0005
3.357
Counts
Frequency (normalized to 143)

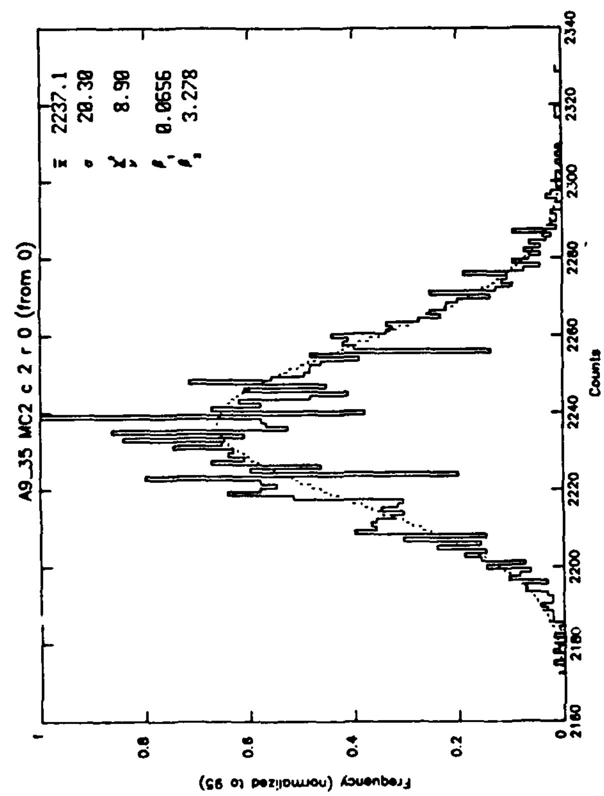

A9_35 MC2 c 2 r 0 (from 0)
2237.1
20.30
8.90
0.0656
3.278
Counts
Frequency (normalized to 95)

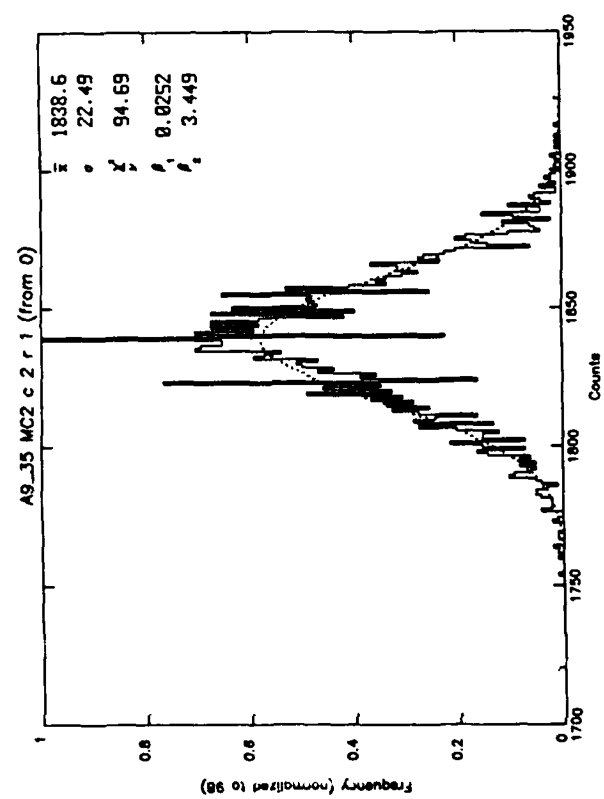

A9_35 MC2 c 2 r 1 (from 0)
1838.6
22.49
94.69
0.0252
3.449
Counts
Frequency (normalized to 98)

A9_35 MC2 c 2 r 2 (from 0)

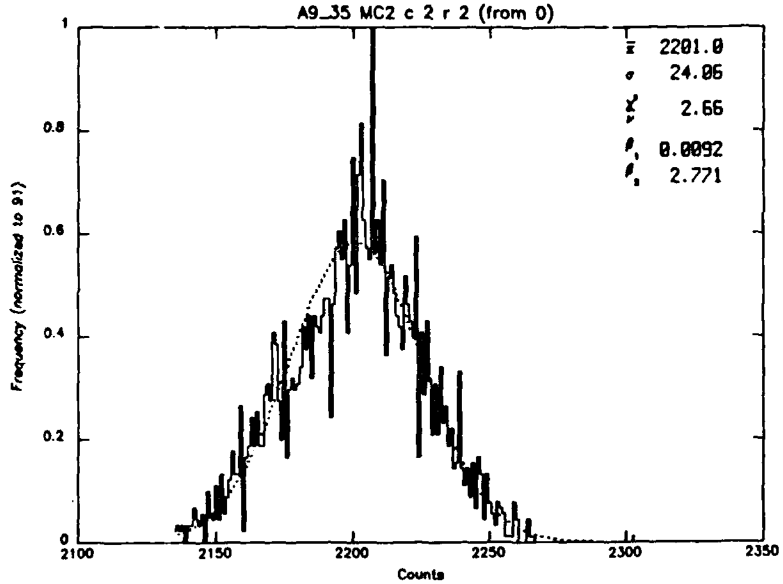

A9_35 MC2 c 3 r 2 (from 0)

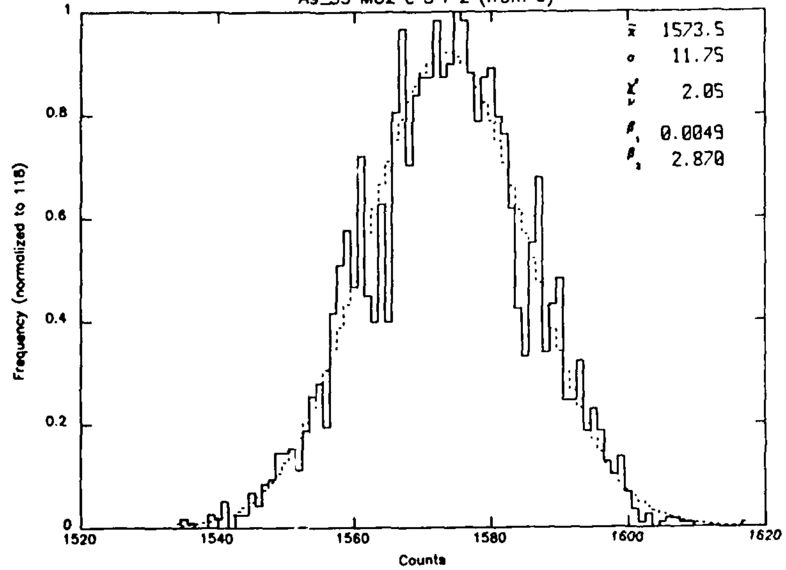

A9_35 MC2 c 2 r 15 (from 0)

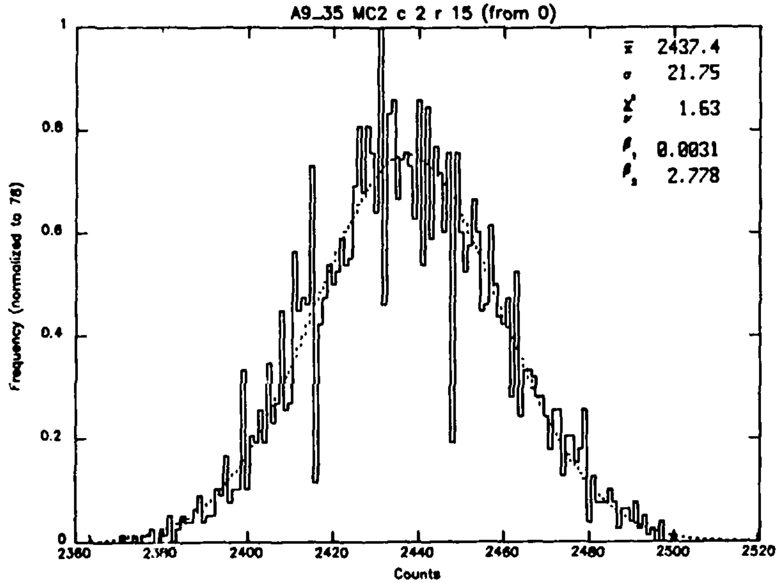

A9_35 MC2 c 3 r 15 (from 0)

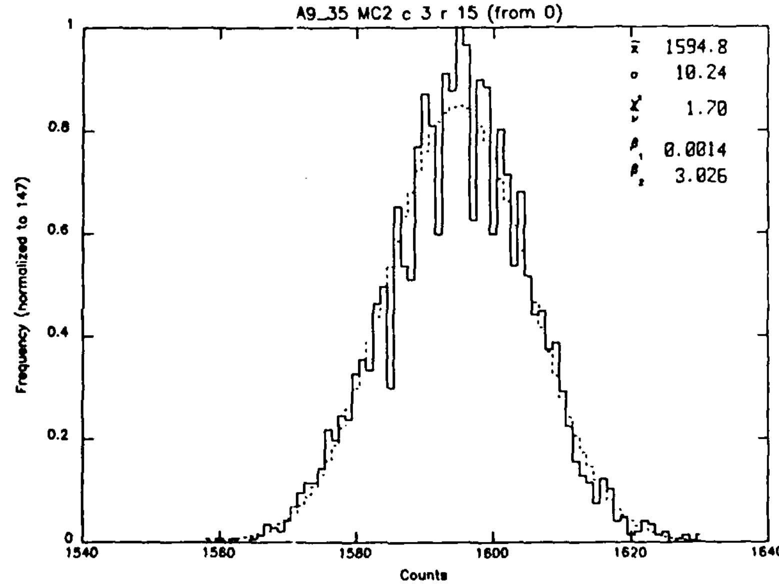

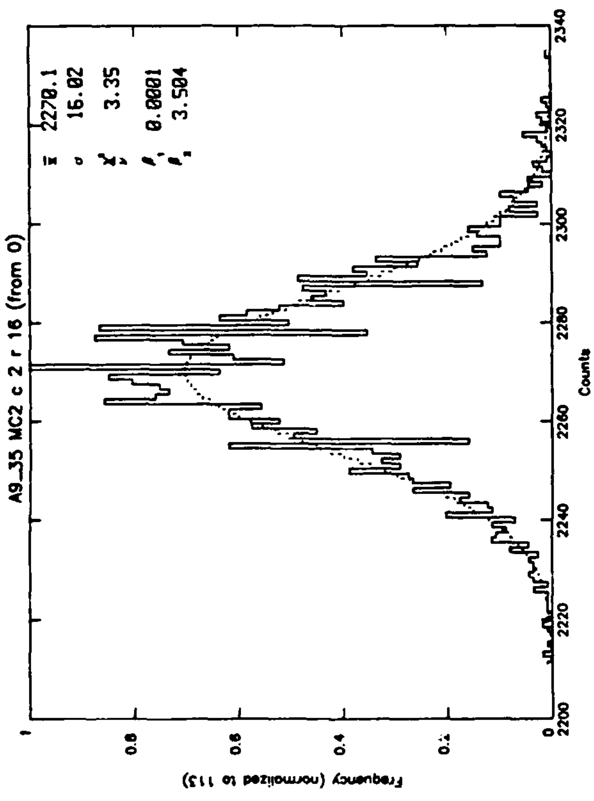
A9_35 MC2 c 2 r 16 (from 0)
x̄ 2270.1
σ 16.02
χ²ν 3.35
β1 0.0001
β2 3.504
Frequency (normalized to 113)
Counts

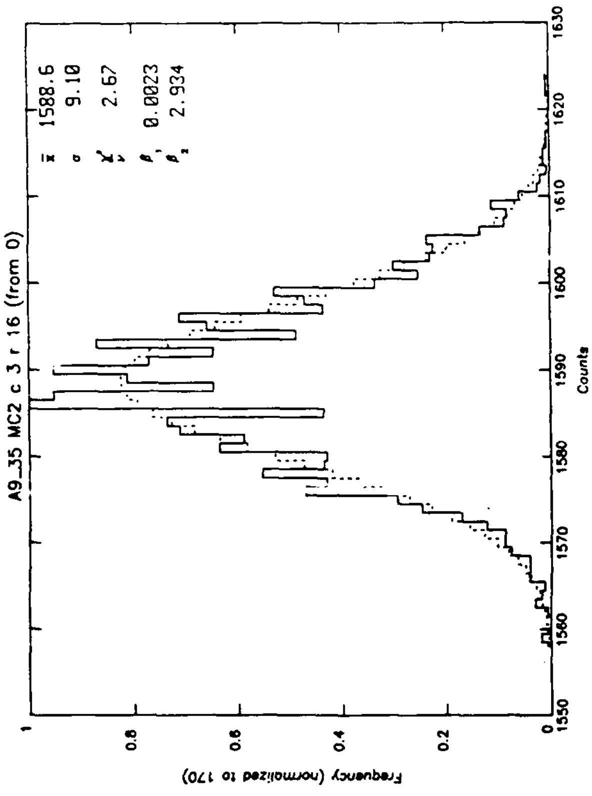
A9_35 MC2 c 3 r 16 (from 0)
x̄ 1588.6
σ 9.10
χ²ν 2.67
β1 0.0023
β2 2.934
Frequency (normalized to 170)
Counts

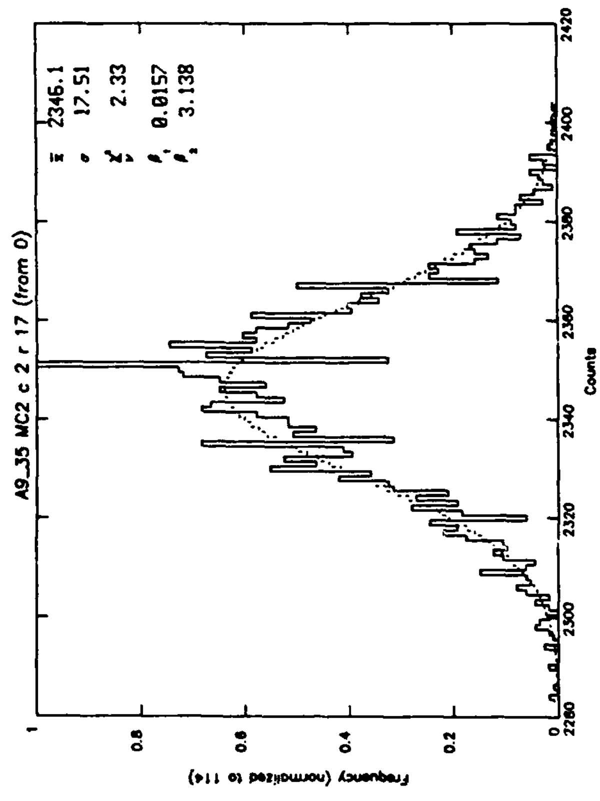
A9_35 MC2 c 2 r 17 (from 0)
x̄ 2346.1
σ 17.51
χ²ν 2.33
β1 0.0157
β2 3.138
Frequency (normalized to 114)
Counts

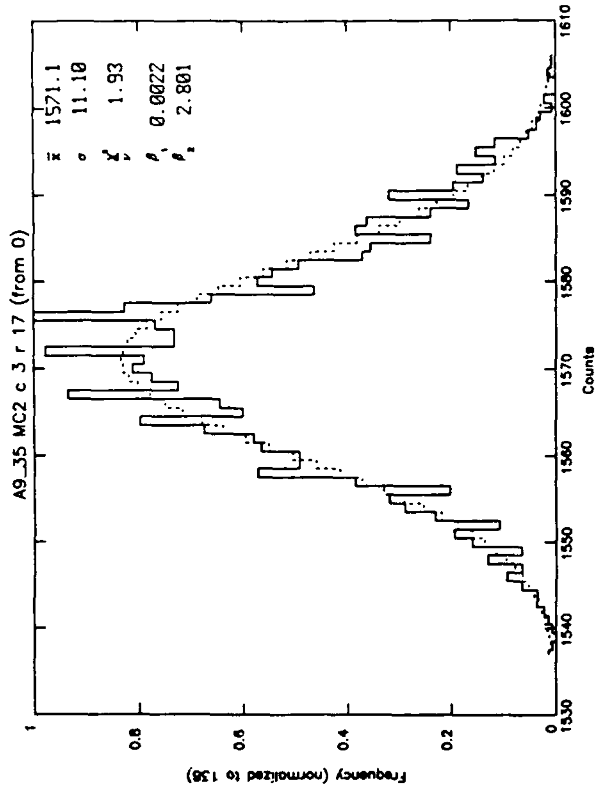
A9_35 MC2 c 3 r 17 (from 0)
x̄ 1571.1
σ 11.10
χ²ν 1.93
β1 0.0022
β2 2.801
Frequency (normalized to 138)
Counts

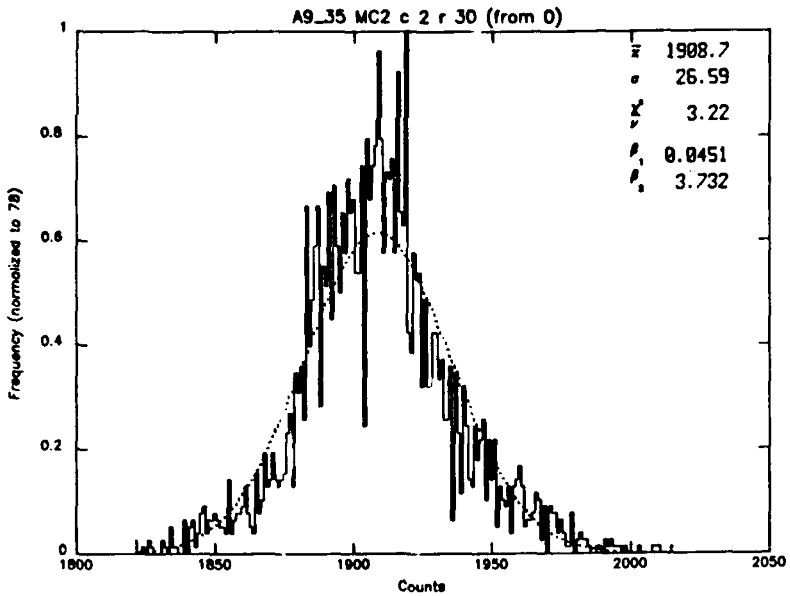
A9_35 MC2 c 2 r 30 (from 0)
x̄ 1908.7
σ 26.59
χ²ν 3.22
β1 0.0451
β2 3.732
Frequency (normalized to 78)
Counts

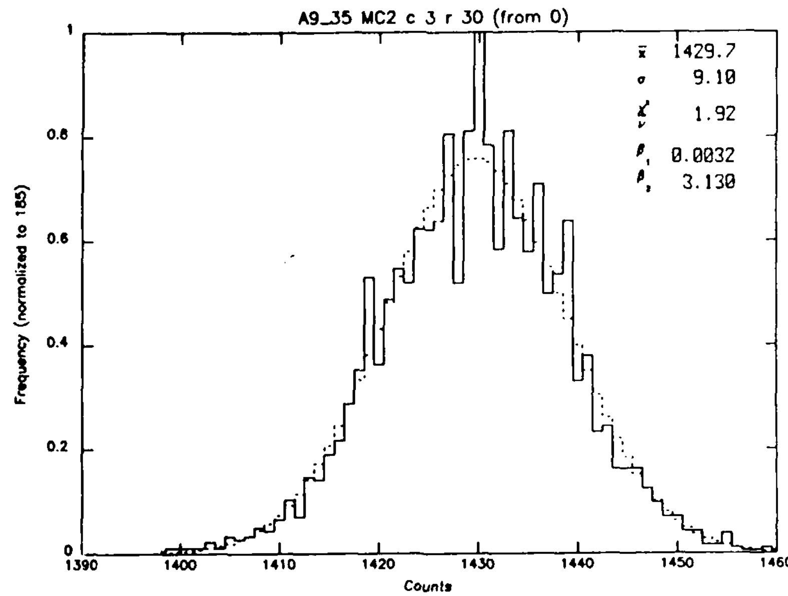
A9_35 MC2 c 3 r 30 (from 0)
x̄ 1429.7
σ 9.10
χ²ν 1.92
β1 0.0032
β2 3.130
Frequency (normalized to 185)
Counts

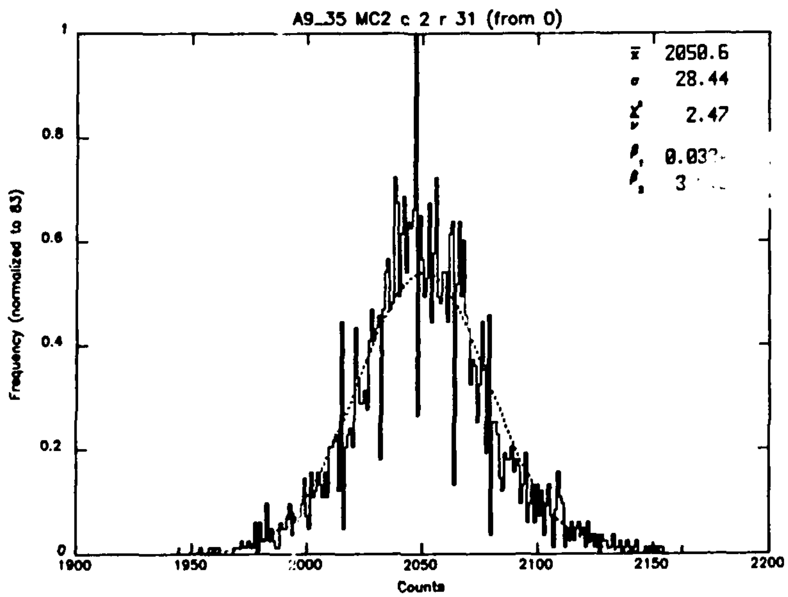
A9_35 MC2 c 2 r 31 (from 0)
x̄ 2050.6
σ 28.44
χ²ν 2.47
Frequency (normalized to 83)
Counts

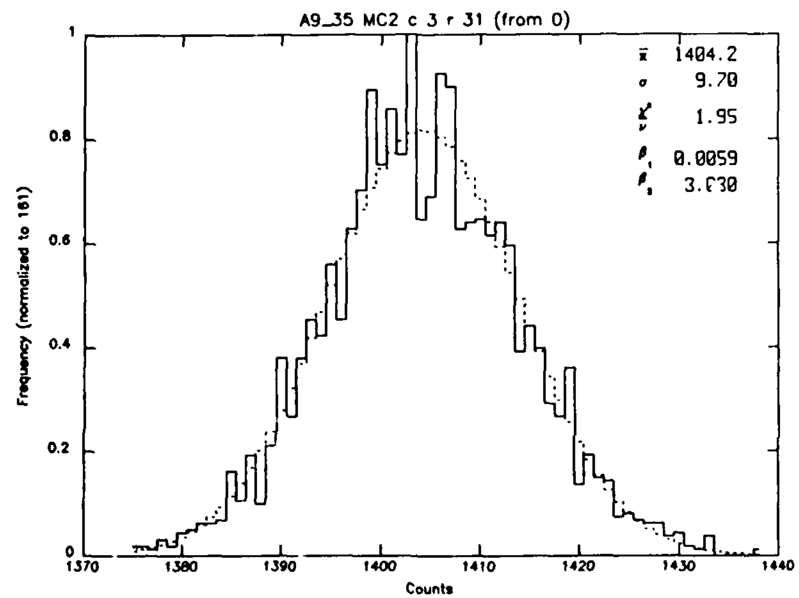
A9_35 MC2 c 3 r 31 (from 0)
x̄ 1404.2
σ 9.70
χ²ν 1.95
β1 0.0059
Frequency (normalized to 161)
Counts

APPENDIX A-9

Array: Aerojet MC^2

	Left	Right
Elements:	Column 4; Rows 0-2, 15-17, 30, 31	Column 7, Rows 0-2, 15-17, 30, 31
Data Run:	Background a9_35	Background a9_35

Purpose: Comparison of column (even vs odd)/row behavior for normal background. Compare also with Appendices A-8 and A-10 for other columns on the same run. The full set (A-8 to A-10) gives representative results across the whole array from top to bottom and left to right. Compare also with Appendices A-11 to A-13 from a different run.

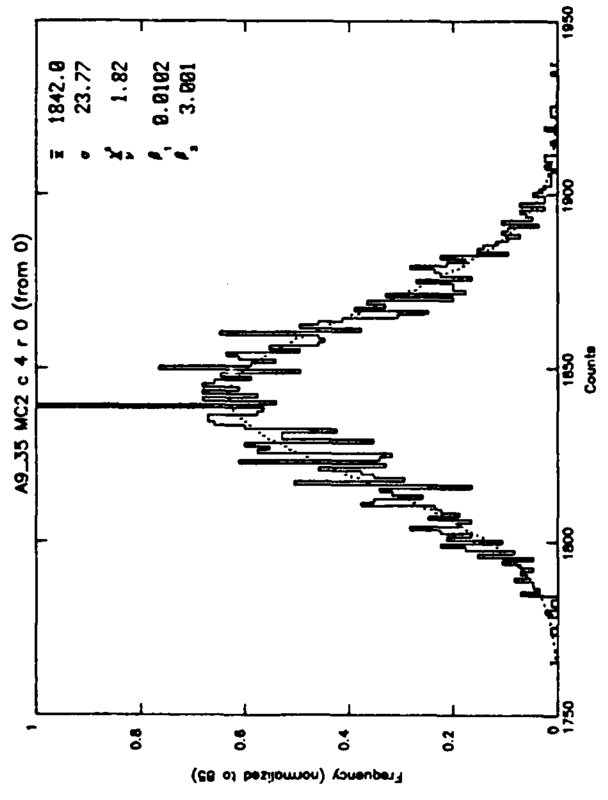
A9_35 MC2 c 4 r 0 (from 0)
x̄ 1842.0
σ 23.77
χ²ν 1.82
β1 0.0102
β2 3.001
Frequency (normalized to 85)
Counts

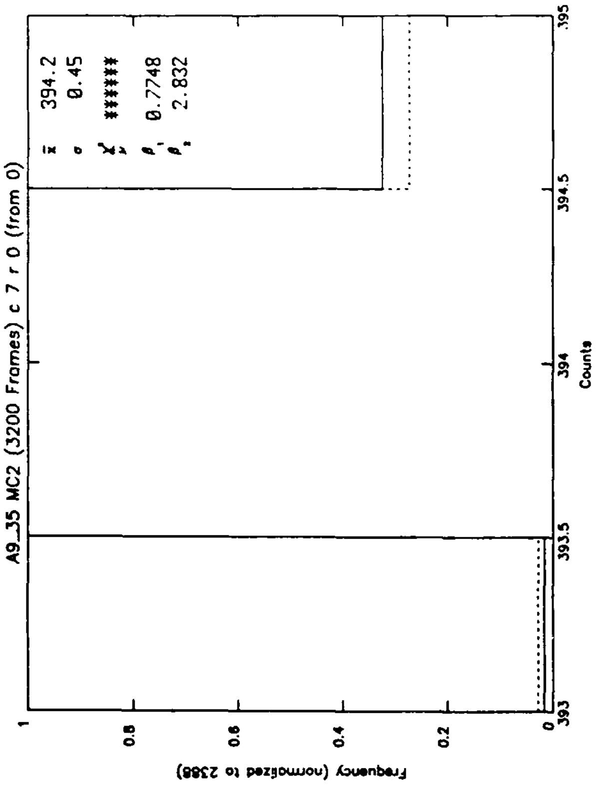
A9_35 MC2 (3200 Frames) c 7 r 0 (from 0)
x̄ 394.2
σ 0.45
χ²ν *****
β1 0.7748
β2 2.832
Frequency (normalized to 2388)
Counts

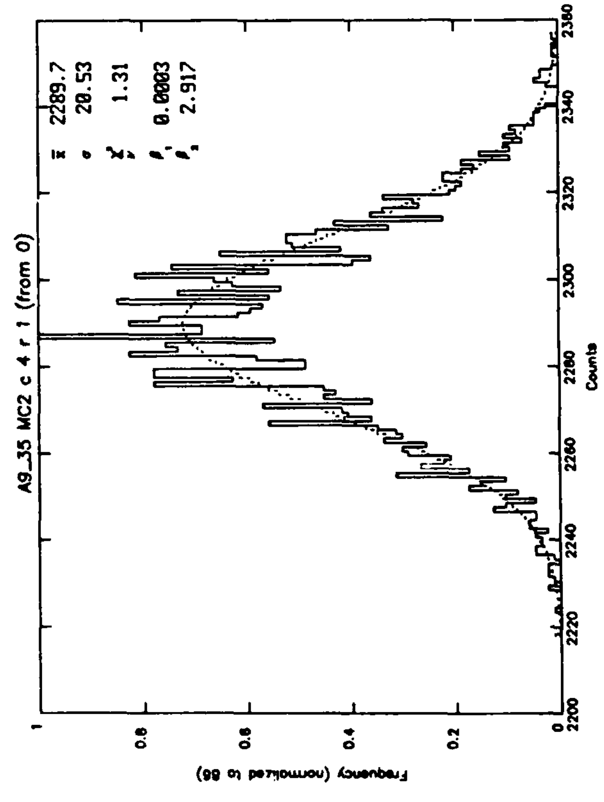
A9_35 MC2 c 4 r 1 (from 0)
x̄ 2289.7
σ 20.53
χ²ν 1.31
β1 0.0003
β2 2.917
Frequency (normalized to 86)
Counts

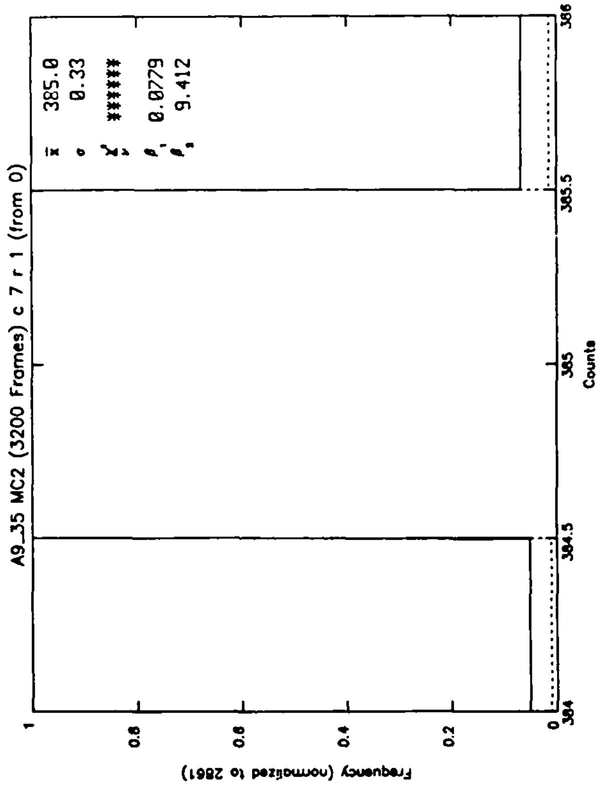
A9_35 MC2 (3200 Frames) c 7 r 1 (from 0)
x̄ 385.0
σ 0.33
χ²ν *****
β1 0.0779
β2 9.412
Frequency (normalized to 2861)
Counts

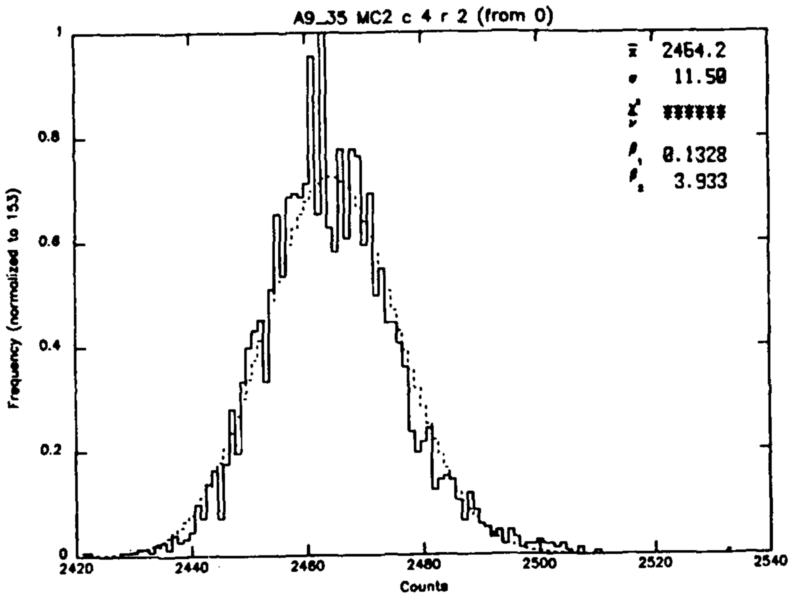
A9_35 MC2 c 4 r 2 (from 0)
x̄ 2464.2
σ 11.50
χ^2_ν ******
β_1 0.1328
β_2 3.933
Frequency (normalized to 153)
Counts

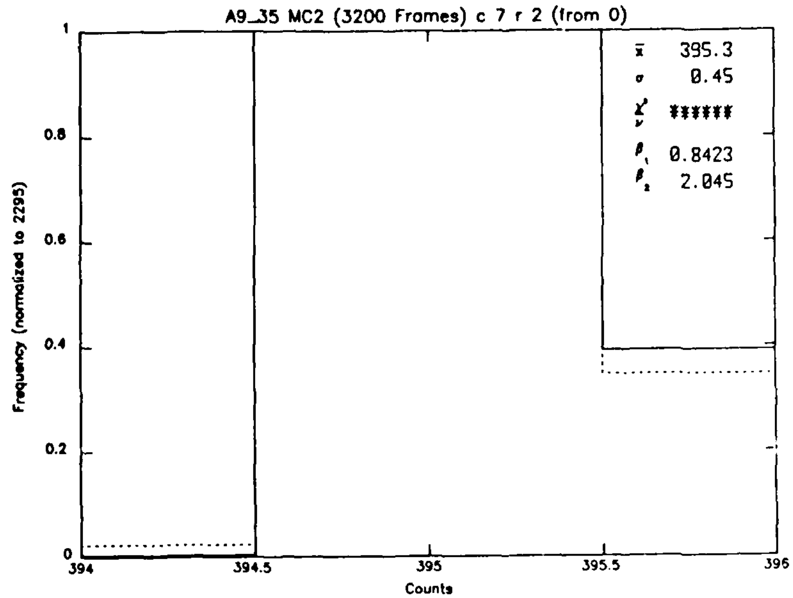
A9_35 MC2 (3200 Frames) c 7 r 2 (from 0)
x̄ 395.3
σ 0.45
χ^2_ν ******
β_1 0.8423
β_2 2.045
Frequency (normalized to 2295)
Counts

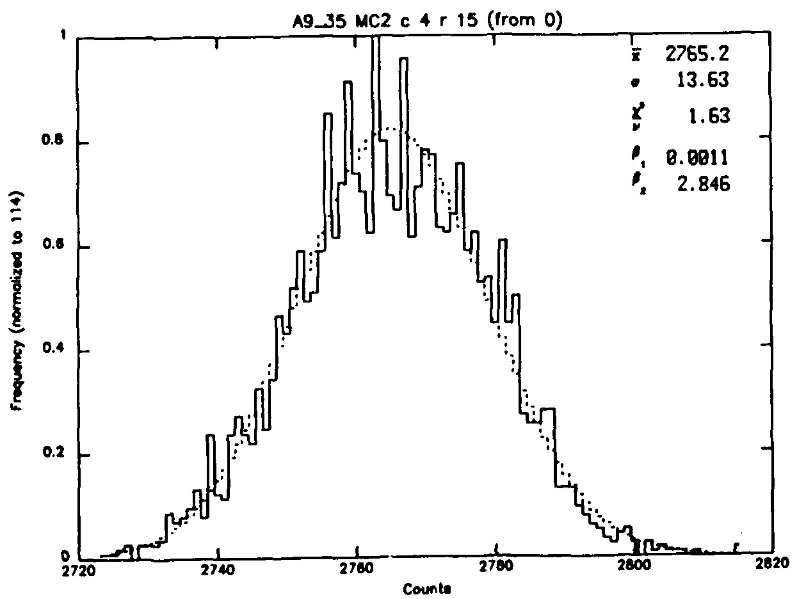
A9_35 MC2 c 4 r 15 (from 0)
x̄ 2765.2
σ 13.63
χ^2_ν 1.63
β_1 0.0011
β_2 2.846
Frequency (normalized to 114)
Counts

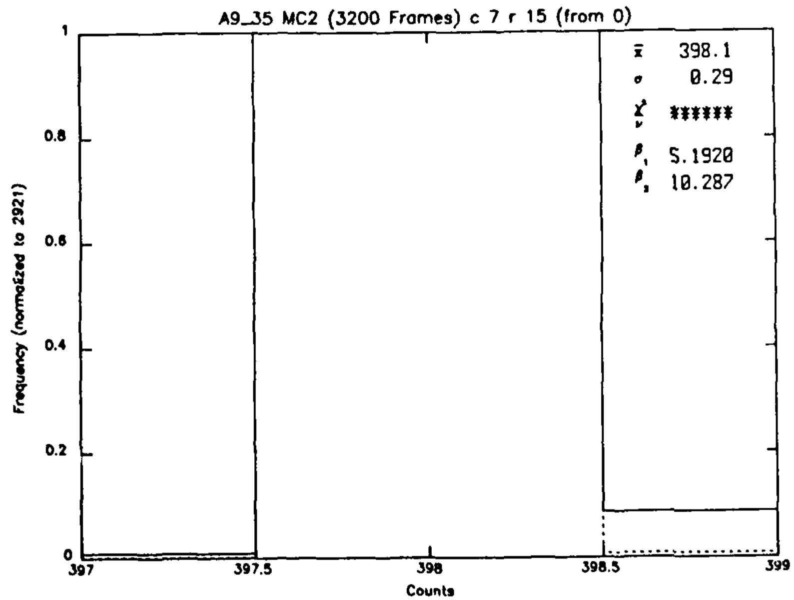
A9_35 MC2 (3200 Frames) c 7 r 15 (from 0)
x̄ 398.1
σ 0.29
χ^2_ν ******
β_1 5.1920
β_2 10.287
Frequency (normalized to 2921)
Counts

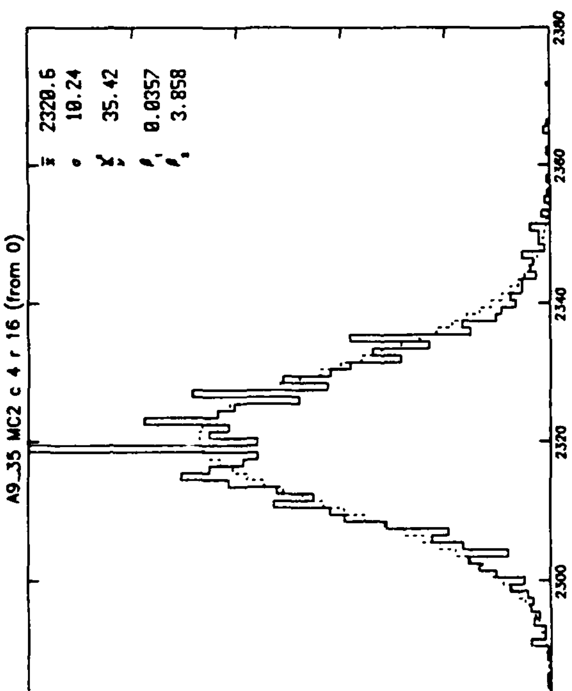
A9_35 MC2 c 4 r 16 (from 0)
x̄ 2320.6
σ 10.24
χ^2_ν 35.42
β_1 0.0357
β_2 3.858
Counts
Frequency (normalized to 185)

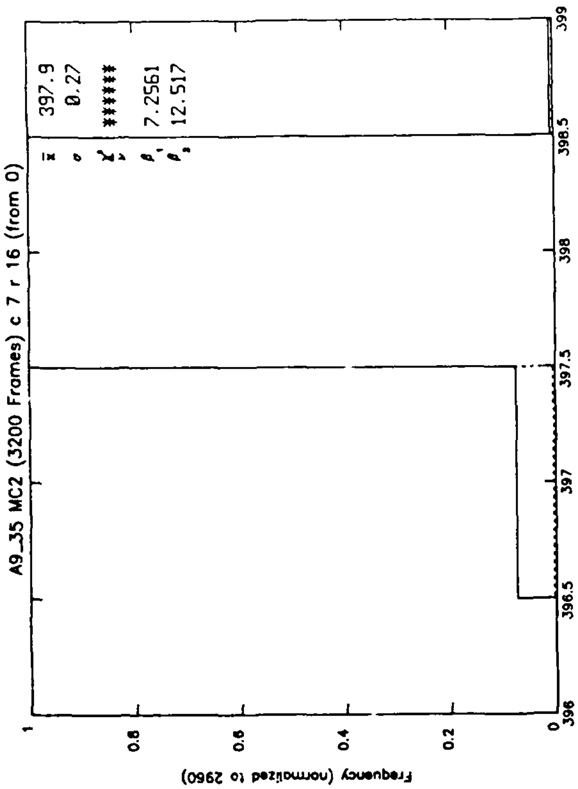
A9_35 MC2 (3200 Frames) c 7 r 16 (from 0)
x̄ 397.9
σ 0.27
χ^2_ν ******
β_1 7.2561
β_2 12.517
Counts
Frequency (normalized to 2960)

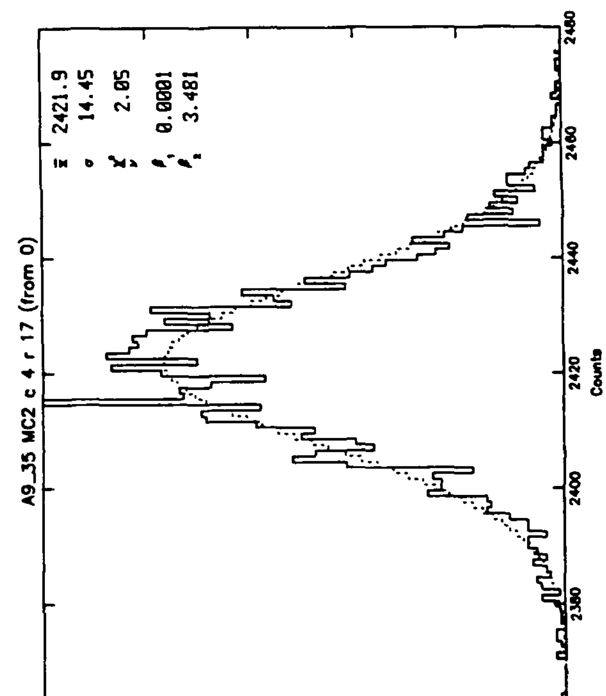
A9_35 MC2 c 4 r 17 (from 0)
x̄ 2421.9
σ 14.45
χ^2_ν 2.05
β_1 0.0001
β_2 3.481
Counts
Frequency (normalized to 115)

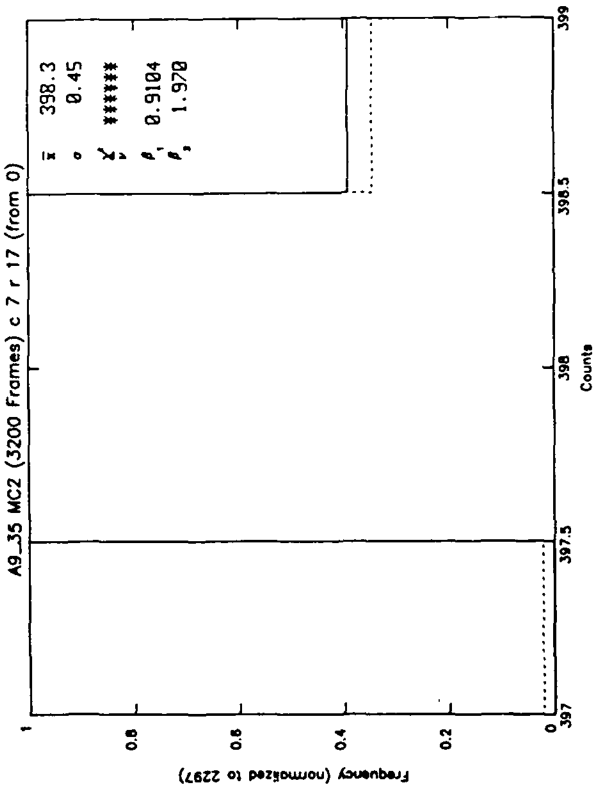
A9_35 MC2 (3200 Frames) c 7 r 17 (from 0)
x̄ 398.3
σ 0.45
χ^2_ν ******
β_1 0.9104
β_2 1.970
Counts
Frequency (normalized to 2297)

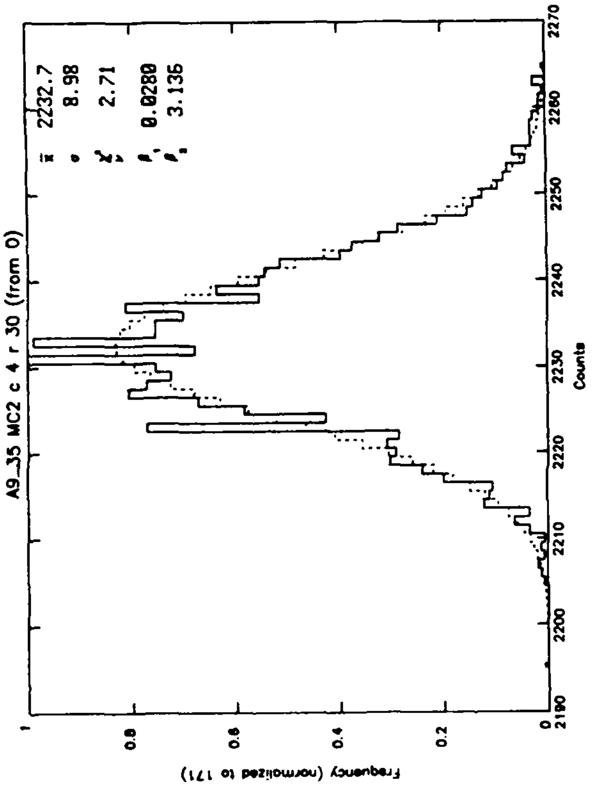
A9_35 MC2 c 4 r 30 (from 0)
Counts
Frequency (normalized to 171)
x̄ 2232.7
σ 8.98
χ²ν 2.71
β1 0.0280
β2 3.136

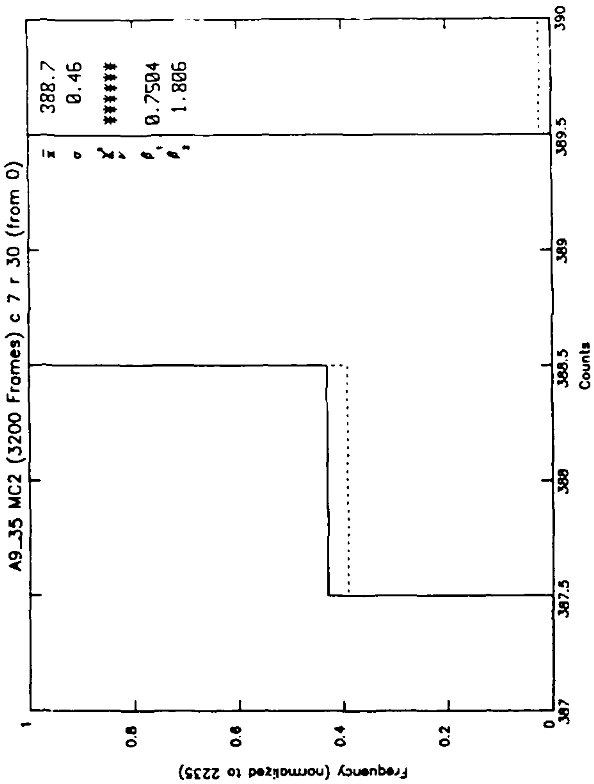
A9_35 MC2 (3200 Frames) c 7 r 30 (from 0)
Counts
Frequency (normalized to 2235)
x̄ 388.7
σ 0.46
χ²ν ******
β1 0.7504
β2 1.806

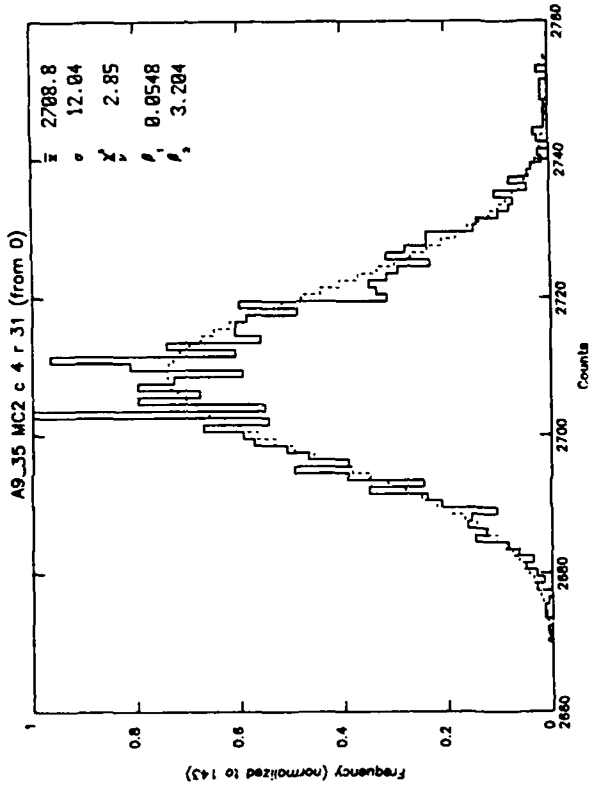
A9_35 MC2 c 4 r 31 (from 0)
Counts
Frequency (normalized to 143)
x̄ 2708.8
σ 12.04
χ²ν 2.85
β1 0.0548
β2 3.204

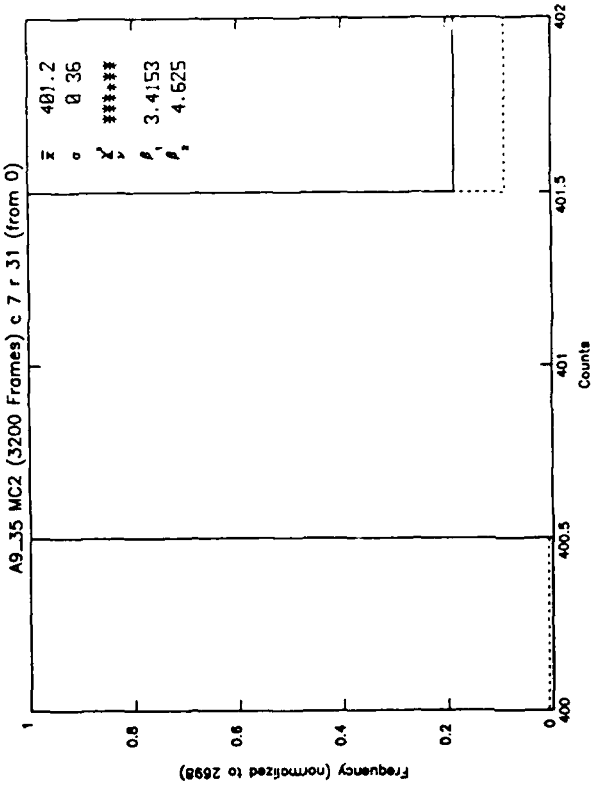
A9_35 MC2 (3200 Frames) c 7 r 31 (from 0)
Counts
Frequency (normalized to 2698)
x̄ 401.2
σ 0.36
χ²ν ******
β1 3.4153
β2 4.625

APPENDIX A-10

Array: Aerojet MC^2

	Left	Right
Elements:	Column 11; Rows 0-2, 15-17, 30, 31	Column 15, Rows 0-2, 15-17, 30, 31
Data Run:	Background a9_35	Background a9_35

Purpose: Comparison of column/row behavior for *normal background.* Compare also with Appendices A-8 and A-9 for other columns on the same run. The full set (A-8 to A-10) gives representative results across the whole array from top to bottom and left to right. Compare also with Appendices A-11 to A-13 from a different run.

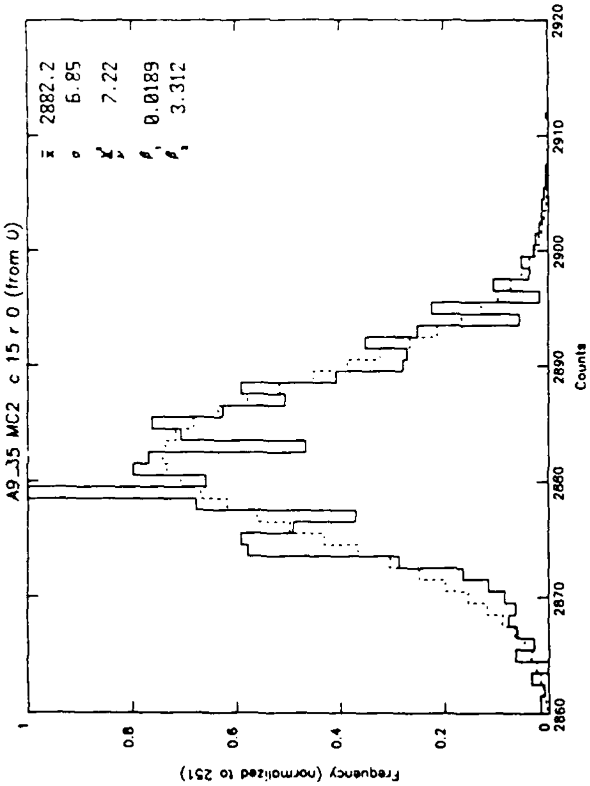

A9_35 MC2 c 15 r 0 (from 0)
x̄ 2882.2
σ 6.85
χ²ν 7.22
β1 0.0189
β2 3.312
Frequency (normalized to 251)
Counts

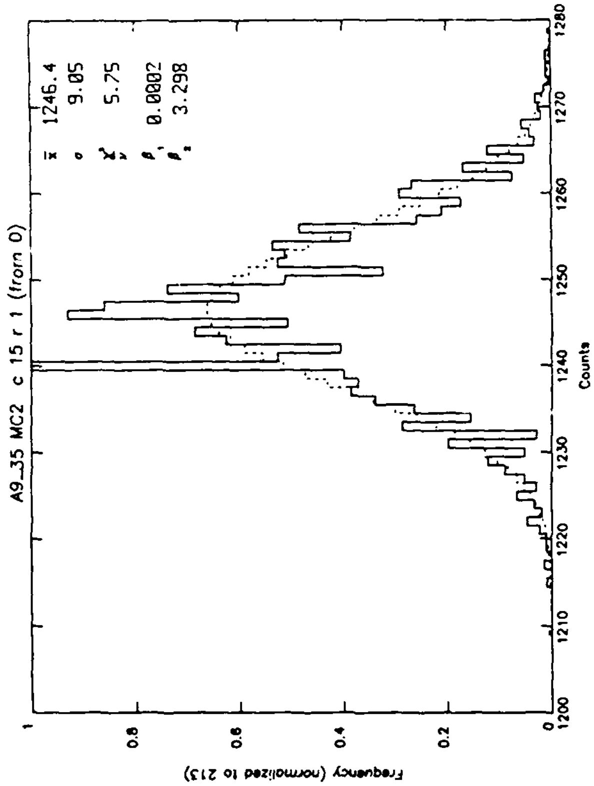

A9_35 MC2 c 15 r 1 (from 0)
x̄ 1246.4
σ 9.05
χ²ν 5.75
β1 0.0082
β2 3.298
Frequency (normalized to 213)
Counts

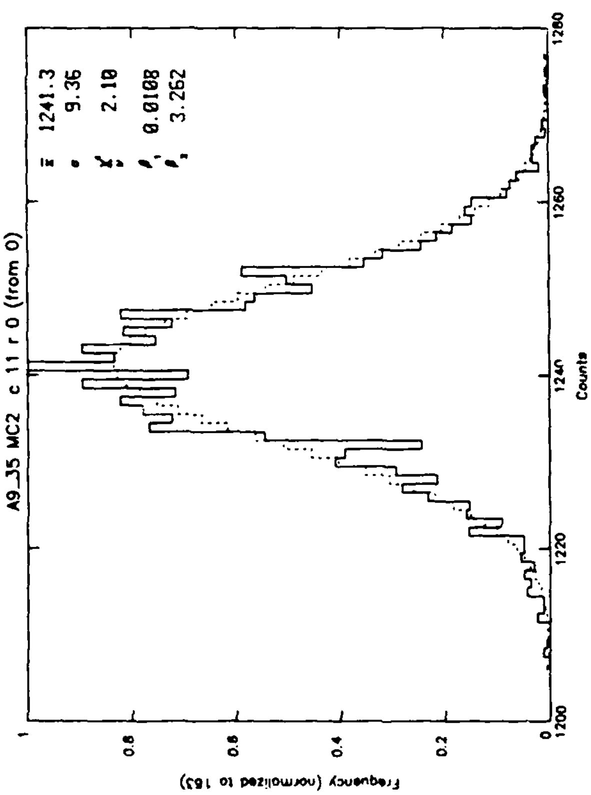

A9_35 MC2 c 11 r 0 (from 0)
x̄ 1241.3
σ 9.36
χ²ν 2.10
β1 0.0108
β2 3.262
Frequency (normalized to 163)
Counts

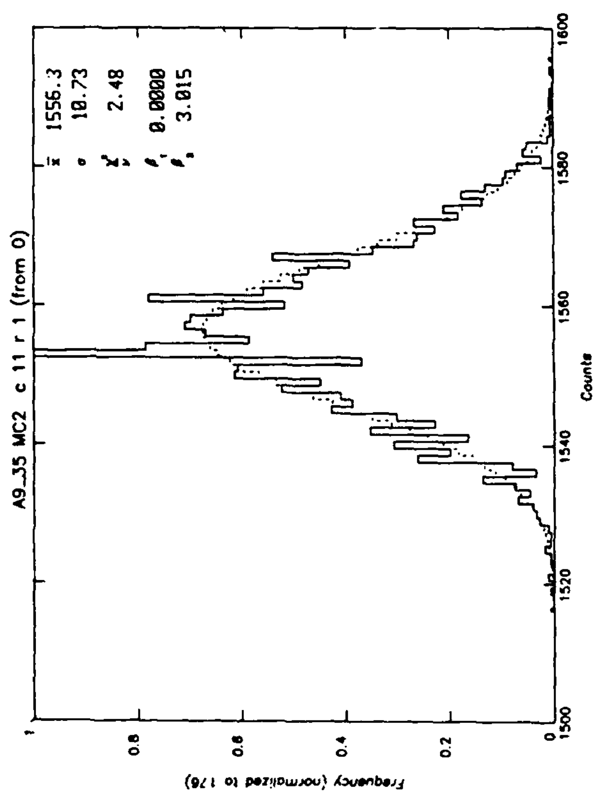

A9_35 MC2 c 11 r 1 (from 0)
x̄ 1556.3
σ 10.73
χ²ν 2.48
β1 0.0000
β2 3.015
Frequency (normalized to 176)
Counts

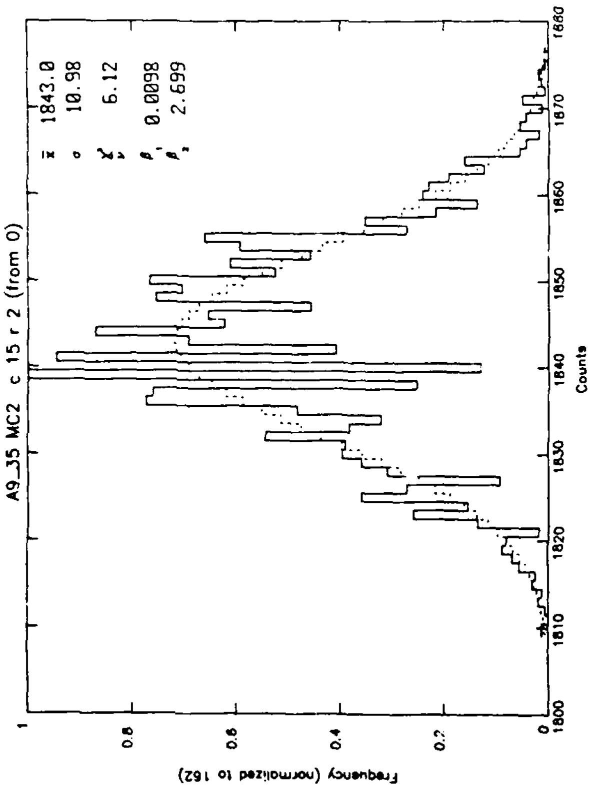
A9_35 MC2 c 15 r 2 (from 0)
x̄ 1843.0
σ 10.98
χ²ν 6.12
β₁ 0.0098
β₂ 2.699
Frequency (normalized to 162)
Counts

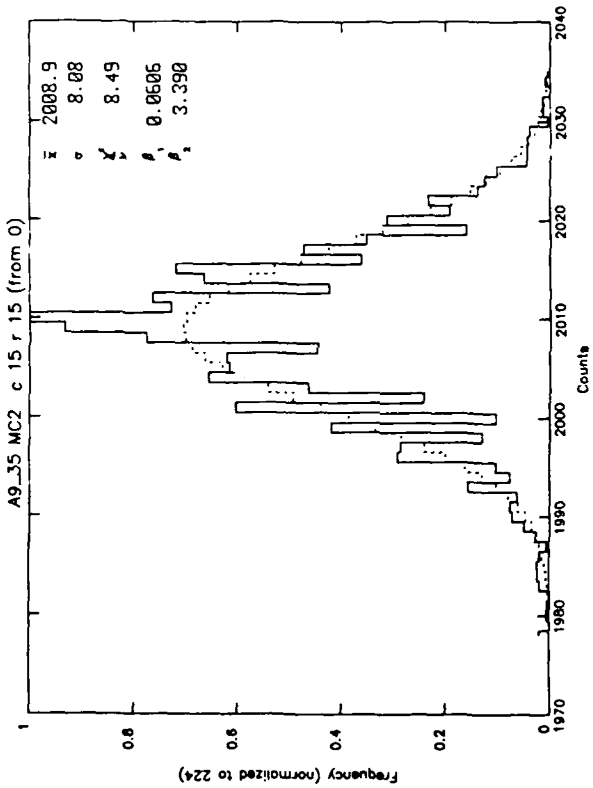
A9_35 MC2 c 15 r 15 (from 0)
x̄ 2008.9
σ 8.08
χ²ν 8.49
β₁ 0.0606
β₂ 3.390
Frequency (normalized to 224)
Counts

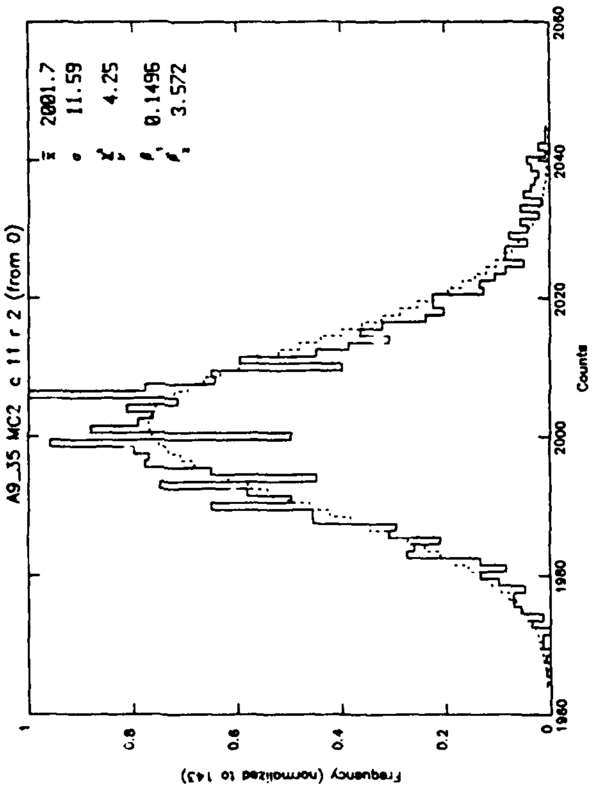
A9_35 MC2 c 11 r 2 (from 0)
x̄ 2001.7
σ 11.59
χ²ν 4.25
β₁ 0.1496
β₂ 3.572
Frequency (normalized to 143)
Counts

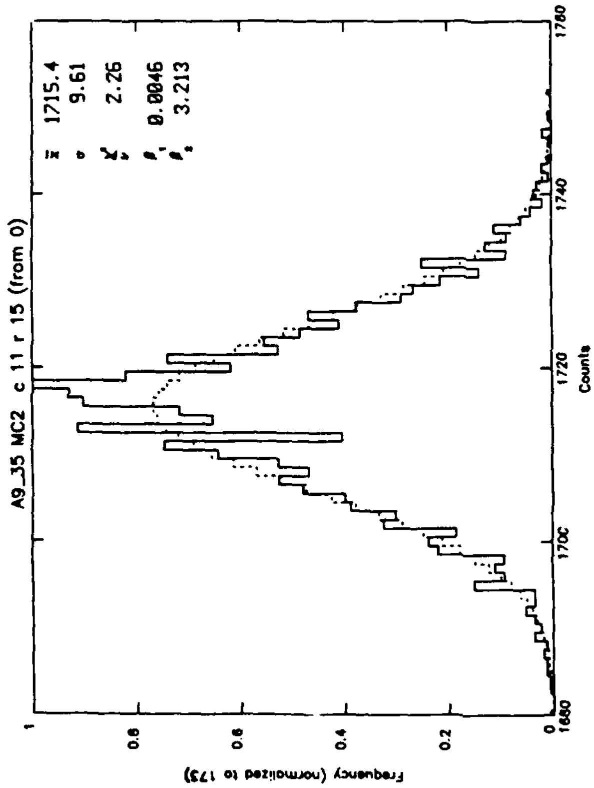
A9_35 MC2 c 11 r 15 (from 0)
x̄ 1715.4
σ 9.61
χ²ν 2.26
β₁ 0.0046
β₂ 3.213
Frequency (normalized to 173)
Counts

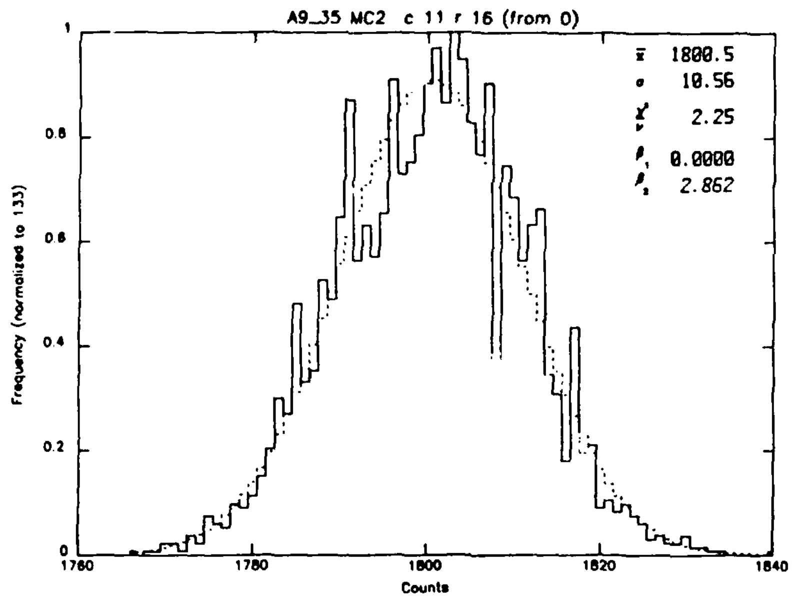
A9_35 MC2 c 11 r 16 (from 0)
$\bar{x}$ 1800.5
σ 10.56
χ^2_ν 2.25
β_1 0.0000
β_2 2.862
Frequency (normalized to 133)
Counts

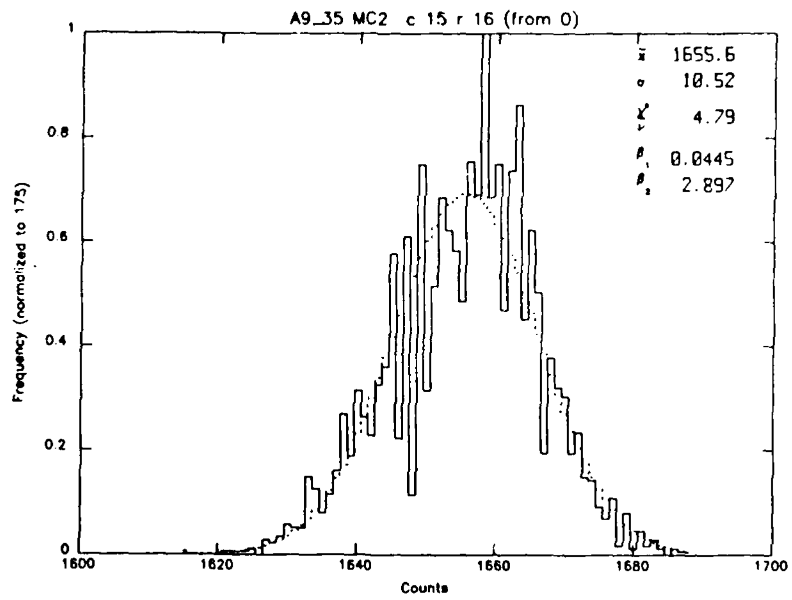
A9_35 MC2 c 15 r 16 (from 0)
$\bar{x}$ 1655.6
σ 10.52
χ^2_ν 4.79
β_1 0.0445
β_2 2.897
Frequency (normalized to 175)
Counts

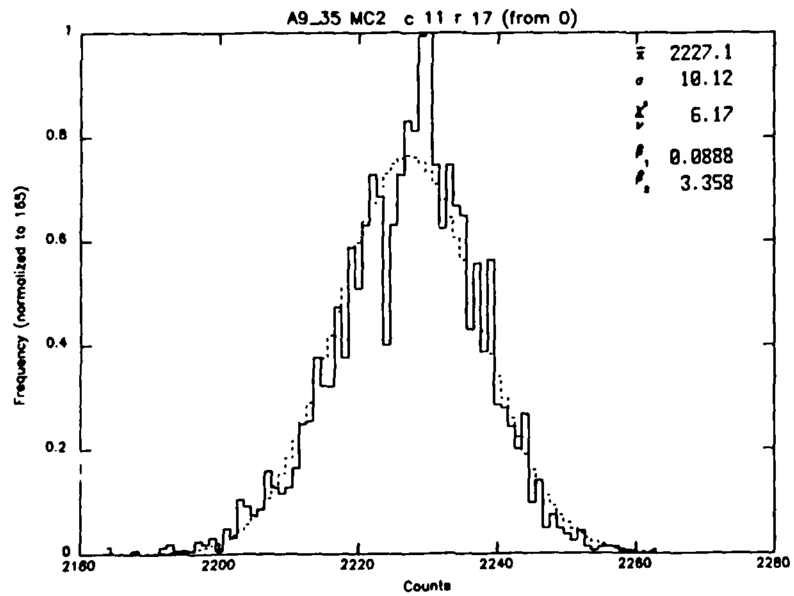
A9_35 MC2 c 11 r 17 (from 0)
$\bar{x}$ 2227.1
σ 10.12
χ^2_ν 6.17
β_1 0.0888
β_2 3.358
Frequency (normalized to 165)
Counts

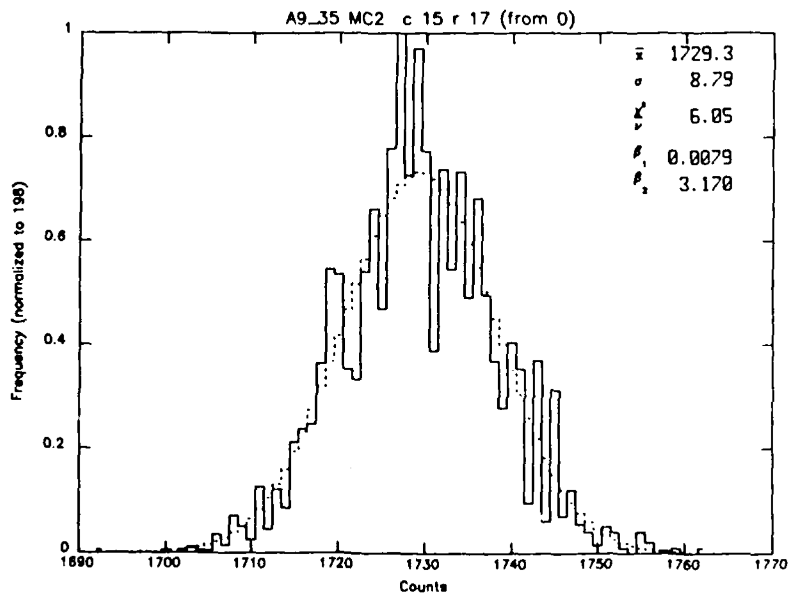
A9_35 MC2 c 15 r 17 (from 0)
$\bar{x}$ 1729.3
σ 8.79
χ^2_ν 6.05
β_1 0.0079
β_2 3.170
Frequency (normalized to 198)
Counts

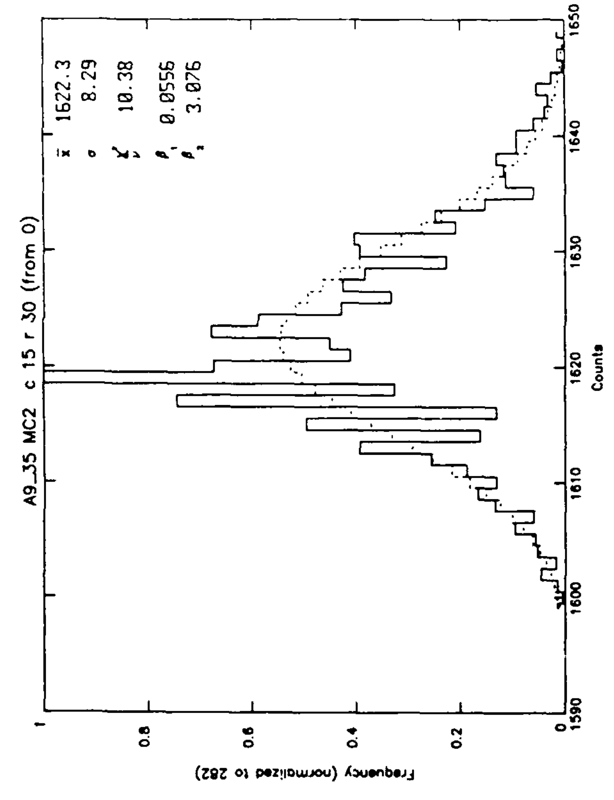
A9_35 MC2 c 15 r 30 (from 0)
x̄ 1622.3
σ 8.29
χ²ν 10.38
β1 0.0556
β2 3.076
Frequency (normalized to 282)
Counts

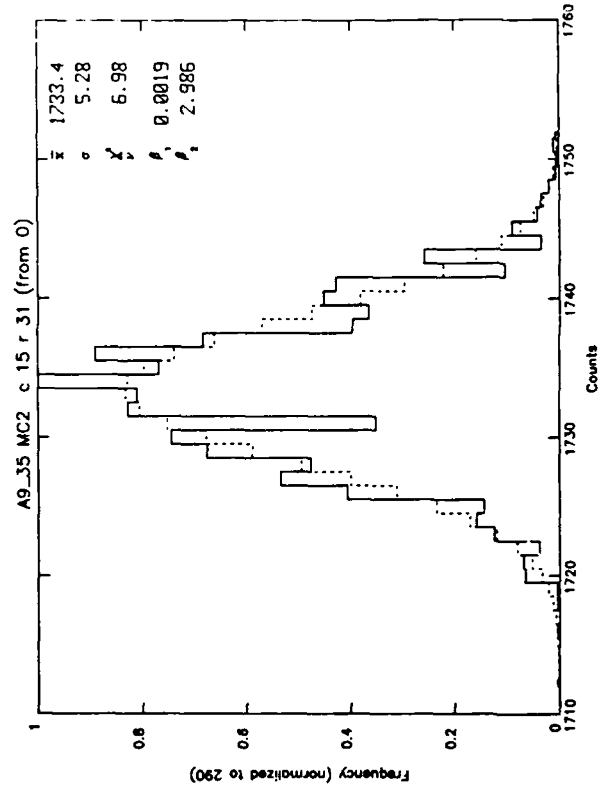
A9_35 MC2 c 15 r 31 (from 0)
x̄ 1733.4
σ 5.28
χ²ν 6.98
β1 0.0019
β2 2.986
Frequency (normalized to 290)
Counts

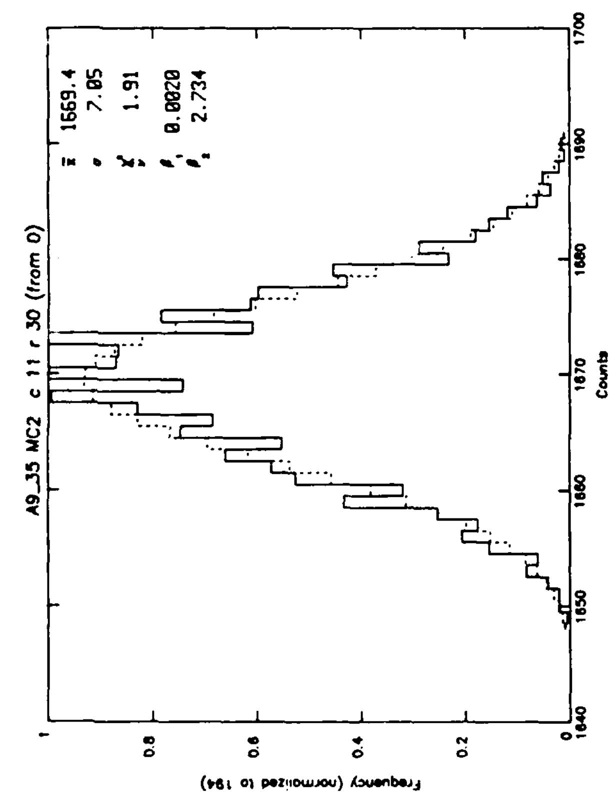
A9_35 MC2 c 11 r 30 (from 0)
x̄ 1669.4
σ 7.05
χ²ν 1.91
β1 0.0020
β2 2.734
Frequency (normalized to 194)
Counts

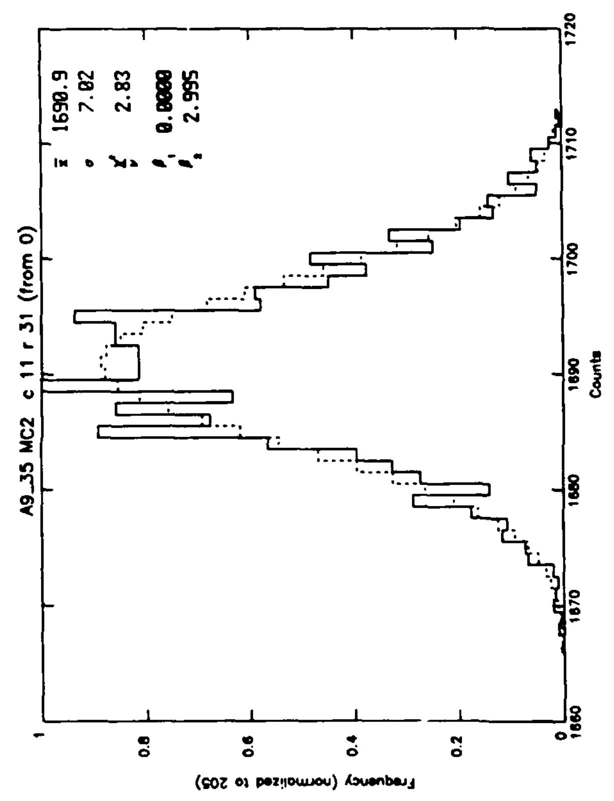
A9_35 MC2 c 11 r 31 (from 0)
x̄ 1690.9
σ 7.02
χ²ν 2.83
β1 0.0000
β2 2.995
Frequency (normalized to 205)
Counts

APPENDIX A-11

Array: Aerojet MC^2

	Left	Right
Elements:	Column 2; Rows 0-2, 15-17, 30, 31	Column 4, Rows 0-2, 15-17, 30, 31
Data Run:	Background a9_36	Background a9_36

Purpose: Comparison of column (both even)/row behavior for normal background. Compare also with Appendices A-12 and A-13 for other columns on the same run. The full set (A-11 to A-13) gives representative results across the whole array from top to bottom and left to right. Compare also with Appendices A-8 to A-10 from a different run.

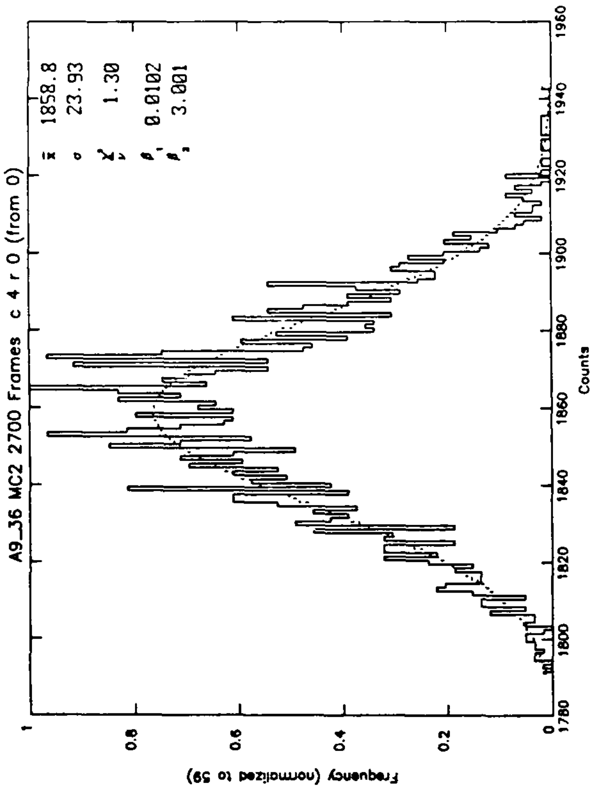
A9_36 MC2 2700 Frames c 4 r 0 (from 0)
Frequency (normalized to 59)
Counts
1780
1800
1820
1840
1860
1880
1900
1920
1940
1960
0
0.2
0.4
0.6
0.8
1
$\bar{x}$ 1858.8
σ 23.93
χ^2_ν 1.30
β_1 0.0102
β_2 3.001

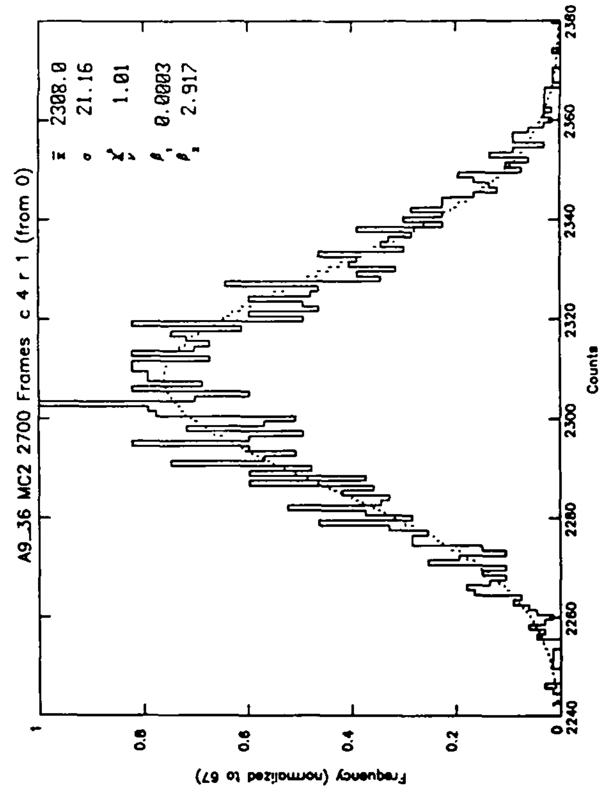
A9_36 MC2 2700 Frames c 4 r 1 (from 0)
Frequency (normalized to 67)
Counts
2240
2260
2280
2300
2320
2340
2360
2380
0
0.2
0.4
0.6
0.8
1
$\bar{x}$ 2308.0
σ 21.16
χ^2_ν 1.01
β_1 0.0003
β_2 2.917

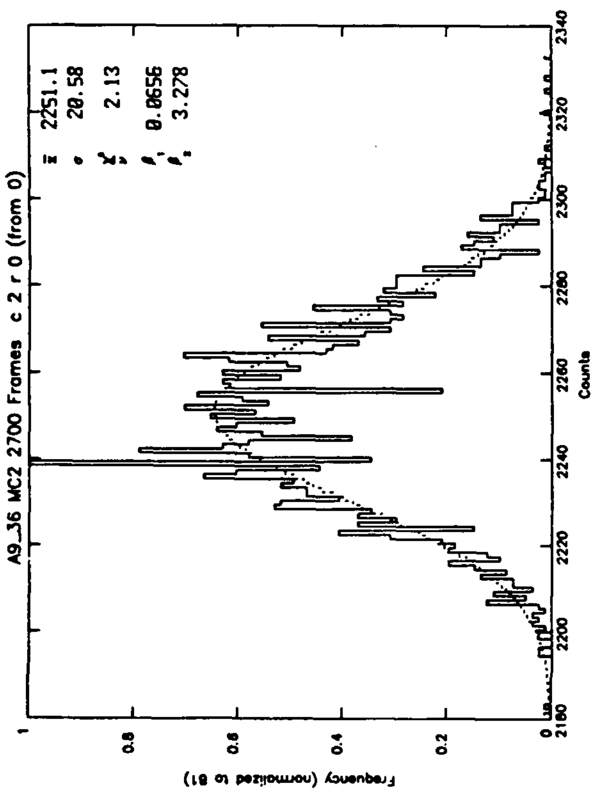
A9_36 MC2 2700 Frames c 2 r 0 (from 0)
Frequency (normalized to 61)
Counts
2180
2200
2220
2240
2260
2280
2300
2320
2340
0
0.2
0.4
0.6
0.8
1
$\bar{x}$ 2251.1
σ 20.58
χ^2_ν 2.13
β_1 0.0656
β_2 3.278

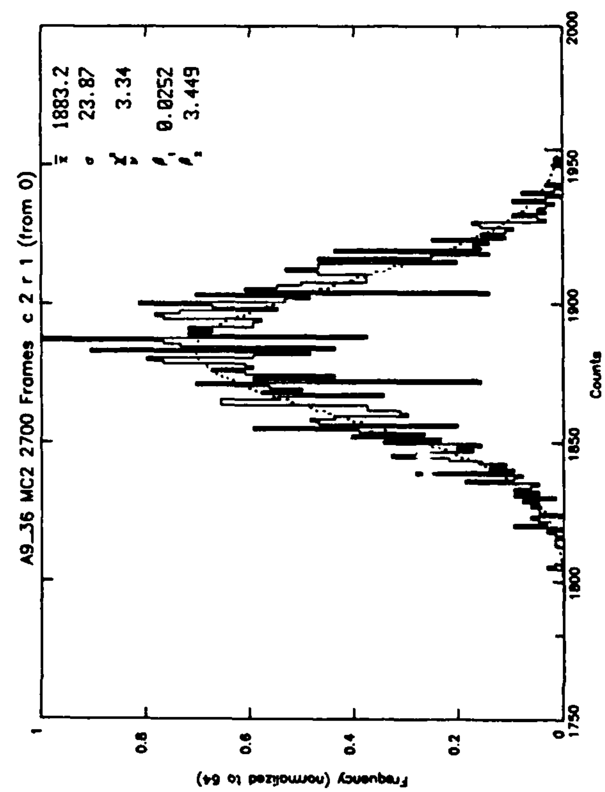
A9_36 MC2 2700 Frames c 2 r 1 (from 0)
Frequency (normalized to 64)
Counts
1750
1800
1850
1900
1950
2000
0
0.2
0.4
0.6
0.8
1
$\bar{x}$ 1883.2
σ 23.87
χ^2_ν 3.34
β_1 0.0252
β_2 3.449

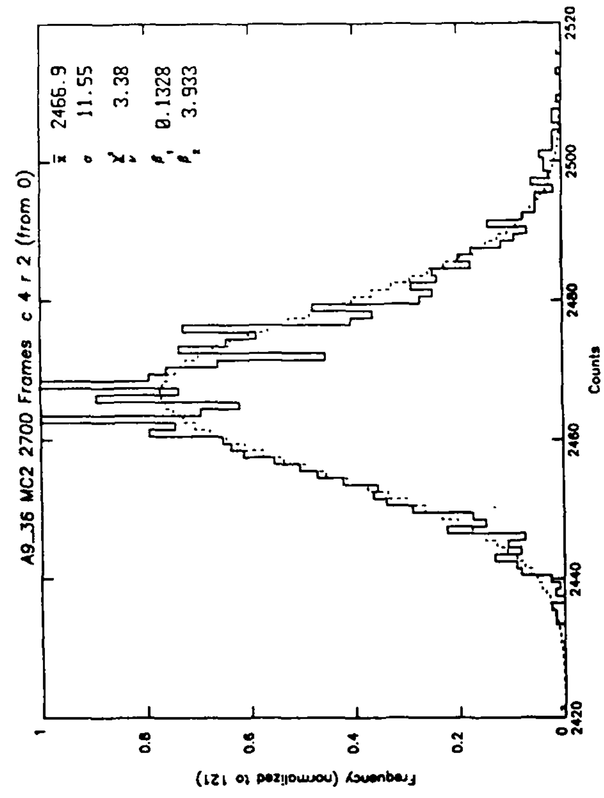
A9_36 MC2 2700 Frames c 4 r 2 (from 0)
x̄ 2466.9
σ 11.55
χ²ν 3.38
β1 0.1328
β2 3.933
Frequency (normalized to 121)
Counts

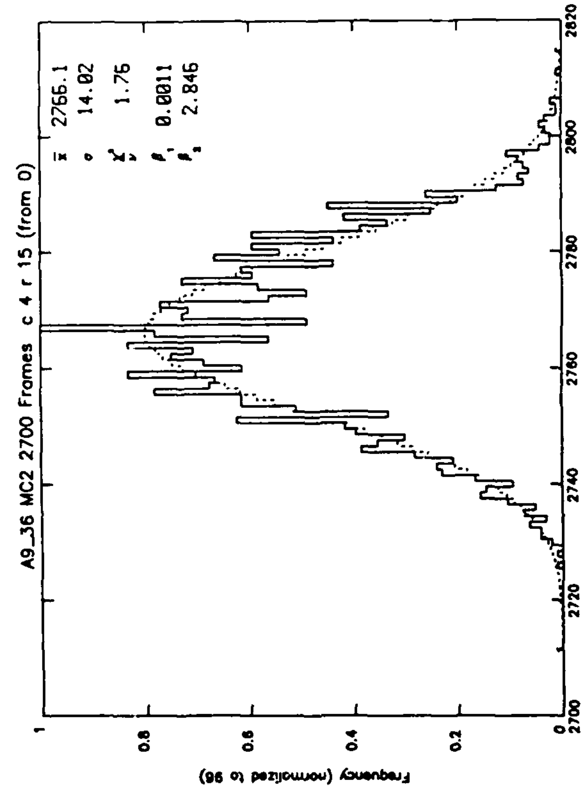
A9_36 MC2 2700 Frames c 4 r 15 (from 0)
x̄ 2766.1
σ 14.02
χ²ν 1.76
β1 0.0011
β2 2.846
Frequency (normalized to 96)
Counts

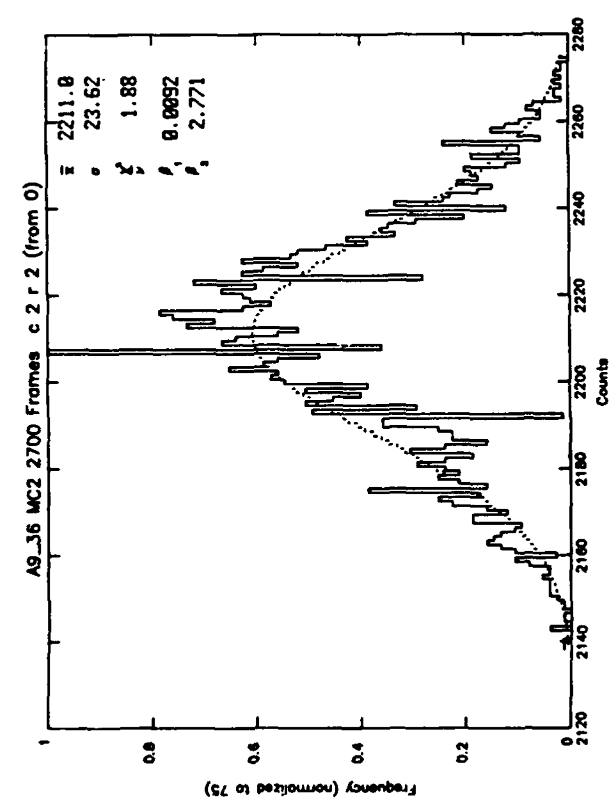
A9_36 MC2 2700 Frames c 2 r 2 (from 0)
x̄ 2211.0
σ 23.62
χ²ν 1.88
β1 0.0092
β2 2.771
Frequency (normalized to 73)
Counts

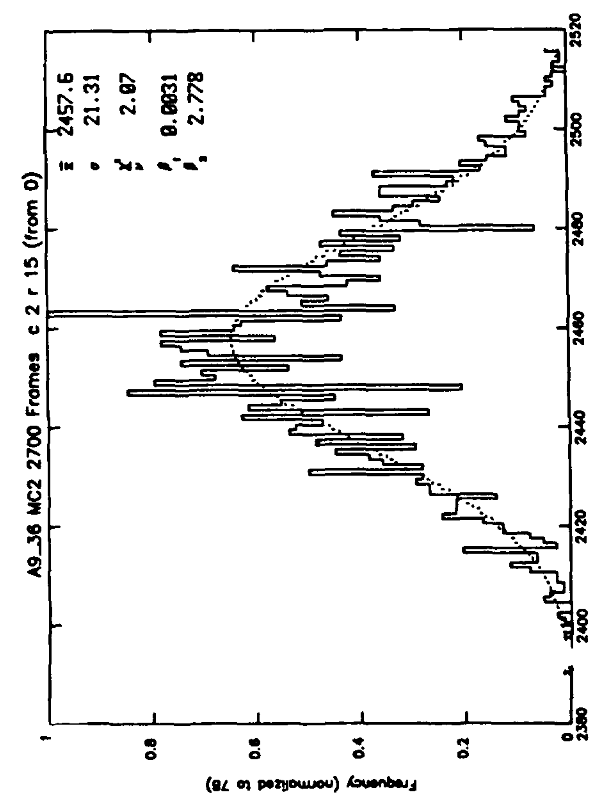
A9_36 MC2 2700 Frames c 2 r 15 (from 0)
x̄ 2457.6
σ 21.31
χ²ν 2.07
β1 0.0031
β2 2.778
Frequency (normalized to 78)
Counts

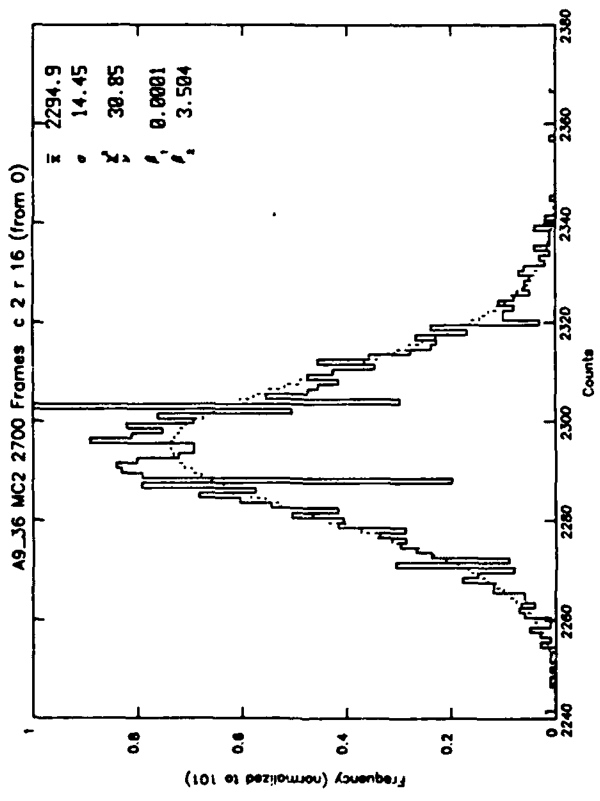
A9_36 MC2 2700 Frames c 2 r 16 (from 0)
x̄ 2294.9
σ 14.45
χ²ν 30.85
β1 0.0001
β2 3.504
Frequency (normalized to 101)
Counts

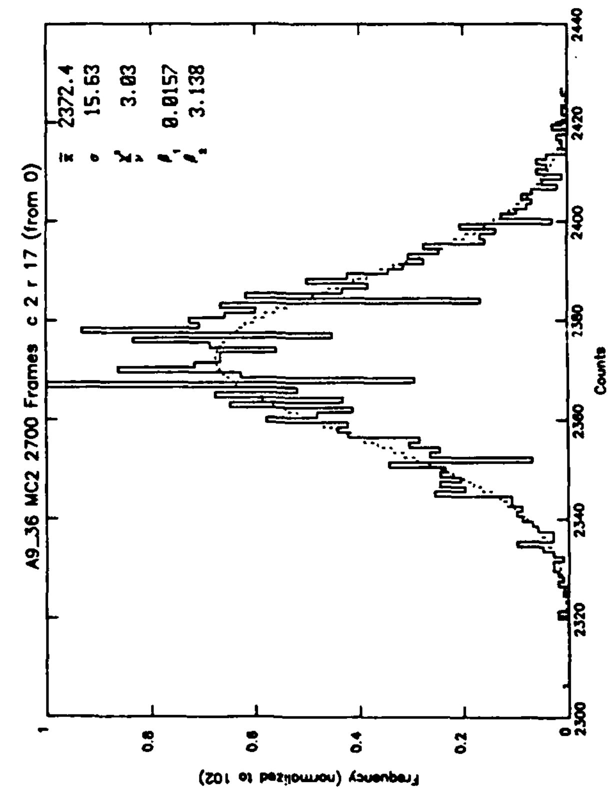
A9_36 MC2 2700 Frames c 2 r 17 (from 0)
x̄ 2372.4
σ 15.63
χ²ν 3.03
β1 0.0157
β2 3.138
Frequency (normalized to 102)
Counts

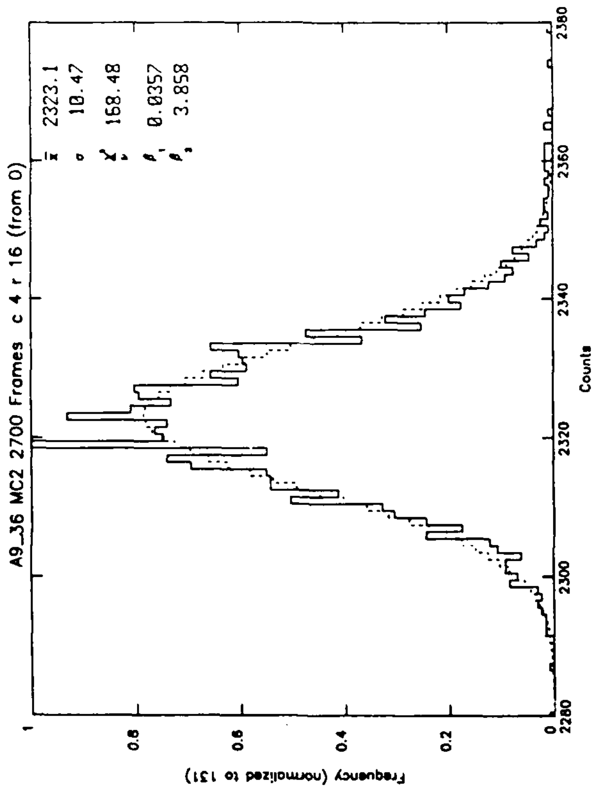
A9_36 MC2 2700 Frames c 4 r 16 (from 0)
x̄ 2323.1
σ 10.47
χ²ν 168.48
β1 0.0357
β2 3.858
Frequency (normalized to 131)
Counts

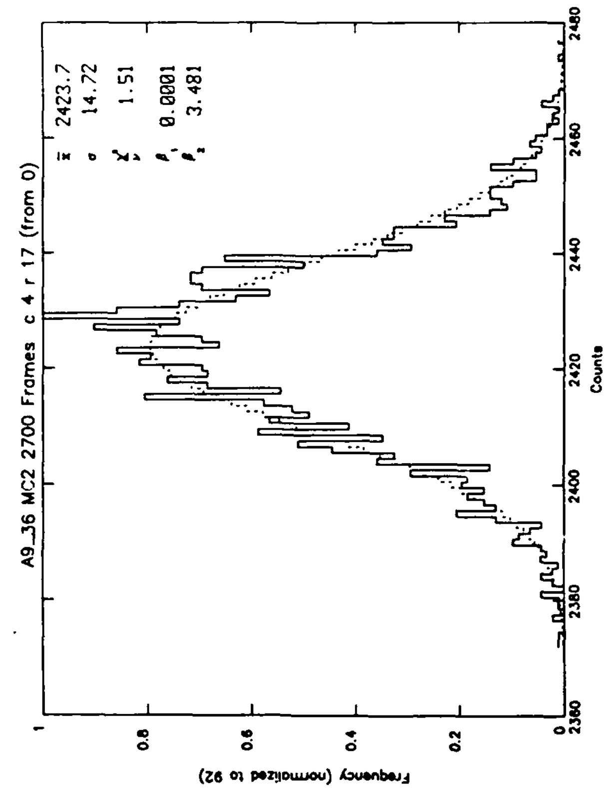
A9_36 MC2 2700 Frames c 4 r 17 (from 0)
x̄ 2423.7
σ 14.72
χ²ν 1.51
β1 0.0001
β2 3.481
Frequency (normalized to 92)
Counts

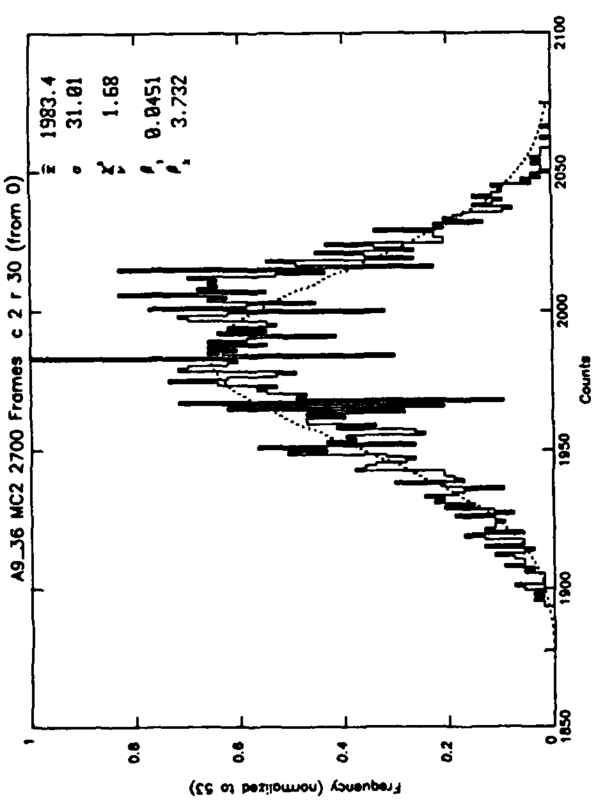
A9_36 MC2 2700 Frames c 2 r 30 (from 0)
1983.4
31.01
1.68
0.0451
3.732
Frequency (normalized to 53)
Counts

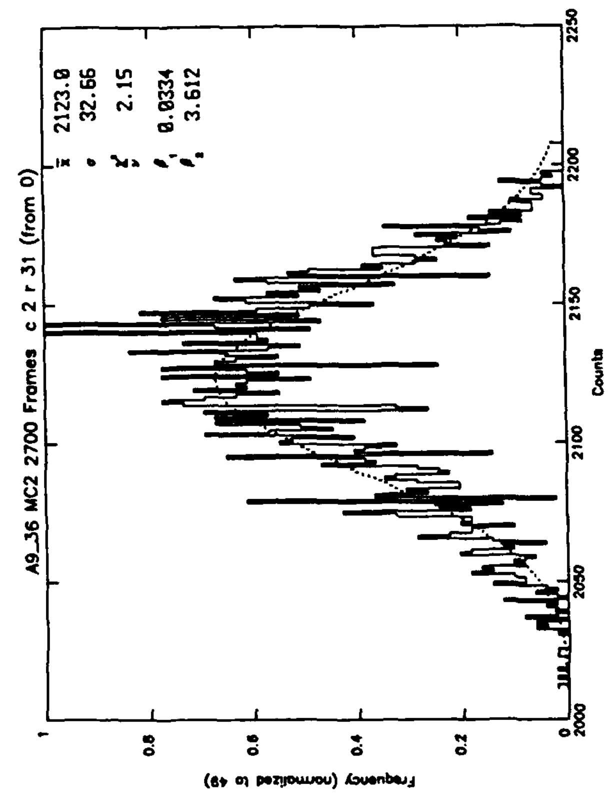
A9_36 MC2 2700 Frames c 2 r 31 (from 0)
2123.0
32.66
2.15
0.0334
3.612
Frequency (normalized to 49)
Counts

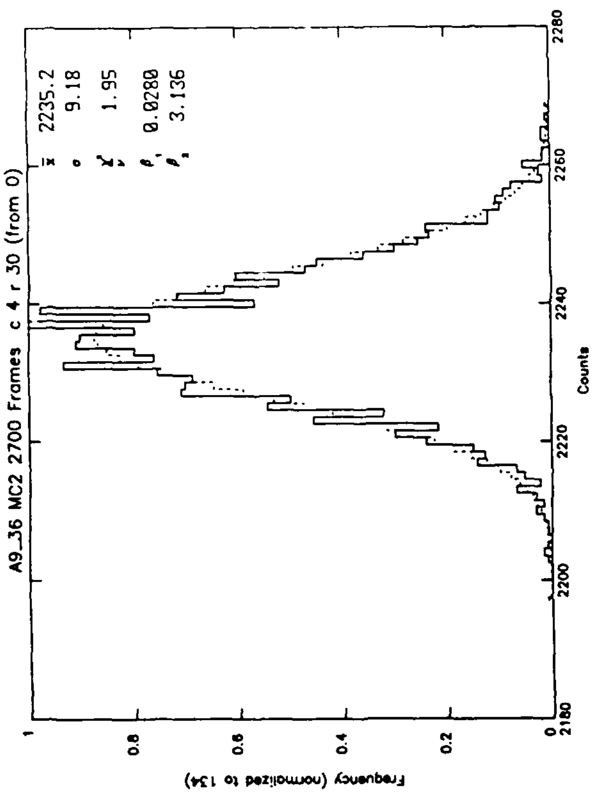
A9_36 MC2 2700 Frames c 4 r 30 (from 0)
2235.2
9.18
1.95
0.0280
3.136
Frequency (normalized to 134)
Counts

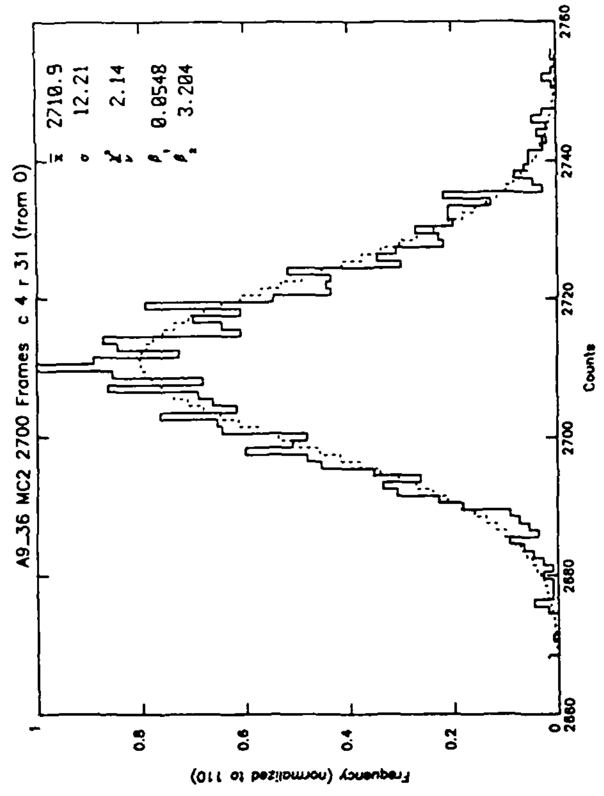
A9_36 MC2 2700 Frames c 4 r 31 (from 0)
2710.9
12.21
2.14
0.0548
3.204
Frequency (normalized to 110)
Counts

APPENDIX A-12

Array: Aerojet MC^2

	Left	Right
Elements:	Column 3; Rows 0-2, 15-17, 30, 31	Column 11, Rows 0-2, 15-17, 30, 31
Data Run:	Background a9_36	Background a9_36

Purpose: Comparison of column (from near left and near right sides of array)/row behavior for normal background. Compare also with Appendices A-11 and A-13 for other columns on the same run. The full set (A-11 to A-13) gives representative results across the whole array from top to bottom and left to right. Compare also with Appendices A-8 to A-10 from a different run.

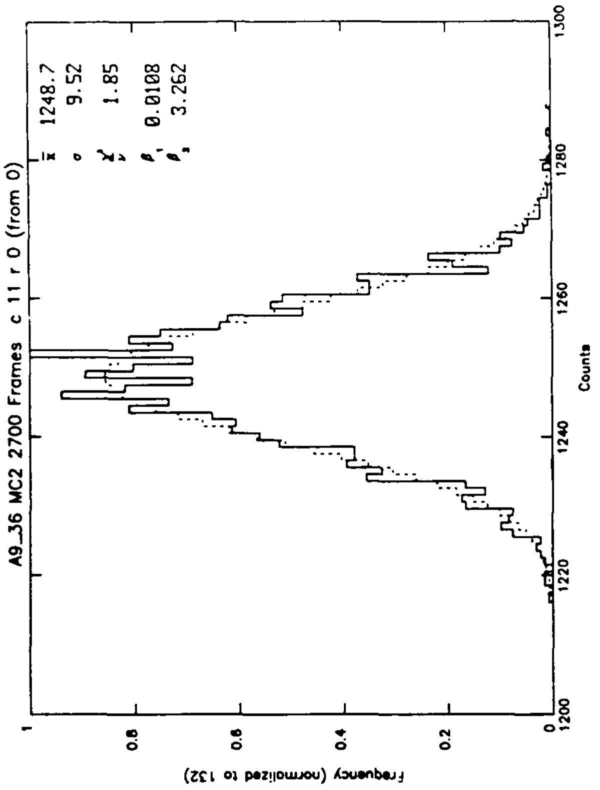
A9_36 MC2 2700 Frames c 11 r 0 (from 0)
x̄ 1248.7
σ 9.52
χ^2_ν 1.85
β_1 0.0108
β_2 3.262
Frequency (normalized to 132)
Counts

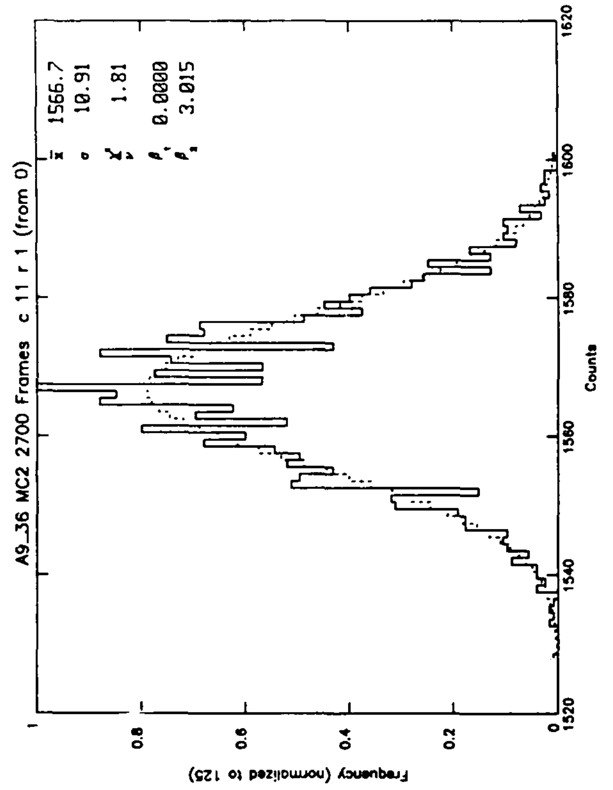
A9_36 MC2 2700 Frames c 11 r 1 (from 0)
x̄ 1566.7
σ 10.91
χ^2_ν 1.81
β_1 0.0000
β_2 3.015
Frequency (normalized to 125)
Counts

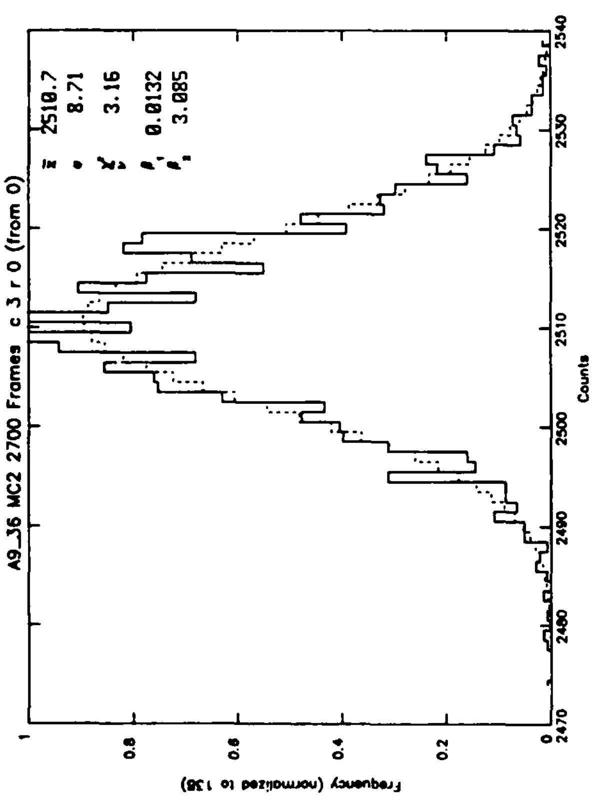
A9_36 MC2 2700 Frames c 3 r 0 (from 0)
x̄ 2510.7
σ 8.71
χ^2_ν 3.16
β_1 0.0132
β_2 3.085
Frequency (normalized to 136)
Counts

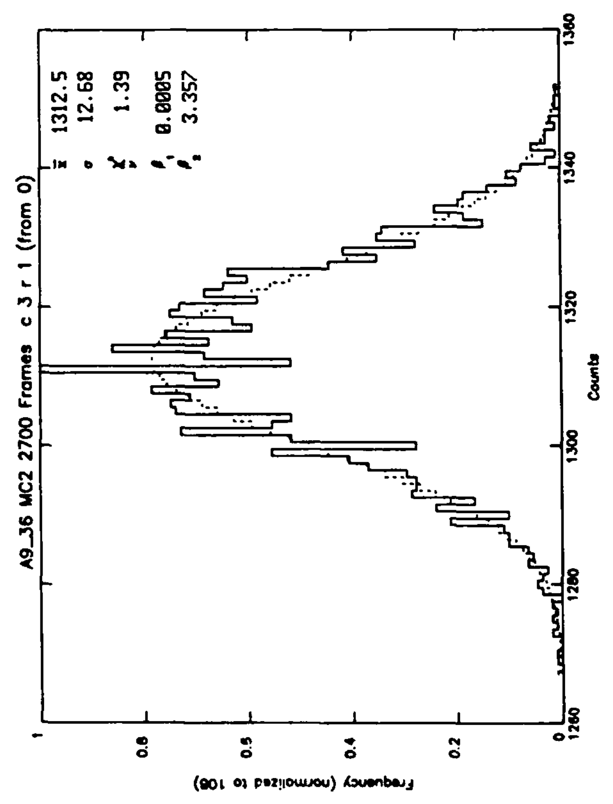
A9_36 MC2 2700 Frames c 3 r 1 (from 0)
x̄ 1312.5
σ 12.68
χ^2_ν 1.39
β_1 0.0005
β_2 3.357
Frequency (normalized to 108)
Counts

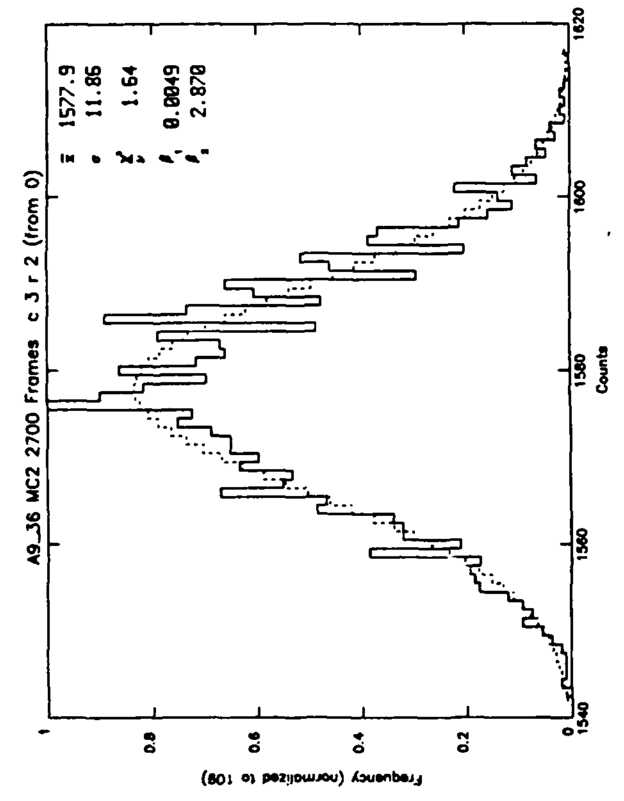
A9_36 MC2 2700 Frames c 3 r 2 (from 0)
x̄ 1577.9
σ 11.86
χ²ν 1.64
β1 0.0049
β2 2.870
Frequency (normalized to 108)
Counts

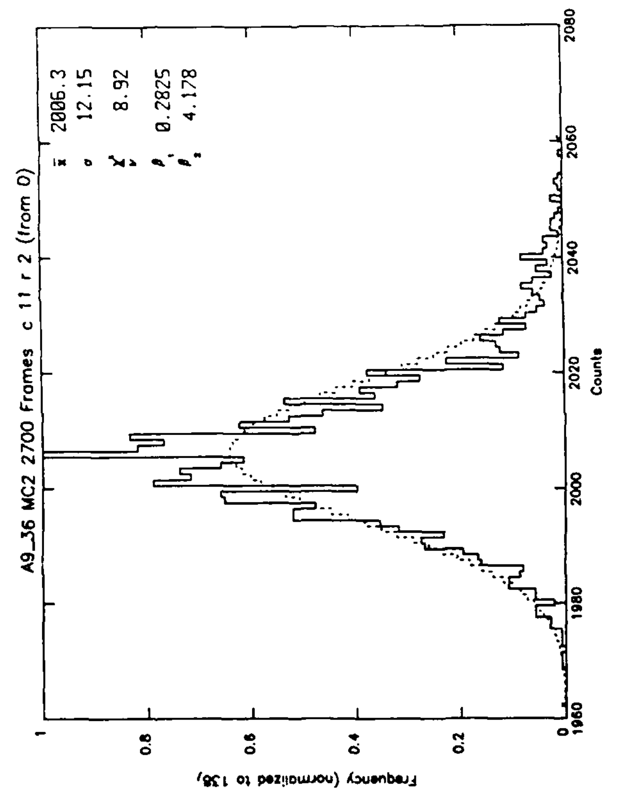
A9_36 MC2 2700 Frames c 11 r 2 (from 0)
x̄ 2006.3
σ 12.15
χ²ν 8.92
β1 0.2825
β2 4.178
Frequency (normalized to 138)
Counts

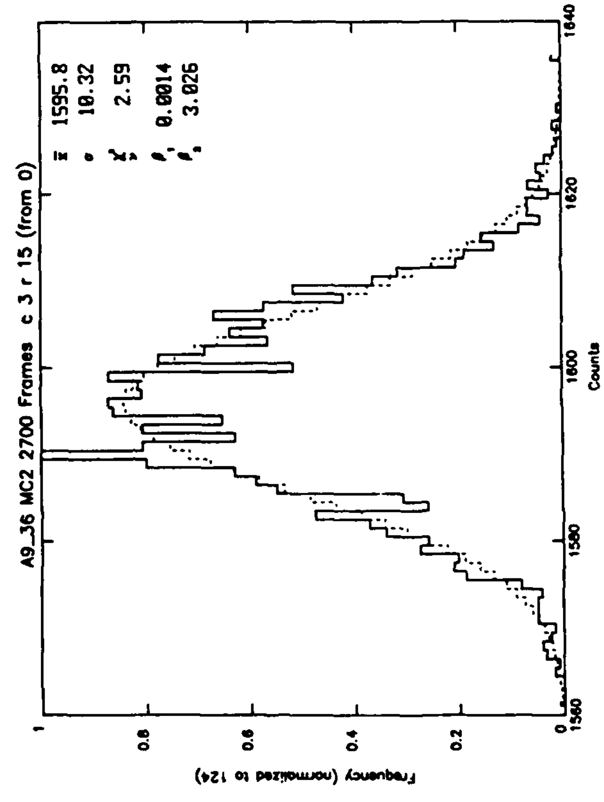
A9_36 MC2 2700 Frames c 3 r 15 (from 0)
x̄ 1595.8
σ 10.32
χ²ν 2.59
β1 0.0014
β2 3.026
Frequency (normalized to 124)
Counts

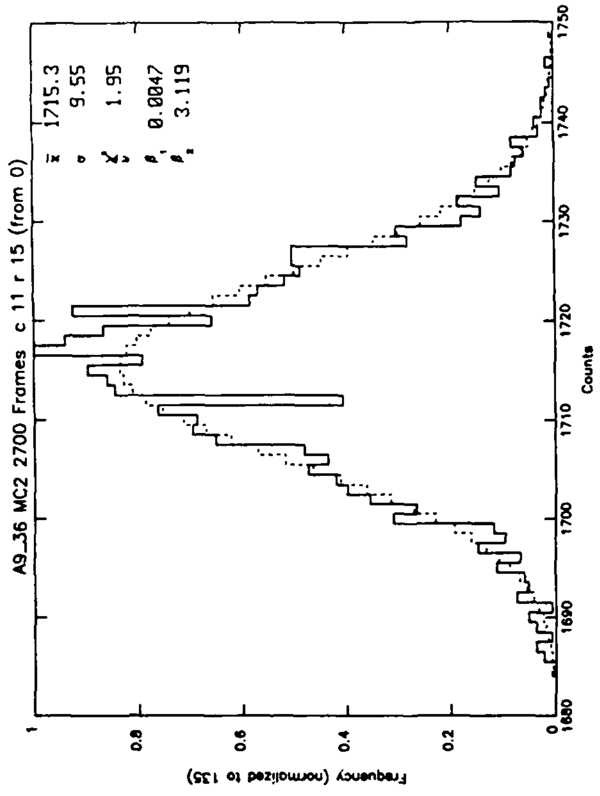
A9_36 MC2 2700 Frames c 11 r 15 (from 0)
x̄ 1715.3
σ 9.55
χ²ν 1.95
β1 0.0047
β2 3.119
Frequency (normalized to 135)
Counts

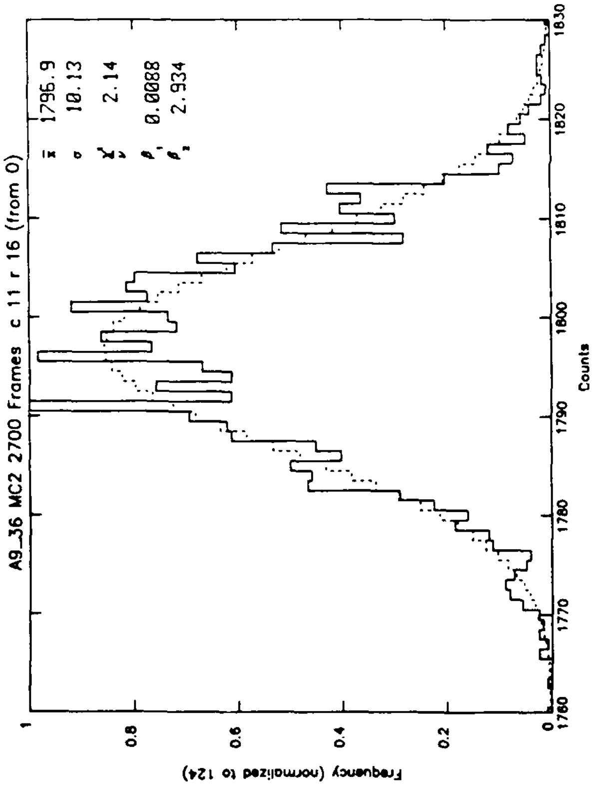
A9_36 MC2 2700 Frames c 11 r 16 (from 0)
x̄ 1796.9
σ 10.13
χ^2_ν 2.14
β_1 0.0088
β_2 2.934
Frequency (normalized to 124)
Counts

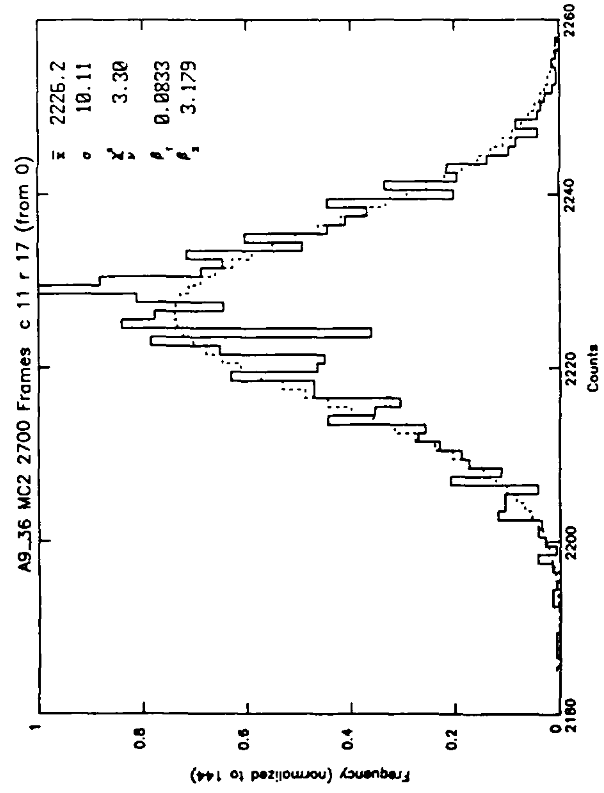
A9_36 MC2 2700 Frames c 11 r 17 (from 0)
x̄ 2226.2
σ 10.11
χ^2_ν 3.30
β_1 0.0833
β_2 3.179
Frequency (normalized to 144)
Counts

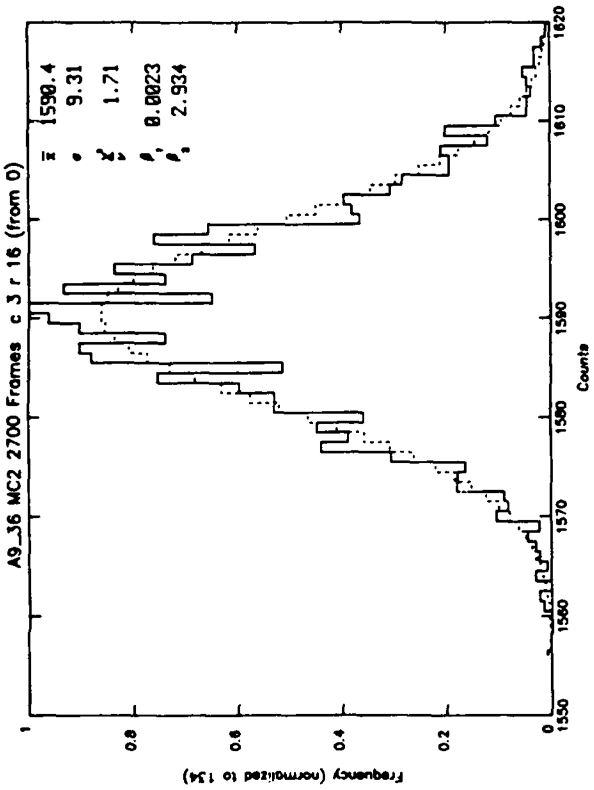
A9_36 MC2 2700 Frames c 3 r 16 (from 0)
x̄ 1590.4
σ 9.31
χ^2_ν 1.71
β_1 0.0023
β_2 2.934
Frequency (normalized to 134)
Counts

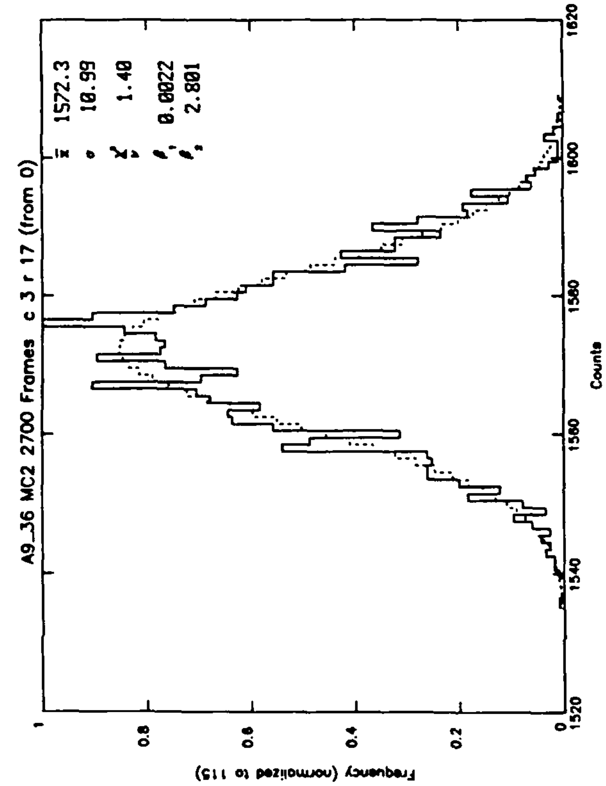
A9_36 MC2 2700 Frames c 3 r 17 (from 0)
x̄ 1572.3
σ 10.99
χ^2_ν 1.40
β_1 0.0022
β_2 2.801
Frequency (normalized to 115)
Counts

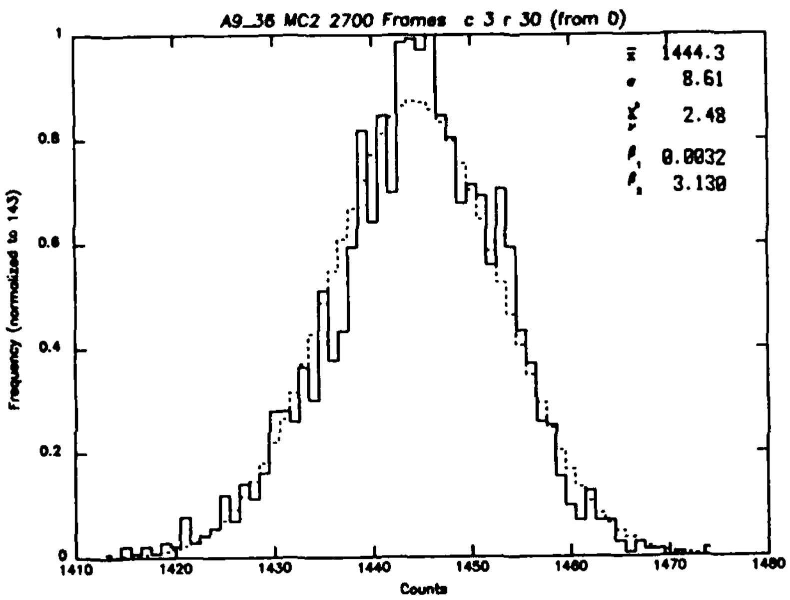
A9_36 MC2 2700 Frames c 3 r 30 (from 0)
$\bar{x}$ 1444.3
σ 8.61
χ^2_ν 2.48
β_1 0.0032
β_2 3.130
Frequency (normalized to 143)
Counts

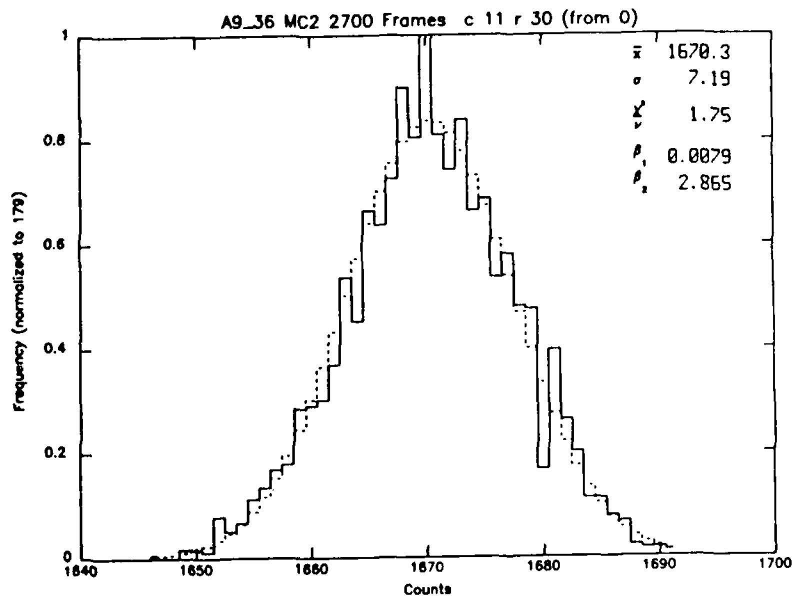
A9_36 MC2 2700 Frames c 11 r 30 (from 0)
$\bar{x}$ 1670.3
σ 7.19
χ^2_ν 1.75
β_1 0.0079
β_2 2.865
Frequency (normalized to 179)
Counts

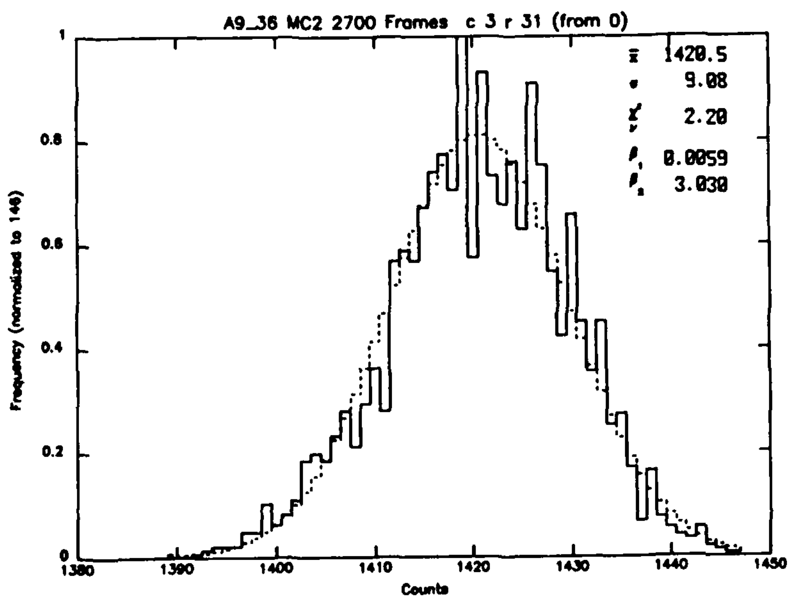
A9_36 MC2 2700 Frames c 3 r 31 (from 0)
$\bar{x}$ 1420.5
σ 9.08
χ^2_ν 2.20
β_1 0.0059
β_2 3.030
Frequency (normalized to 146)
Counts

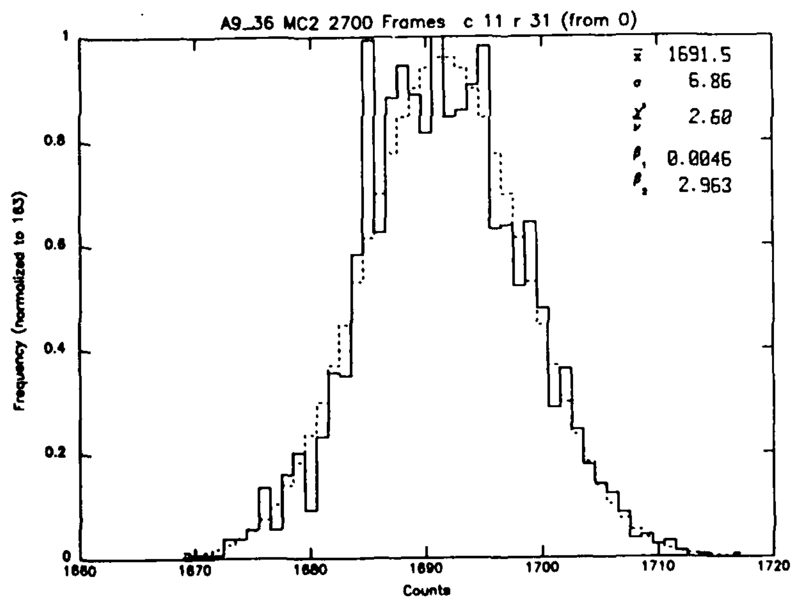
A9_36 MC2 2700 Frames c 11 r 31 (from 0)
$\bar{x}$ 1691.5
σ 6.86
χ^2_ν 2.60
β_1 0.0046
β_2 2.963
Frequency (normalized to 163)
Counts

APPENDIX A-13

Array: Aerojet MC^2

	Left	Right
Elements:	Column 7; Rows 0-2, 15-17, 30, 31	Column 15, Rows 0-2, 15-17, 30, 31
Data Run:	Background a9_36	Background a9_36

Purpose: Comparison of column/row for normal background. Note that column 7 was abnormal with 1) low count values, and 2) all samples falling in one or two count bins. Column 15 is normal as can be seen from comparison with Appendices A-12 and A-13 for other columns on the same run. Compare also with Appendices A-11 and A-13 for other columns on the same run. The full set (A-11 to A-13) gives representative results across the whole array from top to bottom and left to right. Compare also with Appendices A-8 to A-10 from a different run.

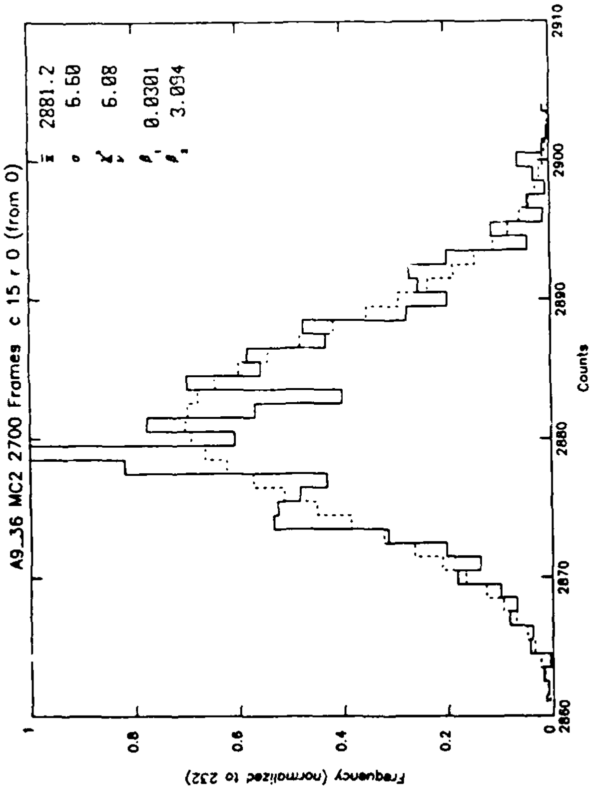
A9_36 MC2 2700 Frames c 15 r 0 (from 0)
2881.2
6.60
6.08
0.0301
3.094
Counts
Frequency (normalized to 232)

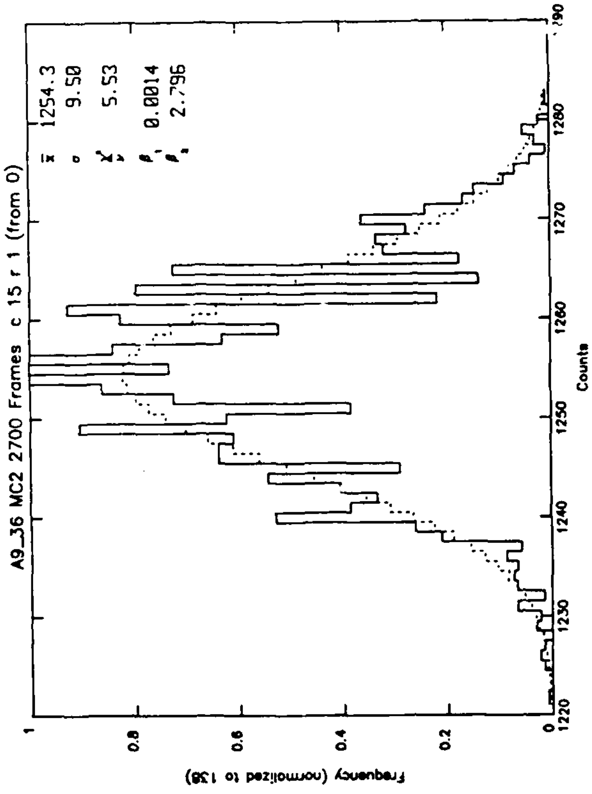
A9_36 MC2 2700 Frames c 15 r 1 (from 0)
1254.3
9.50
5.53
0.0014
2.796
Counts
Frequency (normalized to 138)

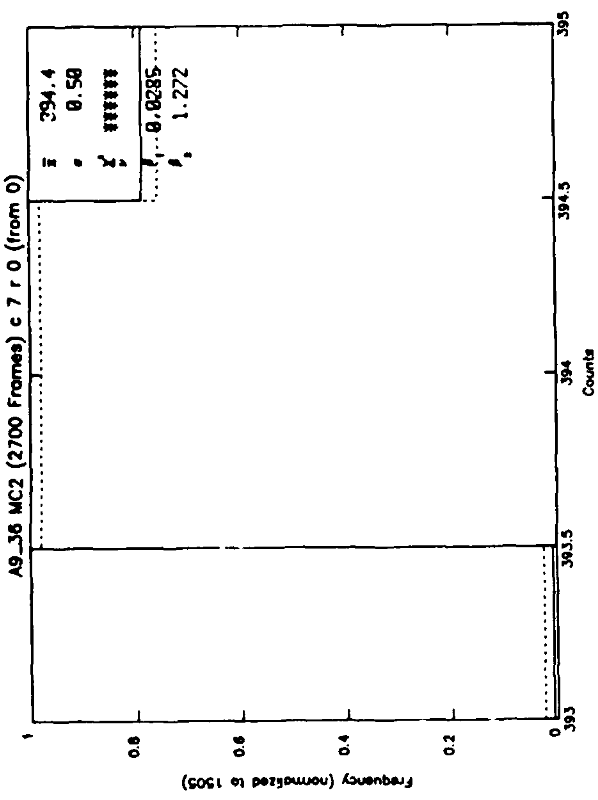
A9_36 MC2 (2700 Frames) c 7 r 0 (from 0)
394.4
0.50
######
0.0285
1.272
Counts
Frequency (normalized to 1503)

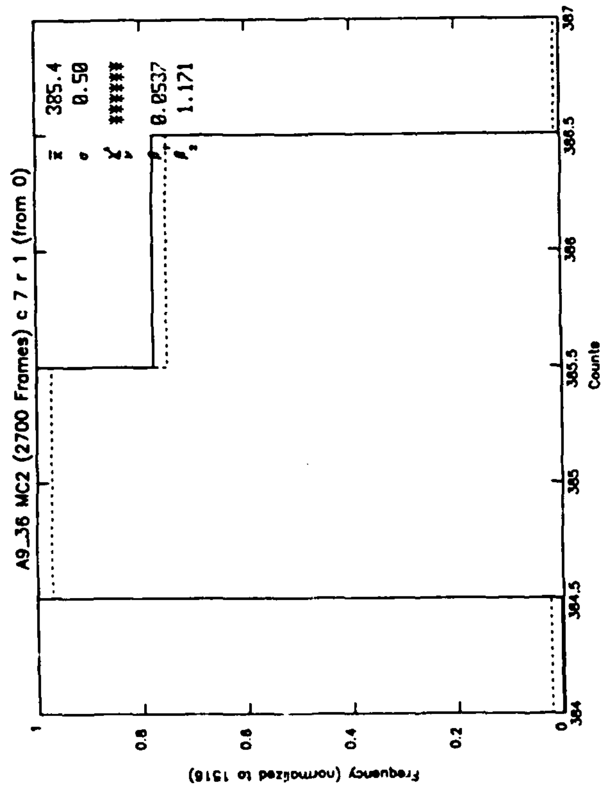
A9_36 MC2 (2700 Frames) c 7 r 1 (from 0)
385.4
0.50
######
0.0537
1.171
Counts
Frequency (normalized to 1318)

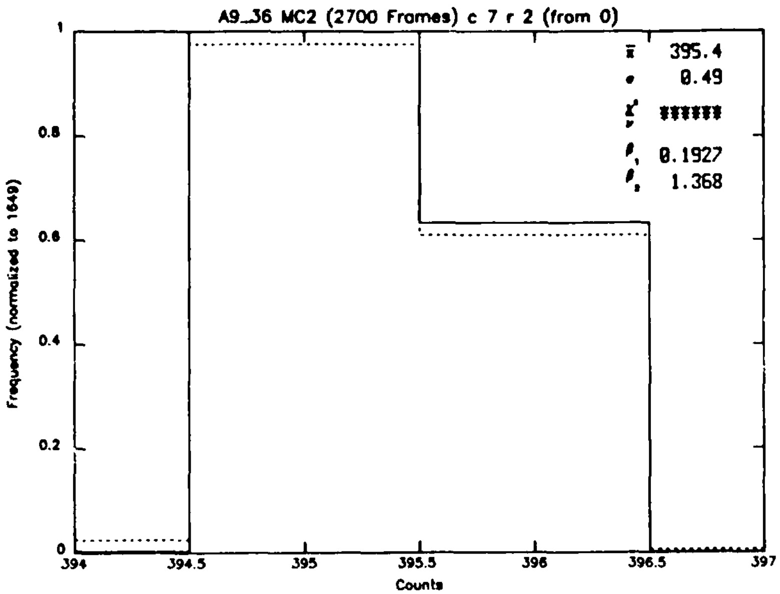
A9_36 MC2 (2700 Frames) c 7 r 2 (from 0)
x̄ 395.4
σ 0.49
χ²ν ######
β1 0.1927
β2 1.368
Frequency (normalized to 1649)
Counts

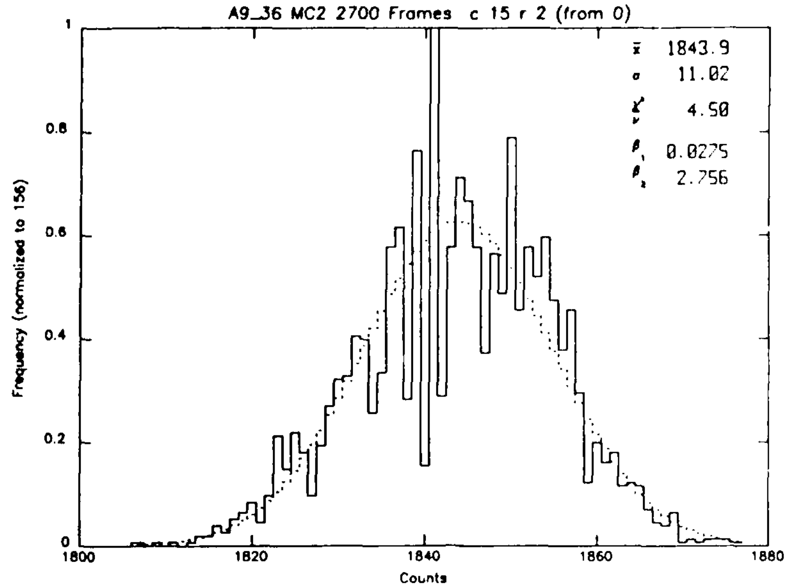
A9_36 MC2 2700 Frames c 15 r 2 (from 0)
x̄ 1843.9
σ 11.02
χ²ν 4.50
β1 0.0275
β2 2.756
Frequency (normalized to 156)
Counts

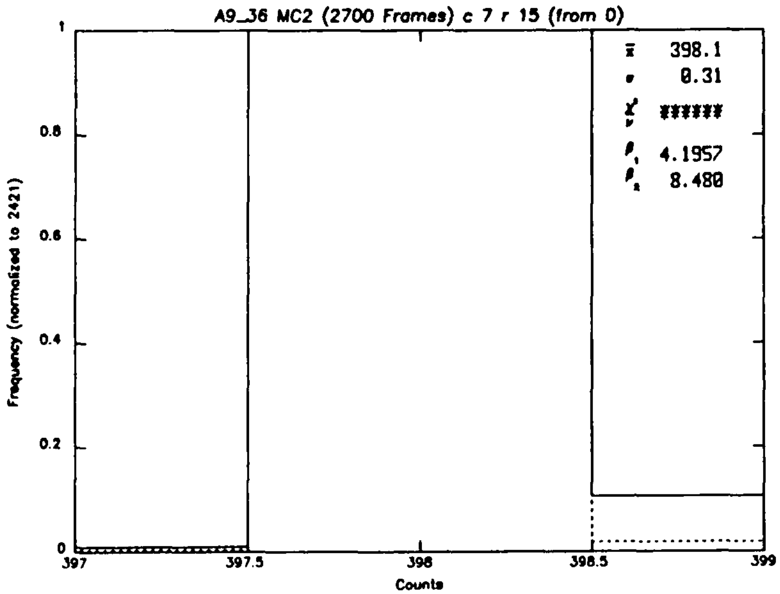
A9_36 MC2 (2700 Frames) c 7 r 15 (from 0)
x̄ 398.1
σ 0.31
χ²ν ######
β1 4.1957
β2 8.480
Frequency (normalized to 2421)
Counts

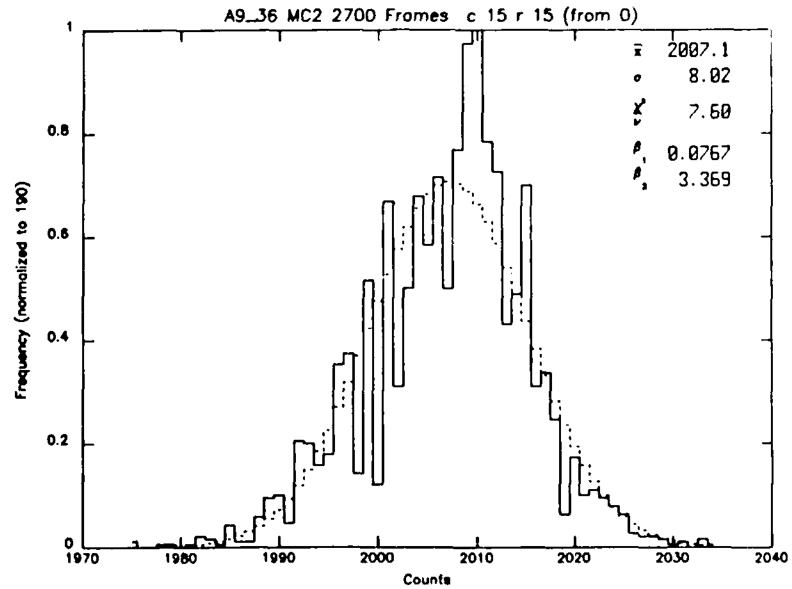
A9_36 MC2 2700 Frames c 15 r 15 (from 0)
x̄ 2007.1
σ 8.02
χ²ν 7.60
β1 0.0767
β2 3.369
Frequency (normalized to 190)
Counts

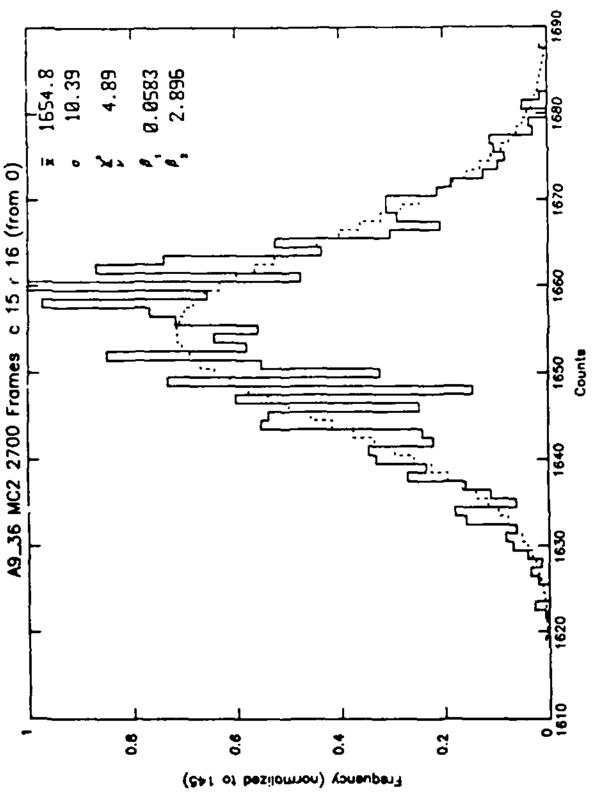
A9_36 MC2 2700 Frames c 15 r 16 (from 0)
Frequency (normalized to 145)
Counts
x̄ 1654.8
σ 10.39
χ²ν 4.89
β1 0.0583
β2 2.896

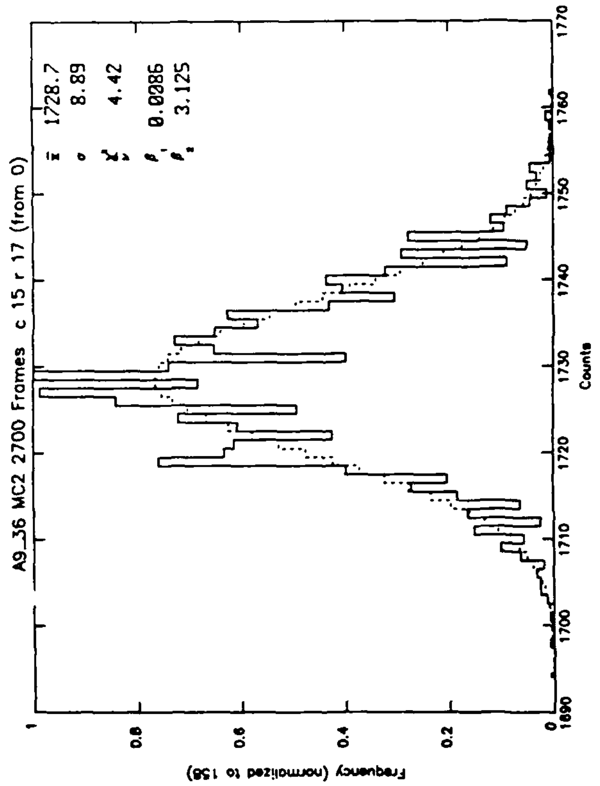
A9_36 MC2 2700 Frames c 15 r 17 (from 0)
Frequency (normalized to 158)
Counts
x̄ 1728.7
σ 8.89
χ²ν 4.42
β1 0.0086
β2 3.125

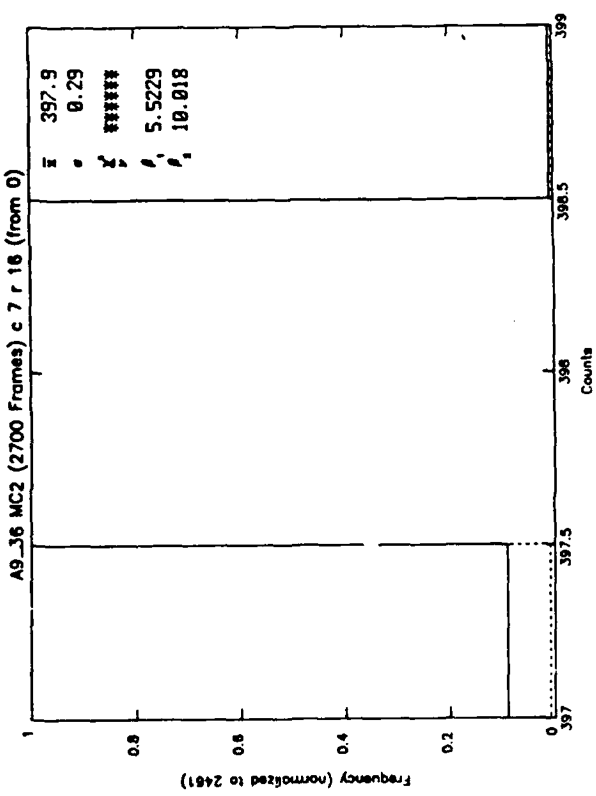
A9_36 MC2 (2700 Frames) c 7 r 16 (from 0)
Frequency (normalized to 2461)
Counts
x̄ 397.9
σ 0.29
χ²ν ******
β1 5.5229
β2 10.018

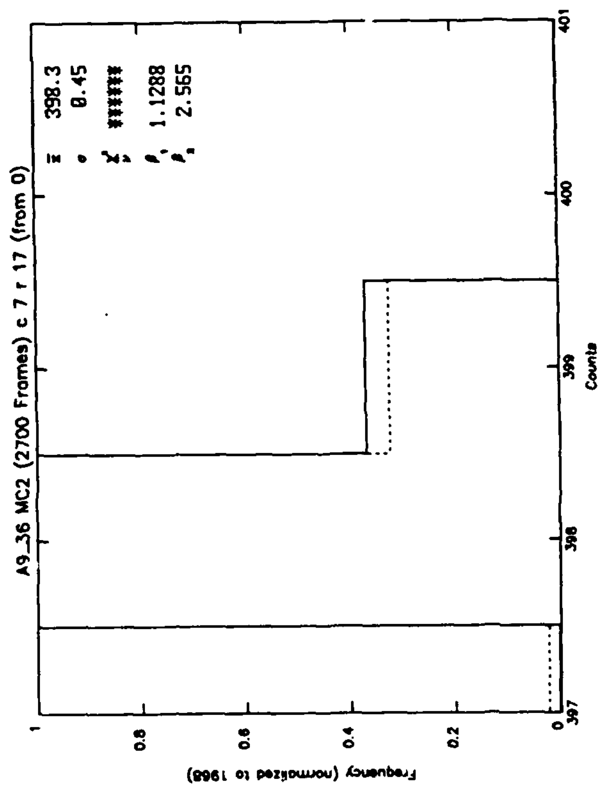
A9_36 MC2 (2700 Frames) c 7 r 17 (from 0)
Frequency (normalized to 1968)
Counts
x̄ 398.3
σ 0.45
χ²ν ******
β1 1.1288
β2 2.565

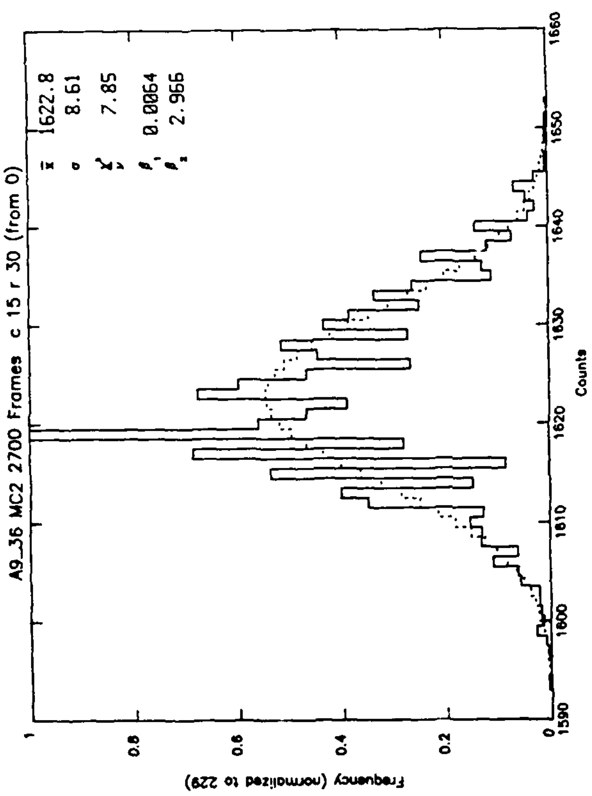
A9_36 MC2 2700 Frames c 15 r 30 (from 0)
x̄ 1622.8
σ 8.61
χ^2_ν 7.85
ρ_1 0.0064
ρ_2 2.966
Counts
Frequency (normalized to 229)

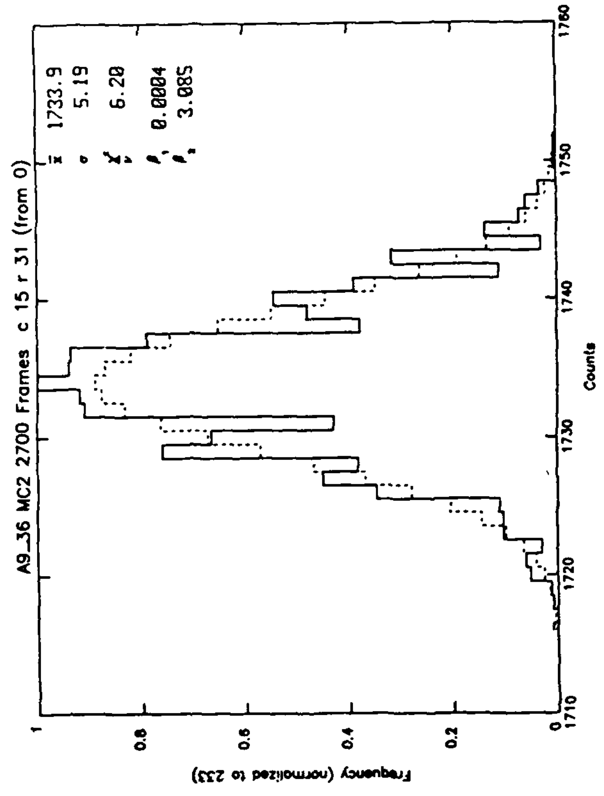
A9_36 MC2 2700 Frames c 15 r 31 (from 0)
x̄ 1733.9
σ 5.19
χ^2_ν 6.20
ρ_1 0.0004
ρ_2 3.085
Counts
Frequency (normalized to 233)

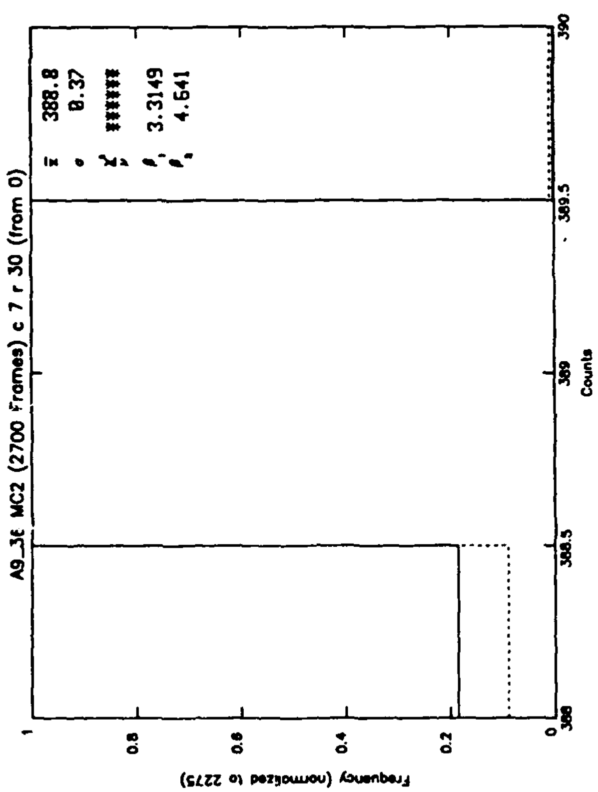
A9_36 MC2 (2700 Frames) c 7 r 30 (from 0)
x̄ 388.8
σ 0.37
χ^2_ν ######
ρ_1 3.3149
ρ_2 4.641
Counts
Frequency (normalized to 2275)

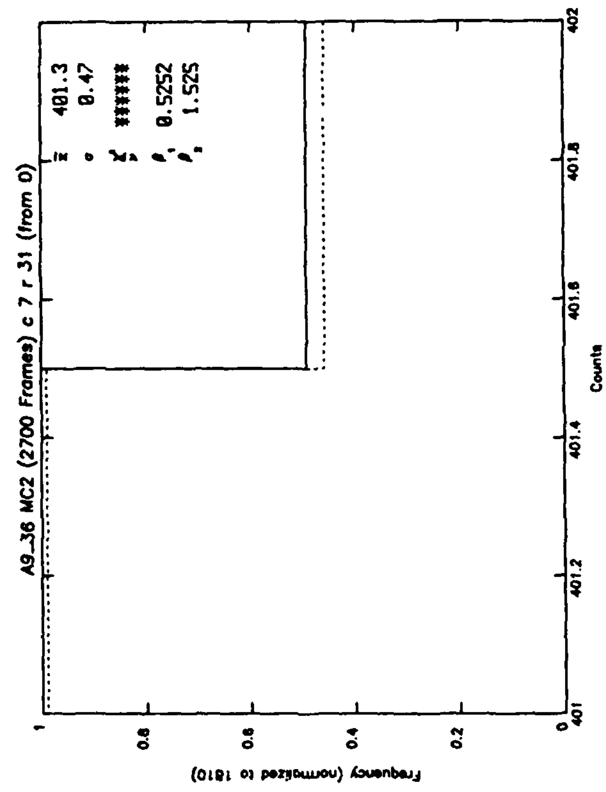
A9_36 MC2 (2700 Frames) c 7 r 31 (from 0)
x̄ 401.3
σ 0.47
χ^2_ν ######
ρ_1 0.5252
ρ_2 1.525
Counts
Frequency (normalized to 1810)

APPENDIX A-14

Array: Aerojet MC^2 (left) and Aerojet Bulk (right) Arrays

	Left	Right
Elements:	Column 0, Rows 0-31	Column 0, Rows 0-31
Data Run:	Star a9_35	Background a11_17

Purpose: Comparison of MC^2 and Bulk arrays. Rows in identical locations in the representative dewars are chosen. Compare also with Appendix A-15 where column 5 (nearer the middle of the array) is selected and with Appendix A-16 where full sets of data from columns 0 and 5 are used. Note that Appendix A-15 uses a different data run (a9_36) for the MC^2 array. The same data run (a9_35) is used for Appendix A-16.

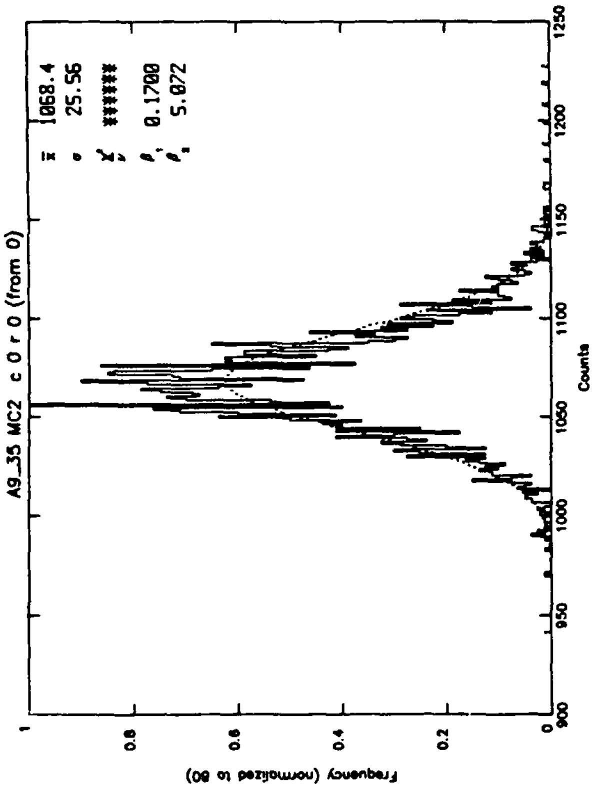
A9_35 MC2 c 0 r 0 (from 0)
x̄ 1068.4
σ 25.56
χ²ν ######
β₁ 0.1700
β₂ 5.072
Frequency (normalized to 80)
Counts

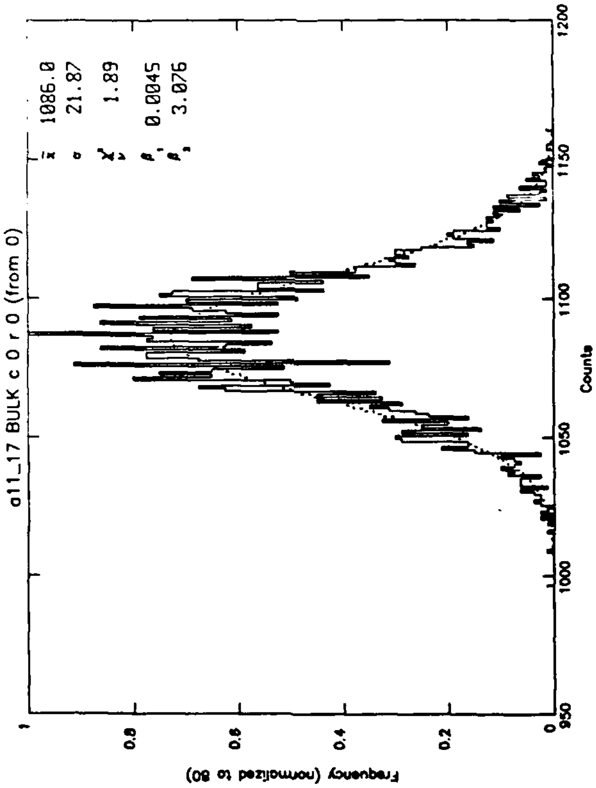
a11_17 BULK c 0 r 0 (from 0)
x̄ 1086.0
σ 21.87
χ²ν 1.89
β₁ 0.0045
β₂ 3.076
Frequency (normalized to 80)
Counts

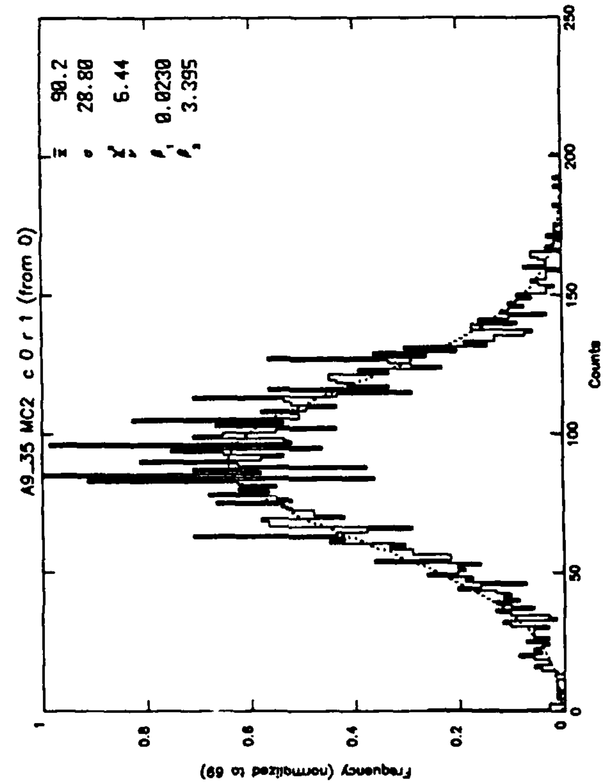
A9_35 MC2 c 0 r 1 (from 0)
x̄ 90.2
σ 28.80
χ²ν 6.44
β₁ 0.0230
β₂ 3.395
Frequency (normalized to 69)
Counts

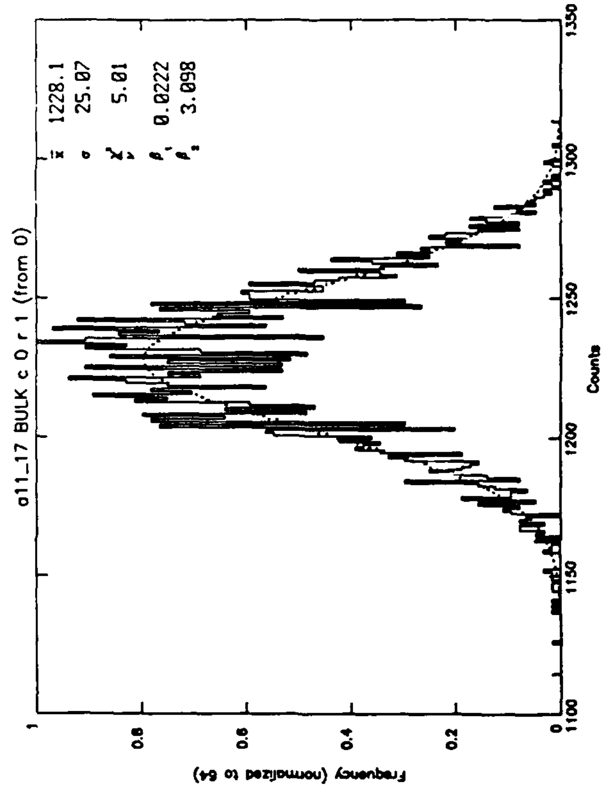
a11_17 BULK c 0 r 1 (from 0)
x̄ 1228.1
σ 25.07
χ²ν 5.01
β₁ 0.0222
β₂ 3.098
Frequency (normalized to 64)
Counts

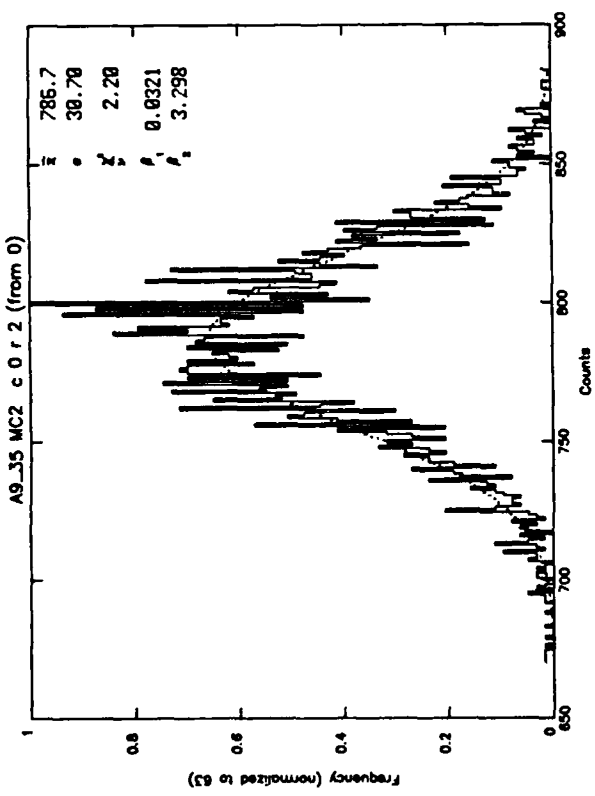
A9_35 MC2 c 0 r 2 (from 0)
x̄ 786.7
σ 30.70
χ^2_ν 2.20
β_1 0.0321
β_2 3.298
Frequency (normalized to 63)
Counts

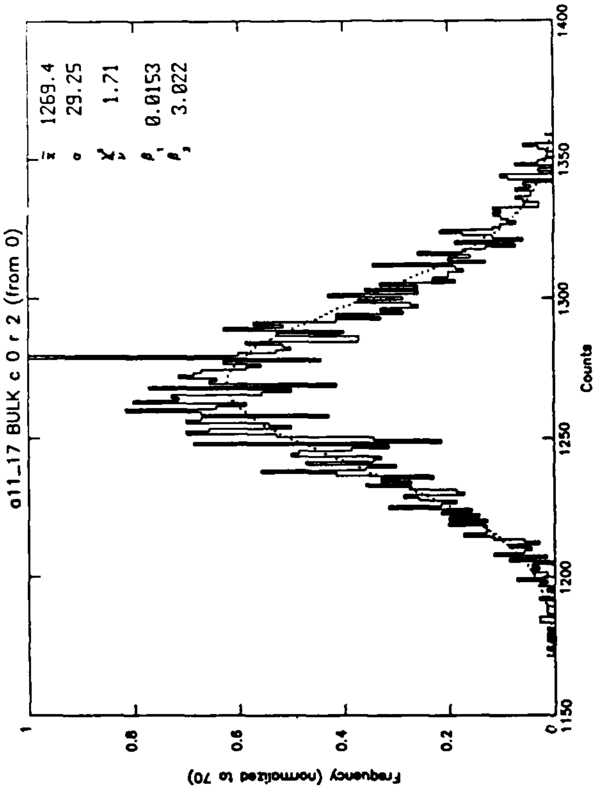
a11_17 BULK c 0 r 2 (from 0)
x̄ 1269.4
σ 29.25
χ^2_ν 1.71
β_1 0.0153
β_2 3.022
Frequency (normalized to 70)
Counts

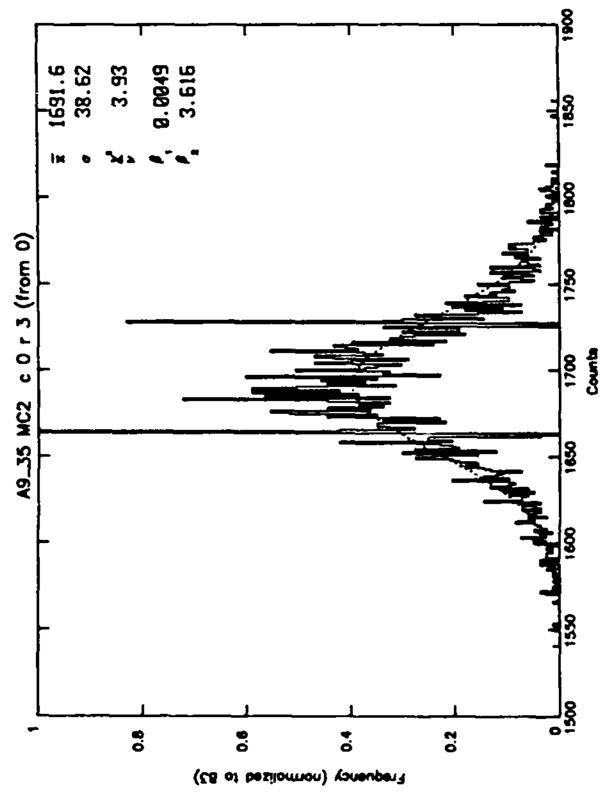
A9_35 MC2 c 0 r 3 (from 0)
x̄ 1691.6
σ 38.62
χ^2_ν 3.93
β_1 0.0049
β_2 3.616
Frequency (normalized to 83)
Counts

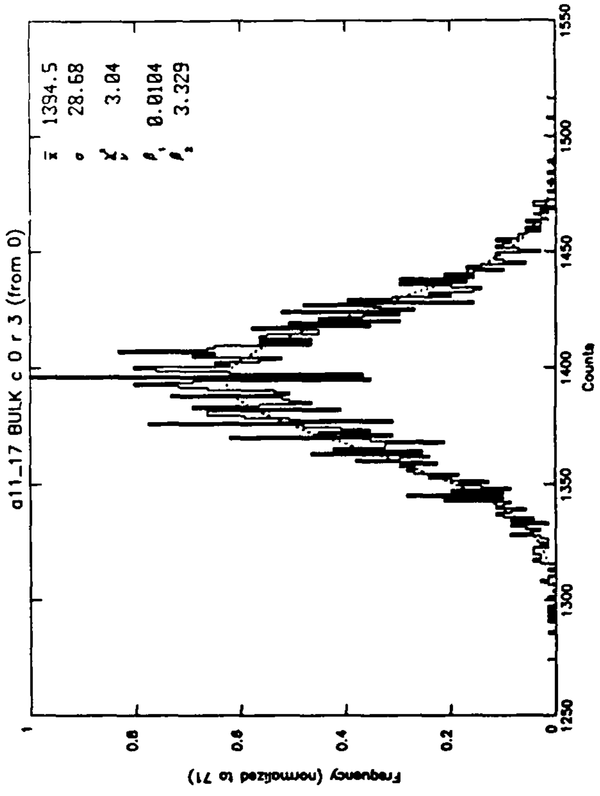
a11_17 BULK c 0 r 3 (from 0)
x̄ 1394.5
σ 28.68
χ^2_ν 3.04
β_1 0.0104
β_2 3.329
Frequency (normalized to 71)
Counts

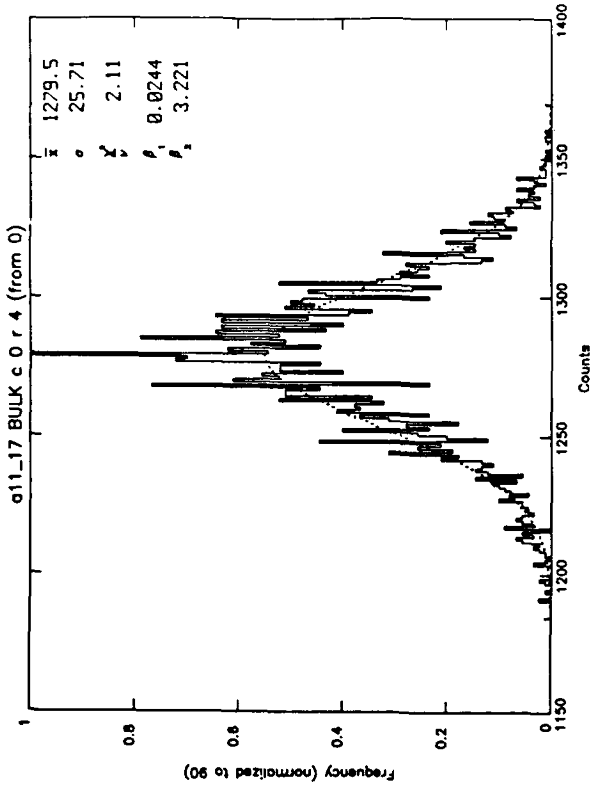
a11_17 BULK c 0 r 4 (from 0)
x̄ 1279.5
σ 25.71
χ^2_ν 2.11
β_1 0.0244
β_2 3.221
Counts
Frequency (normalized to 90)

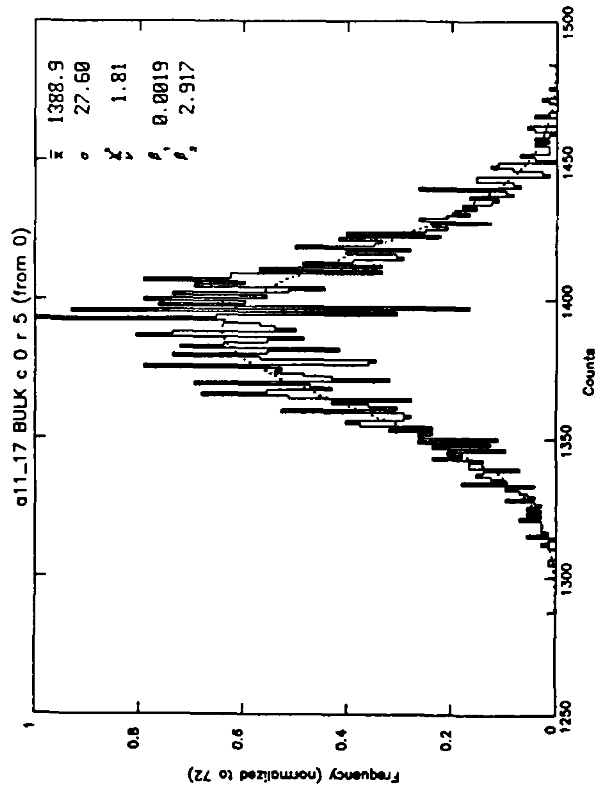
a11_17 BULK c 0 r 5 (from 0)
x̄ 1388.9
σ 27.60
χ^2_ν 1.81
β_1 0.0019
β_2 2.917
Counts
Frequency (normalized to 72)

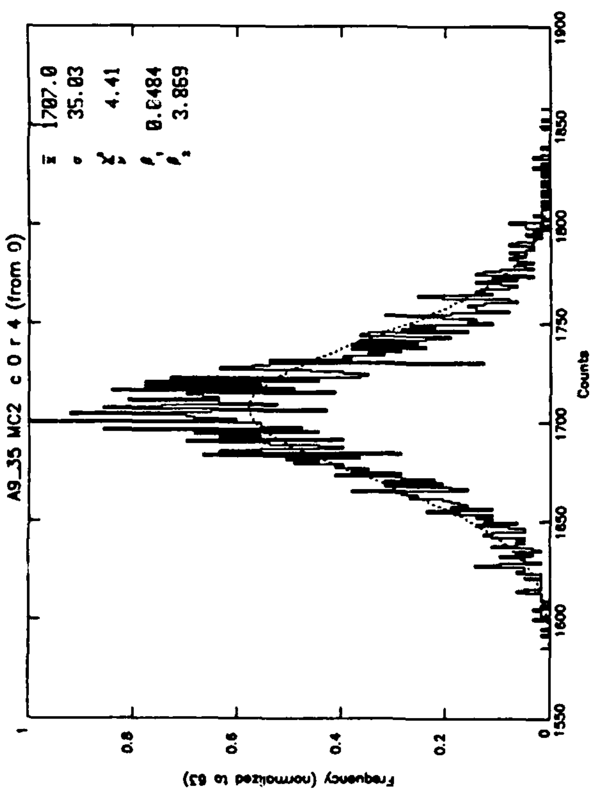
A9_35 MC2 c 0 r 4 (from 0)
x̄ 1707.0
σ 35.03
χ^2_ν 4.41
β_1 0.0484
β_2 3.869
Counts
Frequency (normalized to 63)

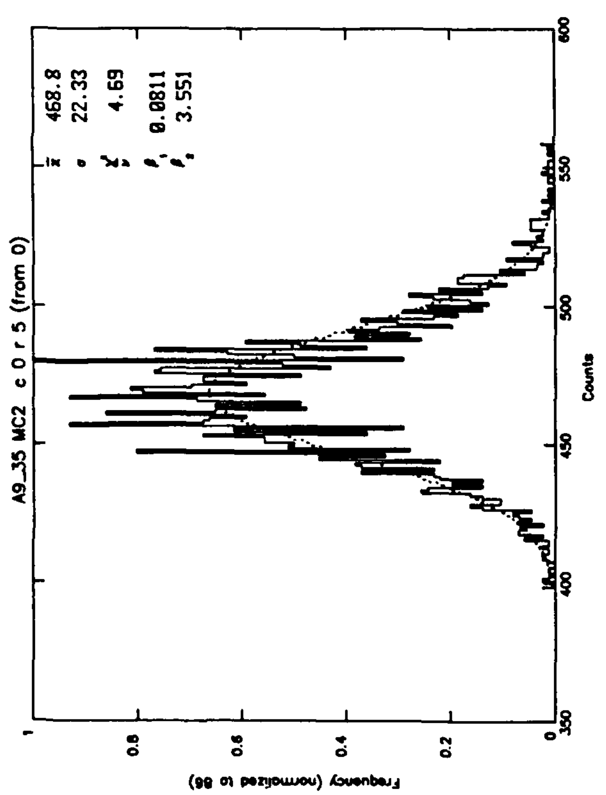
A9_35 MC2 c 0 r 5 (from 0)
x̄ 468.8
σ 22.33
χ^2_ν 4.69
β_1 0.0811
β_2 3.551
Counts
Frequency (normalized to 86)

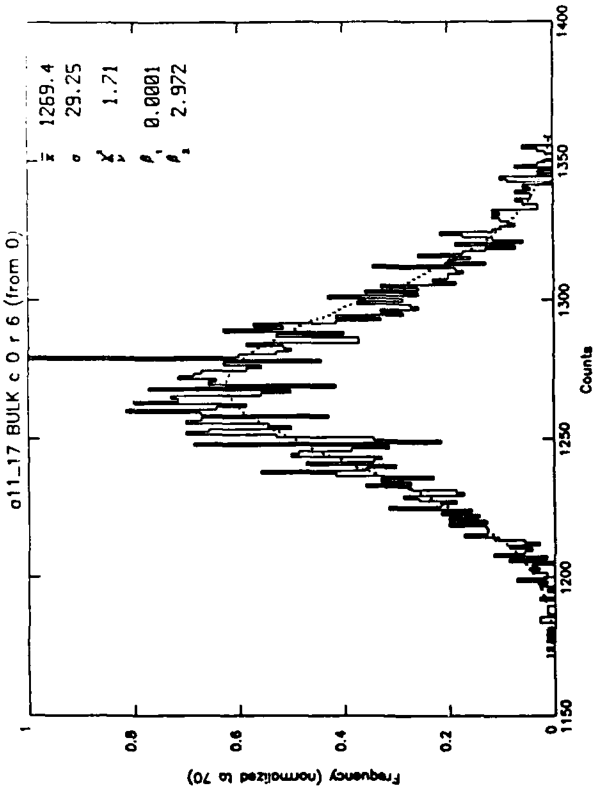

a11_17 BULK c 0 r 6 (from 0)
x̄ 1269.4
σ 29.25
χ²ν 1.71
β1 0.0001
β2 2.972
Frequency (normalized to 70)
Counts

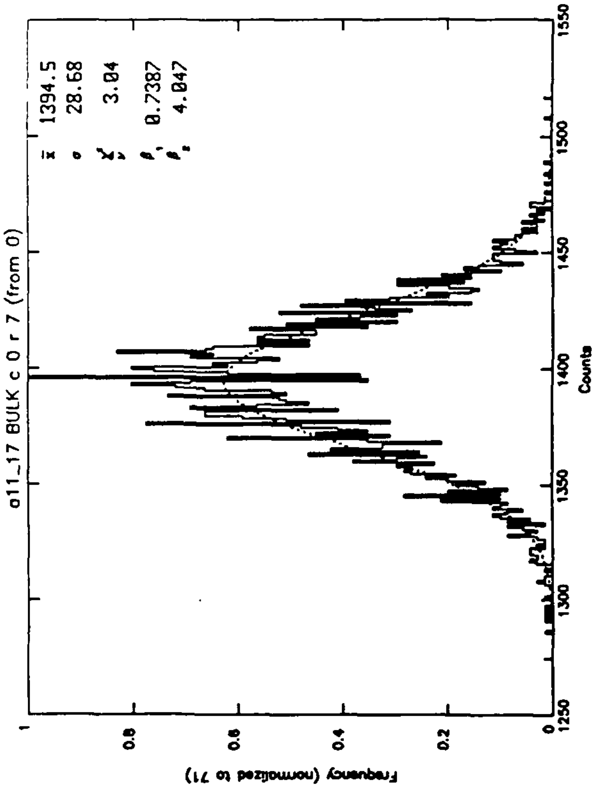

a11_17 BULK c 0 r 7 (from 0)
x̄ 1394.5
σ 28.68
χ²ν 3.04
β1 0.7387
β2 4.047
Frequency (normalized to 71)
Counts

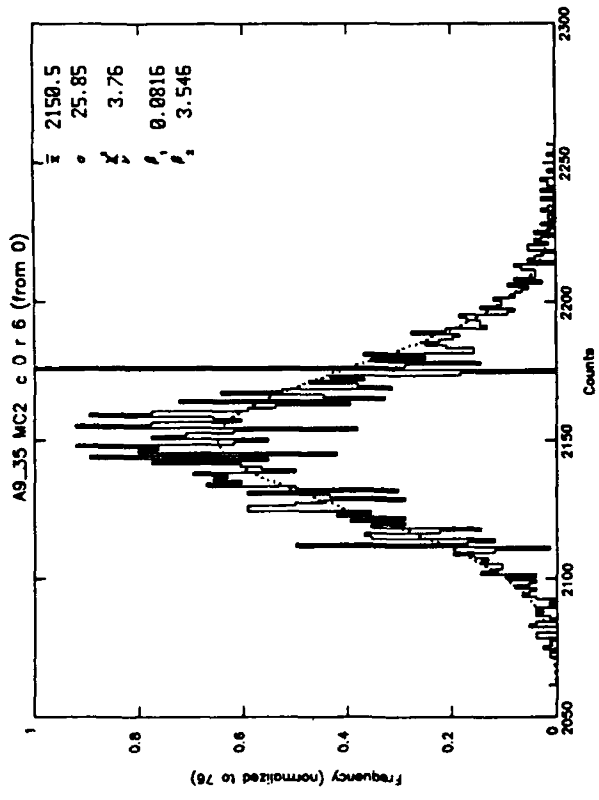

A9_35 MC2 c 0 r 6 (from 0)
x̄ 2150.5
σ 25.85
χ²ν 3.76
β1 0.0816
β2 3.546
Frequency (normalized to 76)
Counts

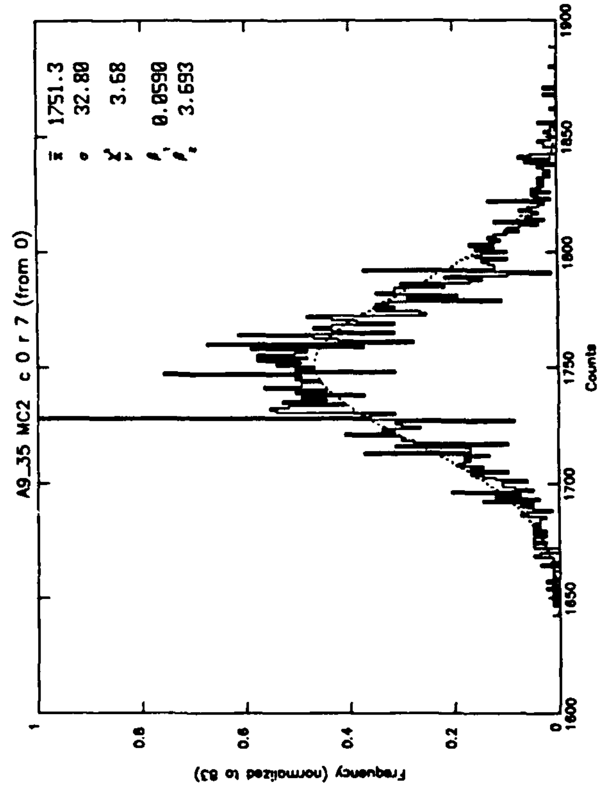

A9_35 MC2 c 0 r 7 (from 0)
x̄ 1751.3
σ 32.80
χ²ν 3.68
β1 0.0590
β2 3.693
Frequency (normalized to 83)
Counts

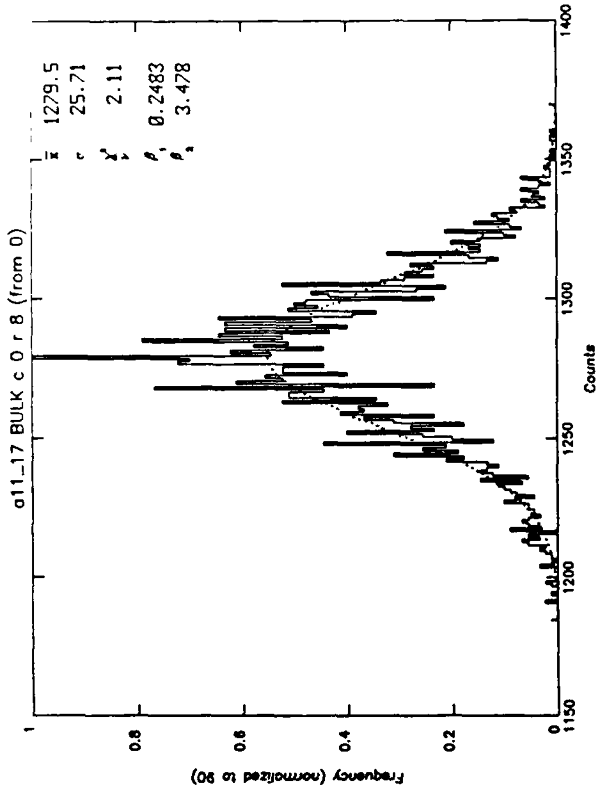

a11_17 BULK c 0 r 8 (from 0)
x̄ 1279.5
σ 25.71
χ²ν 2.11
β1 0.2483
β2 3.478
Frequency (normalized to 90)
Counts

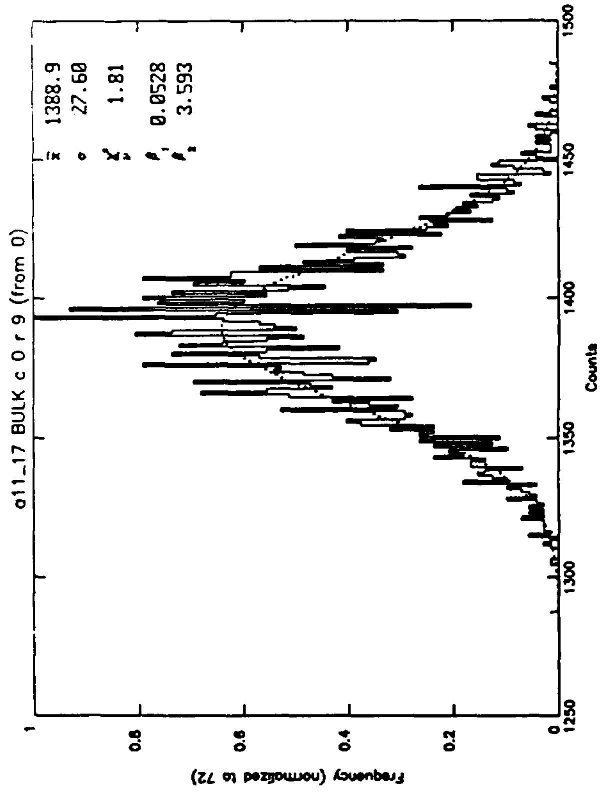

a11_17 BULK c 0 r 9 (from 0)
x̄ 1388.9
σ 27.60
χ²ν 1.81
β1 0.0528
β2 3.593
Frequency (normalized to 72)
Counts

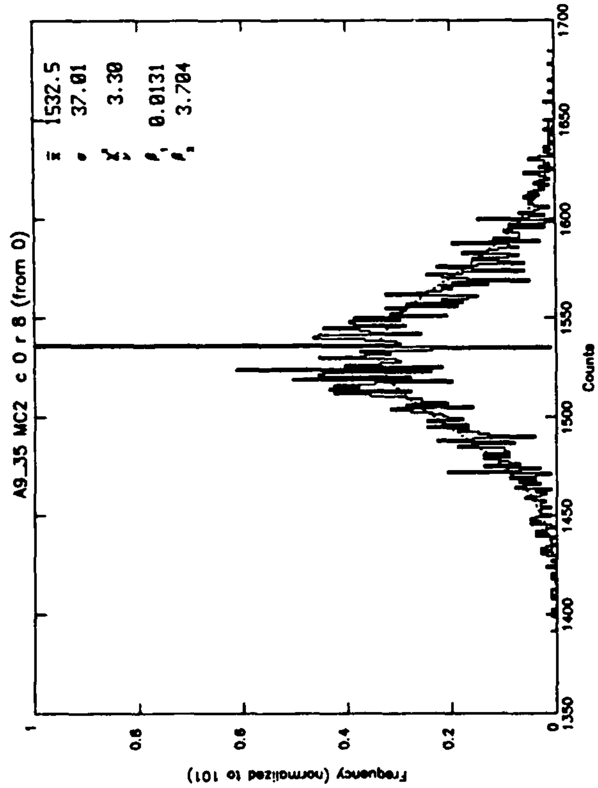

A9_35 MC2 c 0 r 8 (from 0)
x̄ 1532.5
σ 37.01
χ²ν 3.30
β1 0.0131
β2 3.704
Frequency (normalized to 101)
Counts

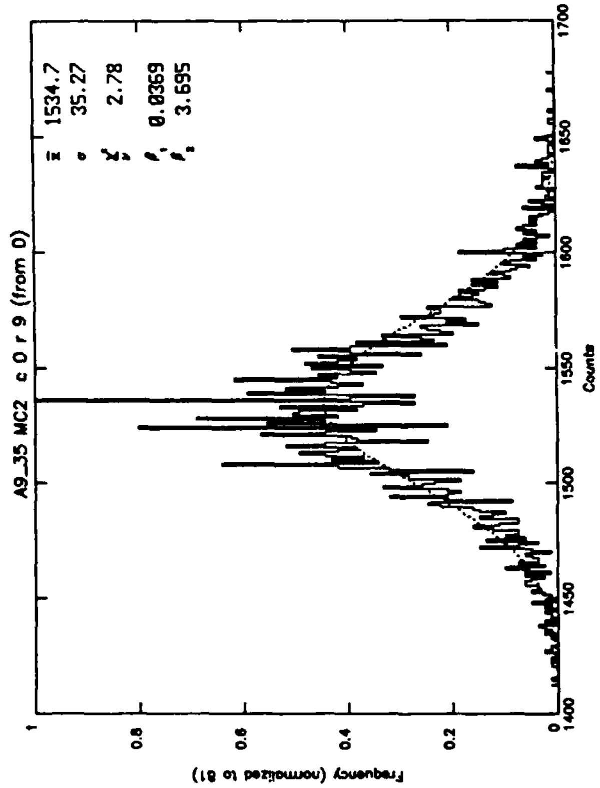

A9_35 MC2 c 0 r 9 (from 0)
x̄ 1534.7
σ 35.27
χ²ν 2.78
β1 0.0369
β2 3.695
Frequency (normalized to 81)
Counts

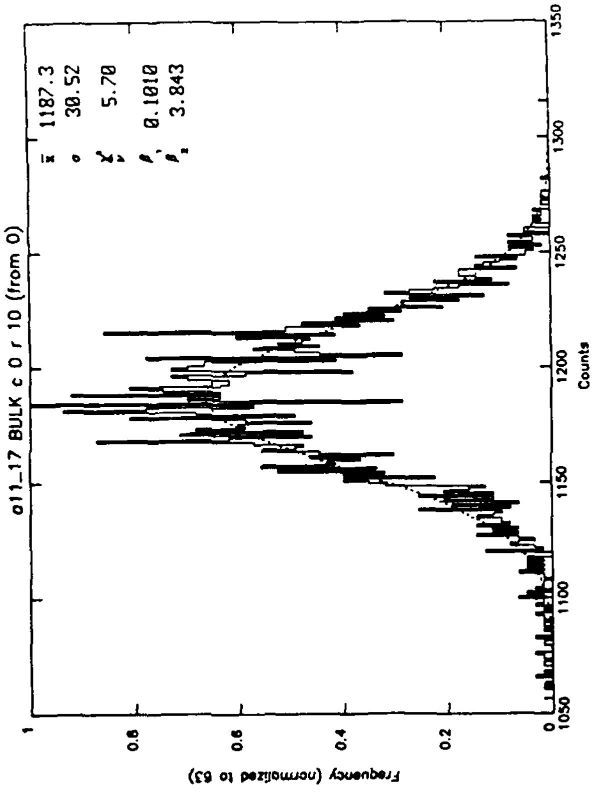
a11_17 BULK c 0 r 10 (from 0)
x̄ 1187.3
σ 30.52
χ^2_ν 5.70
β_1 0.1010
β_2 3.843
Counts
Frequency (normalized to 63)

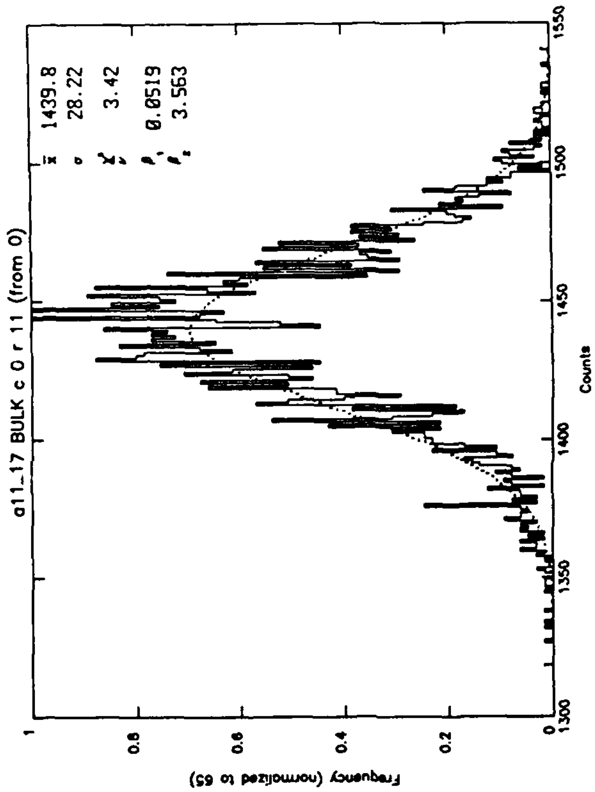
a11_17 BULK c 0 r 11 (from 0)
x̄ 1439.8
σ 28.22
χ^2_ν 3.42
β_1 0.0519
β_2 3.563
Counts
Frequency (normalized to 65)

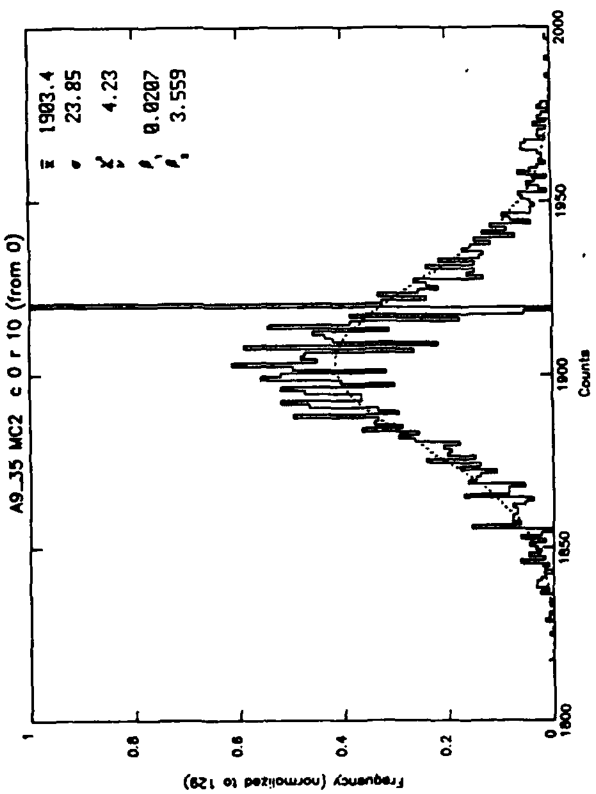
A9_35 MC2 c 0 r 10 (from 0)
x̄ 1903.4
σ 23.85
χ^2_ν 4.23
β_1 0.0207
β_2 3.559
Counts
Frequency (normalized to 129)

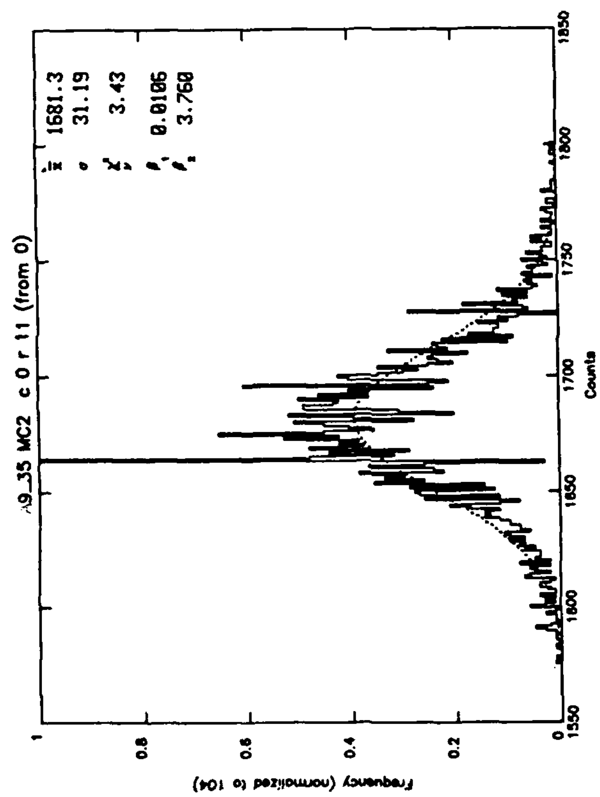
A9_35 MC2 c 0 r 11 (from 0)
x̄ 1681.3
σ 31.19
χ^2_ν 3.43
β_1 0.0106
β_2 3.760
Counts
Frequency (normalized to 104)

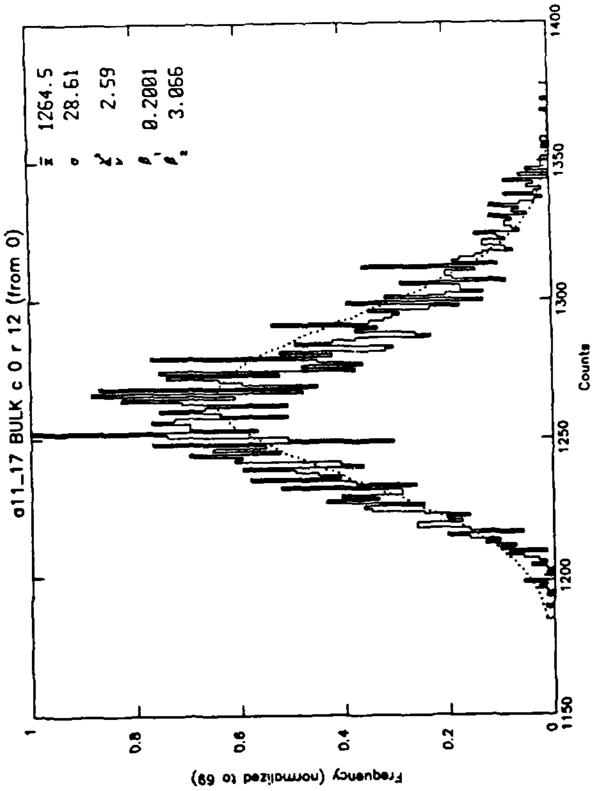

a11_17 BULK c 0 r 12 (from 0)
$\bar{x}$ 1264.5
σ 28.61
χ^2_ν 2.59
β_1 0.2081
β_2 3.066
Counts
Frequency (normalized to 69)

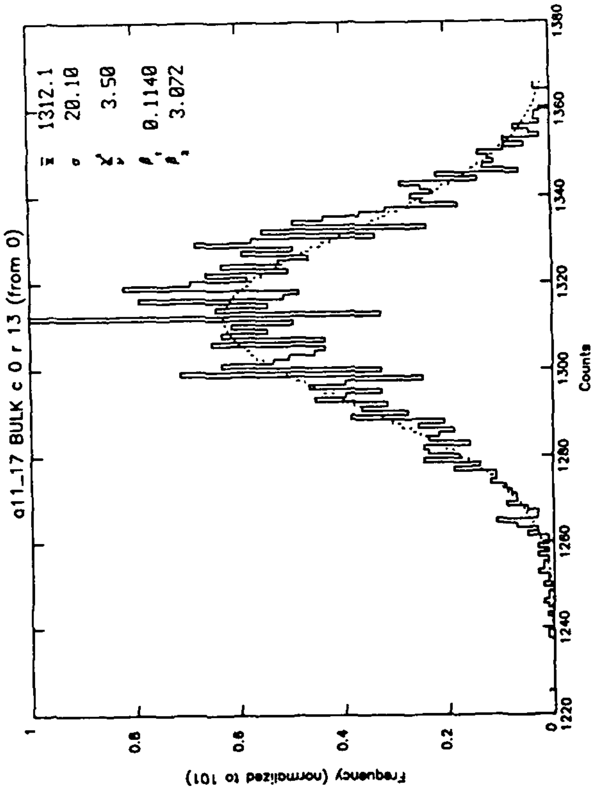

a11_17 BULK c 0 r 13 (from 0)
$\bar{x}$ 1312.1
σ 20.10
χ^2_ν 3.50
β_1 0.1140
β_2 3.072
Counts
Frequency (normalized to 101)

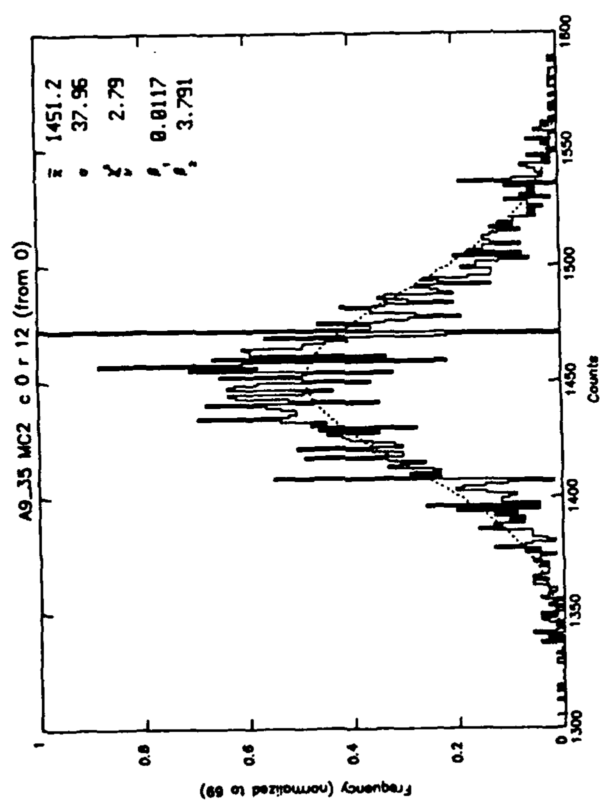

A9_35 MC2 c 0 r 12 (from 0)
$\bar{x}$ 1451.2
σ 37.96
χ^2_ν 2.79
β_1 0.0117
β_2 3.791
Counts
Frequency (normalized to 69)

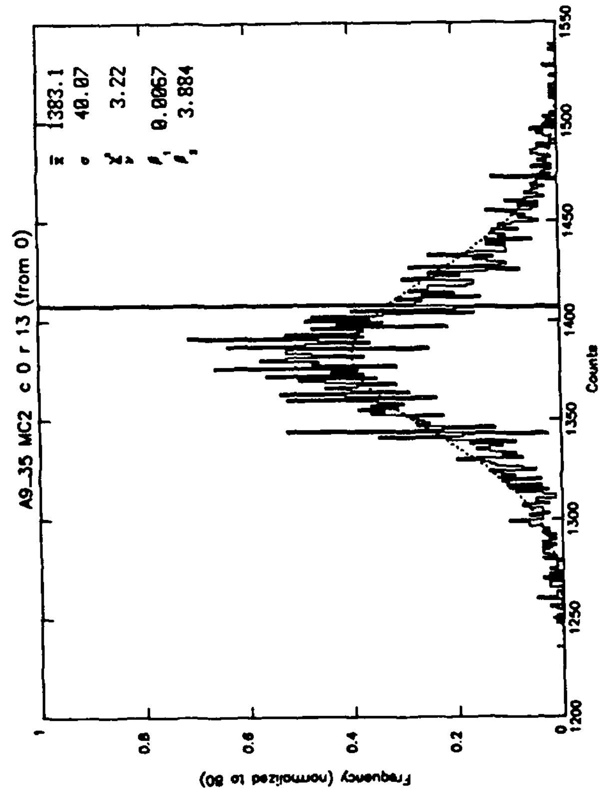

A9_35 MC2 c 0 r 13 (from 0)
$\bar{x}$ 1383.1
σ 40.07
χ^2_ν 3.22
β_1 0.0067
β_2 3.884
Counts
Frequency (normalized to 80)

A9_35 MC2 c 0 r 14 (from 0)

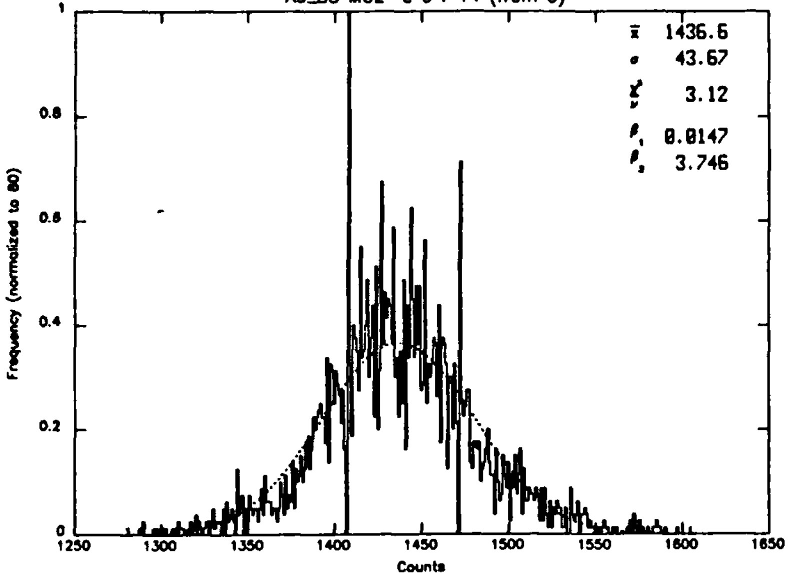

a11_17 BULK c 0 r 14 (from 0)

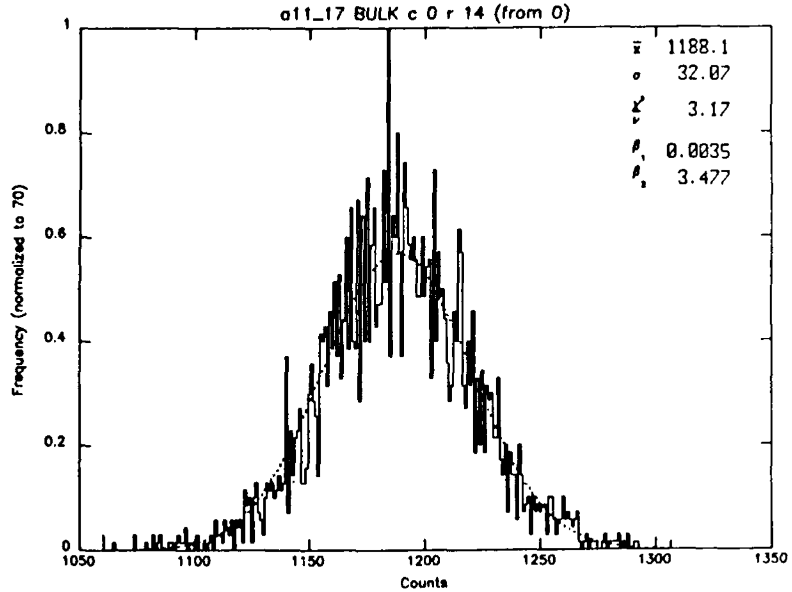

A9_35 MC2 c 0 r 15 (from 0)

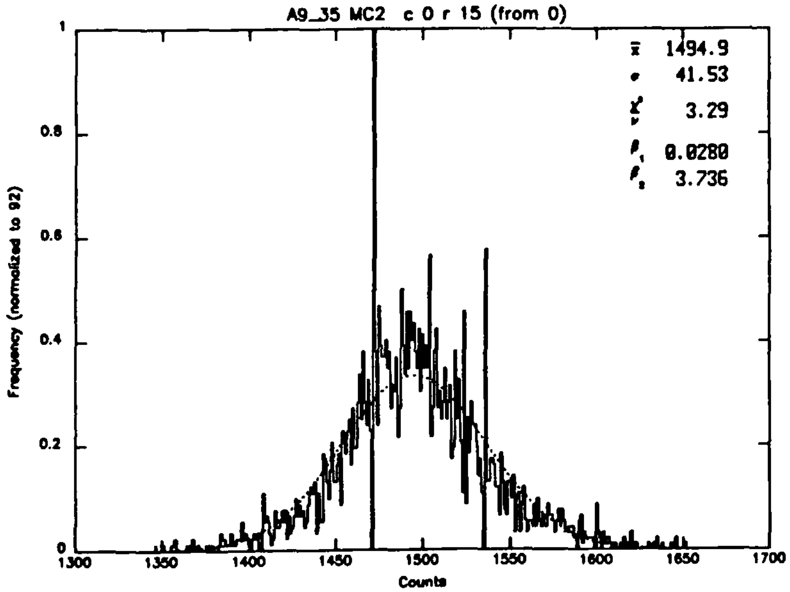

a11_17 BULK c 0 r 15 (from 0)

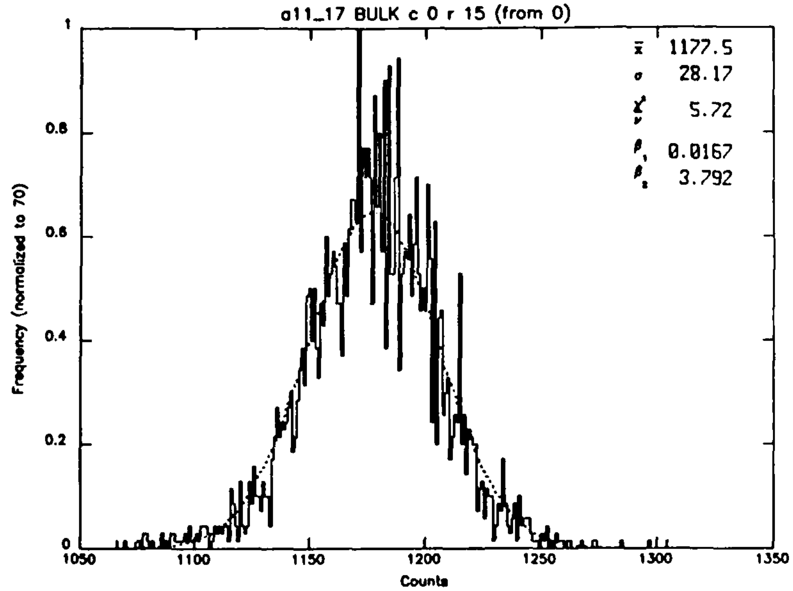

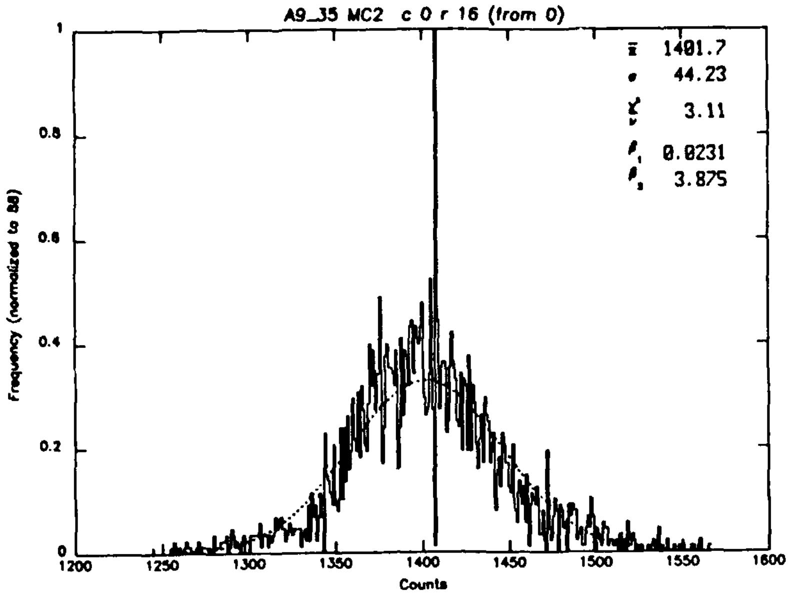
A9_35 MC2 c 0 r 16 (from 0)
Frequency (normalized to 88)
Counts
x̄ 1401.7
σ 44.23
χ^2_ν 3.11
β_1 0.0231
β_2 3.875

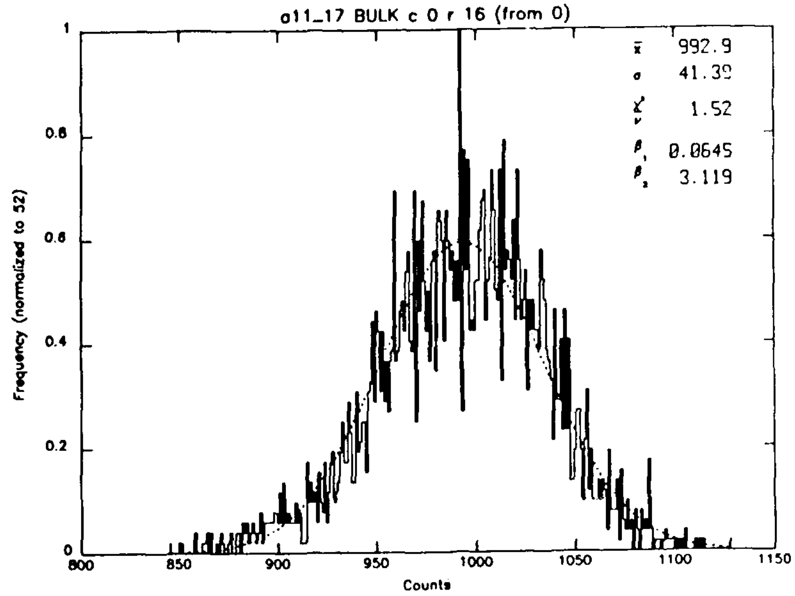
a11_17 BULK c 0 r 16 (from 0)
Frequency (normalized to 52)
Counts
x̄ 992.9
σ 41.39
χ^2_ν 1.52
β_1 0.0645
β_2 3.119

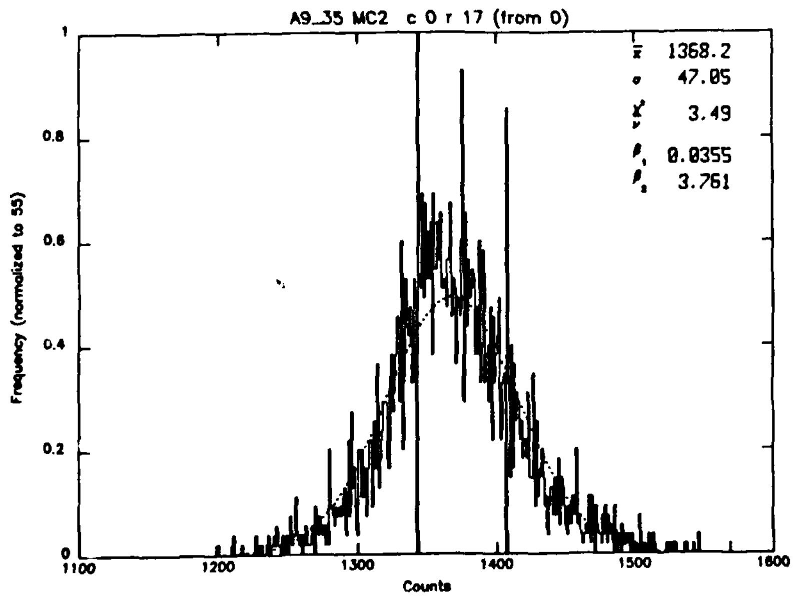
A9_35 MC2 c 0 r 17 (from 0)
Frequency (normalized to 55)
Counts
x̄ 1368.2
σ 47.05
χ^2_ν 3.49
β_1 0.0355
β_2 3.761

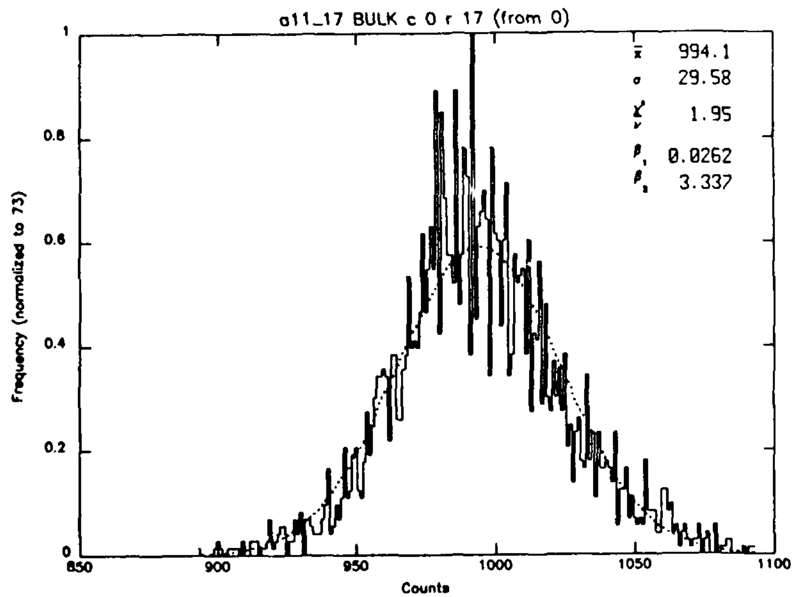
a11_17 BULK c 0 r 17 (from 0)
Frequency (normalized to 73)
Counts
x̄ 994.1
σ 29.58
χ^2_ν 1.95
β_1 0.0262
β_2 3.337

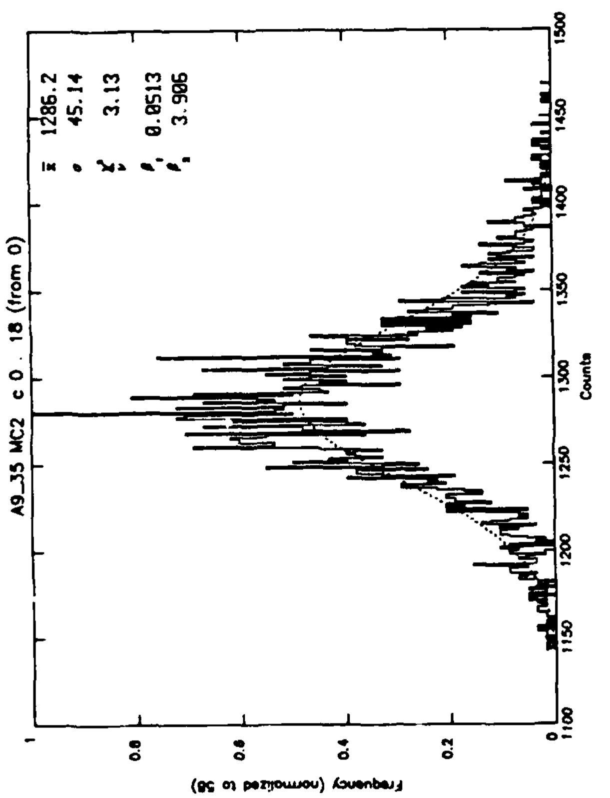

A9_35 MC2 c 0 . 18 (from 0)
x̄ 1286.2
σ 45.14
χ²ν 3.13
β1 0.0513
β2 3.906
Counts
Frequency (normalized to 58)

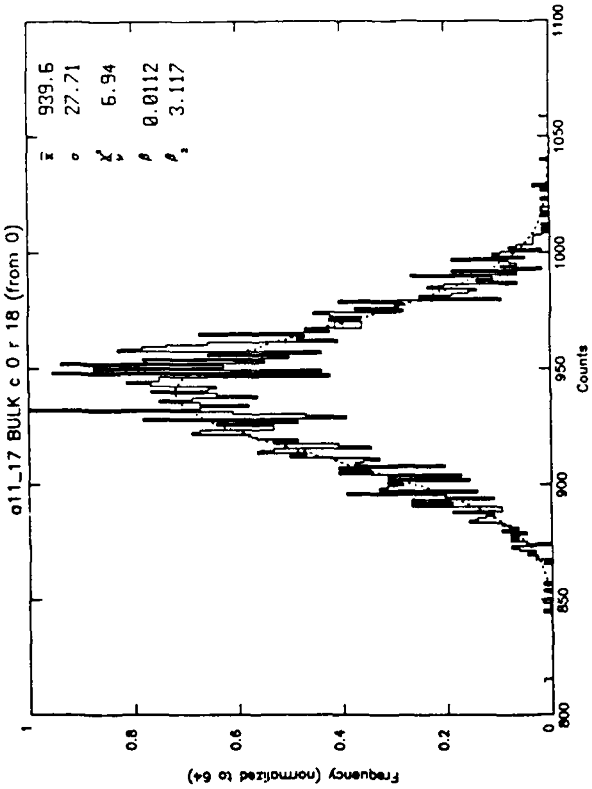

a11_17 BULK c 0 r 18 (from 0)
x̄ 939.6
σ 27.71
χ²ν 6.94
β1 0.0112
β2 3.117
Counts
Frequency (normalized to 64)

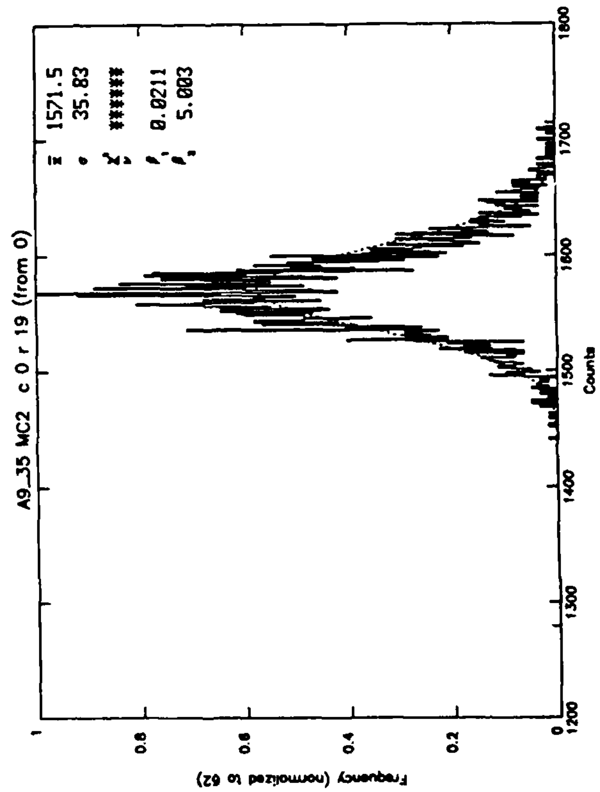

A9_35 MC2 c 0 r 19 (from 0)
x̄ 1571.5
σ 35.83
χ²ν ******
β1 0.0211
β2 5.003
Counts
Frequency (normalized to 62)

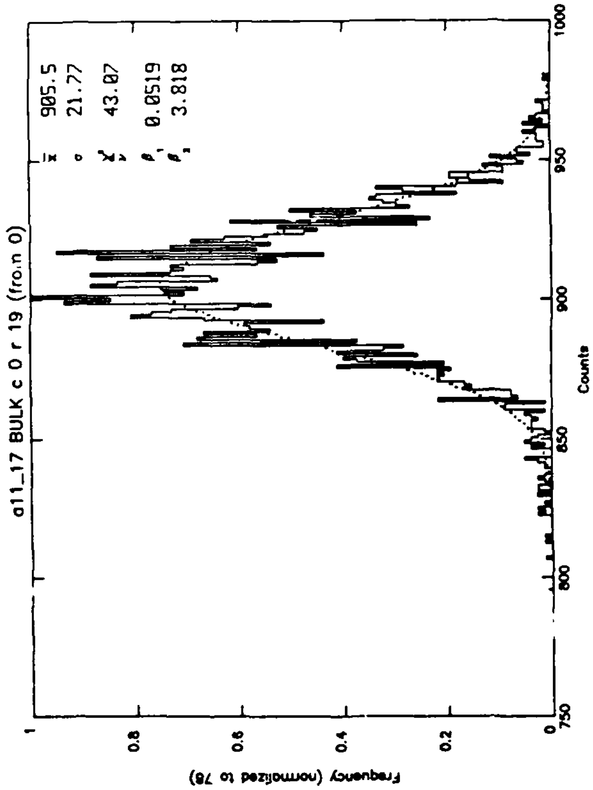

a11_17 BULK c 0 r 19 (from 0)
x̄ 905.5
σ 21.77
χ²ν 43.07
β1 0.0519
β2 3.818
Counts
Frequency (normalized to 78)

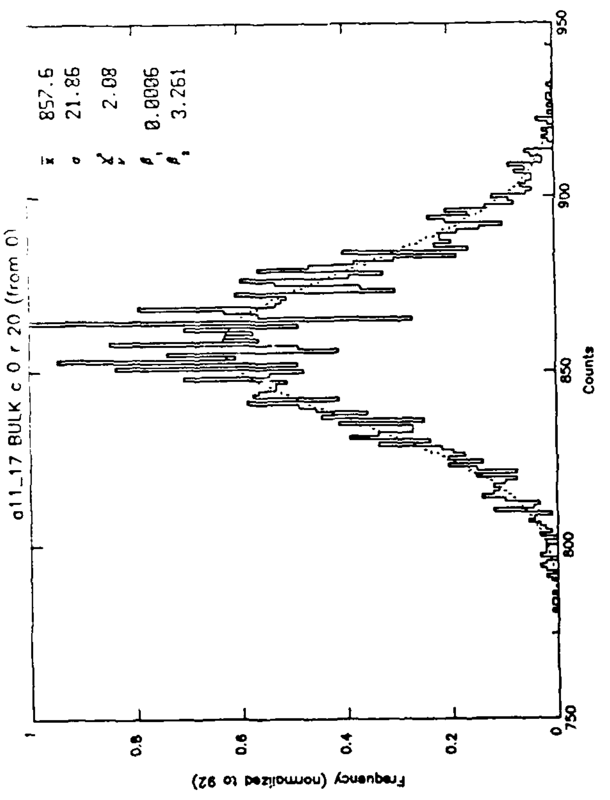
a11_17 BULK c 0 r 20 (from 0)
x̄ 857.6
σ 21.86
χ^2_ν 2.08
β_1 0.0006
β_2 3.261
Frequency (normalized to 92)
Counts

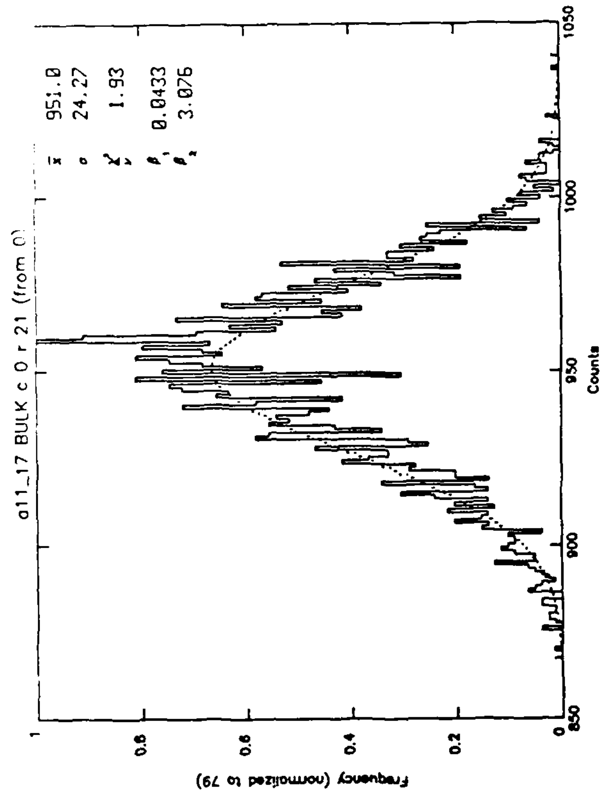
a11_17 BULK c 0 r 21 (from 0)
x̄ 951.0
σ 24.27
χ^2_ν 1.93
β_1 0.0433
β_2 3.076
Frequency (normalized to 79)
Counts

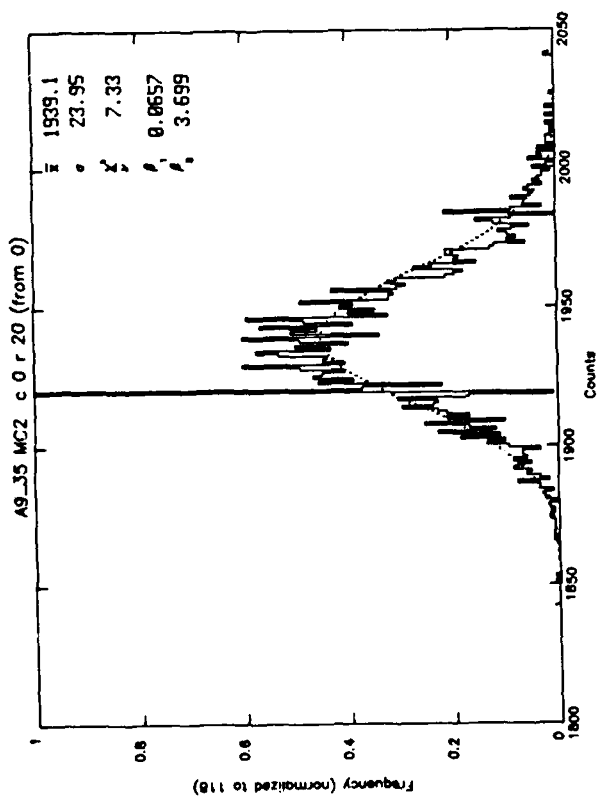
A9_35 MC2 c 0 r 20 (from 0)
x̄ 1939.1
σ 23.95
χ^2_ν 7.33
β_1 0.0657
β_2 3.699
Frequency (normalized to 118)
Counts

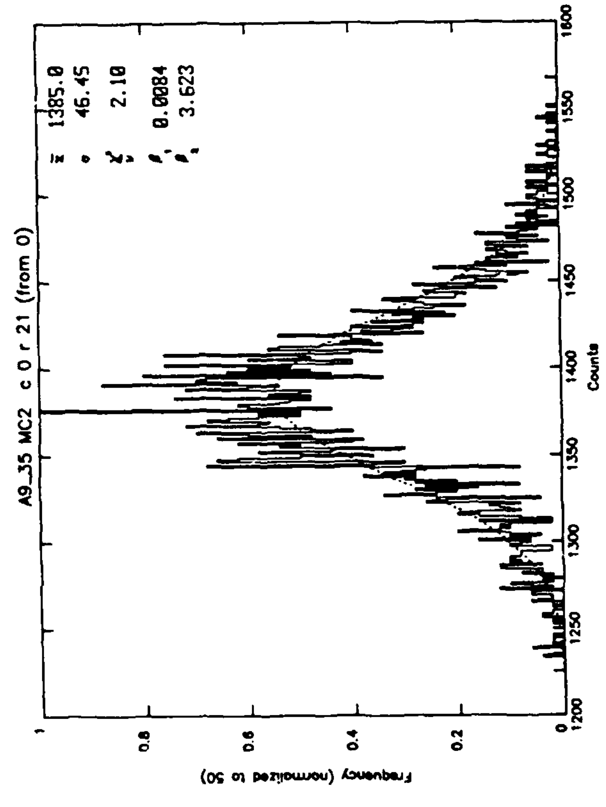
A9_35 MC2 c 0 r 21 (from 0)
x̄ 1385.0
σ 46.45
χ^2_ν 2.10
β_1 0.0084
β_2 3.623
Frequency (normalized to 50)
Counts

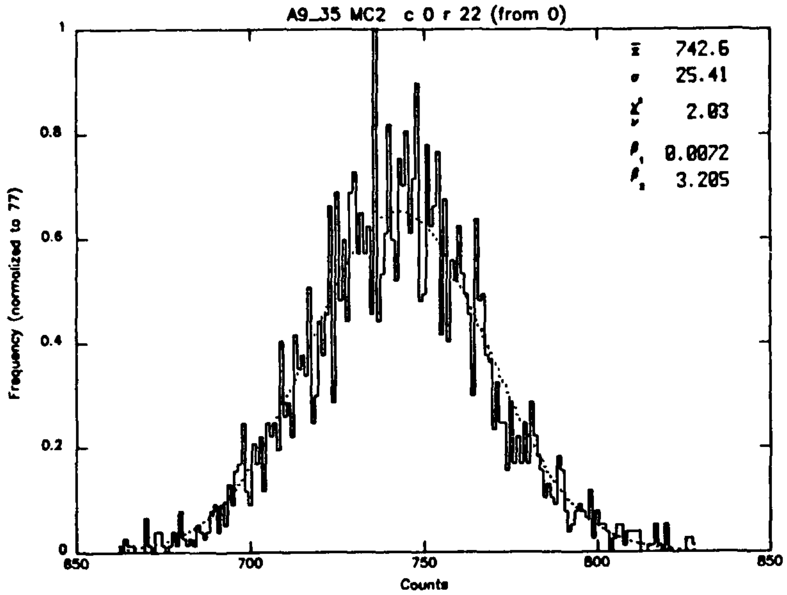
A9_35 MC2 c 0 r 22 (from 0)
Frequency (normalized to 77)
Counts
x̄ 742.6
σ 25.41
χ²ν 2.03
β1 0.0072
β2 3.205

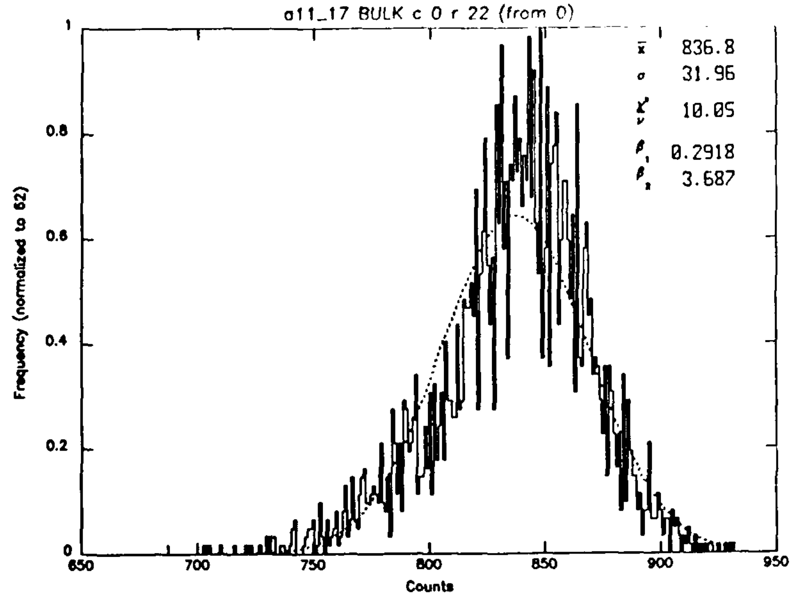
a11_17 BULK c 0 r 22 (from 0)
Frequency (normalized to 62)
Counts
x̄ 836.8
σ 31.96
χ²ν 10.05
β1 0.2918
β2 3.687

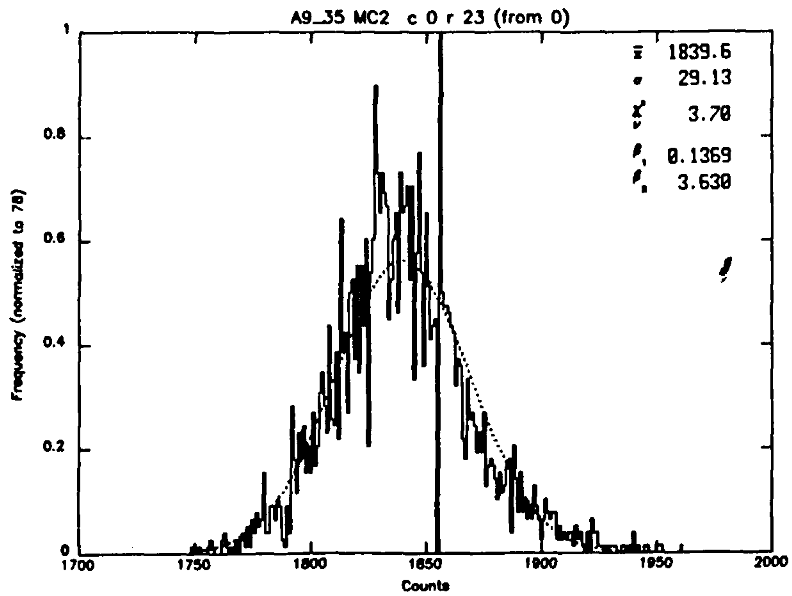
A9_35 MC2 c 0 r 23 (from 0)
Frequency (normalized to 78)
Counts
x̄ 1839.6
σ 29.13
χ²ν 3.70
β1 0.1369
β2 3.630

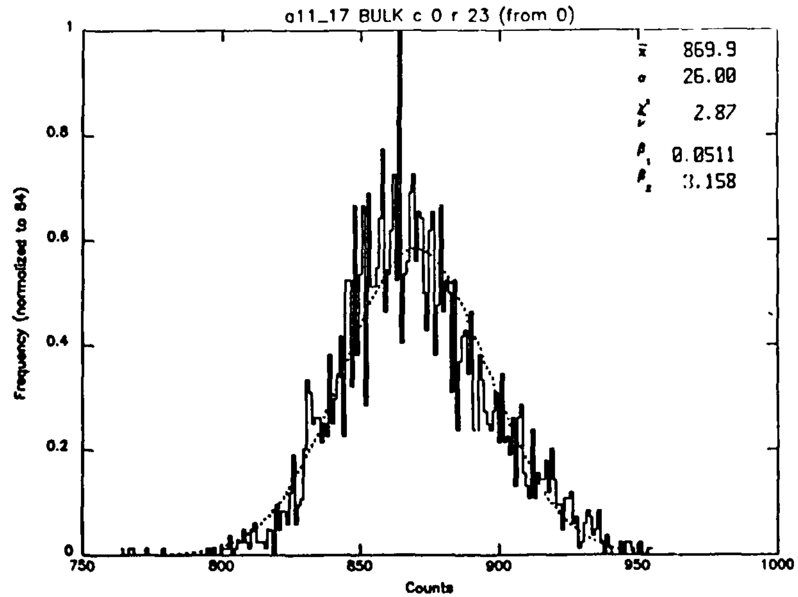
a11_17 BULK c 0 r 23 (from 0)
Frequency (normalized to 84)
Counts
x̄ 869.9
σ 26.00
χ²ν 2.87
β1 0.0511
β2 3.158

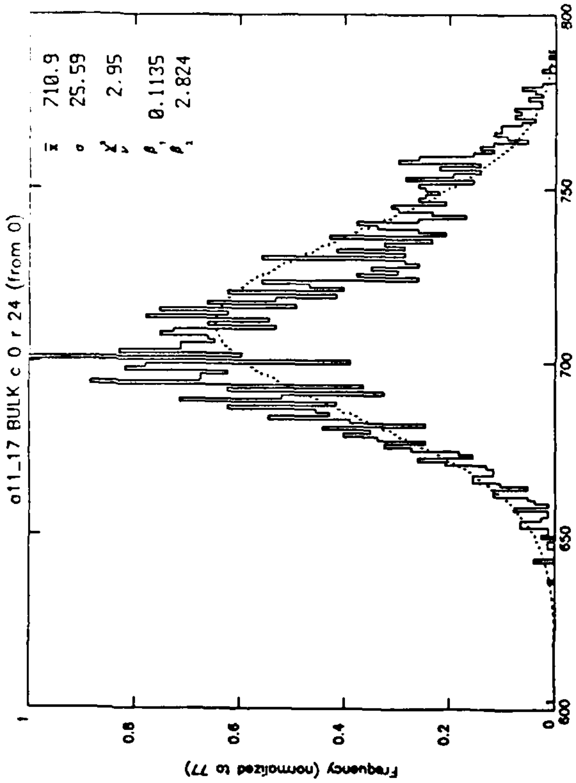
a11_17 BULK c 0 r 24 (from 0)
x̄ 710.9
σ 25.59
χ² 2.95
β₁ 0.1135
β₂ 2.824
Frequency (normalized to 77)
Counts

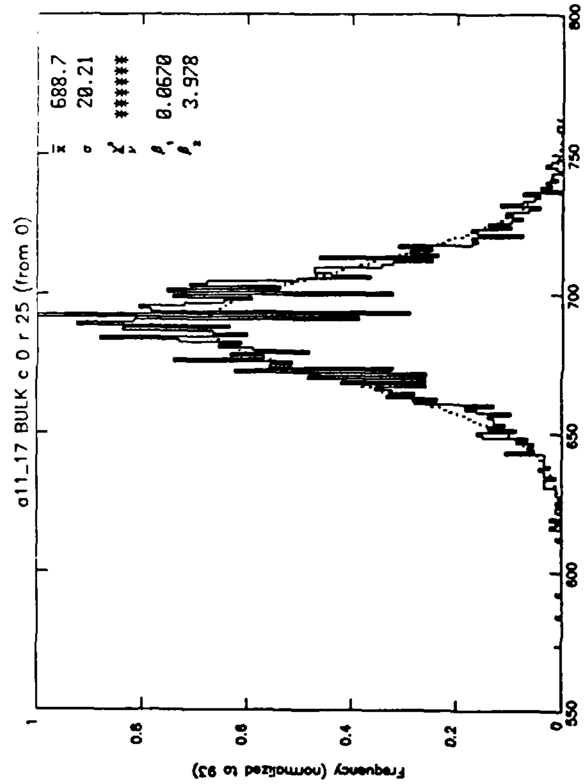
a11_17 BULK c 0 r 25 (from 0)
x̄ 688.7
σ 20.21
χ² ******
β₁ 0.0670
β₂ 3.978
Frequency (normalized to 93)
Counts

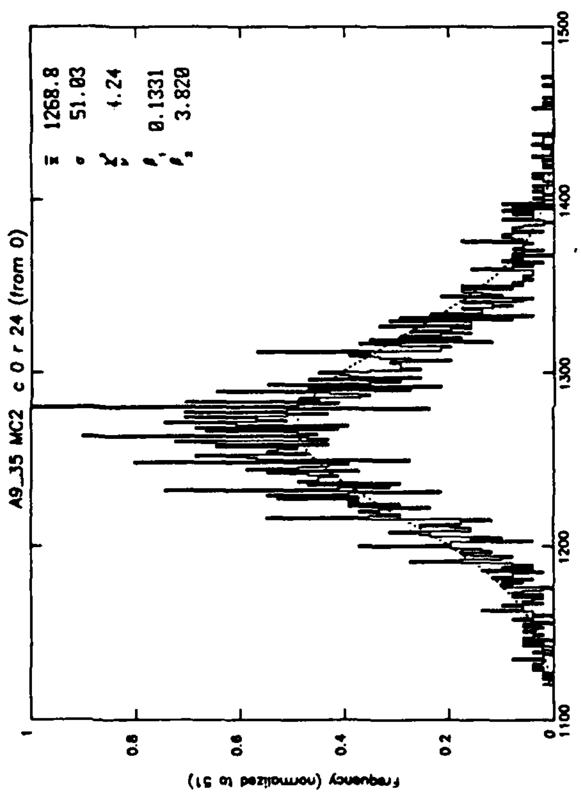
A9_35 MC2 c 0 r 24 (from 0)
x̄ 1268.8
σ 51.03
χ² 4.24
β₁ 0.1331
β₂ 3.820
Frequency (normalized to 51)
Counts

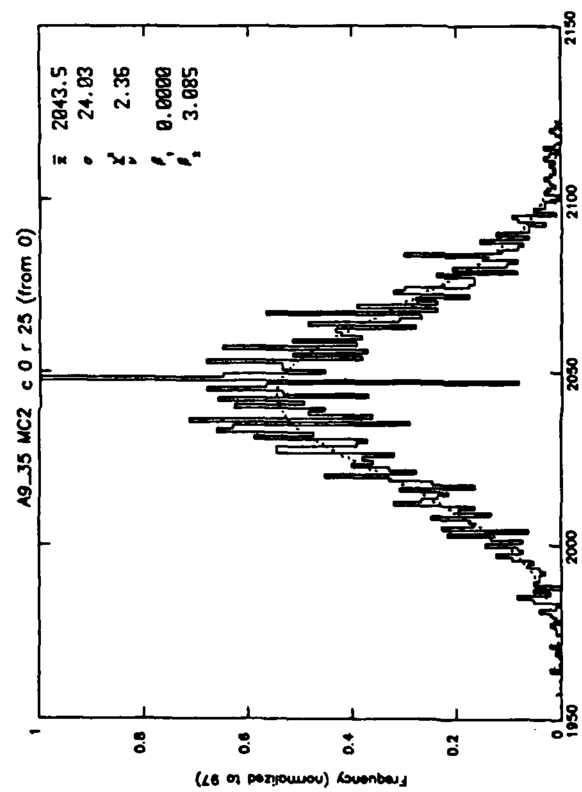
A9_35 MC2 c 0 r 25 (from 0)
x̄ 2043.5
σ 24.03
χ² 2.36
β₁ 0.0000
β₂ 3.085
Frequency (normalized to 97)
Counts

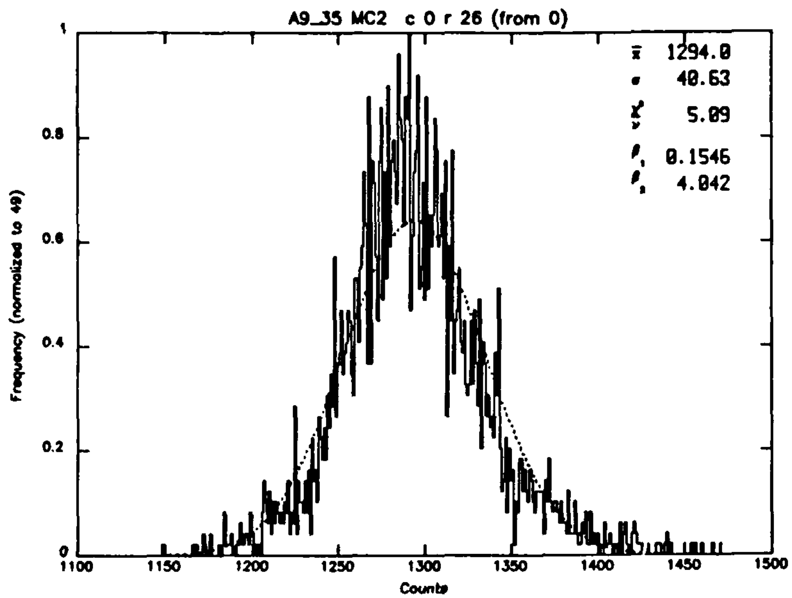
A9_35 MC2 c 0 r 26 (from 0)
Frequency (normalized to 49)
Counts
x̄ 1294.0
σ 40.63
χ²ν 5.09
β1 0.1546
β2 4.042

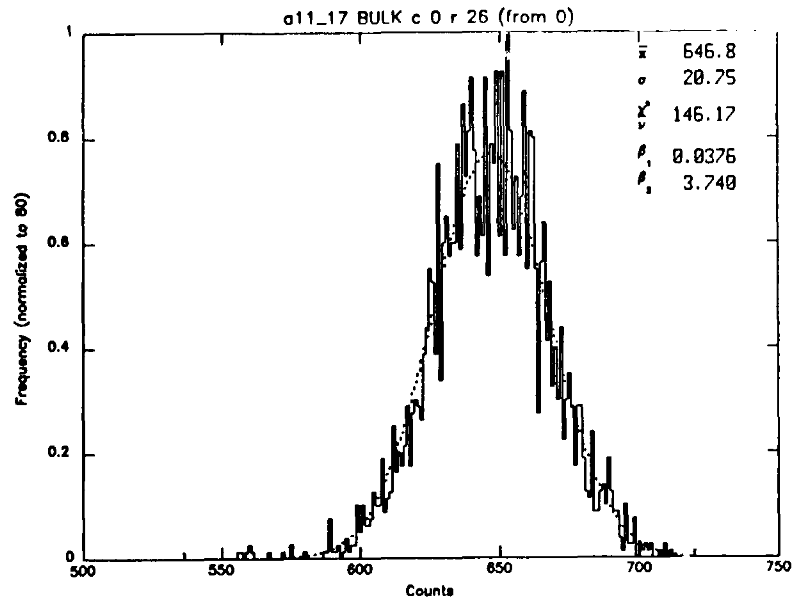
a11_17 BULK c 0 r 26 (from 0)
Frequency (normalized to 80)
Counts
x̄ 646.8
σ 20.75
χ²ν 146.17
β1 0.0376
β2 3.740

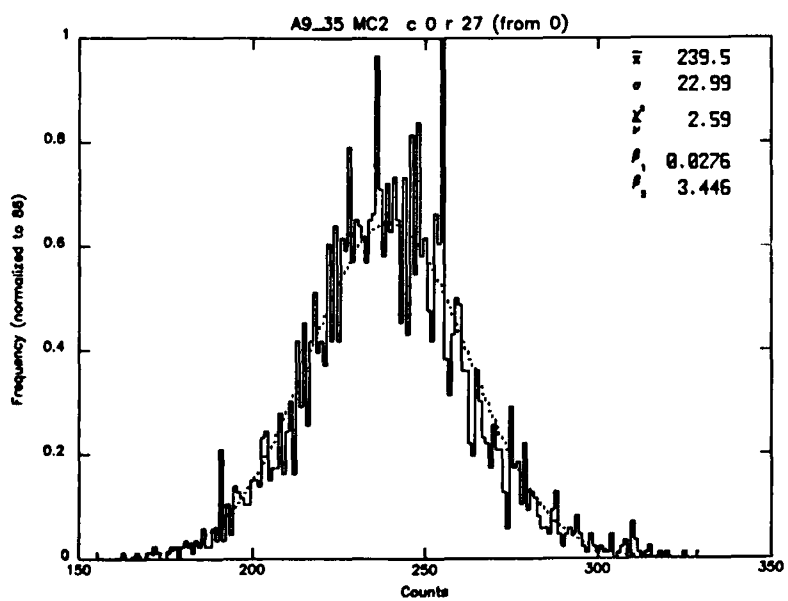
A9_35 MC2 c 0 r 27 (from 0)
Frequency (normalized to 86)
Counts
x̄ 239.5
σ 22.99
χ²ν 2.59
β1 0.0276
β2 3.446

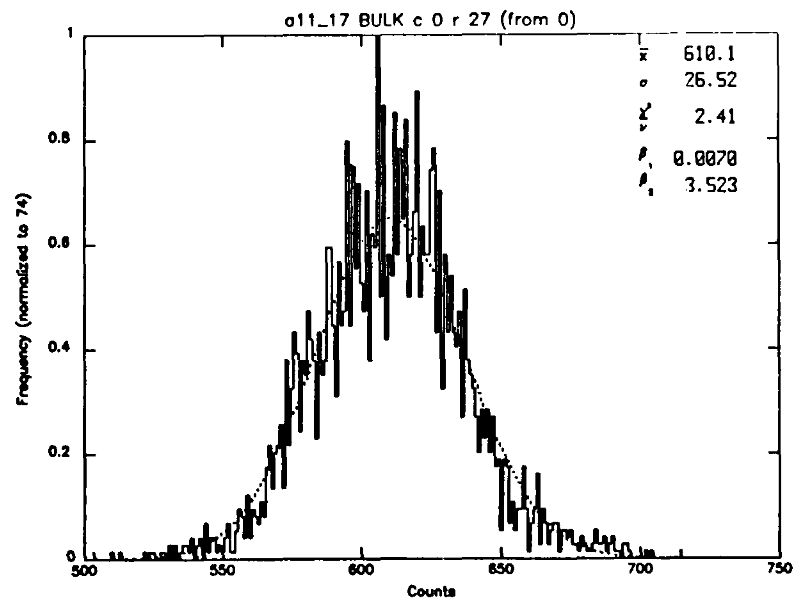
a11_17 BULK c 0 r 27 (from 0)
Frequency (normalized to 74)
Counts
x̄ 610.1
σ 26.52
χ²ν 2.41
β1 0.0070
β2 3.523

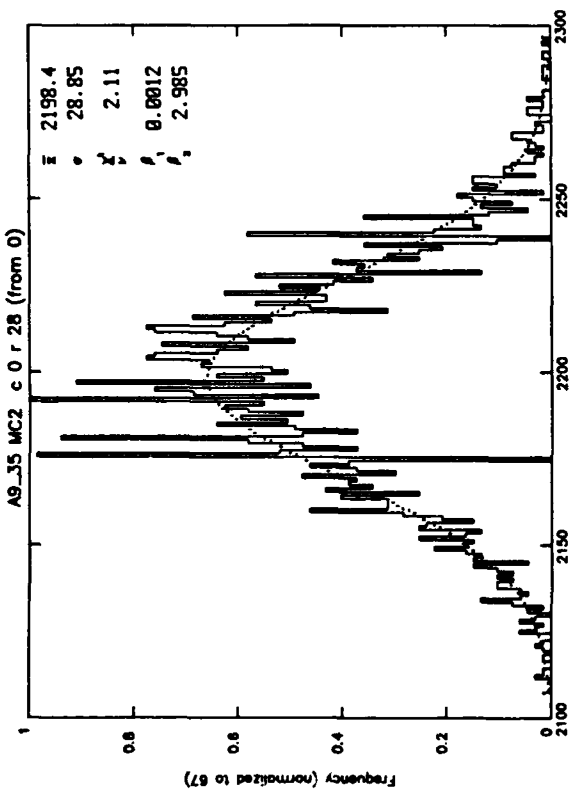
A9_35 MC2 c 0 r 28 (from 0)
Frequency (normalized to 67)
Counts
x̄ 2198.4
σ 28.85
χ²ν 2.11
β1 0.0012
β2 2.985

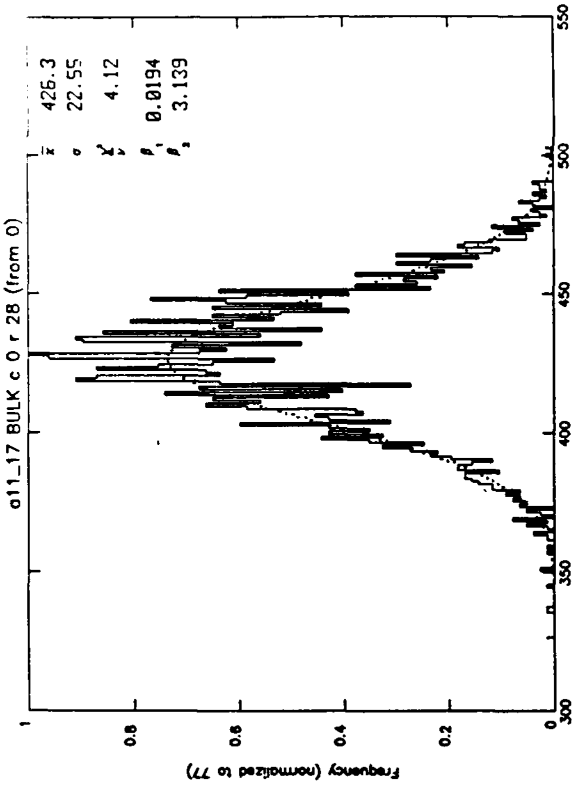
a11_17 BULK c 0 r 28 (from 0)
Frequency (normalized to 77)
Counts
x̄ 426.3
σ 22.55
χ²ν 4.12
β1 0.0194
β2 3.139

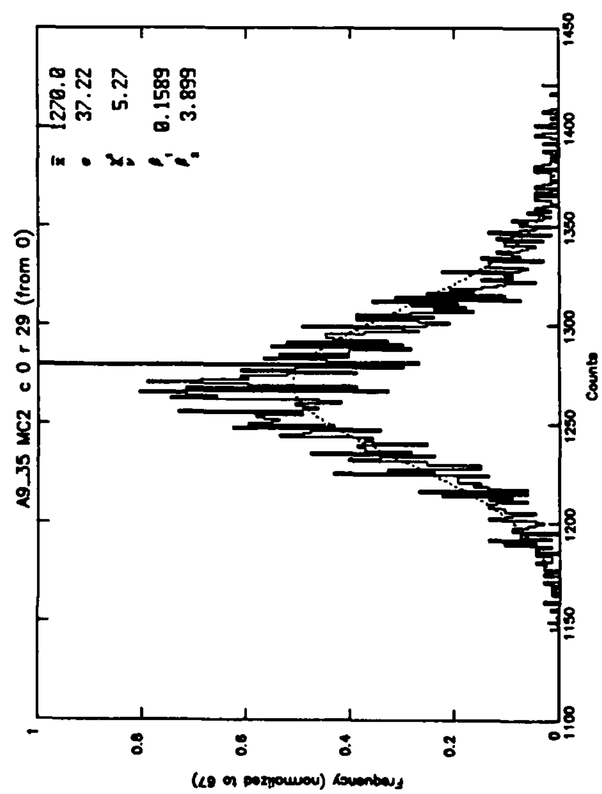
A9_35 MC2 c 0 r 29 (from 0)
Frequency (normalized to 67)
Counts
x̄ 1270.0
σ 37.22
χ²ν 5.27
β1 0.1589
β2 3.899

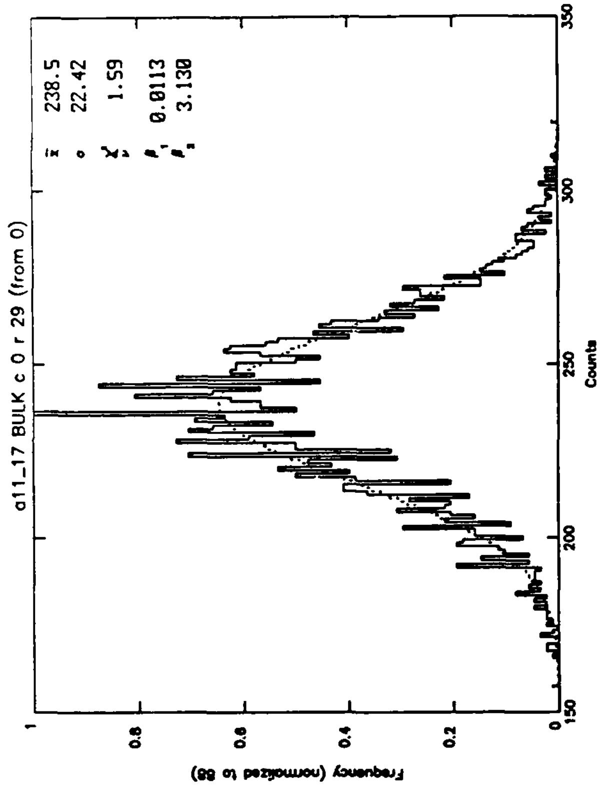
a11_17 BULK c 0 r 29 (from 0)
Counts
x̄ 238.5
σ 22.42
χ²ν 1.59
β1 0.0113
β2 3.130

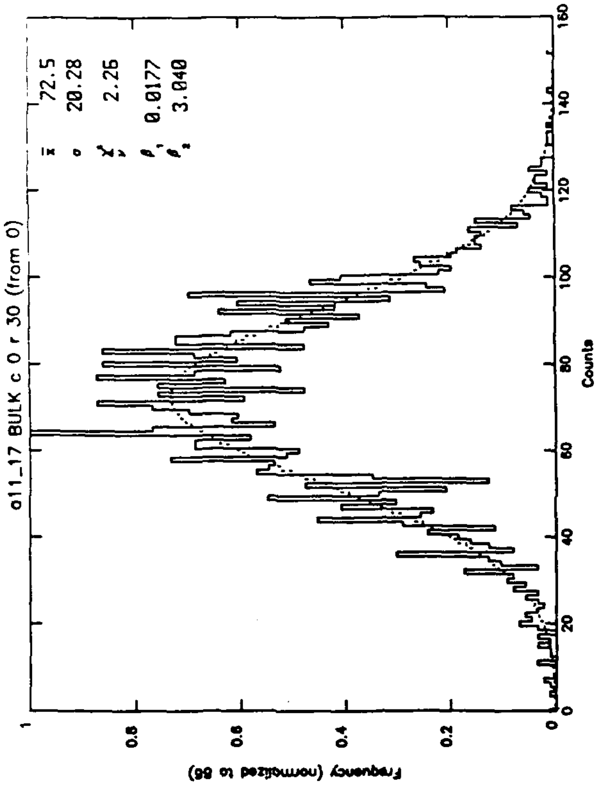
a11_17 BULK c 0 r 30 (from 0)
$\bar{x}$ 72.5
σ 20.28
χ^2_ν 2.26
β_1 0.0177
β_2 3.040
Frequency (normalized to 66)
Counts

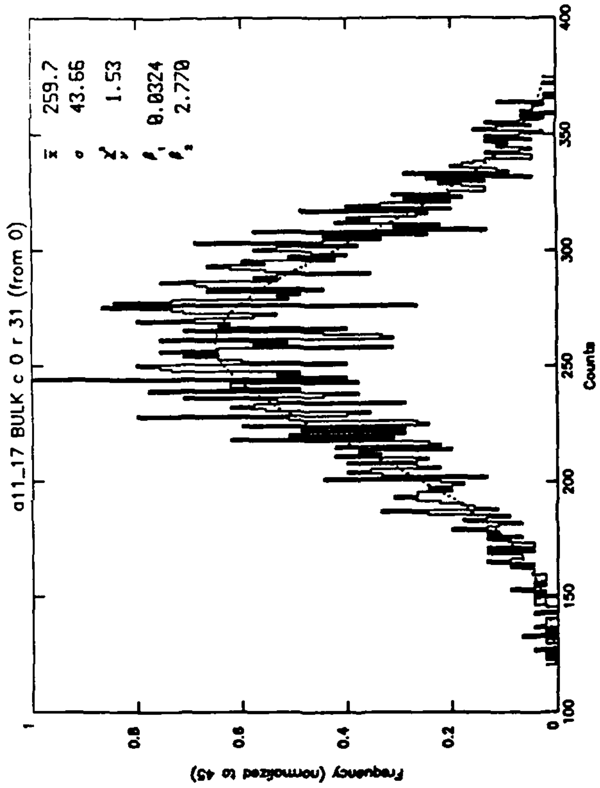
a11_17 BULK c 0 r 31 (from 0)
$\bar{x}$ 259.7
σ 43.66
χ^2_ν 1.53
β_1 0.0324
β_2 2.770
Frequency (normalized to 45)
Counts

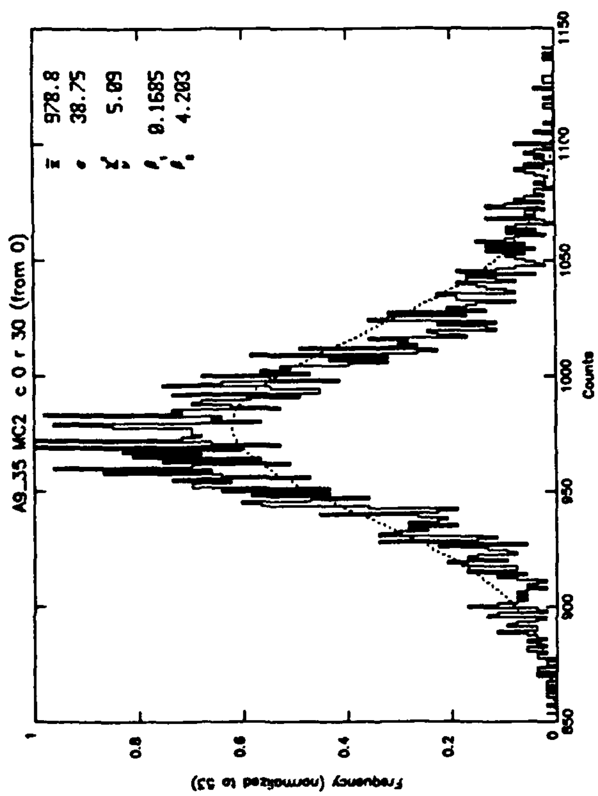
A9_35 MC2 c 0 r 30 (from 0)
$\bar{x}$ 978.8
σ 38.75
χ^2_ν 5.09
β_1 0.1685
β_2 4.203
Frequency (normalized to 53)
Counts

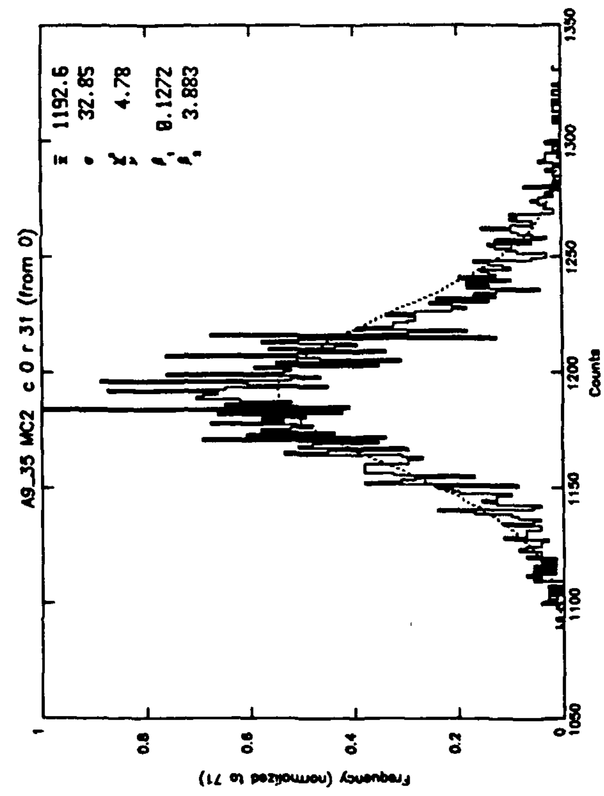
A9_35 MC2 c 0 r 31 (from 0)
$\bar{x}$ 1192.6
σ 32.85
χ^2_ν 4.78
β_1 0.1272
β_2 3.883
Frequency (normalized to 71)
Counts

APPENDIX A-15

Array: Aerojet MC^2 (left) and Aerojet Bulk (right) Arrays

	Left	Right
Elements:	Column 5, Rows 0-31	Column 5, Rows 0-31
Data Run:	Background a9_36	Background al1_17

Purpose: Comparison of MC^2 and Bulk arrays. Columns in identical locations in the representative dewars are chosen. Compare also with Appendix A-14 where column 0 is selected and with Appendix A-16 where full sets of data from columns 0 and 5 are used. Note that Appendices A-14 and A-16 use a different data run (a9_35) for the MC^2 array. The same data run (al1_17) is used for the Bulk array in all three Appendices (14-16).

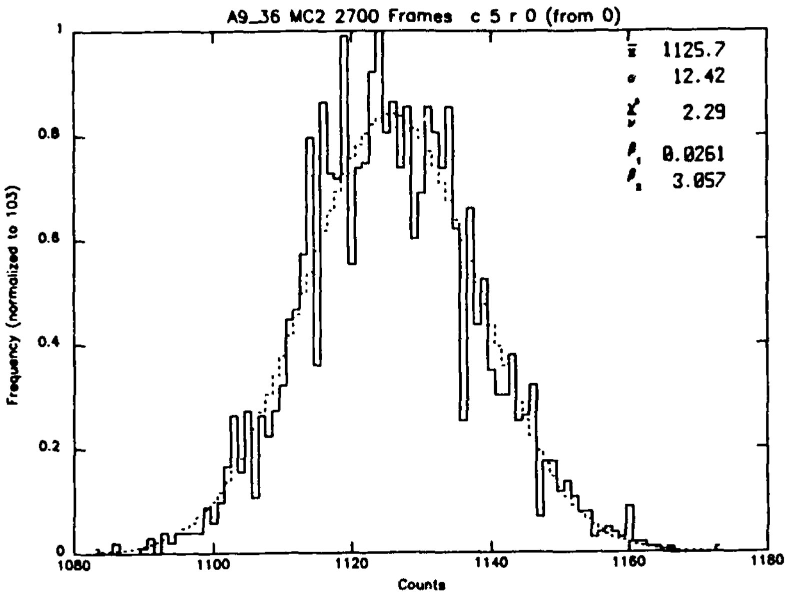
A9_36 MC2 2700 Frames c 5 r 0 (from 0)
x̄ 1125.7
σ 12.42
χ²ν 2.29
β₁ 0.0261
β₂ 3.057
Frequency (normalized to 103)
Counts

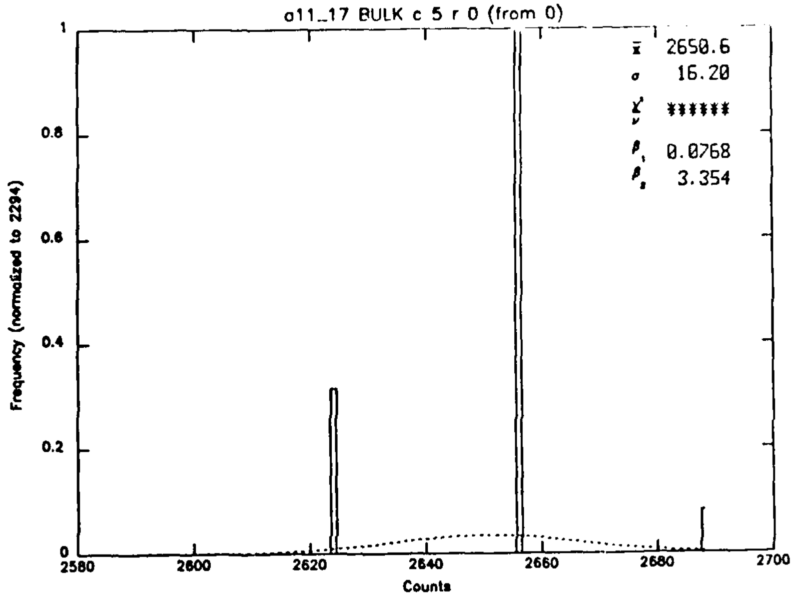
a11_17 BULK c 5 r 0 (from 0)
x̄ 2650.6
σ 16.20
χ²ν ******
β₁ 0.0768
β₂ 3.354
Frequency (normalized to 2294)
Counts

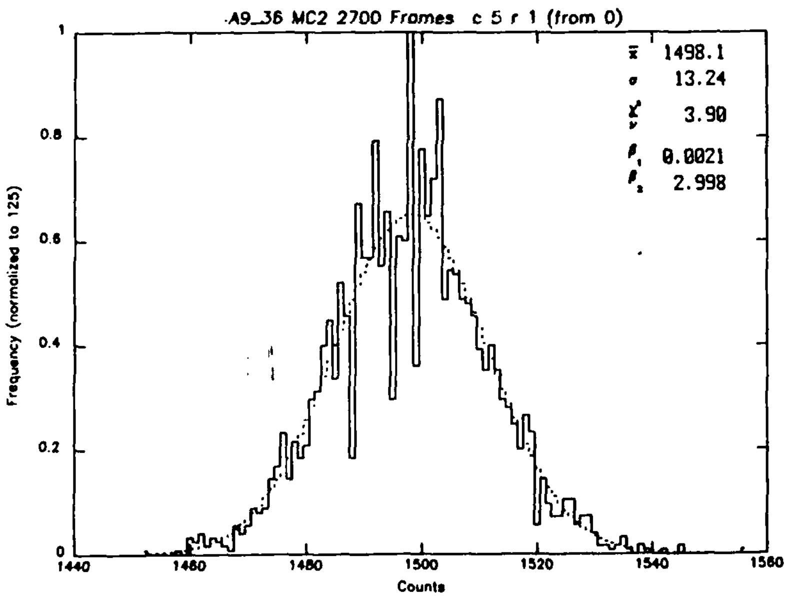
A9_36 MC2 2700 Frames c 5 r 1 (from 0)
x̄ 1498.1
σ 13.24
χ²ν 3.90
β₁ 0.0021
β₂ 2.998
Frequency (normalized to 125)
Counts

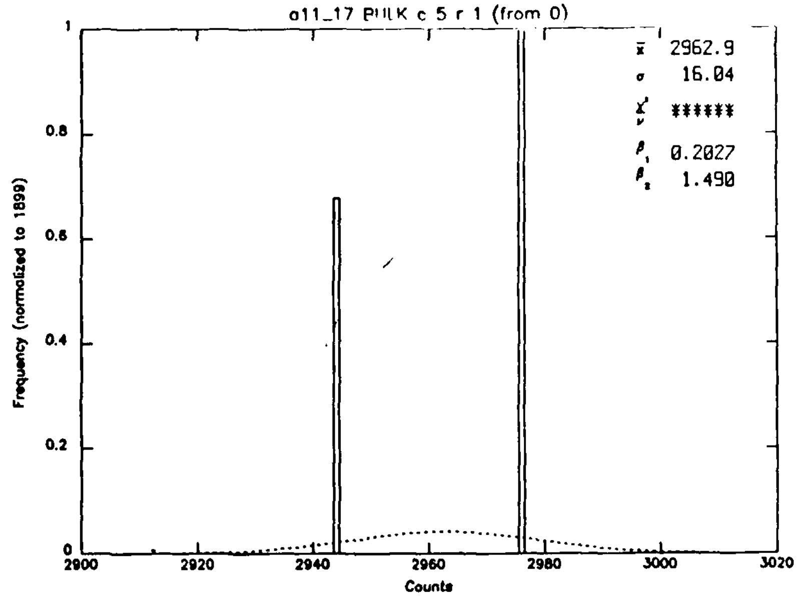
a11_17 BULK c 5 r 1 (from 0)
x̄ 2962.9
σ 16.04
χ²ν ******
β₁ 0.2027
β₂ 1.490
Frequency (normalized to 1899)
Counts

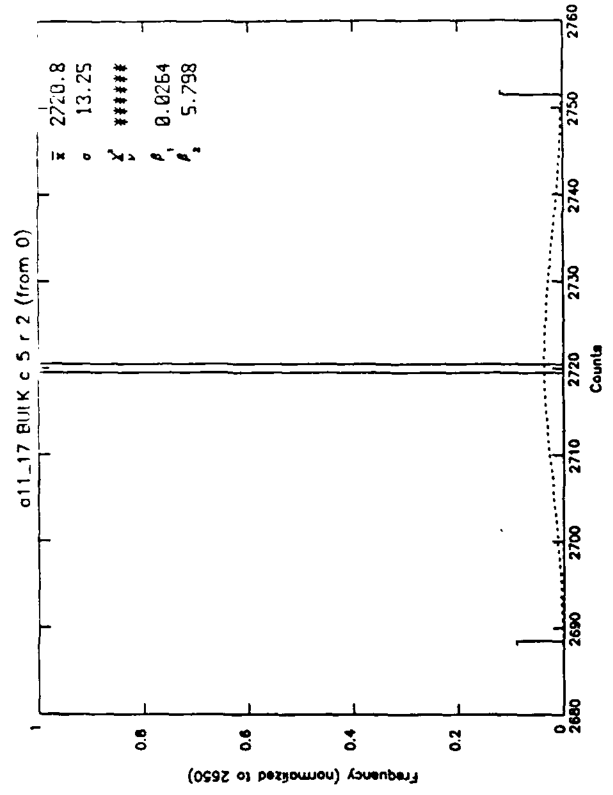

a11_17 BULK c 5 r 2 (from 0)
x̄ 2720.8
σ 13.25
χ^2_ν ******
β_1 0.0264
β_2 5.798
Frequency (normalized to 2650)
Counts

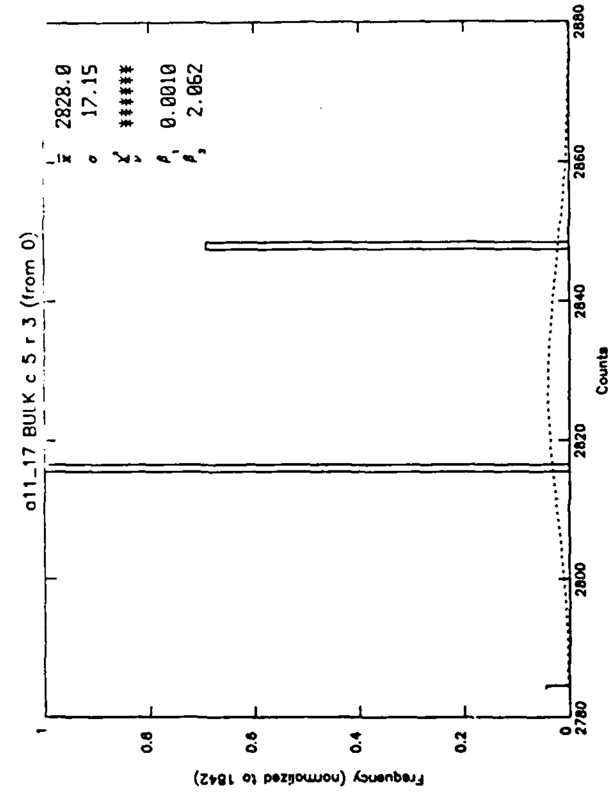

a11_17 BULK c 5 r 3 (from 0)
x̄ 2828.0
σ 17.15
χ^2_ν ******
β_1 0.0010
β_2 2.062
Frequency (normalized to 1842)
Counts

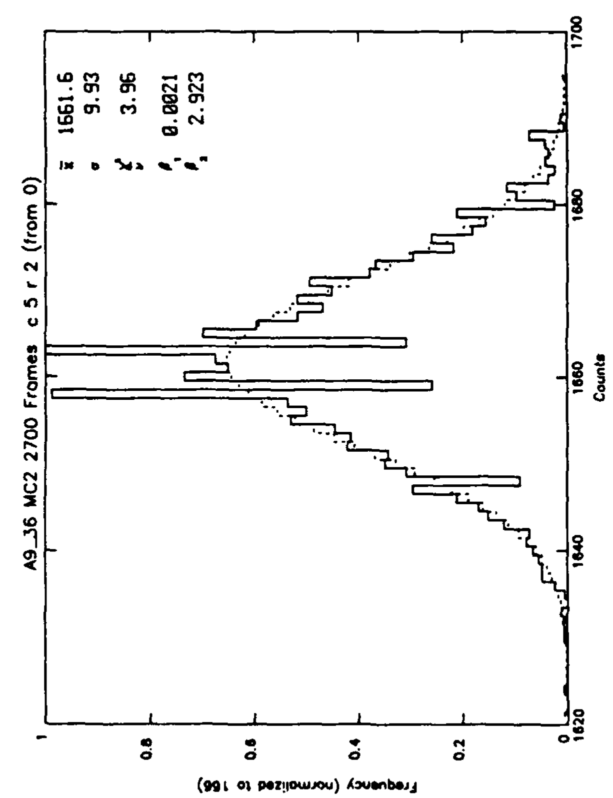

A9_36 MC2 2700 Frames c 5 r 2 (from 0)
x̄ 1661.6
σ 9.93
χ^2_ν 3.96
β_1 0.0021
β_2 2.923
Frequency (normalized to 166)
Counts

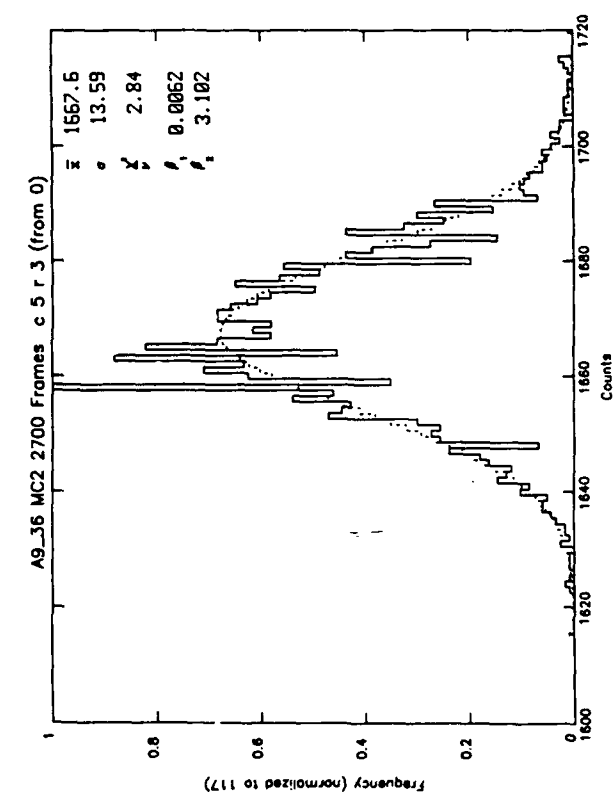

A9_36 MC2 2700 Frames c 5 r 3 (from 0)
x̄ 1667.6
σ 13.59
χ^2_ν 2.84
β_1 0.0062
β_2 3.102
Frequency (normalized to 117)
Counts

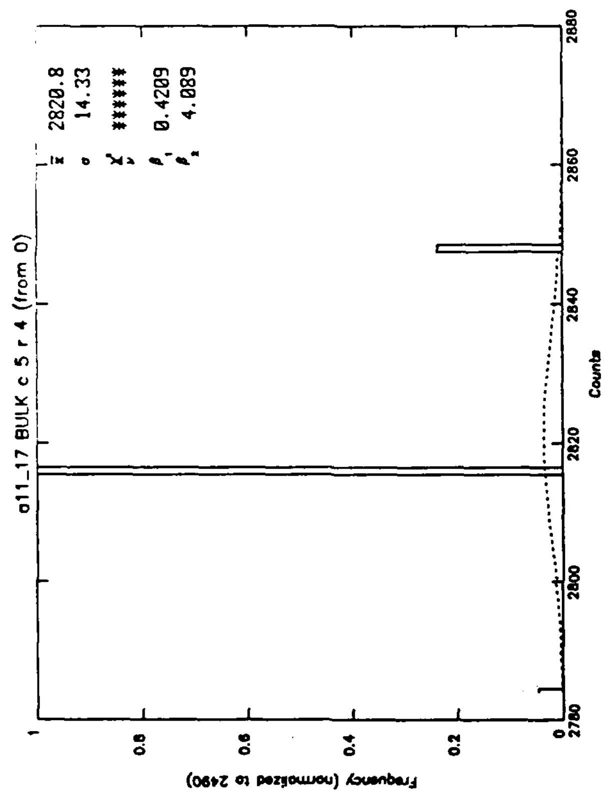
a11_17 BULK c 5 r 4 (from 0)
Frequency (normalized to 2490)
Counts
x̄ 2820.8
σ 14.33
χ² ν ######
β1 0.4209
β2 4.089

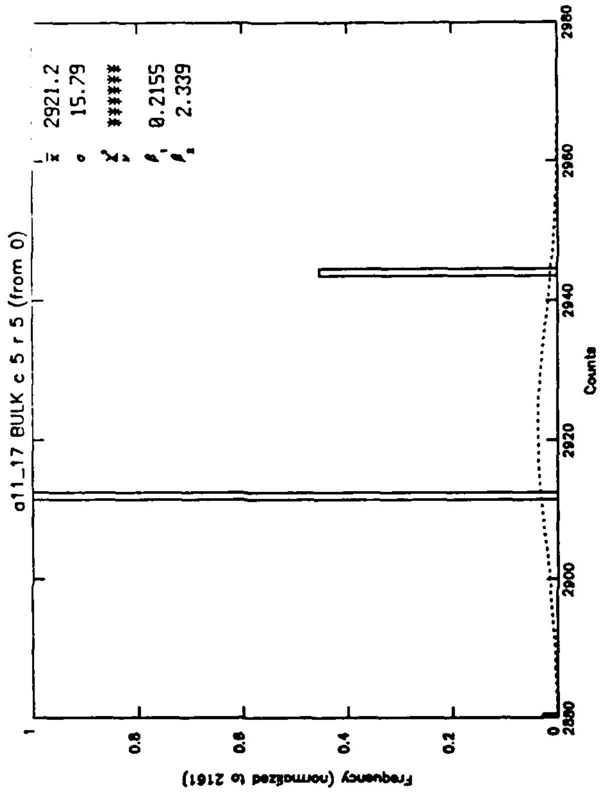
a11_17 BULK c 5 r 5 (from 0)
Frequency (normalized to 2161)
Counts
x̄ 2921.2
σ 15.79
χ² ν ######
β1 0.2155
β2 2.339

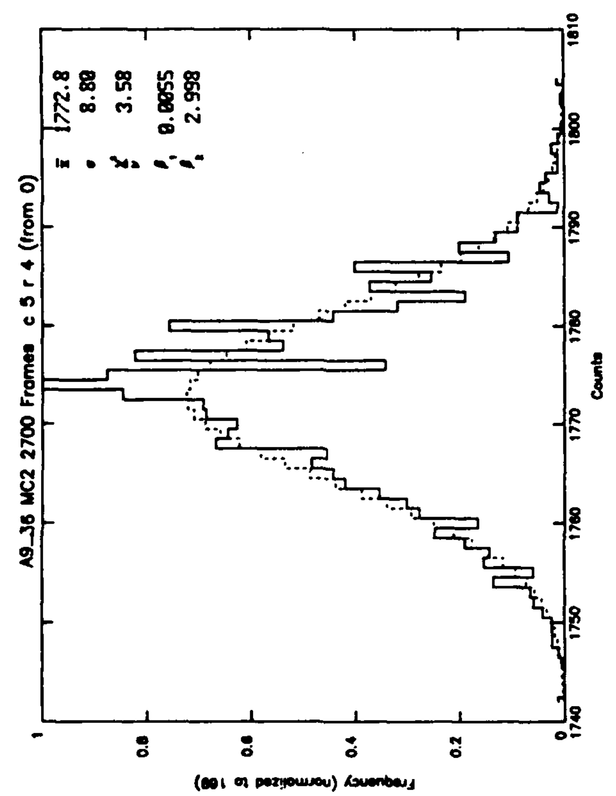
A9_36 MC2 2700 Frames c 5 r 4 (from 0)
Frequency (normalized to 168)
Counts
x̄ 1772.8
σ 8.80
χ² ν 3.58
β1 0.0055
β2 2.998

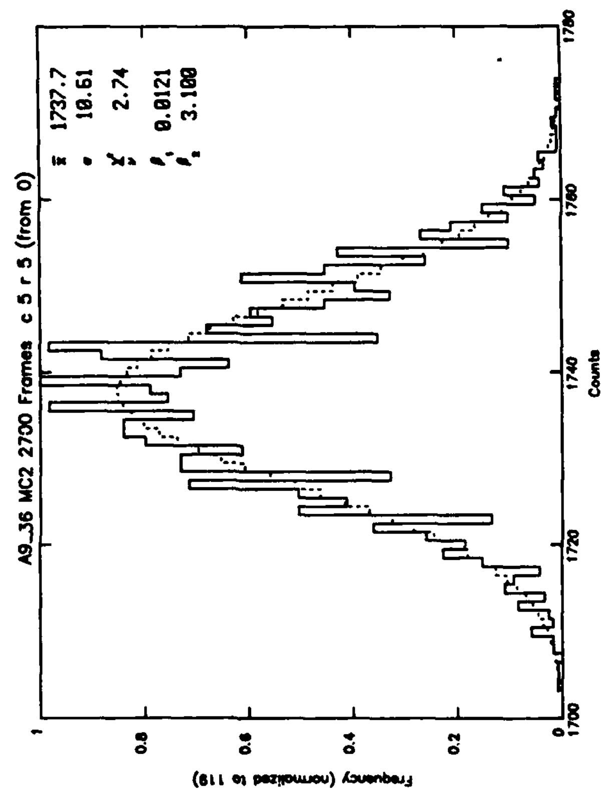
A9_36 MC2 2700 Frames c 5 r 5 (from 0)
Frequency (normalized to 119)
Counts
x̄ 1737.7
σ 10.61
χ² ν 2.74
β1 0.0121
β2 3.100

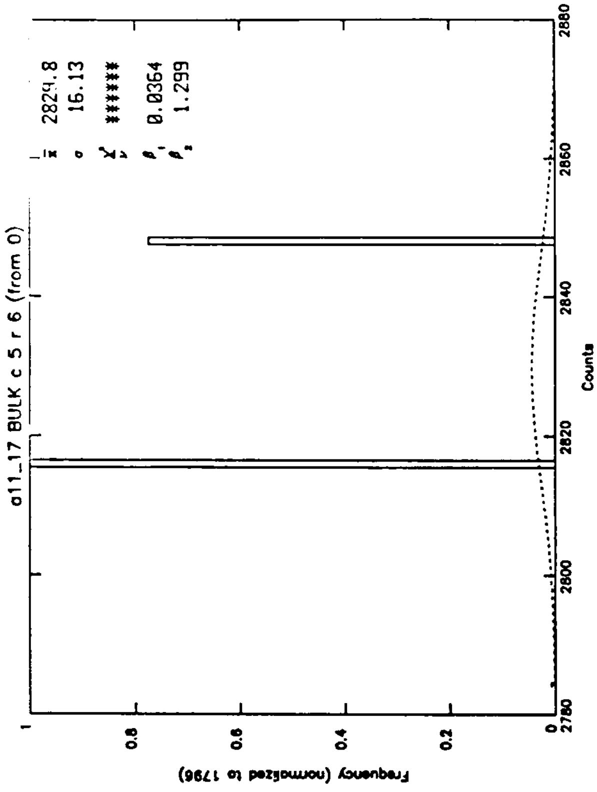
a11_17 BULK c 5 r 6 (from 0)
x̄ 2829.8
σ 16.13
χ^2_ν *****
β_1 0.0364
β_2 1.299
Counts
Frequency (normalized to 1796)

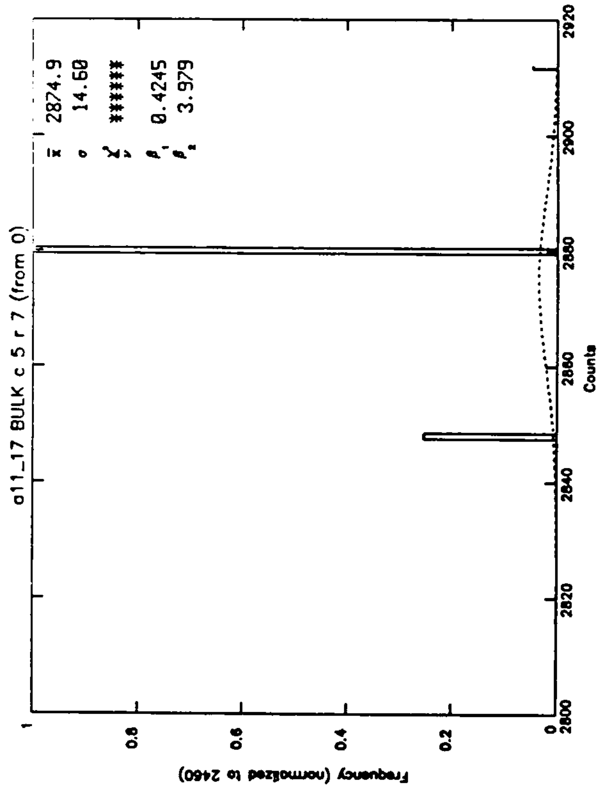
a11_17 BULK c 5 r 7 (from 0)
x̄ 2874.9
σ 14.60
χ^2_ν *****
β_1 0.4245
β_2 3.979
Counts
Frequency (normalized to 2460)

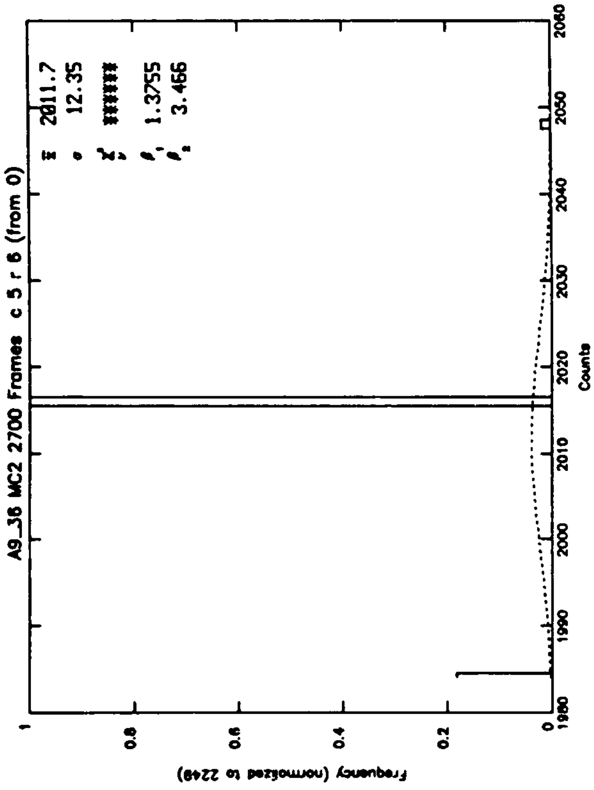
A9_36 MC2 2700 Frames c 5 r 6 (from 0)
x̄ 2011.7
σ 12.35
χ^2_ν *****
β_1 1.3755
β_2 3.466
Counts
Frequency (normalized to 2248)

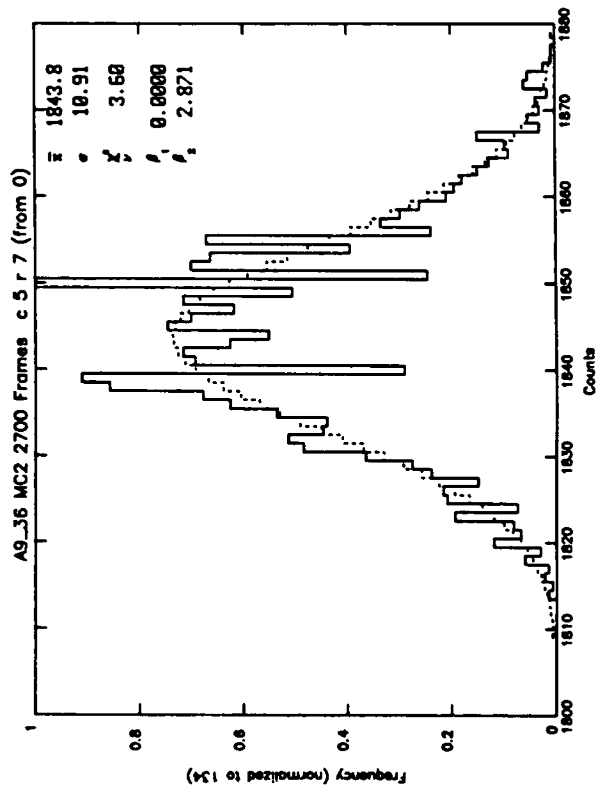
A9_36 MC2 2700 Frames c 5 r 7 (from 0)
x̄ 1843.8
σ 10.91
χ^2_ν 3.60
β_1 0.0000
β_2 2.871
Counts
Frequency (normalized to 134)

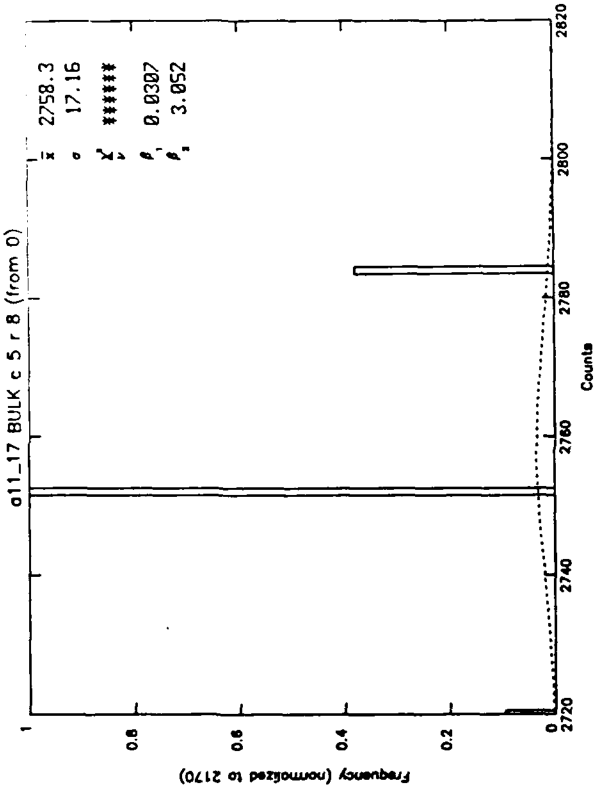
a11_17 BULK c 5 r 8 (from 0)
$\bar{x}$ 2758.3
σ 17.16
χ^2_ν ******
β_1 0.0307
β_2 3.052
Counts
Frequency (normalized to 2170)

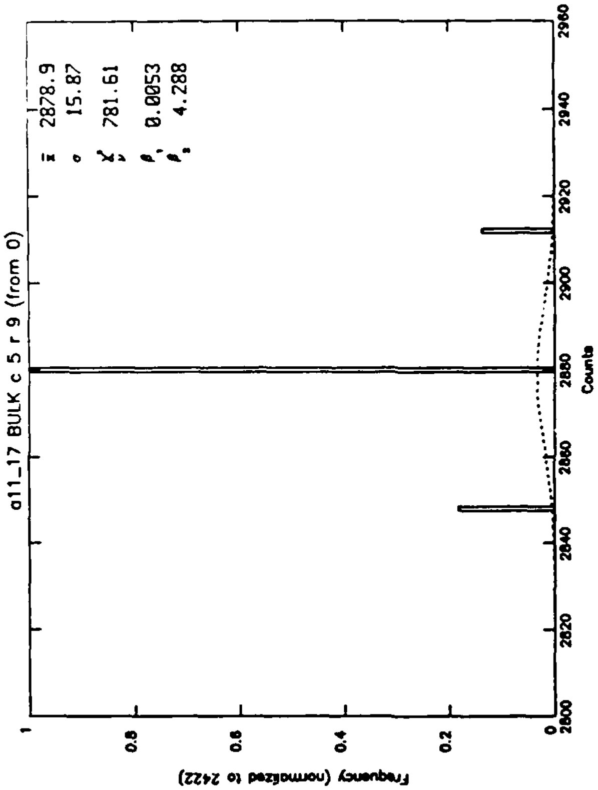
a11_17 BULK c 5 r 9 (from 0)
$\bar{x}$ 2878.9
σ 15.87
χ^2_ν 781.61
β_1 0.0053
β_2 4.288
Counts
Frequency (normalized to 2422)

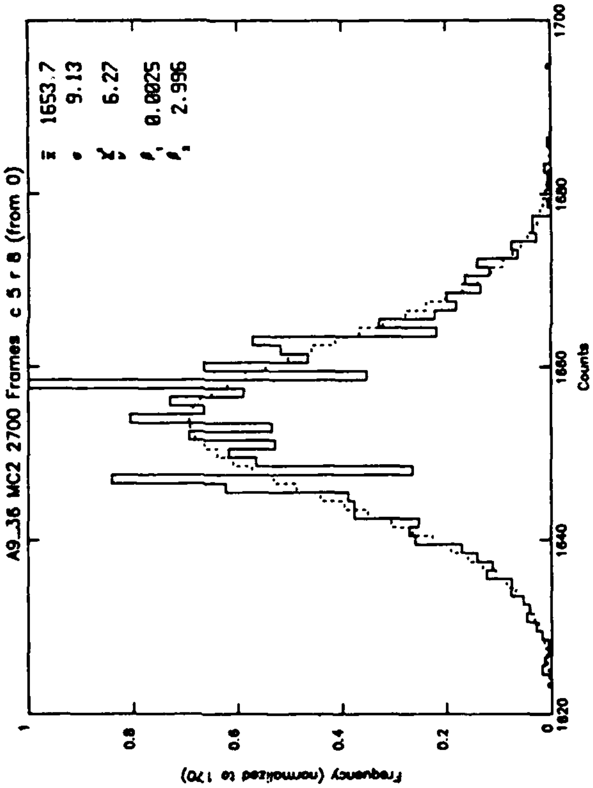
A9_36 MC2 2700 Frames c 5 r 8 (from 0)
$\bar{x}$ 1653.7
σ 9.13
χ^2_ν 6.27
β_1 0.0025
β_2 2.996
Counts
Frequency (normalized to 170)

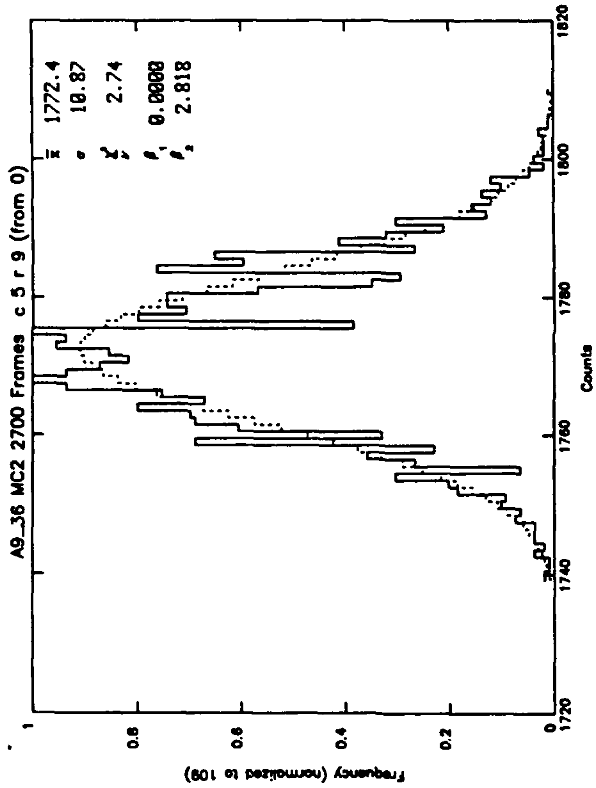
A9_36 MC2 2700 Frames c 5 r 9 (from 0)
$\bar{x}$ 1772.4
σ 10.87
χ^2_ν 2.74
β_1 0.0000
β_2 2.818
Counts
Frequency (normalized to 108)

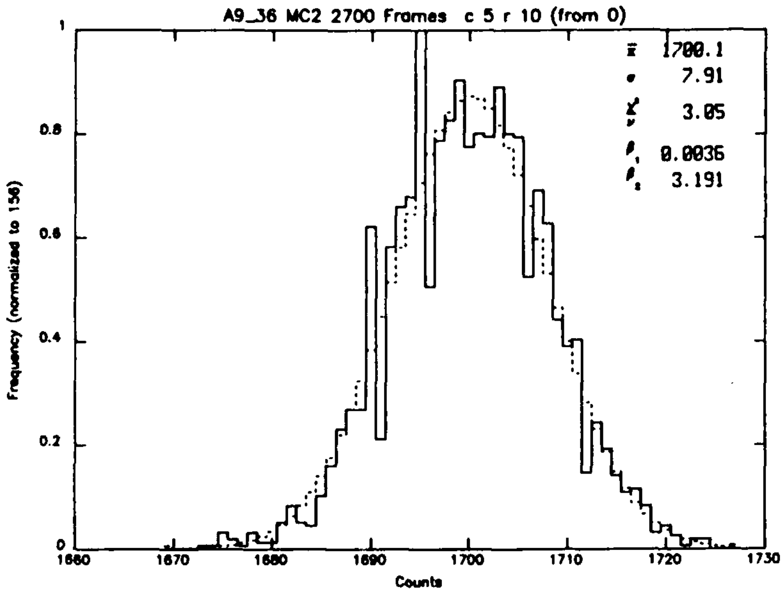
A9_36 MC2 2700 Frames c 5 r 10 (from 0)
$\bar{x}$ 1700.1
σ 7.91
χ^2_ν 3.05
β_1 0.0036
β_2 3.191
Frequency (normalized to 156)
Counts
0
0.2
0.4
0.6
0.8
1
1660
1670
1680
1690
1700
1710
1720
1730

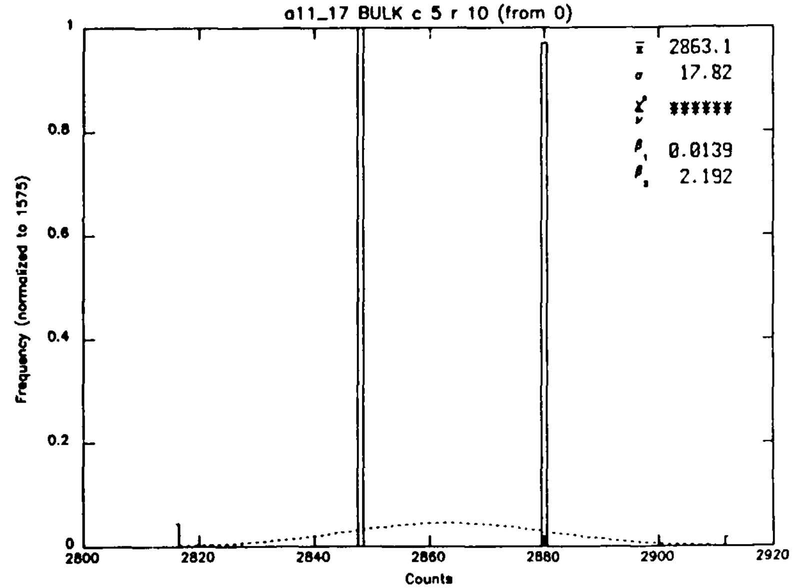
a11_17 BULK c 5 r 10 (from 0)
$\bar{x}$ 2863.1
σ 17.82
χ^2_ν ******
β_1 0.0139
β_2 2.192
Frequency (normalized to 1575)
Counts
0
0.2
0.4
0.6
0.8
1
2800
2820
2840
2860
2880
2900
2920

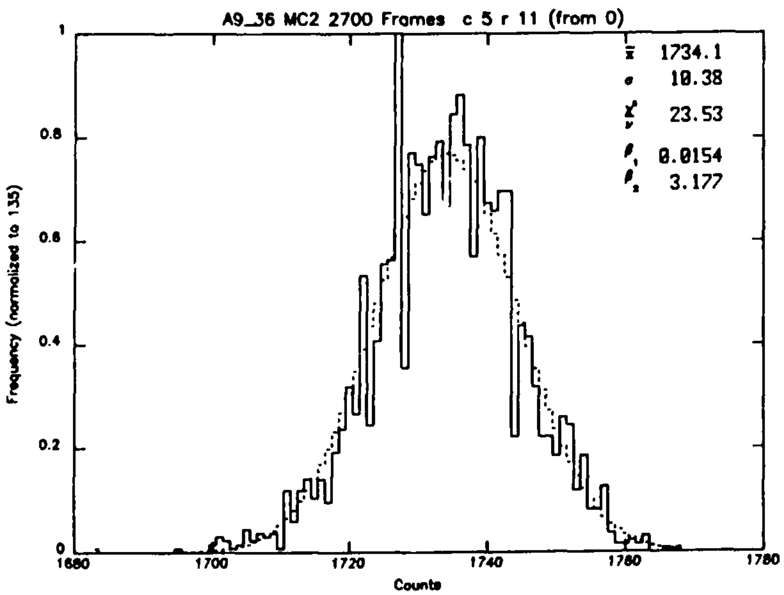
A9_36 MC2 2700 Frames c 5 r 11 (from 0)
$\bar{x}$ 1734.1
σ 10.38
χ^2_ν 23.53
β_1 0.0154
β_2 3.177
Frequency (normalized to 135)
Counts
0
0.2
0.4
0.6
0.8
1
1680
1700
1720
1740
1760
1780

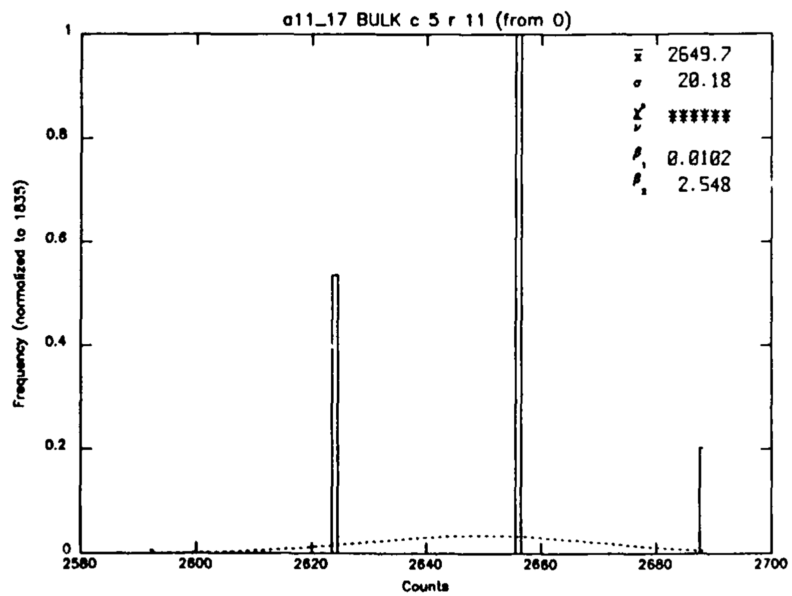
a11_17 BULK c 5 r 11 (from 0)
$\bar{x}$ 2649.7
σ 20.18
χ^2_ν ******
β_1 0.0102
β_2 2.548
Frequency (normalized to 1835)
Counts
0
0.2
0.4
0.6
0.8
1
2580
2600
2620
2640
2660
2680
2700

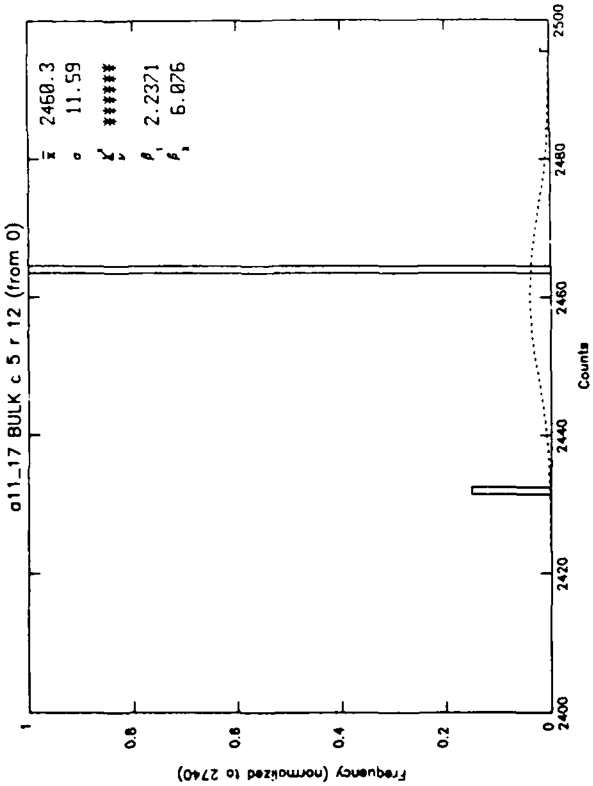
a11_17 BULK c 5 r 12 (from 0)
x̄ 2460.3
σ 11.59
χ²ν ******
β₁ 2.2371
β₂ 6.076
Frequency (normalized to 2740)
Counts

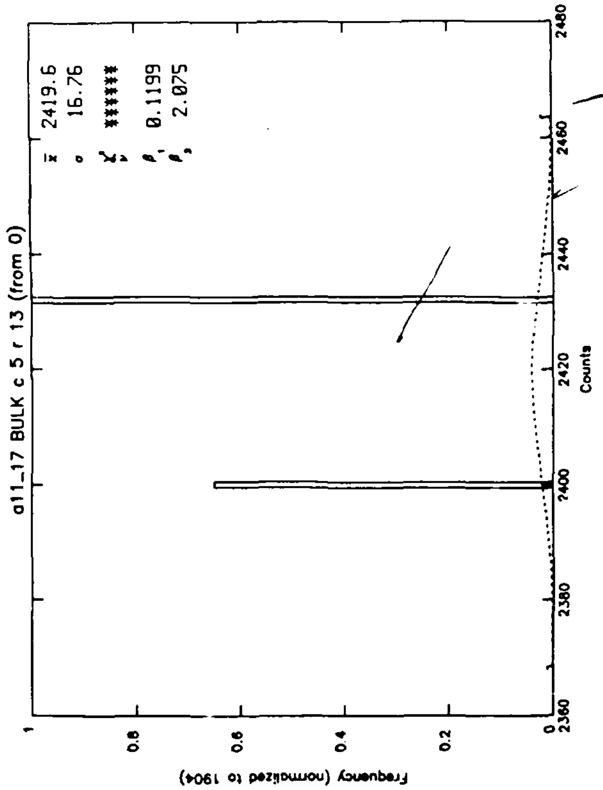
a11_17 BULK c 5 r 13 (from 0)
x̄ 2419.6
σ 16.76
χ²ν ******
β₁ 0.1199
β₂ 2.075
Frequency (normalized to 1904)
Counts

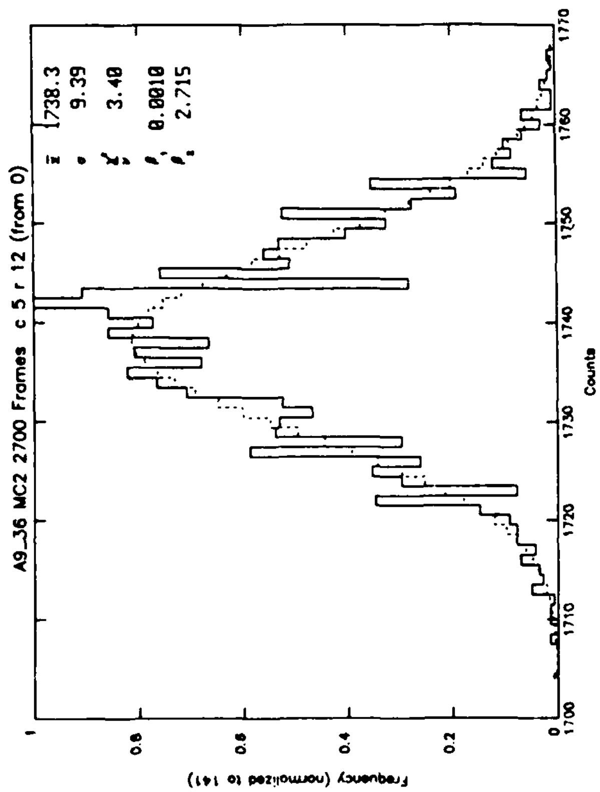
A9_36 MC2 2700 Frames c 5 r 12 (from 0)
x̄ 1738.3
σ 9.39
χ²ν 3.40
β₁ 0.0010
β₂ 2.715
Frequency (normalized to 141)
Counts

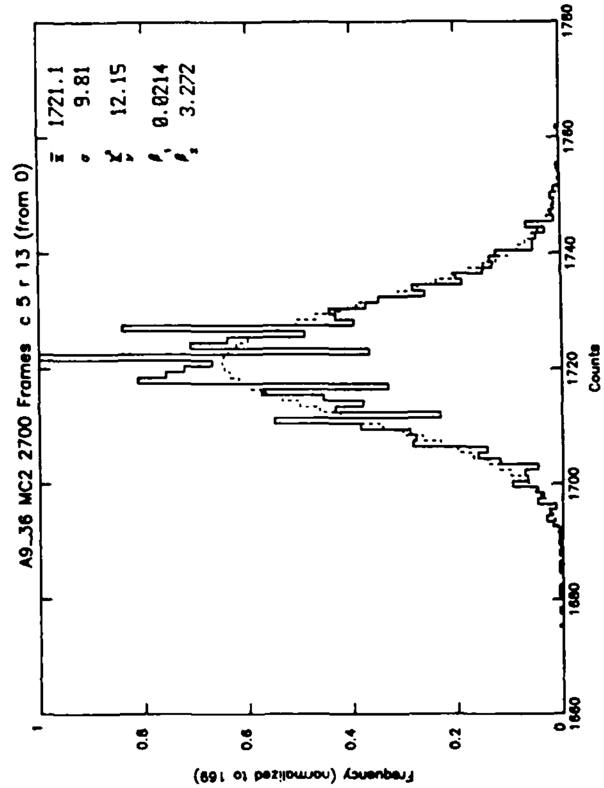
A9_36 MC2 2700 Frames c 5 r 13 (from 0)
x̄ 1721.1
σ 9.81
χ²ν 12.15
β₁ 0.0214
β₂ 3.272
Frequency (normalized to 169)
Counts

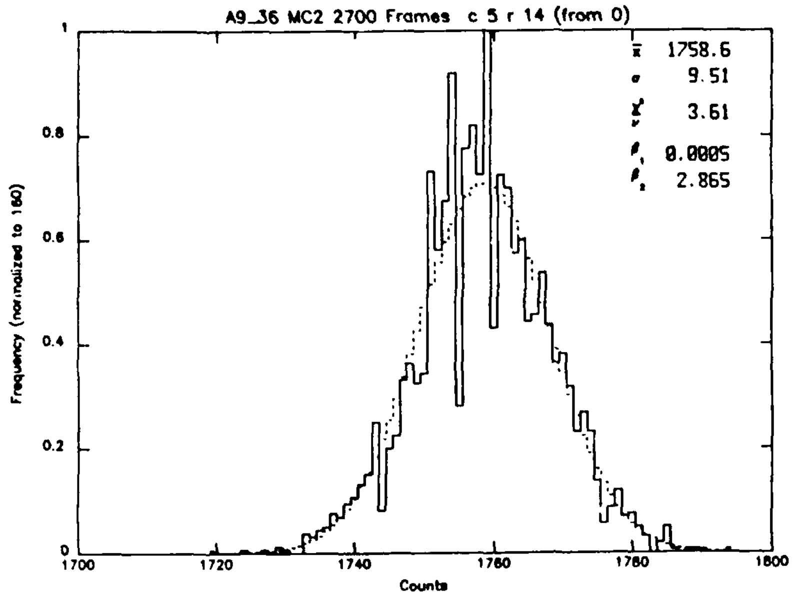
A9_36 MC2 2700 Frames c 5 r 14 (from 0)
x̄ 1758.6
σ 9.51
χ²ν 3.61
β1 0.0005
β2 2.865
Frequency (normalized to 160)
Counts

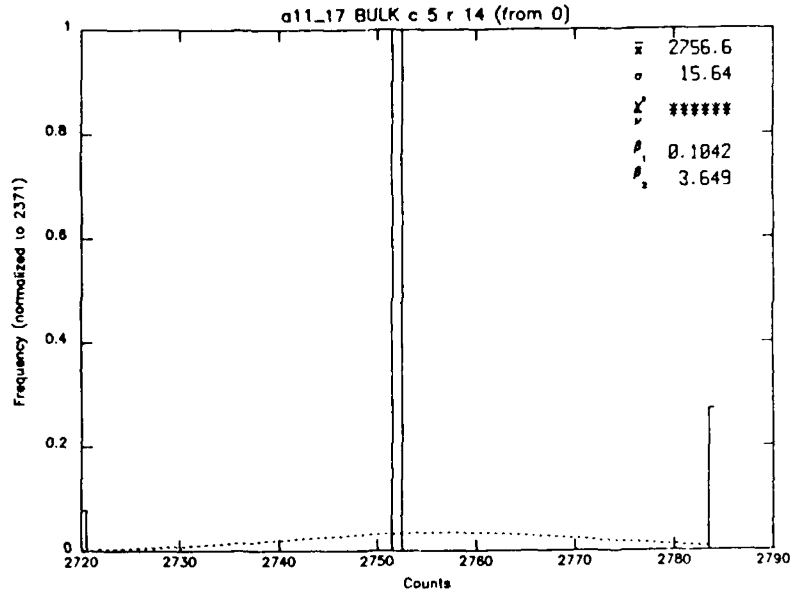
a11_17 BULK c 5 r 14 (from 0)
x̄ 2756.6
σ 15.64
χ²ν ******
β1 0.1042
β2 3.649
Frequency (normalized to 2371)
Counts

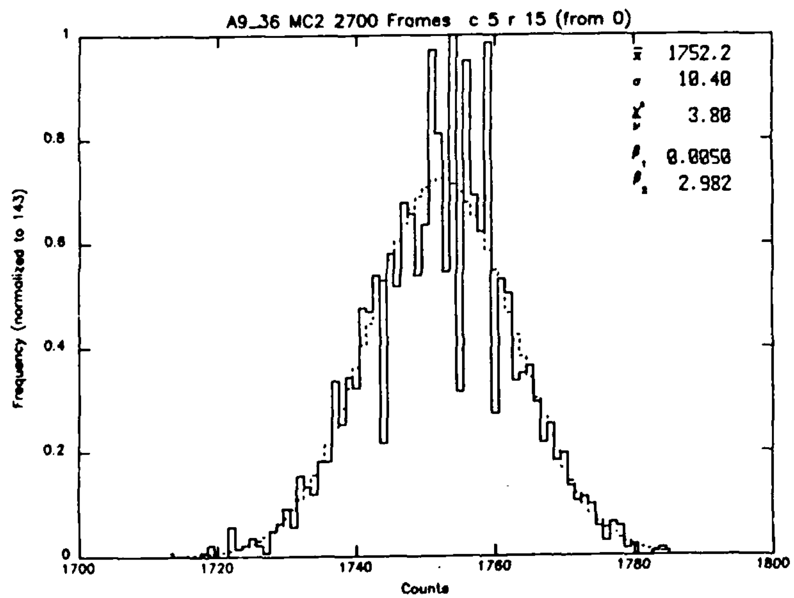
A9_36 MC2 2700 Frames c 5 r 15 (from 0)
x̄ 1752.2
σ 10.40
χ²ν 3.80
β1 0.0050
β2 2.982
Frequency (normalized to 143)
Counts

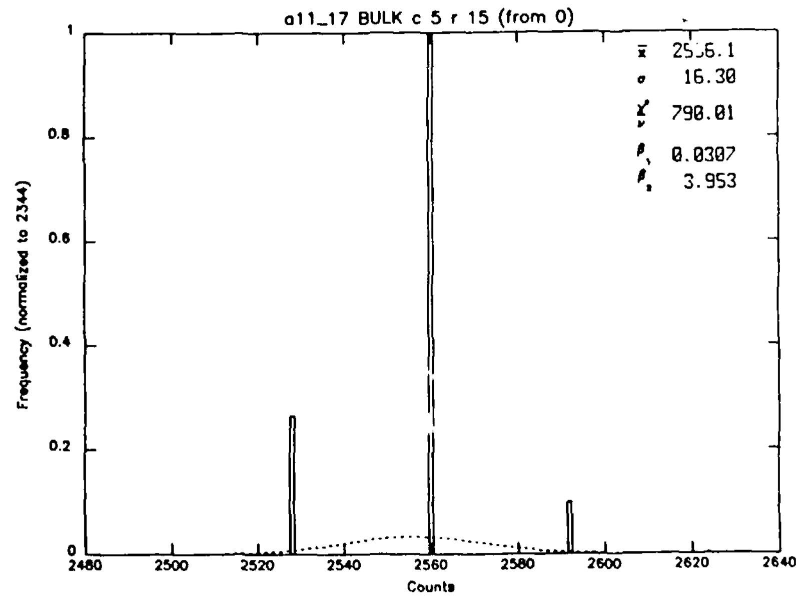
a11_17 BULK c 5 r 15 (from 0)
σ 16.30
χ²ν 790.01
β1 0.0307
β2 3.953
Frequency (normalized to 2344)
Counts

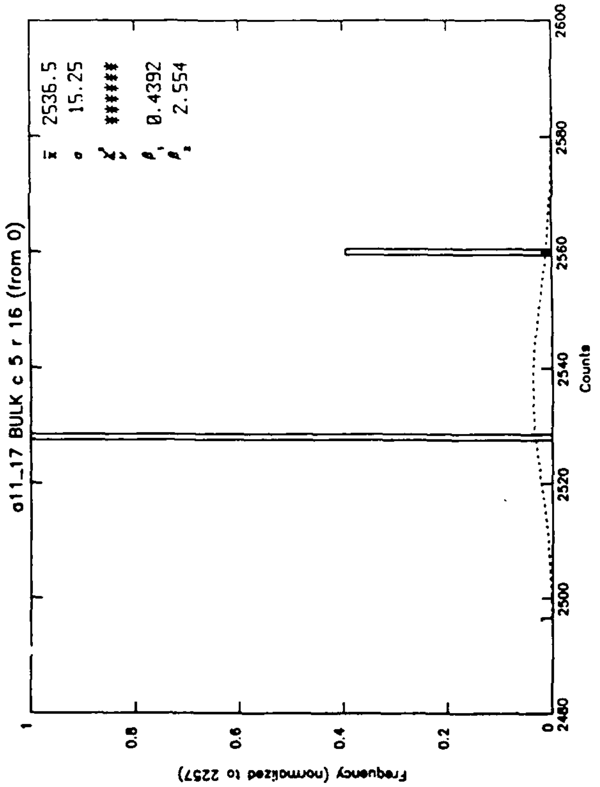
a11_17 BULK c 5 r 16 (from 0)
Frequency (normalized to 2257)
Counts
x̄ 2536.5
σ 15.25
χ² ν ######
β₁ 0.4392
β₂ 2.554

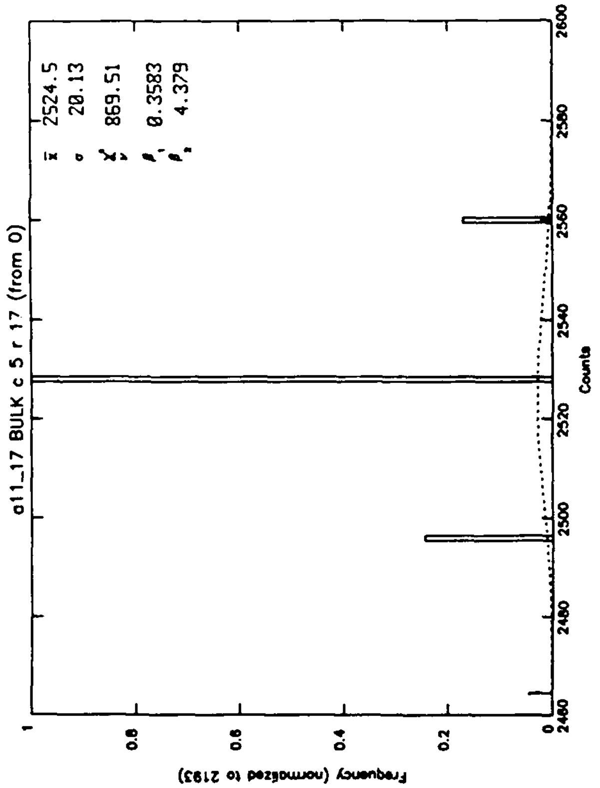
a11_17 BULK c 5 r 17 (from 0)
Frequency (normalized to 2193)
Counts
x̄ 2524.5
σ 20.13
χ² ν 869.51
β₁ 0.3583
β₂ 4.379

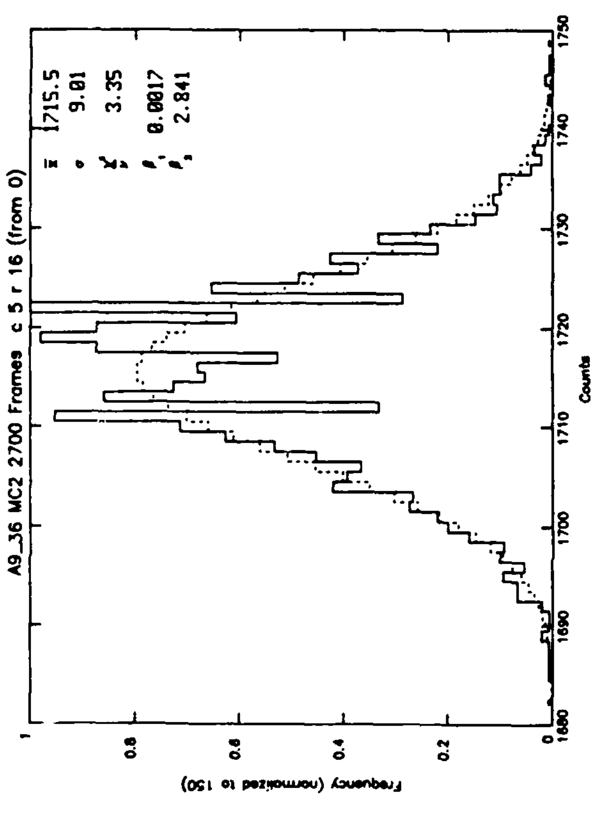
A9_36 MC2 2700 Frames c 5 r 16 (from 0)
Frequency (normalized to 150)
Counts
x̄ 1715.5
σ 9.01
χ² ν 3.35
β₁ 0.0017
β₂ 2.841

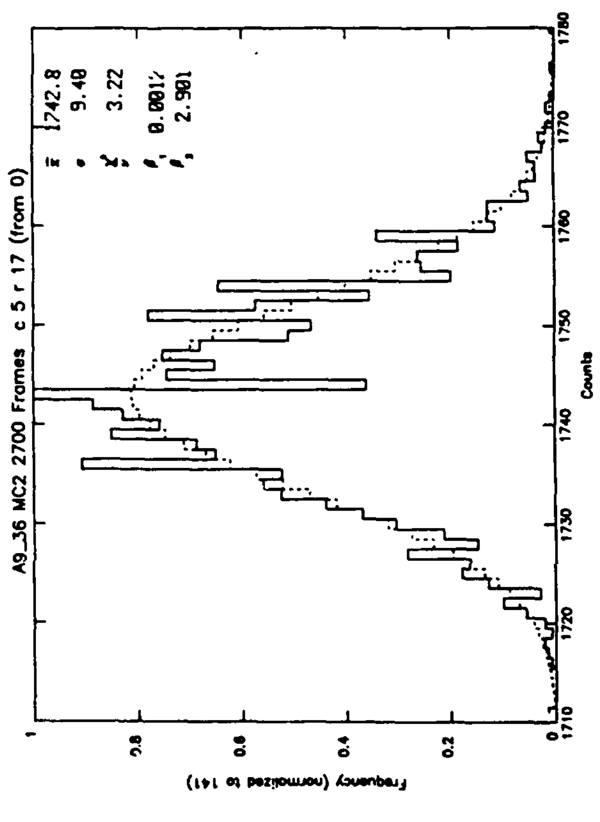
A9_36 MC2 2700 Frames c 5 r 17 (from 0)
Frequency (normalized to 141)
Counts
x̄ 1742.8
σ 9.40
χ² ν 3.22
β₁ 0.0017
β₂ 2.981

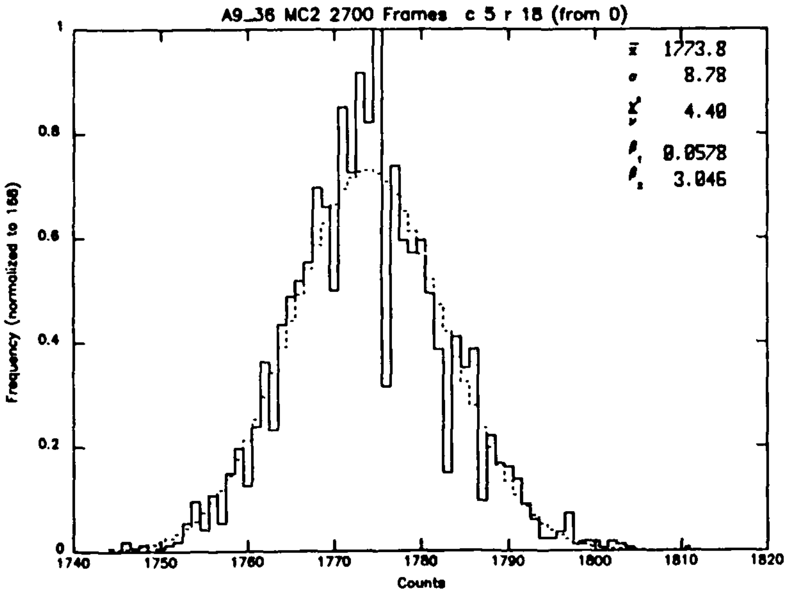
A9_36 MC2 2700 Frames c 5 r 18 (from 0)
x̄ 1773.8
σ 8.78
χ²ν 4.40
β1 0.0578
β2 3.046
Frequency (normalized to 168)
Counts

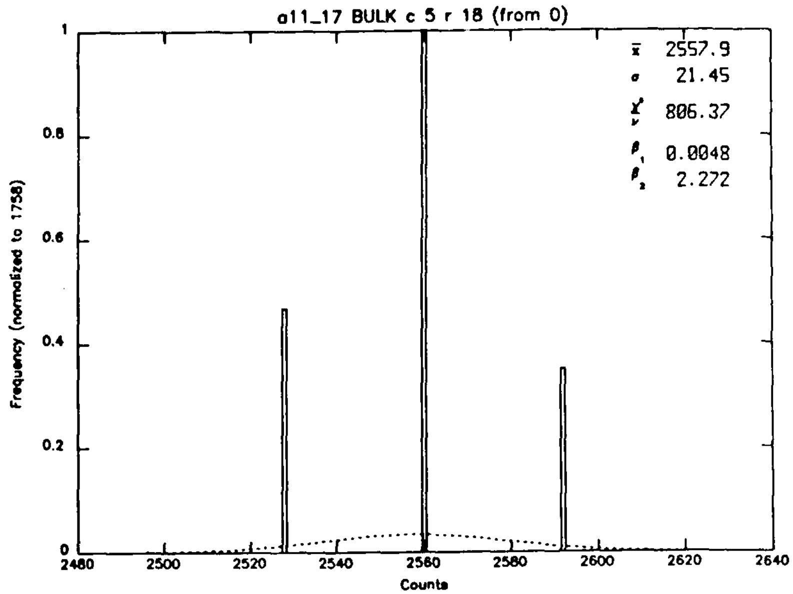
a11_17 BULK c 5 r 18 (from 0)
x̄ 2557.9
σ 21.45
χ²ν 806.37
β1 0.0048
β2 2.272
Frequency (normalized to 1758)
Counts

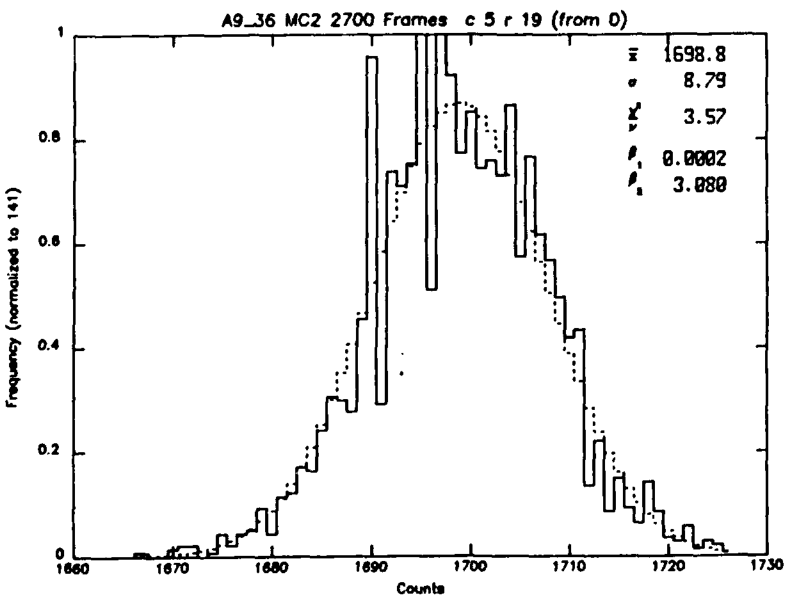
A9_36 MC2 2700 Frames c 5 r 19 (from 0)
x̄ 1698.8
σ 8.79
χ²ν 3.57
β1 0.0002
β2 3.080
Frequency (normalized to 141)
Counts

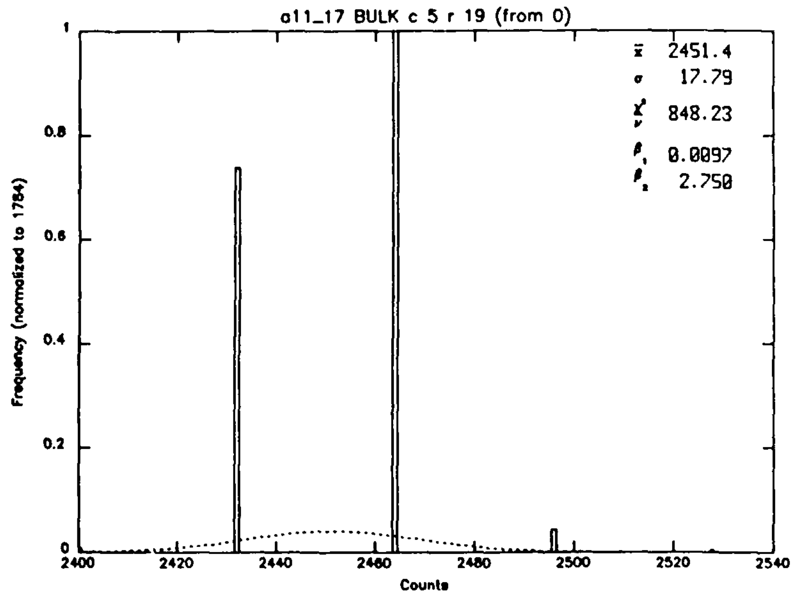
a11_17 BULK c 5 r 19 (from 0)
x̄ 2451.4
σ 17.79
χ²ν 848.23
β1 0.0097
β2 2.750
Frequency (normalized to 1784)
Counts

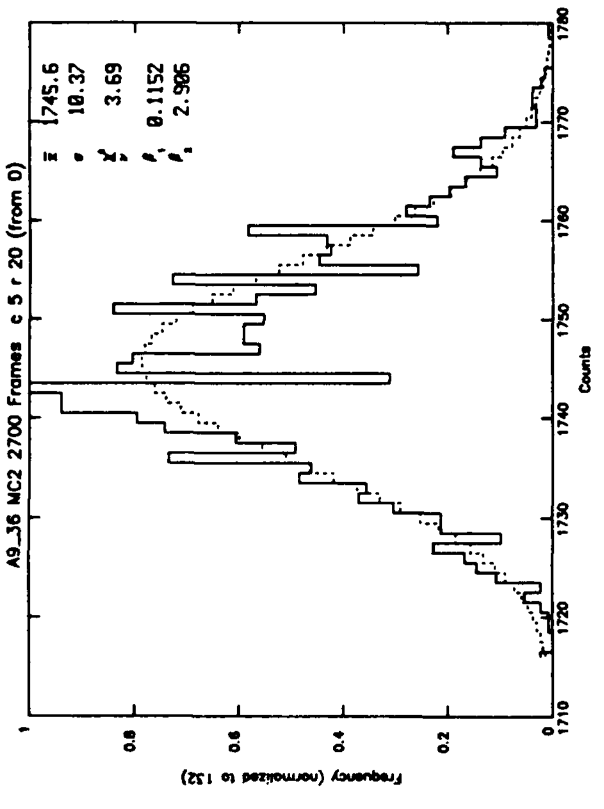
A9_36 MC2 2700 Frames c 5 r 20 (from 0)
$\bar{x}$ 1745.6
σ 10.37
χ^2_ν 3.69
β_1 0.1152
β_2 2.906
Frequency (normalized to 132)
Counts

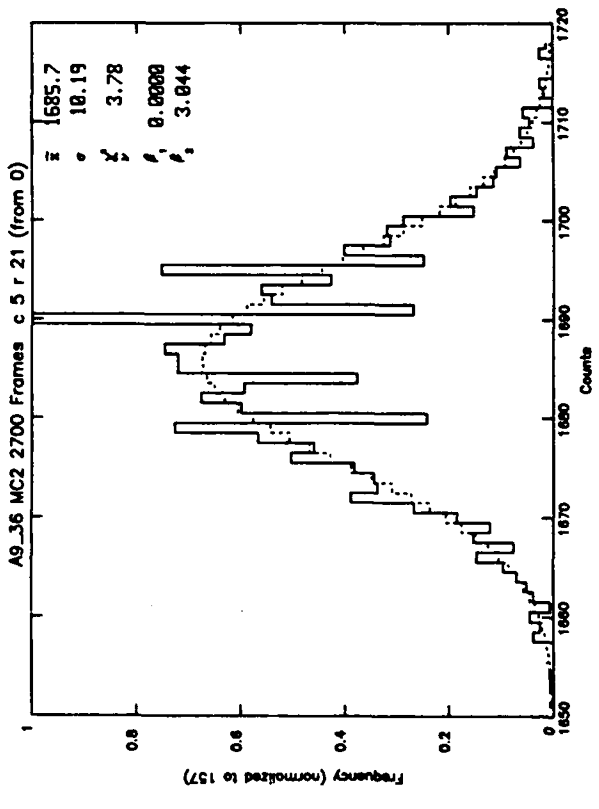
A9_36 MC2 2700 Frames c 5 r 21 (from 0)
$\bar{x}$ 1685.7
σ 10.19
χ^2_ν 3.78
β_1 0.0000
β_2 3.044
Frequency (normalized to 157)
Counts

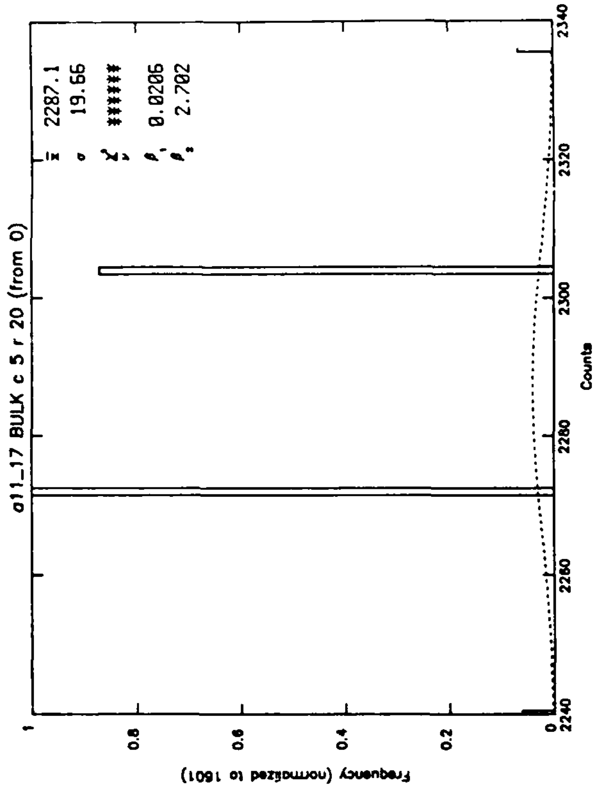
a11_17 BULK c 5 r 20 (from 0)
$\bar{x}$ 2287.1
σ 19.66
χ^2_ν ******
β_1 0.0206
β_2 2.702
Frequency (normalized to 1601)
Counts

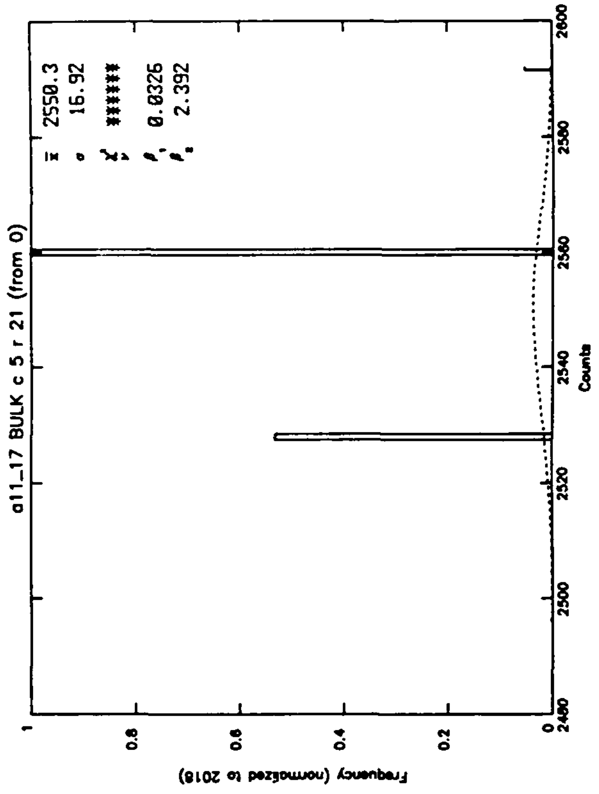
a11_17 BULK c 5 r 21 (from 0)
$\bar{x}$ 2550.3
σ 16.92
χ^2_ν ******
β_1 0.0326
β_2 2.392
Frequency (normalized to 2018)
Counts

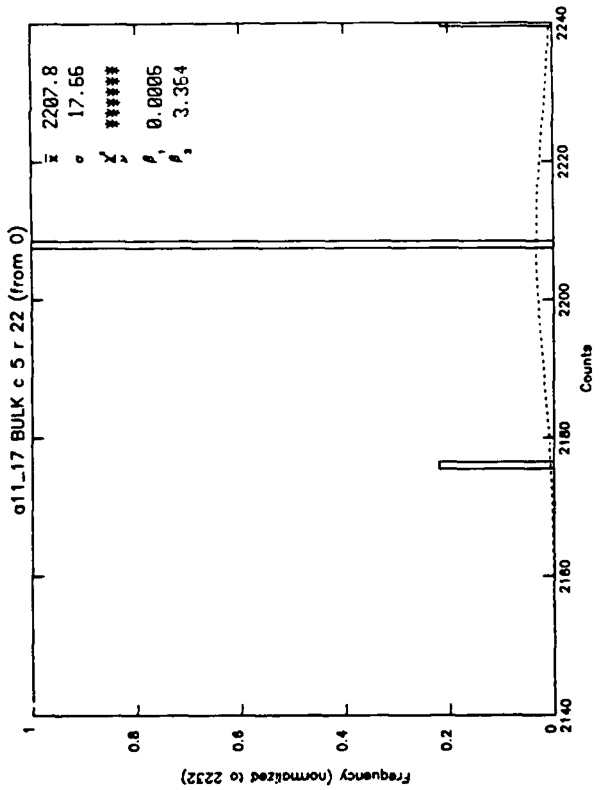
a11_17 BULK c 5 r 22 (from 0)
x̄ 2207.8
σ 17.66
χ² *****
β₁ 0.0006
β₂ 3.364
Frequency (normalized to 2232)
Counts

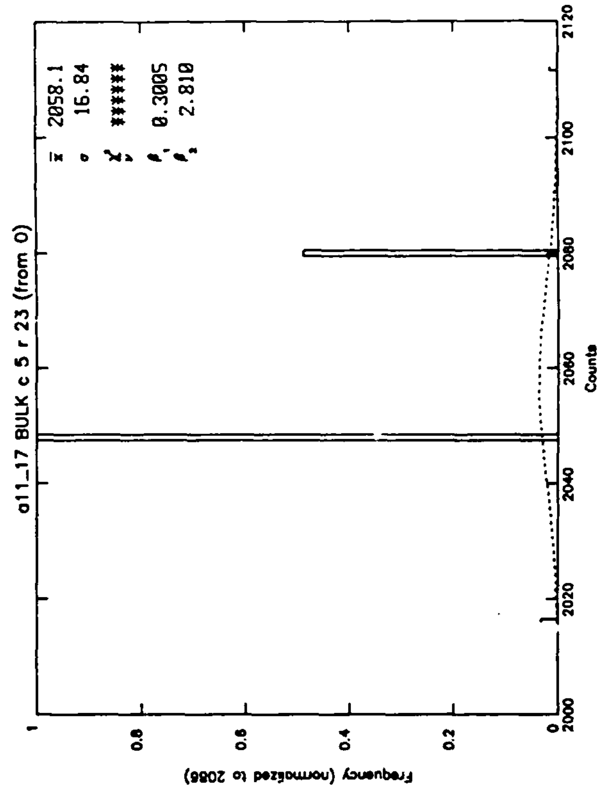
a11_17 BULK c 5 r 23 (from 0)
x̄ 2058.1
σ 16.84
χ² *****
β₁ 0.3005
β₂ 2.810
Frequency (normalized to 2086)
Counts

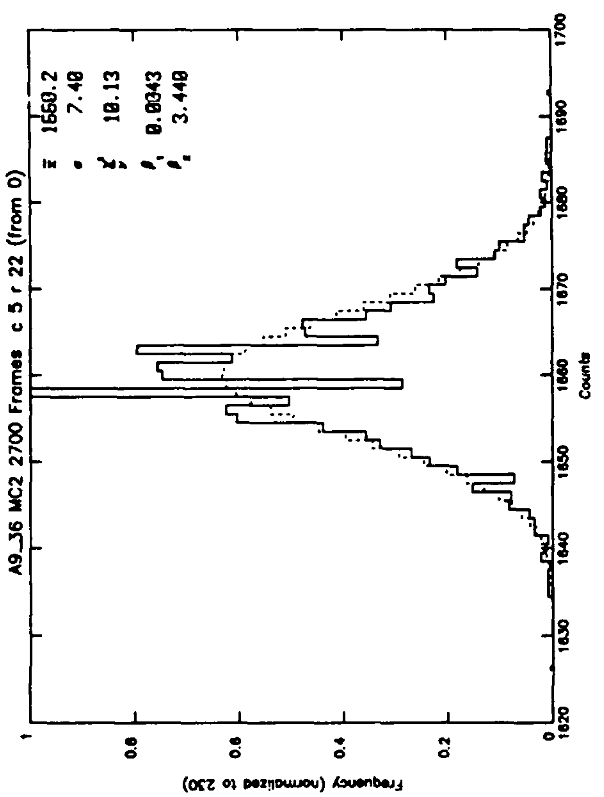
A9_36 MC2 2700 Frames c 5 r 22 (from 0)
x̄ 1660.2
σ 7.40
χ² 10.13
β₁ 0.0043
β₂ 3.440
Frequency (normalized to 230)
Counts

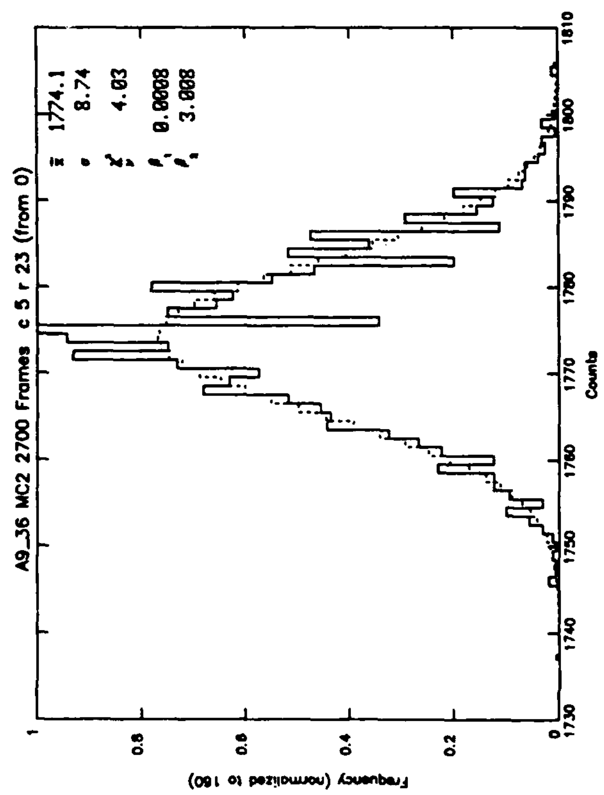
A9_36 MC2 2700 Frames c 5 r 23 (from 0)
x̄ 1774.1
σ 8.74
χ² 4.03
β₁ 0.0008
β₂ 3.008
Frequency (normalized to 160)
Counts

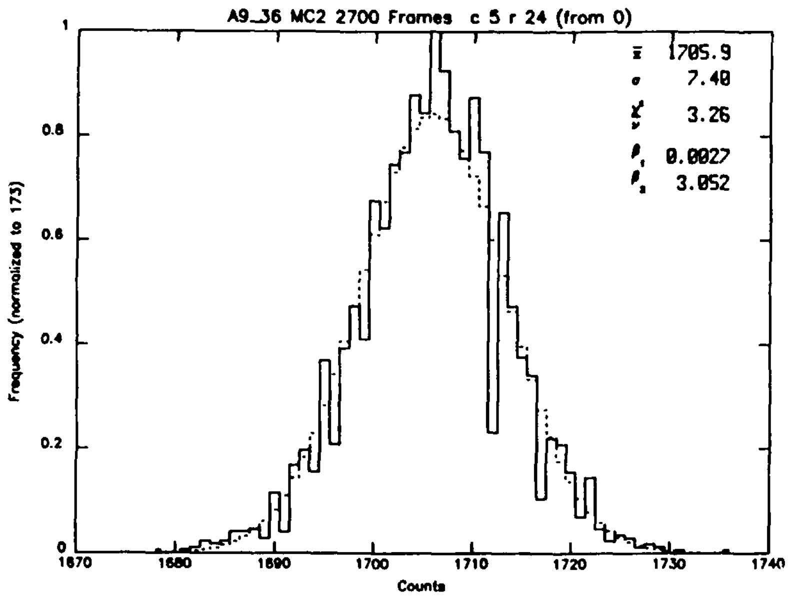
A9_36 MC2 2700 Frames c 5 r 24 (from 0)
Frequency (normalized to 173)
Counts
x̄ 1705.9
σ 7.40
χ^2_ν 3.26
β_1 0.0027
β_2 3.052

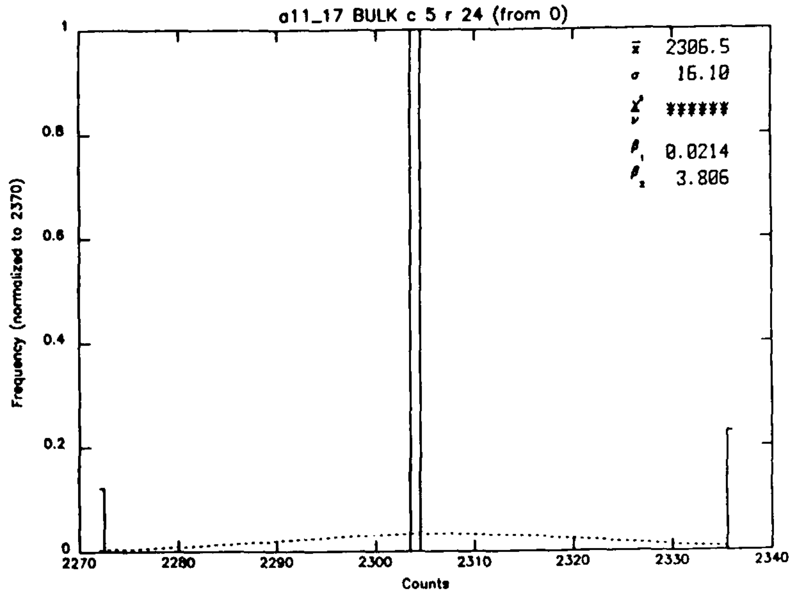
a11_17 BULK c 5 r 24 (from 0)
Frequency (normalized to 2370)
Counts
x̄ 2306.5
σ 16.10
χ^2_ν ******
β_1 0.0214
β_2 3.806

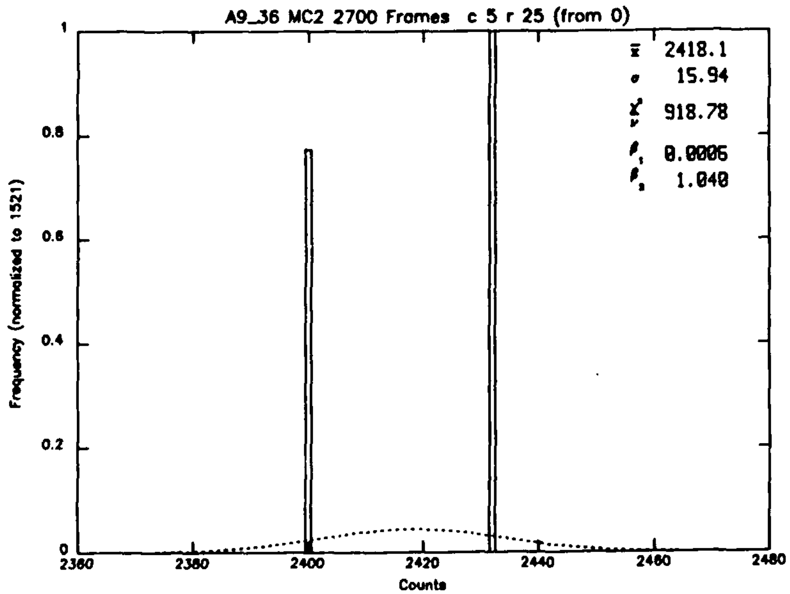
A9_36 MC2 2700 Frames c 5 r 25 (from 0)
Frequency (normalized to 1521)
Counts
x̄ 2418.1
σ 15.94
χ^2_ν 918.78
β_1 0.0006
β_2 1.040

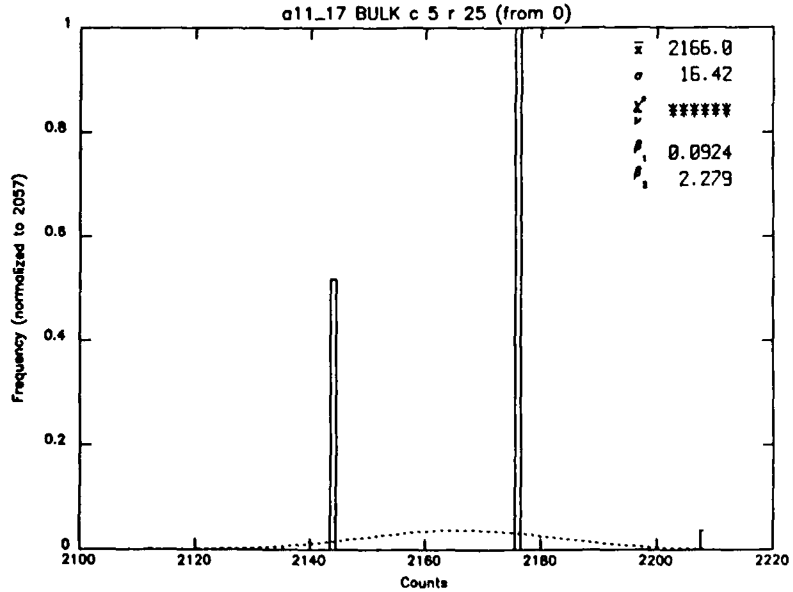
a11_17 BULK c 5 r 25 (from 0)
Frequency (normalized to 2057)
Counts
x̄ 2166.0
σ 16.42
χ^2_ν ******
β_1 0.0924
β_2 2.279

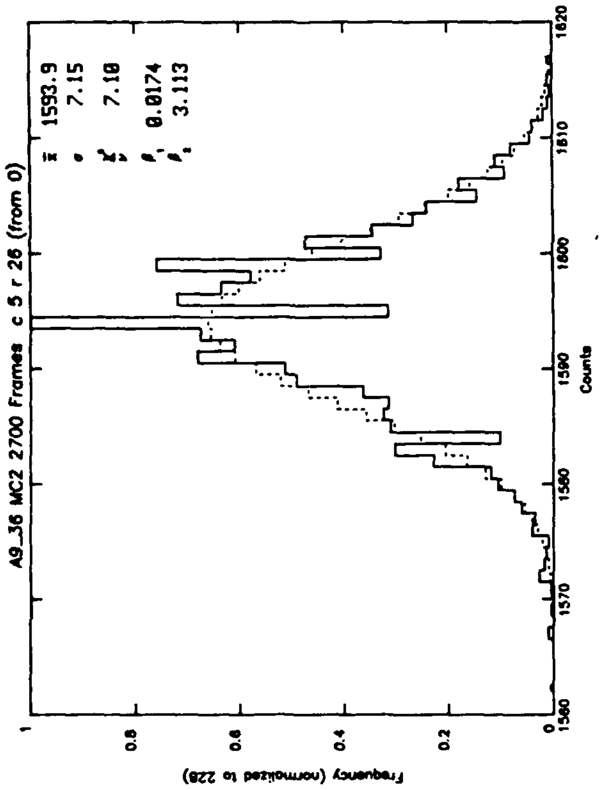

A9_36 MC2 2700 Frames c 5 r 26 (from 0)
x̄ 1593.9
σ 7.15
χ² 7.10
β1 0.0174
β2 3.113
Frequency (normalized to 228)
Counts

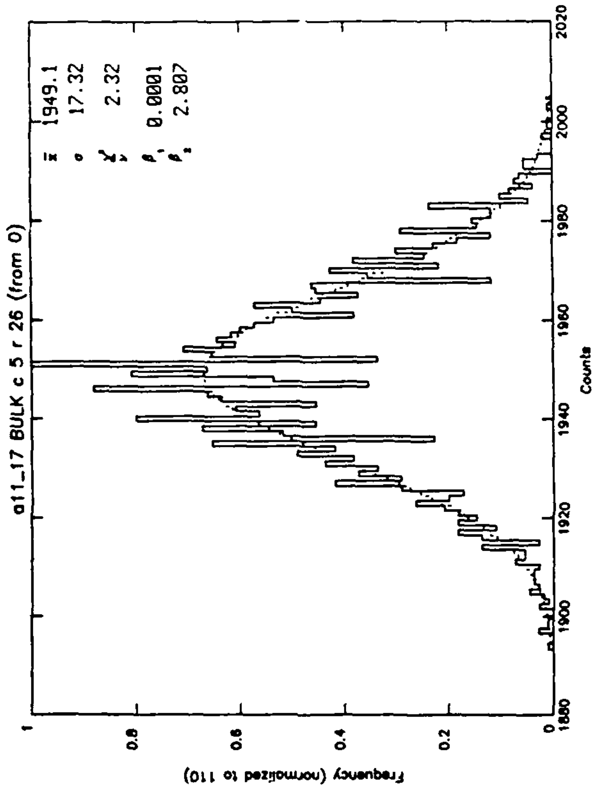

a11_17 BULK c 5 r 26 (from 0)
x̄ 1949.1
σ 17.32
χ² 2.32
β1 0.0001
β2 2.807
Frequency (normalized to 110)
Counts

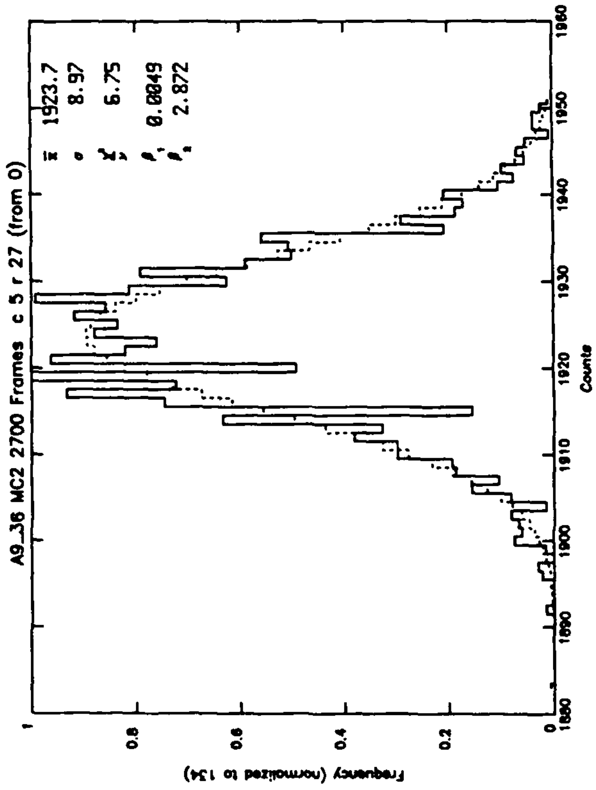

A9_36 MC2 2700 Frames c 5 r 27 (from 0)
x̄ 1923.7
σ 8.97
χ² 6.75
β1 0.0049
β2 2.872
Frequency (normalized to 134)
Counts

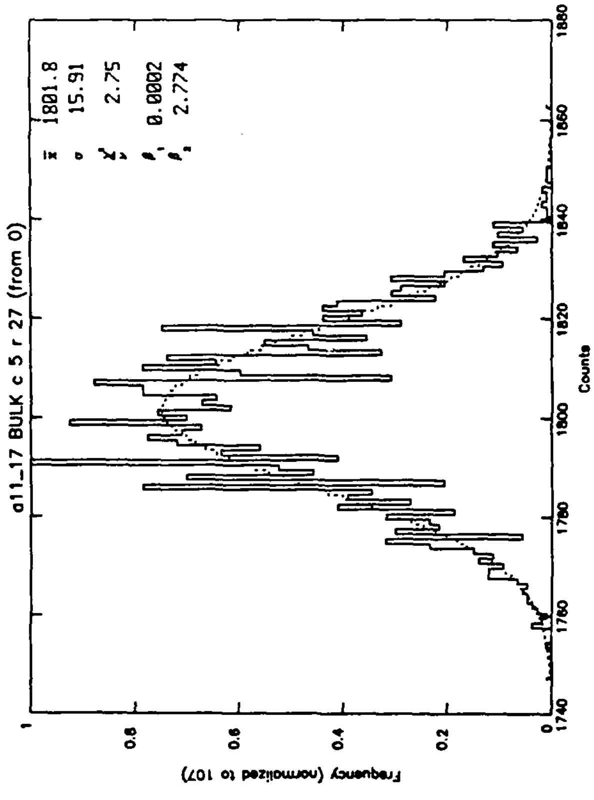

a11_17 BULK c 5 r 27 (from 0)
x̄ 1801.8
σ 15.91
χ² 2.75
β1 0.0002
β2 2.774
Frequency (normalized to 107)
Counts

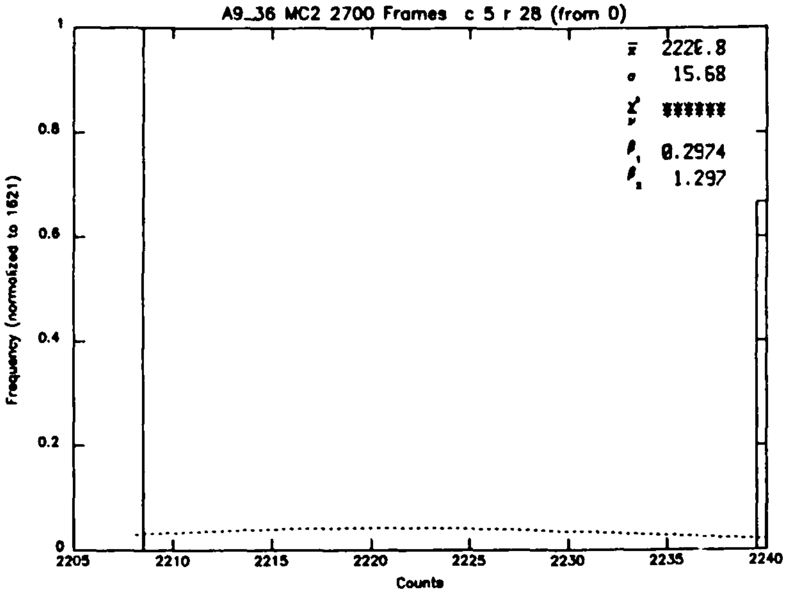
A9_36 MC2 2700 Frames c 5 r 28 (from 0)
$\bar{x}$ 222?.8
σ 15.68
χ^2_ν ******
β_1 0.2974
β_2 1.297
Frequency (normalized to 1621)
Counts

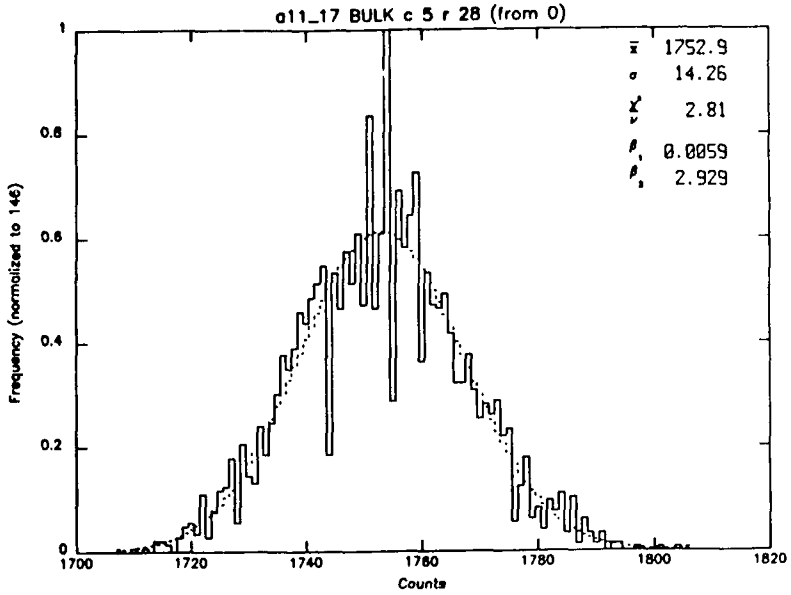
a11_17 BULK c 5 r 28 (from 0)
$\bar{x}$ 1752.9
σ 14.26
χ^2_ν 2.81
β_1 0.0059
β_2 2.929
Frequency (normalized to 146)
Counts

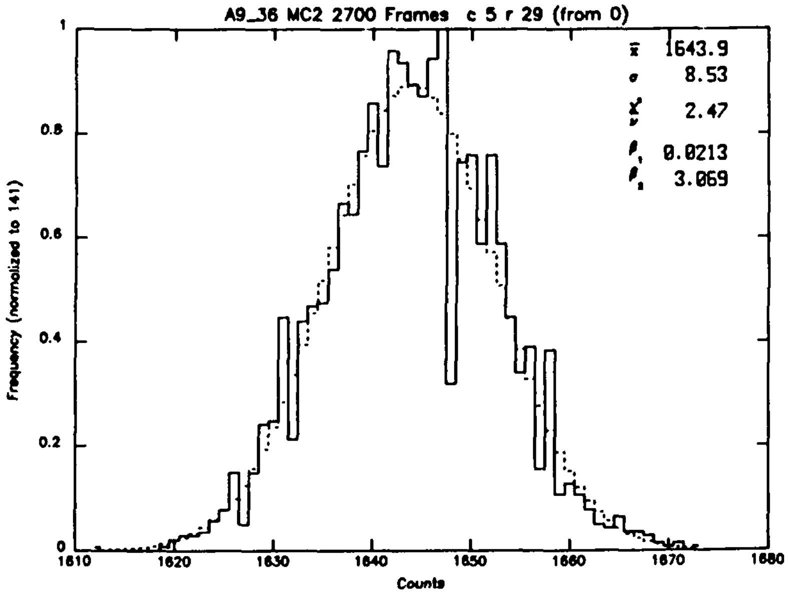
A9_36 MC2 2700 Frames c 5 r 29 (from 0)
$\bar{x}$ 1643.9
σ 8.53
χ^2_ν 2.47
β_1 0.0213
β_2 3.069
Frequency (normalized to 141)
Counts

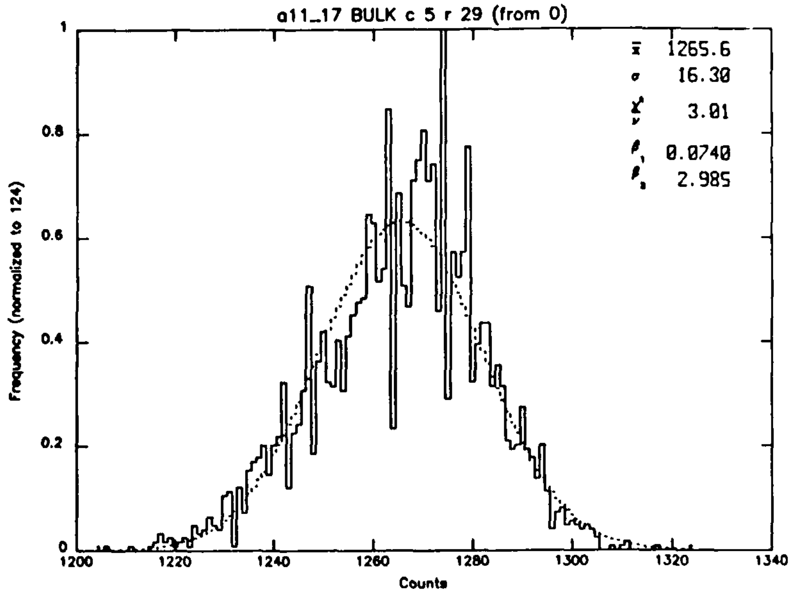
a11_17 BULK c 5 r 29 (from 0)
$\bar{x}$ 1265.6
σ 16.30
χ^2_ν 3.01
β_1 0.0740
β_2 2.985
Frequency (normalized to 124)
Counts

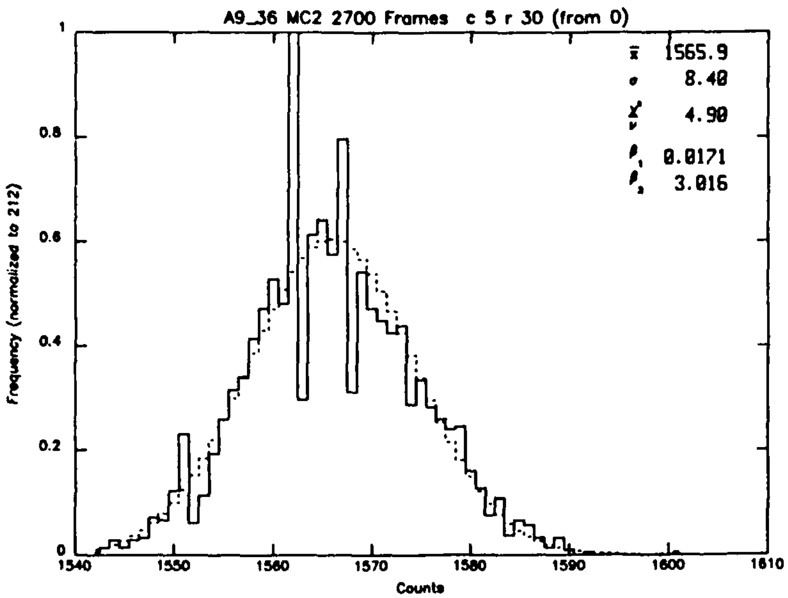
A9_36 MC2 2700 Frames c 5 r 30 (from 0)
x̄ 1565.9
σ 8.40
χ²ν 4.90
β1 0.0171
β2 3.016
Frequency (normalized to 212)
Counts

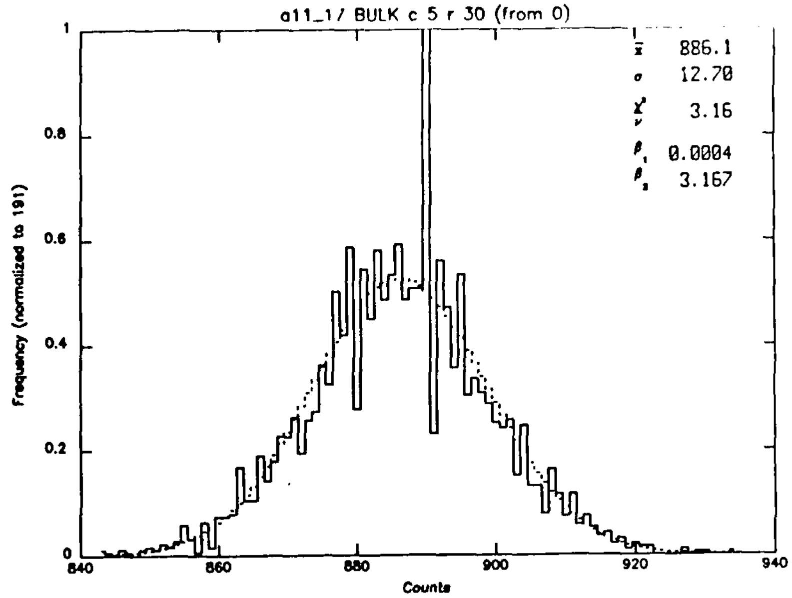
a11_17 BULK c 5 r 30 (from 0)
x̄ 886.1
σ 12.70
χ²ν 3.16
β1 0.0004
β2 3.167
Frequency (normalized to 191)
Counts

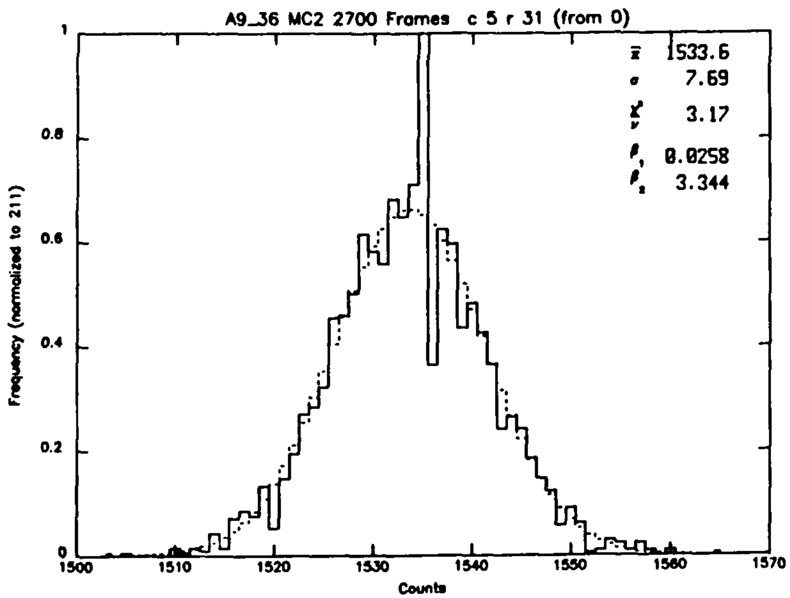
A9_36 MC2 2700 Frames c 5 r 31 (from 0)
x̄ 1533.6
σ 7.69
χ²ν 3.17
β1 0.0258
β2 3.344
Frequency (normalized to 211)
Counts

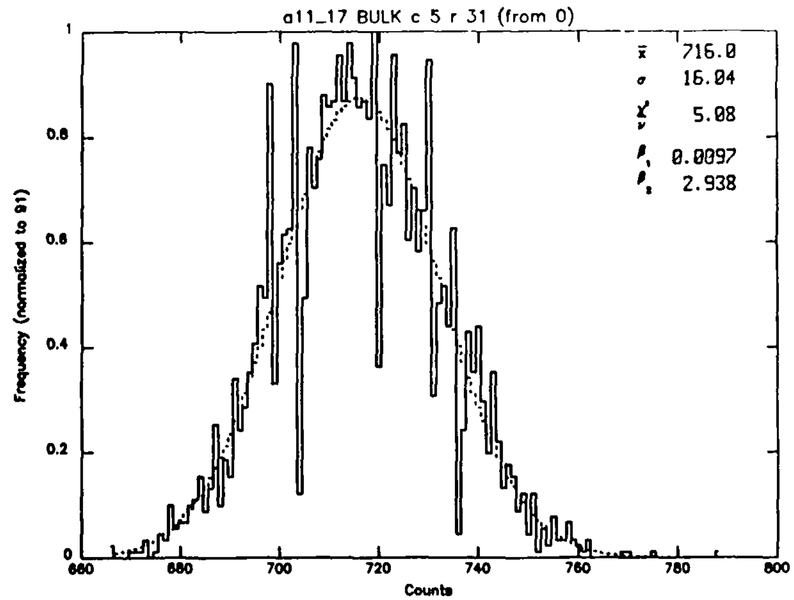
a11_17 BULK c 5 r 31 (from 0)
x̄ 716.0
σ 16.04
χ²ν 5.08
β1 0.0097
β2 2.938
Frequency (normalized to 91)
Counts

APPENDIX A-16

Array: Aerojet MC^2 (left) and Aerojet Bulk (right) Arrays

	Left	Right
Elements:	Column 5, Rows 0-31	Column 0, Rows 0-31
Data Run:	Star a9_35	Background a11_17

Purpose: Comparison of MC^2 and Bulk arrays. Note that different columns are used. Direct comparisons with equivalent columns may be made using Appendices A-14 and A-15. Note that Appendix A-15 uses a different data run (a9_36) for the MC^2 array.

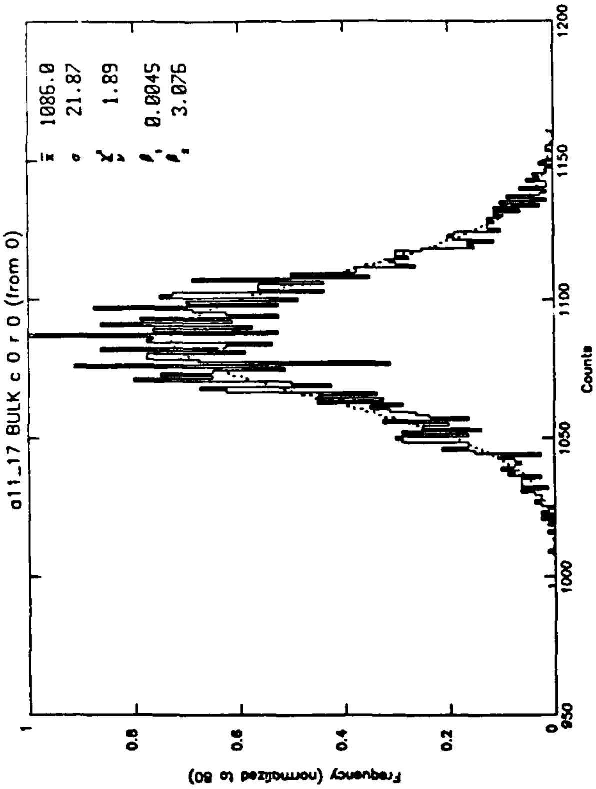
a11_17 BULK c 0 r 0 (from 0)
x̄ 1086.0
σ 21.87
χ²ν 1.89
β1 0.0045
β2 3.076
Counts
Frequency (normalized to 80)

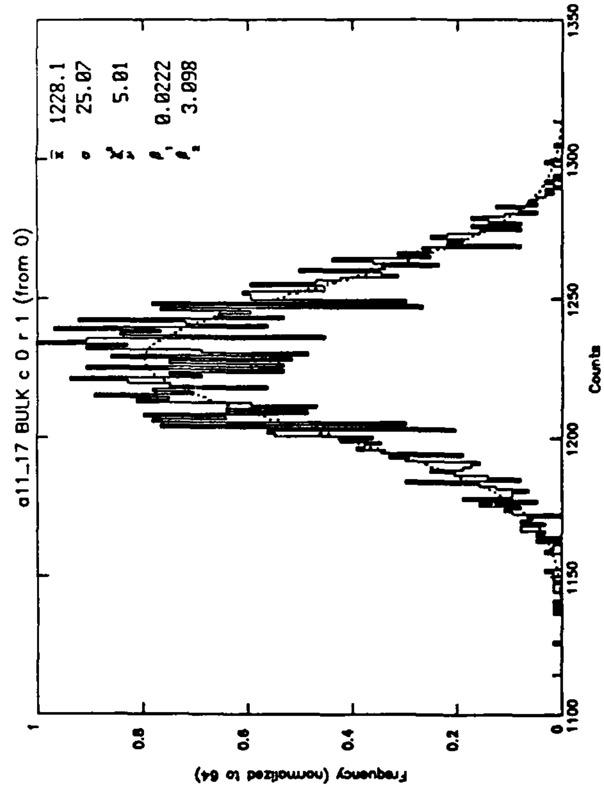
a11_17 BULK c 0 r 1 (from 0)
x̄ 1228.1
σ 25.07
χ²ν 5.01
β1 0.0222
β2 3.098
Counts
Frequency (normalized to 64)

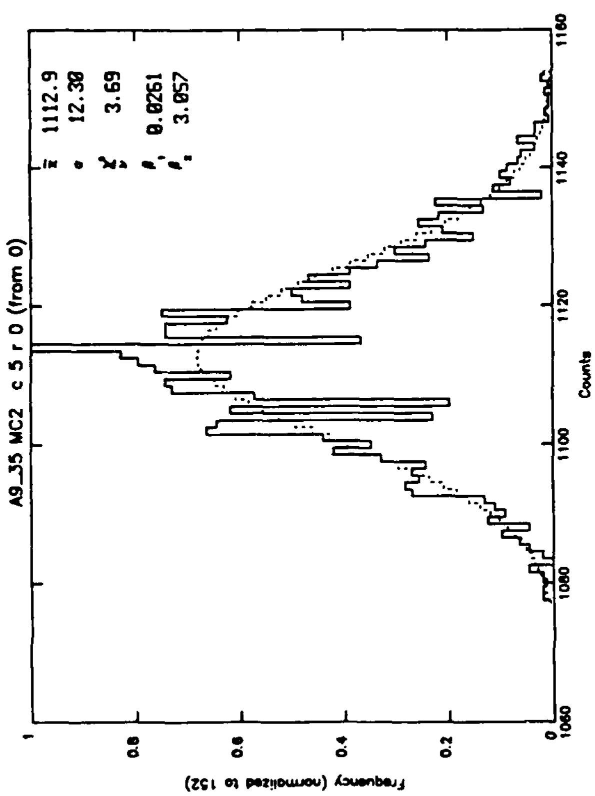
A9_35 MC2 c 5 r 0 (from 0)
x̄ 1112.9
σ 12.30
χ²ν 3.69
β1 0.0261
β2 3.057
Counts
Frequency (normalized to 152)

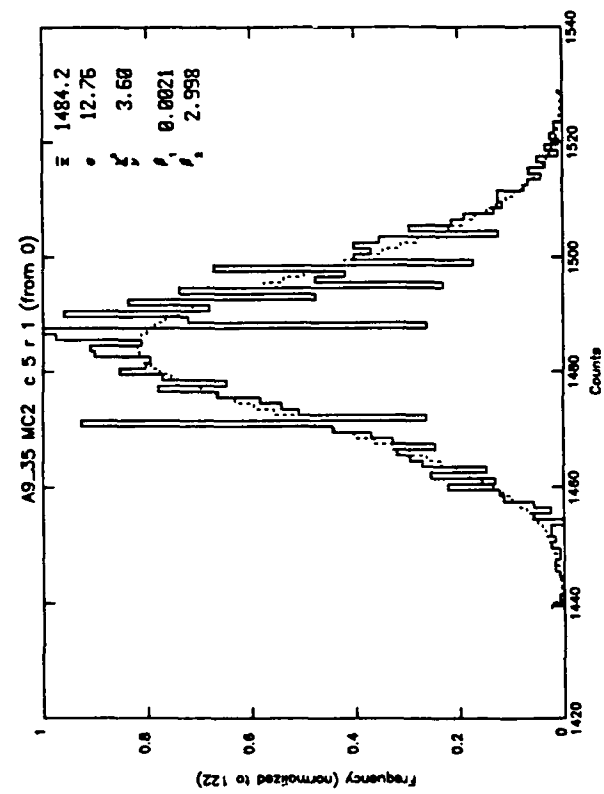
A9_35 MC2 c 5 r 1 (from 0)
x̄ 1484.2
σ 12.76
χ²ν 3.60
β1 0.0021
β2 2.998
Counts
Frequency (normalized to 122)

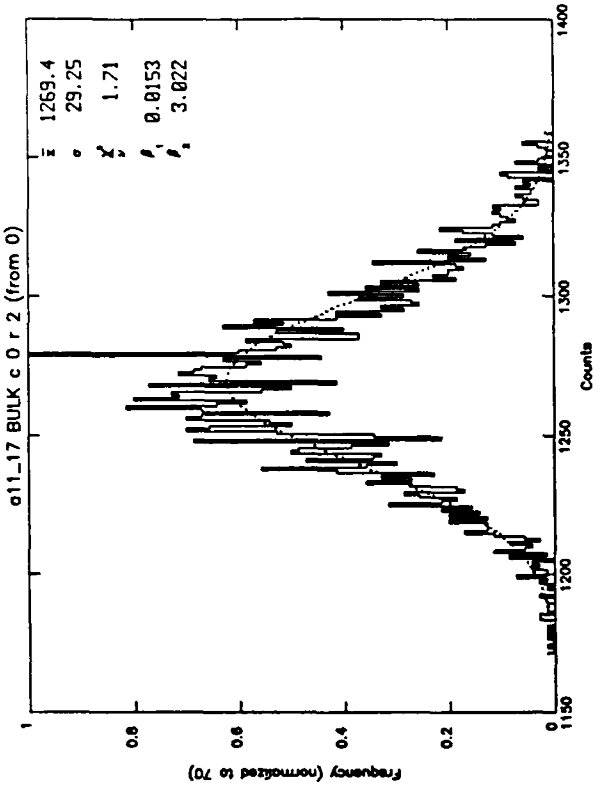
a11_17 BULK c 0 r 2 (from 0)
x̄ 1269.4
σ 29.25
χ²ν 1.71
β1 0.0153
β2 3.022
Counts
Frequency (normalized to 70)

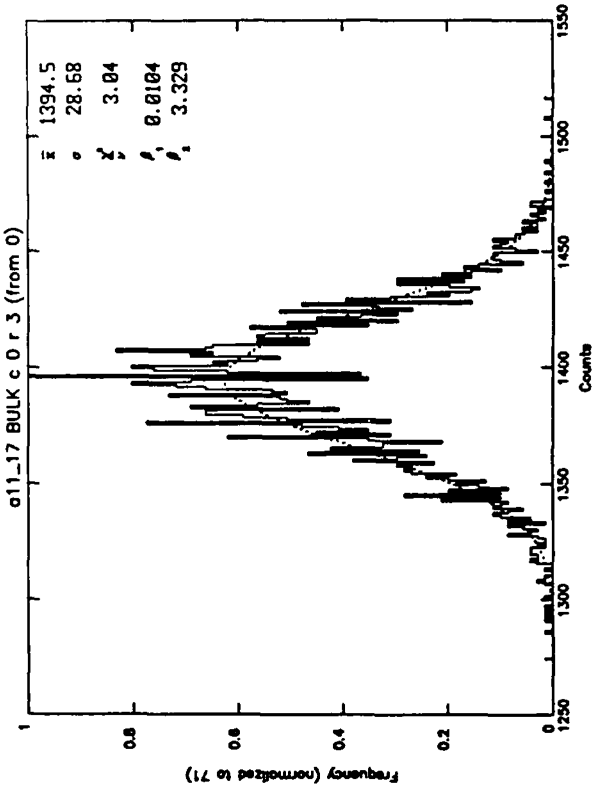
a11_17 BULK c 0 r 3 (from 0)
x̄ 1394.5
σ 28.68
χ²ν 3.04
β1 0.0104
β2 3.329
Counts
Frequency (normalized to 71)

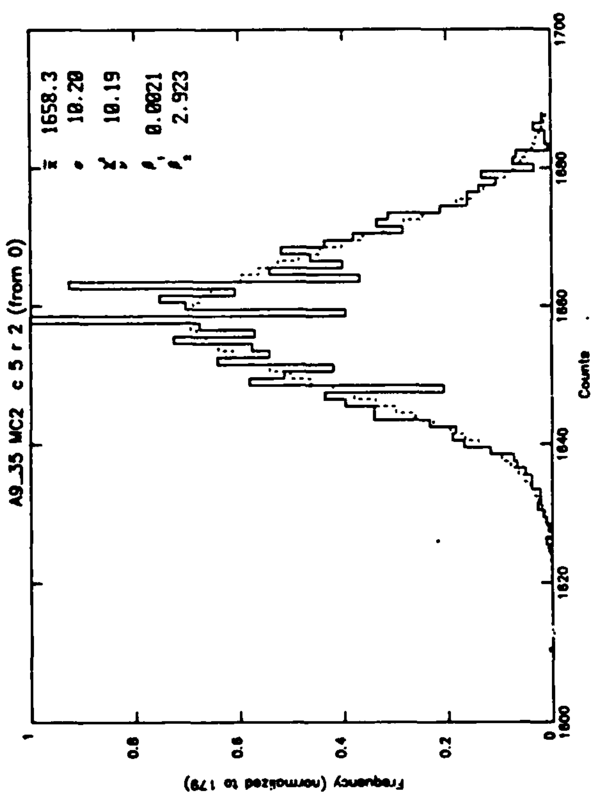
A9_35 MC2 c 5 r 2 (from 0)
x̄ 1658.3
σ 10.20
χ²ν 10.19
β1 0.0021
β2 2.923
Counts
Frequency (normalized to 179)

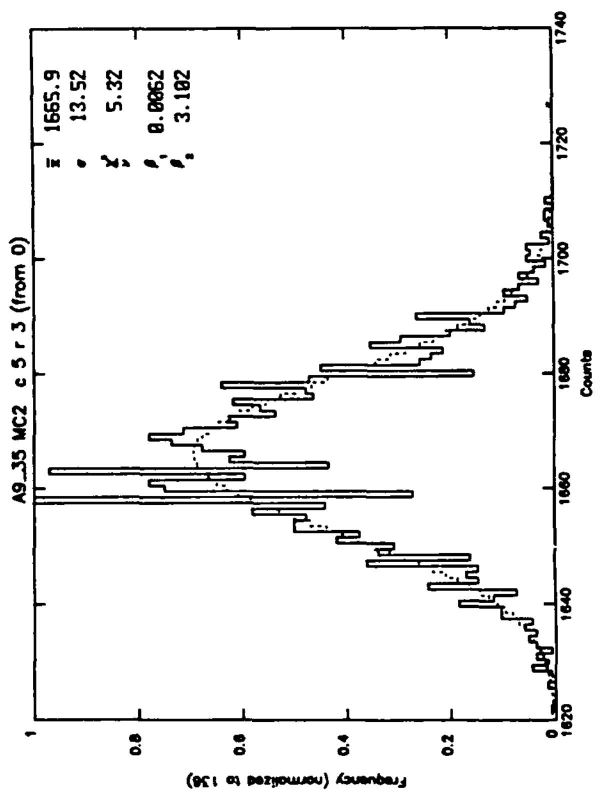
A9_35 MC2 c 5 r 3 (from 0)
x̄ 1665.9
σ 13.52
χ²ν 5.32
β1 0.0062
β2 3.102
Counts
Frequency (normalized to 136)

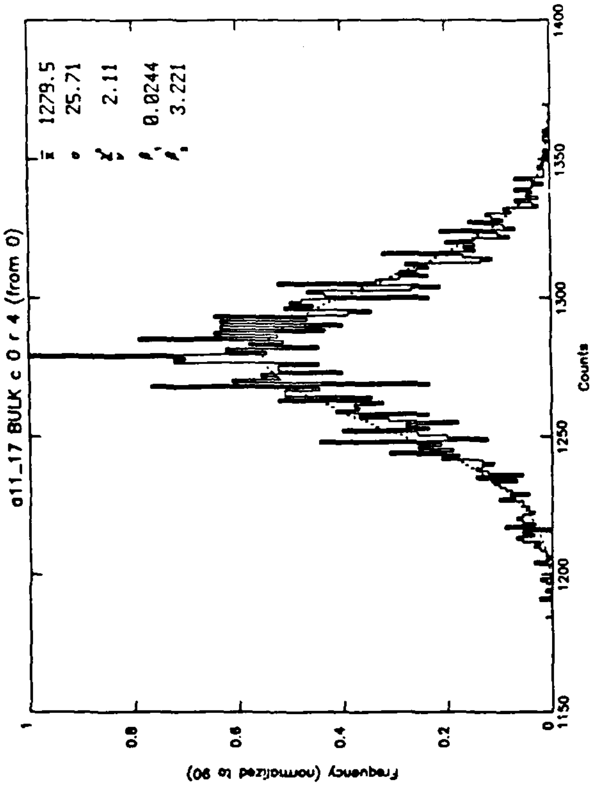

a11_17 BULK c 0 r 4 (from 0)
x̄ 1279.5
σ 25.71
χ^2_ν 2.11
β_1 0.0244
β_2 3.221
Frequency (normalized to 90)
Counts

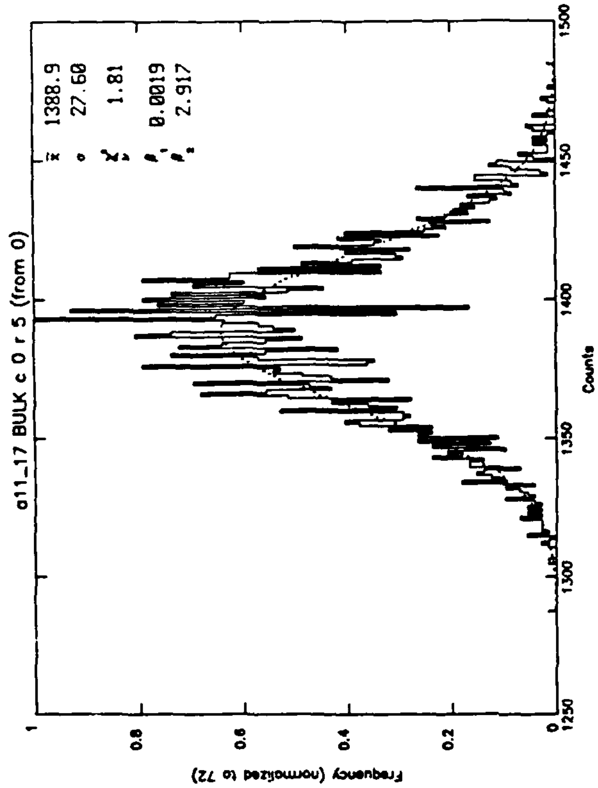

a11_17 BULK c 0 r 5 (from 0)
x̄ 1388.9
σ 27.60
χ^2_ν 1.81
β_1 0.0019
β_2 2.917
Frequency (normalized to 72)
Counts

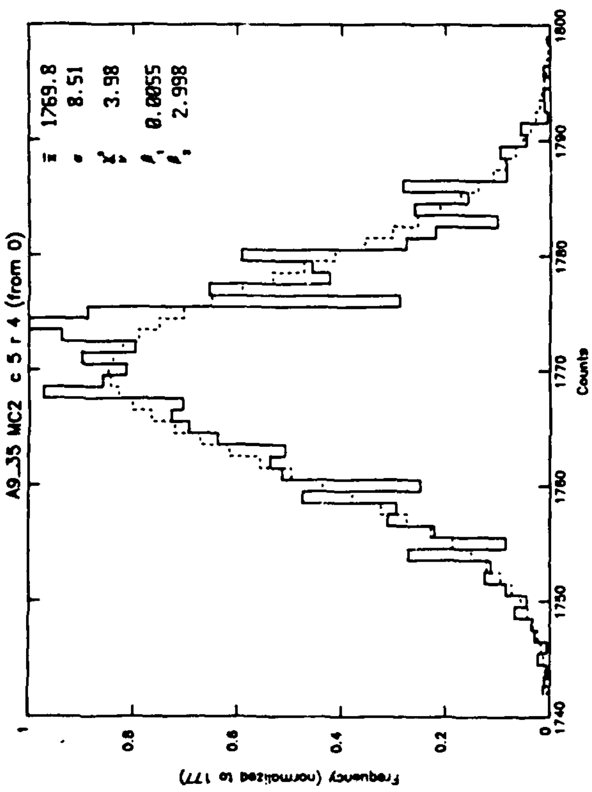

A9_35 MC2 c 5 r 4 (from 0)
x̄ 1769.8
σ 8.51
χ^2_ν 3.98
β_1 0.0055
β_2 2.998
Frequency (normalized to 177)
Counts

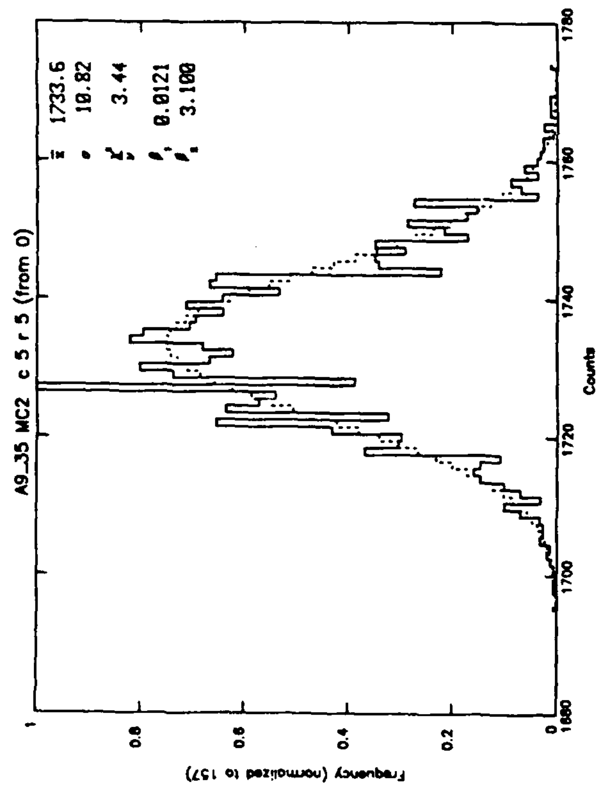

A9_35 MC2 c 5 r 5 (from 0)
x̄ 1733.6
σ 10.82
χ^2_ν 3.44
β_1 0.0121
β_2 3.100
Frequency (normalized to 157)
Counts

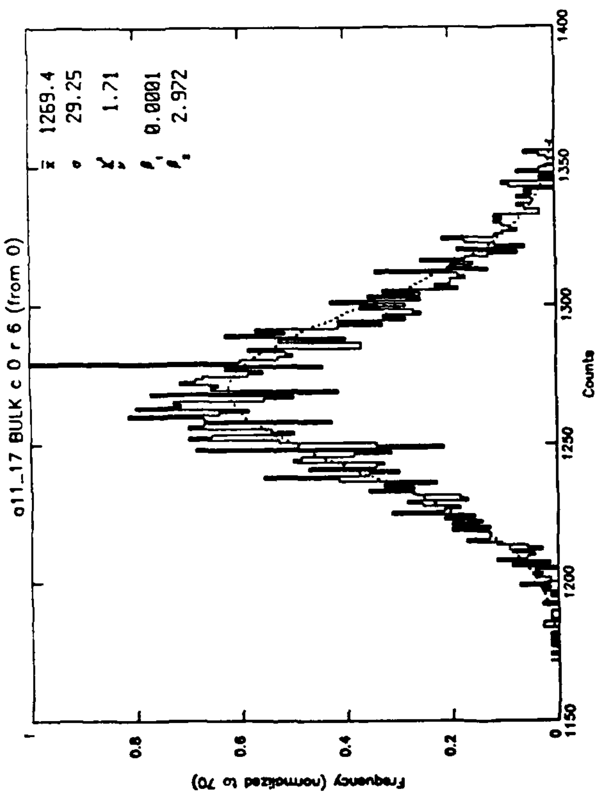
a11_17 BULK c 0 r 6 (from 0)
Frequency (normalized to 70)
Counts
x̄ 1269.4
σ 29.25
χ^2_ν 1.71
β_1 0.0001
β_2 2.972

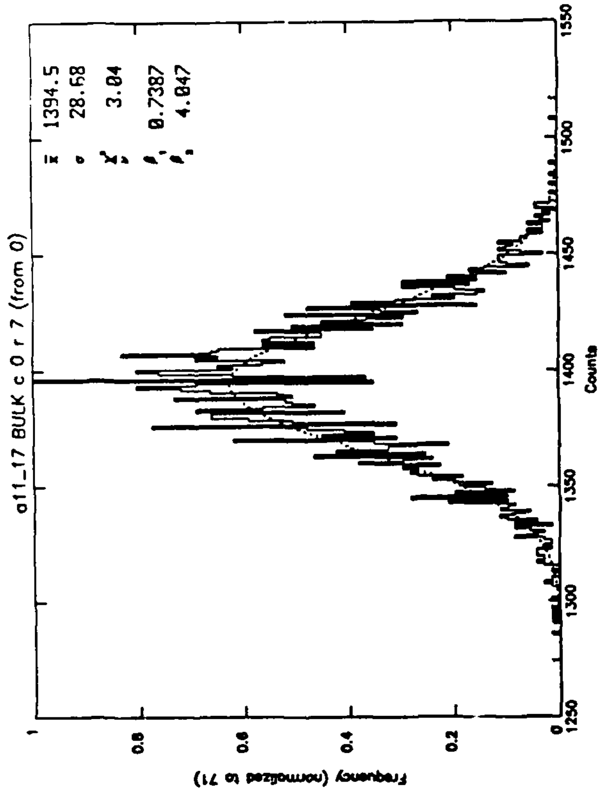
a11_17 BULK c 0 r 7 (from 0)
Frequency (normalized to 71)
Counts
x̄ 1394.5
σ 28.68
χ^2_ν 3.04
β_1 0.7387
β_2 4.047

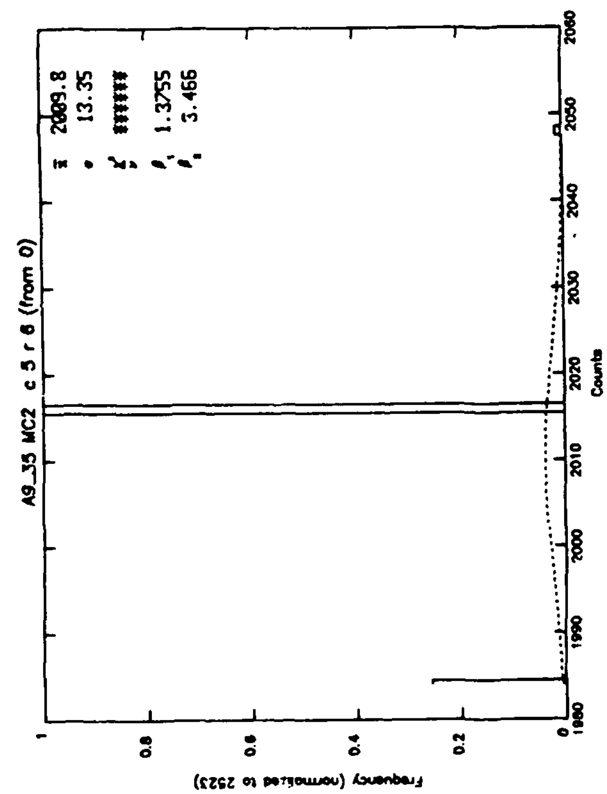
A9_35 MC2 c 5 r 6 (from 0)
Frequency (normalized to 2523)
Counts
x̄ 2009.8
σ 13.35
χ^2_ν ######
β_1 1.3755
β_2 3.466

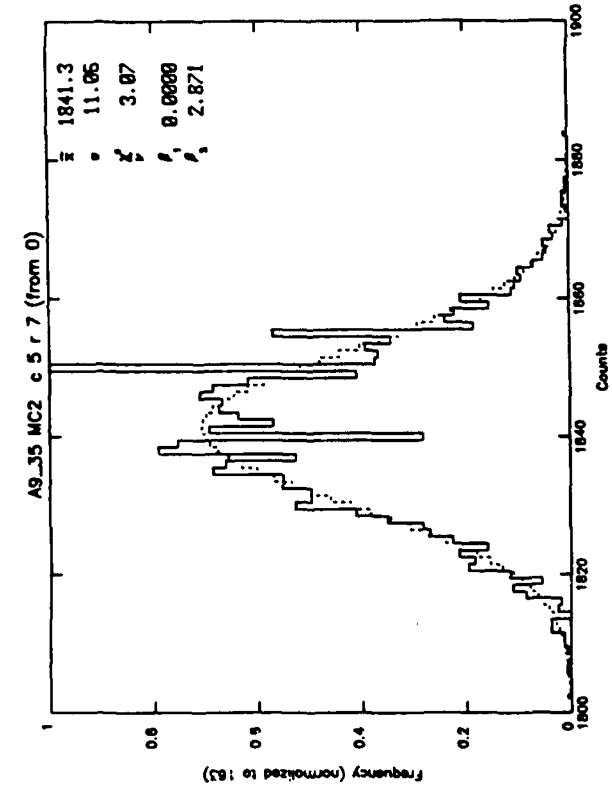
A9_35 MC2 c 5 r 7 (from 0)
Frequency (normalized to 163)
Counts
x̄ 1841.3
σ 11.06
χ^2_ν 3.07
β_1 0.0000
β_2 2.871

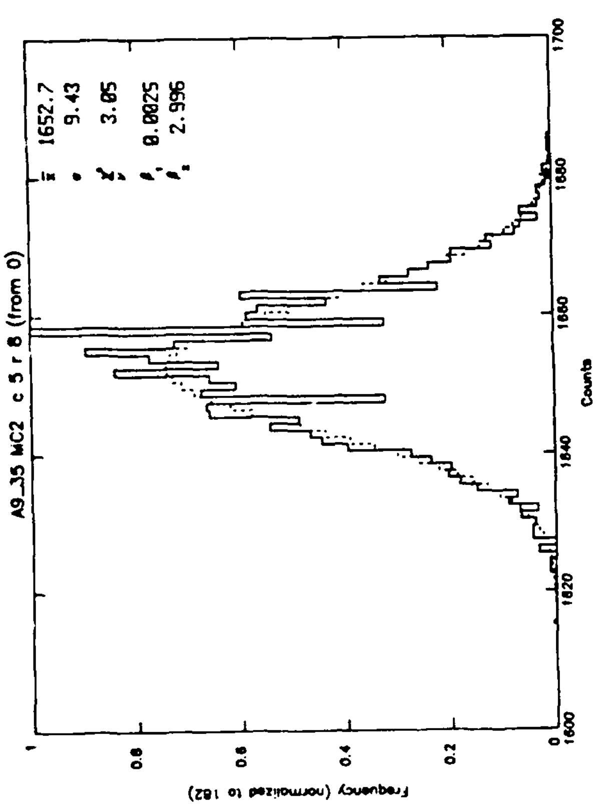
A9_35 MC2 c 5 r 8 (from 0)
$\bar{x}$ 1652.7
σ 9.43
χ^2_ν 3.05
β_1 0.0025
β_2 2.996
Counts
Frequency (normalized to 162)

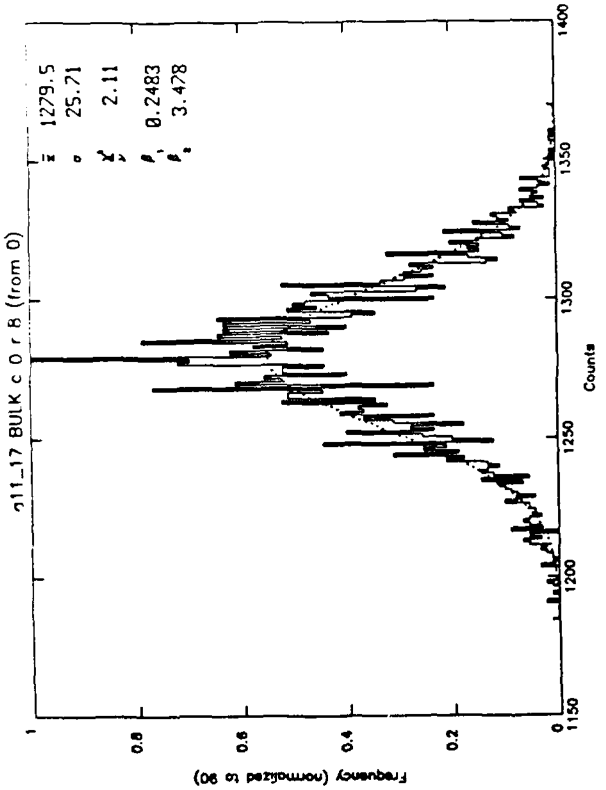
a11_17 BULK c 0 r 8 (from 0)
$\bar{x}$ 1279.5
σ 25.71
χ^2_ν 2.11
β_1 0.2483
β_2 3.478
Counts
Frequency (normalized to 90)

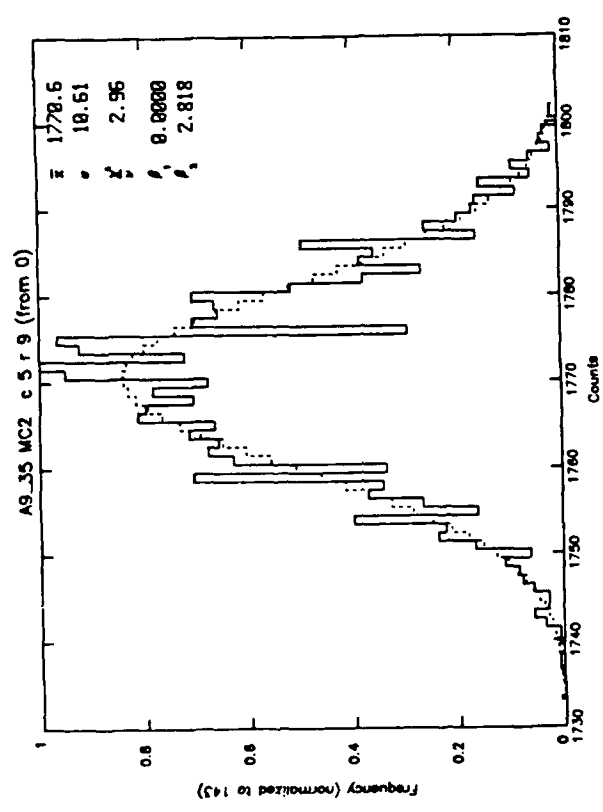
A9_35 MC2 c 5 r 9 (from 0)
$\bar{x}$ 1770.6
σ 10.61
χ^2_ν 2.96
β_1 0.0000
β_2 2.818
Counts
Frequency (normalized to 143)

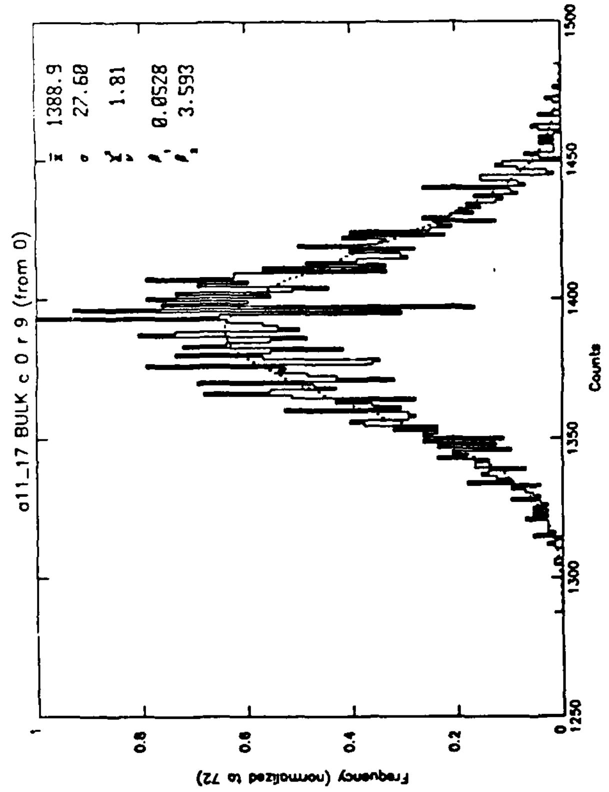
a11_17 BULK c 0 r 9 (from 0)
$\bar{x}$ 1388.9
σ 27.60
χ^2_ν 1.81
β_1 0.0528
β_2 3.593
Counts
Frequency (normalized to 72)

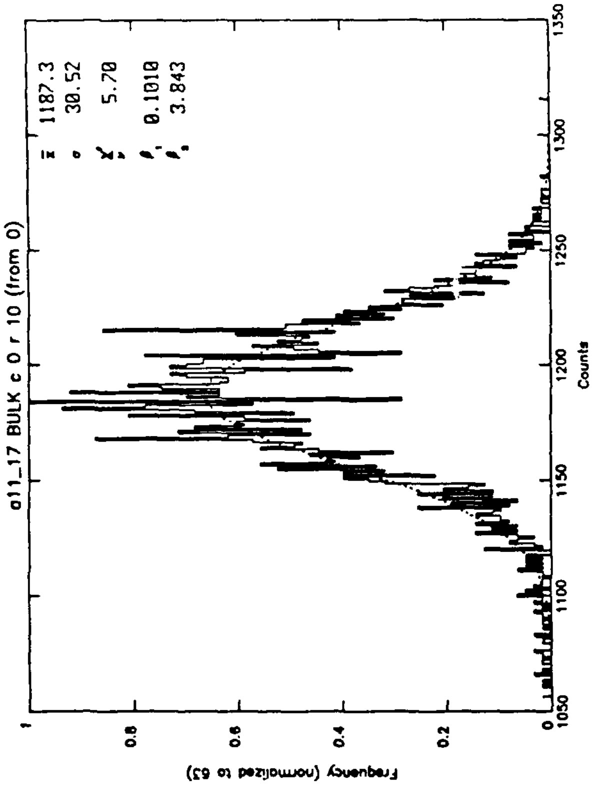
a11_17 BULK c 0 r 10 (from 0)
x̄ 1187.3
σ 30.52
χ² 5.70
0.1010
3.843
Counts
Frequency (normalized to 63)

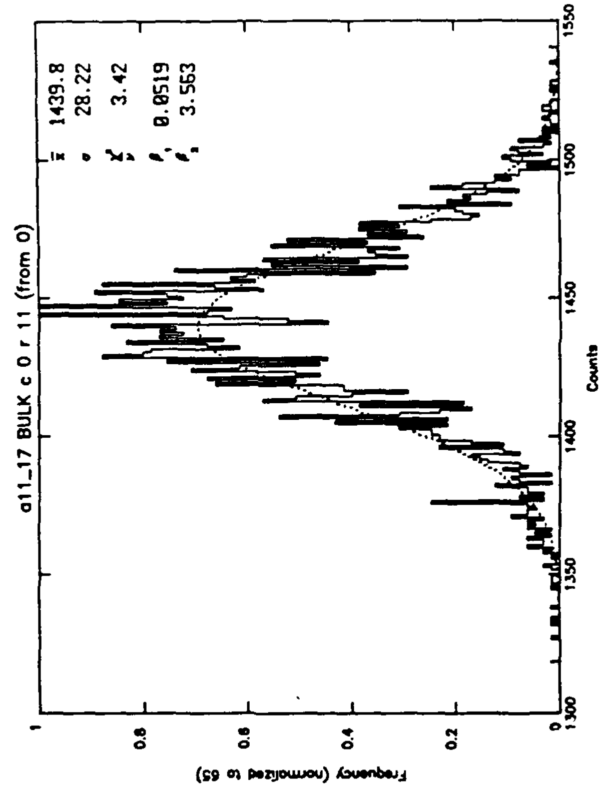
a11_17 BULK c 0 r 11 (from 0)
x̄ 1439.8
σ 28.22
χ² 3.42
0.0519
3.563
Counts
Frequency (normalized to 65)

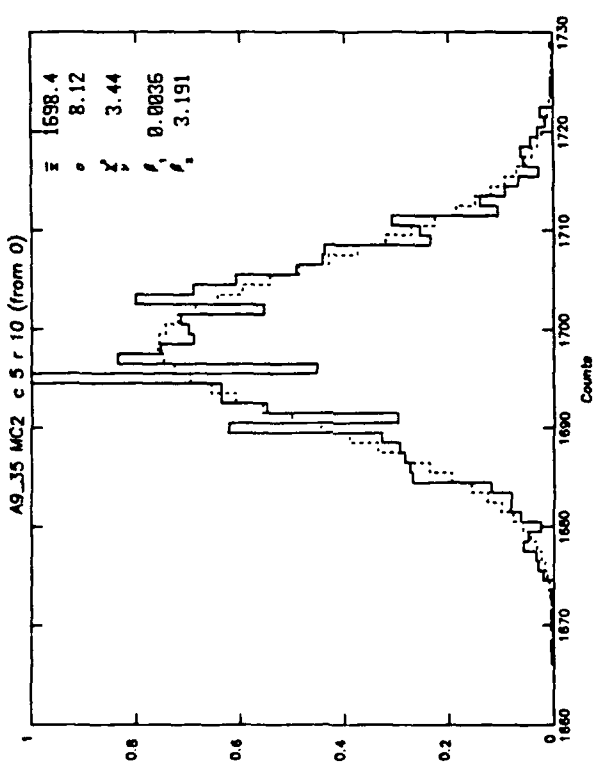
A9_35 MC2 c 5 r 10 (from 0)
x̄ 1698.4
σ 8.12
χ² 3.44
0.0036
3.191
Counts
Frequency (normalized to 207)

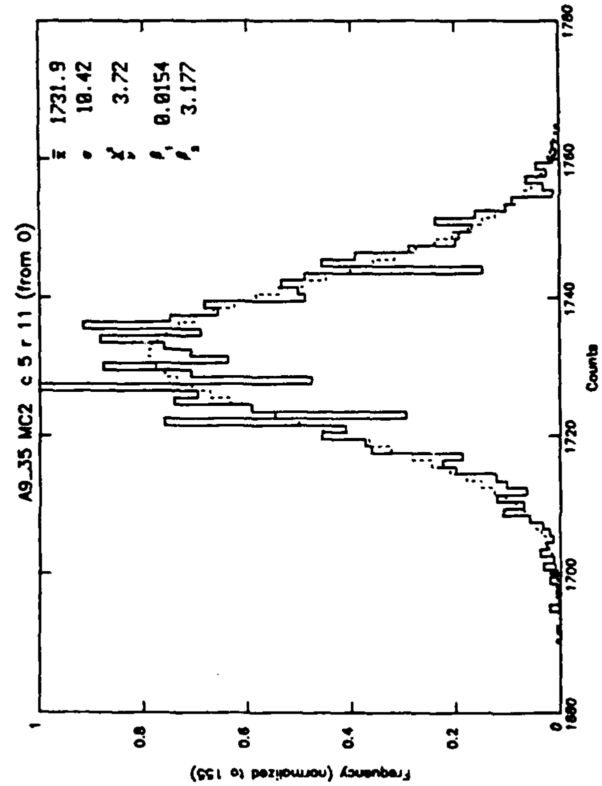
A9_35 MC2 c 5 r 11 (from 0)
x̄ 1731.9
σ 10.42
χ² 3.72
0.0154
3.177
Counts
Frequency (normalized to 155)

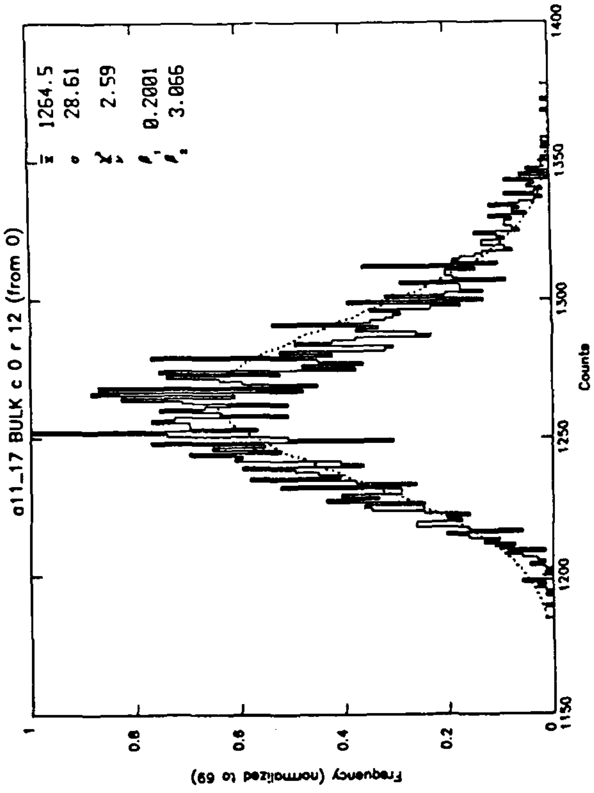

a11_17 BULK c 0 r 12 (from 0)
x̄ 1264.5
σ 28.61
χ²ν 2.59
β1 0.2001
β2 3.066
Counts
Frequency (normalized to 69)

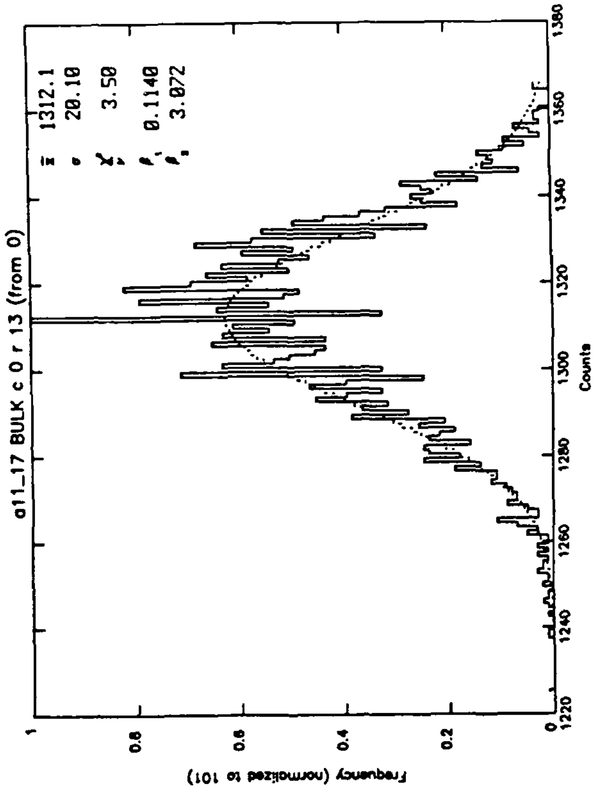

a11_17 BULK c 0 r 13 (from 0)
x̄ 1312.1
σ 20.10
χ²ν 3.50
β1 0.1140
β2 3.072
Counts
Frequency (normalized to 101)

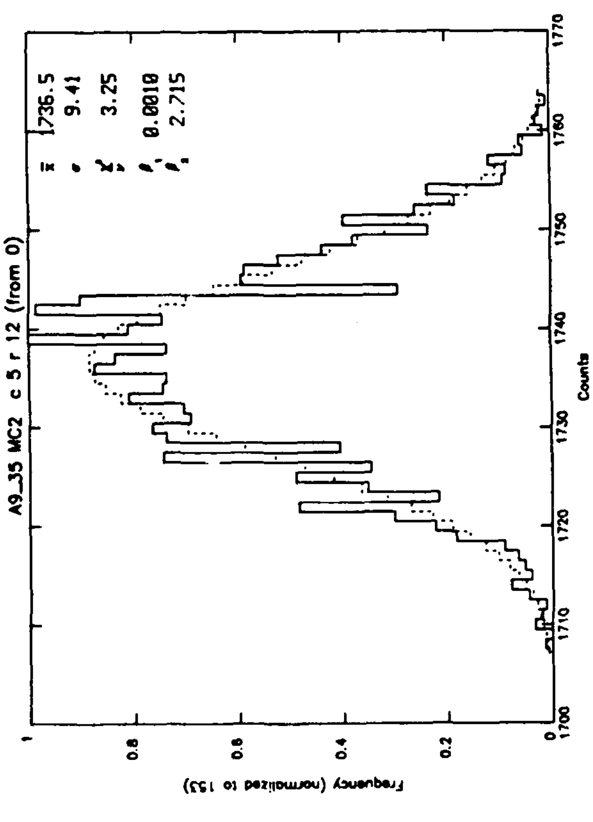

A9_35 MC2 c 5 r 12 (from 0)
x̄ 1736.5
σ 9.41
χ²ν 3.25
β1 0.0010
β2 2.715
Counts
Frequency (normalized to 153)

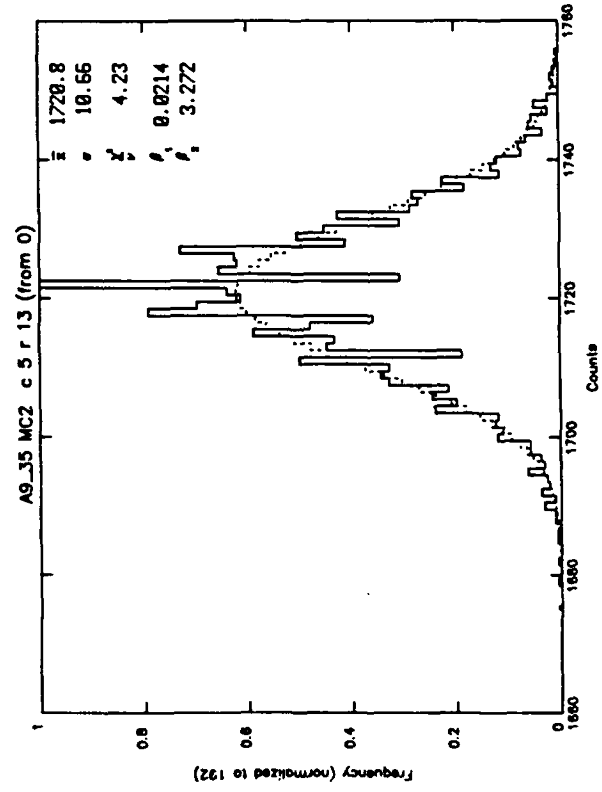

A9_35 MC2 c 5 r 13 (from 0)
x̄ 1720.8
σ 10.66
χ²ν 4.23
β1 0.0214
β2 3.272
Counts
Frequency (normalized to 132)

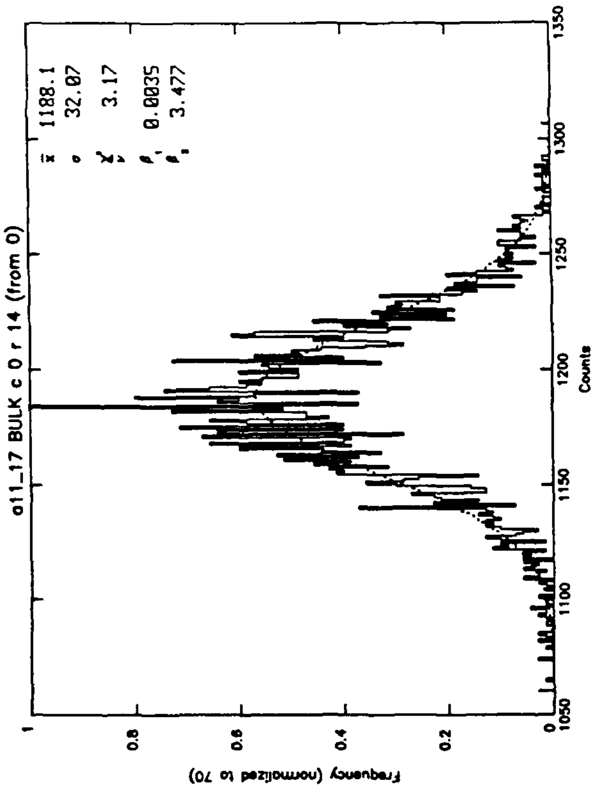
a11_17 BULK c 0 r 14 (from 0)
x̄ 1188.1
σ 32.07
χ^2_ν 3.17
β_1 0.0035
β_2 3.477
Frequency (normalized to 70)
Counts

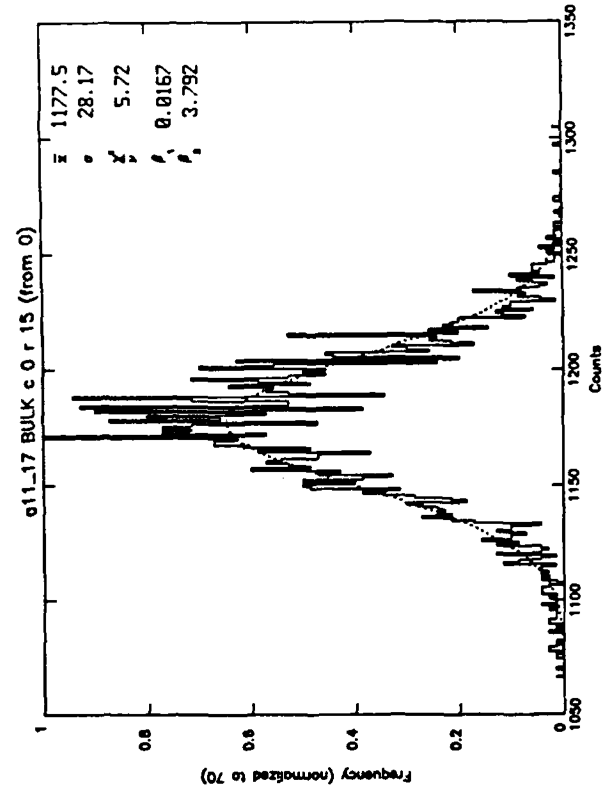
a11_17 BULK c 0 r 15 (from 0)
x̄ 1177.5
σ 28.17
χ^2_ν 5.72
β_1 0.0167
β_2 3.792
Frequency (normalized to 70)
Counts

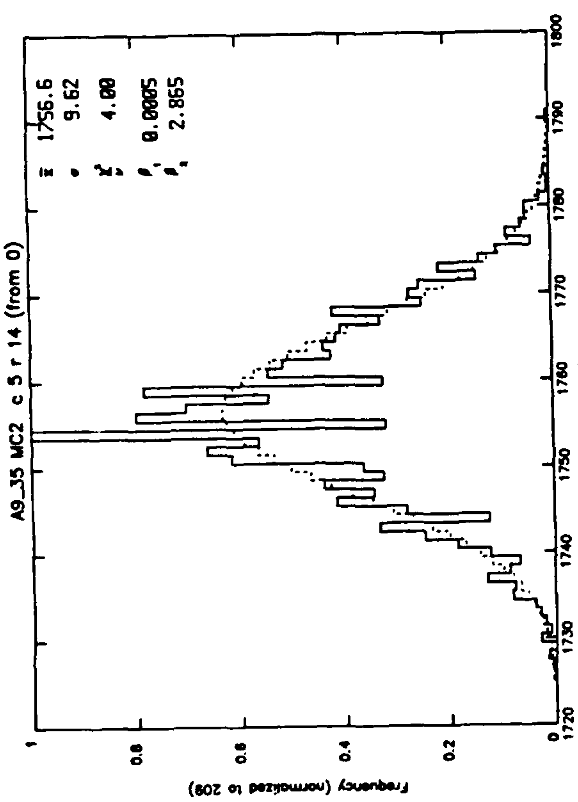
A9_35 MC2 c 5 r 14 (from 0)
x̄ 1756.6
σ 9.62
χ^2_ν 4.00
β_1 0.0005
β_2 2.865
Frequency (normalized to 208)
Counts

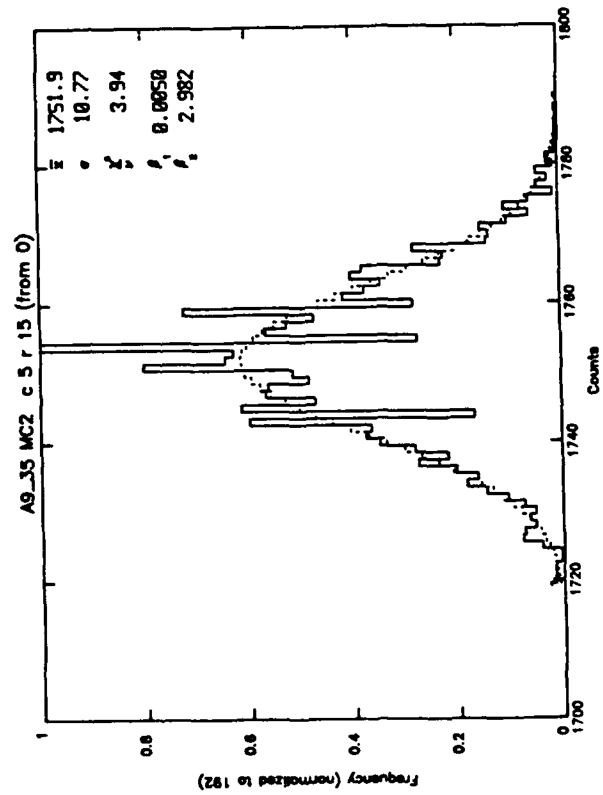
A9_35 MC2 c 5 r 15 (from 0)
x̄ 1751.9
σ 10.77
χ^2_ν 3.94
β_1 0.0050
β_2 2.982
Frequency (normalized to 192)
Counts

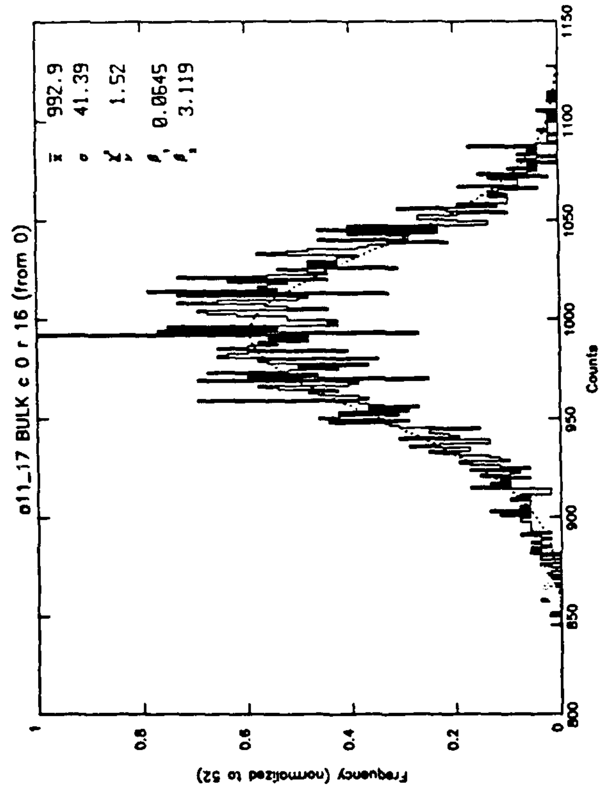
a11_17 BULK c 0 r 16 (from 0)
x̄ 992.9
σ 41.39
χ^2_ν 1.52
β_1 0.0645
β_2 3.119
Frequency (normalized to 52)
Counts

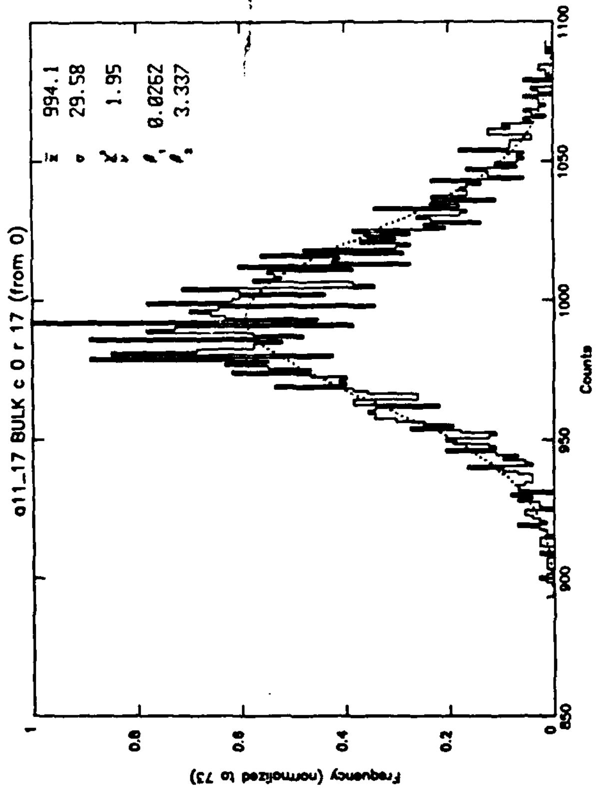
a11_17 BULK c 0 r 17 (from 0)
x̄ 994.1
σ 29.58
χ^2_ν 1.95
β_1 0.0262
β_2 3.337
Frequency (normalized to 73)
Counts

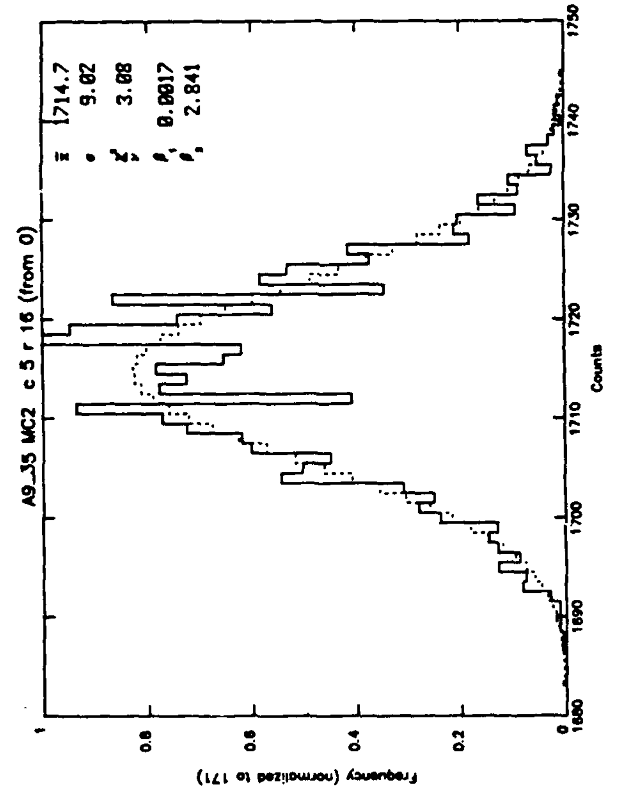
A9_35 MC2 c 5 r 16 (from 0)
x̄ 1714.7
σ 9.02
χ^2_ν 3.08
β_1 0.0017
β_2 2.841
Frequency (normalized to 171)
Counts

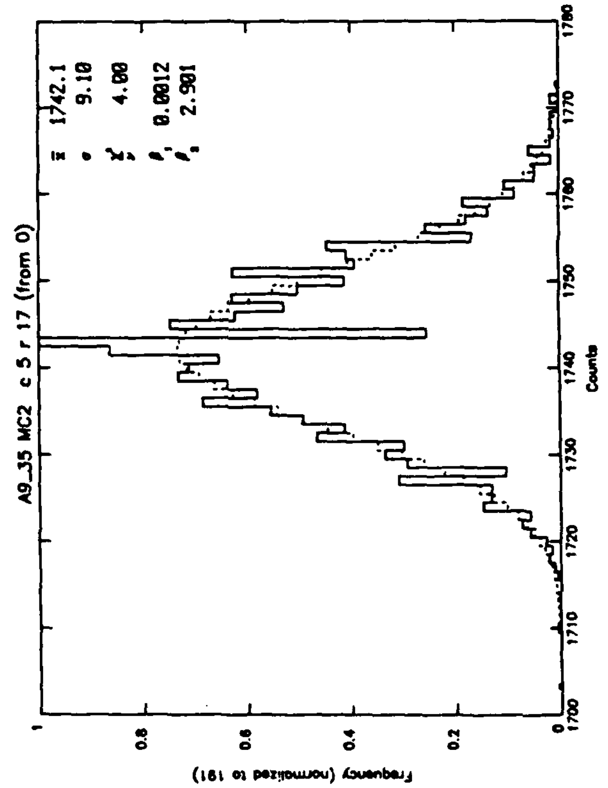
A9_35 MC2 c 5 r 17 (from 0)
x̄ 1742.1
σ 9.10
χ^2_ν 4.00
β_1 0.0012
β_2 2.981
Frequency (normalized to 191)
Counts

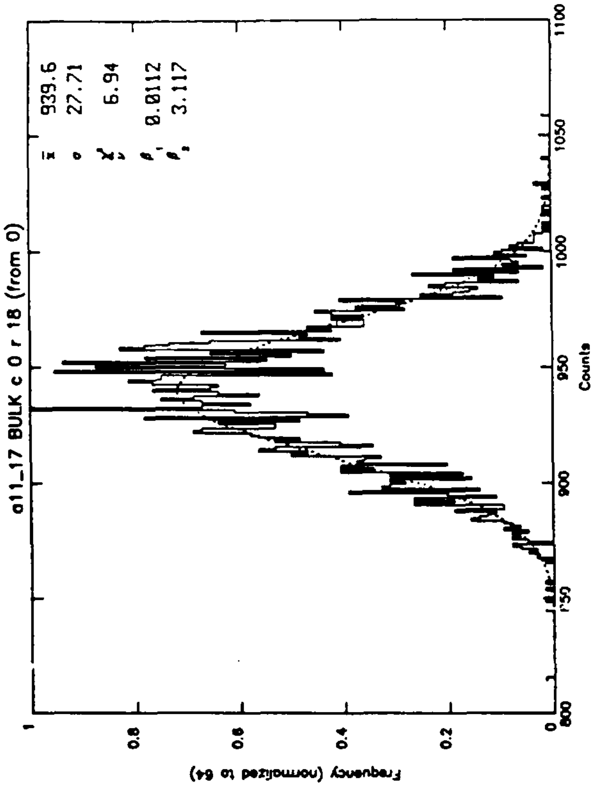
a11_17 BULK c 0 r 18 (from 0)
x̄ 939.6
σ 27.71
χ^2_ν 6.94
β_1 0.0112
β_2 3.117
Counts
Frequency (normalized to 64)

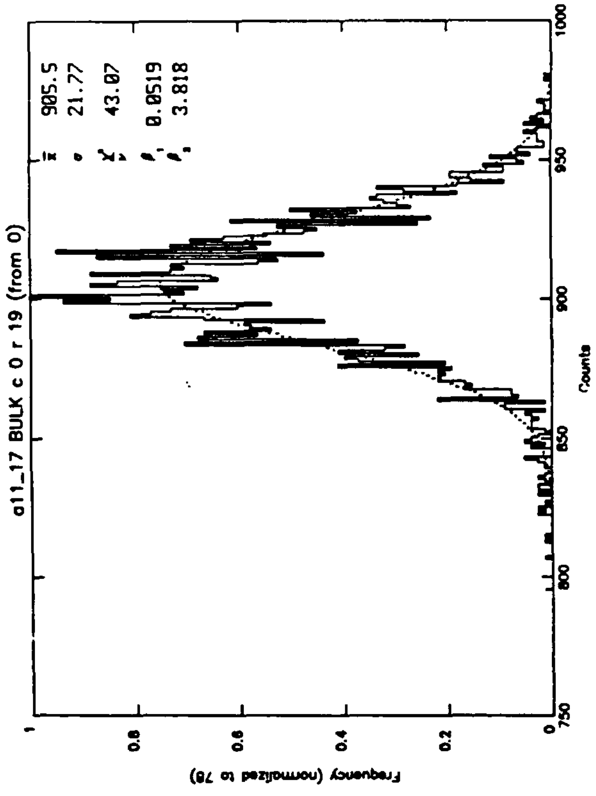
a11_17 BULK c 0 r 19 (from 0)
x̄ 905.5
σ 21.77
χ^2_ν 43.07
β_1 0.0519
β_2 3.818
Counts
Frequency (normalized to 78)

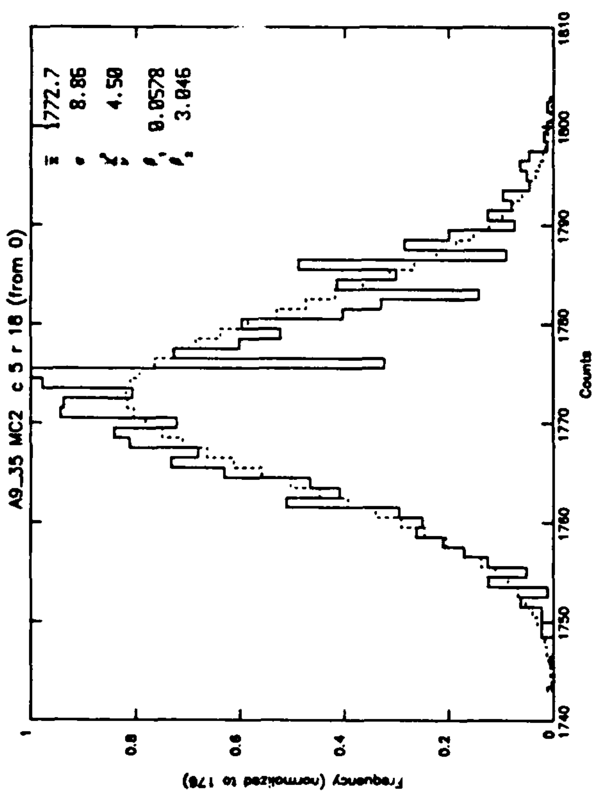
A9_35 MC2 c 5 r 18 (from 0)
x̄ 1772.7
σ 8.86
χ^2_ν 4.50
β_1 0.0578
β_2 3.046
Counts
Frequency (normalized to 178)

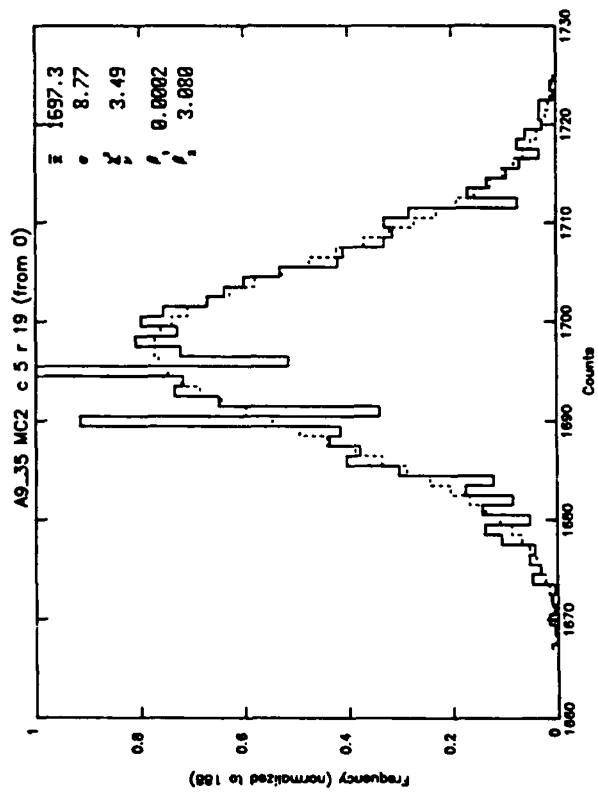
A9_35 MC2 c 5 r 19 (from 0)
x̄ 1697.3
σ 8.77
χ^2_ν 3.49
β_1 0.0002
β_2 3.080
Counts
Frequency (normalized to 188)

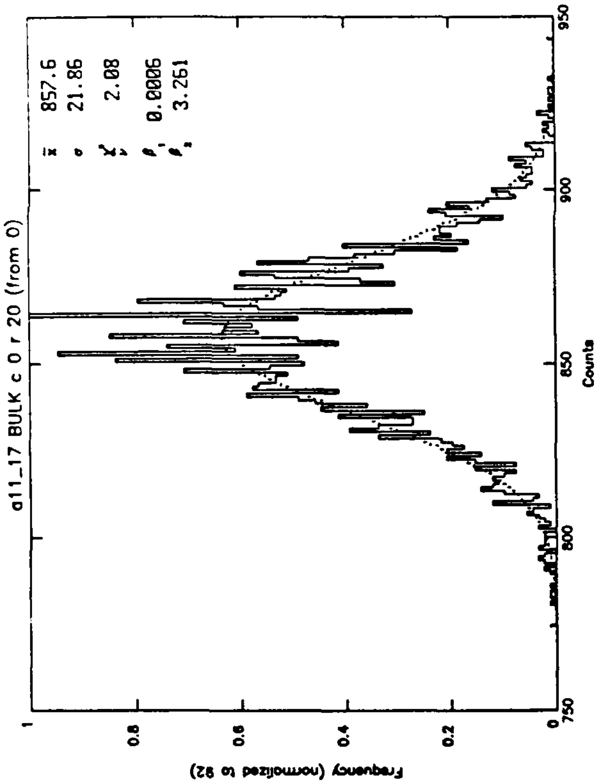
a11_17 BULK c 0 r 20 (from 0)
857.6
21.86
2.08
0.0006
3.261
Counts
Frequency (normalized to 92)

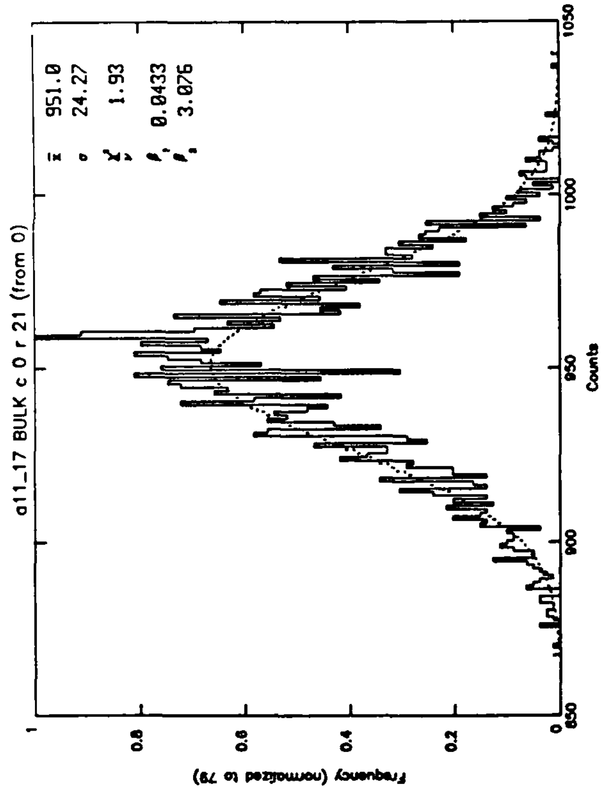
a11_17 BULK c 0 r 21 (from 0)
951.0
24.27
1.93
0.0433
3.076
Counts
Frequency (normalized to 79)

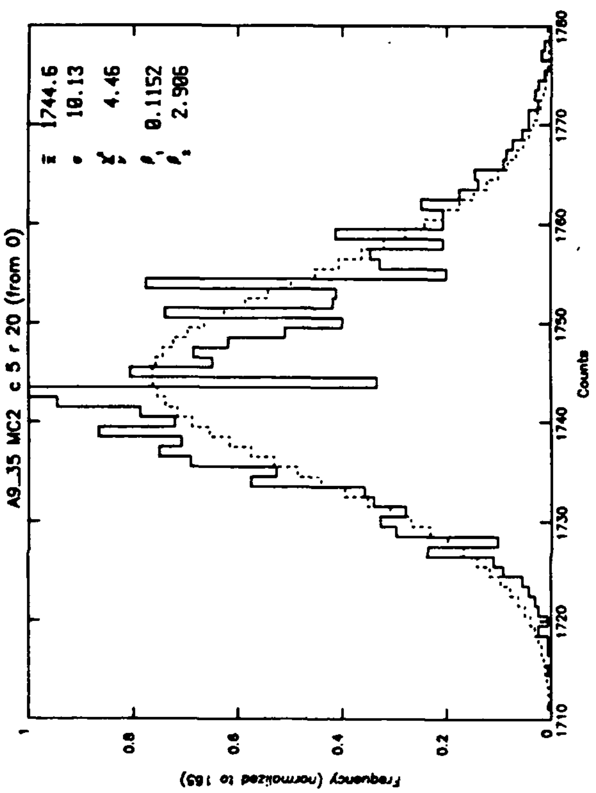
A9_35 MC2 c 5 r 20 (from 0)
1744.6
10.13
4.46
0.1152
2.906
Counts
Frequency (normalized to 163)

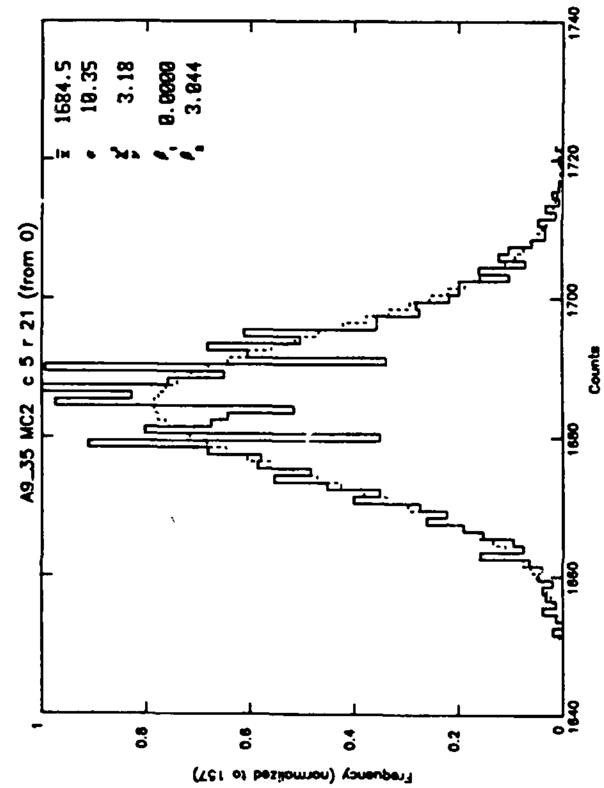
A9_35 MC2 c 5 r 21 (from 0)
1684.5
10.35
3.18
0.0000
3.044
Counts
Frequency (normalized to 157)

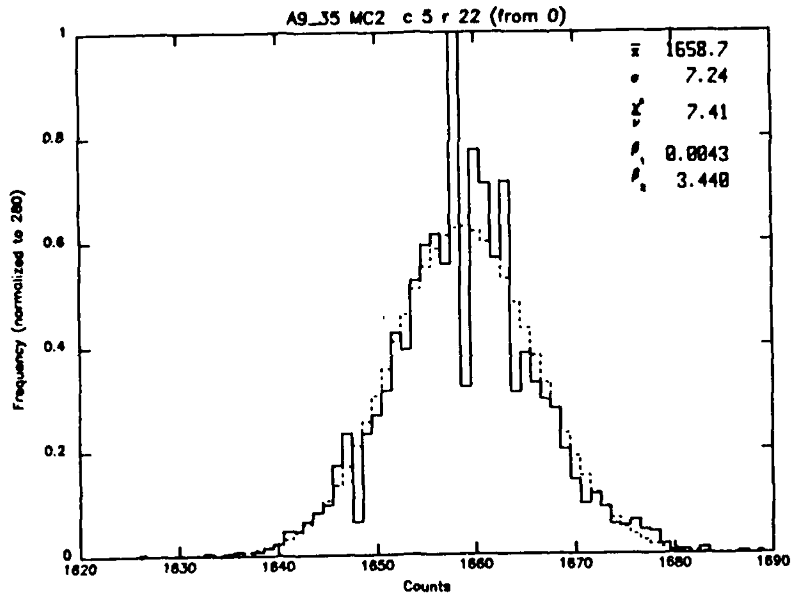
A9_35 MC2 c 5 r 22 (from 0)
$\bar{x}$ 1658.7
σ 7.24
χ^2_ν 7.41
β_1 0.0043
β_2 3.440
Frequency (normalized to 280)
Counts

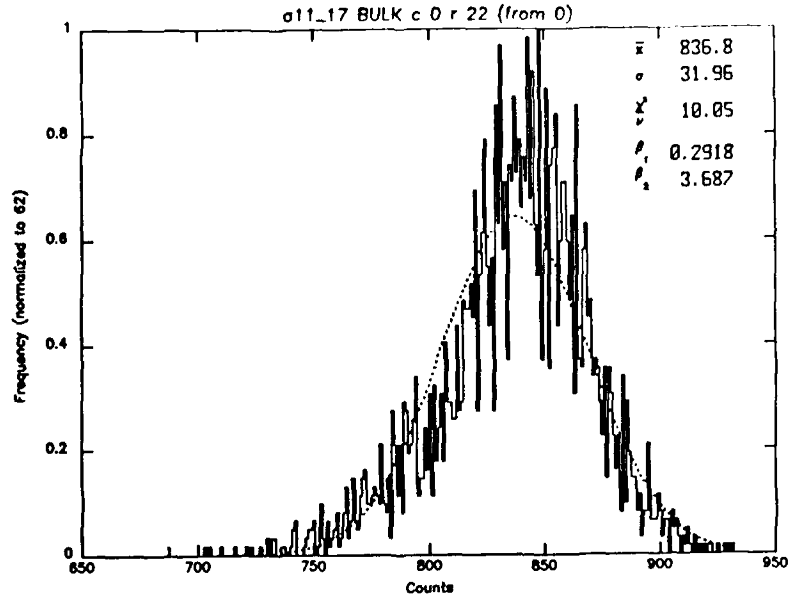
a11_17 BULK c 0 r 22 (from 0)
$\bar{x}$ 836.8
σ 31.96
χ^2_ν 10.05
β_1 0.2918
β_2 3.687
Frequency (normalized to 62)
Counts

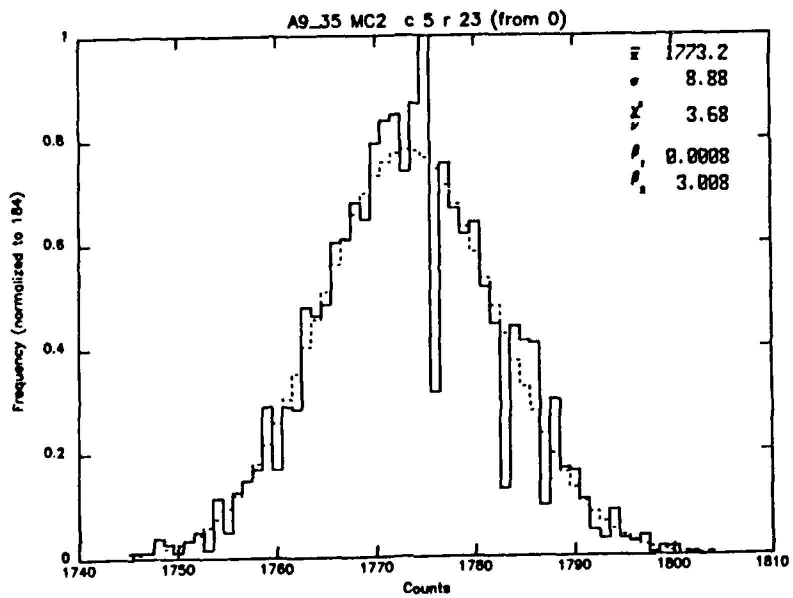
A9_35 MC2 c 5 r 23 (from 0)
$\bar{x}$ 1773.2
σ 8.88
χ^2_ν 3.68
β_1 0.0008
β_2 3.008
Frequency (normalized to 184)
Counts

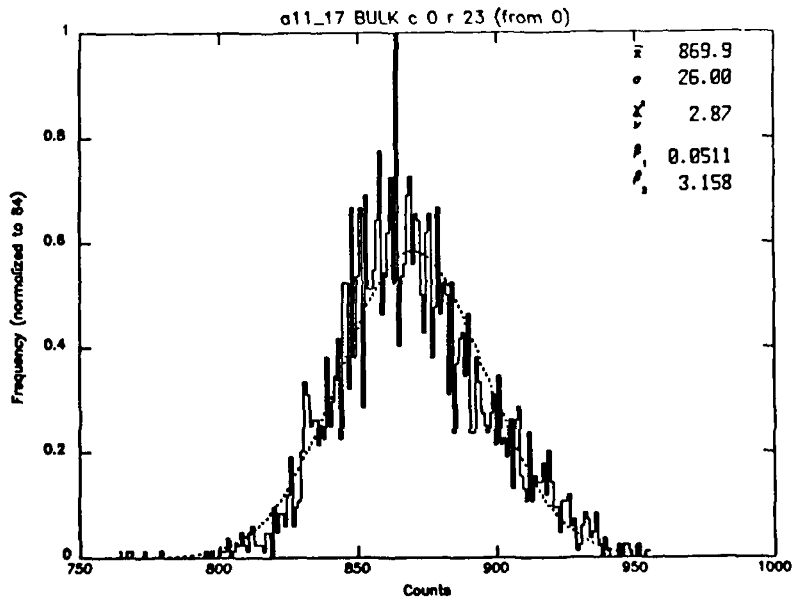
a11_17 BULK c 0 r 23 (from 0)
$\bar{x}$ 869.9
σ 26.00
χ^2_ν 2.87
β_1 0.0511
β_2 3.158
Frequency (normalized to 84)
Counts

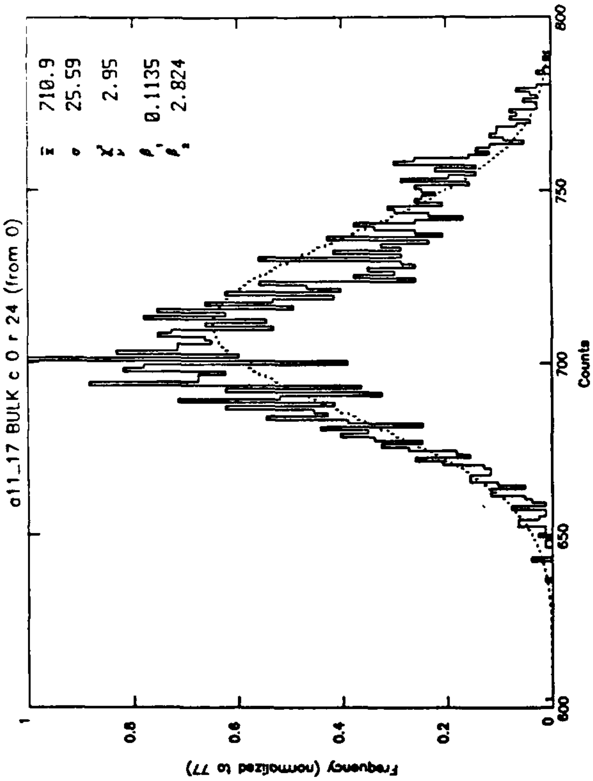
a11_17 BULK c 0 r 24 (from 0)
x̄ 710.9
σ 25.59
χ² 2.95
β₁ 0.1135
β₂ 2.824
Frequency (normalized to 77)
Counts

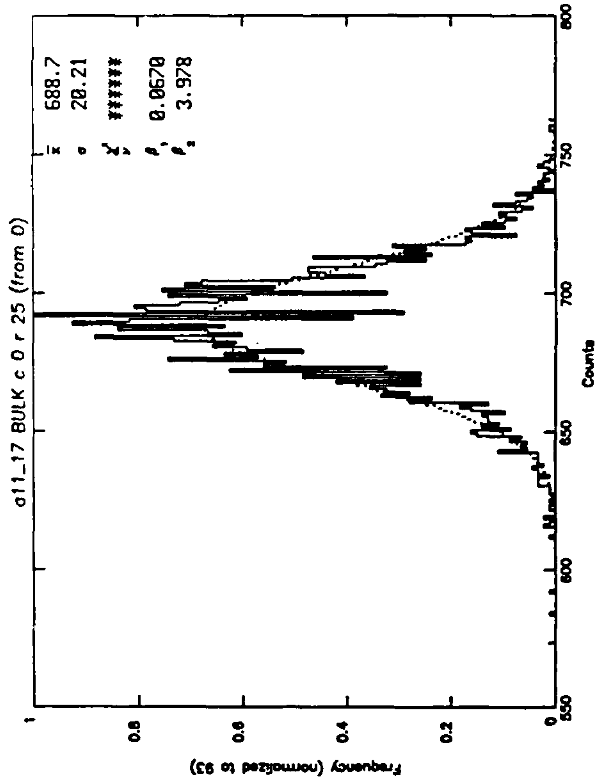
a11_17 BULK c 0 r 25 (from 0)
x̄ 688.7
σ 20.21
χ² ######
β₁ 0.0670
β₂ 3.978
Frequency (normalized to 93)
Counts

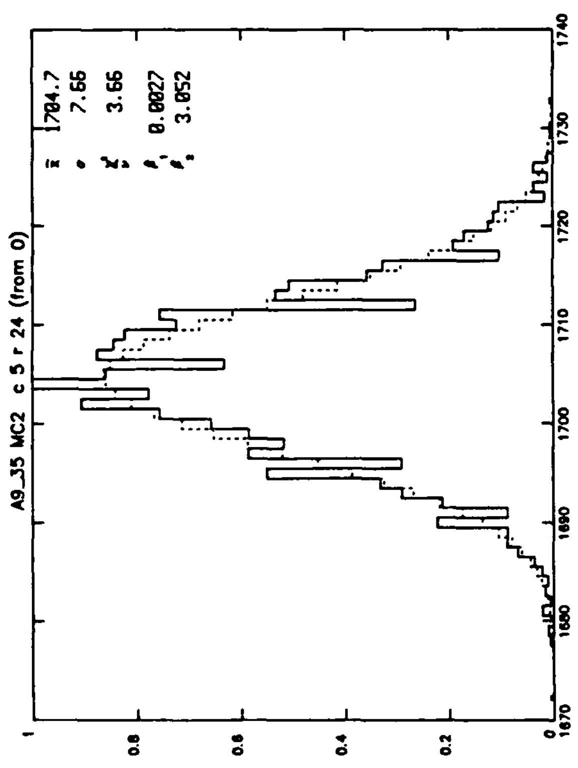
A9_35 MC2 c 5 r 24 (from 0)
x̄ 1704.7
σ 7.66
χ² 3.66
β₁ 0.0027
β₂ 3.052
Frequency (normalized to 193)
Counts

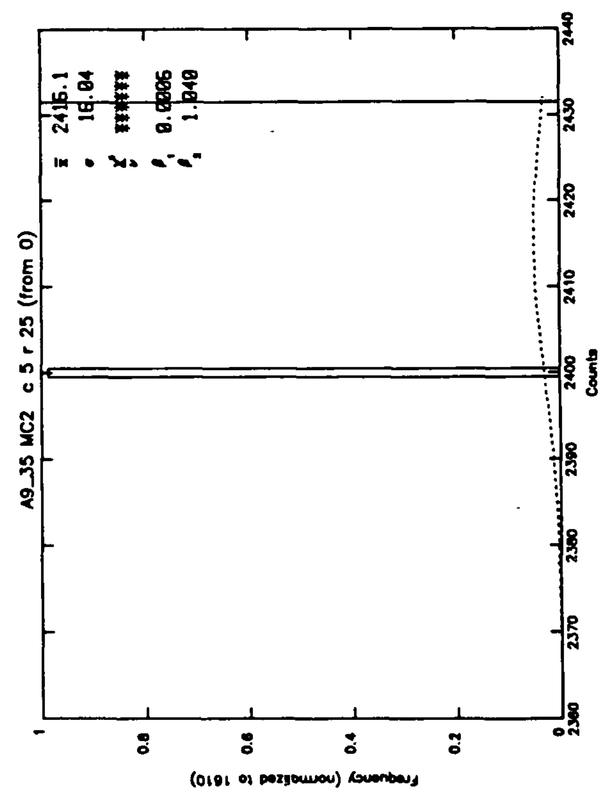
A9_35 MC2 c 5 r 25 (from 0)
x̄ 2416.1
σ 16.04
χ² ######
β₁ 0.0006
β₂ 1.040
Frequency (normalized to 1610)
Counts

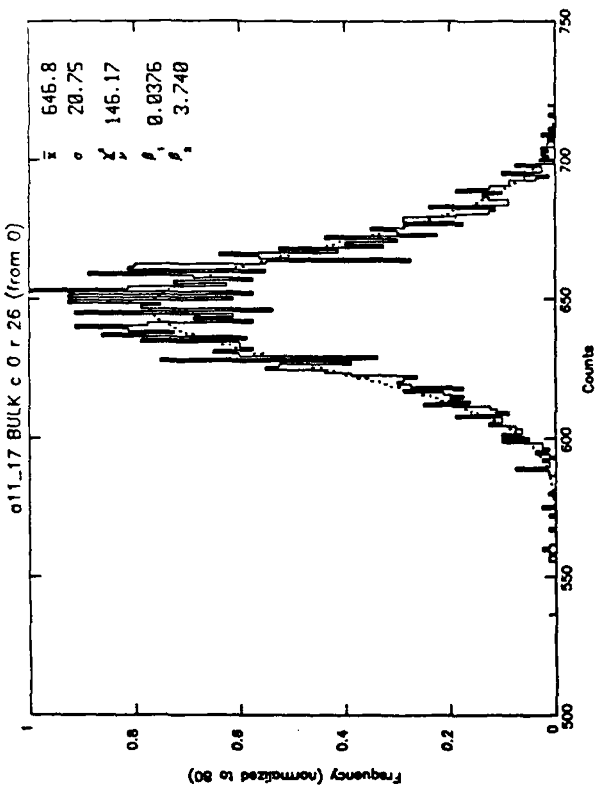
a11_17 BULK c 0 r 26 (from 0)
x̄ 646.8
σ 20.75
χ^2_ν 145.17
β_1 0.0376
β_2 3.740
Counts
Frequency (normalized to 80)

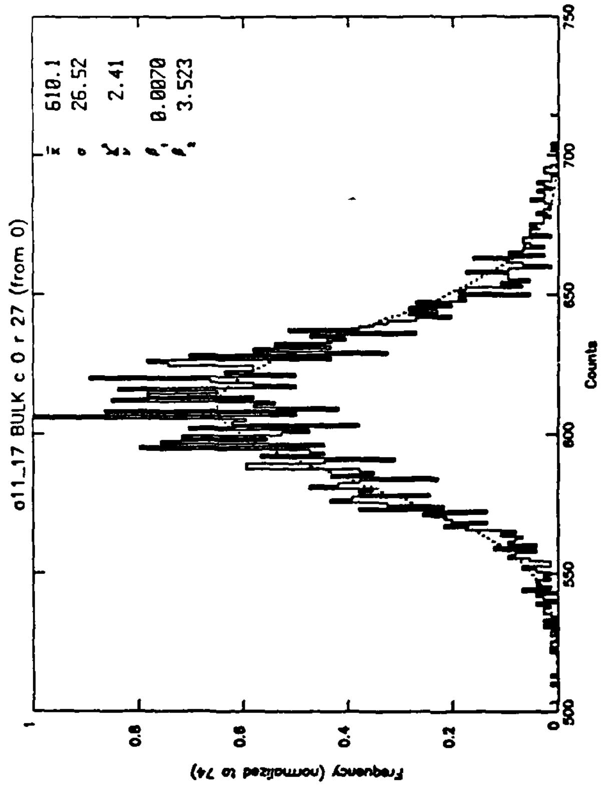
a11_17 BULK c 0 r 27 (from 0)
x̄ 610.1
σ 26.52
χ^2_ν 2.41
β_1 0.0070
β_2 3.523
Counts
Frequency (normalized to 74)

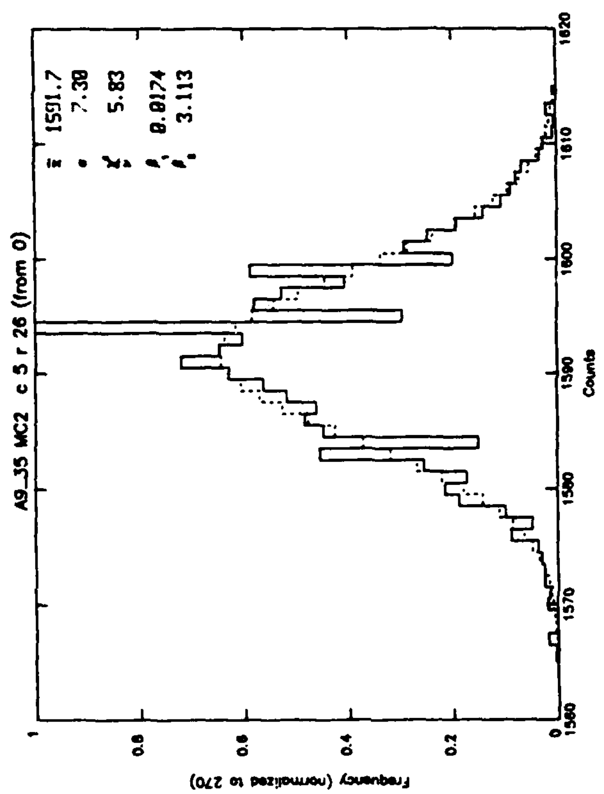
A9_35 MC2 c 5 r 26 (from 0)
x̄ 1591.7
σ 7.30
χ^2_ν 5.83
β_1 0.0174
β_2 3.113
Counts
Frequency (normalized to 270)

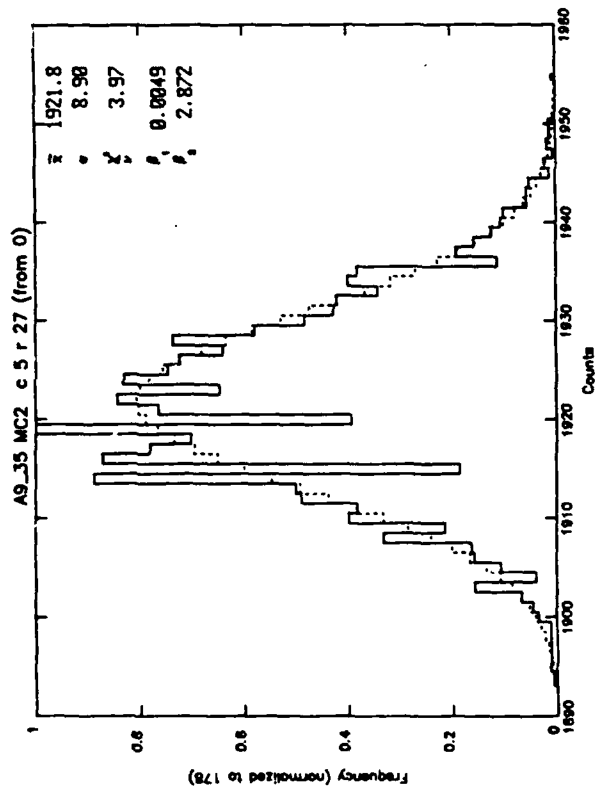
A9_35 MC2 c 5 r 27 (from 0)
x̄ 1921.8
σ 8.98
χ^2_ν 3.97
β_1 0.0049
β_2 2.872
Counts
Frequency (normalized to 178)

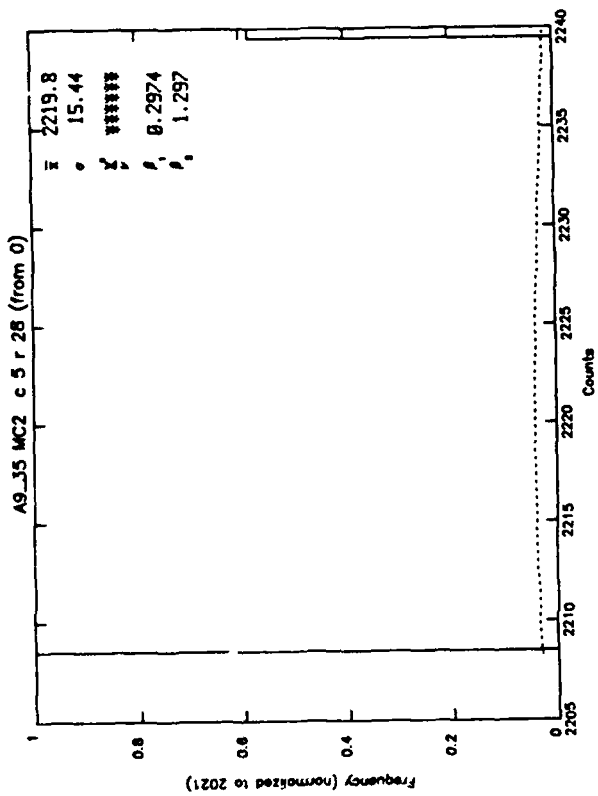
A9_35 MC2 c 5 r 28 (from 0)
x̄ 2219.8
σ 15.44
χ²ν ######
β₁ 0.2974
β₂ 1.297
Counts
Frequency (normalized to 2021)

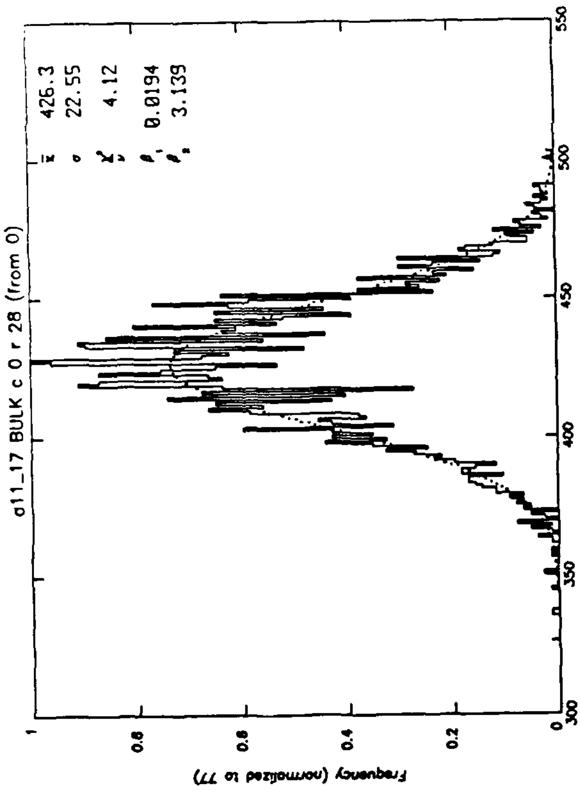
a11_17 BULK c 0 r 28 (from 0)
x̄ 426.3
σ 22.55
χ²ν 4.12
β₁ 0.0194
β₂ 3.139
Counts
Frequency (normalized to 77)

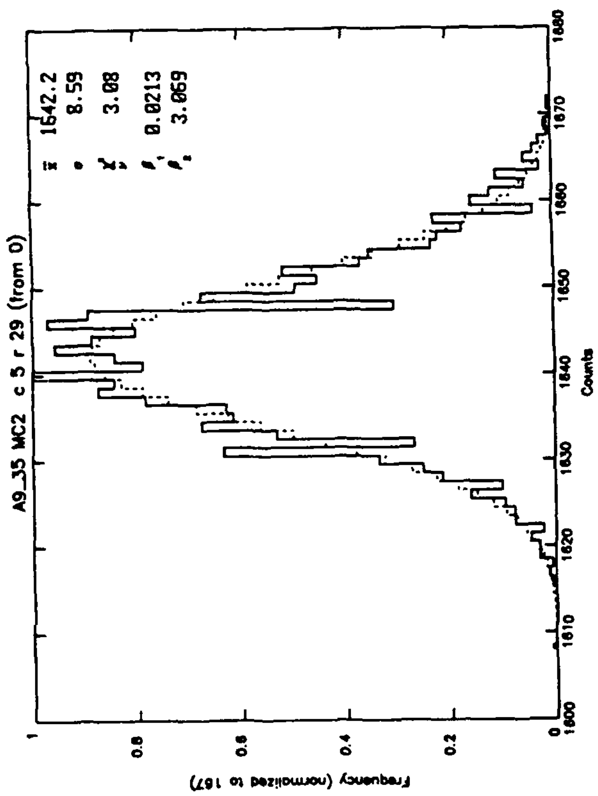
A9_35 MC2 c 5 r 29 (from 0)
x̄ 1642.2
σ 8.59
χ²ν 3.08
β₁ 0.0213
β₂ 3.069
Counts
Frequency (normalized to 167)

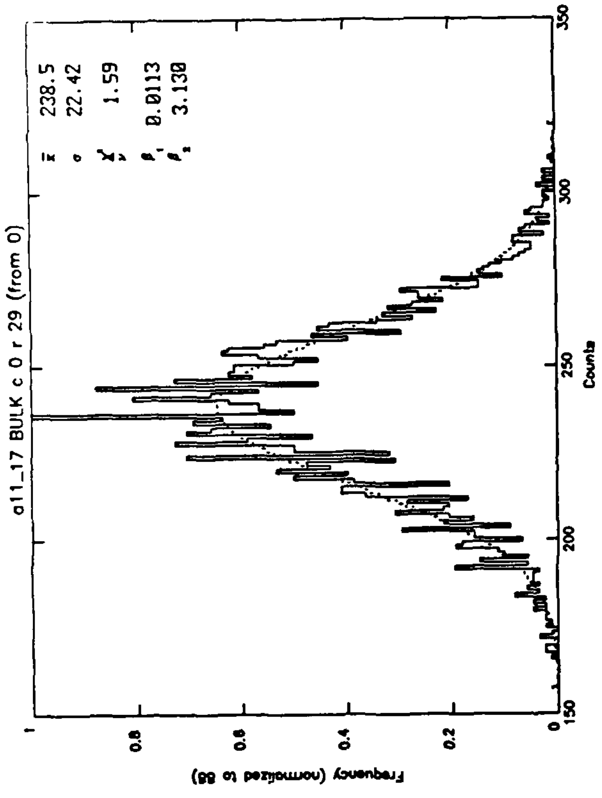
a11_17 BULK c 0 r 29 (from 0)
x̄ 238.5
σ 22.42
χ²ν 1.59
β₁ 0.0113
β₂ 3.130
Counts
Frequency (normalized to 66)

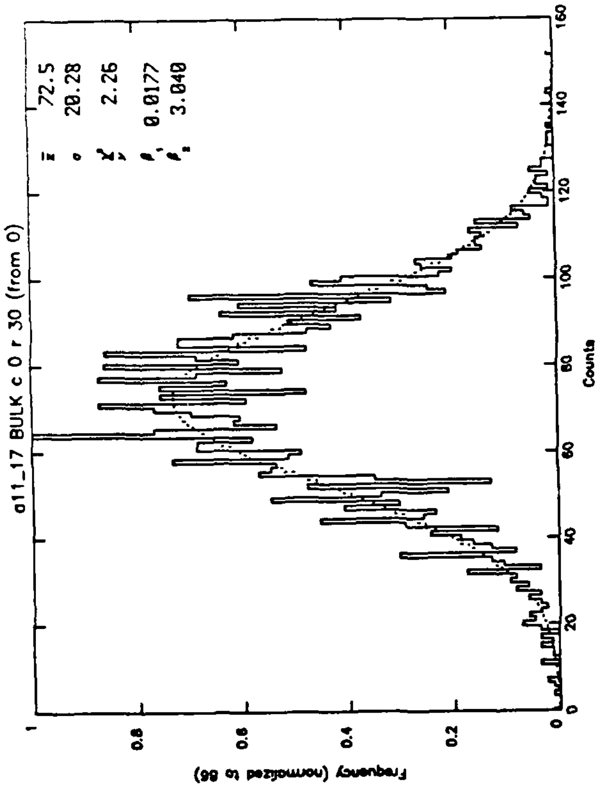
a11_17 BULK c 0 r 30 (from 0)
x̄ 72.5
σ 20.28
χ^2_ν 2.26
β_1 0.0177
β_2 3.040
Counts
Frequency (normalized to 66)

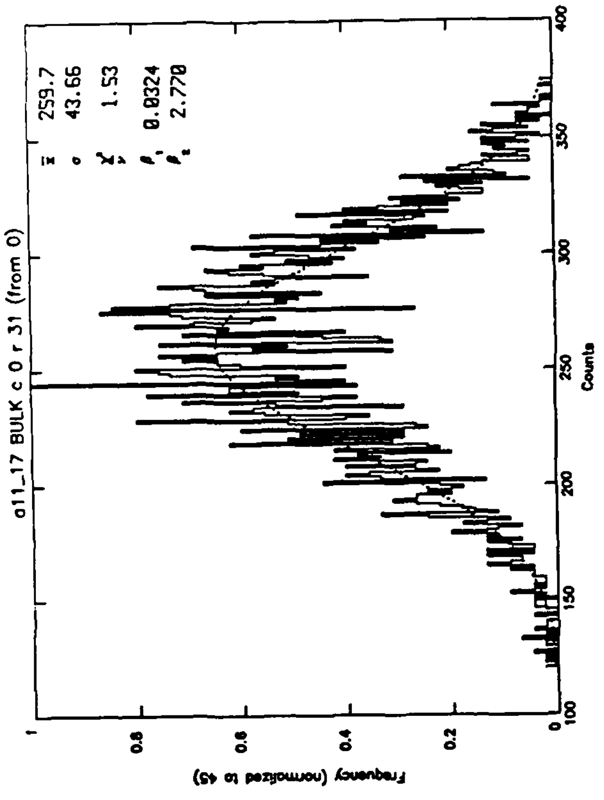
a11_17 BULK c 0 r 31 (from 0)
x̄ 259.7
σ 43.66
χ^2_ν 1.53
β_1 0.0324
β_2 2.770
Counts
Frequency (normalized to 45)

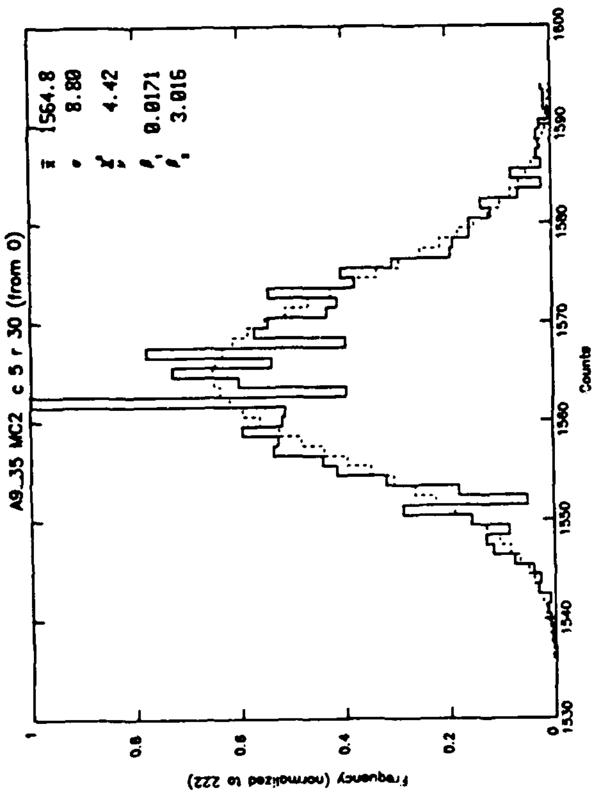
A9_35 MC2 c 5 r 30 (from 0)
x̄ 1564.8
σ 8.80
χ^2_ν 4.42
β_1 0.0171
β_2 3.016
Counts
Frequency (normalized to 222)

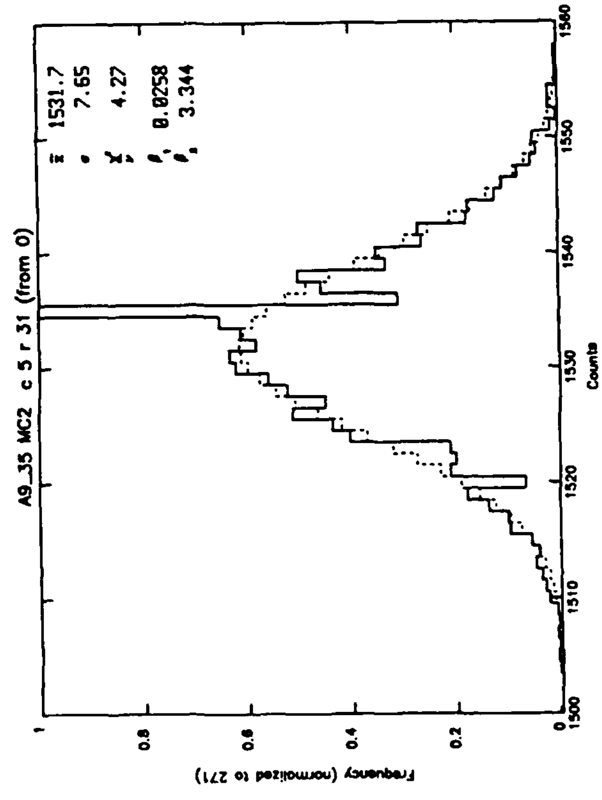
A9_35 MC2 c 5 r 31 (from 0)
x̄ 1531.7
σ 7.65
χ^2_ν 4.27
β_1 0.0258
β_2 3.344
Counts
Frequency (normalized to 271)

Appendix B
Array Performance

The tables which are the principal part of this section display parameters which define the array performance pixel-by-pixel for a variety of different conditions. In each case, a file of data which includes 3200 frames (at 307 microseconds per frame, this is 0.98 seconds of data) is used to determine the statistical parameters described in the section on noise estimation in the main body of the text. For each parameter, a table is constructed in which the value for each pixel is entered in a position representing its location in the array. The reader must be careful to note however that our use of computer format to number the columns and rows could introduce some confusion. Thus for the Rockwell BIBIB array which has 10 columns and 50 rows, the array is listed as 10 columns of 50 numbers; the upper left and lower right numbers are for pixels c0, r0 and c9, r49, respectively, with the 10^{th} number down the 5^{th} column corresponding to c4, r9. The Aerojet arrays have 16 columns and 32 rows; this different aspect ratio necessitates laying out the equivalent table in a sideways configuration, but in all other respects the tables are the same format.

Table B1 is a summary of relevant test conditions for each of the tables to follow. The conditions apply to the same files when they are used for the plots in Appendix A, of course, and thus Table B1 is a reference for that data as well.

Figures 2-7 in the main text show some of the data from the tables which make certain features of the arrays easy to see. For each of the two Aerojet arrays for which we have been able to locate a star sighting, these gray-scale plots show a background measurement, a similar measurement with the star in the field of view, and the result of dividing the former by the latter. In addition to showing the impossibility of seeing the star without the flat-fielding and removal of local background, these figures also graphically display optical characteristics of the array mountings in the dewars. The MC^2 array is vignetted on the top two rows and left three columns due to a slight internal misalignment. The bulk array is vignetted on the bottom and right for a similar reason. Examining Figures 6 and 7 shows that the Rockwell array also suffered from vignetting; in this case, however, the optics were not

TABLE B1
Summary of Array Tables

Table numbering code follows the convention:
a = average   b = variance   c = skewness   d = kurtosis

Rockwell BIBIB Array

Tables B-R1(a-d)	Background Run #1 (BG #1)
Tables B-R2(a-d)	Background Run #2 (BG #2)
Tables B-R3(a-d)	Background Run #3 (BG #3)
Tables B-R4(a-d)	Background Run #4 (BG #4)
Tables B-R5(a-d)	Background Run #5 (BG #5)
Table B-R6	(Average BG #1)/(Average BG #2)
Table B-R7	(Average BG #3)/(Average BG #2)
Table B-R8	(Average BG #4)/(Average BG #2)
Table B-R9	(Average BG #5)/(Average BG #2)

Aerojet MC^2 Array

Tables B-AM1(a-d)	Background Run #1 (BGM #1) Before Star Sighting
Tables B-AM2(a-d)	Star (α Ori) at top; Bias = 2.0v (Star M #1)
Tables B-AM3(a-d)	Star (α Ori) at bottom; Bias = 1.8v (Star M #2)
Tables B-AM4(a-d)	Background Run #2 (BGM #2) After Star Sighting
Tables B-AM5(a-d)	Background Run #3 (BGM #3) After Star Sighting
Tables B-AM6(a-d)	Background Run #4 (BGM #4) After Star Sighting

Aerojet Bulk SiBi Array

Tables B-AB1(a-d)	Star (CW Leo) at center (Star B #1)
Tables B-AB2(a-d)	Background Run #1 (BGB #1)
Table B-AB3	(Average Star B #1)/(Average BGB #1)

large enough for the relatively long BIBIB array, with the result that there was vignetting both at the top and the bottom of the array.

Noise

During the flights, attempts were made to measure the noise on the arrays in several ways. One pixel's output, as a DC signal, was fed into an Ithaco lock-in amplifier which could be set to display the rms noise at a frequency between ~ 10 and 100 Hz, with a user-set bandwidth of 1 Hz. This same input was fed into an HP 3582A spectrum analyzer which uses an FFT algorithm to get the noise spectrum. In the course of making chopped observations of a star, the array outputs were displayed as a colored "checkerboard" display, and watching the ~ 15 Hz frame rate, one could watch the pixels change color and gain a qualitative idea of how good the signal-to-noise (S/N) ratio really was in terms of the ability to "see" the star on the screen.

The trace shown on the spectrum analyzer occasionally exhibited a peak near 120 Hz, and when playing the frames back in a movie fashion, it appeared (to at least one of the authors) that there might be a low frequency modulation of the general background level, such as might arise from the off-axis response of the instrument to seeing different parts of the telescope cavity, e.g., as the plane moved relative to the telescope in flight.

As different analysts saw different effects (or none at all) it became apparent that an objective evaluation was necessary. Procedures were written in IDL (Interactive Data Language) on the Space Sciences Laboratory VAX to compute the moments of the distributions of the ADCs (analog to digital counts) for each pixel over a file of nominally 3200 frames or pictures or images. If these 3200 frames were down-loaded from a 28 track tape, they would represent 300 μsec/frame x 3200 frames/file or about 1 sec. If they were stored directly by The Aerospace Corporation 16 bit computer onto 9 track tape, it would still represent about 1 sec of actual integration, but over an elapsed time of about 4 sec. Moreover, these frames were not uniformly sampled in time; sometimes they were stored as 1 of every 3, sometimes as 1 of every 4 frames. The exact number is stored in the frame's header information, but it is a tedious and long task to recover the information and process the data accordingly. Thus, it was deemed inappropriate to attempt FFT analysis

on the non-consecutive 9 track data frames, but entirely appropriate to use FFT techniques on the downloaded 28 track data which were sequential, consecutive frames.

However, the 28 track data are not in the same format as the 9 track data, i.e., they are not stored by frame. Thus, software had to be written to search for a sync pulse, scan ahead and see if another sync pulse occurred exactly 500 pixels later (for RI data), and if so, then begin writing the resulting frames into a file. If not, the search was continued pixel by pixel. In view of the known spurious sync pulses (which were so numerous in the AESC data to render it effectively impossible to process), this was a critical operation which could be fooled by bad data some of the time, and needed to be checked quickly and well. We found that calculating the higher moments of the distribution served as an excellent test of the quality of the data, as the data can be in error many ways, but it can only be correct one way and thus give reasonable values for the moments.

The moments used were the first, the average; the second, computed as the variance (σ^2) or the standard deviation (σ); the third, the skew, and the fourth, the Kurtosis. These can be represented in equation form as

$$\bar{x} = \frac{\Sigma\, x_i}{N}$$

$$V = \sigma^2 = \frac{\Sigma(x_i - \bar{x})^2}{N - 1}$$

$$s = \beta_1 = \frac{[\Sigma(x_i - \bar{x})^3]^2}{[\Sigma(x_i - \bar{x})^2]^3}$$

$$k = \beta_2 = \frac{\Sigma(x_i - \bar{x})^4}{[\Sigma(x_i - \bar{x})^2]^2} .$$

Due to the fact that the background nearly fills the "wells," modest differences in multiplexer read noise do not usually have any noticeable effect. If the noise were due tc random fluctuations in the background, we

would expect the histogram displaying the frequency of occurrence of a particular ADC vs the ADCs observed for a given pixel to approximate a normal distribution. (This does assume enough gain and enough bits so that the noise will trigger several ADC levels. For the good columns of the ACSC arrays, this was certainly the case. For the RI array, it was marginal.)

This average or mean should represent the most likely value to use to represent the signal. When we are searching for IR stars, we are often looking for signals from a few counts to a fraction of a count. The standard deviation represents the half-width of the Gaussian fit to the histogram; $\sigma_{mean} = \sigma/\sqrt{n}$ is the uncertainty in the average. The skew represents the "shift" of the distribution asymmetrically from the mean, and the kurtosis how peaked the distribution is (see, e.g., Cangelosi, Taylor and Rice, p. 54-57, 1979). For most of the good pixels on any of the arrays, the skews were close to zero and the kurtosis ~ 2-5. In the instances where there were frames of zeroes (which occurred for unknown reasons in the AESC 9 track tapes) mixed with valid frames or where the sync had been erroneously identified (as happened occasionally on RI down-loaded 18 track data), the skew and kurtosis parameters assumed values *orders of magnitude too large*.

If one calculates one additional quality parameter, the χ^2/degree of freedom for the fit of an optimized Gaussian to the histogram, we can judge quite well whether the data have odd frequency components, electrical pickup, variable width A/D bins, etc. Inasmuch as we do not have a well defined error associated with the number of times we measure a particular ADC, we adopt the formal definition of the reduced χ^2 (see, e.g., Introduction to Error Analysis by Taylor; Univ Sci 1982)

$$= \frac{\sum_{i=1}^{N} \frac{(\text{expected-observed})^2}{\text{expected}}}{N - \nu}$$

This essentially assumes the uncertainty in a given measurement of occurrence of an ADC level is the square root of the fit value. Note that while this definition does result in unnaturally high values of χ^2/degree of freedom for any distribution with even one or two ADC levels measured where the fit is close to zero, it is a uniform way of assessing the fit. The reader is given ample opportunity to assess the fits himself; see the figures of the histo-

grams. The discussion of our interpretation of the noise is contained in the body of this report in Sections III, IV, and V.

Some specific problems did show up in these data. For the AESC MC^2 array, one column (12) went dead, and one was definitely not well behaved (7) as can be seen in Figure 2 of the main body of the report. Note that all pixel identifications and matrix identifications (column and row) follow the computer convention of starting at zero.

Table B-R1a
Rockwell BIBIB Array
Background Run #1 (BG #1)

AVERAGE COUNT/FRAME FOR 3200 FRAMES

Rock bg1 Ave

405.160	440.624	538.557	995.082	454.910	474.295	468.800	20.089	20.601	463.270
387.761	414.612	421.925	420.595	427.157	15.746	442.338	11.340	441.389	14.427
416.728	444.108	442.398	446.256	447.134	476.058	462.797	462.558	457.388	524.226
446.827	691.267	471.542	472.818	471.309	496.518	886.949	482.169	517.500	485.541
471.534	492.455	490.757	489.297	487.661	557.564	501.789	498.331	490.107	497.425
461.313	488.818	495.343	492.557	495.996	512.188	547.749	502.937	496.335	497.510
474.478	507.963	518.611	519.365	516.516	534.535	528.692	20.945	520.099	522.661
475.776	523.125	536.431	533.062	531.029	554.195	545.514	545.119	536.655	542.425
526.074	537.107	552.526	826.541	549.246	568.124	563.358	559.291	547.803	20.105
47.373	548.741	563.138	557.672	560.390	26.992	572.966	569.338	561.556	567.309
520.636	571.902	585.814	579.823	580.627	602.757	595.376	591.615	576.524	579.080
526.446	585.171	635.813	594.227	651.739	612.417	605.307	605.943	869.826	595.928
527.454	586.211	600.922	726.658	836.426	619.382	788.542	619.553	602.295	610.623
520.677	580.571	595.346	643.433	594.663	615.786	609.012	609.866	608.140	622.354
524.633	581.169	900.125	598.446	597.180	618.853	614.464	614.551	610.986	635.550
515.135	572.126	585.522	593.497	591.089	612.551	609.345	609.785	610.891	630.915
510.251	568.103	586.721	590.549	591.549	613.028	610.919	612.233	790.079	637.607
623.623	561.123	582.045	587.289	587.346	609.882	605.709	609.876	608.787	636.231
498.882	556.235	581.691	582.202	592.524	608.795	607.687	609.901	613.052	845.866
496.268	555.370	578.741	585.946	590.989	686.380	609.141	611.433	614.782	866.037
497.765	557.413	583.093	590.755	592.912	615.162	610.883	859.298	611.180	780.138
503.770	559.427	586.674	596.111	597.933	619.338	641.918	905.183	624.790	641.084
519.618	846.086	582.447	591.341	590.015	611.476	608.198	675.132	608.188	620.086
657.750	542.600	580.925	589.426	589.919	614.882	611.749	614.368	607.992	617.942
511.883	589.476	584.540	943.172	593.770	584.266	608.926	613.176	608.999	617.715
507.972	565.255	583.118	585.444	592.039	613.548	608.031	611.900	608.393	615.038
521.204	576.518	591.442	893.989	592.619	616.173	614.816	615.633	609.200	616.695
517.209	570.443	586.008	588.004	587.948	610.883	608.797	610.668	617.381	923.317
518.981	569.073	586.399	586.231	584.504	606.736	605.471	606.989	603.063	609.012
516.637	571.134	948.693	586.328	590.047	607.214	603.581	604.966	604.379	612.193
516.674	569.748	580.888	589.097	588.287	607.213	603.698	607.164	613.141	631.611
514.120	564.582	580.692	584.237	584.399	604.200	601.131	606.742	609.997	620.392
514.304	563.980	574.244	583.104	912.491	602.256	601.555	606.098	606.556	611.248
587.621	558.704	571.305	572.496	572.029	595.359	596.767	600.972	600.798	607.009
506.196	558.823	574.168	576.065	791.700	598.601	601.272	605.345	605.839	613.078
496.727	547.653	563.375	568.668	564.522	832.050	592.635	596.646	598.098	644.590
497.015	553.230	563.179	569.493	563.206	588.435	591.817	593.916	601.587	847.970
493.782	785.563	730.832	572.088	569.660	709.495	589.064	591.442	604.397	614.453
491.559	541.721	559.355	566.041	566.677	830.105	585.366	617.284	638.858	613.079
485.544	540.677	555.049	555.288	558.861	569.675	578.448	579.387	741.061	606.959
492.083	520.698	555.701	560.311	558.864	582.003	579.732	580.076	580.733	590.615
484.069	43.724	547.740	555.541	550.409	574.956	572.954	572.647	572.788	579.774
502.996	719.079	564.262	568.985	634.570	587.791	587.043	585.640	586.919	598.337
485.752	535.570	543.547	554.813	554.801	574.728	571.328	722.423	574.816	583.796
517.401	608.818	551.788	576.966	555.375	587.982	567.316	562.678	567.740	774.038
475.916	524.123	538.655	545.279	541.877	559.884	553.626	553.012	554.396	562.984
471.479	515.211	530.143	531.478	528.627	548.670	543.682	541.708	859.235	554.844
463.193	504.652	517.807	519.411	520.387	539.057	533.854	531.567	535.968	546.620
452.261	495.812	742.775	506.160	507.819	526.330	520.503	518.154	523.531	530.257
429.698	469.425	476.370	483.774	484.508	523.807	525.977	528.151	531.603	694.743

Table B-R1b
Rockwell BIBIB Array
Background Run #1 (BG #1)

VARIANCE

Rock bg1 Sig^2

4.102	4.222	4.272	1.925	1.929	5.268	5.125	8.195	9.247	5.427
3.132	2.956	3.238	3.632	1.934	6.869	4.330	9.729	3.933	14.842
3.376	3.245	3.356	3.870	5.003	3.873	4.258	4.015	4.234	4.289
4.318	14.112	3.163	3.732	1.530	2.946	2.127	4.247	3.663	3.431
3.472	3.667	3.872	4.343	1.886	4.699	4.251	4.241	4.092	4.555
4.131	4.450	4.450	4.881	1.860	495.568	6.333	5.523	5.607	6.654
3.004	3.097	3.098	3.537	2.001	3.688	3.859	7.953	3.648	3.796
3.781	3.466	3.644	4.247	2.229	4.005	4.849	4.248	4.256	4.912
3.969	3.983	4.315	7.825	2.192	4.654	5.764	5.018	4.912	13.922
2.665	3.071	3.203	3.419	1.965	10.547	4.131	3.861	3.794	3.744
5.896	6.162	6.372	7.535	3.122	7.110	8.169	7.205	7.244	7.788
2.954	3.165	3.171	3.439	1.774	3.333	4.702	4.944	1.242	4.367
3.438	3.312	3.397	3.329	1.746	3.738	3.818	4.017	3.803	4.055
5.606	5.739	5.982	7.331	2.795	6.621	7.830	7.409	7.176	8.230
5.709	5.467	4.632	6.308	2.931	6.058	7.429	6.567	6.968	6.833
5.376	5.611	6.253	6.700	2.762	6.901	7.546	7.670	7.081	6.874
3.535	3.940	4.034	4.226	1.819	4.698	4.955	4.510	5.361	4.598
5.230	5.591	6.123	6.362	4.187	6.348	6.508	5.566	7.350	4.964
4.447	4.459	4.673	5.367	2.454	6.512	5.849	5.199	4.884	11.681
3.574	3.584	3.721	4.285	1.766	4.195	4.431	4.244	4.106	3.682
3.282	3.043	3.274	3.475	1.756	3.691	4.284	4.146	3.752	6.465
2.746	2.622	2.907	3.324	1.939	3.687	3.693	1.058	3.268	3.326
3.276	2.535	3.034	3.329	1.751	3.155	3.752	3.258	4.256	3.535
4.798	5.322	5.717	6.552	3.164	7.102	6.416	6.428	7.346	6.596
3.466	3.588	3.964	2.714	2.239	4.743	4.560	4.744	6.067	4.545
3.805	3.609	3.604	3.951	2.103	3.795	5.100	3.894	4.154	4.156
3.789	3.983	3.859	14.264	1.943	4.464	4.947	4.811	5.112	4.590
3.790	3.566	3.983	4.303	2.213	4.169	4.985	4.898	4.538	3.408
5.403	5.643	5.745	6.270	2.700	7.166	6.814	7.313	6.837	6.752
2.804	2.766	0.902	3.303	1.787	3.590	3.995	3.764	3.585	3.770
3.313	3.182	3.199	3.500	2.058	4.403	3.971	3.823	3.489	3.515
83.901	3.404	3.515	3.943	1.970	4.569	4.428	4.967	4.055	4.241
165.945	4.555	4.669	5.292	0.548	5.158	5.943	5.653	6.947	5.649
3.238	3.028	3.426	3.722	1.949	3.563	4.118	4.003	3.628	4.642
3.388	3.209	3.760	4.444	1.662	3.804	4.655	4.552	4.877	4.382
3.331	3.204	3.462	3.623	1.964	3.057	4.071	3.887	3.818	3.777
3.272	3.456	3.530	3.764	1.872	3.754	3.726	3.674	3.545	6.032
2.697	3.046	2.607	3.274	1.968	3.090	3.520	3.091	3.247	3.222
2.976	2.783	2.879	3.421	1.966	4.378	3.621	3.835	3.823	3.595
3.394	3.300	3.520	3.821	1.632	4.059	4.591	4.195	3.561	4.390
4.677	5.303	5.208	5.757	2.131	6.432	5.394	4.775	4.292	4.739
3.973	5.256	4.270	4.665	2.369	5.776	5.479	4.899	4.794	5.497
2.729	2.378	3.003	3.286	1.714	3.557	3.717	3.678	3.235	3.432
2.429	2.444	2.739	2.632	1.561	2.802	2.996	3.113	2.935	2.929
3.159	2.716	2.645	3.337	1.721	3.266	3.447	3.364	3.159	3.267
2.676	2.608	2.775	2.971	1.652	2.503	3.732	3.527	3.352	4.285
3.524	84.646	3.912	4.228	1.644	4.504	4.640	4.432	1.485	4.596
6.419	6.670	6.917	7.741	2.962	7.589	9.326	8.567	8.141	8.514
6.054	5.702	5.476	6.662	3.780	5.910	8.279	7.799	7.489	8.772
8.791	8.460	9.109	9.024	6.811	8.420	9.348	9.644	9.455	7.514

Table B-R1c
Rockwell BIBIB Array
Background Run #1 (BG #1)

SKEWNESS

Rock bg1 Skew

0.001	0.010	0.048	0.005	0.115	0.003	0.112	0.114	0.277	0.104
0.005	0.030	0.004	0.000	0.012	0.137	0.004	0.149	0.000	0.105
3.096	0.018	0.014	0.004	211.053	0.022	0.001	0.016	0.019	0.002
86.369	16.551	0.015	0.005	0.000	0.045	0.552	6.921	0.002	0.010
0.009	0.016	0.001	0.009	0.026	0.001	0.003	0.000	0.002	0.008
0.013	0.005	0.041	0.010	0.006	513.421	0.015	0.022	0.037	0.001
0.073	0.088	0.120	0.085	0.150	0.045	0.089	0.712	0.094	0.158
0.008	0.042	0.011	0.002	0.014	0.044	0.002	0.004	0.018	0.028
0.063	0.040	0.114	0.059	0.000	0.114	0.140	0.104	0.048	0.091
0.046	0.011	0.000	0.004	0.002	0.131	0.019	0.025	0.045	0.082
0.001	0.001	0.000	0.008	0.026	0.003	0.005	0.007	0.013	0.049
0.043	0.077	0.035	0.079	0.009	0.069	4.261	14.839	0.304	0.123
0.149	0.127	0.042	0.029	0.077	0.128	0.015	0.098	0.071	0.045
0.029	0.022	0.016	0.005	0.003	0.011	0.406	0.884	0.027	0.154
0.113	0.147	0.063	0.088	0.127	0.111	0.188	0.165	0.088	0.203
0.007	0.004	0.003	0.008	0.001	0.000	0.002	1.304	0.006	0.005
0.013	0.008	0.013	0.007	0.013	0.018	0.014	0.005	0.034	0.003
0.167	0.136	0.085	0.055	0.081	1.368	2.365	0.077	6.981	0.012
0.000	0.001	0.002	0.018	0.032	4.998	4.507	0.627	0.000	0.005
0.293	0.130	0.172	0.200	0.006	0.776	0.206	0.183	0.155	2.477
0.000	0.011	0.003	0.001	0.000	0.002	0.753	0.003	0.000	0.035
0.106	0.113	0.100	0.092	0.206	0.087	0.168	0.567	0.129	0.130
0.011	0.000	0.000	0.071	0.039	0.003	1.759	0.003	9.328	0.001
0.071	0.095	0.060	0.101	0.170	0.143	0.025	0.044	1.314	0.050
0.012	0.009	0.001	0.076	0.003	0.000	0.036	0.014	7.739	0.027
0.025	0.037	0.047	0.072	0.198	0.056	9.406	0.064	0.077	0.071
0.007	0.016	0.004	620.340	0.021	0.004	0.003	0.001	1.620	0.014
0.000	0.003	0.001	0.000	0.021	0.004	0.740	0.436	0.000	0.013
0.003	0.001	0.000	0.003	0.034	0.032	0.009	0.998	0.008	0.075
0.001	0.008	0.108	0.004	0.217	7.998	2.746	2.363	0.036	0.065
0.004	0.016	0.028	0.026	0.006	17.739	0.048	1.473	0.049	0.066
2872.932	0.006	0.017	0.011	0.017	6.470	0.014	13.079	0.046	0.005
1482.072	0.041	0.047	0.034	0.023	0.041	0.037	3.149	9.115	0.007
0.007	0.001	0.013	0.005	0.107	0.001	0.017	0.000	0.000	8.726
0.005	0.000	0.052	0.007	0.020	0.005	0.030	0.944	4.038	0.046
0.027	0.027	0.061	0.010	0.022	0.022	0.046	0.007	0.015	0.005
0.011	0.001	0.018	0.000	0.007	0.013	0.006	0.008	0.002	0.010
0.533	0.137	0.472	0.673	0.201	0.621	0.855	0.627	0.603	0.776
0.002	0.021	0.003	0.010	0.218	0.002	0.002	0.003	0.059	0.009
0.024	0.037	0.046	0.039	0.037	0.040	0.083	0.041	0.049	1.816
0.007	0.053	0.027	0.020	0.034	0.048	0.021	0.020	0.025	0.020
0.019	0.051	0.056	0.079	0.059	33.301	0.025	0.083	0.052	0.119
0.008	0.027	0.019	0.031	0.027	0.004	0.015	0.014	0.002	0.000
0.091	0.037	0.029	0.049	0.143	0.241	0.147	0.284	0.216	0.218
0.001	3.910	0.015	0.002	0.013	0.002	0.015	0.000	0.042	0.001
0.033	0.034	0.033	0.005	0.130	0.032	0.101	0.063	0.080	0.185
0.008	2761.702	0.002	0.001	0.001	0.011	0.002	0.057	0.000	0.018
0.159	0.133	0.136	0.118	0.045	0.239	0.123	0.197	0.170	0.150
0.005	0.031	0.020	0.021	0.028	0.000	0.042	0.025	0.027	0.005
0.000	0.000	0.006	0.001	0.007	0.011	0.000	0.006	0.001	0.000

Table B-R1d
Rockwell BIBIB Array
Background Run #1 (BG #1)

KURTOSIS

Rock bg1 Kurt

4.466	4.493	4.730	2.892	4.640	5.147	4.941	4.570	4.700	4.298
3.002	3.225	2.948	2.867	3.204	3.862	2.804	3.325	2.880	3.180
33.864	3.018	2.768	3.023	416.326	2.763	2.891	3.145	2.830	2.885
285.921	24.500	2.936	2.860	3.921	3.206	4.896	37.765	2.821	3.020
2.796	2.631	2.588	2.614	2.927	3.866	2.734	2.699	2.729	4.024
2.813	2.652	3.794	2.841	3.455	519.965	2.712	2.984	3.501	2.680
3.351	3.678	3.638	3.409	3.752	3.528	3.409	4.743	3.714	3.609
2.761	2.922	2.932	3.015	2.959	2.882	2.695	2.942	2.893	2.959
5.382	3.732	3.964	3.538	3.322	4.190	4.300	4.066	3.827	3.308
3.036	2.914	3.430	5.251	3.166	2.797	3.086	2.766	2.970	3.277
2.926	2.885	2.819	2.877	2.944	2.779	2.704	2.909	2.812	2.823
3.129	3.050	3.015	3.083	3.056	3.002	38.654	62.790	2.795	3.131
4.748	3.377	3.359	3.535	3.461	3.333	3.559	3.565	3.228	3.255
2.876	2.900	2.688	2.822	2.801	2.860	6.771	10.664	2.793	3.702
2.877	2.979	2.710	3.072	3.281	2.797	2.975	3.007	10.633	2.957
2.718	2.845	2.832	2.937	3.255	2.660	2.734	13.812	2.684	2.922
3.164	3.429	3.233	3.353	4.188	3.432	3.031	3.272	3.264	3.334
4.089	3.265	2.958	2.927	2.731	13.609	20.559	2.950	30.622	3.007
3.577	3.400	3.384	3.582	3.419	27.143	28.893	11.371	3.389	2.868
4.649	3.589	3.654	3.506	3.876	7.663	3.508	3.610	3.771	19.258
3.079	3.172	3.121	3.079	2.961	2.963	13.278	2.894	3.281	3.064
3.533	3.520	3.282	3.147	3.381	3.053	3.397	4.108	3.329	3.281
3.080	3.031	3.089	4.532	2.883	2.825	22.488	2.849	48.366	3.019
3.005	3.128	3.023	3.043	3.034	2.987	2.852	3.015	18.333	3.002
3.162	3.036	2.976	5.700	2.944	2.908	3.098	3.031	36.134	3.109
3.221	3.291	3.603	3.393	4.104	3.498	46.404	3.175	3.282	3.624
3.082	2.998	3.123	851.469	3.552	3.123	3.000	3.057	21.287	3.145
2.804	2.872	2.808	2.782	3.241	2.833	13.028	11.010	2.871	2.683
3.019	3.026	2.894	3.021	3.219	3.125	3.018	14.846	2.936	8.361
3.329	4.031	3.233	3.764	3.707	52.329	33.988	32.894	4.131	3.850
2.890	3.218	2.915	3.152	3.003	67.489	3.177	25.019	3.320	3.846
2977.886	2.830	2.799	2.960	3.168	45.828	2.761	56.568	2.924	4.856
1520.265	2.991	3.182	3.003	2.796	2.940	2.895	25.432	37.673	3.008
2.906	5.547	3.048	3.051	3.632	2.915	3.014	2.799	3.076	47.530
2.873	4.939	2.821	2.606	3.437	3.090	2.538	21.615	33.822	2.544
4.270	3.052	3.723	3.134	3.017	3.244	3.432	3.414	3.702	3.128
3.937	2.795	3.337	2.918	3.194	2.843	2.995	2.827	2.901	2.806
4.559	3.962	4.746	5.169	3.875	5.185	5.206	5.430	4.884	5.008
3.199	3.208	3.271	3.526	3.706	2.727	3.362	3.029	3.436	3.578
2.920	2.945	3.014	2.921	3.237	2.892	3.121	2.930	2.932	19.866
2.703	2.375	2.545	2.593	2.972	2.444	2.850	2.658	2.755	2.881
2.861	2.839	3.039	2.946	3.049	149.104	2.966	3.068	2.976	3.118
3.591	3.611	3.111	3.311	3.182	2.928	3.151	3.148	3.292	3.614
3.327	3.425	3.347	3.585	3.701	3.837	3.929	6.947	4.101	4.694
2.755	7.707	2.978	2.722	3.399	2.712	3.059	2.908	3.823	3.064
2.990	3.102	3.190	2.921	3.116	5.808	3.096	3.066	3.29[illegible]	4.159
3.230	2900.710	2.961	2.921	3.234	3.102	3.227	3.299	3.162	3.256
3.059	2.747	2.766	2.759	3.082	2.811	2.816	2.856	2.948	2.892
3.265	3.973	3.421	3.386	3.313	3.598	3.299	3.286	3.179	2.990
3.017	2.733	2.787	2.775	2.477	2.778	2.877	2.814	2.883	2.940

Table B-R2a
Rockwell BIBIB Array
Background Run #2 (BG #2)

AVERAGE COUNT/FRAME FOR 3200 FRAMES

Rock BG #2 AVE of 3200 frames

405.221	440.667	538.737	995.083	454.527	474.339	468.788	21.147	21.814	463.847
387.640	414.615	421.963	420.824	426.767	16.192	442.438	11.954	441.610	15.313
416.790	444.311	442.497	446.446	446.896	476.321	463.242	462.848	457.849	525.088
446.305	690.581	471.044	472.363	470.566	496.349	886.896	481.941	517.210	485.391
471.822	492.536	490.980	489.566	487.483	557.739	502.169	498.750	490.549	497.777
461.412	488.858	495.633	492.752	495.507	511.723	548.322	503.254	496.690	498.044
474.293	507.757	518.534	519.274	516.108	534.482	528.761	22.011	520.300	523.131
475.688	523.189	536.426	533.042	530.453	554.370	545.656	545.247	536.778	542.914
525.853	536.812	552.131	826.833	548.656	567.818	563.010	559.259	547.677	21.331
47.192	548.380	562.748	557.359	559.461	27.211	572.646	569.178	561.375	567.327
519.983	571.380	585.384	579.287	579.917	602.325	594.890	591.192	576.261	579.268
526.261	584.818	635.616	593.848	651.009	612.064	605.081	605.813	869.732	596.074
527.270	585.929	600.747	726.649	835.988	619.159	788.415	619.559	602.398	610.727
520.202	580.079	595.001	643.300	593.868	615.536	608.713	609.761	608.090	622.372
524.541	581.133	900.618	598.809	596.575	618.980	614.632	614.823	611.363	635.998
514.800	571.631	585.063	593.198	590.281	612.328	609.147	609.618	610.867	630.922
510.489	568.195	586.719	590.586	590.999	613.163	611.204	612.325	790.423	637.846
623.943	560.915	581.891	587.275	586.643	609.835	605.820	610.068	608.836	636.348
498.834	556.096	581.615	582.061	591.917	608.676	607.431	609.747	613.125	846.054
496.177	555.320	578.590	585.813	590.317	686.362	608.994	611.525	614.805	866.412
497.942	557.539	583.263	590.999	592.594	615.403	611.392	859.675	611.514	780.846
503.834	559.404	586.651	596.145	597.482	619.439	641.930	905.234	625.067	641.403
519.389	846.196	582.350	591.046	589.400	611.228	608.047	674.956	608.009	619.993
658.825	542.531	580.812	589.447	589.470	614.951	611.899	614.606	607.998	617.964
511.886	589.223	584.459	943.180	593.317	584.172	609.013	613.216	608.872	617.904
507.827	565.127	582.967	585.507	591.258	613.507	607.967	611.902	608.584	615.341
521.173	576.151	591.203	894.231	591.905	616.047	614.779	615.794	609.036	616.747
517.378	570.466	586.086	587.996	587.403	610.952	608.822	610.853	617.654	923.130
518.933	569.122	586.372	586.278	583.934	606.892	605.524	607.131	603.329	609.286
516.317	570.852	948.814	586.270	589.205	607.038	603.322	604.887	604.525	612.220
516.625	569.592	580.787	589.222	587.471	607.270	603.656	607.279	613.364	631.897
513.543	564.211	580.398	583.836	583.601	603.809	600.822	606.503	609.758	620.165
513.643	563.810	574.085	582.978	911.932	602.034	601.391	605.957	606.620	611.287
587.158	558.598	571.216	572.327	571.199	595.404	596.750	600.939	600.787	607.061
506.057	558.887	574.390	576.251	791.271	598.792	601.444	605.717	606.109	613.478
496.342	547.384	563.041	568.477	563.653	832.444	592.576	596.418	597.995	644.800
496.924	552.944	563.336	569.580	562.795	588.543	592.039	596.018	601.847	848.564
493.516	786.602	731.006	571.965	568.894	709.618	589.051	591.387	604.460	614.611
491.560	541.448	559.244	566.094	566.096	828.530	585.499	617.470	639.203	613.333
485.313	540.487	554.826	555.235	558.250	569.742	578.321	579.200	741.194	606.977
491.650	520.104	555.323	559.808	558.158	581.810	579.347	579.859	580.433	590.587
484.004	43.615	547.654	555.502	549.692	575.007	573.062	572.613	572.865	579.912
503.209	719.783	564.397	569.264	634.191	587.903	587.262	585.975	587.309	598.544
485.799	535.507	543.526	554.803	554.391	574.676	571.511	722.998	574.969	584.039
517.190	608.582	551.501	576.892	554.645	587.916	567.092	562.724	567.722	774.585
475.707	524.019	538.541	545.184	541.247	559.836	553.601	553.164	554.493	562.969
471.870	515.515	530.722	532.000	528.526	549.001	544.231	542.223	859.577	555.517
462.989	504.485	517.870	519.633	519.966	539.083	534.057	531.841	536.271	547.010
452.798	496.030	743.393	506.522	507.964	526.664	520.747	518.481	524.149	531.001
430.580	470.214	477.294	484.700	484.768	524.793	526.742	529.025	532.457	695.888

Table B-R2b
Rockwell BIBIB Array
Background Run #2 (BG #2)

VARIANCE

Rock BG #2 - VAR of 3200 frames

4.584	4.675	4.991	1.933	2.292	5.850	5.693	7.221	7.650	5.864
3.109	2.624	3.109	3.577	1.815	5.729	4.170	7.849	3.678	11.607
2.950	3.154	3.427	4.029	4.633	3.709	4.044	3.757	3.878	4.036
4.046	7.923	2.851	3.500	1.449	2.971	1.872	3.989	3.703	3.220
3.490	3.678	3.870	4.391	1.894	4.695	4.591	4.181	3.930	4.394
3.750	3.945	3.892	4.310	1.758	167.961	5.370	4.674	4.830	5.369
3.012	3.085	3.052	3.564	1.839	3.760	3.913	5.671	3.460	3.522
3.456	3.292	3.414	3.987	2.045	3.457	4.611	3.835	3.939	4.316
3.824	4.079	4.059	7.334	2.188	4.499	5.476	5.091	4.665	10.070
2.739	3.341	3.473	3.695	2.065	10.602	4.481	4.270	3.964	4.099
4.806	5.056	5.340	6.293	2.581	5.742	6.761	5.773	5.759	6.446
2.690	2.817	2.791	3.161	1.700	3.089	4.291	3.819	1.219	3.768
2.814	2.813	2.862	2.969	1.493	3.089	3.285	3.259	3.020	3.303
5.515	5.737	6.012	7.437	2.747	6.620	8.007	7.909	8.228	8.042
4.849	4.728	3.993	5.510	2.479	5.272	6.448	5.603	5.402	5.585
4.730	5.208	5.670	6.075	2.597	6.544	7.476	6.406	6.623	6.094
85.480	3.623	3.906	4.270	1.645	4.416	4.987	4.356	5.330	4.184
5.673	5.733	6.452	6.659	4.127	6.532	6.432	6.336	6.456	5.346
4.254	4.388	4.501	5.119	2.255	5.374	4.645	4.570	4.394	11.341
3.572	3.671	3.901	4.282	1.820	4.326	4.960	4.344	3.978	3.511
3.218	3.275	3.303	3.511	1.657	3.744	4.236	4.204	3.552	5.060
2.279	2.018	2.322	2.598	1.619	2.800	2.848	0.881	2.605	2.724
2.721	2.221	2.630	2.875	1.624	2.778	3.687	3.069	4.251	3.245
4.399	4.671	5.034	5.620	2 922	5.853	5.932	5.467	6.814	5.623
85.035	3.262	3.705	2.488	2.002	4.157	4.598	4.175	5.269	3.993
3.921	3.586	3.700	4.203	1.937	3.857	4.181	4.187	5.125	4.144
3.772	3.915	3.902	19.500	1.688	4.376	4.891	4.709	5.853	4.451
3.321	3.292	3.582	3.876	2.068	3.961	4.234	4.168	3.888	3.083
4.173	4.427	4.421	4.758	1.991	5.766	5.453	5.581	5.431	4.589
2.780	2.730	0.895	3.130	1.841	4.157	3.466	3.605	3.510	3.439
3.276	3.290	3.166	3.490	1.963	3.500	3.959	4.348	3.379	3.388
2.814	3.253	3.418	3.828	1.787	3.657	3.970	3.937	4.187	3.823
3.606	4.036	4.175	4.793	0.521	4.610	5.285	4.618	5.057	5.078
3.028	2.868	3.414	3.603	1.788	3.420	3.967	3.763	3.437	4.243
3.489	3.308	3.939	4.656	1.579	4.229	4.777	5.920	5.279	4.218
2.922	2.894	2.956	3.363	1.753	2.880	3.527	3.488	3.274	3.299
3.240	3.498	3.574	3.801	1.754	3.968	4.121	3.869	3.573	6.026
2.556	2.954	2.501	2.897	1.646	2.875	3.203	2.813	3.288	2.858
2.571	2.555	2.763	3.009	1.615	4.172	3.349	3.366	3.135	2.930
3.049	3.048	3.333	3.661	1.619	3.708	4.492	3.973	3.429	4.849
4.561	5.144	5.174	5.768	2.284	6.260	5.541	4.823	4.395	4.991
3.718	5.150	4.120	4.459	2.232	4.323	5.243	4.631	4.491	4.854
2.720	2.625	3.179	3.559	1.629	3.741	3.901	3.851	3.475	3.490
2.091	2.131	2.298	2.383	1.396	2.376	2.592	2.738	2.340	2.321
2.865	2.816	2.298	3.080	1.501	2.874	3.056	2.939	2.673	2.711
2.659	2.526	2.800	2.954	1.692	2.898	3.466	3.194	3.059	3.602
3.897	84.694	4.205	4.668	1.782	4.789	4.742	4.636	1.706	4.501
6.748	6.564	7.310	7.885	3.003	7.704	9.400	8.819	8.245	8.894
5.938	5.683	6.261	6.715	3.333	6.222	8.543	8.041	7.595	9.176
6.830	6.571	6.940	6.869	5.088	6.592	7.474	7.686	7.505	6.229

Table B-R2c
Rockwell BIBIB Array
Background Run #2 (BG #2)

SKEWNESS

Rock BG #2 - Skew of 3200 frames

0.190	0.271	0.385	0.001	0.074	0.307	0.470	0.022	0.002	0.289
0.008	0.036	0.016	0.021	0.037	0.155	0.006	0.219	0.005	0.203
0.002	0.002	0.002	0.025	272.557	0.009	0.001	0.006	0.010	0.001
108.935	24.552	0.033	0.014	0.029	0.681	0.407	8.753	0.005	0.003
0.006	0.026	0.004	0.025	0.031	0.019	0.000	0.001	0.009	0.018
0.013	0.005	0.059	0.010	0.007	1473.315	0.022	0.028	0.111	0.004
0.133	0.058	0.077	0.094	0.085	0.011	0.091	0.598	0.035	0.111
0.001	0.021	0.001	0.000	0.000	0.018	0.000	0.000	0.002	0.015
0.160	0.067	0.119	0.023	0.000	0.146	0.104	0.450	0.081	0.058
0.029	0.007	0.000	0.001	0.017	0.052	0.000	0.000	0.002	0.007
0.007	0.002	0.001	0.012	0.015	0.006	0.003	0.008	0.008	0.059
0.054	0.035	0.015	0.020	0.018	0.035	6.368	7.681	0.341	0.135
0.004	0.031	0.004	0.001	0.013	0.043	0.000	0.022	0.037	0.006
0.030	0.023	0.053	0.009	0.007	0.027	0.396	2.431	2.801	0.155
0.122	0.053	0.075	0.061	0.077	0.067	0.077	0.087	0.139	0.139
0.014	0.001	0.000	0.001	0.012	0.071	1.556	0.239	0.082	0.006
2835.158	0.171	0.116	0.138	0.016	0.197	0.704	0.087	0.082	0.036
0.112	0.129	0.055	0.064	0.079	1.239	0.028	1.284	1.330	0.058
0.040	0.065	0.088	0.123	0.148	1.298	0.223	0.177	0.061	0.013
0.331	0.202	0.212	0.296	0.027	0.916	3.853	0.246	0.204	0.376
0.007	0.186	0.000	0.001	0.005	0.002	0.591	0.001	0.008	[illegible]
0.030	0.056	0.056	0.054	0.069	0.117	0.062	0.233	0.085	0.069
0.051	0.012	0.023	0.026	0.009	0.044	7.850	0.026	18.429	0.027
0.026	0.094	0.075	0.146	0.113	0.194	0.049	0.059	3.389	0.050
2832.865	0.004	0.001	0.391	0.000	0.001	0.985	0.004	7.793	0.025
0.000	0.003	0.001	0.003	0.106	0.009	0.002	0.564	8.726	0.003
0.007	0.008	0.010	540.292	0.050	0.001	0.001	0.000	8.045	0.004
0.018	0.013	0.003	0.005	0.016	0.681	0.004	0.008	0.010	0.000
0.003	0.014	0.019	0.000	0.004	0.994	0.798	2.564	1.462	0.000
0.009	0.000	0.042	0.000	0.089	22.438	0.001	2.854	3.672	0.005
0.006	0.002	0.009	0.006	0.001	2.138	0.019	10.260	0.038	0.016
0.018	0.001	0.005	0.000	0.007	0.017	0.000	6.843	2.674	0.043
0.070	0.036	0.026	0.027	0.019	0.028	0.053	1.519	1.227	0.027
0.001	0.009	0.001	0.000	0.021	0.011	0.000	0.003	0.019	5.196
0.026	0.038	0.081	0.064	0.092	0.008	0.077	13.991	6.693	0.150
0.070	0.006	0.011	0.001	0.001	0.010	0.026	0.001	0.000	0.018
0.002	0.013	0.017	0.010	0.013	0.000	0.045	0.013	0.019	0.013
0.414	0.171	0.391	0.395	0.057	0.509	0.694	0.514	2.483	0.594
0.000	0.024	0.521	0.001	0.102	0.001	0.006	0.001	0.007	0.023
0.018	0.028	0.045	0.280	0.016	0.026	0.038	0.052	0.037	9.132
0.001	0.006	0.003	0.002	0.065	0.012	0.001	0.000	0.001	0.070
0.015	0.023	0.040	0.045	0.052	0.044	0.026	0.040	0.025	0.096
0.080	0.167	0.154	0.156	0.004	0.063	0.123	0.084	0.088	0.083
0.044	0.010	0.001	0.006	0.026	0.024	0.009	0.011	0.016	0.019
0.003	13.663	0.002	0.005	0.013	0.006	0.018	0.007	0.024	0.001
0.019	0.038	0.012	0.016	0.030	2.920	0.087	0.025	0.113	0.283
0.014	2747.406	0.023	0.025	0.038	0.007	0.009	0.703	0.025	0.109
0.051	0.042	0.042	0.031	0.001	0.086	0.052	0.064	0.063	0.039
0.077	0.112	0.151	0.121	0.000	0.041	0.143	0.102	0.102	0.025
0.010	0.004	0.005	0.007	0.038	0.039	0.002	0.006	0.009	0.004

Table B-R2d
Rockwell BIBIB Array
Background Run #2 (BG #2)

KURTOSIS

Rock BG #2 - Kurt of 3200 frames

5.801	5.840	5.911	3.055	5.218	6.938	6.052	6.298	6.625	4.928
2.947	2.990	2.978	2.942	3.082	3.872	2.808	3.549	2.877	3.542
2.907	3.068	2.947	3.082	492.512	2.890	3.007	3.110	2.880	3.237
335.988	40.710	3.340	3.002	3.130	9.156	5.250	43.873	2.912	3.027
2.861	2.872	2.842	2.851	3.067	4.080	2.969	2.786	2.772	3.194
2.936	2.740	4.056	2.946	3.392	1514.333	2.837	3.046	4.287	3.067
3.416	3.455	3.358	3.393	3.448	3.608	3.274	5.717	3.362	3.493
2.717	2.889	2.869	2.878	2.893	2.963	2.866	2.834	3.019	3.076
4.991	3.657	3.955	3.624	3.287	4.256	3.899	6.528	3.608	4.006
3.143	2.954	2.888	2.908	3.321	2.592	3.024	2.723	2.780	2.950
2.850	2.982	2.915	2.913	3.081	2.814	2.906	3.055	2.897	2.895
3.210	2.985	2.927	3.030	3.234	2.908	47.009	54.176	2.895	3.376
3.105	3.142	3.211	3.720	3.450	3.364	3.209	3.413	3.371	3.374
2.916	2.907	2.807	2.868	2.823	2.867	6.801	16.760	18.927	3.247
3.198	3.051	2.831	3.079	2.944	2.918	3.015	3.083	3.056	2.972
2.744	2.844	2.757	2.683	2.957	6.191	15.517	8.177	7.020	2.954
2951.669	3.424	3.374	3.611	4.127	3.631	10.357	3.303	3.240	3.446
3.849	3.284	2.947	2.880	2.718	13.028	3.030	13.349	14.816	3.084
3.707	3.647	3.650	3.833	4.035	12.834	3.997	3.681	3.729	3.227
4.714	3.716	3.735	3.731	3.662	7.477	23.484	3.689	4.015	3.541
3.772	7.930	2.984	2.942	3.162	2.956	12.573	2.861	3.070	3.233
3.524	3.338	3.168	3.299	3.005	3.388	3.232	3.806	3.351	3.269
3.277	3.452	3.428	3.235	2.735	3.046	[illegible]	3.016	65.322	3.141
3.270	3.279	2.986	3.196	3.150	3.308	2.931	3.176	26.945	3.059
2950.266	3.046	3.042	9.114	2.960	3.067	14.685	3.330	38.900	3.285
3.071	3.020	3.260	3.123	3.808	3.141	3.301	12.460	42.597	3.449
3.142	2.880	3.225	678.196	3.855	2.982	3.162	3.049	38.481	3.144
2.730	2.938	2.811	2.747	3.204	14.671	2.892	2.794	2.747	2.655
3.193	3.029	3.199	3.153	3.371	12.868	16.079	23.314	19.917	3.060
3.257	3.660	3.318	3.511	3.334	77.327	3.553	35.486	38.908	3.767
2.853	2.995	2.914	3.007	3.413	28.373	3.053	52.232	3.091	3.585
3.091	2.755	2.719	2.870	3.548	2.795	2.849	47.187	28.421	5.585
3.096	2.930	3.025	3.028	2.726	2.926	2.869	20.135	16.016	2.950
2.886	3.081	3.026	2.979	3.375	2.778	3.050	2.726	2.863	38.338
2.842	2.999	2.778	2.673	3.325	3.043	2.563	56.143	41.154	2.606
4.692	3.107	3.151	3.072	3.096	3.194	3.322	3.243	3.445	3.071
2.867	2.786	2.885	2.925	2.997	2.823	2.966	2.803	2.802	2.689
4.272	3.754	4.596	4.539	3.582	4.593	5.082	4.907	44.783	4.688
3.134	2.886	10.185	3.045	3.331	2.973	2.933	2.816	3.209	3.165
2.936	2.936	3.059	6.423	2.965	3.041	3.017	3.163	3.042	44.009
2.727	2.342	2.563	2.621	7.661	2.384	2.990	2.781	2.824	3.225
2.778	2.569	2.928	2.826	2.848	2.954	2.983	2.964	2.917	2.971
3.310	3.136	3.156	3.210	2.882	2.751	3.278	3.068	3.295	3.577
3.143	3.279	3.071	3.227	3.131	3.303	3.204	2.995	3.544	3.760
2.675	69.382	3.093	2.772	3.311	2.767	3.331	2.965	3.840	3.176
2.933	3.099	3.094	2.995	2.905	17.901	3.192	3.056	3.208	3.650
3.256	2890.528	3.114	3.221	3.435	3.175	3.402	15.145	3.111	5.449
2.676	2.666	2.621	2.598	2.990	2.636	2.725	2.749	2.710	2.566
3.431	3.572	3.591	3.538	3.671	3.739	3.210	3.378	3.331	3.204
3.191	3.092	3.143	3.037	2.967	3.051	3.201	3.022	3.064	3.187

Table B-R3a
Rockwell BIBIB Array
Background Run #3 (BG #3)

AVERAGE COUNT/FRAME FOR 3200 FRAMES

AVE

404.63	440.09	539.31	995.16	453.99	473.81	468.24	19.38	19.90	463.29
387.31	414.04	421.38	420.44	426.29	14.88	441.96	10.57	441.12	13.78
416.15	443.65	442.03	445.89	446.18	476.01	462.65	462.28	457.26	524.71
446.33	691.60	470.95	472.28	470.15	496.07	887.60	481.86	517.25	485.37
471.26	492.06	490.36	489.15	486.79	557.22	501.62	498.29	490.05	497.35
460.73	488.05	494.84	492.06	494.74	511.12	548.03	502.57	495.95	497.10
473.67	507.13	517.92	518.97	515.28	534.02	528.12	20.38	519.57	522.65
475.10	522.33	535.62	532.44	529.80	553.76	544.92	544.60	536.09	542.07
526.21	536.71	552.03	827.39	548.39	567.74	563.18	559.26	547.65	20.00
46.73	548.16	562.42	557.08	559.04	26.12	572.31	568.88	560.93	567.12
519.53	570.84	584.82	578.74	579.15	601.81	594.63	590.99	575.83	578.93
525.53	584.29	635.27	593.33	650.48	611.67	604.43	605.27	869.79	595.54
526.44	585.37	600.17	727.05	836.05	618.60	788.86	618.98	601.75	610.27
519.71	579.64	594.49	643.15	593.22	615.01	608.09	609.12	607.35	621.88
524.48	580.98	901.22	598.75	596.27	618.96	614.65	614.68	611.20	636.04
514.52	571.48	584.91	593.19	589.85	612.13	608.92	609.47	610.58	630.69
509.80	567.57	586.18	590.13	590.44	612.53	610.64	611.95	790.88	637.56
624.06	560.54	581.42	587.00	586.14	609.59	605.46	609.82	608.63	636.05
498.48	555.71	581.20	581.78	591.45	608.52	607.28	609.49	612.92	845.91
495.65	554.86	578.13	585.49	589.69	686.29	608.58	610.99	614.29	866.61
497.41	557.05	582.94	590.65	592.05	615.13	610.90	859.92	611.32	781.03
503.17	558.77	586.02	595.46	596.73	618.74	641.53	905.12	624.40	640.82
519.02	846.59	581.92	590.79	589.00	610.95	607.84	674.68	607.80	619.58
658.21	541.67	580.19	588.79	588.81	614.29	611.27	614.08	607.16	617.29
511.26	588.83	583.84	943.18	592.73	583.68	608.47	612.55	608.25	617.48
507.07	564.28	582.25	584.75	590.47	612.94	607.59	611.40	608.08	614.83
520.74	575.77	590.91	894.89	591.40	615.72	614.57	615.64	608.96	616.51
516.78	569.65	585.43	587.44	586.72	610.51	608.33	610.21	617.16	923.34
518.75	568.63	586.10	586.15	583.45	606.75	605.18	606.90	602.96	609.09
515.74	570.00	948.63	585.65	588.34	606.27	602.95	604.13	603.67	611.64
516.02	568.83	579.90	588.72	586.74	606.55	603.10	606.62	612.80	631.46
513.20	563.53	579.76	583.33	582.89	603.42	600.26	605.79	609.26	619.75
513.10	563.11	573.40	582.32	911.80	601.44	600.71	605.37	606.16	610.70
587.36	558.16	570.76	572.05	570.54	595.03	596.28	600.53	600.45	606.94
505.86	558.65	573.96	576.07	791.11	598.58	601.12	605.21	605.67	613.22
496.01	546.95	562.45	568.00	563.05	831.92	592.03	595.85	597.58	644.57
496.68	553.38	562.86	569.30	562.19	588.16	591.71	595.57	601.45	848.85
492.88	786.06	731.11	571.31	568.14	709.40	588.41	590.69	603.77	614.02
490.86	541.00	558.81	565.46	565.33	828.41	584.87	617.20	638.98	612.93
484.68	540.02	554.46	554.62	557.62	569.25	577.89	578.77	740.97	606.50
491.03	519.77	554.74	559.29	557.30	581.22	578.86	579.32	579.91	589.89
483.30	42.85	547.06	554.74	548.93	574.23	572.20	571.83	571.97	579.10
502.52	719.43	563.80	568.53	633.99	587.31	586.66	585.39	586.77	598.04
485.21	534.86	542.79	554.23	553.45	574.20	570.67	722.59	574.27	583.22
516.79	608.72	551.15	576.41	554.26	587.73	566.82	562.45	567.49	774.72
475.21	523.29	538.14	544.62	540.73	559.30	553.00	552.50	553.84	562.32
471.43	514.81	530.24	531.57	528.01	548.53	543.67	541.71	859.86	555.03
462.02	503.29	516.66	518.54	519.04	538.02	532.94	530.54	535.03	546.01
452.05	495.49	743.68	506.34	507.28	526.26	520.51	518.18	523.86	530.81
430.30	470.00	476.97	484.48	484.59	524.51	526.61	528.99	532.50	696.36

The minimum and maximum are 10.572500 995.15969

Table B-R3b
Rockwell BIBIB Array
Background Run #3 (BG #3)

VARIANCE

VAR

5.05	5.10	5.21	1.95	3.11	6.99	6.51	17.79	21.09	8.10
3.87	3.42	3.71	4.34	2.79	11.83	5.18	16.68	5.32	26.46
3.85	4.09	4.37	6.34	4.92	5.55	5.44	5.63	6.06	6.64
4.31	8.05	3.21	3.68	2.00	3.26	2.01	3.74	4.16	4.27
3.64	4.22	4.39	4.70	2.66	5.12	5.17	5.33	5.38	6.33
3.95	4.24	4.03	4.47	2.30	250.73	5.59	5.30	5.64	6.97
4.07	4.70	4.62	5.07	3.44	5.35	5.58	19.05	6.11	6.41
3.83	3.97	3.86	4.35	2.51	4.46	5.16	4.93	5.40	6.56
8.04	7.65	8.10	11.07	4.00	9.71	10.35	9.46	9.14	25.24
2.78	3.21	3.23	3.84	2.29	12.76	4.43	4.21	4.26	4.22
5.47	5.96	6.06	7.16	3.88	6.84	7.87	7.23	7.30	8.50
3.06	3.14	3.06	3.48	1.93	3.74	4.85	3.97	1.25	5.37
4.09	4.23	4.34	3.85	2.22	4.87	3.98	5.14	5.04	5.59
6.08	6.62	6.97	7.93	3.48	7.90	9.04	8.36	9.60	9.89
5.76	5.68	4.40	6.80	3.45	6.76	7.88	7.22	7.71	8.08
5.24	5.74	6.08	6.45	3.44	7.37	7.51	7.13	8.00	7.57
5.07	5.50	5.73	6.12	3.59	7.07	7.06	6.86	6.75	7.43
6.22	6.51	7.18	7.49	5.36	7.26	7.53	7.53	8.39	7.15
5.31	5.50	5.75	6.39	3.54	7.94	6.33	6.61	6.39	11.68
4.00	4.25	4.17	4.73	2.86	4.58	4.96	4.92	4.85	3.66
4.12	4.37	4.58	4.78	2.64	5.07	5.44	4.64	5.63	7.32
2.99	3.17	3.30	3.71	2.83	3.98	4.34	0.89	4.70	5.33
2.99	2.42	2.99	3.10	1.82	2.93	4.02	3.17	4.16	3.62
4.44	5.07	5.53	6.28	3.41	7.47	6.79	7.09	8.25	8.09
85.52	3.64	3.80	2.40	2.95	4.72	4.76	4.59	5.34	4.97
5.27	4.88	5.14	5.58	3.54	5.21	6.06	6.11	6.82	6.82
3.99	4.16	4.12	24.56	2.57	4.74	5.21	5.13	6.38	5.41
4.56	4.52	4.82	5.11	3.77	5.05	6.55	6.69	6.41	3.59
6.38	6.86	6.80	7.13	4.16	9.13	8.50	9.02	8.26	8.35
3.52	4.05	1.18	4.29	2.84	5.30	4.98	4.81	5.30	6.07
3.85	4.06	4.10	4.04	3.04	4.06	5.22	4.75	5.20	5.52
84.17	3.44	3.59	3.82	2.23	4.04	4.43	4.41	6.01	4.73
4.09	4.74	6.22	5.26	0.47	5.66	6.46	5.51	6.46	6.82
3.49	3.85	4.07	4.27	3.01	4.13	4.81	4.77	4.53	5.73
3.63	3.58	4.05	4.73	1.85	4.49	4.70	4.62	5.39	4.97
3.30	3.23	3.56	3.68	2.18	4.46	4.13	4.35	4.38	4.28
3.79	4.21	4.43	4.54	2.63	4.85	4.82	4.78	4.77	6.73
3.27	3.13	2.76	3.72	2.65	3.48	4.05	3.90	4.46	4.74
3.37	3.48	3.55	3.98	2.89	3.89	4.46	4.44	4.51	5.04
3.26	3.20	3.49	3.66	2.20	4.00	4.60	4.34	3.37	5.24
4.39	5.03	4.81	5.66	2.72	5.87	5.49	4.71	4.50	5.17
4.19	5.41	4.96	5.20	2.92	5.66	5.98	5.82	6.16	6.80
3.28	3.14	3.88	4.01	2.44	4.48	4.51	4.57	4.54	4.56
3.07	3.22	3.47	3.72	2.54	3.98	4.28	4.47	4.69	5.03
3.22	3.04	2.87	3.49	2.26	3.59	3.74	3.88	3.91	3.30
3.25	3.42	3.59	3.76	2.39	3.65	5.00	4.84	4.76	6.32
4.87	5.47	5.38	5.82	2.75	6.26	6.41	6.45	1.79	6.95
8.49	8.91	9.66	10.26	4.26	10.43	12.82	12.53	12.14	13.58
7.93	7.76	6.90	92.23	6.68	8.44	10.49	10.62	10.06	11.85
16.33	15.31	17.17	16.69	13.34	15.47	16.82	17.31	17.81	13.79

The minimum and maximum are 0.46958337 250.72690

Table B-R3c
Rockwell BIBIB Array
Background Run #3 (BG #3)

SKEWNESS

SKEW

0.111	0.182	0.250	0.000	0.078	1.367	0.233	0.393	0.596	0.073
0.048	0.084	0.032	0.018	0.098	0.514	0.034	0.441	0.079	0.450
0.080	0.076	0.074	27.929	55.921	0.479	0.074	0.188	0.184	0.128
90.626	20.431	0.006	0.010	0.059	0.333	0.271	0.005	0.001	0.014
0.022	0.042	0.008	0.035	0.207	0.038	0.013	0.019	0.056	0.105
0.030	0.029	0.012	0.007	0.096	1003.651	0.012	0.012	0.011	0.001
0.071	0.125	0.191	0.147	0.359	0.086	0.140	1.143	0.276	0.303
0.002	0.028	0.001	0.017	0.017	0.068	0.005	0.043	0.066	0.199
3.191	1.330	1.535	1.126	0.094	2.173	1.557	1.460	0.819	0.849
0.000	0.001	0.000	0.177	0.252	0.056	0.007	0.001	0.027	0.028
0.011	0.008	0.005	0.023	0.217	0.005	0.011	0.040	0.059	0.150
0.032	0.014	0.018	0.011	0.027	0.490	4.725	0.135	0.361	0.161
0.269	0.251	0.248	0.110	0.296	0.402	0.108	0.484	0.446	0.479
0.014	0.001	0.006	0.003	0.006	0.000	0.176	0.156	0.976	0.008
0.119	0.123	0.122	0.123	0.220	0.054	0.144	0.138	0.037	0.273
0.022	0.002	0.001	0.000	0.008	0.007	0.267	0.000	0.260	0.015
0.000	0.013	0.006	0.048	0.118	0.359	0.297	0.006	0.093	0.012
0.224	0.082	0.089	0.065	0.068	0.387	0.620	0.838	1.218	0.001
0.049	0.073	0.067	0.136	0.000	5.185	0.096	0.510	0.028	0.034
0.183	0.079	0.185	0.191	0.144	0.582	0.190	0.140	0.090	0.360
0.067	0.172	0.091	0.107	0.197	0.078	0.040	0.011	0.161	0.035
0.202	0.005	0.221	0.208	0.284	0.318	0.273	0.178	0.373	0.442
0.040	0.059	0.023	0.018	0.000	0.039	6.366	0.019	11.449	0.007
0.004	0.026	0.011	0.030	0.070	0.049	0.091	0.034	0.394	0.071
2805.108	0.014	0.000	0.429	0.111	0.003	0.888	0.002	1.791	0.001
0.010	0.031	0.035	0.036	0.348	0.035	0.248	0.043	1.617	0.090
0.034	0.044	0.043	466.271	0.471	0.019	0.010	0.013	5.855	0.071
0.075	0.089	0.054	0.077	0.284	0.072	0.648	0.004	0.179	0.011
0.079	0.066	0.048	0.062	0.648	0.069	0.025	0.766	0.127	0.030
0.065	0.171	0.421	0.158	0.274	5.184	0.199	0.271	0.313	0.437
0.000	0.013	0.010	0.014	0.107	0.032	0.037	0.055	0.027	0.125
2876.897	0.000	0.001	0.004	0.083	0.033	0.002	0.933	6.558	0.095
0.039	0.013	21.006	0.017	0.045	0.008	0.022	0.000	0.420	0.006
0.014	0.139	0.052	0.058	0.228	0.020	0.029	0.007	0.012	1.766
0.064	0.012	0.135	0.105	0.044	0.023	0.091	0.182	2.618	0.168
0.031	0.023	0.022	0.009	0.015	72.436	0.048	0.001	0.010	0.008
0.000	0.030	0.012	0.009	0.098	0.063	0.012	0.042	0.038	0.003
0.393	0.292	0.349	0.576	0.378	0.801	0.712	0.664	0.632	0.827
0.045	0.176	0.104	0.042	0.345	0.000	0.125	0.124	0.181	0.339
0.012	0.001	0.023	0.011	0.024	0.002	0.008	0.011	0.007	0.636
0.015	0.003	0.007	0.040	0.098	0.002	0.004	0.011	0.026	0.096
0.005	0.005	0.046	0.030	0.049	0.065	0.020	0.048	0.073	0.148
0.018	0.050	0.106	0.108	0.073	0.020	0.043	0.026	0.003	0.003
0.245	0.195	0.144	0.250	0.323	0.647	0.436	0.324	0.584	0.903
0.013	10.293	0.030	0.022	0.153	0.089	0.016	0.069	0.037	0.092
0.011	0.061	0.033	0.024	0.106	0.317	0.115	0.115	0.218	0.453
0.001	0.015	0.000	0.006	0.068	0.000	0.000	0.038	0.000	0.031
0.007	0.024	0.021	0.014	0.071	0.071	0.043	0.071	0.125	0.098
0.011	0.006	0.050	2368.837	0.264	0.023	0.006	0.000	0.000	0.006
0.296	0.254	0.102	0.215	0.323	0.331	0.208	0.241	0.228	0.176

The minimum and maximum are 6.75653606E-07 2876.8973

Table B-R3d
Rockwell BIBIB Array
Background Run #3 (BG #3)

KURTOSIS

KURT

5.141	5.323	5.604	3.289	3.695	17.348	5.508	3.458	3.371	4.068
2.972	2.939	2.898	2.850	2.921	3.265	2.789	2.863	2.974	2.792
3.336	3.133	2.991	141.602	230.289	17.825	3.084	3.260	2.944	3.119
295.394	37.725	3.295	3.006	3.108	7.379	3.431	3.108	3.020	3.154
2.957	2.839	2.844	2.762	2.946	2.745	3.045	2.792	2.820	2.925
2.981	2.882	3.088	2.976	3.153	1024.200	2.973	3.233	3.808	3.223
2.743	2.873	2.919	2.798	2.986	2.993	2.812	3.206	2.863	2.856
2.875	2.998	3.029	2.856	2.807	2.963	2.933	2.989	2.930	3.011
8.187	5.762	5.904	5.285	3.793	6.993	5.923	5.773	4.995	3.610
2.952	2.849	2.967	6.968	10.409	2.370	3.149	2.800	2.887	3.054
3.011	3.061	2.974	2.940	3.130	2.978	2.957	3.185	2.967	3.084
2.986	2.934	3.000	2.929	2.862	14.919	40.092	3.217	3.006	3.201
3.514	3.317	3.560	3.916	3.868	3.620	3.441	3.661	3.756	3.650
3.277	3.199	3.106	3.197	3.116	3.184	6.526	6.633	12.781	3.164
2.842	2.986	2.847	2.848	3.006	3.805	2.868	2.910	5.923	2.913
2.913	2.989	2.909	3.580	3.049	2.981	7.280	2.965	8.907	3.191
3.021	3.105	3.162	3.325	3.319	6.228	6.848	3.168	3.181	3.117
4.392	2.947	2.981	2.893	2.580	7.182	9.902	10.559	13.757	3.032
3.178	3.277	3.181	3.420	3.164	23.822	3.483	8.504	3.408	3.112
4.519	3.608	3.662	3.672	4.499	6.288	3.772	3.554	3.677	3.767
3.320	3.536	3.355	3.465	3.666	3.230	3.170	3.124	3.312	3.151
3.741	7.657	3.469	3.824	3.248	3.453	3.722	3.737	4.082	3.440
3.198	3.264	3.174	3.093	2.795	2.953	38.809	3.011	53.225	3.171
2.755	2.669	2.586	2.613	2.537	2.476	6.315	2.599	11.548	2.521
2931.013	2.922	3.118	9.613	3.147	3.100	14.779	3.067	21.860	3.015
2.949	2.970	3.064	3.128	3.282	3.069	11.336	7.649	20.830	3.301
3.317	3.296	3.430	558.520	4.070	3.271	3.294	3.304	33.272	3.360
2.728	2.855	2.777	2.789	3.053	2.865	15.395	7.434	2.857	2.688
3.258	3.094	3.180	3.184	3.956	6.981	8.743	14.933	3.339	6.852
3.353	3.389	3.704	3.663	3.247	40.783	3.542	3.459	3.568	3.543
2.887	2.932	2.924	2.959	3.064	2.994	2.851	3.079	8.249	3.242
2980.608	2.833	2.912	3.009	3.446	3.042	3.021	22.382	35.666	3.202
3.501	3.086	117.073	3.153	2.877	2.988	3.076	3.236	11.543	3.116
3.061	3.331	3.137	3.114	3.403	2.939	3.058	2.893	3.141	22.644
3.002	4.649	2.985	2.805	3.850	2.997	2.802	2.892	28.886	2.750
3.261	3.176	3.313	3.191	3.035	264.126	3.357	3.249	3.689	2.939
3.697	2.872	3.754	2.965	2.979	2.946	2.942	2.894	2.982	2.783
4.180	4.429	4.616	4.876	4.172	5.603	4.575	4.683	4.048	4.196
3.241	3.321	3.360	3.215	3.284	3.125	3.402	3.342	3.431	3.308
2.966	3.083	3.242	3.245	2.985	3.155	3.198	3.203	3.209	15.639
2.729	2.440	2.584	3.760	6.709	2.530	2.794	2.727	2.856	3.174
2.674	2.597	2.801	2.749	2.609	2.736	2.809	2.645	2.644	2.764
3.037	3.314	3.646	3.344	2.940	2.901	3.076	2.961	3.018	3.436
3.253	3.505	3.546	3.635	3.400	4.081	3.666	3.465	3.794	4.309
2.908	59.010	3.225	2.979	3.148	3.042	3.485	3.042	3.807	3.528
2.952	3.047	2.913	2.896	3.004	9.907	2.934	3.017	3.032	3.119
3.192	3.055	3.062	3.070	3.314	2.871	3.246	3.071	3.013	3.085
2.398	2.388	2.390	2.423	2.948	2.459	2.420	2.375	2.582	2.487
3.640	3.717	3.739	2618.646	3.133	3.877	3.565	3.611	3.556	3.306
2.481	2.432	3.828	2.537	2.378	2.617	2.613	2.634	2.601	2.743

The minimum and maximum are 2.3701964 2980.6078

Table B-R4a
Rockwell BIBIB Array
Background Run #4 (BG #4)

AVERAGE COUNT/FRAME FOR 3200 FRAMES

AVE

405.06	442.04	555.74	997.53	455.34	474.93	470.61	21.08	22.04	465.26
388.75	416.49	423.34	421.80	429.28	17.36	443.99	13.56	443.19	17.71
417.53	445.11	443.46	447.06	448.59	478.09	463.90	463.66	458.66	535.28
449.07	720.42	473.77	475.01	473.10	498.75	893.67	484.49	524.46	487.28
471.77	492.17	491.09	489.32	488.28	561.82	502.05	498.75	490.68	498.06
462.61	489.88	496.67	493.53	496.84	512.81	554.00	503.96	497.29	498.18
476.03	509.58	520.39	520.78	517.65	535.72	530.38	21.22	521.42	523.96
476.53	524.28	537.65	533.78	531.87	555.10	546.75	546.23	537.71	543.48
535.59	538.93	554.40	849.92	550.53	570.22	564.99	560.47	549.83	21.75
47.54	549.66	563.91	558.24	560.94	26.05	573.75	569.90	562.46	567.72
520.82	572.86	586.81	580.68	581.23	603.78	596.76	592.30	577.45	580.24
526.81	586.62	644.22	595.17	664.78	613.42	606.44	607.15	872.84	597.02
528.00	587.92	602.44	748.23	865.30	620.92	811.05	622.86	604.25	612.29
522.25	582.77	597.48	650.90	595.94	618.10	611.71	612.83	610.88	625.06
525.27	582.37	920.41	599.67	598.62	620.25	615.91	616.12	612.36	636.58
516.72	574.48	587.95	595.60	592.84	614.89	611.88	612.22	613.45	632.99
510.85	569.56	587.71	591.41	592.67	614.11	612.04	613.53	808.02	639.50
643.25	563.10	583.75	588.95	589.16	611.81	607.64	611.84	609.90	636.63
499.93	558.46	583.61	584.20	594.63	612.22	611.38	613.99	615.92	858.31
496.04	556.13	579.07	586.37	592.52	698.04	612.06	616.16	615.53	883.30
498.96	559.32	584.73	592.44	594.98	617.45	614.65	876.85	612.99	795.56
503.07	559.74	586.72	595.86	598.17	619.87	648.25	923.90	624.38	640.35
521.50	872.40	585.65	593.48	591.77	614.46	611.13	690.29	611.04	623.10
685.13	544.73	583.16	590.97	591.47	616.47	614.00	617.62	609.35	619.43
512.52	593.61	586.06	950.78	594.99	584.91	609.71	613.69	609.54	617.91
509.35	567.53	585.17	587.20	593.47	614.82	609.62	613.41	609.93	616.43
521.95	578.37	592.91	915.71	594.44	617.40	616.16	617.11	610.44	618.30
517.67	571.98	587.13	588.50	589.19	611.82	609.65	612.00	620.52	930.29
522.36	573.90	590.49	589.81	587.83	611.81	609.43	611.50	607.61	613.00
518.54	574.53	953.51	588.75	591.86	609.65	606.27	607.69	607.45	614.61
517.31	571.45	582.05	590.18	589.56	608.38	605.17	608.56	614.64	632.61
514.84	566.62	582.55	585.59	586.11	605.54	602.94	608.64	611.62	621.71
515.89	567.07	576.85	585.82	915.42	605.04	604.77	609.23	609.38	613.89
603.14	560.61	573.22	574.37	573.92	597.40	599.00	602.94	602.70	608.36
507.03	561.13	575.73	577.75	818.61	600.61	603.06	607.01	607.22	614.00
498.54	550.31	566.09	571.18	566.56	854.87	595.56	599.53	600.62	654.87
498.45	556.14	565.14	571.30	565.51	590.80	593.94	598.13	603.56	870.87
493.77	814.60	753.61	572.49	570.85	730.80	589.53	592.25	605.11	614.35
491.29	541.89	559.73	566.69	567.24	853.44	585.96	621.72	644.98	613.58
486.53	542.34	556.55	557.06	560.51	571.44	579.91	581.15	760.79	607.99
492.39	521.25	556.56	561.34	560.16	582.68	580.76	581.57	581.61	591.71
484.92	43.65	549.40	557.39	551.88	576.81	574.41	574.24	574.10	580.93
503.58	743.84	565.69	570.76	648.49	589.54	588.46	587.39	588.40	599.78
486.73	537.40	545.79	556.82	556.61	576.65	573.23	741.15	576.85	585.91
520.86	616.14	553.11	580.59	556.18	590.28	568.57	563.66	568.90	798.16
477.27	526.54	540.82	547.45	543.76	561.60	555.96	555.56	556.42	565.49
472.90	517.28	532.26	533.39	530.78	550.67	545.80	543.97	865.33	556.78
463.74	506.02	518.85	520.31	521.21	539.94	535.12	532.89	536.83	547.66
454.36	498.45	769.75	508.74	510.77	528.73	523.06	521.05	526.20	533.43
433.47	474.09	480.79	487.90	488.92	527.58	529.82	532.27	535.34	719.50

The minimum and maximum are 13.562500 997.53031

Table B-R4b
Rockwell BIBIB Array
Background Run #4 (BG #4)

VARIANCE

VAR

10.98	11.14	10.93	2.93	5.80	15.64	13.00	21.05	22.17	15.24
3.14	2.77	2.97	3.71	2.20	6.72	3.96	9.32	3.94	14.65
3.79	7.96	4.08	5.01	5.74	6.00	5.23	4.89	5.16	5.54
4.47	3.68	3.52	3.77	1.88	3.74	1.58	4.12	4.40	4.68
2.67	2.94	3.01	3.56	1.80	3.83	3.64	3.80	3.65	4.65
3.26	3.69	3.52	4.11	1.88	85.49	5.04	4.62	5.09	5.77
3.26	86.08	3.50	3.95	2.39	4.14	4.58	11.35	4.67	5.46
3.85	3.75	4.01	4.57	2.37	4.22	5.13	4.54	4.73	5.49
3.22	4.08	4.15	5.91	2.56	4.67	5.42	5.46	4.98	21.91
2.67	3.16	3.38	3.51	2.12	11.08	4.24	3.96	3.90	4.06
3.66	3.97	4.20	4.61	2.40	5.24	5.14	4.88	4.80	5.56
3.04	2.99	3.02	3.45	1.69	3.23	5.05	4.07	1.21	4.58
3.70	3.51	3.74	3.67	1.85	4.13	3.70	4.43	4.31	5.01
4.78	5.21	5.35	6.60	2.82	6.38	6.94	6.25	6.54	7.76
4.33	4.24	3.44	4.91	2.07	4.58	5.76	5.21	4.88	5.47
4.51	4.82	5.04	5.49	2.57	5.64	6.13	5.83	5.56	6.04
3.34	3.81	4.04	4.36	2.21	5.02	4.86	4.73	5.00	4.95
5.23	5.83	5.95	6.43	5.09	6.53	7.12	6.69	6.24	5.48
6.65	7.42	7.94	9.42	5.83	12.75	14.96	16.22	12.20	11.52
4.58	4.68	5.25	5.84	3.22	7.17	8.37	11.67	7.90	4.42
3.60	3.36	3.81	4.19	2.42	4.57	6.29	3.95	4.91	6.60
2.99	2.82	3.10	3.29	2.00	4.79	5.69	1.05	3.69	3.91
4.29	3.11	4.27	4.36	2.10	4.12	5.52	4.77	4.97	5.87
5.78	6.37	6.85	8.11	3.66	9.30	8.33	8.34	8.56	9.07
3.27	3.60	3.91	2.77	2.49	4.72	5.46	4.71	5.06	4.84
3.70	3.49	3.61	4.07	2.28	3.93	4.37	4.04	4.37	4.82
4.25	4.19	4.33	3.70	2.46	5.06	5.46	5.75	6.52	6.11
3.33	3.19	3.53	3.87	2.18	3.79	4.77	4.33	4.27	3.15
3.85	3.85	3.94	4.59	2.47	4.45	5.27	5.03	5.99	5.60
2.67	2.89	0.84	3.25	1.74	[illegible]	3.49	4.61	5.59	4.04
3.69	3.39	3.81	4.21	2.71	4.37	5.07	5.01	4.28	5.05
3.51	3.71	3.75	4.57	2.57	5.03	5.12	5.69	4.97	5.94
5.18	5.56	5.88	6.48	0.54	7.10	6.89	6.81	7.72	7.50
3.35	3.23	3.35	3.87	2.20	3.65	4.18	3.96	3.71	4.34
2.89	2.74	3.05	3.72	1.96	3.52	3.82	4.62	5.66	4.39
4.40	4.53	4.83	5.28	2.41	4.53	5.80	5.62	5.48	5.89
2.74	2.87	3.21	3.29	2.13	3.03	3.58	3.36	3.29	3.73
4.08	4.00	3.83	4.98	2.48	4.61	5.42	5.00	5.50	5.87
2.59	2.47	2.82	3.04	1.79	3.63	3.06	2.88	3.19	3.40
3.22	3.33	3.44	3.65	1.75	4.16	4.41	4.05	3.64	4.55
3.95	3.18	4.10	4.55	2.31	4.54	5.36	5.08	4.88	6.84
3.87	4.14	4.26	4.60	2.32	5.70	5.82	5.14	5.16	5.94
2.64	2.61	3.02	3.28	1.70	3.17	3.58	3.70	3.43	3.65
2.45	2.61	2.88	3.09	1.98	3.12	3.48	3.53	4.71	3.67
3.38	3.16	2.98	3.40	2.12	3.08	3.75	3.65	3.47	2.95
2.21	2.04	2.27	2.48	1.46	2.48	2.84	2.94	2.93	3.28
3.92	4.03	4.23	4.87	2.57	4.69	5.12	4.93	1.78	5.72
5.03	5.28	5.68	6.39	2.69	6.09	7.30	6.67	6.49	6.97
5.69	5.47	4.81	89.07	87.43	5.69	7.32	7.77	7.91	9.12
10.01	9.26	10.39	10.69	8.93	8.78	10.88	10.61	11.02	9.77

The minimum and maximum are 0.53627852 89.074061

Table B-R4c
Rockwell BIBIB Array
Background Run #4 (BG #4)

SKEWNESS

SKEW

0.001	0.002	0.008	0.041	0.000	0.046	0.002	0.380	0.549	0.084
0.005	0.001	0.000	0.052	0.207	0.182	0.071	0.712	0.138	1.202
0.046	140.640	0.078	0.036	116.674	11.822	0.092	0.187	0.235	0.356
62.345	0.230	0.001	0.000	0.015	0.028	0.052	0.002	0.000	0.050
0.127	0.033	0.089	0.430	0.023	0.157	0.061	0.039	0.004	0.139
0.021	0.000	0.019	0.060	0.001	2757.983	0.005	0.014	0.163	0.041
0.046	2805.942	0.032	0.084	0.356	0.041	0.068	1.392	0.183	0.266
0.006	0.009	0.000	0.001	0.001	0.021	0.000	0.003	0.004	0.057
0.002	0.004	0.000	0.041	0.558	0.013	0.019	0.050	0.093	1.440
0.000	0.000	0.000	0.341	0.154	0.001	0.001	0.002	0.001	0.023
0.005	0.006	0.000	0.000	0.030	4.884	0.000	0.004	0.029	0.115
0.116	0.087	0.068	0.063	0.010	0.108	12.672	4.509	0.026	0.341
0.295	0.430	0.280	0.302	0.437	0.386	0.094	0.030	0.660	0.635
0.010	0.036	0.007	0.023	0.001	0.076	0.011	0.010	0.000	0.000
0.003	0.002	0.000	0.003	0.061	0.044	0.002	0.007	0.023	0.028
0.003	0.003	0.000	0.002	0.000	0.000	0.000	0.007	0.038	0.078
0.063	0.002	0.000	0.000	0.063	0.003	0.009	0.030	0.007	0.074
0.007	0.001	0.000	0.001	0.037	0.005	0.481	0.069	0.215	0.002
0.001	0.001	0.003	0.000	0.001	0.103	0.125	0.150	0.038	0.008
0.598	0.319	0.562	0.325	0.371	0.307	0.194	0.002	0.305	0.462
0.003	0.024	0.001	0.000	0.007	0.001	0.034	0.011	0.052	0.036
0.014	0.403	0.018	0.040	0.014	0.005	0.024	0.042	0.174	0.005
0.002	0.011	0.001	0.000	0.000	0.000	0.206	0.011	0.127	0.030
0.004	0.006	0.003	0.018	0.070	0.027	0.003	0.015	0.008	0.005
0.001	0.010	0.005	0.015	0.137	0.000	3.908	0.006	1.983	0.011
0.054	0.014	0.032	0.052	0.185	0.039	0.019	0.069	0.168	0.139
0.175	0.151	0.169	0.003	0.765	0.134	0.162	0.237	0.574	0.312
0.004	0.029	0.009	0.016	0.158	0.002	0.837	0.000	0.006	3.722
0.151	0.098	0.173	0.251	0.440	0.115	0.113	0.165	2.556	0.005
0.028	0.000	0.079	0.070	0.138	1.348	0.061	13.831	18.167	0.335
0.075	0.019	0.141	0.152	0.763	0.650	0.553	1.784	0.221	0.301
0.006	0.020	0.039	0.087	0.210	3.073	0.097	5.539	0.204	0.199
0.030	0.041	0.046	0.071	0.019	0.981	0.054	0.085	0.002	0.305
5.365	0.161	0.047	0.003	0.152	0.005	0.000	0.038	0.060	0.121
0.003	0.023	0.000	0.018	0.061	0.000	0.003	16.020	18.850	0.161
0.046	0.047	0.047	0.006	0.059	0.096	0.041	0.060	0.027	0.025
0.008	0.001	0.029	0.002	0.373	0.157	0.001	0.008	0.062	0.003
0.000	0.036	0.012	0.007	0.072	0.001	0.004	0.005	0.644	0.179
0.001	0.083	1.087	0.002	0.215	0.003	0.024	0.043	0.052	0.339
0.004	2.005	0.011	0.099	0.020	0.010	0.019	0.015	0.064	0.934
0.039	0.016	0.080	0.000	0.034	0.105	0.108	0.106	0.237	0.148
0.098	0.217	0.132	0.053	0.016	42.070	0.068	0.168	0.100	0.253
0.000	0.015	0.000	0.000	0.012	0.037	0.002	0.003	0.015	0.016
0.064	0.032	0.064	0.263	0.082	0.052	0.025	0.039	72.988	0.285
0.154	0.071	0.271	0.216	0.295	0.354	0.266	0.356	0.295	0.682
0.043	0.027	0.004	0.009	0.137	0.050	0.252	0.263	0.332	0.426
0.000	0.012	0.002	0.021	0.202	0.013	0.003	0.073	45.926	0.109
0.012	0.001	0.005	0.001	0.000	0.009	0.007	0.009	0.008	0.025
0.647	0.528	0.098	2555.778	2639.127	0.439	0.394	0.541	0.624	0.828
0.601	0.603	0.200	0.446	0.887	0.518	0.358	0.370	0.395	0.162

The minimum and maximum are 1.40781596E-09 2805.9422

Table B-R4d
Rockwell BIBIB Array
Background Run #4 (BG #4)

KURTOSIS

KURT

1.934	1.935	2.231	2.609	1.933	3.861	2.127	3.301	3.558	2.365
3.143	3.551	3.459	3.469	3.608	3.834	3.505	4.232	3.489	4.318
3.171	280.089	3.126	3.022	289.452	52.849	3.305	3.622	3.384	3.854
231.886	6.094	2.849	2.934	2.983	3.211	3.217	2.937	3.153	7.523
3.513	3.131	3.343	8.630	3.124	3.195	3.738	3.776	3.466	3.537
3.058	3.048	2.900	4.482	3.337	2897.953	2.799	3.038	5.515	3.072
3.002	2931.527	3.171	3.237	3.444	3.238	3.037	4.575	3.306	3.527
2.728	2.839	2.836	2.967	2.970	2.809	2.608	2.751	2.768	3.105
3.183	2.974	2.801	3.242	4.310	3.005	3.162	3.260	3.345	4.609
3.074	2.931	2.787	8.574	5.299	2.249	2.924	2.676	3.276	3.124
3.049	2.985	2.942	3.057	3.017	37.099	3.164	3.061	3.101	3.244
4.602	3.079	2.838	2.914	2.957	3.125	56.681	41.190	2.664	3.578
3.745	3.959	3.949	3.842	4.074	6.172	3.339	7.026	4.374	4.205
2.771	2.744	2.783	2.876	2.993	3.976	2.760	2.867	2.948	2.946
3.143	3.247	3.391	3.221	3.548	3.020	3.254	3.164	3.275	3.154
2.753	2.960	2.893	2.841	3.378	2.945	2.799	2.955	3.143	3.348
3.214	3.028	3.132	3.306	3.773	3.211	3.135	3.332	3.135	3.573
2.782	2.744	2.745	2.864	2.863	3.112	8.993	3.559	8.664	3.366
2.748	3.054	2.808	2.682	3.960	3.688	3.011	3.129	3.488	2.877
5.749	4.200	4.387	3.982	4.819	3.715	3.485	2.822	4.009	4.136
3.237	4.846	3.140	3.369	3.614	3.096	2.859	2.959	3.380	3.235
3.189	7.008	3.029	2.855	2.904	2.667	2.822	4.178	4.843	3.010
3.006	2.888	2.885	2.960	3.437	3.058	8.792	2.869	10.566	2.934
2.511	2.683	2.717	2.661	2.937	2.474	2.681	2.572	5.875	3.401
3.318	2.919	2.957	3.221	3.370	3.029	25.403	3.388	20.843	3.278
2.779	3.221	3.212	3.287	3.569	3.405	3.125	3.313	3.448	3.635
3.555	3.524	3.511	3.558	4.531	3.373	3.394	3.615	17.719	3.838
3.284	3.209	3.295	3.346	3.698	3.058	13.241	3.444	3.623	45.939
3.158	3.202	3.345	3.334	3.760	3.098	3.090	3.084	27.692	7.453
3.309	3.350	3.209	3.425	4.027	23.236	3.754	58.670	61.053	4.118
3.061	3.386	3.498	3.651	4.163	17.456	18.885	24.162	3.981	4.106
2.920	3.042	2.929	2.900	3.399	33.210	2.868	34.798	3.098	3.247
2.845	2.912	2.987	2.938	2.860	18.917	3.089	8.135	7.004	3.565
48.305	6.625	3.162	3.073	4.063	3.396	3.100	2.885	3.077	3.373
3.088	4.506	3.218	3.290	3.255	2.906	3.016	63.043	61.104	3.451
2.978	2.943	3.034	3.013	3.190	3.094	2.913	2.997	3.015	2.862
3.204	2.909	2.909	2.954	3.519	3.526	2.859	3.170	3.183	3.088
2.724	4.299	2.863	2.836	3.169	2.722	2.926	2.887	16.279	3.227
3.105	3.193	13.043	3.639	4.125	2.694	3.079	3.217	3.166	3.666
3.096	26.402	2.908	5.171	3.212	2.958	2.992	3.077	3.142	16.865
3.038	3.006	3.101	4.072	9.012	3.436	3.247	3.345	3.502	3.145
2.988	3.309	3.232	4.550	3.349	171.769	3.094	3.323	3.213	3.403
3.195	2.942	2.968	3.059	3.200	2.953	3.056	3.177	3.255	3.307
3.209	2.870	2.869	9.621	3.322	2.947	3.295	3.052	250.459	3.583
3.411	3.178	3.385	3.275	3.414	3.301	3.282	3.404	3.272	3.816
3.052	3.325	3.246	3.281	4.048	4.597	3.860	3.800	3.889	4.436
3.087	3.177	2.923	3.138	3.507	3.059	3.077	3.513	153.624	3.604
2.595	2.675	2.677	2.507	2.656	2.467	2.673	2.756	2.735	2.649
4.444	4.434	3.717	2755.503	2815.710	4.424	4.042	3.977	4.141	4.095
3.308	3.231	5.378	3.108	3.276	3.435	3.044	3.124	3.180	2.732

The minimum and maximum are 1.9328078 2931.5273

Table B-R5a
Rockwell BIBIB Array
Background Run #5 (BG #5)

AVERAGE COUNT/FRAME FOR 3200 FRAMES

AVE

404.23	441.18	555.02	997.13	454.79	473.98	469.58	19.41	20.25	464.00
388.80	416.31	423.22	421.57	429.08	17.13	443.87	13.09	443.09	16.90
417.16	444.74	443.07	446.61	448.14	477.65	463.45	463.09	458.19	534.71
449.09	720.36	473.79	474.92	472.87	498.67	894.10	484.44	524.20	487.24
471.79	492.07	491.01	489.24	488.07	561.91	501.99	498.57	490.54	497.66
462.60	489.91	496.82	493.38	496.83	512.89	554.35	503.82	497.20	497.84
475.72	509.27	520.17	520.39	517.29	535.28	529.94	20.15	521.12	523.38
476.51	524.25	537.55	533.54	531.75	555.01	546.73	546.12	537.50	543.21
535.79	538.80	554.20	849.99	550.11	569.75	564.78	560.26	549.44	20.37
47.61	549.67	563.79	558.23	561.00	25.89	573.81	569.83	562.22	567.54
520.46	572.55	586.36	580.22	580.71	603.30	596.30	591.90	576.96	579.67
526.62	586.16	643.75	594.95	664.40	613.09	606.20	606.74	872.82	596.64
527.37	587.23	601.74	747.87	865.03	620.31	810.86	622.53	603.53	611.54
521.71	582.06	597.02	650.56	595.60	617.51	611.16	612.10	610.10	624.32
524.97	582.20	920.52	599.62	598.06	620.08	615.88	616.06	612.25	636.36
516.54	573.99	587.55	595.21	592.43	614.36	611.50	611.71	612.82	632.39
510.52	568.98	587.47	590.98	592.36	613.66	611.60	612.92	808.23	639.07
642.99	562.74	583.30	588.42	588.57	611.05	606.81	611.06	609.27	636.31
499.48	558.08	583.26	583.61	593.75	610.91	609.29	611.90	614.82	858.11
495.79	556.06	578.91	586.33	592.20	696.58	609.09	611.50	614.37	882.85
498.70	559.09	584.40	592.30	596.30	617.55	612.31	876.04	612.17	795.37
503.20	559.85	586.94	595.91	599.58	623.11	650.60	923.73	624.25	639.94
522.00	872.26	585.99	594.30	592.98	617.84	614.62	690.97	611.10	623.26
684.75	544.43	582.86	590.71	591.69	617.00	614.63	617.72	608.92	618.93
512.43	593.54	585.93	950.85	594.85	585.10	609.70	613.53	609.37	617.50
509.52	567.54	585.29	587.30	593.41	615.07	609.81	613.65	609.86	616.37
521.81	578.09	592.66	915.92	593.99	617.14	615.79	616.93	609.93	617.93
517.61	571.79	587.04	588.37	589.09	611.73	609.44	611.64	620.22	930.77
522.00	573.56	590.29	589.63	587.34	611.50	609.24	611.14	607.15	612.77
518.47	574.41	953.42	588.62	591.78	609.50	606.12	607.42	607.27	614.33
516.89	570.98	581.66	589.62	589.08	607.90	604.62	608.29	614.19	632.16
514.76	566.35	582.13	585.38	585.77	605.39	602.73	608.34	611.15	621.29
515.57	566.44	576.35	585.32	915.41	604.51	604.28	608.79	608.80	613.29
602.97	560.56	572.94	574.11	573.61	597.14	598.84	602.75	602.47	608.19
507.05	560.82	575.48	577.68	818.31	600.42	602.85	606.63	607.00	613.57
498.67	550.12	565.99	571.16	566.46	854.92	595.32	599.36	600.32	654.42
498.11	555.67	564.86	571.05	565.07	590.51	593.70	597.67	603.31	870.80
493.47	814.91	753.56	572.25	570.67	731.17	589.31	591.95	604.84	613.95
491.14	541.70	559.58	566.50	567.07	853.64	585.74	621.22	644.65	612.99
486.59	542.20	556.37	557.05	560.46	571.33	579.85	581.05	761.07	607.71
492.36	521.43	556.32	561.16	560.05	582.35	580.53	581.09	581.38	591.22
485.02	43.68	549.44	557.66	552.01	576.84	574.38	574.30	574.11	580.84
503.38	744.03	565.64	570.51	648.76	589.40	588.32	587.22	588.26	599.59
486.85	537.21	545.69	557.02	556.50	576.50	573.15	740.73	576.77	585.61
520.56	616.04	552.72	580.43	555.79	590.08	568.05	563.31	568.35	797.51
477.43	526.42	540.87	547.24	543.66	561.56	555.81	555.23	556.23	565.39
472.76	517.15	532.14	533.18	530.47	550.36	545.44	543.75	865.37	556.39
463.83	506.12	519.00	520.49	521.10	539.96	535.08	532.87	536.75	547.46
453.87	498.06	769.03	508.48	510.55	528.44	522.50	520.62	525.59	532.83
432.72	473.26	479.95	487.03	488.03	526.96	529.17	531.44	534.64	718.45

The minimum and maximum are 13.088437 997.13469

Table B-R5b
Rockwell BIBIB Array
Background Run #5 (BG #5)

VARIANCE

VAR

9.63	11.36	9.81	2.98	5.23	13.84	12.24	24.59	26.77	15.19
3.92	3.57	3.86	4.60	2.91	10.03	5.19	14.08	6.65	22.22
4.04	9.65	4.48	5.32	4.01	5.61	5.86	5.79	6.28	6.44
4.50	3.85	3.46	3.80	2.14	3.89	1.83	4.56	4.54	5.02
2.84	3.10	3.14	3.51	2.24	4.25	3.94	4.19	4.16	5.43
3.69	3.99	3.95	4.67	2.52	167.20	5.51	5.61	5.49	6.97
4.18	169.56	4.56	5.12	3.25	5.13	6.01	17.80	6.08	6.72
3.73	3.74	3.88	4.58	2.43	4.23	5.32	4.97	5.01	5.95
3.30	4.34	4.55	6.83	3.31	5.10	5.83	6.26	5.84	32.92
2.62	3.06	3.21	3.92	2.01	12.00	4.28	4.12	4.03	4.34
4.02	4.30	4.57	5.39	2.88	5.22	5.80	5.66	7.22	7.13
2.95	3.05	2.87	3.62	1.83	3.50	4.45	4.20	1.20	4.86
4.60	4.32	4.65	4.38	2.57	5.31	4.67	5.70	5.50	6.61
5.04	5.31	5.38	6.78	3.01	6.47	7.15	6.69	7.13	8.34
4.54	4.35	3.60	5.32	2.44	5.02	6.32	5.61	5.47	5.71
4.57	4.71	5.12	5.51	2.72	5.82	6.49	5.95	6.30	6.57
86.15	4.54	4.68	5.19	2.91	5.84	5.77	5.53	5.37	6.15
5.95	6.65	6.94	7.37	5.57	7.30	6.76	6.28	7.28	6.17
7.74	8.29	8.44	9.59	5.77	10.52	10.29	10.21	10.22	12.36
4.68	4.80	5.12	5.82	2.94	6.36	6.70	6.52	6.26	4.44
4.10	3.81	4.07	4.76	5.21	6.70	5.68	4.36	5.35	8.37
2.79	2.76	3.07	3.27	3.32	9.08	11.85	0.80	4.23	4.43
4.76	3.66	4.90	4.93	2.66	6.79	12.55	6.47	6.08	7.06
5.88	6.57	7.05	8.00	3.61	10.03	11.01	8.52	10.97	9.97
3.32	3.73	4.21	2.84	2.35	4.50	4.57	4.48	5.61	5.10
4.09	3.68	3.81	4.28	2.59	3.95	4.66	4.16	4.94	5.35
4.92	4.71	4.90	3.91	3.16	5.71	6.38	6.81	6.53	7.22
3.38	3.27	3.67	4.11	2.53	4.16	4.73	4.65	4.57	2.77
4.53	4.63	4.64	5.37	3.35	5.42	5.73	6.07	8.41	6.31
2.67	2.94	0.83	3.35	2.00	3.45	4.49	4.82	5.57	4.87
4.33	4.30	4.34	4.83	3.46	6.16	5.72	5.56	5.82	6.30
3.63	4.03	4.13	4.94	2.93	5.50	5.64	5.39	5.85	6.98
5.68	6.22	6.62	7.27	0.51	7.38	7.49	7.23	8.85	8.96
3.29	3.48	3.79	4.38	3.73	3.91	4.65	4.46	4.37	5.44
3.16	3.14	3.25	3.97	2.43	3.69	4.08	4.03	5.23	5.02
4.28	4.61	5.01	5.37	2.56	4.97	6.19	5.91	6.03	6.40
3.05	3.28	3.46	3.68	2.86	3.47	3.91	3.68	3.99	3.60
4.47	4.41	4.01	5.37	3.07	5.03	6.23	5.71	6.32	7.12
3.03	3.09	3.35	3.59	2.63	2.94	4.00	3.77	3.78	4.77
3.32	3.37	3.87	4.41	1.92	4.69	4.85	4.60	3.99	5.49
4.62	3.35	4.52	4.94	2.92	5.09	6.16	5.83	5.70	7.92
4.21	4.58	4.53	5.03	2.69	4.77	6.27	5.61	5.91	6.55
2.52	2.62	2.96	3.25	1.78	3.11	3.72	3.70	3.59	3.92
2.55	2.80	3.03	3.20	2.33	3.35	3.66	3.40	3.83	4.23
3.88	3.66	3.63	4.09	2.94	4.06	4.77	4.81	4.35	4.11
2.19	2.14	2.45	2.50	1.96	2.64	3.34	3.67	3.72	4.15
4.69	4.92	5.14	5.91	3.67	5.70	6.48	6.31	1.46	8.08
5.29	5.18	5.64	6.27	2.75	6.04	7.00	6.69	6.22	6.94
8.38	7.81	5.47	91.73	172.31	7.91	10.20	10.41	10.60	12.44
13.22	12.08	13.65	13.19	11.59	10.99	12.73	12.63	12.99	10.67

The minimum and maximum are 0.51470420 172.31468

Table B-R5c
Rockwell BIBIB Array
Background Run #5 (BG #5)

SKEWNESS

SKEW

0.086	9.050	0.098	0.004	0.107	0.304	0.047	0.113	0.204	0.002
0.027	0.001	0.002	0.011	0.001	0.126	0.033	0.350	30.000	0.563
0.017	144.877	0.042	0.007	0.163	0.253	0.045	0.091	0.145	0.200
60.100	4.236	0.006	0.015	0.018	0.003	0.090	0.182	0.004	0.076
0.012	0.000	0.010	0.029	0.006	0.113	0.005	0.002	0.010	0.023
0.003	0.000	0.028	0.396	0.115	1473.024	0.001	0.002	0.023	0.060
0.052	1473.643	0.032	0.056	0.321	0.032	0.064	0.732	0.127	0.163
0.001	0.002	0.001	0.004	0.001	0.007	0.007	0.003	0.000	0.007
0.006	0.008	0.000	0.028	0.273	0.007	0.002	0.016	0.042	0.704
0.160	0.011	0.001	1.464	0.008	0.003	0.000	0.004	0.000	0.016
0.008	0.019	0.034	0.062	0.144	0.057	0.043	0.079	21.761	0.289
0.111	0.098	0.037	0.047	0.008	0.086	4.571	4.612	0.098	0.186
0.300	0.333	0.232	0.204	0.300	0.290	0.062	0.121	0.320	0.029
0.010	0.019	0.004	0.003	0.000	0.004	0.006	0.186	0.133	0.004
0.002	0.001	0.002	0.000	0.105	0.045	0.034	0.004	0.083	0.033
0.005	0.005	0.003	0.000	0.001	0.007	0.133	0.006	0.013	0.046
2768.180	0.007	0.012	0.008	0.172	0.001	0.142	0.025	0.037	0.120
0.001	0.032	0.012	0.002	0.003	0.602	0.429	0.002	1.359	0.005
0.016	0.004	0.010	0.016	0.037	0.186	0.104	0.005	0.012	0.006
0.387	0.221	0.276	0.256	0.030	0.423	1.995	0.664	0.117	0.502
0.002	0.060	0.019	0.036	0.243	0.069	0.025	0.024	0.045	0.001
0.000	0.067	0.001	0.020	0.128	0.367	0.059	0.071	0.000	0.029
0.013	0.002	0.003	0.007	0.011	0.041	0.019	0.003	0.083	0.000
0.073	0.015	0.014	0.009	0.002	0.011	0.233	0.017	2.765	0.056
0.001	0.003	0.000	0.035	0.026	0.005	0.026	0.001	3.025	0.000
0.202	0.098	0.137	0.106	0.171	0.035	0.357	0.087	0.103	0.094
0.123	0.132	0.083	0.009	0.382	0.073	0.121	0.139	0.168	0.174
0.004	0.002	0.002	0.010	0.266	0.013	0.001	0.027	0.000	0.064
0.258	0.199	0.289	0.315	0.518	0.275	0.154	0.001	6.413	0.286
0.025	0.019	0.037	0.110	0.136	0.074	4.213	12.295	7.664	0.336
0.041	0.036	0.056	0.058	0.492	5.284	0.334	0.278	0.088	0.245
0.000	0.016	0.040	0.037	0.087	2.546	0.058	0.309	0.122	0.044
0.001	0.029	0.015	0.032	0.009	0.161	0.048	0.087	0.093	0.158
0.002	0.028	0.033	0.014	106.312	0.022	0.005	0.023	0.034	0.212
0.000	0.021	0.011	0.020	0.087	0.002	0.008	1.249	5.858	0.117
0.116	0.092	0.059	0.053	0.026	0.118	0.098	0.111	0.042	0.030
0.009	0.027	0.022	0.019	0.206	0.159	0.006	0.031	0.076	0.003
0.065	0.103	0.053	0.037	0.039	0.004	0.007	0.011	0.628	0.055
0.043	0.115	0.004	0.039	0.386	0.009	0.115	0.011	0.092	0.303
0.010	0.000	0.125	0.498	0.000	0.012	0.001	0.011	0.072	0.404
0.007	0.005	0.094	0.029	0.205	0.081	0.085	0.129	0.184	0.117
0.060	0.171	0.104	0.012	0.011	0.074	0.054	0.094	0.088	0.212
0.001	0.010	0.000	0.001	0.007	0.021	0.004	0.010	0.027	0.023
0.013	0.011	0.030	0.031	0.074	0.031	0.004	0.025	0.053	0.059
0.155	0.199	0.261	0.255	0.312	0.336	0.305	0.369	0 288	0.550
0.097	0.031	0.025	0.016	0.167	0.006	0.263	0.252	0.352	0.738
0.062	0.067	0.047	0.070	0.385	0.048	0.038	0.101	20.077	0.145
0.006	0.002	0.006	0.000	0.000	0.005	0.007	0.014	0.006	0.025
0.413	0.309	0.004	2346.735	1382.479	0.286	0.278	0.330	0.340	0.498
0.345	0.326	0.093	0.245	0.412	0.304	0.195	0.213	0.209	0.090

The minimum and maximum are 1.44120629E-05 2768.1800

Table B-R5d
Rockwell BIBIB Array
Background Run #5 (BG #5)

KURTOSIS

KURT

2.245	59.197	2.209	2.470	2.238	4.950	2.328	2.732	2.750	2.350
3.126	3.034	3.131	2.994	6.499	2.961	3.219	2.902	151.960	2.787
2.943	259.265	2.691	2.738	2.724	14.934	2.827	2.885	2.753	3.043
228.753	23.709	2.902	2.983	2.822	3.277	3.384	10.145	2.971	3.147
3.503	3.306	3.412	3.305	3.252	4.131	3.820	3.211	3.386	3.952
3.037	2.794	3.660	7.979	6.678	1514.148	2.967	2.992	3.238	3.142
2.912	1514.585	2.859	2.924	2.897	2.981	2.880	2.953	2.879	2.884
2.662	2.942	2.887	2.897	2.967	2.904	2.723	2.775	2.929	2.979
3.165	2.951	2.857	2.842	3.227	2.933	3.054	3.229	2.871	2.783
7.899	3.071	2.910	13.522	2.987	2.558	3.059	2.870	3.384	3.167
3.158	3.267	3.121	3.218	3.046	2.972	3.282	3.245	108.806	3.310
4.568	2.908	2.991	2.988	3.425	3.023	38.699	40.748	4.030	3.481
3.872	3.313	3.300	3.303	3.052	4.704	3.138	4.590	3.146	6.906
2.834	2.921	2.813	2.744	2.923	2.695	2.709	6.354	6.917	2.760
3.112	3.250	3.357	3.254	3.190	5.903	5.279	3.041	8.205	2.998
2.714	2.781	2.815	2.761	3.267	2.889	6.833	2.802	6.445	3.068
2905.274	3.117	3.060	3.158	3.353	3.242	8.085	3.113	3.131	3.304
2.796	2.796	2.679	2.709	2.302	9.575	10.105	2.802	16.149	2.923
2.502	2.465	2.473	2.408	2.441	3.914	4.591	2.416	3.482	3.011
4.335	3.474	3.643	3.541	3.691	3.792	14.201	7.572	3.756	3.801
3.908	3.432	3.086	3.266	2.972	3.020	3.075	4.989	3.141	2.622
3.070	5.148	3.016	3.314	3.429	3.842	2.537	4.146	3.827	3.208
2.951	2.840	2.965	3.009	3.009	3.086	2.888	3.087	7.909	3.123
3.701	2.888	2.827	2.747	2.954	2.747	4.061	2.564	16.654	3.173
3.272	2.859	2.872	3.453	3.024	2.866	2.864	3.105	25.017	2.943
3.163	3.149	3.212	3.239	3.198	3.307	13.210	3.300	12.031	3.163
3.151	3.186	3.117	3.568	3.151	3.050	3.203	3.106	3.156	3.177
3.142	3.292	3.082	3.129	3.581	3.045	3.269	3.255	5.041	3.103
3.465	3.378	3.547	3.375	3.406	3.276	3.156	8.062	33.587	3.038
3.364	3.341	3.617	3.530	3.555	3.565	38.986	55.564	42.784	3.599
2.898	3.248	3.222	3.177	3.358	32.962	16.331	11.941	9.910	3.416
2.743	2.765	2.791	2.674	2.818	28.486	2.571	11.919	2.742	3.271
2.564	2.719	2.691	2.734	2.925	10.514	2.720	7.588	9.062	2.789
2.863	3.153	3.104	3.153	325.466	2.857	3.185	2.813	2.785	12.190
2.980	3.036	3.026	3.084	2.892	2.950	2.913	23.840	37.853	2.871
3.155	2.941	2.821	2.742	2.866	2.971	2.950	2.911	2.789	2.765
3.040	2.970	2.823	2.852	2.874	3.194	2.834	3.033	2.885	3.217
4.193	4.092	2.949	2.858	2.766	2.844	3.034	2.918	13.227	2.758
3.327	3.123	6.244	3.513	3.637	3.629	3.282	5.490	3.197	3.156
3.208	3.040	5.378	9.140	3.306	3.106	2.988	3.234	3.124	12.737
4.772	2.704	2.912	3.491	3.334	3.021	3.065	3.094	3.118	2.864
3.095	3.209	3.370	5.371	3.199	3.292	3.073	3.190	3.063	3.220
3.008	2.669	2.769	3.027	2.943	2.780	2.877	2.785	2.831	3.002
3.311	2.787	2.994	5.919	2.898	2.987	3.095	2.945	2.934	2.986
3.251	3.116	3.187	3.249	3.180	3.244	3.256	3.075	3.299	3.216
3.351	3.571	3.254	3.382	3.567	3.184	3.816	3.515	3.720	4.175
3.106	3.120	2.951	3.042	3.135	2.979	3.010	3.149	115.056	3.549
2.744	2.776	2.813	2.769	2.770	2.787	2.924	2.949	2.984	2.966
3.268	3.109	3.391	2603.574	1451.997	3.389	3.231	3.092	2.977	3.062
2.565	2.524	3.925	2.554	2.396	2.782	2.610	2.547	2.623	2.591

The minimum and maximum are 2.2089250 2905.2744

Table B-R6
Rockwell BIBIB Array

RATIO = (AVERAGE BG #1)/AVERAGE BG #2)

Ratio R BG 1/R BG 2

0.99985	0.99990	0.99967	1.00000	1.00084	0.99991	1.00003	0.94995	0.94439	0.99875
1.00031	0.99999	0.99991	0.99945	1.00091	0.97248	0.99977	0.94861	0.99950	0.94217
0.99985	0.99954	0.99978	0.99957	1.00053	0.99945	0.99904	0.99937	0.99899	0.99836
1.00117	1.00099	1.00106	1.00096	1.00158	1.00034	1.00006	1.00047	1.00056	1.00031
0.99939	0.99984	0.99954	0.99945	1.00037	0.99969	0.99924	0.99916	0.99910	0.99929
0.99979	0.99992	0.99942	0.99960	1.00099	1.00091	0.99896	0.99937	0.99928	0.99893
1.00039	1.00041	1.00015	1.00018	1.00079	1.00010	0.99987	0.95157	0.99962	0.99910
1.00019	0.99988	1.00001	1.00004	1.00109	0.99968	0.99974	0.99977	0.99977	0.99910
1.00042	1.00055	1.00072	0.99965	1.00108	1.00054	1.00062	1.00006	1.00023	0.94254
1.00383	1.00066	1.00069	1.00056	1.00166	0.99193	1.00056	1.00028	1.00032	0.99997
1.00126	1.00091	1.00073	1.00092	1.00122	1.00072	1.00082	1.00072	1.00046	0.99968
1.00035	1.00060	1.00031	1.00064	1.00112	1.00058	1.00037	1.00022	1.00011	0.99976
1.00035	1.00048	1.00029	1.00001	1.00052	1.00036	1.00016	0.99999	0.99983	0.99983
1.00091	1.00085	1.00058	1.00021	1.00134	1.00041	1.00049	1.00017	1.00008	0.99997
1.00018	1.00006	0.99945	0.99939	1.00101	0.99980	0.99973	0.99956	0.99938	0.99930
1.00065	1.00087	1.00078	1.00050	1.00137	1.00036	1.00032	1.00027	1.00004	0.99999
0.99953	0.99984	1.00000	0.99994	1.00093	0.99978	0.99953	0.99985	0.99956	0.99963
0.99949	1.00037	1.00026	1.00002	1.00120	1.00008	0.99982	0.99969	0.99992	0.99982
1.00010	1.00025	1.00013	1.00024	1.00103	1.00020	1.00042	1.00025	0.99988	0.99978
1.00018	1.00009	1.00026	1.00023	1.00114	1.00003	1.00024	0.99985	0.99996	0.99957
0.99965	0.99977	0.99971	0.99959	1.00054	0.99961	0.99917	0.99956	0.99945	0.99909
0.99987	1.00004	1.00004	0.99994	1.00076	0.99984	0.99998	0.99994	0.99956	0.99950
1.00044	0.99987	1.00017	1.00050	1.00104	1.00040	1.00025	1.00026	1.00030	1.00015
0.99837	1.00013	1.00019	0.99997	1.00076	0.99989	0.99975	0.99961	0.99999	0.99996
1.00000	1.00043	1.00014	0.99999	1.00076	1.00016	0.99986	0.99993	1.00021	0.99969
1.00029	1.00023	1.00026	0.99989	1.00132	1.00007	1.00010	1.00000	0.99969	0.99951
1.00006	1.00064	1.00041	0.99973	1.00121	1.00020	1.00006	0.99974	1.00027	0.99992
0.99967	0.99996	0.99987	1.00001	1.00093	0.99989	0.99996	0.99970	0.99956	1.00020
1.00009	0.99991	1.00005	0.99992	1.00098	0.99974	0.99991	0.99977	0.99956	0.99955
1.00062	1.00049	0.99987	1.00010	1.00143	1.00029	1.00043	1.00013	0.99976	0.99996
1.00010	1.00027	1.00017	0.99979	1.00139	0.99991	1.00007	0.99981	0.99964	0.99955
1.00113	1.00066	1.00051	1.00069	1.00137	1.00065	1.00051	1.00039	1.00039	1.00037
1.00129	1.00030	1.00028	1.00022	1.00061	1.00037	1.00027	1.00023	0.99989	0.99994
1.00079	1.00019	1.00016	1.00030	1.00145	0.99992	1.00003	1.00005	1.00002	0.99992
1.00028	0.99989	0.99961	0.99968	1.00054	0.99968	0.99971	0.99939	0.99956	0.99935
1.00078	1.00049	1.00059	1.00034	1.00154	0.99953	1.00010	1.00038	1.00017	0.99967
1.00018	1.00052	0.99972	0.99985	1.00073	0.99982	0.99962	0.99983	0.99957	0.99930
1.00054	0.99868	0.99976	1.00022	1.00135	0.99983	1.00002	1.00009	0.99990	0.99974
1.00000	1.00050	1.00020	0.99991	1.00103	1.00190	0.99977	0.99970	0.99946	0.99959
1.00048	1.00035	1.00040	1.00010	1.00109	0.99988	1.00022	1.00032	0.99982	0.99997
1.00088	1.00114	1.00068	1.00090	1.00127	1.00033	1.00066	1.00037	1.00052	1.00005
1.00013	1.00250	1.00016	1.00007	1.00130	0.99991	0.99981	1.00006	0.99986	0.99976
0.99958	0.99902	0.99976	0.99951	1.00060	0.99981	0.99963	0.99943	0.99934	0.99965
0.99990	1.00012	1.00004	1.00002	1.00074	1.00009	0.99968	0.99921	0.99973	0.99958
1.00041	1.00039	1.00052	1.00013	1.00132	1.00011	1.00039	0.99992	1.00003	0.99929
1.00044	1.00020	1.00021	1.00017	1.00116	1.00009	1.00005	0.99972	0.99982	1.00003
0.99917	0.99941	0.99891	0.99902	1.00019	0.99940	0.99899	0.99905	0.99960	0.99879
1.00044	1.00033	0.99988	0.99957	1.00081	0.99995	0.99962	0.99949	0.99944	0.99929
0.99881	0.99956	0.99917	0.99929	0.99972	0.99937	0.99953	0.99937	0.99882	0.99860
0.99795	0.99832	0.99806	0.99809	0.99946	0.99812	0.99855	0.99835	0.99840	0.99835

Table B-R7
Rockwell BIBIB Array

RATIO = (AVERAGE BG #3)/AVERAGE BG #2)

Ratio R BG 3/R BG 2

0.99853	0.99868	1.00106	1.00008	0.99882	0.99888	0.99884	0.91661	0.91234	0.99879
0.99915	0.99861	0.99861	0.99909	0.99889	0.91900	0.99892	0.88443	0.99889	0.89998
0.99847	0.99852	0.99895	0.99875	0.99840	0.99935	0.99872	0.99878	0.99871	0.99928
1.00006	1.00147	0.99979	0.99982	0.99911	0.99944	1.00080	0.99983	1.00008	0.99993
0.99881	0.999[illegible]3	0.99874	0.99915	0.99859	0.99907	0.99890	0.99907	0.99899	0.99914
0.99852	0.99835	0.99840	0.99860	0.99845	0.99882	0.99946	0.99865	0.99850	0.99811
0.99869	0.99877	0.99881	0.99941	0.99839	0.99914	0.99879	0.92592	0.99859	0.99908
0.99876	0.99836	0.99849	0.99888	0.99876	0.99890	0.99865	0.99881	0.99872	0.99845
1.00068	0.99980	0.99982	1.00067	0.99951	0.99986	1.00031	1.00001	0.99994	0.93746
0.99021	0.99959	0.99942	0.99950	0.99925	0.95971	0.99941	0.99948	0.99921	0.99963
0.99913	0.99906	0.99903	0.99905	0.99868	0.99914	0.99956	0.99967	0.99925	0.99942
0.99861	0.99910	0.99946	0.99913	0.99919	0.99935	0.99892	0.99911	1.00007	0.99911
0.99842	0.99904	0.99903	1.00055	1.00008	0.99910	1.00056	0.99907	0.99892	0.99925
0.99905	0.99925	0.99913	0.99977	0.99891	0.99914	0.99898	0.99896	0.99878	0.99921
0.99989	0.99974	1.00067	0.99990	0.99949	0.99997	1.00003	0.99976	0.99973	1.00006
0.99946	0.99974	0.99974	0.99999	0.99927	0.99967	0.99962	0.99975	0.99953	0.99963
0.99865	0.99890	0.99908	0.99923	0.99905	0.99896	0.99908	0.99939	1.00057	0.99955
1.00018	0.99933	0.99918	0.99953	0.99915	0.99959	0.99940	0.99960	0.99966	0.99954
0.99929	0.99931	0.99928	0.99951	0.99921	0.99974	0.99975	0.99958	0.99967	0.99983
0.99893	0.99917	0.99920	0.99945	0.99894	0.99989	0.99932	0.99913	0.99916	1.00023
0.99893	0.99912	0.99944	0.99940	0.99908	0.99955	0.99920	1.00029	0.99969	1.00023
0.99868	0.99887	0.99892	0.99886	0.99874	0.99887	0.99937	0.99987	0.99894	0.99910
0.99928	1.00047	0.99925	0.99957	0.99932	0.99954	0.99966	0.99959	0.99965	0.99934
0.99907	0.99841	0.99892	0.99889	0.99887	0.99893	0.99897	0.99914	0.99862	0.99891
0.99877	0.99934	0.99895	1.00000	0.99901	0.99915	0.99911	0.99891	0.99897	0.99931
0.99851	0.99849	0.99877	0.99871	0.99866	0.99908	0.99938	0.99918	0.99918	0.99917
0.99917	0.99934	0.99951	1.00073	0.99914	0.99947	0.99965	0.99975	0.99988	0.99961
0.99884	0.99856	0.99888	0.99905	0.99885	0.99927	0.99919	0.99894	0.99921	1.00023
0.99965	0.99914	0.99953	0.99979	0.99917	0.99977	0.99944	0.99962	0.99939	0.99968
0.99889	0.99851	0.99981	0.99895	0.99853	0.99873	0.99939	0.99875	0.99858	0.99905
0.99883	0.99867	0.99848	0.99915	0.99876	0.99882	0.99907	0.99892	0.99908	0.99931
0.99933	0.99879	0.99890	0.99913	0.99878	0.99935	0.99907	0.99882	0.99918	0.99934
0.99894	0.99876	0.99880	0.99887	0.99986	0.99902	0.99887	0.99903	0.99924	0.99905
1.00035	0.99921	0.99920	0.99952	0.99885	0.99937	0.99922	0.99933	0.99945	0.99980
0.99961	0.99958	0.99925	0.99969	0.99980	0.99965	0.99946	0.99916	0.99927	0.99958
0.99932	0.99920	0.99896	0.99916	0.99893	0.99938	0.99908	0.99905	0.99931	0.99964
0.99952	1.00080	0.99915	0.99951	0.99892	0.99935	0.99945	0.99926	0.99934	1.00034
0.99871	0.99930	1.00014	0.99886	0.99868	0.99969	0.99892	0.99882	0.99886	0.99903
0.99857	0.99917	0.99922	0.99889	0.99865	0.99985	0.99892	0.99956	0.99966	0.99935
0.99869	0.99913	0.99933	0.99890	0.99888	0.99914	0.99926	0.99926	0.99970	0.99922
0.99873	0.99936	0.99895	0.99908	0.99845	0.99898	0.99917	0.99906	0.99910	0.99882
0.99854	0.98241	0.99891	0.99863	0.99861	0.99864	0.99850	0.99864	0.99843	0.99860
0.99863	0.99951	0.99895	0.99871	0.99968	0.99899	0.99898	0.99900	0.99909	0.99916
0.99879	0.99879	0.99865	0.99896	0.99830	0.99917	0.99852	0.99944	0.99878	0.99860
0.99923	1.00023	0.99936	0.99916	0.99930	0.99969	0.99951	0.99951	0.99959	1.00018
0.99895	0.99860	0.99926	0.99897	0.99904	0.99904	0.99892	0.99880	0.99883	0.99884
0.99906	0.99863	0.99909	0.99918	0.99903	0.99915	0.99897	0.99906	1.00033	0.99912
0.99791	0.99764	0.99767	0.99789	0.99822	0.99802	0.99790	0.99756	0.99768	0.99816
0.99835	0.99891	1.00038	0.99965	0.99865	0.99923	0.99955	0.99942	0.99946	0.99964
0.99935	0.99954	0.99932	0.99954	0.99964	0.99946	0.99975	0.99993	1.00008	1.00068

Table B-R8
Rockwell BIBIB Array

RATIO = (AVERAGE ST #1)/AVERAGE BG #2)

Ratio St 1/R BG 2

0.99960	1.00312	1.03156	1.00246	1.00179	1.00124	1.00388	0.99694	1.01049	1.00305
1.00286	1.00451	1.00325	1.00231	1.00590	1.07197	1.00350	1.13455	1.00358	1.15685
1.00178	1.00179	1.00217	1.00138	1.00379	1.00371	1.00141	1.00176	1.00177	1.01941
1.00619	1.04320	1.00579	1.00560	1.00539	1.00484	1.00764	1.00528	1.01401	1.00388
0.99989	0.99927	1.00022	0.99950	1.00164	1.00731	0.99977	1.00000	1.00026	1.00056
1.00259	1.00210	1.00209	1.00159	1.00269	1.00213	1.01036	1.00141	1.00120	1.00027
1.00365	1.00358	1.00357	1.00290	1.00299	1.00231	1.00306	0.96397	1.00216	1.00158
1.00176	1.00208	1.00228	1.00139	1.00268	1.00131	1.00200	1.00180	1.00173	1.00105
1.01852	1.00394	1.00411	1.02792	1.00341	1.00423	1.00352	1.00217	1.00393	1.01947
1.00730	1.00234	1.00206	1.00159	1.00264	0.95720	1.00193	1.00126	1.00194	1.00069
1.00161	1.00260	1.00244	1.00241	1.00226	1.00241	1.00315	1.00187	1.00207	1.00168
1.00104	1.00308	1.01353	1.00222	1.02115	1.00221	1.00225	1.00221	1.00357	1.00158
1.00139	1.00339	1.00282	1.02970	1.03506	1.00285	1.02871	1.00534	1.00308	1.00257
1.00394	1.00464	1.00417	1.01181	1.00349	1.00417	1.00492	1.00503	1.00459	1.00432
1.00139	1.00213	1.02198	1.00143	1.00342	1.00205	1.00207	1.00210	1.00162	1.00092
1.00373	1.00498	1.00494	1.00405	1.00433	1.00419	1.00448	1.00428	1.00422	1.00328
1.00070	1.00241	1.00169	1.00140	1.00282	1.00155	1.00137	1.00196	1.02226	1.00259
1.03094	1.00390	1.00320	1.00286	1.00430	1.00323	1.00301	1.00290	1.00174	1.00045
1.00220	1.00425	1.00343	1.00367	1.00458	1.00582	1.00650	1.00695	1.00456	1.01449
0.99973	1.00146	1.00084	1.00096	1.00373	1.01702	1.00503	1.00758	1.00118	1.01949
1.00204	1.00320	1.00252	1.00244	1.00403	1.00333	1.00533	1.01998	1.00241	1.01884
0.99849	1.00059	1.00012	0.99952	1.00116	1.00069	1.00984	1.02062	0.99890	0.99836
1.00407	1.03096	1.00567	1.00411	1.00402	1.00529	1.00506	1.02271	1.00498	1.00501
1.03993	1.00406	1.00403	1.00258	1.00339	1.00247	1.00343	1.00490	1.00223	1.00237
1.00124	1.00745	1.00275	1.00806	1.00283	1.00126	1.00114	1.00076	1.00110	1.00001
1.00300	1.00426	1.00379	1.00289	1.00374	1.00214	1.00271	1.00246	1.00221	1.00177
1.00150	1.00385	1.00289	1.02402	1.00428	1.00219	1.00224	1.00215	1.00231	1.00251
1.00056	1.00266	1.00179	1.00086	1.00305	1.00142	1.00137	1.00188	1.00465	1.00776
1.00660	1.00839	1.00703	1.00603	1.00667	1.00810	1.00645	1.00719	1.00710	1.00610
1.00430	1.00645	1.00495	1.00423	1.00450	1.00430	1.00488	1.00464	1.00483	1.00390
1.00133	1.00326	1.00217	1.00163	1.00355	1.00183	1.00251	1.00211	1.00208	1.00112
1.00253	1.00427	1.00371	1.00300	1.00429	1.00287	1.00352	1.00353	1.00306	1.00250
1.00438	1.00578	1.00482	1.00487	1.00382	1.00499	1.00563	1.00540	1.00455	1.00426
1.02722	1.00360	1.00352	1.00357	1.00476	1.00335	1.00377	1.00334	1.00318	1.00215
1.00192	1.00401	1.00234	1.00260	1.03454	1.00303	1.00268	1.00214	1.00184	1.00085
1.00443	1.00534	1.00542	1.00475	1.00516	1.02694	1.00504	1.00522	1.00440	1.01561
1.00306	1.00578	1.00320	1.00301	1.00482	1.00383	1.00320	1.00354	1.00284	1.02629
[illegible]	1.03559	1.03093	1.00091	1.00344	1.02985	1.00081	1.00145	1.00107	0.99957
0.99946	1.00082	1.00086	1.00106	1.00201	1.03007	1.00078	1.00688	1.00905	1.00040
1.00250	[illegible]	1.00311	1.00329	1.00405	1.00299	1.00275	1.00338	1.02644	1.00166
[illegible]	1.00221	1.00223	1.00274	1.00359	1.00149	1.00243	1.00295	1.00203	1.00190
1.00180	1.00073	1.00319	1.00339	1.00398	1.00314	1.00236	1.00285	1.00215	1.00176
1.00073	1.03342	1.00229	1.00263	1.02255	1.00278	1.00204	1.00241	1.00186	1.00206
1.00192	1.00353	1.00417	1.00364	1.00400	1.00344	1.00301	1.02510	1.00327	1.00320
1.00710	1.01241	1.00291	1.00642	1.00276	1.00402	1.00261	1.00166	1.00207	1.03043
1.00328	1.00481	1.00422	1.00416	1.00464	1.00315	1.00426	1.00434	1.00347	1.00448
1.00218	1.00342	1.00291	1.00261	1.00427	1.00305	1.00289	1.00322	1.00669	1.00227
1.00162	1.00305	1.00189	1.00130	1.00239	1.00159	1.00199	1.00198	1.00103	1.00118
1.00345	1.00488	1.03545	1.00439	1.00552	1.00391	1.00444	1.00496	1.00392	1.00458
1.00671	1.00824	1.00733	1.00660	1.00857	1.00532	1.00584	1.00613	1.00542	1.03393

Table B-R9
Rockwell BIBIB Array

RATIO = (AVERAGE ST #3)/AVERAGE BG #2)

Star 3/R BG #2

0.99756	1.00116	1.03022	1.00206	1.00057	0.99925	1.00170	0.91782	0.92844	1.00034
1.00299	1.00409	1.00299	1.00178	1.00542	1.05823	1.00323	1.09489	1.00335	1.10347
1.00090	1.00097	1.00131	1.00037	1.00278	1.00279	1.00044	1.00053	1.00074	1.01832
1.00625	1.04312	1.00584	1.00542	1.00489	1.00467	1.00812	1.00518	1.01352	1.00381
0.99993	0.99905	1.00006	0.99934	1.00120	1.00749	0.99964	0.99964	0.99998	0.99977
1.00257	1.00214	1.00239	1.00127	1.00267	1.00229	1.01099	1.00113	1.00103	0.99960
1.00300	1.00298	1.00315	1.00214	1.00229	1.00149	1.00223	0.91543	1.00158	1.00047
1.00174	1.00202	1.00210	1.00094	1.00245	1.00115	1.00197	1.00161	1.00135	1.00055
1.01889	1.00370	1.00375	1.02801	1.00265	1.00340	1.00315	1.00179	1.00322	0.95499
1.00879	1.00235	1.00185	1.00156	1.00275	0.95132	1.00203	1.00114	1.00150	1.00038
1.00091	1.00205	1.00166	1.00161	1.00137	1.00161	1.00238	1.00120	1.00121	1.00070
1.00068	1.00230	1.01280	1.00186	1.02057	1.00168	1.00185	1.00152	1.00355	1.00095
1.00019	1.00222	1.00166	1.02920	1.03474	1.00186	1.02846	1.00479	1.00187	1.00133
1.00291	1.00342	1.00339	1.01129	1.00292	1.00320	1.00403	1.00383	1.00330	1.00314
1.00081	1.00184	1.02210	1.00136	1.00249	1.00178	1.00202	1.00201	1.00145	1.00057
1.00339	1.00413	1.00424	1.00340	1.00364	1.00331	1.00386	1.00344	1.00320	1.00233
1.00005	1.00138	1.00127	1.00066	1.00229	1.00081	1.00065	1.00098	1.02253	1.00191
1.03052	1.00325	1.00242	1.00196	1.00328	1.00199	1.00164	1.00162	1.00071	0.99993
1.00131	1.00357	1.00282	1.00265	1.00309	1.00367	1.00306	1.00353	1.00276	1.01425
0.99922	1.00133	1.00055	1.00088	1.00320	1.01489	1.00017	0.99996	0.99929	1.01897
1.00152	1.00279	1.00195	1.00220	1.00625	1.00349	1.00150	1.01904	1.00107	1.01860
0.99874	1.00080	1.00050	0.99960	1.00351	1.00593	1.01351	1.02043	0.99870	0.99772
1.00503	1.03080	1.00625	1.00551	1.00608	1.01082	1.01081	1.02373	1.00508	1.00528
1.03935	1.00351	1.00353	1.00214	1.00376	1.00333	1.00447	1.00507	1.00152	1.00156
1.00106	1.00732	1.00252	1.00813	1.00259	1.00159	1.00112	1.00051	1.00082	0.99935
1.00333	1.00427	1.00399	1.00306	1.00364	1.00255	1.00302	1.00286	1.00209	1.00167
1.00123	1.00337	1.00246	1.02426	1.00352	1.00178	1.00165	1.00185	1.00147	1.00191
1.00045	1.00233	1.00163	1.00064	1.00287	1.00128	1.00101	1.00128	1.00415	1.00828
1.00592	1.00780	1.00669	1.00571	1.00583	1.00760	1.00614	1.00661	1.00633	1.00572
1.00417	1.00624	1.00485	1.00401	1.00438	1.00406	1.00463	1.00419	1.00455	1.00344
1.00051	1.00244	1.00150	1.00067	1.00273	1.00103	1.00160	1.00167	1.00134	1.00042
1.00236	1.00379	1.00298	1.00264	1.00372	1.00262	1.00317	1.00303	1.00228	1.00181
1.00376	1.00466	1.00394	1.00402	1.00382	1.00412	1.00481	1.00467	1.00360	1.00328
1.02692	1.00351	1.00301	1.00312	1.00423	1.00292	1.00350	1.00301	1.00280	1.00185
1.00196	1.00346	1.00189	1.00248	1.03417	1.00271	1.00234	1.00151	1.00147	1.00015
1.00469	1.00500	1.00524	1.00472	1.00498	1.02700	1.00463	1.00494	1.00389	1.01492
1.00238	1.00493	1.00270	1.00258	1.00404	1.00334	1.00281	1.00278	1.00243	1.02620
0.99991	1.03599	1.03085	1.00050	1.00313	1.03038	1.00043	1.00095	1.00063	0.99892
0.99915	1.00046	1.00061	1.00071	1.00172	1.03031	1.00041	1.00607	1.00853	0.99944
1.00264	1.00318	1.00279	1.00326	1.00397	1.00278	1.00264	1.00320	1.02681	1.00121
1.00145	1.00256	1.00179	1.00242	1.00339	1.00093	1.00204	1.00212	1.00162	1.00108
1.00210	1.00153	1.00325	1.00388	1.00422	1.00319	1.00229	1.00294	1.00218	1.00160
1.00034	1.03369	1.00220	1.00219	1.02297	1.00254	1.00181	1.00212	1.00162	1.00176
1.00215	1.00319	1.00398	1.00399	1.00380	1.00318	1.00287	1.02453	1.00313	1.00268
1.00652	1.01225	1.00222	1.00613	1.00206	1.00368	1.00168	1.00103	1.00110	1.02960
1.00363	1.00457	1.00432	1.00378	1.00445	1.00307	1.00399	1.00374	1.00314	1.00431
1.00188	1.00318	1.00266	1.00222	1.00368	1.00248	1.00222	1.00282	1.00674	1.00158
1.00182	1.00325	1.00219	1.00165	1.00219	1.00163	1.00191	1.00194	1.00089	1.00082
1.00237	1.00408	1.03448	1.00386	1.00510	1.00337	1.00337	1.00413	1.00274	1.00345
1.00497	1.00648	1.00557	1.00481	1.00674	1.00413	1.00461	1.00457	1.00409	1.03242

Table B-AM1a
Aerojet MC^2 Array
Background Run #1 (BGM #1) Before Star Sighting

AVERAGE COUNT/FRAME FOR 3200 FRAMES

AVE

1020.61	944.93	2219.80	2505.32	1838.59	1116.93	1544.94	391.40	1417.12	972.03	1842.06	1244.07	0.00	899.55	1596.35	2871.51
64.63	838.55	1817.38	1301.13	2292.28	1494.67	2478.32	382.87	1861.24	1691.77	2449.05	1566.65	0.00	1219.63	1875.14	1265.18
731.52	7.02	2198.74	1592.22	2477.19	1678.90	2389.00	393.44	2305.38	1707.50	2392.13	2016.56	0.00	1381.98	2627.92	1858.92
1587.92	1455.34	2295.54	1628.43	2523.86	1692.55	2401.66	396.38	2503.01	1794.59	3034.37	1889.18	0.00	1649.59	2426.70	1501.32
1614.24	1601.74	2099.03	1546.91	2332.01	1792.53	2842.63	400.75	2719.81	1968.61	2450.91	1808.25	0.00	1825.26	2386.18	1565.90
413.59	1322.53	2465.09	1557.13	2245.35	1757.98	2698.69	394.23	2430.22	1736.12	2448.69	1826.92	0.00	1672.04	2461.77	1240.78
2096.32	1316.72	2633.32	1521.33	2791.02	2018.59	2451.04	398.87	2601.59	1764.68	2538.12	1987.83	0.00	1821.98	2417.81	1783.37
1665.96	1393.80	2160.24	1638.45	2304.29	1863.04	2316.29	396.83	2400.76	2026.53	2470.04	1647.29	0.00	1846.82	2599.83	1769.93
1435.40	1328.57	2145.76	1733.26	2515.40	1679.14	2399.81	398.04	2665.82	1740.05	2458.86	1751.91	0.00	1724.22	2405.56	1871.39
1441.83	1404.60	2281.94	1671.18	2543.94	1799.71	2570.00	398.19	2586.22	1806.11	2460.72	1737.07	0.00	1903.72	2397.79	1721.83
1834.38	1412.64	2184.17	1800.97	2299.89	1725.83	2296.54	403.27	2189.24	1889.49	2491.20	1955.94	0.00	2280.54	2392.16	2223.44
1587.13	1329.92	2019.21	1803.60	2306.84	1760.99	2618.00	401.09	2347.57	1938.82	2507.29	1848.71	0.00	2037.32	2450.97	1951.46
1336.14	1308.34	2269.94	1577.23	2246.27	1765.61	2393.08	396.98	2415.43	1846.11	2469.65	1989.09	0.00	1812.82	2448.80	1799.99
1270.90	2016.65	2243.10	2990.07	2349.30	1749.96	2770.44	410.83	2429.28	2255.74	2784.85	1942.68	0.00	1741.30	2465.46	1764.81
1318.84	1749.13	2496.69	1856.06	2373.17	1780.37	2408.52	394.95	2390.18	1849.09	2438.57	1869.11	0.00	1985.86	2498.74	1623.34
1377.23	1268.95	2418.87	1618.92	2780.24	1779.73	2391.46	396.27	2390.63	1662.46	2705.96	1745.35	0.00	1713.48	2463.43	2022.24
1273.51	1370.13	2247.08	1609.99	2352.79	1741.82	2421.10	396.12	2426.74	1753.98	2473.51	1828.08	0.00	1858.05	2431.12	1688.99
1241.13	1162.86	2325.43	1595.32	2456.14	1765.46	2373.62	396.59	2477.99	1727.49	2443.51	2209.40	0.00	1760.69	2503.12	1764.32
1160.58	1207.99	2056.19	1617.81	2568.65	1794.46	1442.94	396.19	2528.90	1877.51	2524.52	1771.75	0.00	2091.22	2403.12	1773.23
1479.09	1396.91	2139.19	1959.53	2264.71	1723.84	2330.95	394.33	2470.13	1769.70	2560.82	1692.22	0.00	1801.61	2414.17	2231.60
1882.56	1489.58	2062.57	1643.42	2341.45	1769.05	2555.18	401.96	2632.69	1903.62	2465.05	1754.35	0.00	1862.17	2542.99	2467.25
1259.01	1102.39	2112.06	1671.29	2861.20	1711.13	2456.18	395.32	2518.97	1679.58	2394.20	1865.21	0.00	1955.13	2474.01	1817.87
679.69	1075.25	2411.56	1642.87	2460.65	1684.36	2761.20	392.77	0.80	1893.58	2457.18	1782.04	0.00	1877.24	2585.25	1785.70
1764.18	1400.40	1122.60	2298.29	1665.54	1799.96	3162.20	403.15	2541.71	1626.64	2585.48	1824.03	0.00	1741.35	2675.81	1836.09
1132.34	1357.91	2363.62	1444.56	2392.29	1730.85	2354.97	390.72	2422.66	1907.99	2546.95	2003.46	0.00	1713.45	2454.30	1585.34
2001.82	1033.24	2096.36	1556.78	2414.39	2426.67	2740.19	396.04	2437.45	1788.42	12.38	1885.14	0.00	2127.81	2353.48	1759.72
1184.58	1303.71	1884.39	1816.34	2292.87	1620.01	1035.84	393.92	2349.88	1711.48	2627.66	1758.43	0.00	1782.17	2696.56	1737.25
189.12	1055.11	1997.74	1525.07	2353.94	1938.70	2428.76	394.29	2425.74	2334.39	653.02	1761.40	0.00	1776.05	1097.79	1676.50
2150.14	1224.39	2340.75	1563.21	2307.26	2235.13	2403.67	397.25	2421.13	1746.03	1394.55	1836.80	0.00	1804.88	590.20	1876.25
1174.68	1133.12	1891.74	1464.40	2281.64	1671.88	2303.45	394.45	2375.91	2085.48	2422.74	1624.42	0.00	1652.00	1459.96	1665.61
880.02	1058.18	1853.34	1428.40	2264.77	1592.27	2225.68	386.87	2355.12	1555.79	2399.28	1699.66	0.00	1744.03	2418.85	1654.86
1108.99	3134.95	1998.77	1401.52	2723.31	1557.61	2792.88	398.93	2321.54	1647.83	2439.76	1725.73	0.00	1643.50	1584.38	1768.16

The minimum and maximum are 0.00000000E+00 3162.1975

Table B-AMIb
Aerojet MC^2 Array
Background Run #1 (BGM #1) Before Star Sighting

VARIANCE

VAR

1314.79	299.42	456.75	78.13	605.13	181.13	263.71	0.24	129.75	172.49	141.26	82.37	0.00	130.93	128.24	44.61
813.65	3494.95	1264.29	220.54	503.97	197.12	236.65	0.13	257.48	172.55	243.31	130.10	0.00	204.45	293.58	91.06
2017.94	96.47	687.76	139.34	128.85	108.85	483.81	0.25	368.10	110.35	636.70	152.09	0.00	206.28	269.30	119.00
4904.33	1453.28	446.95	97.03	450.60	171.42	129.78	0.24	447.31	118.33	281.81	173.18	0.00	89.85	233.25	61.05
3585.30	746.85	508.36	180.27	77.37	71.32	225.91	0.20	262.98	141.25	299.64	68.82	0.00	69.95	88.17	88.88
1041.87	1395.63	520.91	102.01	107.96	110.67	297.18	0.19	219.35	85.63	320.23	132.32	0.00	98.19	267.65	456.51
1327.51	1463.19	309.95	68.75	341.27	110.18	316.53	0.13	83.79	55.84	337.39	62.92	0.00	133.85	61.88	69.16
3203.35	1524.27	85.44	125.05	284.62	122.94	273.32	0.16	145.87	83.07	165.21	98.68	0.00	109.56	257.70	79.35
4247.83	1673.38	795.12	156.12	203.50	85.11	542.79	0.10	216.17	81.74	324.23	95.08	0.00	120.54	227.81	81.29
3772.33	1491.53	649.95	144.39	121.04	108.14	316.74	0.16	185.84	57.80	149.64	76.87	0.00	65.72	518.30	91.38
1634.47	1564.76	952.12	83.03	142.99	63.22	420.16	0.22	226.14	47.60	209.03	54.41	0.00	60.76	337.92	65.23
3352.05	1475.82	3674.66	69.35	181.04	100.42	268.53	0.10	151.40	81.87	275.02	66.40	0.00	66.42	166.79	92.67
5232.41	1589.00	453.61	72.40	106.40	83.59	217.72	0.09	65.41	46.01	109.61	50.82	0.00	78.97	152.40	64.20
5593.52	673.16	1025.54	65.85	338.62	93.67	344.81	0.16	226.10	79.32	149.28	113.83	0.00	110.61	135.69	92.51
5791.96	611.80	524.27	84.88	375.01	91.77	312.48	0.09	148.76	90.35	60.83	41.58	0.00	89.27	122.03	57.47
4987.72	1523.69	807.31	101.58	191.12	114.19	152.61	0.20	227.77	94.86	382.76	88.09	0.00	84.46	306.03	64.39
5818.72	940.83	918.42	82.25	107.12	79.21	526.89	0.13	96.34	80.51	357.17	103.34	0.00	81.35	111.26	101.42
5750.63	1554.32	912.84	122.54	184.96	83.16	283.55	0.24	259.39	54.09	200.43	91.51	0.00	83.49	363.47	74.64
5309.11	1625.98	1313.78	71.74	217.44	68.93	125.35	0.16	150.79	88.74	155.12	75.54	0.00	77.23	229.96	91.44
2717.42	1140.94	1559.40	119.89	155.41	73.48	175.89	0.22	176.25	102.27	124.52	84.15	0.00	77.89	152.43	64.31
1022.52	999.44	1741.88	74.74	258.20	115.13	155.36	0.06	77.41	57.79	144.32	45.88	0.00	55.15	233.02	104.84
5340.85	1602.46	1760.96	98.09	78.63	102.57	101.38	0.22	93.97	97.05	439.29	81.33	0.00	123.01	575.73	86.88
1054.84	1693.63	897.03	80.00	100.00	53.32	96.06	0.18	0.16	42.70	98.52	73.93	0.00	84.55	309.46	73.44
1605.09	1152.28	413.48	103.27	443.17	76.24	95.12	0.18	122.07	59.99	155.09	67.20	0.00	117.01	274.63	90.43
5189.93	1295.49	1218.01	121.28	114.12	54.25	97.56	0.21	100.18	363.11	75.80	84.76	0.00	79.44	131.37	82.41
667.67	1953.64	1474.04	141.07	277.34	158.20	153.54	0.10	137.77	71.07	5.28	49.63	0.00	52.32	383.94	87.28
3236.86	1143.55	1898.02	100.38	176.59	51.17	226.59	0.13	89.33	69.02	110.72	52.35	0.00	66.05	77.68	42.05
716.60	2206.38	1756.83	176.49	194.93	78.65	90.65	0.21	98.14	49.94	241.52	65.50	0.00	92.49	302.87	73.43
1058.55	1479.90	772.97	189.28	282.67	132.80	69.12	0.19	71.38	69.82	254.73	52.95	0.00	167.33	24221.86	144.69
2580.85	1977.00	2110.32	271.15	105.80	76.24	139.27	0.25	95.57	130.94	105.11	46.81	0.00	74.30	228.72	61.53
3228.45	1931.42	1963.17	294.79	83.94	76.58	79.34	0.15	116.26	54.45	78.68	50.08	0.00	60.98	62.62	70.73
2207.62	57.70	1824.74	330.91	140.81	59.50	93.68	0.11	214.60	62.58	153.93	47.53	0.00	62.00	346.88	27.61

The minimum and maximum are 0.00000000E+00 24221.858

Table B-AMIc
Aerojet MC^2 Array
Background Run #1 (BGM #1) Before Star Sighting

SKEWNESS

SKEW

0.001	0.007	0.033	0.008	0.017	0.002	0.021	0.165	0.020	0.003	0.016	0.001	0.000	0.007	0.008	0.013
0.000	0.082	0.041	0.037	0.010	0.001	0.023	2.778	0.037	0.018	0.015	0.005	0.000	0.000	0.053	0.047
0.010	3.045	0.027	0.017	0.041	0.010	0.001	0.073	0.000	0.018	0.004	0.435	0.000	0.267	0.052	0.011
0.073	0.024	0.044	0.001	0.000	0.005	0.009	0.210	0.000	0.053	0.019	0.082	0.000	0.016	0.010	0.033
0.046	0.016	0.023	0.007	0.020	0.039	0.317	1.733	0.002	0.022	0.001	0.022	0.000	0.218	0.178	0.030
0.025	0.018	0.006	0.002	0.009	0.000	0.001	1.114	0.001	0.016	0.001	0.008	0.000	0.000	0.002	0.058
0.008	0.021	0.000	0.003	0.003	2.375	0.003	2.386	0.009	0.002	0.009	0.008	0.000	0.193	0.006	0.000
0.099	0.014	0.103	0.001	0.010	0.011	0.003	1.732	0.003	0.009	0.104	0.001	0.000	0.001	0.018	0.016
0.068	0.011	0.048	0.010	0.083	0.004	0.021	0.941	0.028	0.014	0.052	0.059	0.000	0.006	0.011	0.000
0.060	0.005	0.010	0.006	0.014	0.001	0.014	2.007	0.065	0.007	0.014	0.020	0.000	0.005	0.000	0.035
0.021	0.005	0.064	0.001	0.027	0.000	0.000	0.516	0.022	0.003	0.006	0.003	0.000	0.007	0.025	0.003
0.047	0.001	0.241	0.029	0.031	0.018	0.127	4.010	0.028	0.010	0.054	0.044	0.000	0.000	0.000	0.014
0.047	0.005	0.178	0.008	0.002	0.004	0.051	0.514	0.001	0.002	0.069	0.001	0.000	0.003	0.003	0.000
0.044	2.408	0.112	0.001	0.001	0.024	0.000	1.769	0.016	0.010	0.012	0.003	0.000	0.000	0.005	0.000
0.019	0.002	0.087	0.038	0.000	0.003	0.000	1.597	0.020	0.002	0.006	0.020	0.000	0.001	0.006	0.041
0.014	0.018	0.038	0.000	0.003	0.001	0.002	0.887	0.002	0.002	0.022	0.010	0.000	0.011	0.002	0.006
0.005	0.026	0.103	0.000	0.022	[illegible]	0.028	2.143	0.001	0.037	0.000	0.001	0.000	0.056	0.002	0.042
0.004	0.028	0.079	0.000	0.002	0.001	0.037	0.120	0.008	0.000	0.010	0.006	0.000	0.005	0.007	0.014
0.000	0.055	0.106	0.003	0.023	0.076	0.012	2.145	0.003	0.003	0.083	0.038	0.000	0.038	0.000	0.014
0.001	0.055	0.103	0.057	0.034	0.005	0.002	0.451	0.061	0.007	0.014	0.016	0.000	0.000	0.017	0.079
0.007	0.042	0.054	0.025	0.000	0.097	0.217	5.228	0.000	0.003	0.002	0.010	0.000	0.010	0.010	0.010
0.000	0.062	0.059	0.017	0.012	0.002	0.010	0.488	0.004	0.014	0.000	0.001	0.000	0.004	0.025	0.105
0.002	0.071	0.056	0.054	0.002	0.004	0.002	1.502	2.309	0.003	0.130	0.074	0.000	0.021	0.000	0.030
0.001	0.064	0.015	0.002	0.008	0.000	0.270	0.712	0.118	0.001	0.003	0.021	0.000	0.171	0.001	0.004
0.004	0.056	0.054	0.092	0.001	0.007	0.079	0.777	0.001	1.593	0.001	0.001	0.000	0 027	0.024	0.004
0.019	0.047	0.054	0.038	0.054	1.950	0.197	0.685	0.122	0.005	65.876	0.009	0.000	0.001	0.001	0.002
0.006	0.056	0.036	0.005	0.082	0.042	0.019	1.180	0.000	0.002	0.005	0.041	0.000	0.009	0.022	0.000
0.015	0.066	0.029	0.083	0.049	0.003	0.010	0.703	0.003	0.000	0.001	0.017	0.000	0.027	0.035	0.001
0.003	0.047	0.003	0.067	0.005	3.672	0.015	1.117	0.000	0.002	0.025	0.030	0.000	0.176	1.332	0.080
0.017	0.066	0.019	0.113	0.015	0.008	0.080	0.051	0.121	0.197	0.006	0.000	0.000	0.016	0.185	0.006
0.003	0.071	0.007	0.120	0.005	0.001	0.008	1.314	0.043	0.003	0.092	0.002	0.000	0.117	0.001	0.000
0.004	0.022	0.006	0.153	0.005	0.046	0.002	1.601	0.020	0.000	0.021	0.027	0.000	0.008	0.010	0.001

The minimum and maximum are 0.00000000E+00 65.876286

Table B-AM1d
Aerojet MC^2 Array
Background Run #1 (BGM #1) Before Star Sighting

KURTOSIS

KURT

3.015	2.813	2.927	3.303	2.987	3.034	4.233	1.311	3.076	2.892	3.010	3.002	1.000	3.002	3.745	3.324
2.920	2.474	2.599	2.945	2.815	2.833	3.365	5.472	3.620	2.950	3.067	2.926	1.000	3.062	3.071	3.079
2.762	5.633	3.051	2.786	3.516	2.729	2.495	1.114	3.268	3.181	2.559	3.669	1.000	3.500	3.197	2.768
2.685	2.696	3.023	2.991	2.883	3.106	3.308	1.360	2.753	3.331	3.112	3.052	1.000	3.101	3.333	3.204
2.746	2.669	3.235	2.836	3.730	3.286	3.908	3.469	2.841	2.557	2.951	3.185	1.000	4.284	4.649	3.502
2.802	2.677	3.112	3.208	3.214	2.997	3.036	2.771	3.705	2.919	3.355	2.998	1.000	3.190	3.433	3.262
2.935	2.703	3.338	3.102	2.525	7.976	3.438	5.864	4.185	3.031	2.714	3.002	1.000	3.612	3.036	3.053
2.840	2.639	3.511	3.119	3.521	2.716	3.323	3.980	3.426	3.130	3.067	3.069	1.000	2.958	2.988	3.012
2.668	2.597	2.873	3.059	3.829	2.877	2.896	9.764	3.197	3.367	3.659	3.567	1.000	3.200	3.947	3.108
2.659	2.671	2.978	2.906	3.221	2.883	3.109	3.568	3.336	3.274	3.907	2.874	1.000	3.341	2.862	3.767
2.646	2.647	3.010	3.024	3.487	3.141	2.649	2.281	4.009	2.843	3.462	2.948	1.000	3.207	3.050	2.839
2.608	2.765	3.172	3.156	3.498	3.429	3.265	8.711	3.730	3.051	3.708	3.487	1.000	3.247	4.332	2.945
2.561	2.756	2.870	3.207	3.359	2.962	3.935	11.345	3.812	2.989	3.584	2.859	1.000	2.883	4.220	3.281
2.596	5.831	2.820	3.054	3.267	3.420	2.584	4.218	3.268	3.245	3.552	3.052	1.000	3.031	4.356	3.042
2.576	2.726	2.829	3.126	3.376	2.839	2.932	9.997	3.304	2.791	3.456	2.882	1.000	2.869	3.640	3.045
2.578	2.717	2.921	3.109	2.743	2.922	4.395	2.212	3.058	2.914	2.964	2.855	1.000	3.096	3.107	3.093
2.629	2.683	2.726	3.032	3.781	2.837	2.656	5.684	3.403	3.121	3.280	2.645	1.000	3.514	3.212	3.059
2.706	2.828	2.744	2.880	3.169	2.983	3.788	1.182	3.066	2.850	3.533	3.355	1.000	3.024	2.798	3.126
2.695	2.736	2.687	3.046	3.553	3.615	2.973	3.574	3.411	2.684	3.625	2.998	1.000	3.306	3.807	3.004
2.763	2.785	2.755	3.098	4.027	3.172	3.558	1.572	3.419	2.677	3.513	3.132	1.000	3.103	3.926	2.998
2.793	2.703	2.628	3.082	3.678	2.760	3.881	15.462	3.099	3.043	3.297	3.016	1.000	3.222	3.351	3.061
2.636	2.620	2.675	2.874	3.087	3.039	2.971	1.709	2.991	2.719	2.861	2.852	1.000	2.815	2.925	3.224
2.909	2.696	2.597	3.114	3.076	3.427	3.260	2.577	3.308	2.934	4.211	3.216	1.000	2.895	2.815	3.121
2.828	2.702	2.890	2.984	3.243	2.877	4.018	4.299	3.465	3.159	3.104	3.054	1.000	3.712	2.819	2.712
2.816	2.684	2.712	2.904	3.409	3.320	3.366	2.265	3.128	5.529	3.204	3.264	1.000	3.212	4.508	2.859
3.050	2.636	2.628	2.728	2.705	4.159	3.689	9.313	3.198	2.782	81.815	3.293	1.000	2.984	3.079	3.195
2.764	2.626	2.579	2.819	3.416	3.376	3.444	6.966	3.206	3.208	3.048	2.972	1.000	2.980	3.254	2.913
2.933	2.664	2.644	2.826	3.128	2.959	2.811	1.975	2.942	3.026	3.033	3.047	1.000	2.881	3.718	2.876
2.872	2.757	2.678	2.866	3.439	4.746	2.947	2.477	3.261	2.967	3.012	3.096	1.000	2.893	2.602	2.797
2.819	2.639	2.590	2.823	3.205	3.092	3.856	1.111	3.425	4.645	3.155	3.076	1.000	3.100	2.897	3.331
2.793	2.659	2.696	2.723	2.982	2.783	3.101	4.934	3.256	3.111	3.564	2.791	1.000	3.433	3.043	2.833
2.797	3.301	2.749	2.834	3.048	3.278	2.972	8.625	2.658	3.121	3.692	3.091	1.000	3.361	2.874	3.139

The minimum and maximum are 1.0000000 81.814911

Table B-AM2a
Aerojet MC² Array
Star (α Ori) at top; Bias = 2.0v (Star M #1)

AVERAGE COUNT/FRAME FOR 3200 FRAMES

AVE

850.50	722.54	1861.64	2571.10	1513.83	901.99	1254.13	388.02	1138.05	770.42	1512.92	973.33	0.00	713.86	1309.76	2615.56
17.06	715.15	1504.62	1065.29	1911.54	1200.86	2078.52	378.93	1518.14	1353.42	2157.60	1237.82	0.00	972.57	1517.40	1039.91
600.96	6.50	1871.32	1299.01	2335.56	1373.61	1991.59	387.35	1920.14	1394.02	1995.10	1645.27	0.00	1127.88	2215.22	1508.13
1336.75	1220.74	1918.14	1335.65	2126.13	1385.44	2004.85	389.89	2096.33	1470.78	2612.29	1540.13	0.00	1331.56	2010.59	1218.81
1367.49	1292.30	1780.47	1257.26	1948.22	1456.76	2422.32	393.00	2292.99	1597.94	2055.82	1494.54	0.00	1483.50	1983.18	1277.94
292.77	1097.68	2076.40	1269.34	2191.05	1441.01	2278.75	388.17	2026.59	1416.53	2047.95	1486.83	0.00	1356.61	2044.72	949.05
1784.40	1086.94	2235.30	1232.89	2380.45	1723.74	2043.31	391.78	2185.49	1443.52	2124.47	1621.33	0.00	1475.49	2003.08	1446.06
1379.86	1158.44	2065.86	1337.09	1922.79	1517.91	1926.62	389.68	2002.04	1666.54	2061.38	1334.67	0.00	1507.26	2171.84	1414.71
1210.36	1100.24	1805.42	1415.96	2118.29	1371.02	2003.07	391.77	2248.63	1425.21	2054.59	1431.71	0.00	1403.00	2006.50	1559.66
1222.64	1163.95	1931.52	1370.28	2141.13	1476.48	2159.47	391.48	2158.94	1478.21	2059.00	1407.56	0.00	1553.00	1990.68	1410.69
1550.69	1181.64	1838.60	1474.76	1918.23	1410.74	1910.35	395.84	1815.13	1560.03	2079.87	1601.63	0.00	1898.10	1986.67	1842.96
1374.11	1115.45	2367.16	1482.01	1924.09	1446.06	2206.63	393.84	1947.76	1579.98	2091.37	1511.75	0.00	1664.54	2039.81	1580.13
1138.67	1088.77	1946.80	1291.90	1872.78	1450.05	2000.19	390.82	2025.96	1519.35	2063.03	1632.11	0.00	1484.94	2042.91	1475.12
1099.98	2044.61	1907.95	2592.76	1973.78	1435.37	2351.73	403.02	2029.89	2140.85	2360.61	1586.41	0.00	1416.07	2055.96	1448.78
1128.16	1428.35	2120.08	1522.10	1989.88	1457.10	2014.92	389.22	1991.55	1523.80	2038.33	1536.52	0.00	1624.09	2088.91	1330.96
1172.54	1055.26	2049.60	1322.12	2363.88	1456.50	1991.94	389.59	1991.21	1354.17	2291.53	1424.16	0.00	1396.41	2049.96	1617.27
1087.35	1106.79	1891.37	1313.85	1966.76	1429.03	2022.63	389.46	2024.63	1436.67	2068.57	1497.78	0.00	1527.05	2029.30	1394.36
1057.92	957.24	1970.79	1302.76	2061.13	1432.50	1998.83	390.06	2076.29	1412.81	2042.98	2176.88	0.00	1437.07	2087.93	1442.79
993.48	1003.78	1736.10	1328.40	2167.19	1477.33	1404.81	390.14	2116.01	1538.97	2113.84	1453.29	0.00	1713.64	1997.11	1469.79
1243.38	1119.85	1805.00	1615.68	1885.34	1401.83	1955.29	387.96	2074.52	1434.56	2148.68	1379.02	0.00	1470.20	2010.00	1847.23
1558.04	1212.34	1741.56	1351.87	1961.80	1441.04	2147.18	395.00	2224.96	1557.23	2063.98	1439.66	0.00	1536.41	2147.19	2314.26
1025.80	909.34	1788.26	1287.60	2496.31	1397.67	2060.24	389.00	2117.06	1365.99	1996.47	1526.88	0.00	1610.41	2065.27	1478.46
525.76	884.05	2047.01	1334.80	2065.96	1375.38	2339.76	386.46	0.11	1547.78	2057.51	1455.24	0.00	1545.22	2161.59	1482.66
1479.18	1129.38	867.93	2041.50	1402.37	1474.70	2725.53	394.92	2137.03	1308.55	2165.66	1490.79	0.00	1418.50	2249.34	1527.70
926.10	1096.15	2016.81	1170.07	2008.79	1417.80	1967.69	388.23	2032.52	2455.29	2148.79	1923.76	0.00	1406.30	2044.02	1298.61
1678.52	858.65	1764.96	1269.54	2027.86	2008.16	2323.12	392.03	2037.99	1483.36	14.01	1549.97	0.00	1745.24	1954.49	1433.07
974.35	1041.72	1586.09	1471.90	1910.21	1320.71	848.43	388.82	2156.62	1404.29	2220.66	1441.46	0.00	1455.14	2273.27	1438.79
105.57	877.49	1673.54	1243.08	1968.91	1579.09	2035.58	388.04	2036.98	1935.30	467.96	1449.73	0.00	1459.90	871.13	1366.55
1815.69	990.67	1972.65	1263.02	1921.56	1913.95	2007.25	390.64	2029.56	1432.31	1172.17	1502.08	0.00	1486.91	380.59	1565.44
955.56	926.38	1597.05	1196.08	1903.81	1367.58	1914.88	389.32	1995.90	2122.74	2026.39	1317.36	0.00	1340.03	1233.92	1358.22
734.19	898.94	1554.17	1167.77	1891.66	1294.89	1845.61	382.15	1955.53	1266.83	2003.60	1379.97	0.00	1428.84	2011.97	1364.65
961.40	2809.17	1709.15	1150.99	2311.73	1262.40	2364.39	392.49	1933.47	1346.19	2041.73	1410.04	0.00	1338.87	1337.30	1468.73

The minimum and maximum are 0.00000000E+00 2809.1712

Table B-AM2b
Aerojet MC^2 Array
Star (α Ori) at top; Bias = 2.0v (Star M #1)

VARIANCE

VAR

527.43	137.97	358.21	98.11	516.70	158.12	228.99	0.09	104.54	172.64	112.57	77.83	0.00	97.23	117.92	49.96
424.53	2017.70	475.52	141.47	470.31	170.58	173.63	0.18	176.85	180.02	229.97	120.00	0.00	170.99	190.00	75.07
770.76	88.80	485.11	134.66	201.69	112.58	457.77	0.25	291.81	112.37	621.81	153.59	0.00	205.24	280.58	118.19
1429.31	431.35	231.01	101.41	481.60	196.78	128.86	0.15	510.49	134.31	279.27	157.32	0.00	95.52	204.83	62.94
1053.31	267.70	260.96	186.38	72.41	72.16	217.70	0.07	287.51	147.98	210.67	102.67	0.00	76.81	71.71	91.75
384.44	392.25	481.13	108.58	79.84	116.53	372.78	0.16	189.00	86.74	282.83	158.01	0.00	118.29	214.94	397.70
674.61	421.16	226.85	70.77	352.58	77.46	264.71	0.19	77.35	58.78	274.74	68.63	0.00	139.56	60.07	63.10
1467.07	467.33	99.31	139.09	226.06	120.37	214.66	0.26	184.77	98.17	218.49	114.03	0.00	144.90	248.65	83.89
1197.54	517.58	412.77	168.41	173.79	86.66	516.82	0.18	249.49	86.83	253.01	96.94	0.00	130.12	208.87	80.06
1051.19	437.43	421.34	167.09	133.18	115.37	303.33	0.26	166.71	63.95	134.28	82.50	0.00	76.83	455.76	101.27
570.78	447.98	503.87	89.62	123.96	64.59	430.03	0.17	174.22	50.35	210.23	58.42	0.00	66.60	293.40	63.91
945.66	430.49	91.38	69.07	143.23	115.03	231.83	0.17	147.38	86.07	281.65	77.77	0.00	76.39	157.89	96.19
1378.86	427.31	144.16	69.77	95.60	88.70	189.71	0.16	60.40	49.78	86.21	54.49	0.00	78.57	146.62	57.00
1816.11	149.81	378.57	71.62	324.68	101.45	366.58	0.15	239.47	88.29	169.96	128.39	0.00	115.69	136.78	87.92
2004.68	283.12	224.40	89.47	360.06	91.21	265.46	0.17	168.33	101.56	111.66	54.14	0.00	103.54	121.73	62.67
1757.74	439.61	488.47	119.74	189.51	116.90	134.11	0.25	244.72	89.72	440.69	114.36	0.00	102.27	311.74	65.68
1607.19	281.60	332.50	82.83	113.13	83.16	503.68	0.26	92.45	89.38	275.03	100.04	0.00	73.60	115.20	110.25
2217.76	473.86	351.90	131.39	173.54	88.16	293.72	0.14	299.66	63.52	221.22	63.90	0.00	105.70	348.52	77.18
1539.98	423.18	358.48	66.31	223.30	75.14	118.40	0.17	152.27	105.59	147.06	83.28	0.00	93.85	202.91	83.06
983.23	341.63	450.50	106.74	133.85	76.56	161.01	0.13	170.34	114.94	130.45	92.42	0.00	77.58	140.87	66.19
527.24	276.75	541.00	56.04	242.68	103.66	154.57	0.10	91.82	52.60	132.93	48.05	0.00	51.65	277.08	112.20
1536.23	384.67	507.10	67.16	94.90	118.54	98.46	0.07	109.97	99.51	448.13	80.84	0.00	122.04	644.22	94.41
741.26	399.67	287.37	59.08	111.43	55.92	101.61	0.25	0.10	60.98	142.11	97.49	0.00	98.04	318.53	77.65
874.50	371.75	269.02	95.68	397.78	73.57	88.09	0.10	158.62	70.07	197.78	86.60	0.00	122.29	304.51	90.78
1533.06	376.66	370.09	36.44	111.44	61.15	125.03	0.20	112.26	58.82	95.39	43.37	0.00	89.48	113.05	84.67
550.89	503.68	431.69	74.20	272.02	221.17	137.82	0.09	156.18	79.12	0.01	52.97	0.00	58.70	355.35	84.16
1564.97	384.50	591.95	76.79	158.38	59.41	209.33	0.15	102.15	74.69	167.09	67.31	0.00	80.43	84.10	50.27
346.50	560.15	526.76	88.91	196.44	81.79	86.34	0.08	104.02	51.47	199.76	66.42	0.00	97.27	324.18	70.59
748.67	442.26	300.59	91.49	373.43	47.00	71.56	0.23	75.28	77.36	214.17	45.35	0.00	220.70	21125.92	177.80
917.96	494.82	603.93	109.76	108.08	78.07	132.95	0.22	96.28	100.21	122.63	57.01	0.00	76.89	265.79	64.79
898.12	436.27	546.43	39.18	76.57	72.31	83.25	0.17	108.42	51.70	78.21	50.71	0.00	53.90	63.26	68.91
706.23	38.15	633.72	102.46	133.31	60.17	102.39	0.25	242.60	74.44	172.51	48.75	0.00	62.67	266.48	27.87

The minimum and maximum are 0.00000000E+00 21125.920

Table B-AM2c
Aerojet MC^2 Array
Star (α Ori) at top; Bias = 2.0v (Star M #1)

SKEWNESS

SKEW

0.000	0.044	0.009	0.046	0.052	0.079	0.047	0.389	0.002	0.007	0.000	0.005	0.000	0.005	0.000	0.054
2.863	0.001	0.243	0.015	0.001	0.015	0.036	0.164	0.009	0.003	0.003	0.012	0.000	0.000	0.045	0.031
0.075	3.087	0.086	0.002	0.000	0.025	0.008	0.152	0.043	0.000	0.006	0.382	0.000	0.424	0.019	0.002
0.477	0.369	0.012	0.000	0.001	0.016	0.013	0.913	0.014	0.070	0.000	0.036	0.000	0.006	0.006	0.000
0.550	0.333	0.012	0.027	0.007	0.015	0.286	0.011	0.003	0.017	0.085	0.005	0.000	0.473	0.009	0.014
0.168	0.447	0.007	0.000	0.008	0.000	0.001	1.845	0.027	0.031	0.035	0.004	0.000	0.002	0.001	0.005
0.345	0.435	0.004	0.000	0.009	0.000	0.001	0.956	0.001	0.030	0.059	0.012	0.000	0.243	0.022	0.000
0.354	0.209	0.180	0.014	0.000	0.001	0.000	0.109	0.030	0.068	0.103	0.000	0.000	0.004	0.000	0.014
0.521	0.321	0.003	0.003	0.148	0.000	0.027	1.318	0.003	0.044	0.003	0.110	0.000	0.007	0.005	0.010
0.558	0.527	0.002	0.018	0.013	0.005	0.002	0.001	0.005	0.013	0.004	0.004	0.000	0.016	0.003	0.084
0.416	0.478	0.067	0.003	0.006	0.001	0.011	1.068	0.021	0.001	0.012	0.014	0.000	0.000	0.087	0.010
0.698	0.432	0.027	0.003	0.024	0.013	0.088	1.270	0.000	0.006	0.072	0.001	0.000	0.017	0.015	0.008
0.827	0.387	0.376	0.001	0.025	0.023	0.011	1.856	0.005	0.022	0.111	0.000	0.000	0.005	0.092	0.000
0.514	0.140	0.066	0.017	0.000	0.001	0.001	0.137	0.000	0.000	0.031	0.005	0.000	0.007	0.083	0.014
0.412	0.211	0.083	0.000	0.005	0.008	0.026	1.681	0.008	0.003	0.006	0.001	0.000	0.000	0.000	0.011
0.219	0.316	0.010	0.004	0.004	0.000	0.003	0.076	0.019	0.021	0.000	0.003	0.000	0.004	0.026	0.013
0.580	0.226	0.282	0.000	0.062	0.012	0.081	0.048	0.003	0.027	0.017	0.001	0.000	0.009	0.006	0.022
0.199	0.211	0.146	0.000	0.057	0.001	0.024	0.580	0.000	0.019	0.005	0.002	0.000	0.016	0.002	0.000
0.424	0.496	0.585	0.011	0.006	0.037	0.002	0.855	0.003	0.009	0.009	0.040	0.000	0.019	0.047	0.000
0.187	0.412	0.449	0.000	0.002	0.001	0.000	0.250	0.013	0.000	0.000	0.004	0.000	0.008	0.061	0.056
0.045	0.528	0.389	0.026	0.017	0.064	0.167	0.001	0.079	0.000	0.000	0.002	0.000	0.001	0.161	0.035
0.361	0.648	0.613	0.002	0.059	0.001	0.012	0.038	0.041	0.009	0.015	0.026	0.000	0.008	0.013	0.015
0.008	0.567	0.475	0.000	0.007	0.002	0.007	0.045	6.180	0.008	0.047	0.000	0.000	0.006	0.001	0.001
0.026	0.388	0.014	0.011	0.004	0.000	0.170	2.657	0.013	0.008	0.000	0.000	0.000	0.014	0.006	0.007
0.338	0.516	0.459	0.011	0.000	0.001	0.156	0.834	0.020	0.008	0.032	0.018	0.000	0.019	0.022	0.000
0.005	0.391	0.434	0.023	0.044	0.504	0.177	0.804	0.160	0.022	128.535	0.000	0.000	0.001	0.060	0.016
0.136	0.469	0.417	0.032	0.013	0.000	0.016	2.750	0.000	0.010	0.010	0.017	0.000	0.003	0.039	0.005
0.010	0.582	0.345	0.017	0.050	0.001	0.000	1.785	0.002	0.012	0.038	0.014	0.000	0.026	0.060	0.047
0.029	0.382	0.189	0.039	0.001	0.002	0.003	0.306	0.008	0.002	0.004	0.033	0.000	0.427	1.191	0.269
0.205	0.528	0.437	0.178	0.027	0.005	0.012	0.601	0.075	0.012	0.012	0.005	0.000	0.001	0.351	0.002
0.329	0.688	0.514	0.237	0.008	0.008	0.002	1.084	0.021	0.003	0.035	0.006	0.000	0.030	0.002	0.015
0.227	0.002	0.241	0.224	0.034	0.000	0.007	0.001	0.031	0.004	0.169	0.032	0.000	0.001	0.081	0.000

The minimum and maximum are 0.00000000E+00 128.53517

Table B-AM2d
Aerojet MC^2 Array
Star (α Ori) at top; Bias = 2.0v (Star M #1)

KURTOSIS

KURT

5.426	3.206	3.260	3.352	3.299	3.102	4.103	10.815	2.992	2.871	3.093	2.933	1.000	3.106	3.196	3.170
10.572	2.356	3.692	2.932	2.627	3.113	3.227	5.215	3.114	2.947	3.277	3.363	1.000	3.240	3.391	3.161
3.420	5.460	3.407	2.903	2.929	2.911	2.633	1.753	3.561	2.954	2.803	3.881	1.000	3.881	3.189	3.052
4.010	3.773	3.610	2.784	2.650	2.974	2.968	5.542	2.919	3.479	3.035	3.255	1.000	2.944	3.658	3.057
4.096	3.817	3.549	2.732	2.936	3.161	4.046	14.360	2.651	2.717	3.521	3.229	1.000	4.853	4.261	3.278
3.436	3.946	3.039	3.355	3.253	2.949	2.690	4.099	3.761	3.074	3.389	2.986	1.000	3.051	3.529	2.919
3.882	3.984	3.910	2.939	2.608	3.375	4.138	2.980	3.461	3.022	3.419	3.183	1.000	3.862	3.184	3.028
3.648	3.675	3.745	3.093	3.777	2.925	3.660	2.096	3.330	3.328	3.445	3.064	1.000	2.855	3.646	2.854
4.195	3.674	3.423	2.879	4.731	2.867	3.034	2.728	3.292	3.733	4.049	3.777	1.000	3.029	4.293	3.224
4.262	4.003	3.075	2.833	3.036	2.954	3.372	1.313	3.501	3.209	3.546	2.955	1.000	3.098	3.146	3.711
3.896	3.978	3.096	2.916	3.134	3.134	2.509	4.263	4.421	3.237	4.136	2.996	1.000	3.194	3.512	2.878
4.332	3.878	2.978	2.990	3.555	3.169	3.670	4.203	3.388	3.025	3.683	3.117	1.000	3.028	4.416	2.931
4.480	3.776	4.180	3.131	3.293	2.770	4.280	3.852	3.509	3.084	4.032	2.906	1.000	3.071	4.354	3.398
3.908	3.257	3.470	2.892	3.275	3.262	2.709	7.867	3.218	2.717	3.373	3.078	1.000	2.892	4.967	2.760
3.606	3.434	3.630	3.052	3.411	2.887	3.411	2.889	3.175	2.788	2.569	3.077	1.000	2.842	3.403	2.865
3.687	3.750	2.991	3.064	2.779	3.078	4.008	1.276	2.904	2.958	3.062	3.091	1.000	3.002	3.257	3.180
4.078	3.668	4.047	2.836	3.739	2.993	2.719	1.328	3.165	3.040	3.662	2.976	1.000	3.148	3.364	2.701
3.373	3.637	3.426	2.995	3.454	2.927	3.878	6.866	3.198	3.074	3.009	2.831	1.000	2.970	3.199	3.108
3.950	4.111	4.412	2.976	3.470	3.325	3.395	4.543	3.396	2.583	3.716	2.789	1.000	2.878	4.084	3.147
3.595	3.866	4.312	2.828	4.463	3.038	3.514	7.647	3.478	2.899	3.352	2.828	1.000	3.188	3.277	2.991
3.453	4.147	3.800	3.190	3.915	2.962	4.007	9.838	4.113	2.950	3.665	2.837	1.000	3.022	3.589	2.958
3.801	4.564	4.323	3.028	3.351	2.916	3.080	14.607	3.148	2.734	2.825	3.144	1.000	2.943	2.907	3.289
2.801	4.203	4.033	3.205	2.964	3.312	3.410	1.193	7.179	2.952	3.415	2.704	1.000	2.875	2.981	3.125
3.141	3.707	2.976	3.174	[illegible].426	3.099	4.014	8.287	3.076	3.007	3.111	3.111	1.000	3.179	2.560	2.771
3.658	4.121	3.936	3.195	3.188	3.176	3.761	2.828	2.842	2.955	3.301	2.961	1.000	3.207	4.243	2.933
3.050	4.031	3.963	3.194	2.746	2.685	3.568	11.168	3.284	2.995	129.535	2.994	1.000	2.892	3.427	3.099
3.415	4.136	4.015	3.060	3.023	3.059	3.235	3.898	2.962	2.940	2.782	2.831	1.000	2.973	3.354	3.126
3.010	4.216	3.639	2.931	2.947	3.172	2.802	11.995	2.964	2.995	3.318	3.069	1.000	2.843	3.458	2.949
2.861	3.832	3.607	3.267	3.252	3.305	3.097	1.393	3.341	2.767	3.052	2.960	1.000	2.692	2.323	2.843
3.565	4.064	3.889	3.449	3.209	3.051	3.107	1.665	3.302	3.252	2.856	2.935	1.000	2.987	2.941	3.129
3.689	4.308	3.998	3.835	3.194	2.755	2.887	4.434	3.193	3.195	3.241	2.859	1.000	3.115	3.166	2.766
3.467	2.516	3.404	3.652	3.493	2.845	3.051	1.000	2.545	2.752	3.609	2.921	1.000	2.921	3.510	3.252

The minimum and maximum are 1.0000000 129.53477

Table B-AM3a
Aerojet MC^2 Array
Star (α Ori) at top; Bias = 1.8v (Star M #2)

AVERAGE COUNT/FRAME FOR 3200 FRAMES

AVE

723.60	556.89	1521.91	2453.32	1232.14	733.85	1021.12	382.70	923.26	618.71	1183.85	750.42	0.00	574.70	1081.00	2390.59
2.10	608.32	1258.08	879.04	1578.80	963.59	1721.67	373.70	1240.73	1056.98	1794.89	962.26	0.00	778.61	1233.67	860.87
510.59	6.20	1586.28	1059.01	1992.58	1119.51	1663.02	380.63	1601.00	1142.38	1652.26	1322.57	0.00	924.78	1849.05	1214.37
1144.85	1040.19	1593.31	1095.33	1768.45	1132.74	1670.17	382.51	1745.04	1203.05	2200.20	1233.37	0.00	1076.37	1667.48	999.43
1173.44	1041.07	1510.65	1022.93	1628.66	1181.81	2035.17	385.03	1915.35	1271.24	1716.41	1214.31	0.00	1200.05	1656.00	1056.72
195.25	922.71	1730.32	1033.91	2039.33	1180.49	1898.38	381.01	1695.32	1158.22	1703.73	1187.07	0.00	1099.93	1699.57	724.61
1489.32	907.07	1867.62	994.48	1989.00	1391.80	1696.39	383.42	1823.26	1185.07	1779.08	1308.66	0.00	1181.54	1661.20	1167.27
1150.94	974.33	1945.71	1086.62	1604.64	1226.91	1604.89	381.97	1672.35	1348.67	1717.72	1081.88	0.00	1229.69	1796.33	1130.94
1041.66	921.88	1516.13	1140.71	1757.09	1117.45	1669.95	383.97	1878.02	1170.31	1718.73	1168.73	0.00	1144.78	1677.63	1303.79
1066.06	981.17	1620.86	1124.16	1783.58	1212.50	1800.20	383.46	1782.62	1210.07	1712.94	1136.90	0.00	1260.84	1656.48	1165.86
1288.80	1000.94	1543.83	1201.68	1596.17	1153.90	1589.24	387.77	1510.91	1285.90	1739.55	1303.08	0.00	1544.86	1656.79	1496.21
1195.08	949.19	2056.61	1194.83	1605.55	1191.41	1840.80	385.66	1625.17	1281.52	1750.92	1243.85	0.00	1351.17	1703.23	1258.46
987.32	921.58	1624.76	1054.67	1557.16	1190.23	1671.23	383.49	1699.67	1253.12	1715.88	1332.11	0.00	1218.61	1709.12	1213.04
977.00	1675.52	1623.87	2177.81	1659.53	1178.54	1973.29	394.05	1691.34	1995.75	1980.27	1280.80	0.00	1156.78	1715.03	1195.02
991.18	1140.81	1775.26	1233.79	1661.50	1191.00	1684.61	382.59	1659.28	1253.39	1702.08	1264.51	0.00	1317.19	1750.78	1103.55
1044.85	894.84	1722.80	1081.12	1981.10	1194.66	1665.31	382.73	1647.10	1105.74	1909.67	1156.20	0.00	1137.07	1708.40	1288.08
977.03	899.92	1591.13	1074.46	1649.54	1176.19	1696.91	382.28	1682.83	1181.11	1725.94	1228.83	0.00	1257.26	1698.72	1163.24
945.43	800.10	1663.42	1063.56	1729.07	1152.97	1687.22	382.81	1730.64	1156.53	1698.22	1973.16	0.00	1170.59	1742.72	1188.31
880.33	846.15	1468.90	1089.52	1810.13	1208.22	1396.36	382.98	1772.74	1254.10	1767.04	1194.69	0.00	1380.02	1662.44	1229.19
1085.87	914.19	1541.29	1335.91	1576.05	1145.69	1650.07	381.00	1737.51	1150.11	1795.49	1124.36	0.00	1139.59	1675.68	1505.21
1266.56	982.26	1477.10	1109.90	1640.30	1168.59	1789.84	387.16	1857.52	1257.59	1724.83	1183.08	0.00	1271.08	1812.93	2173.34
862.35	760.48	1521.27	1052.05	2098.62	1137.44	1729.62	381.73	1784.54	1108.80	1665.39	1244.05	0.00	1328.89	1725.02	1221.41
412.53	736.47	1736.66	1085.85	1736.68	1123.60	1960.60	379.93	0.00	1245.18	1722.36	1188.24	0.00	1277.59	1799.52	1246.68
1257.72	909.42	676.71	1850.61	1191.75	1205.45	2316.03	386.97	1801.66	1060.63	1799.00	1224.50	0.00	1160.87	1870.59	1275.87
793.91	883.64	1724.06	947.59	1691.36	1160.15	1646.02	381.48	1706.50	2086.37	1815.28	1525.81	0.00	1156.30	1707.41	1075.10
1387.41	728.81	1493.48	1039.18	1677.28	1693.37	1951.01	383.85	1703.73	1222.04	12.98	1257.48	0.00	1398.06	1627.16	1162.45
836.89	832.15	1351.48	1171.74	1593.20	1081.86	691.64	382.21	1898.14	1145.86	1886.16	1181.76	0.00	1193.35	1905.43	1205.04
52.63	742.41	1413.70	1009.98	1646.89	1264.82	1714.21	380.90	1720.55	1586.00	326.15	1197.14	0.00	1207.70	681.59	1122.66
1513.22	802.58	1641.15	1012.87	1593.04	1548.13	1680.60	382.99	1713.07	1185.28	987.98	1233.18	0.00	1241.07	89.58	1338.28
795.29	769.71	1368.37	977.76	1587.60	1120.39	1596.67	383.00	1684.90	2079.07	1709.91	1072.94	0.00	1089.43	1072.15	1119.71
647.48	768.76	1321.49	955.60	1580.22	1054.27	1533.90	376.77	1625.77	1033.67	1678.14	1121.60	0.00	1175.58	1680.84	1140.58
860.87	2538.63	1463.91	950.25	1931.20	1025.00	1974.83	385.24	1614.04	1106.25	1712.29	1157.95	0.00	1093.72	1137.19	1234.68

The minimum and maximum are 0.00000000E+00 2538.6322

Table B-AM3b
Aerojet MC^2 Array
Star (α Ori) at top; Bias = 1.8v (Star M #2)

VARIANCE

VAR

676.40	152.07	301.37	76.05	447.07	150.46	205.67	0.21	114.12	166.56	119.60	79.81	0.00	98.89	108.83	44.17
49.59	1813.31	403.48	132.63	379.04	164.07	166.12	0.22	171.01	182.50	191.81	113.30	0.00	168.96	170.14	81.19
945.71	84.75	380.88	136.06	305.72	105.94	306.78	0.23	205.69	108.82	570.46	153.50	0.00	199.27	215.16	115.32
1618.80	456.84	181.99	101.26	356.42	186.09	123.45	0.26	499.86	130.23	240.33	170.06	0.00	99.39	179.40	66.41
1312.41	322.05	210.36	171.91	75.33	71.72	195.68	0.08	281.67	140.92	117.98	70.78	0.00	74.58	61.80	88.96
408.98	419.01	533.79	106.30	78.16	113.55	324.58	0.06	135.97	96.65	196.20	145.90	0.00	106.57	175.65	378.74
902.79	447.59	161.29	66.73	330.17	77.82	204.34	0.25	77.36	57.68	168.73	61.25	0.00	129.86	59.80	62.80
1220.00	509.28	78.82	128.77	181.83	127.45	163.65	0.15	134.65	89.63	160.47	100.29	0.00	118.85	196.64	77.95
1349.83	596.83	251.55	164.49	148.24	79.87	388.79	0.19	201.01	86.18	239.17	94.28	0.00	124.78	156.45	87.11
1275.89	525.83	336.36	178.28	127.45	121.79	241.76	0.26	137.84	66.31	144.94	84.72	0.00	79.86	331.87	114.30
694.96	533.32	476.16	84.50	116.27	64.19	376.88	0.19	136.35	50.17	169.05	51.98	0.00	65.52	170.38	62.41
1104.31	542.72	90.87	69.43	130.69	120.59	188.31	0.23	134.96	83.38	233.09	73.19	0.00	79.15	109.85	97.24
1477.17	567.24	104.73	69.18	95.36	82.91	136.20	0.25	61.62	49.43	94.77	52.03	0.00	84.53	97.19	53.01
1545.06	176.41	278.06	69.82	271.40	99.44	344.28	0.11	186.45	72.36	124.78	113.53	0.00	95.29	124.66	91.68
1664.10	373.84	144.13	79.83	295.26	82.91	196.22	0.24	127.41	95.09	62.47	43.32	0.00	83.68	107.80	63.68
1596.56	552.56	383.08	116.60	173.47	111.29	110.08	0.20	185.38	84.31	369.05	100.51	0.00	91.02	210.61	67.80
1807.41	398.82	248.34	81.74	111.05	79.01	413.19	0.22	77.03	82.93	222.96	93.04	0.00	84.61	98.01	113.18
2054.29	564.71	265.06	114.23	142.97	79.35	257.59	0.16	219.90	60.82	158.23	50.03	0.00	92.10	257.14	80.40
1803.32	490.27	269.19	70.32	176.12	70.94	134.25	0.03	137.92	95.52	118.51	73.29	0.00	83.95	148.96	82.62
1321.36	435.86	350.48	98.67	107.23	81.59	142.27	0.05	153.06	115.63	121.96	86.47	0.00	75.44	138.34	68.31
838.07	356.04	430.93	57.76	254.91	116.38	129.82	0.16	96.42	51.39	133.50	49.94	0.00	59.42	240.19	98.25
1770.71	415.37	418.50	64.46	92.32	119.72	101.57	0.22	103.69	100.82	304.89	85.20	0.00	127.23	656.32	97.89
533.57	417.78	296.82	58.66	106.00	54.68	98.48	0.08	0.00	48.39	96.71	87.93	0.00	92.71	243.98	63.45
1170.97	410.18	235.06	99.19	384.08	73.67	82.08	0.13	135.50	68.81	166.36	84.16	0.00	107.75	277.57	90.52
2202.72	419.46	389.23	59.73	111.40	66.47	149.71	0.25	105.79	57.14	78.78	39.28	0.00	83.23	82.65	80.01
702.79	474.60	454.44	59.67	251.61	123.40	144.12	0.20	143.93	80.19	0.06	55.24	0.00	62.68	274.63	93.93
1639.57	358.95	583.08	49.98	145.15	50.93	190.49	0.19	91.98	71.24	108.18	59.51	0.00	66.94	75.95	48.48
289.34	545.07	619.96	70.39	183.59	85.42	89.31	0.10	109.76	50.56	183.56	67.97	0.00	97.25	239.50	73.10
987.41	443.20	355.60	69.79	364.37	49.24	72.05	0.02	88.73	97.37	193.44	43.97	0.00	119.07	7221.46	126.75
1442.74	489.45	706.43	93.04	102.99	79.34	126.21	0.02	102.11	88.89	134.24	56.96	0.00	86.97	148.28	65.07
1209.66	411.80	680.19	75.87	75.78	70.73	77.84	0.18	106.19	51.46	77.84	50.13	0.00	57.91	52.97	66.67
1054.63	30.97	760.57	80.10	136.06	55.58	101.29	0.19	262.21	66.73	184.57	50.28	0.00	63.72	165.68	26.95

The minimum and maximum are 0.00000000E+00 7221.4596

Table B-AM3c
Aerojet MC^2 Array
Star (α Ori) at top; Bias = 1.8v (Star M #2)

SKEWNESS

SKEW

1.325	0.038	0.016	0.038	0.186	0.053	0.010	0.739	0.000	0.002	0.005	0.028	0.000	0.008	0.005	0.021
19.838	0.349	0.028	0.004	0.005	0.027	0.008	0.581	0.001	0.008	0.009	0.010	0.000	0.032	0.036	0.038
0.009	3.848	0.164	0.000	0.004	0.006	0.118	0.296	0.042	0.007	0.026	0.231	0.000	0.299	0.020	0.006
0.000	0.002	0.002	0.004	0.040	0.029	0.010	0.021	0.012	0.032	0.010	0.091	0.000	0.028	0.016	0.003
0.000	0.000	0.001	0.008	0.012	0.013	0.014	0.891	0.021	0.027	0.031	0.008	0.000	0.428	0.017	0.008
0.002	0.001	0.008	0.017	0.001	0.009	0.000	0.084	0.025	0.032	0.015	0.002	0.000	0.002	0.054	0.004
0.001	0.002	0.005	0.001	0.024	0.014	0.118	0.116	0.001	0.002	0.055	0.000	0.000	0.197	0.000	0.000
0.001	0.000	0.043	0.001	0.001	0.027	0.002	0.098	0.003	0.092	0.048	0.002	0.000	0.000	0.001	0.005
0.002	0.002	0.004	0.016	0.241	0.013	0.163	0.030	0.000	0.073	0.007	0.033	0.000	0.004	0.002	0.037
0.000	0.001	0.012	0.000	0.001	0.012	0.000	0.053	0.007	0.005	0.002	0.015	0.000	0.004	0.054	0.035
0.000	0.001	0.074	0.001	0.000	0.003	0.078	1.262	0.080	0.000	0.001	0.000	0.000	0.002	0.143	0.009
0.000	0.000	0.005	0.039	0.005	0.000	0.027	0.444	0.002	0.000	0.001	0.002	0.000	0.005	0.012	0.019
0.000	0.011	0.014	0.007	0.000	0.000	0.002	0.010	0.009	0.007	0.004	0.005	0.000	0.000	0.103	0.000
0.001	0.002	0.002	0.019	0.005	0.005	0.000	0.961	0.001	0.001	0.010	0.010	0.000	0.003	0.068	0.000
0.001	0.019	0.002	0.010	0.001	0.008	0.016	0.138	0.014	0.000	0.001	0.029	0.000	0.002	0.008	0.000
0.000	0.009	0.011	0.000	0.030	0.001	0.004	1.030	0.049	0.001	0.012	0.001	0.000	0.003	0.017	0.006
0.000	0.016	0.003	0.007	0.013	0.013	0.136	0.477	0.020	0.009	0.014	0.031	0.000	0.019	0.002	0.007
0.003	0.005	0.027	0.000	0.045	0.033	0.005	2.339	0.004	0.005	0.011	0.045	0.000	0.016	0.054	0.000
0.000	0.020	0.033	0.003	0.001	0.046	0.000	14.860	0.012	0.011	0.009	0.011	0.000	0.008	0.020	0.013
0.005	0.009	0.034	0.000	0.001	0.003	0.008	0.017	0.012	0.004	0.001	0.021	0.000	0.002	0.002	0.033
0.010	0.004	0.005	0.001	0.107	0.034	0.051	1.567	0.069	0.004	0.010	0.001	0.000	0.006	0.171	0.020
0.004	0.017	0.024	0.000	0.012	0.007	0.001	0.428	0.048	0.0[illegible]1	0.029	0.000	0.000	0.005	0.007	0.007
0.025	0.001	0.001	0.004	0.000	0.025	0.028	4.834	0.000	0.002	0.154	0.007	0.000	0.000	0.001	0.010
0.019	0.001	0.001	0.000	0.005	0.002	0.108	0.194	0.039	0.000	0.006	0.001	0.000	0.091	0.007	0.014
0.021	0.002	0.002	0.009	0.000	0.001	0.304	0.008	0.004	0.044	0.010	0.022	0.000	0.004	0.012	0.020
0.000	0.002	0.002	0.000	0.069	0.000	0.141	0.468	0.124	0.010	455.483	0.006	0.000	0.023	0.024	0.024
0.030	0.004	0.001	0.026	0.003	0.014	0.016	0.862	0.017	0.002	0.002	0.019	0.000	0.000	0.001	0.025
0.005	0.000	[illegible].000	0.015	0.065	0.007	0.019	5.522	0.010	0.012	0.014	0.000	0.000	0.030	0.001	0.000
0.001	0.000	0.000	0.002	0.035	0.000	0.000	13.045	0.004	0.005	0.004	0.000	0.000	0.293	3.385	0.244
0.014	0.000	0.001	0.006	0.008	0.023	0.002	0.178	0.060	0.029	0.001	0.008	0.000	0.013	0.183	0.020
0.024	0.001	0.000	0.040	0.030	0.005	0.006	1.641	0.007	0.005	0.029	0.004	0.000	0.040	0.005	0.000
0.016	0.017	0.003	0.007	0.000	0.004	0.010	1.299	0.023	0.011	0.232	0.003	0.000	0.006	0.016	0.012

The minimum and maximum are 0.00000000E+00 455.48313

Table B-AM3d
Aerojet MC^2 Array
Star (α Ori) at top; Bias = 1.8v (Star M #2)

KURTOSIS

KURT

12.275	2.994	3.858	3.252	3.781	3.005	3.412	1.821	3.005	2.883	2.886	3.058	1.000	3.112	3.149	2.904
26.500	3.201	2.851	2.908	3.033	3.338	3.067	1.963	3.122	2.919	3.315	2.915	1.000	3.070	2.962	3.202
3.042	6.547	3.894	2.862	2.519	2.957	3.353	1.319	3.777	3.100	2.989	3.638	1.000	3.796	3.189	2.900
2.606	2.679	3.834	3.111	3.104	3.188	3.099	1.271	3.658	3.421	3.325	3.182	1.000	3.142	3.047	3.153
2.556	2.467	3.568	2.750	3.105	3.092	4.064	11.739	2.769	2.724	4.042	2.992	1.000	4.965	3.255	3.081
3.000	2.695	2.583	3.425	2.895	3.103	3.069	17.004	3.630	3.028	3.696	2.886	1.000	2.921	3.706	3.198
2.555	2.594	4.210	3.015	2.882	3.554	7.183	1.255	3.332	3.116	4.101	3.022	1.000	3.605	2.993	2.777
2.503	2.543	3.950	3.036	3.898	2.708	3.533	6.597	3.066	3.160	3.270	2.958	1.000	2.984	3.244	3.028
2.688	2.642	4.264	3.032	4.420	3.129	3.524	5.279	3.538	3.511	3.484	3.467	1.000	3.047	4.523	3.307
2.558	2.552	3.096	2.908	3.043	2.971	3.344	1.256	3.202	3.003	3.020	3.054	1.000	3.047	3.667	3.331
2.633	2.506	3.244	2.953	2.934	3.135	2.793	2.715	4.096	2.942	4.553	3.167	1.000	2.900	4.132	3.044
2.623	2.560	2.719	3.140	3.359	3.258	3.618	1.493	3.303	2.906	3.491	3.300	1.000	2.853	3.738	2.881
2.474	2.426	3.368	2.931	3.061	2.911	4.240	1.162	3.008	3.039	3.463	3.277	1.000	3.035	4.801	3.362
2.476	2.768	3.005	2.945	3.388	3.338	2.580	8.437	3.668	2.865	4.212	2.820	1.000	2.991	4.720	2.775
2.488	2.695	3.345	2.893	3.741	2.850	3.689	1.200	3.360	2.763	3.171	2.985	1.000	3.049	3.317	2.962
2.504	2.500	3.024	2.949	2.812	2.863	3.696	2.029	3.205	3.195	3.345	2.969	1.000	3.106	3.717	2.985
2.532	2.579	3.173	2.993	3.470	3.133	3.140	2.179	3.311	3.096	3.327	3.174	1.000	3.198	3.078	2.744
2.475	2.861	3.000	2.857	3.345	3.057	4.005	3.389	3.189	2.866	2.938	3.113	1.000	3.166	3.864	3.516
2.382	2.592	2.907	2.984	3.761	3.228	2.960	36.333	3.779	2.649	3.553	3.080	1.000	2.900	4.246	2.820
2.535	2.596	2.726	2.922	3.749	3.163	3.453	19.039	3.288	2.799	3.150	2.925	1.000	3.140	3.199	3.078
2.712	2.580	2.943	2.899	4.160	2.718	4.107	4.420	3.513	3.095	3.344	2.936	1.000	3.160	3.627	3.132
2.442	2.642	2.699	3.013	3.065	3.038	3.200	2.384	3.368	2.779	3.459	2.966	1.000	2.939	2.813	2.930
2.916	2.644	2.668	3.239	3.199	3.106	3.374	9.962	1.000	2.886	4.397	2.812	1.000	2.897	3.439	3.367
2.566	2.592	2.993	2.968	3.255	2.937	3.843	7.546	3.018	2.828	3.497	3.019	1.000	3.398	2.744	2.824
2.404	2.719	2.585	3.446	3.166	3.119	3.757	1.047	3.028	2.974	3.435	2.937	1.000	3.266	3.803	2.872
2.753	2.595	2.509	3.059	2.759	2.940	3.453	4.018	3.284	2.992	979.008	3.024	1.000	3.195	3.880	2.920
2.521	2.630	2.867	3.540	2.867	3.281	3.350	3.129	3.042	2.872	2.913	2.779	1.000	3.003	3.764	3.077
2.973	2.620	2.629	3.379	3.094	2.755	2.959	7.669	3.088	2.985	3.145	3.144	1.000	2.843	3.368	3.330
2.776	2.731	2.742	3.218	3.186	3.129	2.899	47.166	2.987	2.830	3.033	3.141	1.000	3.316	4.883	3.204
2.550	2.649	2.545	2.975	3.099	3.187	3.302	43.813	3.498	2.936	2.949	3.154	1.000	2.963	3.354	3.470
2.539	2.561	2.500	2.932	3.553	2.802	3.204	2.640	3.285	2.977	3.298	2.875	1.000	3.361	3.193	3.002
2.572	2.988	2.606	2.893	3.494	3.180	3.143	2.545	2.491	3.049	3.795	2.932	1.000	3.026	3.050	2.997

The minimum and maximum are 1.0000000 979.00818

Table B-AM4a
Aerojet MC^2 Array
Background Run #2 (BGM #2) Before Star Sighting

AVERAGE COUNT/FRAME FOR 3200 FRAMES

AVE

710.97	550.45	1516.68	2453.70	1227.14	730.45	1016.90	382.65	918.94	615.63	1180.64	747.60	0.00	571.80	1077.66	2390.83
1.76	610.83	1244.66	874.02	1572.17	958.94	1715.99	373.54	1235.17	1053.01	1790.43	958.43	0.00	774.08	1227.84	858.32
496.75	6.08	1579.81	1058.36	1992.25	1119.65	1663.30	380.61	1600.15	1141.31	1650.29	1320.53	0.00	923.78	1848.32	1213.75
1122.19	1029.74	1590.13	1095.32	1769.23	1132.60	1670.03	382.50	1745.19	1202.89	2201.37	1234.67	0.00	1076.96	1668.65	1000.85
1152.78	1033.06	1506.84	1022.60	1628.89	1181.73	2035.73	385.02	1915.46	1272.19	1716.32	1215.34	0.00	1201.04	1656.94	1057.37
186.98	912.71	1726.96	1033.18	2039.70	1179.46	1898.17	381.01	1694.91	1158.31	1703.96	1187.74	0.00	1100.38	1699.69	744.37
1474.28	897.09	1864.33	994.42	1987.94	1390.92	1696.04	383.42	1823.64	1184.83	1779.21	1308.53	0.00	1181.27	1662.18	1168.03
1130.95	883.11	1944.78	1086.54	1604.34	1226.83	1605.47	381.98	1672.07	1348.46	1717.68	1082.49	0.00	1229.99	1797.03	1131.47
1021.16	910.14	1510.68	1140.24	1756.79	1117.75	1668.91	383.97	1878.04	1170.52	1718.98	1168.55	0.00	1145.14	1678.55	1304.60
1046.43	969.46	1618.42	1123.46	1783.23	1212.48	1801.38	383.47	1784.03	1209.99	1713.12	1137.00	0.00	1260.32	1657.77	1166.49
1273.45	989.09	1538.80	1201.66	1596.17	1153.96	1589.19	387.78	1511.14	1286.21	1739.70	1303.65	0.00	1545.52	1657.37	1496.89
1175.69	937.62	2056.70	1194.49	1605.34	1191.72	1841.83	385.65	1625.20	1281.50	1750.72	1243.85	0.00	1352.17	1703.90	1259.08
964.12	909.41	1619.95	1053.87	1556.80	1190.21	1670.81	383.49	1699.61	1252.81	1715.96	1331.90	0.00	1218.81	1710.40	1213.66
952.40	1670.16	1617.33	2177.68	1659.33	1178.67	1972.80	394.05	1691.69	1995.66	1980.54	1281.22	0.00	1158.40	1716.29	1195.24
966.58	1131.67	1771.15	1233.63	1661.79	1191.28	1684.32	382.60	1659.70	1253.59	1702.13	1264.91	0.00	1317.42	1751.44	1104.20
1020.50	883.36	1717.41	1080.70	1979.55	1194.80	1665.47	382.71	1647.41	1105.92	1909.25	1156.43	0.00	1137.57	1708.59	1288.46
950.84	889.93	1584.31	1073.43	1648.78	1175.82	1695.96	382.29	1683.17	1181.24	1725.43	1229.00	0.00	1257.99	1699.33	1164.51
919.95	789.20	1656.37	1062.54	1728.97	1153.05	1687.09	382.77	1730.04	1156.47	1698.12	1971.53	0.00	1170.74	1742.65	1188.85
854.50	835.25	1460.46	1088.72	1808.31	1208.21	1396.27	382.98	1773.09	1253.97	1766.37	1194.30	0.00	1379.63	1662.87	1229.86
1064.20	903.48	1532.22	1333.70	1575.76	1145.34	1649.34	380.98	1737.10	1149.72	1795.02	1124.49	0.00	1199.62	1676.35	1505.04
1251.97	972.54	1466.55	1108.22	1640.66	1168.07	1789.56	387.16	1857.44	1257.53	1724.74	1183.27	0.00	1271.31	1813.25	2173.60
837.08	749.86	1510.52	1050.18	2098.70	1137.33	1728.59	381.69	1784.44	1108.26	1666.24	1244.66	0.00	1328.97	1724.97	1221.87
406.19	725.98	1728.77	1084.53	1737.37	1123.63	1960.33	379.91	0.00	1245.50	1722.57	1188.36	0.00	1277.62	1800.22	1247.20
1239.86	898.64	672.82	1850.09	1191.53	1204.96	2316.85	386.96	1801.13	1060.47	1798.66	1224.29	0.00	1160.99	1870.72	1275.93
767.99	873.20	1714.45	945.28	1691.26	1169.89	1645.96	381.44	1706.59	2086.38	1814.82	1526.38	0.00	1156.34	1707.56	1074.94
1376.46	717.13	1482.90	1036.52	1676.66	1692.33	1950.29	383.78	1703.68	1221.37	12.97	1256.73	0.00	1397.76	1627.41	1162.68
816.65	821.57	1339.82	1168.65	1593.55	1081.59	690.94	382.20	1897.18	1145.48	1884.82	1181.60	0.00	1193.32	1905.57	1205.52
46.21	730.03	1400.61	1006.49	1646.71	1264.15	1713.79	380.85	1711.75	1583.69	329.24	1197.06	0.00	1207.32	682.40	1122.71
1502.92	791.47	1632.41	1009.39	1593.62	1647.74	1679.80	382.96	1701.17	1172.67	982.14	1232.60	0.00	1242.63	68.55	1339.60
775.55	737.42	1354.62	973.72	1587.67	1119.53	1596.18	382.98	1674.49	2077.59	1699.98	1071.86	0.00	1089.35	1074.31	1119.99
627.84	756.71	1308.17	951.29	1579.21	1053.66	1533.12	376.67	1623.06	1031.10	1674.97	1120.97	0.00	1175.72	1681.19	1140.67
843.58	2538.00	1471.51	945.60	1931.14	1024.49	1975.00	385.23	1613.15	1105.51	1711.73	1157.97	0.00	1094.07	1134.62	1235.00

The minimum and maximum are 0.00000000E+00 2538.0048

Table B-AM4b
Aerojet MC^2 Array
Background Run #2 (BGM #2) Before Star Sighting

VARIANCE

VAR

902.18	231.09	324.05	70.76	445.83	162.70	202.81	0.23	125.60	166.93	128.04	87.87	0.00	103.01	118.69	43.55
38.78	2463.41	654.40	159.06	424.74	180.45	173.94	0.25	185.70	192.51	195.95	117.63	0.00	180.85	185.41	80.99
1351.67	86.64	451.38	136.86	304.01	118.59	303.48	0.24	232.39	112.30	568.83	144.87	0.00	196.55	229.58	121.43
3036.11	852.27	215.63	98.69	348.70	175.04	120.43	0.26	537.37	131.99	236.90	176.30	0.00	97.83	179.66	65.86
2538.26	569.70	237.43	170.89	76.50	67.98	188.62	0.10	271.08	141.14	123.76	66.50	0.00	73.72	62.13	86.05
607.04	795.06	549.78	107.00	72.73	117.03	318.49	0.07	148.35	91.49	191.85	144.16	0.00	113.43	171.33	327.93
1638.91	825.48	171.14	66.49	336.12	75.68	211.33	0.25	78.08	55.54	166.09	61.65	0.00	130.74	56.04	68.77
2418.26	930.21	81.49	137.58	186.27	119.81	158.58	0.17	133.52	88.67	162.89	95.74	0.00	121.53	195.05	78.34
2483.70	1036.72	339.23	167.11	150.54	80.58	445.59	0.20	195.59	84.76	251.00	95.16	0.00	129.26	165.80	84.98
2469.79	1053.10	393.68	180.99	124.98	116.71	234.40	0.26	144.19	67.49	139.04	82.80	0.00	77.75	323.64	106.13
1424.51	1061.43	521.01	86.16	121.62	64.68	387.96	0.19	142.85	53.24	169.85	51.78	0.00	62.64	180.84	58.24
2200.53	1047.79	102.56	64.66	135.99	121.80	204.64	0.23	143.92	84.17	282.24	76.77	0.00	83.22	120.24	102.87
3021.36	1092.48	170.96	67.18	91.39	89.68	140.82	0.25	63.28	49.51	93.64	54.27	0.00	79.33	93.06	53.46
3116.34	283.65	400.54	69.44	266.45	99.43	358.16	0.11	164.88	74.47	117.33	113.87	0.00	97.79	105.30	89.62
3302.24	632.09	217.29	80.30	300.76	84.88	199.31	0.25	131.51	102.36	60.97	45.30	0.00	83.46	108.81	68.10
3188.34	1039.52	433.55	117.03	175.98	112.74	110.15	0.21	185.05	83.57	364.99	95.47	0.00	90.83	190.78	66.52
3622.30	735.04	402.34	81.34	112.09	76.40	437.47	0.23	80.41	86.58	231.88	98.04	0.00	82.52	100.00	108.72
3794.11	941.27	404.89	124.48	152.19	79.26	230.97	0.18	219.27	63.89	154.85	50.19	0.00	89.39	262.27	80.34
3590.25	931.89	489.12	66.03	187.99	75.52	131.46	0.03	131.44	99.58	117.95	68.44	0.00	86.21	153.86	82.06
2533.69	822.46	631.97	96.84	109.98	78.96	143.85	0.06	170.15	120.99	133.46	84.32	0.00	75.08	141.34	70.27
1442.06	687.72	759.50	61.60	249.85	114.43	122.57	0.16	92.81	55.16	137.49	48.52	0.00	58.39	234.49	95.40
3416.90	808.28	824.78	69.25	93.85	123.42	106.28	0.24	106.24	101.96	318.68	83.85	0.00	133.90	695.61	90.95
743.89	770.17	521.33	60.95	102.98	54.91	100.30	0.10	0.00	42.65	101.06	89.37	0.00	87.72	267.63	64.52
2132.69	732.90	281.76	98.12	368.45	76.71	79.42	0.15	132.91	73.57	181.16	82.36	0.00	107.65	290.64	92.62
4125.11	781.80	750.97	66.66	111.62	63.15	146.34	0.25	101.24	58.36	82.40	38.96	0.00	79.68	79.87	76.22
1042.09	904.80	855.34	72.19	250.13	130.51	135.36	0.22	140.56	76.76	0.03	52.86	0.00	57.97	268.39	94.58
3114.63	705.35	1096.03	59.07	141.24	49.73	192.15	0.19	86.81	67.29	107.83	60.06	0.00	65.76	74.74	48.92
360.44	1050.74	1183.07	86.79	179.91	83.94	87.92	0.13	110.08	52.97	189.96	72.12	0.00	102.53	225.63	71.06
1434.80	812.92	650.03	86.09	345.46	50.88	68.79	0.04	71.20	76.57	183.23	43.02	0.00	97.99	3444.17	96.94
2588.57	946.31	1380.63	123.01	108.45	81.44	126.92	0.04	92.76	85.50	107.56	57.77	0.00	88.17	115.86	64.42
2289.70	824.43	1379.14	110.45	78.36	72.20	75.64	0.22	100.18	51.00	70.02	47.08	0.00	55.02	54.74	62.75
1937.63	31.43	1357.00	123.24	144.56	54.17	92.76	0.19	259.91	67.33	187.30	51.40	0.00	60.44	164.96	26.63

The minimum and maximum are 0.00000000E+00 4125.1122

Table B-AM4c
Aerojet MC^2 Array
Background Run #2 (BGM #2) Before Star Sighting

SKEWNESS

SKEW

0.140	0.045	0.000	0.098	0.115	0.082	0.039	0.490	0.000	0.002	0.000	0.016	0.000	0.005	0.000	0.027
20.971	0.174	0.003	0.001	0.000	0.033	0.037	0.011	0.002	0.013	0.003	0.009	0.000	0.011	0.005	0.051
0.026	4.441	0.072	0.001	0.000	0.009	0.190	0.194	0.012	0.000	0.035	0.273	0.000	0.318	0.016	0.001
0.076	0.063	0.017	0.011	0.014	0.011	0.016	0.021	0.002	0.048	0.004	0.132	0.000	0.013	0.024	0.004
0.087	0.069	0.009	0.002	0.033	0.012	0.054	0.222	0.035	0.042	0.195	0.000	0.000	0.457	0.001	0.008
0.019	0.061	0.003	0.003	0.001	0.001	0.001	0.048	0.011	0.009	0.002	0.005	0.000	0.006	0.035	0.016
0.084	0.073	0.016	0.005	0.034	0.007	0.008	0.131	0.010	0.012	0.078	0.001	0.000	0.219	0.007	0.003
0.092	0.091	0.097	0.001	0.023	0.015	0.012	0.024	0.003	0.009	0.077	0.000	0.000	0.002	0.000	0.002
0.079	0.058	0.012	0.004	0.160	0.002	0.099	0.018	0.001	0.019	0.018	0.048	0.000	0.013	0.004	0.002
0.075	0.109	0.009	0.007	0.001	0.010	0.003	0.036	0.043	0.010	0.006	0.024	0.000	0.006	0.055	0.007
0.065	0.122	0.066	0.005	0.001	0.001	0.073	1.268	0.098	0.000	0.001	0.000	0.000	0.003	0.122	0.020
0.072	0.136	0.012	0.036	0.014	0.002	0.009	0.383	0.001	0.001	0.004	0.006	0.000	0.020	0.004	0.007
0.069	0.145	0.001	0.010	0.000	0.000	0.006	0.008	0.000	0.022	0.001	0.005	0.000	0.002	0.095	0.000
0.052	0.067	0.003	0.014	0.000	0.000	0.002	0.760	0.002	0.000	0.010	0.035	0.000	0.003	0.000	0.004
0.071	0.112	0.004	0.004	0.005	0.005	0.043	0.155	0.031	0.002	0.000	0.004	0.000	0.011	0.010	0.000
0.080	0.154	0.001	0.001	0.024	0.001	0.000	0.864	0.051	0.002	0.002	0.000	0.000	0.001	0.013	0.002
0.098	0.167	0.001	0.000	0.043	0.000	0.089	0.405	0.020	0.003	0.026	0.006	0.000	0.029	0.002	0.007
0.073	0.143	0.011	0.001	0.046	0.005	0.000	1.673	0.014	0.014	0.001	0.047	0.000	0.026	0.149	0.018
0.114	0.165	0.000	0.006	0.012	0.039	0.010	19.979	0.004	0.002	0.000	0.009	0.000	0.027	0.034	0.006
0.129	0.147	0.000	0.016	0.036	0.006	0.000	0.747	0.015	0.002	0.009	0.016	0.000	0.001	0.029	0.023
0.129	0.174	0.010	0.003	0.058	0.075	0.160	1.462	0.094	0.021	0.027	0.002	0.000	0.000	0.202	0.021
0.133	0.132	0.003	0.006	0.008	0.000	0.013	0.219	0.014	0.007	0.070	0.002	0.000	0.004	0.020	0.008
0.152	0.093	0.012	0.001	0.001	0.002	0.012	3.689	0.000	0.001	0.025	0.014	0.000	0.006	0.050	0.005
0.176	0.081	0.002	0.000	0.003	0.003	0.141	0.109	0.052	0.001	0.001	0.000	0.000	0.226	0.040	0.005
0.209	0.077	0.065	0.000	0.002	0.001	0.215	0.062	0.001	0.048	0.042	0.019	0.000	0.025	0.119	0.001
0.068	0.069	0.038	0.000	0.065	0.004	0.100	0.382	0.074	0.016	30.011	0.021	0.000	0.016	0.048	0.010
0.210	0.082	0.045	0.000	0.010	0.003	0.000	0.858	0.019	0.000	0.012	0.027	0.000	0.011	0.002	0.015
0.028	0.083	0.079	0.036	0.026	0.000	0.001	3.349	0.000	0.049	0.000	0.003	0.000	0.010	0.000	0.014
0.067	0.074	0.081	0.019	0.021	0.001	0.006	11.731	0.008	0.000	0.027	0.002	0.000	0.241	10.233	0.173
0.213	0.068	0.103	0.006	0.024	0.002	0.000	6.196	0.104	0.057	0.005	0.025	0.000	0.005	0.109	0.011
0.225	0.066	0.129	0.000	0.002	0.001	0.003	0.554	0.002	0.000	0.093	0.000	0.000	0.054	0.001	0.001
0.213	0.015	0.090	0.000	0.015	0.000	0.001	1.165	0.029	0.001	0.221	0.007	0.000	0.007	0.000	0.007

The minimum and maximum are 0.00000000E+00 30.011155

Table B-AM4d
Aerojet MC^2 Array
Background Run #2 (BGM #2) Before Star Sighting

KURTOSIS

KURT

3.564	2.778	3.585	3.507	3.649	3.246	3.743	1.697	3.025	2.876	3.094	3.216	1.000	3.053	3.361	3.012
27.908	2.702	2.611	2.865	3.056	3.353	3.076	1.184	3.335	2.950	3.428	2.920	1.000	3.448	3.265	2.922
2.733	7.316	3.618	2.884	2.548	2.910	3.640	1.238	3.263	2.834	2.966	3.696	1.000	3.933	3.197	2.938
2.294	2.357	3.479	2.902	3.191	3.133	2.836	1.338	3.507	3.335	3.336	3.183	1.000	3.200	3.183	3.017
2.312	2.383	3.361	2.742	3.267	3.155	4.155	10.110	2.823	2.771	4.655	2.933	1.000	4.898	3.101	3.309
2.646	2.433	2.612	3.300	2.957	3.020	3.015	13.380	3.492	3.083	3.694	2.994	1.000	3.133	3.805	3.010
2.370	2.372	4.021	2.919	2.877	3.582	4.213	1.253	3.193	2.966	4.083	3.171	1.000	3.831	3.011	2.693
2.307	2.402	4.091	3.040	3.933	2.900	3.172	5.986	3.390	2.901	3.491	3.009	1.000	2.994	3.314	3.054
2.339	2.440	3.772	2.871	4.031	3.005	3.614	5.019	3.565	3.410	3.547	3.292	1.000	3.113	4.293	3.331
2.399	2.298	3.134	2.820	3.190	3.016	3.399	1.225	3.455	3.090	3.607	3.014	1.000	2.996	3.918	3.294
2.326	2.301	3.214	2.996	2.973	2.911	2.813	2.907	4.206	2.951	4.412	3.290	1.000	3.113	4.148	3.044
2.391	2.327	2.955	3.285	3.097	3.060	3.538	1.407	3.463	2.840	3.752	3.287	1.000	3.119	3.757	2.955
2.277	2.263	2.660	2.950	3.087	2.968	4.597	1.124	3.047	2.951	3.602	3.269	1.000	3.045	5.265	3.572
2.292	2.662	3.030	2.820	3.475	3.033	2.548	8.726	3.369	2.890	4.003	2.873	1.000	2.854	4.548	2.791
2.268	2.408	2.935	3.011	3.753	2.850	4.038	1.450	3.243	2.699	2.882	3.034	1.000	3.039	3.626	2.764
2.276	2.369	2.922	3.103	2.675	2.968	3.552	2.005	3.174	2.991	3.349	2.885	1.000	2.908	3.519	2.951
2.245	2.344	2.864	2.997	3.526	2.958	2.939	2.133	3.216	2.830	3.719	2.790	1.000	2.952	3.202	2.715
2.308	2.491	2.739	2.792	3.026	3.173	3.708	2.672	3.302	3.037	3.174	3.117	1.000	3.106	3.915	3.197
2.224	2.422	2.458	2.959	3.932	3.229	3.148	34.389	3.753	2.863	3.517	3.045	1.000	2.938	4.544	2.751
2.311	2.414	2.622	3.107	3.620	2.987	3.688	16.206	3.251	2.839	3.388	2.983	1.000	3.176	3.257	3.245
2.365	2.416	2.511	3.036	4.070	2.827	4.496	4.153	3.899	2.984	3.687	3.047	1.000	3.530	3.855	3.012
2.253	2.398	2.473	3.137	2.980	2.941	3.015	2.105	2.959	2.755	3.559	3.262	1.000	3.005	2.703	3.004
2.831	2.462	2.430	3.040	3.094	3.574	3.211	8.313	1.000	2.873	3.855	2.821	1.000	2.853	3.371	3.156
2.360	2.442	3.011	3.157	3.309	2.964	3.845	6.508	3.020	2.887	3.179	2.992	1.000	3.812	2.774	2.935
2.311	2.302	2.344	3.017	2.999	3.431	3.713	1.082	2.900	2.814	3.549	2.873	1.000	3.353	5.065	2.914
2.690	2.469	2.354	2.927	2.888	2.899	3.396	3.024	3.295	2.999	31.011	2.984	1.000	3.220	3.964	2.850
2.384	2.371	2.400	3.097	3.321	3.063	3.191	3.378	3.048	3.155	3.069	2.875	1.000	3.029	3.450	2.968
2.863	2.348	2.323	3.286	3.199	2.764	2.990	4.632	2.838	3.263	3.079	3.248	1.000	2.933	3.330	3.401
2.781	2.448	2.401	3.140	3.424	3.214	2.795	21.020	3.144	2.933	3.001	3.159	1.000	3.754	12.394	3.339
2.485	2.352	2.353	2.955	3.291	3.222	3.206	24.103	3.381	3.204	2.989	3.010	1.000	2.894	3.754	3.228
2.397	2.346	2.298	2.827	3.333	2.832	3.053	1.629	3.153	2.848	3.618	2.881	1.000	3.237	2.938	2.870
2.395	3.036	2.447	2.823	3.424	3.226	2.917	2.712	2.508	3.063	3.765	2.846	1.000	3.171	3.116	2.886

The minimum and maximum are 1.0000000 34.389135

Table B-AM5a
Aerojet MC^2 Array
Background Run #3 (BGM #3) Before Star Sighting

AVERAGE COUNT/FRAME FOR 3200 FRAMES

AVE

1068.44	966.17	2237.13	2511.73	1842.01	1112.90	1531.39	394.23	1403.28	964.37	1841.13	1241.30	0.00	893.28	1584.52	2882.16
90.16	867.48	1838.56	1292.87	2289.73	1484.24	2471.35	385.01	1838.30	1681.23	2443.06	1556.35	0.00	1204.26	1853.92	1246.41
786.70	7.51	2200.95	1573.46	2464.23	1658.29	2356.52	395.28	2276.58	1681.67	2366.68	2001.73	0.00	1361.73	2611.78	1842.98
1691.63	1502.24	2293.45	1602.73	2501.34	1665.94	2367.89	398.10	2475.87	1764.37	3025.24	1867.58	0.00	1619.47	2389.12	1472.49
1707.00	1638.48	2094.64	1520.74	2297.90	1769.81	2827.50	402.27	2698.92	1948.73	2415.84	1774.56	0.00	1799.26	2345.32	1533.65
468.79	1366.87	2458.94	1531.96	2239.31	1733.57	2675.99	396.02	2393.13	1702.87	2411.40	1800.72	0.00	1639.21	2427.20	1195.00
2150.54	1363.58	2634.71	1497.23	2776.79	2009.81	2418.12	401.00	2575.93	1732.19	2501.99	1965.00	0.00	1800.51	2379.43	1759.32
1751.26	1443.47	2161.72	1615.20	2270.01	1841.28	2278.34	398.42	2364.19	2007.75	2432.76	1615.99	0.00	1813.42	2573.83	1746.35
1532.54	1382.24	2148.11	1712.78	2494.81	1652.70	2363.53	399.97	2644.53	1709.06	2424.89	1721.40	0.00	1694.71	2365.29	1840.33
1534.75	1458.11	2285.68	1645.82	2520.85	1770.62	2544.67	400.29	2561.71	1774.42	2425.61	1704.96	0.00	1875.12	2355.45	1685.74
1903.39	1468.97	2186.71	1780.73	2268.83	1698.37	2261.37	405.05	2155.15	1858.73	2456.32	1932.07	0.00	2271.64	2349.77	2209.84
1681.33	1383.15	2001.15	1783.99	2272.74	1731.91	2593.62	403.02	2309.04	1913.30	2474.03	1813.47	0.00	2013.62	2409.97	1932.99
1451.20	1363.90	2278.80	1551.58	2213.20	1736.54	2355.09	398.50	2379.31	1811.73	2437.21	1961.95	0.00	1778.97	2407.23	1769.61
1383.08	2036.24	2256.11	2996.90	2316.07	1720.79	2749.75	412.81	2394.66	2258.56	2762.40	1917.67	0.00	1707.73	2424.76	1729.25
1436.55	1789.14	2514.75	1838.73	2345.08	1756.57	2374.59	396.83	2356.48	1822.94	2404.71	1837.54	0.00	1962.36	2457.98	1589.84
1494.87	1323.71	2437.40	1594.79	2765.16	1751.88	2354.32	398.07	2360.54	1638.17	2686.62	1715.45	0.00	1681.87	2423.31	2008.86
1401.66	1416.75	2270.08	1588.59	2320.59	1714.74	2384.05	397.94	2395.75	1733.72	2457.60	1800.45	0.00	1825.98	2391.87	1655.57
1368.21	1213.76	2346.15	1571.11	2421.86	1742.10	2337.58	398.28	2445.37	1705.48	2422.39	2227.10	0.00	1727.68	2464.99	1729.33
1286.19	1263.36	2086.09	1596.41	2547.36	1772.74	1416.47	398.04	2493.21	1853.48	2496.29	1743.54	0.00	2075.31	2366.90	1737.48
1571.51	1445.00	2171.32	1935.69	2230.18	1697.33	2296.37	396.05	2436.58	1743.75	2523.87	1660.11	0.00	1769.11	2375.88	2215.13
1939.11	1536.40	2099.60	1623.69	2304.17	1744.63	2527.21	403.95	2608.85	1879.83	2430.48	1721.73	0.00	1829.50	2505.80	2471.77
1384.96	1157.43	2153.91	1553.30	2851.26	1684.45	2419.20	396.99	2484.17	1649.68	2363.14	1838.46	0.00	1923.14	2436.61	1789.65
742.62	1133.28	2446.60	1632.45	2426.37	1658.74	2740.14	394.66	0.94	1872.58	2421.57	1753.25	0.00	1845.14	2553.71	1751.06
1839.64	1450.73	1141.96	2309.72	1643.87	1773.23	3151.41	405.05	2503.99	1594.04	2557.21	1789.84	0.00	1708.84	2650.45	1807.35
1268.76	1414.59	2406.30	1433.87	2357.95	1704.72	2321.36	392.73	2386.35	1910.20	2509.19	2002.76	0.00	1681.66	2413.28	1551.43
2043.50	1097.71	2139.13	1547.52	2392.34	2416.08	2720.61	398.02	2400.89	1757.38	15.42	1861.78	0.00	2114.48	2314.46	1734.75
1293.97	1356.50	1931.13	1814.50	2255.77	1591.68	1017.72	395.91	2328.42	1679.00	2582.26	1723.70	0.00	1747.91	2668.91	1702.46
239.47	1123.28	2047.62	1520.19	2318.13	1921.84	2388.52	396.08	2389.45	2319.54	648.61	1727.05	0.00	1742.76	1080.46	1643.19
2198.35	1282.90	2376.42	1560.38	2276.28	2219.79	2364.29	399.00	2382.61	1711.44	1377.27	1800.51	0.00	1769.58	577.16	1839.24
1270.02	1197.68	1944.77	1461.59	2247.33	1642.20	2263.43	396.33	2342.28	2091.25	2383.22	1590.47	0.00	1619.00	1431.91	1629.91
978.76	1126.35	1908.68	1429.68	2232.68	1564.85	2187.55	388.70	2320.39	1528.03	2362.94	1669.42	0.00	1712.46	2379.47	1622.27
1192.64	3146.16	2050.58	1404.24	2708.80	1531.74	2774.95	401.16	2285.21	1615.48	2400.78	1690.93	0.00	1612.35	1554.98	1733.40

The minimum and maximum are 0.00000000E+00 3151.4084

Table B-AM5b
Aerojet MC^2 Array
Background Run #3 (BGM #3) Before Star Sighting

VARIANCE

VAR

653.46	155.35	412.10	72.78	565.19	151.37	258.80	0.20	111.07	165.92	137.63	87.67	0.00	100.63	119.25	46.96
829.26	2941.10	506.02	132.39	421.61	162.84	237.90	0.11	227.12	176.18	228.69	115.19	0.00	175.21	257.32	81.90
942.47	102.87	578.79	138.04	132.22	103.94	480.57	0.21	404.35	109.98	591.83	134.26	0.00	215.15	296.15	120.63
1491.12	513.74	251.71	105.68	458.56	182.87	137.04	0.11	435.50	112.17	303.86	169.14	0.00	93.99	237.29	59.38
1226.76	291.13	319.10	178.06	70.61	72.40	258.66	0.19	269.02	141.96	328.61	81.00	0.00	84.51	96.34	87.30
498.56	488.25	377.35	102.32	106.87	117.17	300.49	0.09	237.18	91.87	327.37	138.65	0.00	101.35	281.03	425.18
668.36	520.27	251.00	72.28	340.43	178.32	321.21	0.07	91.00	56.31	349.36	73.14	0.00	148.19	61.18	68.52
1076.02	56[illegible].99	83.08	125.21	283.22	122.42	310.53	0.24	143.07	80.63	151.50	100.03	0.00	115.34	292.23	76.70
1370.06	645.44	467.65	161.93	220.74	88.99	570.62	0.35	232.30	90.85	350.36	99.88	0.00	128.64	240.76	83.17
1244.19	550.16	430.99	148.96	136.11	112.67	337.45	0.33	192.59	57.23	169.97	83.16	0.00	71.06	501.47	97.63
568.62	590.98	496.09	88.14	146.63	65.94	443.23	0.07	228.78	49.74	217.25	57.26	0.00	66.05	367.92	62.68
972.51	598.16	2074.24	73.80	192.34	108.59	255.57	0.13	167.02	86.92	308.29	71.06	0.00	81.28	211.64	96.19
1440.77	648.90	134.17	77.85	113.97	88.63	240.34	0.25	66.63	50.29	102.36	53.35	0.00	80.40	175.79	66.06
1605.48	984.61	345.79	69.89	376.78	113.64	355.73	0.16	244.78	85.82	149.92	107.57	0.00	100.38	143.64	85.57
1906.75	289.63	193.38	87.56	405.00	92.53	329.35	0.15	145.15	94.93	64.62	46.23	0.00	86.63	134.71	56.97
1724.33	621.73	472.99	104.79	185.70	116.08	149.60	0.08	255.99	97.81	408.35	92.32	0.00	87.27	340.07	65.26
1956.60	382.32	256.74	82.78	104.81	81.40	575.65	0.07	92.89	106.60	394.66	111.41	0.00	81.87	119.92	110.76
2214.01	607.49	306.54	123.16	208.71	82.83	306.55	0.20	272.68	66.67	218.22	102.51	0.00	87.81	408.74	77.33
2037.89	585.86	310.93	61.97	242.51	78.42	130.45	0.06	151.90	98.14	147.77	71.93	0.00	83.92	233.94	84.94
1283.69	410.84	426.12	93.04	148.98	76.98	194.24	0.08	177.94	107.92	137.07	90.27	0.00	80.70	167.81	70.74
573.55	337.96	540.29	57.03	265.82	102.53	158.61	0.08	81.41	56.20	142.39	45.66	0.00	57.18	278.47	108.63
2157.34	509.78	494.11	67.21	84.54	107.15	103.80	0.09	102.67	107.41	425.71	82.26	0.00	116.68	582.30	85.02
645.51	505.08	274.36	57.09	106.26	52.45	101.65	0.23	0.05	44.12	97.88	76.14	0.00	87.57	314.03	71.62
848.34	366.63	267.38	96.13	380.49	78.84	85.45	0.06	135.60	62.95	152.55	72.28	0.00	119.76	276.09	90.70
2604.34	397.58	379.35	65.03	123.74	58.75	123.99	0.20	109.49	378.57	92.67	90.10	0.00	83.04	135.95	78.23
577.22	629.86	461.97	69.04	279.26	257.35	136.14	0.09	141.96	78.57	13.37	57.11	0.00	54.43	426.85	88.33
1651.14	354.46	628.85	57.26	168.90	53.23	231.44	0.10	90.14	68.94	111.67	54.18	0.00	69.45	84.98	43.56
528.36	662.74	601.32	80.15	201.74	79.16	92.39	0.09	100.61	55.20	219.09	68.54	0.00	101.26	336.80	74.99
832.20	475.51	322.07	87.88	325.72	238.35	71.91	0.06	70.84	76.19	202.38	48.94	0.00	161.44	23391.02	144.93
1385.69	571.13	737.27	95.36	109.75	73.72	132.44	0.23	102.87	134.17	113.04	50.93	0.00	76.35	229.26	62.97
1501.78	550.41	706.92	82.84	80.59	77.43	87.67	0.21	114.81	54.01	75.54	49.73	0.00	60.81	58.35	68.70
1079.36	43.47	808.58	94.04	145.08	58.50	101.84	0.13	220.94	65.42	167.49	49.33	0.00	64.35	397.98	27.84

The minimum and maximum are 0.00000000E+00 23391.022

Table B-AM5c
Aerojet MC^2 Array
Background Run #3 (BGM #3) Before Star Sighting

SKEWNESS

SKEW

0.170	0.004	0.066	0.013	0.010	0.026	0.045	0.775	0.001	0.001	0.013	0.011	0.000	0.009	0.000	0.019
0.023	0.011	0.025	0.000	0.000	0.002	0.050	0.078	0.068	0.002	0.005	0.000	0.000	0.055	0.067	0.000
0.032	2.714	0.009	0.005	0.133	0.002	0.002	0.842	0.000	0.013	0.001	0.150	0.000	0.305	0.044	0.010
0.005	0.008	0.002	0.029	0.000	0.006	0.009	3.752	0.016	0.025	0.031	0.064	0.000	0.024	0.014	0.020
0.048	0.015	0.025	0.007	0.006	0.006	0.258	1.134	0.000	0.020	0.015	0.000	0.000	0.837	0.211	0.078
0.081	0.016	0.017	0.005	0.000	0.012	0.001	0.493	0.000	0.006	0.000	0.001	0.000	0.000	0.000	0.009
0.082	0.018	0.097	0.007	0.000	1.376	0.013	0.046	0.096	0.000	0.006	0.023	0.000	0.221	0.011	0.001
0.059	0.026	0.108	0.002	0.011	0.000	0.001	0.115	0.045	0.038	0.096	0.000	0.000	0.000	0.000	0.015
0.013	0.020	0.004	0.007	0.086	0.002	0.001	0.000	0.044	0.042	0.002	0.040	0.000	0.003	0.010	0.005
0.037	0.061	0.001	0.019	0.006	0.000	0.000	0.012	0.049	0.000	0.000	0.027	0.000	0.021	0.006	0.006
0.021	0.070	0.001	0.012	0.003	0.004	0.001	6.636	0.004	0.000	0.019	0.000	0.000	0.001	0.003	0.011
0.011	0.059	0.125	0.025	0.004	0.015	0.116	0.079	0.066	0.001	0.035	0.011	0.000	0.018	0.000	0.003
0.012	0.083	0.001	0.001	0.005	0.001	0.002	0.000	0.005	0.003	0.060	0.004	0.000	0.000	0.000	0.000
0.007	2.039	0.002	0.003	0.002	0.021	0.006	2.135	0.016	0.000	0.082	0.000	0.000	0.001	0.008	0.000
0.015	0.115	0.043	0.020	0.010	0.000	0.007	2.214	0.016	0.005	0.008	0.006	0.000	0.000	0.000	0.040
0.028	0.083	0.003	0.001	0.001	0.005	0.000	5.192	0.002	0.002	0.045	0.005	0.000	0.006	0.005	0.061
0.023	0.095	0.000	0.002	0.036	0.002	0.031	7.256	0.006	0.016	0.005	0.000	0.000	0.033	0.011	0.044
0.036	0.091	0.016	0.002	0.000	0.001	0.016	0.910	0.000	0.019	0.025	0.089	0.000	0.016	0.000	0.008
0.051	0.086	0.022	0.006	0.012	0.058	0.039	4.864	0.004	0.004	0.110	0.053	0.000	0.023	0.004	0.024
0.021	0.059	0.028	0.001	0.001	0.000	0.009	2.848	0.048	0.002	0.001	0.012	0.000	0.002	0.001	0.001
0.066	0.068	0.012	0.003	0.001	0.115	0.335	2.435	0.032	0.001	0.000	0.005	0.000	0.021	0.045	0.035
0.008	0.061	0.010	0.006	0.010	0.000	0.000	0.071	0.033	0.004	0.004	0.004	0.000	0.002	0.002	0.073
0.007	0.024	0.000	0.000	0.003	0.004	0.000	0.425	14.932	0.000	0.028	0.021	0.000	0.003	0.006	0.008
0.137	0.039	0.006	0.002	0.040	0.001	0.156	7.861	0.100	0.000	0.000	0.004	0.000	0.111	0.001	0.002
0.133	0.016	0.025	0.013	0.000	0.003	0.188	1.005	0.002	1.425	0.052	0.002	0.000	0.014	0.038	0.005
0.000	0.013	0.011	0.003	0.033	0.001	0.173	0.180	0.105	0.011	33.225	0.027	0.000	0.002	0.000	0.006
0.155	0.016	0.020	0.015	0.035	0.017	0.013	3.881	0.001	0.000	0.014	0.016	0.000	0.018	0.024	0.002
0.028	0.004	0.023	0.019	0.068	0.005	0.007	3.822	0.004	0.008	0.011	0.024	0.000	0.031	0.017	0.002
0.001	0.004	0.025	0.007	0.005	0.297	0.000	0.001	0.000	0.004	0.009	0.002	0.000	0.226	1.177	0.112
0.159	0.003	0.048	0.014	0.014	0.021	0.024	0.445	0.157	0.236	0.002	0.005	0.000	0.021	0.188	0.000
0.168	0.034	0.045	0.003	0.028	0.017	0.010	0.750	0.066	0.000	0.070	0.002	0.000	0.066	0.003	0.056
0.127	0.015	0.033	0.006	0.055	0.026	0.006	3.415	0.019	0.005	0.046	0.000	0.000	0.010	0.056	0.002

The minimum and maximum are 0.00000000E+00 33.224529

Table B-AM5d
Aerojet MC^2 Array
Background Run #3 (BGM #3) Before Star Sighting

KURTOSIS

KURT

5.072	3.269	[illegible].278	3.085	3.001	3.057	4.244	2.832	3.346	2.937	3.078	3.262	1.000	2.949	3.562	3.312
3.395	2.188	3.449	3.357	2.917	2.998	3.387	9.412	3.477	2.878	2.880	3.015	1.000	3.441	3.440	3.298
3.298	5.194	2.771	2.870	3.933	2.923	2.433	2.045	3.091	3.196	2.779	3.572	1.000	3.596	3.207	2.699
3.616	3.463	3.677	3.157	2.886	3.102	3.119	7.484	2.902	3.342	2.897	3.023	1.000	2.883	3.912	3.327
3.869	3.493	3.576	2.814	3.556	2.998	3.485	2.133	2.760	2.594	2.800	2.895	1.000	5.778	5.053	3.194
3.551	3.472	3.312	3.194	2.965	3.100	3.110	11.146	3.772	2.884	3.231	2.944	1.000	3.086	3.408	3.144
3.546	3.470	3.637	2.952	2.513	3.466	3.796	16.018	4.352	3.023	2.844	3.135	1.000	3.752	2.872	3.097
3.693	3.522	3.744	3.151	3.786	2.871	3.214	1.114	3.378	3.118	3.211	2.922	1.000	3.005	2.970	3.100
3.704	3.451	3.037	2.954	4.068	2.996	2.867	2.860	3.431	3.501	3.484	3.514	1.000	3.264	4.260	3.142
3.695	3.838	2.942	2.858	2.992	2.818	3.114	2.442	3.662	3.309	3.426	2.883	1.000	3.010	2.870	3.515
3.559	3.862	2.827	3.141	3.565	3.191	2.511	13.421	3.912	2.921	3.857	2.774	1.000	2.984	2.866	3.297
3.760	3.775	3.347	3.117	3.466	3.177	3.195	7.352	3.575	2.787	3.415	3.240	1.000	3.132	4.020	2.894
3.791	3.789	3.870	3.094	3.665	2.715	3.754	1.000	3.891	2.97[illegible]	3.717	2.783	1.000	3.053	4.036	3.031
3.884	4.201	3.343	2.996	3.008	3.272	2.636	3.472	3.212	3.114	3.879	3.045	1.000	2.984	4.317	2.784
3.746	3.694	3.357	3.183	3.691	2.865	2.930	4.205	3.398	2.631	3.425	2.868	1.000	2.906	4.053	3.172
3.736	3.770	2.778	3.026	2.846	2.982	3.845	10.287	3.210	3.120	3.075	3.213	1.000	3.029	3.002	3.390
3.875	3.738	3.504	2.934	3.858	2.841	2.632	12.517	3.508	2.959	3.080	2.862	1.000	3.285	3.761	2.897
3.761	3.742	3.138	2.801	3.481	2.901	3.777	1.970	3.115	3.040	3.383	3.358	1.000	3.323	2.878	3.170
3.906	3.810	3.537	3.048	3.663	3.046	3.534	15.092	3.524	2.658	4.037	3.189	1.000	2.892	3.922	3.068
5.003	3.798	3.470	3.087	4.273	3.080	3.419	11.451	3.304	2.850	3.450	2.941	1.000	2.947	3.539	2.986
3.699	3.826	3.280	3.058	3.309	2.906	3.920	11.216	3.789	3.230	3.765	3.332	1.000	2.985	3.122	3.141
3.623	3.857	3.451	2.978	3.177	3.044	3.081	11.473	3.559	2.821	3.064	3.014	1.000	2.807	3.017	3.120
3.205	3.805	3.780	3.145	2.945	3.440	3.332	1.449	15.931	3.068	4.067	2.968	1.000	2.929	2.689	3.104
3.630	3.504	3.021	3.293	3.450	3.008	3.877	13.984	3.184	2.961	3.340	3.057	1.000	3.409	2.864	2.739
3.820	3.563	3.572	3.136	3.155	3.052	3.733	2.098	3.035	5.188	3.522	2.870	1.000	3.352	4.826	2.976
3.085	3.757	3.451	3.184	2.792	1.040	3.468	10.510	3.293	3.057	45.016	2.931	1.000	2.946	2.969	2.976
4.042	3.734	3.667	3.387	3.241	3.113	3.939	7.915	3.107	3.074	2.978	3.036	1.000	2.900	3.490	3.045
3.446	3.765	3.694	3.277	3.159	2.872	2.930	9.241	3.220	3.101	3.465	3.039	1.000	2.801	3.711	2.834
2.985	3.573	3.275	2.992	3.381	1.297	3.059	16.321	2.831	2.907	3.084	2.995	1.000	2.939	2.446	2.878
3.899	3.700	3.767	3.237	3.155	3.069	3.280	1.566	3.586	5.651	3.118	3.272	1.000	2.921	3.033	3.138
4.203	3.710	3.732	3.130	3.136	3.016	3.061	1.806	3.634	3.016	3.338	2.734	1.000	3.325	3.095	3.076
3.883	3.142	3.612	3.030	3.204	3.344	2.884	4.625	2.621	3.116	3.625	2.995	1.000	3.002	3.050	2.986

The minimum and maximum are 0.99982419 45.016131

Table B-AM6a
Aerojet MC^2 Array
Background Run #4 (BGM #4) Before Star Sighting

AVERAGE COUNT/FRAME FOR 3200 FRAMES

AVE

1133.76	994.61	2251.13	2610.70	1858.84	1125.75	1645.76	394.43	1418.85	976.72	1849.13	1248.68	0.00	906.15	1592.33	2881.24
116.65	926.60	1883.24	1312.48	2307.99	1498.06	2483.11	385.44	1855.94	1691.14	2454.17	1566.70	0.00	1220.87	1872.81	1254.32
839.87	7.60	2210.98	1577.91	2466.87	1661.64	2360.04	395.39	2282.28	1687.94	2372.48	2006.32	0.00	1366.98	2616.67	1843.86
1789.65	1561.54	2302.14	1603.06	2502.35	1667.61	2369.56	398.14	2477.20	1766.38	3025.60	1868.88	0.00	1620.96	2389.62	1472.83
1796.29	1680.09	2103.01	1522.38	2300.69	1772.82	2829.07	402.39	2699.77	1950.26	2418.81	1777.18	0.00	1800.32	2345.13	1533.37
516.70	1424.39	2467.17	1534.07	2240.44	1737.73	2676.65	396.08	2396.52	1705.16	2413.72	1802.40	0.00	1640.68	2427.60	1172.81
2209.77	1422.31	2640.20	1498.88	2778.48	2011.65	2417.86	401.04	2577.97	1734.55	2503.88	1966.17	0.00	1800.96	2379.44	1759.69
1831.16	1505.13	2162.91	1616.74	2272.79	1843.81	2278.27	398.53	2366.75	2010.05	2434.98	1617.10	0.00	1815.12	2574.26	1745.81
1624.11	1446.63	2164.24	1714.03	2496.61	1653.68	2365.43	400.07	2646.56	1711.44	2427.79	1723.07	0.00	1695.12	2365.78	1840.08
1622.41	1523.45	2298.87	1648.46	2522.70	1772.43	2546.81	400.43	2564.84	1776.40	2427.33	1706.21	0.00	1876.27	2357.42	1686.23
1963.28	1538.05	2205.54	1783.28	2271.99	1700.12	2262.95	405.10	2156.22	1861.05	2468.10	1932.84	0.00	2273.23	2350.72	2209.66
1761.91	1452.27	1974.90	1784.60	2275.28	1734.06	2594.54	403.11	2310.07	1914.08	2474.37	1814.92	0.00	2014.12	2410.55	1932.72
1550.59	1437.46	2295.53	1552.73	2215.25	1738.32	2357.83	398.58	2379.91	1812.80	2439.18	1963.34	0.00	1779.68	2408.60	1770.13
1488.06	2044.89	2280.48	2997.40	2317.66	1721.10	2750.94	412.81	2393.61	2257.88	2763.53	1919.32	0.00	1708.40	2426.03	1729.22
1546.83	1832.83	2530.43	1839.06	2347.73	1758.59	2375.81	396.87	2354.33	1822.45	2405.01	1838.35	0.00	1962.54	2458.43	1589.84
1600.62	1394.90	2457.57	1595.84	2766.13	1752.24	2356.10	398.09	2354.77	1630.76	2686.21	1715.33	0.00	1682.19	2423.72	2007.13
1519.48	1470.64	2294.90	1590.37	2323.13	1715.55	2385.08	397.92	2392.56	1723.27	2439.05	1796.87	0.00	1826.89	2391.91	1654.83
1488.68	1280.80	2372.38	1572.31	2423.75	1742.84	2338.74	398.27	2442.79	1694.16	2406.39	2226.19	0.00	1728.17	2464.35	1728.68
1407.70	1331.98	2123.50	1597.89	2551.10	1773.80	1417.58	398.12	2492.03	1852.19	2494.42	1743.54	0.00	2076.31	2368.43	1736.61
1665.81	1501.46	2212.59	1938.17	2233.03	1698.84	2297.62	396.13	2435.95	1744.12	2525.01	1660.67	0.00	1770.67	2377.24	2215.25
1995.93	1587.27	2144.25	1625.89	2307.15	1745.65	2529.21	403.97	2609.37	1881.04	2431.69	1722.22	0.00	1830.36	2507.24	2471.47
1503.34	1221.28	2201.49	1555.72	2851.94	1685.70	2419.74	397.08	2485.11	1650.26	2364.92	1839.41	0.00	1924.76	2437.93	1789.92
801.09	1195.02	2484.48	1634.72	2427.39	1660.17	2742.07	394.74	0.94	1872.82	2423.44	1754.93	0.00	1846.10	2553.98	1751.43
1921.13	1499.46	1161.33	2308.90	1646.65	1774.14	3151.70	405.07	2504.56	1594.38	2559.01	1791.74	0.00	1710.04	2653.29	1807.37
1412.91	1465.90	2454.18	1438.76	2360.74	1705.92	2322.99	392.81	2387.03	1910.11	2509.14	2002.92	0.00	1682.55	2415.12	1551.87
2081.65	1163.38	2194.49	1553.40	2394.04	2418.06	2721.76	398.07	2402.01	1757.23	18.43	1862.94	0.00	2114.26	2316.30	1735.29
1413.75	1407.78	1994.18	1819.29	2258.27	1593.91	1032.57	395.97	2330.18	1679.79	2582.58	1724.67	0.00	1748.73	2669.37	1702.61
293.14	1191.66	2112.19	1528.74	2320.55	1923.74	2390.18	396.16	2390.40	2319.70	648.15	1728.29	0.00	1743.84	1079.74	1644.00
2250.66	1336.62	2420.83	1569.12	2278.22	2220.79	2366.28	399.02	2383.96	1711.48	1378.44	1801.76	0.00	1770.13	581.79	1839.35
1376.11	1260.90	2019.21	1474.62	2249.89	1643.93	2264.67	396.56	2343.67	2091.88	2384.06	1591.38	0.00	1620.23	1432.27	1630.70
1093.26	1191.18	1983.43	1444.31	2235.15	1565.95	2189.92	388.85	2322.06	1528.69	2363.96	1670.26	0.00	1713.81	2380.83	1622.79
1287.47	3141.61	2123.03	1420.54	2710.94	1533.64	2777.32	401.33	2286.44	1615.76	2400.98	1691.50	0.00	1613.59	1552.24	1733.90

The minimum and maximum are 0.00000000E+00 3151.7022

Table B-AM6b
Aerojet MC^2 Array
Background Run #4 (BGM #4) Before Star Sighting

VARIANCE

VAR

989.41	210.92	423.47	75.86	572.56	154.28	281.62	0.25	129.39	173.02	137.99	90.67	0.00	114.22	124.61	43.57
857.74	3386.76	569.74	160.89	447.75	175.38	252.24	0.25	269.94	185.82	229.67	118.96	0.00	179.90	292.73	90.29
1236.98	101.67	557.81	140.55	133.39	98.68	476.53	0.24	407.73	112.46	604.83	147.58	0.00	222.61	288.29	121.47
1852.11	617.45	234.61	98.01	435.60	184.73	135.32	0.13	429.33	113.24	293.40	165.46	0.00	96.17	249.22	66.00
1544.59	349.05	317.57	178.66	74.36	77.39	228.85	0.24	270.58	140.50	329.14	77.86	0.00	80.79	89.24	86.37
601.91	562.13	355.24	106.27	111.34	112.56	303.17	0.10	244.55	92.20	336.43	141.71	0.00	110.90	280.76	494.04
942.43	601.12	212.79	68.91	355.88	152.45	358.86	0.06	88.34	57.34	350.73	71.66	0.00	135.70	62.30	68.25
1409.01	706.34	83.94	117.42	281.61	119.03	322.13	0.25	142.20	80.31	159.17	106.33	0.00	122.76	311.36	79.70
1702.53	820.41	420.66	163.58	205.27	83.44	533.42	0.35	238.12	87.55	336.89	98.72	0.00	131.29	249.00	86.63
1600.79	743.24	396.05	152.70	133.94	118.19	340.44	0.32	208.79	59.56	186.73	84.20	0.00	79.00	532.00	104.74
768.96	808.32	471.78	92.15	144.67	62.52	430.50	0.10	263.36	49.57	227.88	58.10	0.00	67.15	386.32	65.08
1195.82	823.69	1893.86	71.11	193.01	107.76	282.50	0.17	165.82	84.89	314.84	69.47	0.00	78.43	199.13	98.52
1726.37	941.98	123.45	79.56	106.74	88.08	234.65	0.25	69.88	49.07	106.31	52.11	0.00	86.03	194.48	66.83
1926.06	1495.24	303.72	70.63	360.71	96.28	344.34	0.16	224.87	84.22	148.22	110.29	0.00	94.81	147.74	89.76
2260.48	430.27	175.47	86.03	401.16	90.38	320.69	0.14	140.81	93.03	64.53	46.92	0.00	86.29	123.06	53.19
2064.86	982.90	453.99	106.50	196.46	108.07	146.51	0.10	239.01	91.17	418.00	91.20	0.00	88.45	343.75	64.27
2392.43	616.18	208.72	86.77	109.72	81.23	553.64	0.08	91.51	89.92	362.80	102.65	0.00	81.79	114.77	108.02
2655.39	921.25	244.21	120.73	216.79	88.31	332.43	0.20	266.88	57.16	195.47	102.28	0.00	88.90	395.98	79.00
2528.51	927.72	240.72	61.25	230.70	77.03	133.80	0.12	155.80	95.47	145.39	72.11	0.00	81.92	268.07	85.18
1648.67	640.12	318.67	87.48	147.78	77.26	199.74	0.12	175.72	105.14	143.47	89.11	0.00	81.28	170.13	68.35
780.22	552.45	438.20	56.46	278.57	107.59	164.57	0.08	91.73	59.29	152.40	46.82	0.00	57.80	284.61	109.83
2260.38	810.02	406.62	65.81	82.06	103.77	104.25	0.12	101.18	108.84	440.89	85.75	0.00	125.05	611.15	85.63
888.06	743.82	251.39	56.88	109.63	54.81	101.58	0.19	0.06	40.93	102.79	78.61	0.00	90.84	322.58	72.11
1430.89	517.11	270.05	103.38	418.53	76.47	95.46	0.08	139.69	65.14	151.75	75.18	0.00	116.42	272.61	88.76
3889.06	556.97	415.43	63.49	121.71	54.69	108.00	0.15	108.95	397.32	91.56	96.85	0.00	84.10	127.14	79.75
722.46	873.58	498.67	67.11	284.57	254.12	136.65	0.11	135.01	71.79	60.00	53.12	0.00	54.08	431.82	86.84
2983.61	503.48	686.64	55.16	179.83	51.09	252.04	0.08	89.31	64.36	117.34	54.16	0.00	67.62	82.45	44.64
821.02	913.38	702.67	74.94	189.44	80.43	89.84	0.14	97.36	52.98	233.61	66.40	0.00	106.80	317.01	76.87
1117.97	620.11	410.45	80.87	336.44	245.78	70.61	0.06	73.24	78.01	199.67	48.12	0.00	158.98	22275.82	143.18
2612.08	735.55	914.86	83.86	111.33	72.79	145.02	0.25	99.14	131.31	112.64	47.24	0.00	76.55	219.27	61.63
2714.66	770.97	961.62	74.15	84.30	70.48	87.47	0.13	112.39	49.71	77.39	51.35	0.00	60.52	60.05	74.17
1926.76	36.28	1066.77	82.47	149.13	59.11	96.90	0.22	224.21	66.37	169.69	47.07	0.00	63.64	271.62	26.98

The minimum and maximum are 0.00000000E+00 22275.820

Table B-AM6c
Aerojet MC^2 Array
Background Run #4 (BGM #4) Before Star Sighting

SKEWNESS

SKEW

0.021	0.037	0.024	0.006	0.003	0.018	0.012	0.028	0.009	0.001	0.028	0.004	0.000	0.002	0.032	0.030
0.037	0.000	0.051	0.012	0.006	0.003	0.013	0.054	0.066	0.005	0.011	0.000	0.000	0.006	0.071	0.001
0.075	2.363	0.041	0.000	0.088	0.001	0.000	0.193	0.000	0.002	0.006	0.282	0.000	0.400	0.010	0.027
0.076	0.163	0.002	0.003	0.033	0.019	0.015	3.124	0.004	0.013	0.053	0.036	0.000	0.030	0.014	0.081
0.057	0.069	0.026	0.005	0.006	0.006	0.321	0.219	0.000	0.016	0.001	0.018	0.000	0.654	0.209	0.071
0.017	0.091	0.026	0.007	0.013	0.002	0.001	2.966	0.000	0.004	0.002	0.000	0.000	0.009	0.005	0.023
0.016	0.105	0.098	0.000	0.002	1.589	0.000	4.056	0.022	0.004	0.003	0.014	0.000	0.290	0.036	0.002
0.037	0.090	0.090	0.000	0.002	0.013	0.002	0.009	0.000	0.003	0.110	0.005	0.000	0.000	0.019	0.008
0.086	0.103	0.001	0.000	0.176	0.000	0.016	0.000	0.038	0.058	0.015	0.002	0.000	0.000	0.004	0.008
0.038	0.119	0.000	0.016	0.014	0.007	0.002	0.097	0.049	0.000	0.029	0.021	0.000	0.002	0.000	0.055
0.071	0.106	0.009	0.003	0.006	0.002	0.000	5.278	0.027	0.000	0.016	0.005	0.000	0.005	0.017	0.001
0.123	0.117	0.066	0.020	0.017	0.027	0.170	0.606	0.012	0.009	0.015	0.009	0.000	0.002	0.007	0.019
0.152	0.112	0.022	0.000	0.002	0.009	0.014	0.070	0.001	0.008	0.134	0.006	0.000	0.000	0.000	0.001
0.139	0.421	0.001	0.005	0.002	0.020	0.000	2.270	0.002	0.005	0.093	0.000	0.000	0.001	0.000	0.000
0.141	0.066	0.038	0.006	0.001	0.000	0.000	2.170	0.006	0.002	0.002	0.030	0.000	0.003	0.012	0.018
0.146	0.080	0.008	0.001	0.000	0.012	0.000	4.196	0.006	0.002	0.026	0.005	0.000	0.000	0.007	0.077
0.175	0.050	0.011	0.001	0.065	0.013	0.032	5.523	0.001	0.013	0.003	0.009	0.000	0.007	0.006	0.058
0.152	0.039	0.004	0.000	0.007	0.014	0.005	1.129	0.002	0.000	0.021	0.083	0.000	0.027	0.000	0.009
0.182	0.057	0.072	0.003	0.024	0.034	0.014	3.620	0.001	0.004	0.075	0.050	0.000	0.016	0.000	0.025
0.131	0.051	0.072	0.006	0.039	0.002	0.000	3.423	0.062	0.005	0.006	0.021	0.000	0.015	0.005	0.000
0.025	0.039	0.079	0.000	0.003	0.035	0.179	0.741	0.033	0.000	0.000	0.003	0.000	0.006	0.025	0.025
0.245	0.036	0.135	0.005	0.007	0.000	0.000	1.523	0.008	0.002	0.000	0.001	0.000	0.007	0.009	0.104
0.116	0.066	0.178	0.008	0.000	0.015	0.005	1.122	12.671	0.006	0.325	0.021	0.000	0.003	0.003	0.004
0.057	0.045	0.024	0.003	0.024	0.000	0.202	6.950	0.088	0.001	0.005	0.001	0.000	0.240	0.003	0.007
0.145	0.026	0.113	0.002	0.002	0.002	0.073	2.566	0.002	1.848	0.019	0.030	0.000	0.041	0.036	0.001
0.000	0.054	0.143	0.000	0.026	0.063	0.121	1.694	0.131	0.017	5.030	0.012	0.000	0.002	0.000	0.020
0.038	0.069	0.103	0.009	0.071	0.044	0.006	0.903	0.001	0.001	0.029	0.018	0.000	0.020	0.101	0.009
0.011	0.071	0.145	0.012	0.078	0.015	0.018	2.974	0.000	0.006	0.031	0.008	0.000	0.013	0.021	0.015
0.006	0.069	0.077	0.012	0.002	0.168	0.000	1.925	0.007	0.003	0.032	0.012	0.000	0.248	1.470	0.133
0.016	0.108	0.107	0.036	0.037	0.001	0.008	0.048	0.158	0.028	0.003	0.014	0.000	0.033	0.245	0.002
0.035	0.071	0.104	0.062	0.003	0.023	0.000	3.315	0.054	0.001	0.061	0.008	0.000	0.081	0.031	0.006
0.034	0.000	0.133	0.038	0.036	0.002	0.003	0.525	0.017	0.022	0.034	0.005	0.000	0.002	0.006	0.000

The minimum and maximum are 0.00000000E+00 12.670702

Table B–AM6d
Aerojet MC^2 Array
Background Run #4 (BGM #4) Before Star Sighting

KURTOSIS

KURT

4.399	2.748	2.844	3.171	2.787	3.066	3.841	1.272	3.116	2.952	3.151	3.011	1.000	2.963	4.273	3.094
3.322	2.079	2.863	2.885	2.790	3.164	3.513	1.171	3.445	3.006	3.056	2.877	1.000	3.055	3.470	2.796
2.891	4.652	2.854	2.699	3.477	3.048	2.463	1.368	3.027	3.329	2.676	4.178	1.000	3.616	3.412	2.756
2.807	2.880	3.704	3.115	2.937	3.295	3.224	5.024	2.798	3.482	3.142	3.008	1.000	3.161	3.491	3.369
2.776	2.845	3.634	2.885	3.276	3.151	3.665	1.270	2.854	2.643	2.990	2.971	1.000	5.428	4.649	3.103
2.794	2.825	3.509	3.388	3.270	2.880	3.011	8.741	3.456	2.973	3.053	2.841	1.000	3.129	3.290	2.814
2.782	2.782	4.022	2.829	2.648	5.031	3.637	15.255	3.450	3.021	2.926	2.901	1.000	3.906	2.991	2.965
2.745	2.799	3.914	3.097	3.739	2.833	3.305	1.078	3.123	2.994	3.425	3.145	1.000	2.991	2.842	2.969
2.826	2.853	2.943	2.849	4.194	3.095	2.860	2.836	3.125	3.511	3.352	3.195	1.000	3.073	4.084	3.224
2.714	2.720	2.849	2.887	3.117	2.841	3.006	2.145	3.536	3.221	3.697	2.876	1.000	2.963	2.912	3.584
2.768	2.646	2.767	2.915	3.761	3.105	2.561	7.591	3.734	2.744	3.835	2.864	1.000	3.127	2.892	3.234
2.730	2.677	3.171	2.943	3.383	3.351	3.698	5.212	3.695	2.738	3.616	3.311	1.000	2.978	4.188	2.728
2.708	2.626	3.852	3.307	3.496	2.935	4.074	1.333	4.241	3.024	3.616	2.891	1.000	2.927	3.696	3.357
2.764	2.075	3.113	2.926	3.025	3.636	2.611	3.741	3.366	3.229	3.935	2.939	1.000	2.877	4.858	2.916
2.852	2.724	3.426	2.928	3.035	3.200	3.011	5.304	3.113	2.798	3.281	3.020	1.000	3.036	3.443	3.129
2.820	2.605	2.645	3.004	2.668	3.060	4.283	8.480	3.157	2.914	2.955	3.119	1.000	2.875	2.941	3.369
2.809	2.709	3.502	3.034	4.041	3.025	2.632	10.018	3.459	3.011	3 .36	2.934	1.000	3.191	3.635	2.898
2.851	2.785	3.214	2.815	3.191	2.928	3.691	2.565	3.191	2.976	3.696	3.179	1.000	3.223	2.899	3 125
2.801	2.607	3.427	3.079	3.470	3.276	3.152	6.007	3.698	2.596	4.009	3.202	1.000	2.942	3.930	2.981
2.767	2.668	3.034	3.008	4.242	3.140	3.472	5.725	3.220	2.827	3.900	3.196	1.000	3.075	3.488	2.988
2.823	2.603	3.101	3.099	3.403	2.687	3.798	11.515	3.563	2.932	3.361	3.218	1.000	3.357	3.016	3.059
2.937	2.662	2.999	3.069	3.106	2.905	3.025	7.476	2.920	2.621	2.738	2.880	1.000	2.850	2.978	3.434
3.019	2.716	3.049	2.954	2.972	3.635	3.132	2.200	13.670	3.224	5.430	2.951	1.000	2.915	2.733	3.006
2.692	2.888	3.337	3.397	3.348	3.123	3.714	10.768	3.147	3.118	3.591	3.043	1.000	3.807	2.964	2.833
2.698	2.645	2.845	2.957	3.393	3.352	3.662	3.755	3.044	5.617	2.992	3.151	1.000	3.229	4.547	2.909
3.052	2.715	2.997	3.011	2.725	1.135	3.282	8.132	3.108	2.928	8.142	2.940	1.000	3.161	3.022	2.997
2.588	2.776	2.936	3.196	3.249	3.262	3.433	12.131	3.003	2.970	2.987	3.104	1.000	2.863	3.981	2.925
2.803	2.802	2.808	2.919	3.289	3.232	2.885	4.503	3.045	3.164	3.272	3.140	1.000	2.857	3.727	2.841
2.708	2.998	2.842	2.999	3.092	1.168	2.904	17.033	3.097	2.782	3.059	2.945	1.000	2.911	2.759	2.844
2.513	2.855	2.703	2.910	3.189	2.942	3.236	1.095	3.387	3.539	3.119	3.346	1.000	3.105	3.004	3.072
2.565	2.733	2.709	3.245	3.225	2.896	3.016	4.641	3.487	3.127	3.616	2.865	1.000	3.385	2.891	2.966
2.587	3.299	2.780	2.902	3.220	3.283	2.989	1.525	2.694	2.949	3.774	2.963	1.000	3.095	3.096	3.085

The minimum and maximum are 1.0000000 17.033276

Table B-ABla
Aerojet Bulk Si:Bi Array
Star (CW Leo) at center (Star B #1)

AVERAGE COUNT/FRAME FOR 3200 FRAMES

AVE

1085.70	2702.01	1098.04	2588.01	1102.31	2650.05	1101.12	2762.10	947.39	2843.44	1004.79	2904.25	1036.14	2824.01	809.50	1519.92
1227.05	2839.00	1037.46	2707.85	982.24	2962.87	935.26	3021.90	899.82	2653.23	958.82	2688.08	729.93	2369.29	540.32	1316.68
1268.60	2483.25	1109.76	3027.74	1061.23	2720.28	1041.95	2952.74	1048.24	3028.73	1000.17	2869.80	799.76	2678.37	560.21	1516.89
1395.75	2999.34	1086.48	2871.56	912.47	2827.21	942.97	3028.14	1107.18	2799.84	952.07	2575.67	818.56	2577.26	555.05	1145.78
1279.92	2859.69	1070.72	2768.56	1005.68	2820.91	1080.68	2961.52	933.28	2858.65	930.95	2681.51	799.48	2715.61	574.99	1309.22
1389.34	3021.05	1069.68	2572.92	1052.09	2921.28	1052.44	3019.43	1042.00	2960.96	954.00	3060.98	893.11	2512.02	629.66	1467.66
1269.66	2806.87	1117.71	2773.04	1072.55	2830.43	998.05	2911.91	899.31	2776.17	830.05	2668.24	703.61	2657.02	509.26	1441.44
1329.51	2652.28	1148.39	2978.03	1161.25	2875.75	1165.23	3022.90	1038.17	3006.10	947.03	2983.63	873.77	2488.08	604.63	1478.58
1227.65	2686.74	1113.75	2958.81	1191.54	2757.66	1082.24	2727.11	858.63	2635.31	876.88	2854.90	709.43	2473.72	489.84	1493.28
1436.89	2564.90	1161.60	2830.87	1149.16	2879.31	994.53	2823.19	1004.97	2904.14	823.85	2811.23	712.59	2382.97	553.86	1543.71
1186.93	2914.72	1152.85	2751.52	1159.08	2863.53	1046.87	2881.62	1051.28	2689.75	880.46	2831.96	779.75	2405.65	562.66	1423.44
1440.02	2808.60	1124.04	2630.08	1108.32	2649.74	962.29	2727.93	892.80	2603.13	779.10	2431.38	737.08	2527.82	551.49	1397.03
1264.34	2933.59	1084.91	2485.59	1083.32	2459.82	925.99	2931.40	963.45	2741.54	835.38	2633.11	769.35	2343.85	540.57	1359.89
1312.08	2595.71	1064.82	2603.29	970.44	2419.71	945.77	2793.75	1007.15	2645.32	902.20	2536.13	607.99	2083.52	569.35	1659.49
1189.21	2639.95	953.23	2347.93	894.71	2756.12	929.84	2652.98	948.85	2604.77	792.63	2533.85	689.42	2487.19	519.74	1569.07
1177.34	2734.71	916.51	2599.34	975.83	2555.56	961.34	2782.03	893.67	2588.06	888.74	2583.82	685.34	2177.80	497.57	1421.40
993.37	2299.07	978.69	2377.03	957.31	2536.95	1040.71	2548.11	957.13	2610.07	870.23	2593.04	736.74	2473.29	529.00	1500.81
997.37	2067.06	953.24	2420.35	1012.82	2524.63	929.82	2442.17	1014.64	2338.25	859.27	2557.30	716.94	2152.96	449.63	1592.06
944.13	2320.53	1050.31	2324.34	980.69	2559.65	965.51	2595.96	971.01	2348.78	784.75	2362.74	630.74	1836.75	470.89	1166.18
905.88	2017.46	905.81	2115.26	985.53	2450.31	974.33	2652.20	930.25	2443.55	838.91	1957.32	702.76	2353.55	540.42	1444.67
859.66	2099.20	990.26	2614.30	978.11	2286.11	943.33	2005.97	810.93	2436.99	758.25	2334.94	675.80	2034.01	501.17	1483.41
951.78	2297.39	939.68	2022.55	953.48	2550.54	1003.47	2120.43	892.31	2299.12	781.51	2283.44	628.86	1831.15	498.96	1470.09
835.25	1884.13	916.22	2421.87	944.17	2206.97	973.33	2380.80	900.11	2339.43	744.84	2174.41	674.66	1837.59	501.60	1655.43
870.38	1974.64	900.16	2146.49	924.11	2058.25	872.61	462.17	487.06	2256.42	730.13	2250.16	699.21	2096.81	469.49	1125.65
710.82	1973.81	805.70	2018.88	855.61	2306.78	910.54	2450.92	892.14	2393.17	812.47	2241.72	655.85	1972.94	453.97	1402.14
688.78	1548.93	761.36	2103.88	841.06	2165.57	738.58	2153.93	817.63	2254.30	708.44	845.86	560.99	2095.70	477.69	1471.87
646.88	1995.94	764.20	1974.11	792.08	1949.54	731.44	1910.72	752.90	1815.89	737.60	2166.33	591.32	1754.44	370.75	1256.46
609.58	1722.67	648.88	1924.25	701.56	1801.32	645.15	1940.72	731.50	1966.52	602.26	1980.00	481.58	1765.14	379.33	1033.54
426.27	1526.71	577.31	1651.06	518.07	1752.01	538.84	1842.47	505.46	1898.14	474.62	1833.55	311.98	1482.82	271.83	917.58
237.50	1109.56	318.32	1332.87	362.82	1264.80	309.43	1168.59	359.48	1369.21	316.96	1202.83	228.00	1168.83	233.70	696.28
72.24	657.91	198.08	735.06	198.32	885.15	166.05	879.58	203.30	798.89	165.69	913.49	128.76	782.59	110.38	464.52
261.41	731.18	319.03	718.54	250.46	715.47	308.02	672.85	239.88	720.48	245.76	673.07	177.60	598.86	151.63	598.06

The minimum and maximum are 72.240000 3060.9756

Table B-AB1b
Aerojet Bulk Si:Bi Array
Star (CW Leo) at center (Star B #1)

VARIANCE

VAR

468.52	120.71	635.05	178.76	245.56	263.88	202.32	108.97	198.52	93.52	497.64	125.88	664.41	664.27	757.91	540.72
620.64	246.72	415.39	185.29	291.57	258.72	1302.51	177.98	134.84	63.70	177.05	101.03	1687.41	181.90	570.46	245.27
846.55	162.84	376.44	238.72	197.92	180.46	171.49	102.86	146.15	95.77	384.93	110.98	828.51	269.82	1471.23	389.34
850.93	208.14	759.37	213.24	656.79	295.87	288.65	164.03	565.58	159.87	188.41	198.29	1247.17	321.52	673.86	232.49
673.22	146.35	481.78	200.48	187.25	193.23	136.57	123.93	490.12	151.23	174.01	158.60	519.52	231.60	1111.45	533.45
783.64	230.52	179.42	144.44	220.29	242.92	414.98	115.10	951.04	206.51	789.86	203.27	369.61	169.39	523.69	609.52
517.78	106.96	278.95	149.47	308.22	260.66	288.86	219.84	1771.51	262.80	377.22	237.05	336.78	167.64	819.27	266.08
1019.84	158.26	154.48	224.74	207.47	219.13	122.63	248.80	323.34	264.92	794.14	256.69	1284.81	163.12	291.91	272.43
816.99	208.86	532.55	153.18	230.33	291.90	284.54	149.65	275.09	142.45	291.61	253.19	217.78	197.93	2172.08	242.52
709.85	174.59	184.50	228.61	267.95	246.32	519.94	354.72	489.88	210.19	331.64	211.12	473.08	302.87	422.94	251.49
944.35	317.18	377.79	149.49	256.92	327.56	217.16	122.56	229.55	196.51	431.94	259.19	304.49	158.09	185.54	258.64
801.20	289.54	681.47	385.81	480.74	379.49	213.70	221.20	218.21	212.14	325.81	137.45	357.29	372.86	458.25	216.15
811.26	127.78	375.17	209.96	165.58	152.18	594.81	148.91	209.80	129.83	450.75	186.71	376.12	187.67	332.71	253.07
418.35	183.33	793.47	210.79	1203.35	278.16	662.87	184.81	285.88	111.97	523.91	363.47	472.73	181.90	462.49	250.37
1033.59	188.28	173.69	194.56	276.68	245.50	192.81	367.29	178.67	103.13	531.01	473.62	550.64	204.34	514.20	229.24
843.32	141.32	257.03	134.25	243.72	277.33	282.50	309.18	650.64	201.79	347.99	465.76	480.15	594.65	443.47	213.96
1770.28	182.86	309.98	270.57	182.98	250.54	211.69	371.47	242.60	183.10	338.29	480.36	462.99	506.73	1274.17	206.07
1051.35	309.19	448.62	322.88	312.21	438.38	261.34	204.78	252.76	251.85	260.56	275.72	255.16	271.94	317.11	225.70
774.97	186.36	210.12	132.60	178.89	464.34	325.44	160.42	254.05	143.77	260.98	269.62	198.64	168.76	379.12	249.56
505.02	244.52	416.88	266.51	471.22	298.12	310.91	221.77	238.54	242.32	299.99	193.53	479.96	136.84	373.42	161.80
485.18	383.54	244.25	133.75	333.54	401.67	190.94	344.78	999.26	188.13	248.32	135.18	197.09	138.21	261.77	185.56
528.06	198.77	345.50	347.38	362.30	277.96	832.62	239.47	288.39	236.39	222.45	195.61	323.17	136.17	308.61	254.02
1140.62	276.64	274.94	133.30	227.74	296.31	326.10	274.18	305.74	216.14	283.51	515.40	282.80	134.27	253.88	191.16
673.85	192.20	370.25	251.08	314.46	292.15	300.18	372.52	338.12	228.13	368.95	293.13	441.98	171.54	232.21	163.03
652.52	189.68	274.29	229.83	171.08	279.72	334.86	115.40	237.25	271.99	288.14	179.11	252.24	257.00	318.06	206.86
457.71	235.08	193.06	255.76	392.04	274.34	486.39	221.44	181.10	121.06	450.87	207.43	649.34	199.95	466.93	229.88
401.10	120.46	209.32	203.73	305.02	295.37	488.19	202.23	324.93	191.51	372.97	173.22	238.93	121.11	302.11	173.16
710.84	297.10	284.79	230.47	309.88	260.10	461.00	195.92	419.18	200.68	520.98	258.43	322.87	154.71	493.71	168.87
477.57	230.20	247.16	219.11	471.06	209.14	433.94	277.24	234.81	162.77	449.45	177.62	374.98	227.80	343.54	215.72
478.02	241.78	722.83	264.56	792.62	268.69	754.60	338.01	523.53	428.79	1234.02	278.87	573.77	282.95	497.60	373.35
399.33	324.82	400.40	458.29	435.01	158.13	362.15	223.52	545.64	198.31	354.33	209.02	700.03	293.91	342.62	219.47
1948.80	369.34	1607.10	396.25	393.74	257.83	1615.34	310.51	1895.27	217.31	2310.12	380.05	2425.19	346.14	335.84	238.28

The minimum and maximum are 63.702241 2425.1944

Table B-ABIc

Aerojet Bulk Si:Bi Array

Star (CW Leo) at center (Star B #1)

SKEWNESS

SKEW

0.000	0.001	1.561	0.002	0.027	0.075	0.066	0.003	0.155	0.254	0.102	0.086	0.004	0.000	0.001	0.343
0.027	0.015	0.228	0.000	1.288	0.212	0.127	0.000	0.258	0.001	0.186	0.034	0.127	1.480	0.529	0.082
0.037	0.003	0.201	0.069	0.109	0.003	0.936	0.010	0.049	0.127	0.825	0.006	0.006	0.606	0.150	0.245
0.000	0.001	1.187	0.296	1.118	0.012	1.281	0.143	1.450	0.069	0.230	0.014	0.939	0.935	0.052	0.002
0.026	0.022	0.179	0.006	0.215	0.591	1.450	0.027	1.324	0.048	0.176	0.040	0.426	0.464	0.045	0.113
0.004	0.018	0.044	0.006	0.448	0.280	1.470	0.001	0.732	0.021	0.217	0.001	0.969	0.004	0.015	0.116
0.000	0.000	0.374	0.001	0.295	0.017	0.257	0.000	0.045	0.069	0.139	0.057	0.047	0.007	0.035	0.002
0.640	0.011	0.210	0.010	0.345	0.264	0.016	0.000	0.387	0.000	0.915	0.093	0.064	0.330	0.105	0.000
0.230	0.001	0.307	0.003	0.274	0.033	0.112	0.113	0.146	0.234	0.140	0.114	0.095	0.012	0.000	0.009
0.120	0.014	0.111	0.000	0.593	0.000	0.802	0.005	0.537	0.026	0.016	0.014	0.003	0.031	0.000	0.000
0.115	0.000	0.196	0.003	0.004	0.017	0.031	0.003	0.411	0.061	0.064	0.024	0.311	0.025	0.000	0.000
0.053	0.004	0.286	0.023	0.830	0.005	0.554	0.022	0.804	0.021	0.321	0.049	0.352	0.003	0.002	0.006
0.159	0.000	0.003	0.006	0.197	1.502	1.606	0.045	0.245	0.004	0.038	0.000	0.087	0.000	0.000	0.002
0.217	0.003	0.476	0.011	0.097	0.107	0.862	0.002	0.962	0.016	0.489	0.001	0.015	0.012	2.049	0.009
0.029	0.009	0.014	0.051	1.567	0.084	0.059	0.000	0.347	0.030	0.880	0.026	0.027	0.050	0.081	0.004
0.070	0.000	0.008	0.004	0.183	0.032	0.441	0.002	1.313	0.004	0.081	0.100	0.261	0.201	0.006	0.004
0.068	0.003	0.396	0.006	0.085	0.247	0.141	0.025	2.941	0.003	0.000	0.394	0.010	0.175	0.078	0.005
0.027	0.000	0.337	0.012	0.088	0.367	0.630	0.005	0.408	0.006	0.083	0.000	0.055	0.021	0.008	0.000
0.056	0.004	0.411	0.051	0.005	0.000	0.080	0.006	0.070	0.052	0.045	0.000	0.090	0.016	0.512	0.002
0.223	0.013	0.722	0.002	0.545	0.003	0.540	0.001	0.308	0.002	0.021	0.016	1.421	0.000	0.483	0.003
0.000	0.013	0.263	0.054	1.835	0.052	0.321	0.097	0.265	0.002	0.005	0.024	0.002	0.002	0.210	0.000
0.044	0.014	0.362	0.042	0.091	0.087	0.710	0.002	1.057	0.009	0.005	0.010	0.038	0.034	0.001	0.003
0.481	0.001	0.257	0.000	0.342	0.003	0.394	0.015	0.017	0.001	0.021	0.023	0.099	0.001	0.013	0.000
0.108	0.040	0.476	0.022	0.059	0.232	0.902	0.002	0.618	0.005	0.010	0.000	0.025	0.022	0.001	0.002
0.081	0.000	0.041	0.000	0.252	0.009	0.137	0.006	0.035	0.026	0.036	0.000	0.035	0.056	0.028	0.001
0.064	0.034	0.002	0.006	0.692	0.086	0.025	0.005	0.015	0.000	0.269	0.083	0.352	0.022	0.020	0.000
0.024	0.003	0.085	0.000	0.201	0.003	0.485	0.031	0.108	0.002	0.004	0.035	0.014	0.000	0.194	0.000
0.019	0.007	0.096	0.000	0.095	0.000	0.151	0.018	0.636	0.044	0.250	0.011	0.008	0.008	0.062	0.001
0.028	0.011	0.110	0.015	0.021	0.002	0.251	0.013	0.098	0.001	0.069	0.015	0.000	0.003	0.005	0.005
0.019	0.013	0.405	0.041	0.281	0.074	0.258	0.019	0.345	0.002	0.126	0.001	0.001	0.002	0.003	0.001
0.031	0.000	0.007	0.004	0.037	0.008	0.031	0.000	0.029	0.000	0.128	0.001	0.153	0.021	0.026	0.002
0.028	0.002	0.201	0.002	0.099	0.006	0.847	0.161	0.351	0.000	0.013	0.010	0.006	0.032	1.402	0.013

The minimum and maximum are 4.86637924E-07 2.9407460

Table B-AB1d
Aerojet Bulk Si:Bi Array
Star (CW Leo) at center (Star B #1)

KURTOSIS

KURT

2.907	3.092	5.267	2.998	2.905	3.177	3.079	2.998	3.749	4.957	3.060	3.337	2.741	2.563	2.926	3.702
3.425	3.597	3.750	2.953	5.863	1.532	2.161	3.001	4.895	3.504	5.064	4.915	2.526	8.345	4.712	4.491
2.936	3.035	3.318	2.882	3.523	5.670	6.276	2.883	3.212	3.674	4.240	3.338	2.689	4.716	3.564	3.866
3.104	2.982	4.427	4.272	4.245	2.234	5.758	3.045	4.764	4.202	4.942	3.456	3.602	6.450	3.741	3.260
5.738	3.090	2.701	3.085	3.665	4.111	10.627	3.103	5.740	3.202	4.184	3.584	3.990	4.804	2.825	3.033
2.819	2.930	3.275	2.936	4.618	2.263	5.092	2.867	3.602	3.285	3.037	2.839	5.025	2.866	3.170	3.256
3.123	3.144	3.458	2.722	3.671	1.225	3.149	2.685	1.954	3.787	3.461	2.731	3.228	2.821	3.564	3.034
3.904	3.046	3.922	2.820	4.549	4.213	3.053	3.037	4.502	2.841	4.215	2.968	2.555	4.748	3.687	2.962
3.362	2.880	3.006	2.930	4.272	3.167	3.400	3.445	3.904	5.389	3.355	3.245	3.057	2.857	2.308	3.080
4.077	3.327	3.662	2.681	4.702	4.280	4.346	2.787	3.849	3.215	3.217	3.087	2.885	2.946	3.148	3.111
3.731	2.821	3.278	3.075	2.865	2.304	3.196	2.710	4.382	3.282	3.169	2.661	3.354	2.969	3.081	2.928
3.616	2.898	3.346	2.653	4.360	2.630	5.554	3.011	5.591	2.901	4.127	3.335	4.456	2.665	3.192	2.958
2.898	3.036	2.715	2.678	3.616	5.139	5.489	2.935	3.788	2.735	2.670	3.016	3.124	2.895	2.944	3.053
3.465	3.246	3.145	3.134	2.550	2.026	3.947	2.993	5.735	3.118	4.077	2.871	3.598	2.899	6.808	3.198
3.628	2.856	2.944	2.832	7.943	3.735	3.413	2.604	4.160	4.040	5.280	2.827	3.816	3.028	4.328	3.117
4.293	3.097	2.898	3.022	3.694	3.588	4.262	2.568	4.431	2.914	3.786	3.134	3.963	3.063	3.011	3.096
3.080	2.791	3.725	3.057	3.166	2.877	3.812	2.412	12.328	2.956	3.001	3.300	2.802	3.086	3.616	3.022
3.366	2.809	3.990	2.729	3.484	4.204	6.405	2.744	5.030	2.793	3.224	3.221	3.163	2.964	3.420	3.088
3.169	2.897	4.476	3.022	3.017	2.278	3.500	3.151	3.190	3.238	3.074	3.102	3.891	2.906	4.859	3.019
4.818	2.835	4.985	3.148	4.036	2.110	4.588	2.901	4.594	3.007	3.044	2.713	6.046	2.968	5.201	3.234
3.167	2.814	4.527	3.287	6.454	2.805	4.187	2.744	2.412	2.956	3.005	3.262	3.103	3.427	4.231	3.071
3.136	3.045	4.288	2.596	3.299	2.451	3.422	2.910	6.624	2.974	2.877	2.918	3.428	3.206	3.034	2.801
4.007	2.823	4.630	3.056	4.870	3.524	4.772	2.671	2.949	2.893	3.380	2.738	4.051	3.025	3.148	3.067
3.092	3.176	4.254	2.893	3.305	2.798	5.254	2.855	5.661	2.883	2.930	2.689	2.931	2.949	3.164	3.051
2.777	2.822	3.397	2.942	4.106	3.584	2.897	3.113	3.001	3.103	3.154	2.924	3.131	2.653	3.046	2.822
4.554	2.846	3.099	3.037	4.639	2.251	3.086	2.869	3.596	3.372	5.123	3.037	3.875	3.014	3.222	3.208
3.426	2.832	3.737	3.044	3.658	2.827	3.805	3.165	3.567	3.321	2.973	3.057	2.918	2.942	4.283	3.018
3.534	2.977	3.897	2.733	3.238	3.004	3.523	3.104	4.747	2.871	3.855	2.832	3.015	3.005	3.654	3.116
3.132	3.071	3.413	2.978	3.094	3.017	3.376	3.075	3.423	2.976	3.150	2.747	2.774	2.874	3.760	3.143
3.055	2.955	4.089	3.084	3.413	3.065	3.721	2.786	3.908	2.817	2.875	2.766	3.156	2.883	3.105	2.936
3.091	2.773	2.925	2.872	2.993	3.079	3.320	3.539	3.274	3.131	4.268	3.193	3.720	3.004	3.336	2.862
2.732	2.913	2.866	3.098	3.499	2.946	3.601	3.843	2.739	2.909	2.233	3.042	2.181	2.908	7.856	2.974

The minimum and maximum are 1.2245182 12.327769

Table B-AB2a
Aerojet Bulk Si:Bi Array
Background Run #1 (BGB #1)

AVERAGE COUNT/FRAME FOR 3200 FRAMES

AVE

1085.96	2702.47	1096.86	2588.81	1103.48	2650.65	1101.57	2762.30	947.21	2844.12	1004.66	2905.50	1036.58	2827.08	811.81	1524.59
1228.08	2839.29	1036.87	2708.27	982.55	2962.90	937.16	3021.93	899.75	2653.07	959.23	2689.62	732.20	2370.95	542.51	1320.67
1269.36	2483.77	1110.08	3028.02	1061.24	2720.76	1042.48	2953.08	1048.10	3028.88	1000.86	2871.15	800.62	2679.30	562.23	1521.29
1394.46	2999.79	1085.84	2872.31	912.90	2827.97	942.69	3028.49	1107.05	2800.21	952.56	2577.33	820.14	2578.02	556.67	1149.21
1279.46	2860.04	1070.56	2769.70	1006.14	2820.79	1080.45	2962.28	934.54	2858.15	931.15	2682.36	800.21	2715.64	575.18	1312.78
1388.93	3021.15	1069.47	2573.28	1052.00	2921.18	1052.50	3019.99	1042.94	2961.81	954.24	3062.63	893.59	2513.03	631.24	1471.10
1270.10	2806.46	1117.50	2772.62	1071.95	2829.79	998.12	2911.67	899.84	2776.47	830.23	2668.94	704.48	2657.76	509.86	1445.41
1330.18	2652.21	1147.98	2977.48	1150.48	2874.85	1164.65	3022.92	1038.66	3006.40	948.99	2984.45	876.54	2489.10	605.63	1482.55
1227.82	2686.42	1114.51	2958.59	1192.03	2758.26	1081.70	2726.97	859.25	2635.82	877.41	2856.08	710.12	2474.29	491.62	1497.41
1435.77	2555.06	1161.39	2830.71	1147.73	2878.92	994.59	2823.31	1003.99	2904.96	825.46	2811.39	712.77	2384.19	555.55	1548.23
1187.27	2915.03	1151.94	2751.17	1158.04	2863.15	1046.83	2882.05	1050.91	2690.33	880.86	2832.65	779.83	2406.28	563.11	1427.75
1439.81	2808.46	1124.11	2629.75	1108.26	2649.66	961.38	2729.21	892.69	2602.24	778.60	2430.58	737.32	2526.72	551.16	1400.53
1264.46	2933.97	1085.48	2485.80	1084.10	2460.27	926.13	2931.55	962.59	2738.56	832.57	2629.07	767.52	2341.54	540.46	1363.38
1312.10	2596.36	1064.95	2602.89	970.28	2419.59	945.00	2792.96	1005.10	2639.95	892.92	2520.03	599.97	2077.29	568.46	1661.57
1188.09	2640.37	953.20	2347.62	894.73	2756.57	929.41	2651.98	945.69	2596.16	774.04	2475.88	664.92	2471.39	516.84	1570.20
1177.46	2735.24	917.19	2599.92	975.96	2556.13	960.78	2780.93	890.28	2576.86	861.35	2488.09	635.43	2146.75	491.04	1421.43
992.91	2299.02	978.21	2376.61	956.65	2536.50	1039.23	2545.37	952.04	2595.05	834.35	2489.89	681.67	2431.54	520.49	1500.22
994.09	2066.52	952.23	2419.48	1012.69	2524.52	927.78	2439.67	1011.07	2325.82	842.08	2524.15	694.35	2127.86	444.33	1591.58
939.63	2317.49	1047.72	2322.18	979.46	2557.93	963.43	2593.38	969.69	2342.88	779.35	2354.19	623.37	1825.38	466.63	1165.40
905.53	2018.04	906.74	2117.03	987.03	2451.44	975.44	2653.30	930.64	2441.61	837.65	1956.39	700.11	2348.07	537.53	1444.91
857.61	2098.86	990.29	2614.28	978.55	2287.10	943.97	2004.46	811.70	2436.22	756.88	2335.29	674.12	2030.76	499.58	1484.85
951.02	2297.44	940.48	2023.02	953.64	2550.25	1004.05	2120.29	891.91	2298.55	781.54	2285.56	628.35	1829.93	498.10	1472.69
836.78	1884.56	917.18	2421.95	944.44	2207.82	972.25	2380.89	899.68	2339.06	744.16	2177.00	674.02	1837.48	500.42	1658.08
869.86	1974.29	899.67	2146.80	925.34	2058.13	872.79	461.73	487.02	2256.66	730.42	2252.71	699.89	2097.56	469.46	1127.05
710.90	1973.65	804.76	2018.98	855.80	2306.54	912.05	2451.48	891.50	2392.23	812.06	2244.17	656.14	1973.10	464.26	1404.02
688.70	1548.63	760.99	2104.08	841.22	2166.04	738.14	2153.06	817.29	2254.18	709.00	846.11	560.41	2096.43	477.47	1473.34
646.78	1996.33	764.39	1973.35	790.94	1949.14	732.54	1911.08	753.17	1816.03	738.06	2168.95	590.96	1754.81	370.63	1258.23
610.10	1723.12	649.30	1923.09	701.36	1801.78	644.31	1940.93	730.78	1966.98	603.04	1981.25	482.41	1765.49	379.79	1034.56
426.26	1526.65	577.37	1651.19	518.27	1752.90	538.73	1843.43	505.54	1898.41	474.23	1835.33	312.85	1483.07	272.27	919.17
238.54	1109.90	320.74	1333.53	362.73	1265.56	311.47	1169.20	359.34	1370.63	317.24	1204.61	228.35	1169.61	233.69	697.78
72.55	857.43	198.16	735.76	198.57	886.12	166.89	880.23	203.94	790.35	165.69	914.74	131.63	784.13	109.95	464.15
259.72	732.21	320.99	718.82	250.34	715.99	309.05	672.80	240.79	720.42	246.43	673.72	181.21	598.76	152.01	598.28

The minimum and maximum are 72.548438 3062.6328

Table B-AB2b
Aerojet Bulk Si:Bi Array
Background Run #1 (BGB #1)

VARIANCE

VAR

478.46	122.79	714.03	176.51	255.57	262.34	196.98	100.94	204.76	90.60	523.57	123.67	691.44	660.08	753.47	584.05
628.59	243.01	455.27	185.77	294.64	257.27	1257.46	174.26	131.67	62.14	161.27	107.22	1627.07	159.27	534.87	251.23
855.70	168.85	351.09	263.82	195.98	175.48	148.16	96.38	152.06	95.49	369.46	113.91	834.45	267.05	1339.69	377.83
822.66	211.44	779.38	194.84	653.78	294.25	308.72	161.76	558.05	162.67	164.41	182.30	1209.81	285.14	670.81	215.82
660.82	144.61	468.97	195.05	185.24	205.28	138.05	111.50	458.80	160.58	170.34	147.03	537.18	226.77	1105.74	520.11
761.58	236.15	195.91	141.27	189.36	249.25	392.92	120.62	958.43	198.83	819.12	207.53	376.40	182.16	531.16	616.29
503.03	115.73	295.61	148.72	320.24	260.16	288.31	207.27	1681.00	258.36	367.46	237.66	340.11	172.94	841.17	259.95
1126.41	156.51	155.02	219.53	199.12	213.22	128.57	233.08	308.56	275.41	762.48	274.62	1295.59	155.92	309.23	272.69
826.14	207.27	507.15	151.80	226.40	294.34	277.23	159.29	265.67	148.16	291.96	249.78	222.06	193.56	2210.97	229.80
694.40	161.04	197.71	226.40	278.21	251.71	519.10	366.94	490.65	211.60	342.45	224.79	460.51	295.84	473.53	237.58
931.51	317.33	402.96	150.48	263.95	317.46	207.52	127.06	225.72	200.72	404.52	249.29	295.75	155.68	184.83	238.26
796.39	278.44	713.13	366.88	482.92	407.29	222.65	224.78	206.26	209.44	324.63	155.59	340.17	354.10	468.51	217.15
818.79	128.82	373.32	218.62	157.93	134.29	585.51	147.87	200.61	125.79	447.68	196.42	382.43	186.49	329.87	239.82
404.07	184.88	789.96	192.14	1192.79	280.96	662.55	183.55	300.21	114.53	538.12	311.15	439.95	173.96	436.79	249.84
1028.26	180.07	174.25	208.82	271.92	244.47	180.44	362.25	184.44	96.91	473.18	263.60	499.19	147.01	518.56	224.96
793.79	143.38	258.74	137.21	248.03	265.75	278.97	305.68	629.78	184.19	326.10	187.00	412.10	311.05	428.70	205.59
1713.17	177.61	301.23	272.37	183.11	232.46	208.20	372.86	232.93	151.72	225.50	165.51	367.15	195.61	1195.57	210.07
875.15	281.49	413.29	301.73	289.31	405.30	266.55	191.05	251.00	243.57	221.86	151.87	231.04	188.72	324.75	213.47
767.81	185.90	206.52	123.25	172.79	460.18	328.48	155.90	263.08	137.00	268.86	277.46	203.41	167.29	398.06	249.41
474.03	250.53	426.36	265.13	464.65	316.59	300.02	204.16	233.81	240.84	296.62	185.60	440.57	137.94	391.45	164.93
477.70	379.11	244.77	134.33	350.29	386.51	188.13	353.89	896.83	191.77	255.50	131.45	187.83	143.19	267.12	181.53
589.07	207.81	348.86	343.53	389.56	286.15	827.92	233.69	291.39	235.53	223.49	203.41	325.97	141.01	307.66	254.97
1021.46	270.05	270.72	129.15	208.99	311.75	348.62	275.39	309.32	212.42	257.43	486.80	248.36	127.96	268.25	175.15
676.09	183.26	370.89	252.78	315.64	283.71	333.91	371.64	329.92	250.11	367.29	295.39	448.98	151.59	224.27	166.00
655.09	192.96	269.04	218.24	177.01	259.23	304.73	114.68	253.98	270.82	284.10	179.17	254.42	262.35	307.60	211.39
408.55	219.30	191.37	274.25	391.03	269.52	482.85	217.11	197.29	115.27	412.14	211.97	669.69	205.53	485.23	236.30
430.38	123.06	208.64	197.12	326.56	300.02	475.92	201.85	330.22	198.98	375.78	185.10	231.79	126.19	312.50	167.25
703.22	294.26	285.64	234.50	292.79	253.07	497.55	194.43	432.05	190.35	523.82	240.19	326.44	157.99	467.56	172.61
508.32	221.94	248.71	215.11	442.30	203.39	408.36	278.43	229.56	153.51	464.80	182.74	379.29	227.61	346.26	210.92
502.54	235.65	669.48	258.17	810.72	265.66	750.95	341.85	570.81	394.29	1202.33	281.84	582.22	274.69	490.52	338.97
411.39	309.87	385.10	465.75	447.16	161.35	365.81	218.36	531.88	189.16	359.14	211.39	685.32	296.22	319.11	220.56
1906.25	377.93	1607.78	389.92	415.70	257.28	1532.83	337.42	1778.67	216.03	2319.13	371.90	2599.58	336.00	361.45	235.91

The minimum and maximum are 62.139152 2599.5772

Table B-AB2c
Aerojet Bulk Si:Bi Array
Background Run #1 (BGB #1)

SKEWNESS

SKEW

0.005	0.017	1.029	0.004	0.035	0.077	0.037	0.004	0.303	0.057	0.082	0.046	0.016	0.004	0.019	0.284
0.022	0.008	0.343	0.004	1.509	0.203	0.199	0.002	0.178	0.021	0.156	0.069	0.166	1.145	0.076	0.238
0.015	0.027	0.156	0.055	0.210	0.026	0.017	0.001	0.145	0.048	0.783	0.029	0.001	0.075	0.153	0.188
0.010	0.007	1.132	0.293	1.333	0.001	1.499	0.079	1.162	0.149	0.297	0.017	0.944	0.861	0.114	0.001
0.024	0.000	0.155	0.016	0.166	0.421	1.150	0.033	1.508	0.090	0.095	0.031	0.392	0.736	0.029	0.146
0.002	0.002	0.085	0.000	0.241	0.215	1.018	0.004	0.079	0.006	0.248	0.006	0.901	0.003	0.019	0.056
0.000	0.009	0.372	0.000	0.178	0.036	0.276	0.006	0.043	0.000	0.083	0.078	0.028	0.007	0.000	0.012
0.739	0.034	0.194	0.041	0.222	0.425	0.019	0.001	0.428	0.002	0.732	0.072	0.097	0.291	0.221	0.005
0.248	0.001	0.410	0.000	0.306	0.031	0.034	0.165	0.060	0.672	0.138	0.108	0.047	0.001	0.001	0.001
0.053	0.072	0.270	0.001	0.770	0.005	0.748	0.001	0.421	0.030	0.040	0.026	0.004	0.044	0.004	0.019
0.101	0.008	0.147	0.002	0.010	0.014	0.076	0.002	0.264	0.017	0.059	0.049	0.420	0.006	0.000	0.000
0.052	0.002	0.367	0.013	0.056	0.010	0.431	0.027	0.919	0.000	0.268	0.018	0.478	0.009	0.002	0.014
0.200	0.001	0.000	0.036	0.168	2.237	1.535	0.040	0.305	0.005	0.026	0.000	0.134	0.009	0.006	0.002
0.114	0.000	0.394	0.015	0.065	0.120	0.797	0.001	1.193	0.069	0.494	0.005	0.004	0.002	1.771	0.024
0.003	0.002	0.005	0.055	1.263	0.104	0.082	0.003	0.550	0.001	0.791	0.000	0.053	0.001	0.025	0.001
0.017	0.003	0.011	0.005	0.219	0.031	0.364	0.001	1.314	0.056	0.260	0.029	0.213	0.011	0.002	0.017
0.064	0.002	0.430	0.014	0.067	0.439	0.040	0.012	3.302	0.001	0.016	0.147	0.000	0.016	0.106	0.002
0.026	0.000	0.301	0.000	0.097	0.358	0.832	0.005	0.652	0.000	0.137	0.014	0.081	0.002	0.046	0.000
0.011	0.002	0.332	0.005	0.009	0.005	0.043	0.014	0.056	0.025	0.093	0.003	0.100	0.004	0.777	0.005
0.052	0.030	0.605	0.000	0.586	0.010	0.622	0.004	0.330	0.003	0.001	0.001	1.168	0.012	0.572	0.002
0.001	0.006	0.121	0.040	2.455	0.021	0.164	0.111	0.430	0.001	0.000	0.024	0.001	0.005	0.150	0.019
0.043	0.028	0.338	0.059	0.137	0.033	0.792	0.007	0.001	0.010	0.000	0.013	0.021	0.026	0.009	0.004
0.292	0.008	0.165	0.005	0.202	0.001	0.424	0.027	0.020	0.000	0.020	0.013	0.075	0.000	0.022	0.000
0.051	0.048	0.541	0.012	0.058	0.301	1.565	0.000	0.926	0.023	0.014	0.001	0.060	0.014	0.003	0.006
0.113	0.001	0.014	0.002	0.360	0.021	0.181	0.000	0.028	0.027	0.037	0.007	0.029	0.083	0.020	0.009
0.067	0.028	0.001	0.022	0.723	0.092	0.023	0.025	0.134	0.004	0.220	0.116	0.405	0.021	0.008	0.010
0.038	0.001	0.098	0.007	0.279	0.000	0.425	0.012	0.043	0.001	0.020	0.006	0.006	0.002	0.044	0.002
0.007	0.000	0.110	0.032	0.070	0.000	0.266	0.035	0.769	0.043	0.196	0.006	0.026	0.007	0.066	0.001
0.019	0.005	0.109	0.008	0.037	0.006	0.250	0.016	0.054	0.007	0.041	0.003	0.018	0.009	0.042	0.010
0.011	0.022	0.416	0.053	0.289	0.074	0.320	0.000	0.420	0.007	0.098	0.001	0.002	0.005	0.000	0.001
0.018	0.000	0.022	0.000	0.028	0.000	0.004	0.003	0.011	0.004	0.049	0.013	0.125	0.010	0.031	0.000
0.032	0.006	0.196	0.001	0.310	0.010	0.762	0.155	0.269	0.000	0.000	0.012	0.000	0.006	1.320	0.009

The minimum and maximum are 5.55858987E-09 3.3021957

Table B-AB2d
Aerojet Bulk Si:Bi Array
Background Run #1 (BGB #1)

KURTOSIS

KURT

3.076	3.058	5.068	3.115	2.962	3.354	2.944	3.007	3.918	3.874	2.750	3.117	2.624	2.584	3.030	3.595
3.098	3.006	4.170	3.401	6.602	1.490	2.256	2.994	4.790	3.418	4.714	5.832	2.823	7.411	5.300	5.159
3.022	3.478	3.029	2.623	4.430	5.798	4.893	2.809	3.826	3.399	4.045	3.247	2.697	4.704	3.385	4.068
3.329	2.851	4.298	4.388	4.725	2.062	6.165	2.890	4.334	5.405	4.754	3.380	3.685	6.287	3.840	2.951
3.221	2.943	2.689	2.937	3.266	4.089	8.733	3.058	6.316	3.865	3.757	3.487	3.853	5.004	2.790	3.163
2.917	2.889	3.577	2.945	4.135	2.339	5.284	2.956	3.467	3.208	3.027	2.869	4.759	2.995	3.374	3.018
2.972	3.015	3.438	2.887	3.353	1.299	3.202	2.777	1.975	3.096	3.234	2.778	3.075	2.935	3.424	3.367
4.047	2.987	4.545	3.091	3.922	3.979	2.984	3.152	4.737	2.747	4.100	2.756	2.610	4.385	4.603	3.098
3.478	2.919	3.165	2.929	4.304	3.052	3.020	3.366	3.467	6.854	3.668	2.999	3.111	3.079	2.292	3.080
3.593	3.732	4.792	2.744	5.179	4.288	4.182	2.754	3.712	3.131	3.361	3.080	2.863	2.844	3.089	3.029
3.843	2.719	3.068	3.073	2.824	2.192	3.409	2.907	3.941	3.105	3.113	2.738	3.843	2.969	2.829	2.901
3.563	2.802	3.393	2.732	4.430	2.548	5.222	2.909	6.549	3.117	4.010	3.080	4.613	2.688	3.336	3.012
3.066	2.972	2.634	2.829	3.518	6.076	5.428	3.160	4.061	2.917	2.763	3.103	3.362	2.897	2.912	3.027
3.072	2.797	3.093	3.010	2.509	2.075	3.803	2.949	5.854	3.982	4.018	2.783	3.276	2.896	6.650	3.373
3.477	2.815	3.061	2.843	6.901	3.649	3.548	2.602	5.483	3.037	5.590	2.652	3.856	2.924	3.863	3.015
3.792	3.227	2.934	3.108	3.662	3.953	4.299	2.470	4.484	3.216	4.161	3.153	3.807	2.766	2.917	3.050
3.119	3.083	3.798	2.842	3.389	2.554	3.543	2.499	12.782	2.966	3.067	3.595	2.696	2.908	3.735	2.934
3.337	3.001	3.789	2.642	3.283	4.379	5.425	2.891	5.250	2.770	3.605	3.364	3.094	2.801	3.668	2.978
3.117	2.868	5.048	3.120	3.042	2.272	3.126	2.981	3.110	3.110	3.282	2.852	3.871	3.143	5.332	3.118
3.818	2.947	4.340	2.948	4.221	2.750	4.822	2.840	4.485	2.790	2.845	2.704	5.558	3.107	5.574	2.946
3.261	2.838	3.751	3.110	7.714	2.702	3.660	2.790	2.760	2.918	2.862	3.262	3.069	3.140	3.904	3.174
3.076	3.116	4.056	2.765	3.526	2.392	3.556	2.906	5.274	3.082	3.040	2.930	3.173	3.330	2.961	2.812
3.687	2.850	3.659	2.963	3.863	3.364	4.682	2.797	2.921	2.766	3.575	2.608	3.726	3.237	3.041	3.077
3.158	3.173	4.606	3.006	3.279	2.810	6.493	2.852	7.091	3.001	2.774	2.703	2.988	2.946	3.009	3.100
2.824	3.109	2.982	2.985	4.786	3.806	2.999	2.963	3.043	3.107	3.202	2.846	3.188	2.828	3.056	2.999
3.978	2.815	3.269	3.003	5.058	2.279	3.229	2.985	4.362	3.087	4.545	3.219	3.821	3.081	3.042	3.239
3.740	3.011	3.621	3.185	3.493	2.807	3.930	3.136	3.333	3.335	3.093	3.165	2.903	3.096	3.420	2.860
3.523	2.800	4.505	2.874	3.256	2.774	3.920	3.336	4.921	2.955	3.808	2.926	3.316	2.996	3.474	3.017
3.139	2.871	3.483	3.027	3.211	2.929	3.589	2.974	3.313	3.143	3.062	2.904	3.014	2.904	3.066	3.017
3.130	2.804	4.239	3.147	3.340	2.985	3.861	2.682	4.001	2.855	2.905	2.666	3.097	3.013	2.991	2.886
3.040	2.854	3.090	2.782	2.960	3.167	3.193	3.626	3.015	3.031	3.773	3.121	3.692	2.839	3.185	2.887
2.770	2.839	2.813	3.281	4.593	2.938	3.355	3.779	2.602	3.138	2.338	3.104	2.224	2.895	7.200	2.751

The minimum and maximum are 1.2992268 12.781600

Table B-AB3
Aerojet Bulk Si:Bi Array

(Average Star B #1)/Average BGB #1)

Tape 11: Ratio of Star (file 16) over Background (file 17)

1.000	1.000	1.001	1.000	0.999	1.000	1.000	1.000	1.000	1.000	1.000	1.000	1.000	0.999	0.997	0.997
0.999	1.000	1.001	1.000	1.000	1.000	0.998	1.000	1.000	1.000	1.000	0.999	0.997	0.999	0.996	0.997
0.999	1.000	1.000	1.000	1.000	1.000	0.999	1.000	1.000	1.000	0.999	1.000	0.999	1.000	0.996	0.997
1.001	1.000	1.001	1.000	1.000	1.000	1.000	1.000	1.000	1.000	0.999	0.999	0.998	1.000	0.997	0.997
1.000	1.000	1.000	1.000	1.000	1.000	1.000	1.000	0.999	1.000	1.000	1.000	0.999	1.000	1.000	0.997
1.000	1.000	1.000	1.000	1.000	1.000	1.000	1.000	0.999	1.000	1.000	0.999	0.999	1.000	0.997	0.998
1.000	1.000	1.000	1.000	1.001	1.000	1.000	1.000	0.999	1.000	1.000	1.000	0.999	1.000	0.999	0.997
0.999	1.000	1.000	1.000	1.001	1.000	1.000	1.000	1.000	1.000	0.998	1.000	0.997	1.000	0.998	0.997
1.000	1.000	0.999	1.000	1.000	1.000	1.001	1.000	0.999	1.000	0.999	1.000	0.999	1.000	0.996	0.997
1.001	1.000	1.000	1.000	1.001	1.000	1.000	1.000	1.001	1.000	0.998	1.000	1.000	0.999	0.997	0.997
1.000	1.000	1.001	1.000	1.001	1.000	1.000	1.000	1.000	1.000	1.000	1.000	1.000	1.000	0.999	0.997
1.000	1.000	1.000	1.000	1.000	1.000	1.001	1.000	1.000	1.000	1.001	1.000	1.000	1.000	1.001	0.998
1.000	1.000	0.999	1.000	0.999	1.000	1.000	1.000	1.001	1.001	1.003	1.002	1.002	1.001	1.000	0.997
1.000	1.000	1.000	1.000	1.000	1.000	1.001	1.000	1.002	1.002	1.010	1.006	1.013	1.003	1.002	0.999
1.001	1.000	1.000	1.000	1.000	1.000	1.000	1.000	1.003	1.003	1.024	1.023	1.037	1.006	1.006	0.999
1.000	1.000	0.999	1.000	1.000	1.000	1.001	1.000	1.004	1.004	1.032	1.038	1.079	1.014	1.013	1.000
1.000	1.000	1.000	1.000	1.001	1.000	1.001	1.001	1.005	1.006	1.043	1.041	1.081	1.017	1.016	1.000
1.003	1.000	1.001	1.000	1.000	1.000	1.002	1.001	1.004	1.005	1.020	1.013	1.033	1.012	1.012	1.000
1.005	1.001	1.002	1.001	1.001	1.001	1.002	1.001	1.001	1.003	1.007	1.004	1.012	1.006	1.009	1.001
1.000	1.000	0.999	0.999	0.998	1.000	0.999	1.000	1.000	1.001	1.001	1.000	1.004	1.002	1.005	1.000
1.002	1.000	1.000	1.000	1.000	1.000	0.999	1.001	0.999	1.000	1.002	1.000	1.002	1.002	1.003	0.999
1.001	1.000	0.999	1.000	1.000	1.000	0.999	1.000	1.000	1.000	1.000	0.999	1.001	1.001	1.002	0.998
0.998	1.000	0.999	1.000	1.000	1.000	1.001	1.000	1.000	1.000	1.001	0.999	1.001	1.000	1.002	0.998
1.001	1.000	1.001	1.000	0.999	1.000	1.000	1.001	1.000	1.000	1.000	0.999	0.999	1.000	1.000	0.999
1.000	1.000	1.001	1.000	1.000	1.000	0.998	1.000	1.001	1.000	1.001	0.999	1.000	1.000	0.999	0.999
1.000	1.000	1.000	1.000	1.000	1.000	1.001	1.000	1.000	1.000	0.999	1.000	1.001	1.000	1.000	0.999
1.000	1.000	1.000	1.000	1.001	1.000	0.998	1.000	1.000	1.000	0.999	0.999	1.001	1.000	1.000	0.999
0.999	1.000	0.999	1.001	1.000	1.000	1.001	1.000	1.001	1.000	0.999	0.999	0.998	1.000	0.999	0.999
1.000	1.000	1.000	1.000	1.000	0.999	1.000	0.999	1.000	1.000	1.001	0.999	0.997	1.000	0.998	0.998
0.996	1.000	0.992	1.000	1.000	0.999	0.993	0.999	1.000	0.999	0.999	0.999	0.998	0.999	1.000	0.998
0.996	1.001	1.000	0.999	0.999	0.999	0.995	0.999	0.997	0.998	1.000	0.999	0.978	0.998	1.004	1.001
1.006	0.999	0.994	1.000	1.001	0.999	0.997	1.000	0.996	1.000	0.997	0.999	0.980	1.000	0.997	1.000

A Reprint from the

PROCEEDINGS

Of SPIE-The International Society for Optical Engineering

Volume 685

Infrared Technology XII

19-20 August 1986
San Diego, California

Test of IR arrays on the Kuiper Airborne Observatory

R. W. Russell, G. S. Rossano, D. K. Lynch, G. T. Colon-Bonet, J. A. Hackwell, T. C. Morse, R. H. Macklin, D. Murray, D. A. Retig, C. J. Rice, D. A. Roux, R. M. Young
Space Sciences Laboratory, The Aerospace Corporation
P.O. Box 92957, Los Angeles, California 90009

©1986 by the Society of Photo-Optical Instrumentation Engineers
Box 10, Bellingham, Washington 98227 USA. Telephone 206/676-3290

Invited Paper

Test of IR arrays on the Kuiper Airborne Observatory

R. W. Russell, G. S. Rossano, D. K. Lynch, G. T. Colon-Bonet, J. A. Hackwell, T. C. Morse, R. H. Macklin, D. Murray, D. A. Retig, C. J. Rice, D. A. Roux, and R. M. Young

Space Sciences Laboratory, The Aerospace Corporation, P. O. Box 92957, Los Angeles, California 90009

Abstract

The Aerospace Corporation has conducted 5 flight series on the Kuiper Airborne Observatory (KAO) utilizing two-dimensional array infrared cameras. The KAO is operated by NASA Ames Research Center. These flights have several objectives with the primary task being the test in an aircraft environment of state-of-the-art two-dimensional arrays of both blocked impurity band and bulk silicon devices provided by Rockwell International and the Aerojet ElectroSystems Company under contract to the U.S. Army. There is extremely low crosstalk due to the SWIFET (switched FET) readout scheme employed on all three arrays flown to date. The ~ 500-element arrays were operated with a frame time of 307 μsec which placed a large burden on the data recording equipment. The flight data were recorded on 8" floppy disks, a 9-track tape recorder, and a high-speed 28-track flight recorder. System sensitivities have been shown to be good enough to detect astronomical sources, both point-like and extended in nature. Both staring and scanning experiments were performed using several astronomical sources. In the scanning experiments, a star was used as a point source which was scanned across the array at a fixed angle and angular rate using the rocking secondary mirror of the KAO. The data were then processed in a Time Delay and Integrate mode by the Boeing Aircraft Corporation; this TDI simulation achieved close to the theoretically predicted improvement in signal-to-noise ratio.

Introduction

Recently the U.S. Army engaged in an engineering and technology development and demonstration program in concert with wind tunnel and airborne astronomical research programs at the NASA Ames Research Center. The program deals with many issues in such diverse areas as atmospheric seeing effects, aerodynamics effects on images, background radiance from the atmosphere and the platform, and the use of IR arrays on airborne platforms. Because the program is built around the use of the Kuiper Airborne Observatory (KAO) (Figure 1), the project is dubbed the Kuiper Infrared Technology Experiment, or KITE. The KAO itself is a 4-engine C141 jet transport equipped with a 90-cm, all-reflective altazimuth telescope viewing out the left side of the aircraft at elevation angles from about 35° to about 72°. One major thrust of the KITE program includes the integration of existing state-of-the-art infrared detector arrays both of bulk silicon and of Impurity Band Conduction (IBC) architecture into flight-qualified dewars for testing under a variety of conditions on three different telescopes. The goals of the array work are:

1. To take several state-of-the-art IR arrays which have been used only in the laboratory and demonstrate their use in a working flight system which includes data acquisition and subsequent data processing.

2. To collect information on the use of the above arrays in an airborne environment where ground currents, radio transmissions, and mechanical and acoustical vibrations are only a few of many potential sources of performance degradation.

3. To quantify the angular size of the IR image near 11 μm over a variety of time scales, and to measure the amount of motion of that image (blur size and jitter).

4. To collect a database for evaluating the impact of varying aerodynamical parameters (for example, the mach number and cavity turbulence) on the image quality.

5. To attempt an actual demonstration of system performance in a time-delay-and-integrate (TDI) mode.

6. To provide a database for subsequent use in studies of signal processing of extended sources, background variability and subtraction, and closely spaced objects.

All of these goals were met in a 2-year time period, and within 5 months of the ambitious schedule conceived in August 1983, although we have only just begun to process the data and to interpret the results.

A project of this magnitude requires a tremendous amount of manpower. Organizing the effort was complicated in this case by the compressed schedule caused by funding delays and

KUIPER AIRBORNE OBSERVATORY

OPERATING CEILING:	41-45 K ft
ENDURANCE FOR RESEARCH:	7.5 hr
RANGE:	3300 n. mi
PAYLOAD:	60-100 K lb
TELESCOPE APERTURE:	36 in (91 cm)
POINTING PRECISION:	≤1 arcsec
INVESTIGATOR ACCOMMODATION:	5-7

LEAR JET OBSERVATORY

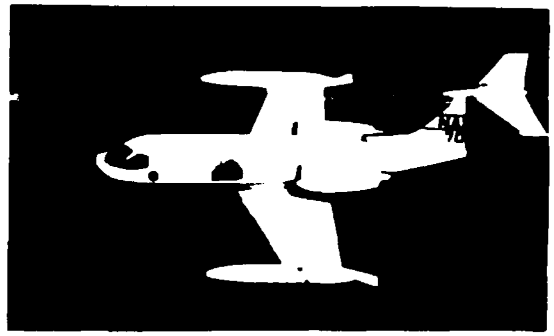

OPERATING CEILING:	45 K ft
ENDURANCE FOR RESEARCH.	2.5 hr
RANGE:	1300 n. mi
PAYLOAD:	1.2 K lb
TELESCOPE APERTURE:	12 in (30 cm)
POINTING PRECISION	15 arcsec
INVESTIGATOR ACCOMMODATION:	2

Figure 1. Description of NASA aircraft.

aircraft problems. Figure 2 shows the organization of the project. We emphasize that this effort was conceived as a systems engineering project and not as a comparative array test and evaluation program. The three different arrays used were operated with different filters under different conditions; no quick comparisons of relative performance can be or should be made. Aerojet ElectroSystems Company (AESC) supplied a Si:Bi bulk array and an MC^2 array, both in a 16 x 32 pixel format, together with a signal processor which could be programmed to do a hardware flat-fielding to correct for offset and gain variations in the array/multiplexer combination. Because the same electronics had to be used for all devices this latter feature was used only in the laboratory. Rockwell International (RI) provided a BIBIB array in a 10 x 50 pixel format together with a signal processor built to identical interface specifications. This meant that the readout devices of the Boeing Aerospace Corporation and The Aerospace Corporation could connect to either set of electronics interchangeably. Boeing Aerospace Corporation (BAC) provided a burst processor and actively participated both in test runs on a telescope at Mt. Lemmon and on KAO flights. The burst processor provides a very useful real-time tool as well as a convenient way to store 128 consecutive frames onto an 8" floppy disc. The Boeing signal processing group has done a great deal of analysis of image size and motion as well as having worked on the TDI demonstration. Teledyne Brown Engineering (TBE) contributed two versions of the optical design for the dewar in its f/16 configuration, worked with Aerospace on the f/6.5 optics, provided the germanium lenses, participated in ground and flight tests, did much of the planning of test procedures, and performed major post-flight data analysis. The University of Denver built and flew a cold-optics radiometer to provide a characterization of the atmospheric radiance which was coincident in space and time with the array observations. The Aerospace Corporation served as principal investigator on the experiment, coordinated the various groups, provided cryogenic dewar specifications, installed and aligned the optics in the dewar, conducted the various observing runs and test programs, provided the primary data acquisition system, and converted the various flight tapes into common 9-track tapes. Recently, Aerospace has also begun to play a major role in data analysis and interpretation.

Dewars and Optics

Overall Goals to be Met by the Mechanical and Optical Design

Two major constraints determined the optical/mechanical design of the KITE detector systems. First, the instruments had to be suitable for use on three different telescopes without moving the detector arrays or the internal wiring. These telescopes are: the Kuiper Airborne Observatory or KAO (f/16, 36-inch primary mirror), the Lear Jet Observatory or LJO (f/6.5, 12-inch mirror), and the ground-based Mt. Lemmon NASA telescope (f/16, 60-inch mirror). Second, the infrared background seen by the detector arrays while observing through a telescope must be low enough not to saturate the detector multiplexer. All of

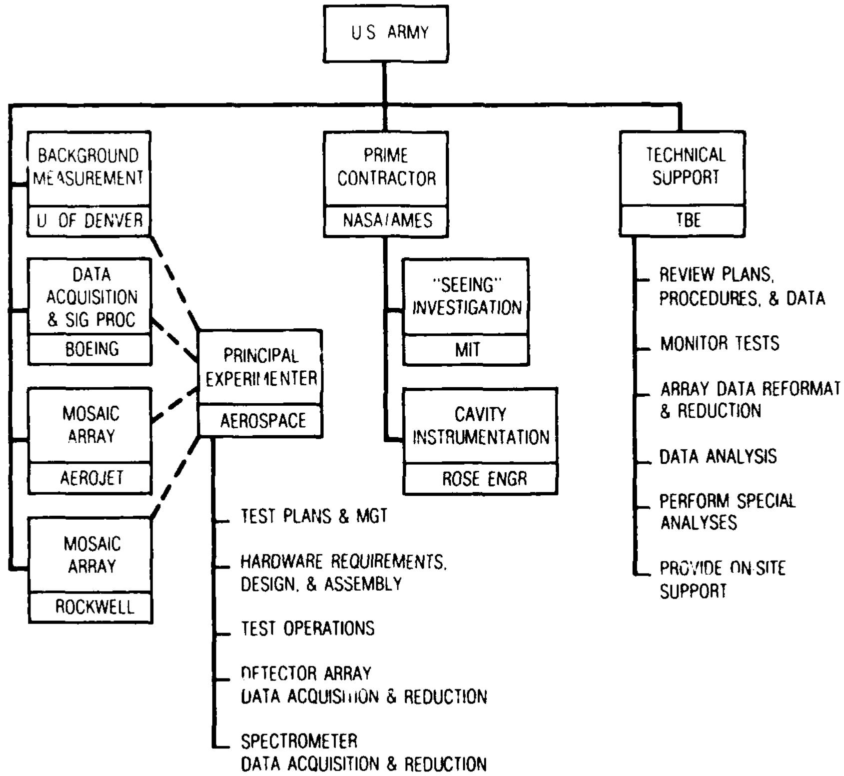

Figure 2. Organization of the KITE project.

the decisions made during the design and implementation of the KITE systems were ultimately driven by one or the other of these two constraints. In addition we wanted the instruments to be simple to use and maintain and to be portable. For practicality we specified that the cryogenic dewars require re-filling a maximum of once per day.

Cryostats

The detector cryostats had to be small enough to fit into the space available on the airborne platforms (a severe constraint in the case of the Lear Jet), and yet have an interior work space large enough to accommodate the relatively bulky elements required by the optical design. Because time was short, a readily available, reliable, and tested cryostat was strongly preferred. These requirements led us to choose the Infrared Laboratories' model HD-3(8) dewar with an expanded workspace and two vacuum-sealed 41-pin connectors. This liquid-nitrogen shielded dewar has been used by a number of other infrared astronomers who have found it to be reliable. Figure 3 shows a cross-section of the HD-3(8); the liquid-helium-cooled work surface is an 8-inch diameter circle, and there is a vertical space of 4-in between the helium-cooled surface and the nitrogen-cooled radiation shield.

The original TBE optical design called for a 2-inch clear hole through the liquid nitrogen shield which placed an unacceptably high thermal radiation load on the helium cryostat. The current design uses two liquid-nitrogen cooled blocking filters and a cooled rectangular focal plane baffle to reduce the amount of thermal radiation which enters the helium-cooled volume. The helium vessel needs to be refilled only once every 60 hours when the arrays have not been turned on. There is significant electrical energy dissipation from the arrays at the cold work surface when they are operating; in this case the hold time falls to about 24 hours. The thermal radiation shield must be refilled with liquid nitrogen approximately once every 24 hours as well. Thus it is not possible to leave an unused cold dewar unattended for an entire weekend.

The dewar is heavy, about 70 lbs with preamp and mounting hardware, which places severe constraints on the hardware which mates it to the telescope. On an aircraft, the mounting hardware must be capable of maintaining the dewar's optical alignment in the presence of strong vibration. On a ground-based telescope, the dewar's optical alignment with respect to the telescope must be maintained even as the telescope is tilted by up to 60°.

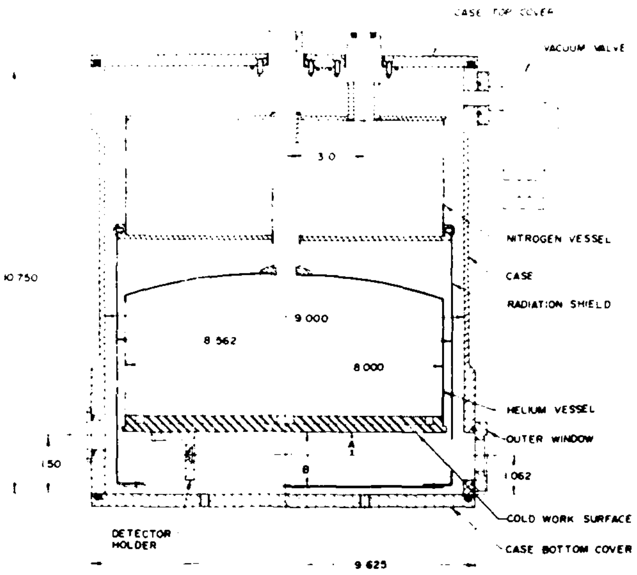

Figure 3. Cross-section of the Infrared Laboratory HD-3(8) dewar used for the detector arrays. Dimensions are in inches. The dimensions marked "A" and "B" are 2" and 4", respectively, for our dewar which necessitated adjustments in some of the other indicated sizes.

Dewar Optical Design

The optics inside the dewar must re-image the focal-plane of the (existing) telescopes onto the detector array at a suitable magnification while introducing as little extra aberration as possible. The design must also include a Lyot stop which is a helium-cooled stop placed at a real image of the pupil to minimize unwanted background radiation reaching the detectors. To minimize thermal background radiation all of the optical train, with the exception of the entrance window, must be cooled to cryogenic temperatures. Additionally, the optics should be kept as simple as possible so that they can be aligned in the laboratory and not lose alignment when cooled or when exposed to shock and vibration on board the aircraft.

The production of compact, high-quality re-imaging optics is a challenging task for the optical designer. Two designs were developed, one for the f/6.5 LJO telescope, the other for use on both the f/16 KAO and the f/16 Mt. Lemmon 60-inch telescope. The f/6.5 design uses a pair of off-axis paraboloids (Figure 4); the system has an overall magnification of unity and serves merely to take the image formed by the telescope focal plane and re-image the light onto the detector focal plane. When used on the LJO 12-inch telescope, each 125 x 125 micron detector subtends an angle of 13 x 13 arcseconds (65 x 65 microradians). The AESC Si:Bi bulk detector array mounted in this optical system was first flown on the LJO in May, 1985 to measure backgrounds and system noise. No star observations were made at that time because of problems with the pointing servo-system of the telescope.

Because we wanted the optical system used on the KAO to have a de-magnification of approximately 2.5, the simple two-mirror system used for the LJO was not adequate. Such a system gives unacceptably large aberrations when used at a magnification other than unity. While Aerospace was awaiting the award of contract, TBE undertook the design of a re-imaging system which would give acceptable optical performance and still fit inside the infrared dewar. Their foresight allowed the acquisition of the optics in a timely fashion and avoided delays in the program. Because of the large amount of special wiring and cabling that is needed to mount the detectors in the dewar, we asked that the new design not require that the detector substrate be moved from its original position on the helium surface. The initial TBE design used a single Ge lens which was mounted just inside the penetration of the liquid nitrogen shield and simply condensed the beam; it is shown in Figure 5. Because there was no Lyot stop, this first design gave a high infrared background which saturated the detector array. The final TBE design is shown in Figure 6. A germanium lens is used to re-image the telescope focal plane and to provide a real image of the pupil for a Lyot stop. Two flat mirrors, one before the lens and one after the lens, fold the optical path so that it fits into the dewar. This optical scheme is used by all three detector systems when they are mounted on the KAO or on the Mt. Lemmon 60-inch telescope. Table 1 summarizes the re-imaging optics and their performance on the telescopes.

Table 1. Performance of Re-Imaging Optics

Telescope	f/ratio	Aperture	Expected Effective Detector Size	Blur Circle[1]
LJO	6.5	12"	~ 70-100 μrad	~ 75-240 μrad
KAO	16	36"	~ 20-24 μrad	~ 40 μrad
Mt. Lemmon	16	60"	~ 13-16 μrad	10-35 μrad

[1]Typical seeing, including diffraction effects, known aberrations, etc.

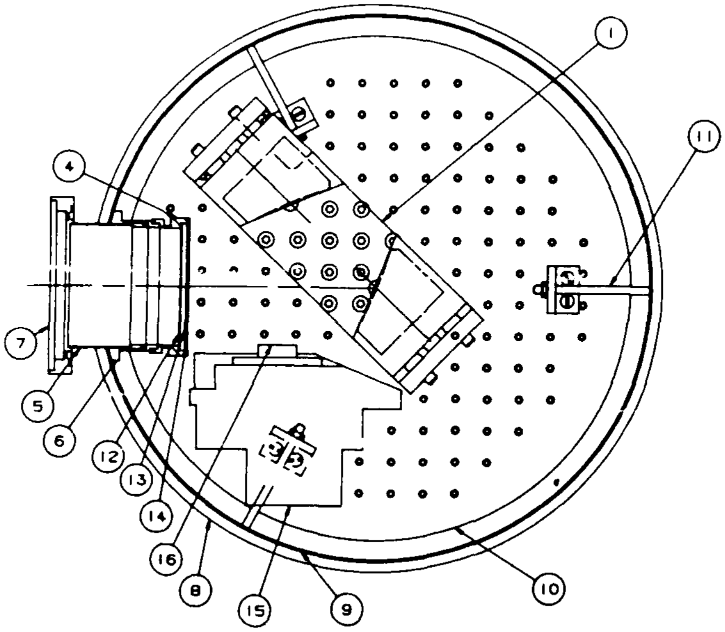

QTY.	PART NAME	ITEM
1	BANDPASS FILTER	16
1	DETECTOR	15
1	PRESSURE RING	14
1	BARIUM FLUORIDE FILTER AND FIELD STOP	13
1	SI FILTER	12
3	SUPPORT ROD ASSEMBLY	11
1	8" COLD PLATE (.50 GRID)	10
1	LN2 SHIELD	9
1	VACUUM HOUSING I.D. (NOM.)	8
1	ENTRANCE WINDOW MOUNTING PLATE	7
1	SADDLE	6
1	SHIELD TUBE	5
1	FILTER MOUNT	4
1	PARABOLA ASSEMBLY	1
1		

PARTS LIST

Figure 4. Off-axis paraboloid re-imaging optics used for the LJO f/6.5 telescope. Cold baffles are omitted for clarity. View is from below the dewar (see Figure 3).

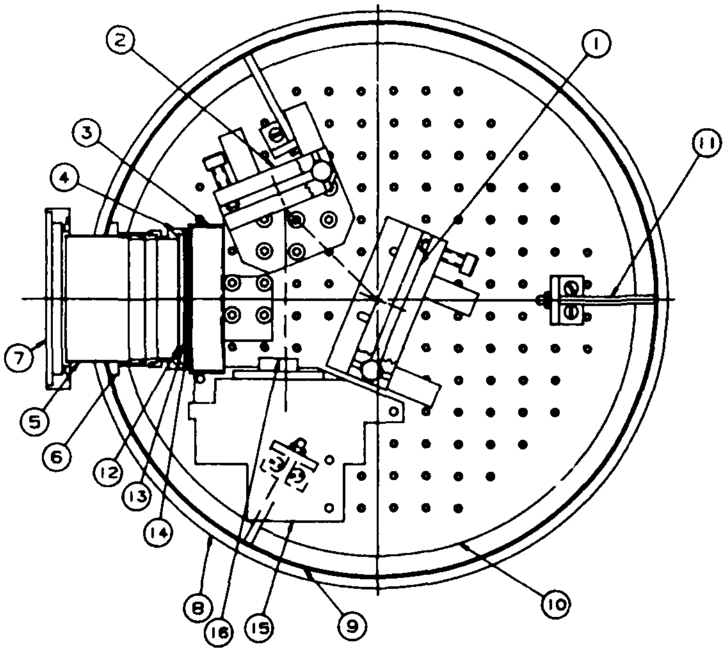

QTY	PART NAME	ITEM
1	BANDPASS FILTER	16
1	DETECTOR	15
1	PRESSURE RING	14
1	BARIUM FLUORIDE FILTER	13
1	SI FILTER	12
1	SUPPORT ROD ASSY.	11
1	8" COLD PLATE	10
1	LN2 SHIELD	9
1	VACUUM HOUSING I.D.	8
1	ENTRANCE WINDOW MOUNT	7
1	SADDLE	6
1	SHIELD TUBE	5
1	FILTER MOUNT	4
1	Ge LENS HOLDER	3
1	MIRROR MOUNT #2 ASSY.	2
1	MIRROR MOUNT #1 ASSY.	1

PARTS LIST

Figure 5. Original condensing lens scheme designed but not used at f/16 because it has no Lyot stop and gives a high background. Cold baffles are omitted.

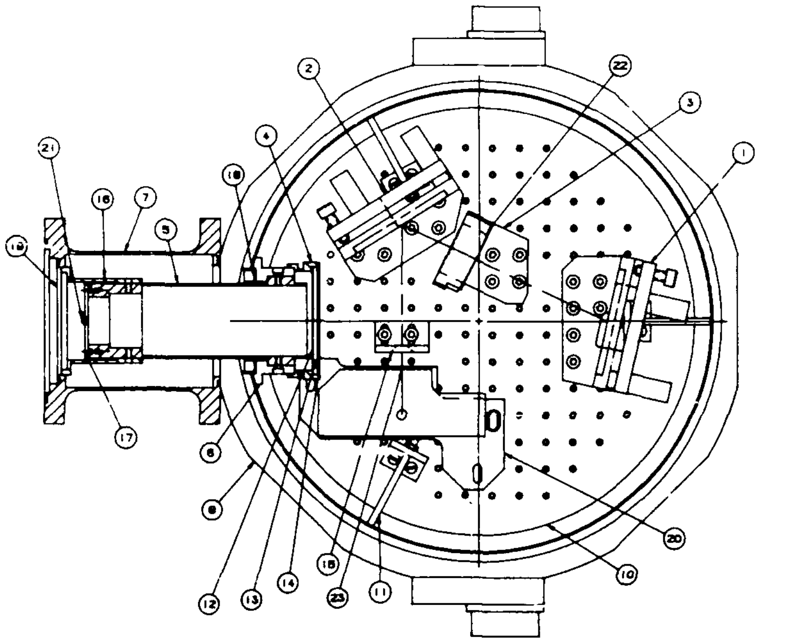

QTY.	PART NAME	ITEM
1	BANDPASS FILTER	23
1	LENS	22
	TELESCOPE FOCUS/DEWAR ROTATION POINT	21
1	ARRAY	20
	ENTRANCE WINDOW MOUNT SURFACE	19
1	GUIDE TUBE KAO/AESC	18
1	APERTURE PLATE KAO/AESC	17
1	SHIELD TUBE SUPPORT KAO/AESC	16
1	PUPIL KAO/AESC	15
1	PRESSURE RING	14
1	BARIUM FLUORIDE FILTER	13
1	SI FILTER	12
3	SUPPORT ROD ASSEMBLY	11
1	8" COLD PLATE (.50 GRID)	10
1	LN2 SHIELD	9
1	VACUUM HOUSING (NOM.)	8
1	EXTENSION ASSY. HD-3(8) DEWAR	7
1	SADDLE KAO/AESC	6
1	SHIELD TUBE KAO/AESC	5
1	FILTER MOUNT	4
1	Ge LENS/MOUNT	3
1	MIRROR MOUNT #2 ASSY.	2
1	MIRROR MOUNT #1 ASSY.	1

PARTS LIST

Figure 6. Final optics used for the Kuiper Airborne Observatory f/16 36-inch telescope and the Mt. Lemmon Observatory 60-inch telescope. This design re-images the pupil onto a cooled Lyot stop, and greatly reduces the background seen by the array. Helium-temperature baffles are omitted.

The Germanium Lens

A germanium lens has a refractive index high enough to give the short focal length demanded by the final optical design without introducing unacceptable aberrations; it also serves as an additional short-wavelength blocking filter. The use of a germanium lens presents two problems, however. First, because germanium does not transmit visible light, the lens must be aligned by "dead reckoning". Second, an uncoated Ge lens transmits only ~ 40% of the incident radiation. Thus the lens must be anti-reflection (A-R) coated to reduce reflection losses. This A-R coating must adhere to the lens at liquid helium temperatures and survive repeated cycling between 4K and 300K. Thermal tests were made of an A-R coating supplied by CVI Laser Corporation on a germanium flat. Adhesion after three cycles between room temperature and liquid helium temperature was found to be excellent, and the coating readily passed an "adhesive tape" and an "eraser" abrasion test. Unfortunately, the lenses that were subsequently coated shed their A-R coatings after only one thermal cycle. These lenses have since been re-coated with acceptable results, although some of them are starting to shed their A-R coating where they are in contact with the clips that hold them in their optical mounts.

Although the HD-3(8) dewars were specially modified to give extra room in the "vertical" direction (perpendicular to the optical axis), the largest germanium lens that can be fitted into the dewar in a rigid mount without obstructing other parts of the optical path has a diameter of only about 2 inches. This is too small to allow all of the detectors in the Rockwell BIBIB 10 x 50 element array to be illuminated by the entire primary mirror. Even with the optics optimally aligned, detectors at the extreme edges of the 50-element columns are vignetted. Any performance figures that we discuss for this array are for fully illuminated detectors near the optical axis.

Optical Mounts, Baffles, and Background Considerations

Mounts for the optical components were designed and constructed at The Aerospace Corporation. The major issues addressed when designing the mounts were differential thermal contraction and the thermal sinking of elements to the helium surface. Even now the most thermally-distant components cool relatively slowly so that the first 3-liter load of liquid helium is lost within 20 minutes. At the end of this time, however, the optics are sufficiently cold that the second 3-liter load of helium will last almost a full 60 hours.

The requirement for using existing array devices was driven by cost and schedule constraints. For example, it was only about 6 months from the time that the first array was

put into a dewar until it had been tested in the laboratory and successfully flown on the LJO and KAO. Unfortunately, the existing arrays were all meant to be used under low background conditions (i.e., had small node capacitances of the order of 0.4 pf) and this required particular attention to spectral filtering and cold baffling if the multiplexers were not to be saturated.

If the background from the liquid-nitrogen cooled radiation shield were allowed to illuminate the entire hemisphere viewed by a detector, each detector would see $\sim 1.3 \times 10^8$ photons per second per micron at 11 microns. Thus, the Rockwell $BIBIB_2$ detector would see $\sim 3.6 \times 10^7$ photons per second in its 0.28-μm bandpass, and the AESC MC^2 detector would see $\sim 2.5 \times 10^8$ photons per second in its 1.9-μm bandpass. The number of photons (7.5×10^4) collected in one frame time (3×10^{-4} sec) is quite small when compared to the saturation level of $\sim 10^6$ electrons. Yet, when blanked-off tests were performed in early stages of the project, the devices were essentially in saturation (i.e., $> 10^6$ photons/detector per frame). This was traced to a long wavelength (> 18 μm) leak which appeared in the bandpass filters when they were operated at 10K. The filters have a transmission of ~ 25% from 20 to 28 μm, a region of strong response for IBC devices. The background due to 77K radiation through the leak would be expected to be too high to be useful as a reference "zero". Thus, liquid-helium cooled baffles were placed between the helium-cooled optics and the nitrogen-cooled radiation shield. Although these baffles are fairly crude and are fabricated from aluminum shim, aluminum foil and aluminum tape, they are readily installed and removed, and greatly reduce the background from the radiation shield.

We also found several "light leaks" in the liquid-nitrogen cooled radiation shield which were letting in an unacceptably large number of photons from the room-temperature vacuum canister. The largest light leak was through the metal caps over the holes for the nylon stabilizing pins in the baseplate. This was cured by placing aluminum tape around the metal caps. Other small radiation leaks were corrected in a like manner. Each detector currently sees a background flux from the dewar alone of less than 5×10^8 photons per second when the helium-cooled baffles around the optics and the light leaks into the radiation shield are blocked. This is adequate to serve as a zero-incident photon (ZIP) background when compared to the background seen by the arrays through the 10 μm filters.

Windows and Filters

The dewar entrance window is made of ZnSe and has been anti-reflection coated to give maximum transmission near 10 microns. Unlike a number of other commonly used infrared window materials, ZnSe is relatively insensitive to degradation in a humid environment. The material also has a very low infrared emissivity (< 1% at 10 microns), which is particularly important as it must be used at "room" temperature and furthermore fills the beam. One disadvantage of ZnSe is that it has a high refractive index and must be anti-reflection coated to avoid unacceptably high (~ 30%) reflection losses.

Infrared filters are placed at two positions inside the dewar. A set consisting of an 8-13 μm interference filter coupled with an uncoated BaF_2 blocking filter is mounted on the liquid-nitrogen cooled radiation shield (see Figures 4 and 6). This filter set prevents unwanted thermal radiation from entering the liquid-helium cooled areas and protects the detectors from seeing unnecessarily high background radiation; the filters also reduce the thermal radiation load borne by the helium cryostat as discussed above. The BaF_2 filter blocks long-wavelength leaks in the 8-13 μm interference filters and radiates like a 77K blackbody as far as leaks in the narrow filter on the array mount are concerned. A helium-cooled filter (or two in the case of the RI array) is placed directly in front of the detector array. This narrow-band interference filter is the primary determinant of the infrared bandpass seen by the detector. For the Rockwell BIBIB array, the limiting filter has a half-power bandpass from 10.5 to 10.7 μm warm. The AESC arrays use filters with a half-power bandpass from 10.5-12.5 μm warm.

Data Acqusition System

The data acquisition system is based on a 16-bit 8086/8087-based S-100 bus computer system assembled from a combination of boards, some of which were commercially available and some of which were designed and built in-house. The functional diagram is shown in Figure 7. Integrated circuits were specifically chosen for high speed operation (8 MHz) because of the extremely high data rates associated with the experiment. For a 307 μsec frame time and 512 pixels at 12 bits each, the full bandwidth is about 3.3 Mbytes/sec of data. Including housekeeping, the data rate is 5 Mbytes/sec. There is no reasonable way to intercept that data stream with a conventional computer, so a number of interface boards were designed and built at The Aerospace Corporation to send the data, together with housekeeping and time code information, directly to the Ampex 28-track high density recorder while sending in parallel the array data to the host computer. The host computer is capable of acquiring approximately 1 out of every 4 frames sent to it at this rate. The computer can display either a color representation of the data at about 15 Hz, or send the

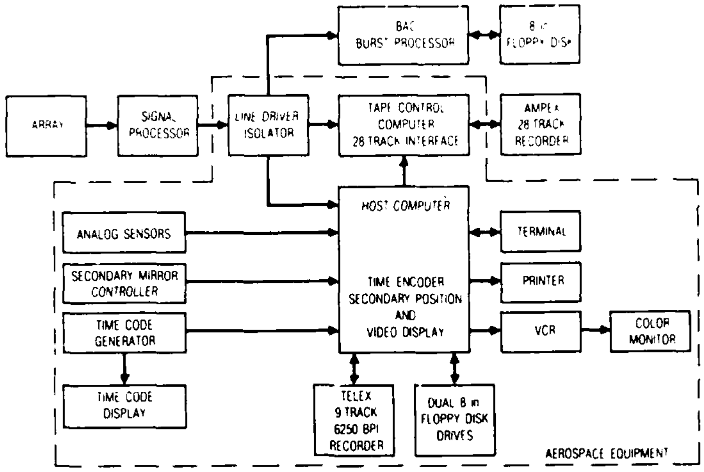

Figure 7. Functional diagram of the 16-bit 8086/8087-based S-100 bus computer system. Aerospace equipment is enclosed by the dotted line; other equipment was GFE or supplied by other contractors.

1 in 4 frames to either a 6250-bpi Telex 9 track tape recorder (3200 frame files) or to an 8" floppy disc (1228 frames/disc). The acquisition of the data in the host computer is done with a buffered interface board and a "frame grabber" (a dual-port memory and video display processor) designed and built at Aerospace. In addition, boards were built to encode the time and the position of the secondary mirror during each frame, to decode the time during 28-track tape playback, to simulate the array output so that hardware and software tests can be done independent of functioning arrays, to interface the 28-track playback electronics to the host computer so that the data quality on the 28-track tapes can be verified, and to interface between the 28-track and 9-track recorders during playback and downloading of the data to 9-track tapes.

Software was written to provide a versatile display in real-time. Corrections for offset and gain variation in the array output (pattern noise) can be applied to the data before display on the color monitor. In addition, the host computer can control the position of the rocking secondary mirror of the telescope providing a background subtraction[1,2] at ~ 27 Hz ("chopping") to enhance a target signal relative to the background. However, on our second KAO series we found a background measurement would typically be valid for up to 10 minutes, which allowed the storage and subtraction of that background without chopping. We believe that the background varied so slowly because of the improvements that NASA had made in the vacuum tightness of the cavity with respect to the plane's cabin; this presented the array with a fairly stable background in the open port cavity. Some residual fluctuations can still be seen in the background data, especially when played back in a "movie" mode on a color terminal. We believe that this is due to small motions of the telescope with respect to the cavity as the servo stabilization system corrects for aircraft motion. That servo correction, incidentally, results in an image motion of < 5 μrad, rms.

To date the most difficult task has been interfacing the 28-track Ampex recorder to the array outputs. A large number of early parts failures made it difficult to get started, but these appear to be resolved now. The recorder requires a pixel clock for control of tape speed, and this clock must meet exacting specifications for symmetry, stability, and absence of noise. Although more than 10^{10} bytes of data were recorded on 28-track tapes during three 7-hour flights, problems with interference on the pixel and frame sync lines have made more than 2/3 of it unrecoverable. Thus far we have used instead the smaller amount of real-time 9-track data which was recorded in parallel. We believe that hardware fixes have corrected this problem for future flights. As it currently exists, line drivers with optical isolators which are capable of driving 3 ports are connected directly to the digital data bus of the array electronics package which was provided by the array manufacturer. One of the outputs is then connected to a buffered interface board which conducts I/O with the time encoder board, the secondary position A/D board, and the frame grabber, which are all located in the host computer. This buffered interface board merges the housekeeping data with the array data and sends it to the 28-track recorder.

We now have two options for playback. We can slow down the 28-track recorder and play the tape directly into the 16-bit system without losing frames, or we can connect the Ampex playback electronics to the buffered interface unit (BIU). The BIU uses a microprocessor as

part of a tape controller and resides on two S-100 bus cards. DMA (direct memory access) is used to transfer the data from the 28-track high density tape to a more common 6250 bpi 9-track tape. The BIU uses interrupt-driven software and First-In-First-Out buffers (FIFOs) to increase system throughput. All of these devices have now been run successfully in the laboratory.

Field Tests

When new devices of any sort are created, one of the first tasks undertaken is to attempt to characterize the device under extremely well-controlled conditions. In the case of an IR detector array, this usually means a laboratory environment with the detector installed in a dewar designed specifically for the array in terms of background, spectral filtering, detector temperature, and detector bias. The electronics may be run by batteries, or at a minimum by carefully regulated power supplies, and the entire system is usually in a room where there is no EMI (electro-magnetic interference). This is as it should be, for only in this manner can one map out the performance of the device as a function of the many variables associated with its operation and identify the ultimate limits on its performance.

Unfortunately, this does not address the operating characteristics of devices in the real world. The following plan was therefore devised to move in reasonable increments from the manufacturer's laboratory to airborne observations from the KAO.

The helium dewars were specified several months in advance of the award of contract to Aerospace and delivered on schedule. Next the optics, provided by TBE, were to be installed at Aerospace and the entire dewar taken to the manufacturer for array installation. Plans allowed for several weeks of operation in the Aerospace laboratories following installation. Because of numerous delays the first dewar, containing the AESC bulk array, was delivered the day before departure for the Mt. Lemmon Observatory. At Mt. Lemmon we had to install the dewar in a mounting cradle, set up a test fixture to simulate the telescope, and align the dewar in its cradle. The 60" aperture of the Mt. Lemmon telescope afforded us enough collecting area to see IR stars such as μ Cep or α Ori with a good signal-to-noise ratio. The spot size was essentially as predicted, but the background was unacceptably high. At this point design and procurement of the second version of the f/16 optics were initiated by TBE.

Two off-axis paraboloids, as discussed earlier, were then installed in the dewar and flown on the Learjet Observatory (LJO). The LJO has a very noisy acoustical environment. It also has ground return currents flowing in the skin of the aircraft and frequent radio transmissions by the pilots. Both of these can produce bad electrical interference. We concluded that the LJO flight would be a good test of the impact of an airborne telescope platform on the noise performance of the arrays and their electronics. In flight, the noise spectra of specific pixels were within a factor of two of those measured in the laboratory. Infrared backgrounds were markedly reduced in the air. In retrospect, we believe that the relatively low noise level was probably due to our operating the arrays in a region of soft saturation (slightly too high a bias voltage for the background) where the noise appears artificially small.

Less than one month after the LJO tests, we installed the system on the KAO, which required a complete changeover of the dewar optics and data acquisition systems. The installation of the new optics, which had a liquid-helium-cooled Lyot stop, was prompted by the tests at Mt. Lemmon which had shown an unacceptably high thermal background. During the first two KAO flights, we used the AESC bulk detector array to collect data on response and noise as a function of bias voltage for four IR stars and for Jupiter, which is an extended source. Although we looked for the effects of changing the operating altitude from 39,000 to 45,000 feet, infrared background radiation from the cavity completely dominated all other effects. On the third flight, degradation of the surfaces of the primary and tertiary mirrors increased the background and further degraded the performance of the array.

The RI BIBIB array and AESC MC^2 array were subsequently taken to Mt. Lemmon for shakedown runs and the RI system, including electronics, was flown on the LJO to look for noise problems. Again, only minor problems were noted during these tests, except that we installed a narrower filter (~ .28 μm) for the RI array in order to reduce the background on the detectors. While at Mt. Lemmon, AESC took laboratory array data with the MC^2 detector system viewing liquid nitrogen, dry ice and acetone, and a room-temperature source to provide information for flat-fielding studies. We are just beginning to use these results in our data reduction.

In September-October 1985, a crack was found by NASA in the bulkhead of the KAO telescope cavity. The repair and subsequent testing forced a delay of over 50 days. Following this delay, we conducted a series of three KAO flights in January, 1986 in an attempt to operate all three arrays (two per flight) with the complete data-acquisition system in-

cluding the 28-track high-density tape recorder, which had not been used on the previous KAO flight series. During the first of these flights the telescope was out of collimation and gave comatic, deformed images. Technical difficulties with the telescope also plagued the second flight, but the third flight was successful. During the seven hours of the third flight, all three dewars were mounted on the telescope in turn and we observed the stars α Ori and CW Leo and the nebula M42, a region with multiple sources and extended emission. During the observations of α Ori with the RI dewar, a scanning experiment sequence was conducted by Boeing and TBE to simulate time-delay-and-integrate (TDI) operation. In this test, the image of the star was scanned across the array at different rates to simulate a moving target. The subsequent analysis of the TDI data by BAC showed an improvement in the signal-to-noise ratio of 2.7 versus the theoretical limit of 3.0 even though the secondary mirror is not designed to do this sort of experiment. To the best of our knowledge, this represents the first demonstration of TDI with an operational system, and is a significant accomplishment of the KITE program.

Preliminary Results

As noted above, we have only begun to scratch the surface of the mass of KITE data, but a few comments may be made at this time. The image core appears to be of the correct size, although the wings of the image extend further than expected. The wings probably do not come from the multiplexer because SWIFET (switched FET) multiplexers are noted for their extremely low crosstalk. We plan further laboratory experiments to assess the effect of misalignment or poor focus of the dewar optics.

While observing a bright celestial point source during the first series of flights we noted a low-level illumination of the focal plane over all but the few rows and columns that were vignetted due to a slight misalignment of the dewar optics. Because the low level flux was visible only on those detectors which were able to see out of the dewar, we concluded that the effect was probably due to scattering off dust on the telescope optics.

To first order, all of the arrays show essentially the same system NEP of $\sim 2 \times 10^{-13}$ W/$\sqrt{\text{Hz}}$. But we have noted some non-photon counting sources of noise as we have learned how to optimize the arrays' performance. We are exploring the nature of the noise to look for pick-up (a 120 Hz peak came and went in flight), level shifts such as one might expect from changing out-of-field illumination caused by the motion of the telescope in its cavity, or noise due to ground loops on the airplane. The array processor electronics were constructed with the capability to move the single point ground around the system. However, aircraft schedule constaints have thus far precluded our doing an extensive test of the noise in the aircraft on the runway to study the effects of moving this single ground point or adding additional grounds.

The motion of the image seems minimal, $\lesssim$ 2.4 μrad, and to within our ability to measure it may be constant. The spot size and motion data are consistent with the results being obtained at visible wavelengths by Dunham and Elliot[3] as part of a separate seeing study being done under KITE.

We have now written and tested software to transfer data from both the realtime 9-track tapes and the down-loaded 9-track tapes which are generated from the original 28-track tapes. Now that the data-transfer problems are solved, more sophisticated and more efficient data analysis will be done on the laboratory's VAX 11/785 computer. The IDL language which we use for this work has proven to be a very valuable tool due to its flexibility, ease of use, and large built-in capability. The data can be output as files on disc or tape, as color images or as a 3-D representation of the array intensity (Figure 8). Hard copies are easily made. We are also able to compute averages and standard deviations for each pixel, to find the image centroid, and to study noise spectra using FFT's. With Boeing, TBE, Aerospace, and U.S. Army analysts all studying the data, we hope to maximize the value we can derive from the approximately 100 billion bytes obtained thus far.

Acknowledgments

The excellent support of the many people at Ames Research Center and elsewhere who helped with many aspects of the flights is gratefully acknowledged. Particular thanks are due those people at Rockwell International and Aerojet ElectroSystems Company who helped us to get the most out of their arrays. This work was supported by NASA Grant NAS2-12155.

References

1. Low, F. J. and Rieke, G. H., "The Instrumentation and Techniques of Infrared Photometry," in Methods of Experimental Physics, Vol. 12A: Astrophysics, ed. N. Carleton, Academic Press, 1974.
2. Allen, D. A., Infrared: The New Astronomy, John Wiley and Sons 1975.
3. Dunham, E. W. and Elliott, J. L., private communication.

AEROJET ELECTRO SYSTEMS COMPANY BULK ARRAY

CW LEO

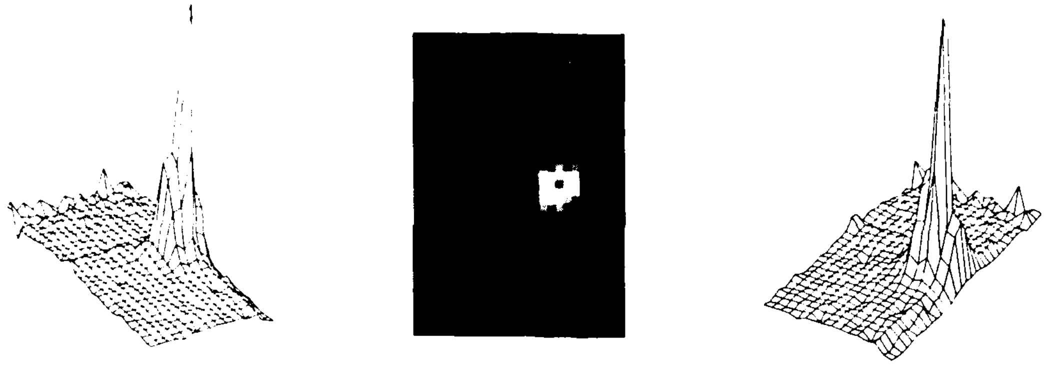

ROCKWELL INTERNATIONAL BIBIB ARRAY

α ORI

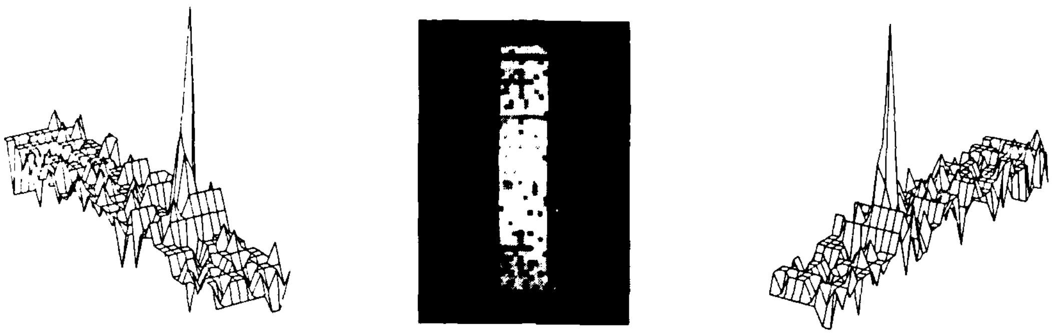

AEROJET ELECTRO SYSTEMS COMPANY MC^2 ARRAY

α ORI

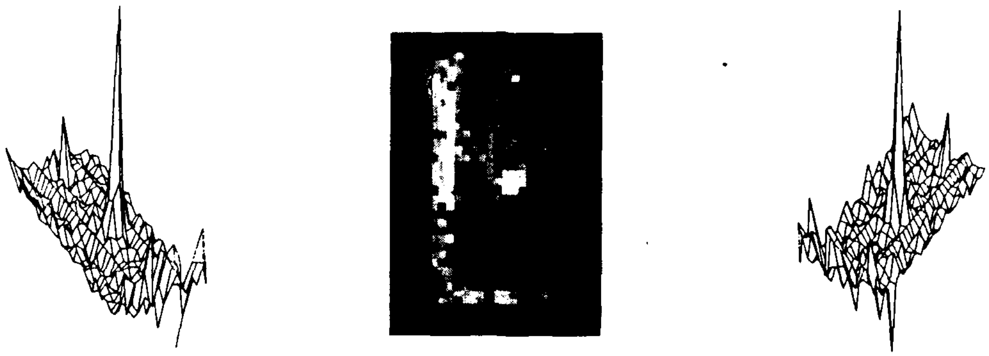

Figure 8. Typical pixel images of point sources (originals are larger and are produced in color) and 3-D contour representations of output for each of the three arrays tested. The data were obtained during the 29-30 January 1986 flight of the KAO. Note that test conditions (e.g., source, integration time, wavelength interval, etc.) differ greatly for each of the arrays so that comparisons should not be made based on these displays.